



Italian Society of Chemistry
Division of Organic Chemistry
Division of Medicinal Chemistry
Division of Mass Spectrometry

TARGETS IN HETEROCYCLIC SYSTEMS

Chemistry and Properties

Volume 17 (2013)

Reviews and Accounts on Heterocyclic Chemistry
http://www.soc.chim.it/it/libriecollane/target_hs

Editors

Prof. Orazio A. Attanasi

University of Urbino "Carlo Bo", Urbino, Italy

and

Prof. Domenico Spinelli

University of Bologna, Bologna, Italy

Published by:

Società Chimica Italiana

Viale Liegi, 48

00198 Roma

Italy

Copyright © 2013 Società Chimica Italiana

All rights reserved. No part of this publication may be reproduced, stored in a retrieval system or transmitted in any form or by any means (electronic, electrostatic, magnetic tape, mechanical, photocopying, recording or otherwise) without permission in writing from the publishers. A person may photocopy an article for personal use.

Volume 1 (1997)	First edition 1997	ISBN 88-86208-24-3	
	Second edition 1999	ISBN 88-86208-24-3	
Volume 2 (1998)	First edition 1999	ISBN 88-86208-11-1	
Volume 3 (1999)	First edition 2000	ISBN 88-86208-13-8	
Volume 4 (2000)	First edition 2001	ISBN 88-86208-16-2	
Volume 5 (2001)	First edition 2002	ISBN 88-86208-19-7	
Volume 6 (2002)	First edition 2003	ISBN 88-86208-23-5	
Volume 7 (2003)	First edition 2004	ISBN 88-86208-28-6	ISSN 1724-9449
Volume 8 (2004)	First edition 2005	ISBN 88 86208-29-4	ISSN 1724-9449
Volume 9 (2005)	First edition 2006	ISBN 88 86208-31-6	ISSN 1724-9449
Volume 10 (2006)	First edition 2007	ISBN 978-88-86208-51-2	ISSN 1724-9449
Volume 11 (2007)	First edition 2008	ISBN 978-88-86208-52-9	ISSN 1724-9449
Volume 12 (2008)	First edition 2009	ISBN 978-88-86208-56-7	ISSN 1724-9449
Volume 13 (2009)	First edition 2010	ISBN 978-88-86208-62-8	ISSN 1724-9449
Volume 14 (2010)	First edition 2011	ISBN 978-88-86208-67-3	ISSN 1724-9449
Volume 15 (2011)	First edition 2012	ISBN 978-88-86208-70-3	ISSN 1724-9449
Volume 16 (2012)	First edition 2013	ISBN 978-88-86208-72-7	ISSN 1724-9449
Volume 17 (2013)	First edition 2014	ISBN 978-88-86208-75-8	ISSN 1724-9449

Printed and bound in Italy by:

Arti Grafiche Editoriali s.r.l.

Via S. Donato, 148/C

61029 Urbino (Pesaro-Urbino)

Italy

June 2014

Editorial Advisory Board Members

Prof. Jan Bergman

*Karolinska Institute
Huddinge, Sweden*

Prof. Robert K. Boeckman Jr.

*University of Rochester
Rochester, USA*

Prof. José A. S. Cavaleiro

*University of Aveiro
Aveiro, Portugal*

Prof. Leopoldo Ceraulo

*University of Palermo
Palermo, Italy*

Prof. Girolamo Cirrincione

*University of Palermo
Palermo, Italy*

Prof. Janine Cossy

*ESPCI
Paris, France*

Dr. Daniele Donati

*Glaxo Wellcome
Verona, Italy*

Prof. José Elguero

*CSIC
Madrid, Spain*

Prof. Dieter Enders

*RWTH
Aachen, Germany*

Prof. Leon Ghosez

*Catholic University of Louvain
Louvain la Neuve, Belgium*

Prof. Gianluca Giorgi

*University of Siena
Siena, Italy*

Prof. Lucedio Greci

*University of Ancona
Ancona, Italy*

Prof. Laurence M. Harwood

*University of Reading
Reading, UK*

Prof. Steven V. Ley

*University of Cambridge
Cambridge, UK*

Prof. Pedro Merino

*University of Zaragoza
Zaragoza, Spain*

Prof. Renato Noto

*University of Palermo
Palermo, Italy*

Prof. Giovanni Sindona

*University of Calabria
Arcavacata di Rende, Italy*

Prof. Branko Stanovnik

*University of Ljubljana
Ljubljana, Slovenia*

Prof. Richard J. K. Taylor

*University of York
York, UK*

Prof. Eric J. Thomas

*University of Manchester
Manchester, UK*

Preface

Heterocyclic derivatives are important in organic chemistry as products (including natural) and/or useful tools in the construction of more complicated molecular entities. Their utilization in polymeric, medicinal and agricultural chemistry is widely documented. Dyestuff, electronic, and tanning structures, as well as life molecules frequently involve heterocyclic rings that play an important role in several chemical and biochemical processes.

Volume 17 (2013) keeps the international standard of TARGETS IN HETEROCYCLIC SYSTEMS – Chemistry and Properties (THS) series and contains eight chapters, covering the synthesis, reactivity, and activity (including medicinal) of different heterorings. Authors from Canada, France, Italy, Spain, and Ukraine are present in this book.

As yet, THS Volumes 1-17 published 229 reviews by 646 authors from 30 different countries for a total of about 7.000 pages.

Comprehensive Reviews reporting the overall state of the art on wide fields as well as personal Accounts highlighting significant advances by research groups dealing with their specific themes have been solicited from leading Authors. The submission of articles having the above-mentioned aims and concerning highly specialistic topics is strongly urged. The publication of Chapters in THS is free of charge. Firstly a brief layout of the contribution proposed, and then the subsequent manuscript, may be forwarded either to a Member of the Editorial Board or to one of the Editors.

The Authors, who contributed most competently to the realization of this Volume, and the Referees, who cooperated unselfishly (often with great patience) spending valuable attention and time in the review of the manuscripts, are gratefully acknowledged.

The Editors thank very much Dr. Lucia De Crescentini for her precious help in the editorial revision of the book.

Orazio A. Attanasi and Domenico Spinelli

Editors

Table of Contents

(for the contents of Volumes 1–16 please visit: <http://www.soc.chim.it>)

Recent advances in pyrimidine derivatives as luminescent, photovoltaic and non-linear optical materials	1
<i>Sylvain Achelle and Christine Baudequin</i>	
1. Introduction	
2. Pyrimidines	
2.1. Arylpyrimidines and arylethynylpyrimidines	
2.2. Arylvinylpyrimidines and aryliminepyrimidines	
2.3. Organometallic and coordinated pyrimidine derivatives	
3. Quinazolines	
4. Pyrrolo[2,3-d]pyrimidines	
5. Other fused pyrimidines	
6. Conclusions	
References	
A unified strategy for the synthesis of bridged indole alkaloids and their close analogues	35
<i>M.-Lluïsa Bennisar</i>	
1. Introduction	
2. Construction of the ervitsine ring system	
3. First total synthesis of apparicine	
3.1. Initial studies	
3.2. Completion of the total synthesis	
4. Synthesis of cleavamine-type indole alkaloids and their 5-nor derivatives	
4.1. Construction of the 5-nor cleavamine skeleton	
4.2. Total synthesis of cleavamines	
5. Conclusion	
Acknowledgments	
References	
Recent advances in the synthesis of selected indolizidine and quinolizidine alkaloids	57
<i>Sunil V. Pansare and Rakesh G. Thorat</i>	
1. Introduction	
2. Scope and organization of the review	
3. Synthetic strategies for selected indolizidine and quinolizidine alkaloids	
3.1. Ring formation <i>via</i> nucleophilic displacement or addition reactions	
3.1.1. Nitrogen-carbon cyclizations with preformed azacycles as starting materials	
3.1.2. Nitrogen-carbon cyclizations with open chain precursors	
3.1.3. Carbon-carbon cyclizations with preformed azacycles as starting materials	

- 3.1.4. Carbon-carbon cyclizations *via* azacyclic intermediates
- 3.2. Syntheses employing ring closing metathesis as a key transformation
- 3.3. Asymmetric cycloaddition-based strategies
- 3.4. Iminium ion-based approaches
- 3.5. Syntheses involving organocatalysis
- 4. Closing remarks
- Acknowledgments
- References

Thiazolo[5,4-*d*]thiazole-based compounds: emerging targets in materials science, organic electronics and photovoltaics

87

Lorenzo Zani, Massimo Calamante, Alessandro Mordini and Gianna Reginato

- 1. Introduction
- 2. Synthesis, elaboration and characterization of thiazolo[5,4-*d*]thiazoles and related materials
 - 2.1. Synthesis and functionalization of thiazolo[5,4-*d*]thiazoles
 - 2.2. Thiazolothiazole-based polymers
 - 2.3. Structural, photophysical and spectroscopic properties
- 3. Applications of thiazolo[5,4-*d*]thiazole-based materials
 - 3.1. Biological activity
 - 3.2. Preparation of metal complexes and crystal engineering
 - 3.3. Non-linear optics and fluorescent sensors/emitters
 - 3.4. Organic light-emitting diodes
 - 3.5. Organic field-effect transistors
 - 3.6. Organic and polymeric solar cells
 - 3.7. Dye-sensitized solar cells
- 4. Conclusions
- Acknowledgments
- References

Synthesis and photophysical properties of the green fluorescent protein chromophore and analogues

125

David Martínez-López and Diego Sampedro

- 1. Introduction
- 2. Synthesis of GFP chromophore analogues
 - 2.1. Synthesis of oxazolones
 - 2.2. Synthesis of imidazolinones
 - 2.3. Synthesis of other derivatives
- 3. Photophysical properties of GFP and GFP derivatives
 - 3.1. Absorption
 - 3.1.1. Oxazolones

- 3.1.2. Imidazolinones
- 3.2. Fluorescence
 - 3.2.1. Oxazolones
 - 3.2.2. Imidazolinones
- 3.3. Photoisomerisation
- 3.4. Photophysical properties of other derivatives
- 4. Applications
- 5. Conclusions
- Acknowledgments
- References

Synthesis, chemical and biological properties of trifluoromethylated pyrimidin-2-ones(thiones) and their fused analogues

147

Veronika M. Shoba, Viktor M. Tkachuk, Volodymyr A. Sukach and Mykhailo V. Vovk

- 1. Introduction
- 2. Synthesis of trifluoromethylated pyrimidin-2-ones(thiones)
 - 2.1. Biginelli reaction
 - 2.2. [NCN]+[CCC] cyclization
 - 2.3. [CCCN]+[CN] cyclization
 - 2.4. [CNC]+[NCC] cyclization
- 3. Chemical properties of trifluoromethylated pyrimidin-2-ones(thiones)
 - 3.1. Nucleophilic addition reactions
 - 3.2. Photochemical reactions and processes involving free radicals
- 4. Biological properties of trifluoromethylated pyrimidin-2-ones(thiones)
- 5. Conclusions
- References

Biocatalysis applied to the synthesis of valuable triazole-containing derivatives

176

Aníbal Cuetos, Fabricio R. Bisogno and Iván Lavandera

- 1. Introduction
- 2. Biocatalytic approaches over triazole-containing derivatives
 - 2.1. 1,2,3-Triazoles
 - 2.1.1. Using hydrolases
 - 2.1.2. Using transferases
 - 2.1.3. Cofactor mimics
 - 2.2. 1,2,4-Triazoles
 - 2.2.1. Using hydrolases: lipases and acylases
 - 2.2.2. Using hydrolases: nucleoside phosphorylases
 - 2.2.3. Using transferases
 - 2.3. Benzotriazoles

- 2.3.1. Using hydrolases
- 2.3.2. Using oxidoreductases
- 3. Biocatalytic approaches over precursors to obtain triazole-containing derivatives
 - 3.1. Using hydrolases
 - 3.2. Using oxidoreductases
 - 3.3. Using transferases
- 4. Novel approaches based on cascade or tandem protocols
- 5. Summary and outlook
- Acknowledgments
- References

**2,5-Diketopiperazines as privileged scaffolds in medicinal chemistry,
Peptidomimetic chemistry and organocatalysis**

215

Umberto Piarulli and Silvia Panzeri

- 1. Introduction
- 2. Synthesis
 - 2.1. Synthesis of the ring
 - 2.2. Functionalization of the DKPs scaffold
- 3. Applications in medicinal chemistry
 - 3.1. DKP as modulator of dopaminergic receptors
 - 3.2. β -turn mimics
 - 3.3. [DKP]integrin ligands
- 4. Application in catalysis
- 5. Conclusion
- References

RECENT ADVANCES IN PYRIMIDINE DERIVATIVES AS LUMINESCENT, PHOTOVOLTAIC AND NON-LINEAR OPTICAL MATERIALS

Sylvain Achelle^{a*} and Christine Baudequin^b

^a Institut des Sciences Chimiques de Rennes, UMR CNRS 6226, I.U.T. Lannion, rue Edouard Branly BP 30219, F-22302 Lannion Cedex, France (e-mail: sylvain.achelle@univ-rennes1.fr)

^b Normandie Univ, COBRA, UMR 6014 et FR 3038; Univ Rouen; INSA Rouen; CNRS, IRCOF, 1 rue Tesnière, F-76821 Mont-Saint-Aignan Cedex, France

Abstract. Through the past few decades, the development of new optical materials has received a lot of attention due to their applications as fluorescent sensors, in biological microscopy and in optoelectronic devices. Most of these applications rely on intramolecular charge transfer (ICT). The presence of electron-withdrawing N-heterocycles such as pyrimidine appeared therefore particularly interesting to be used as electron-attracting part in π -conjugated structures. Moreover, the presence of nitrogen atoms with lone electron pairs allows the pyrimidine to act as effective and stable complexing agent or as base that can be protonated. This review reports the recent examples from the 2010–2013 period of small molecules, oligomers and polymers that bear one or multiple pyrimidine rings in their scaffolds and highlights the applications related to their optical properties.

Contents

1. Introduction
 2. Pyrimidines
 - 2.1. Arylpyrimidines and arylethynylpyrimidines
 - 2.2. Arylvinylpyrimidines and aryliminepyrimidines
 - 2.3. Organometallic and coordinated pyrimidine derivatives
 3. Quinazolines
 4. Pyrrolo[2,3-d]pyrimidines
 5. Other fused pyrimidines
 6. Conclusions
- References

1. Introduction

Diazines which belong to the most important heterocycles are six-membered aromatics with two nitrogen atoms. Three different regioisomers can be distinguished according to the relative position from the nitrogen atoms: pyridazine (1,2-diazine),¹ pyrimidine (1,3-diazine)² and pyrazine (1,4-diazine).³ Among them, the 1,3-diazine derivatives are the most studied because the pyrimidine ring system has wide occurrence in nature as substituted and ring fused compounds and derivatives such as nucleotides and vitamin B1.⁴ The pyrimidine system is also an important pharmacophore.⁵

The elaboration of electro-optical (EO) and nonlinear optical (NLO) materials has attracted considerable attention because of their wide range of potential applications in optical data processing

technologies. Push-pull molecules with large delocalized π -electron systems are also typical second and third order NLO chromophores.⁶ Quadrupolar D- π -A- π -D structures also exhibit third order NLO properties. Second order NLO materials have found applications in green lasers obtained from red sources through frequency doubling, in second harmonic generation microscopy or in terahertz wave generation.⁷ Third order NLO, in particular two-photon absorption (TPA) materials, have also attracted considerable attention due to their applications in photodynamic therapy, confocal microscopy, optical power limiting and 3D data storage and microfabrication.⁸ In analytical chemistry, a variety of fluorescence sensors has been also extensively developed during the past two decades. The synthesis of extended π -conjugated systems has been the key to provide organic materials with required properties. These compounds are often based on a push-pull system, which is constituted by an electron-donating group (D) and an electron-withdrawing group (A) linked through a π -conjugated spacer providing an internal charge transfer (ICT) upon excitation. The molecular properties of the chromophores depend on the strength of the “push-pull” effects which are function of the ability of the donor to provide electrons and the acceptor to withdraw them.

Pyrimidine, which is a highly π -deficient aromatic heterocycle, can therefore be used as electron-withdrawing part in push-pull structures for ICT. An important ICT along the scaffold of the molecule can also induce luminescence properties. The ability of protonation, hydrogen bond formation and chelation of the nitrogen atoms of the pyrimidine ring are also of great importance: such derivatives could be therefore used for the formation of supramolecular assemblies and used as sensors. Moreover, it should be noted that the pyrimidine is also an excellent building block for the synthesis of liquid crystals;⁹ the combination of the optical and thermal advantages of the pyrimidine ring could lead to completely new applications.

The desired optical properties generally require molecules with an extended π -conjugated scaffold. Taking advantage of the availability of a large variety of halogen (and in particular chlorine) pyrimidine derivatives, cross-coupling reactions constitute a method of choice for the synthesis of pyrimidine derivatives that can be used as optical materials. It should be noted that the π -electron deficient character of the pyrimidine ring makes easier the oxidative addition of palladium to a chlorine-carbon bond in position 2, 4 and 6 without the use of specialized and expensive ligands.¹⁰ So, Suzuki,¹¹ Stille,¹² Negishi,¹³ Sonogashira,¹⁴ Heck¹⁵ and Corriu-Kumada¹⁶ cross-couplings carried out with halogenated pyrimidine building blocks have been described.¹⁷ Another synthetic way extensively studied to obtain vinyl pyrimidines consists in the condensation reaction of aldehydes with methylpyrimidines.¹⁸

Recently, we reviewed the use of pyrimidine, pyridazine and pyrazine as building blocks for the synthesis of π -conjugated materials.¹⁹ In the part concerning pyrimidine, we reviewed the literature until the beginning of 2010.^{18a} The present work will be focused on literature from the 2010–2013 period and will provide an overview over pyrimidine derivatives presenting optical applications with a brief description of their properties.

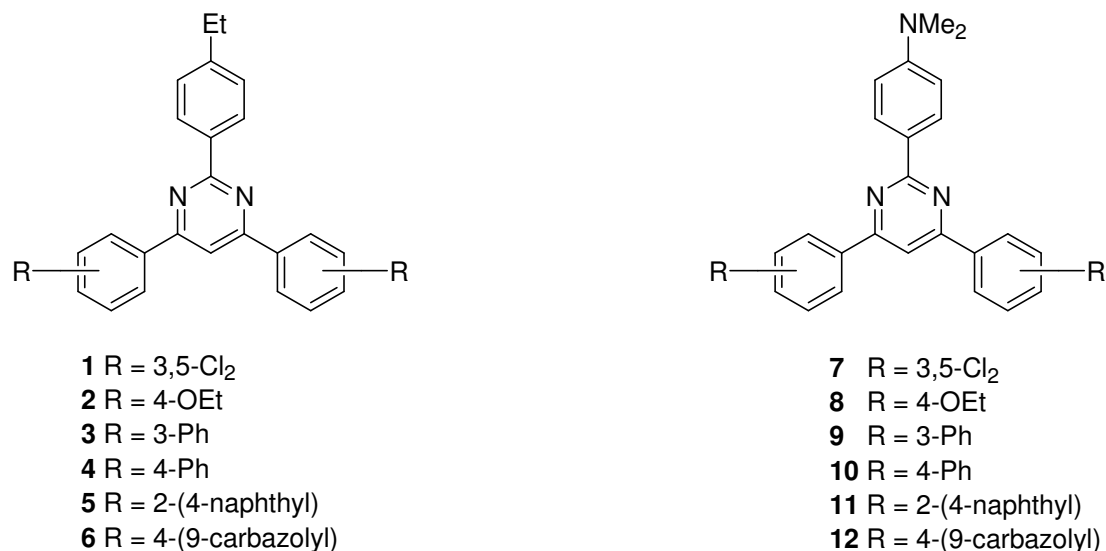
2. Pyrimidines

2.1. Arylpyrimidines and arylolethynylpyrimidines

Arylpyrimidines have been extensively studied as luminescent materials during the last two decades. Ethynylpyrimidines remain less studied. The recent developments of these two classes of compounds still concern luminescence (including fluorescent sensors), NLO materials but also hole/exciton-block layer for light emitting diodes (OLEDs) and dyes for dye-sensitized solar cells (DSSCs).

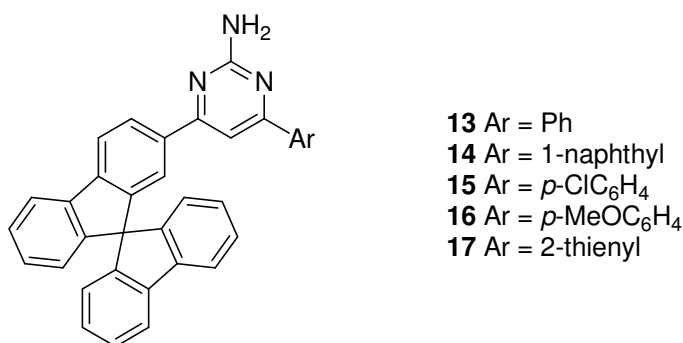
a) Luminescent materials

2,4,6-Triarylpyrimidines are known as good fluorescent dyes.²⁰ Recently, Tumkevičius and co-workers described twelve new compounds in this series (**1–12**, Scheme 1).²¹ As the previously known 2,4,6-triarylpyrimidines, the synthesized derivatives exhibit strong blue fluorescence in THF solution ($\lambda_{em}=345\text{--}436$ nm, Φ_F up to 0.6 for **6**).



Scheme 1

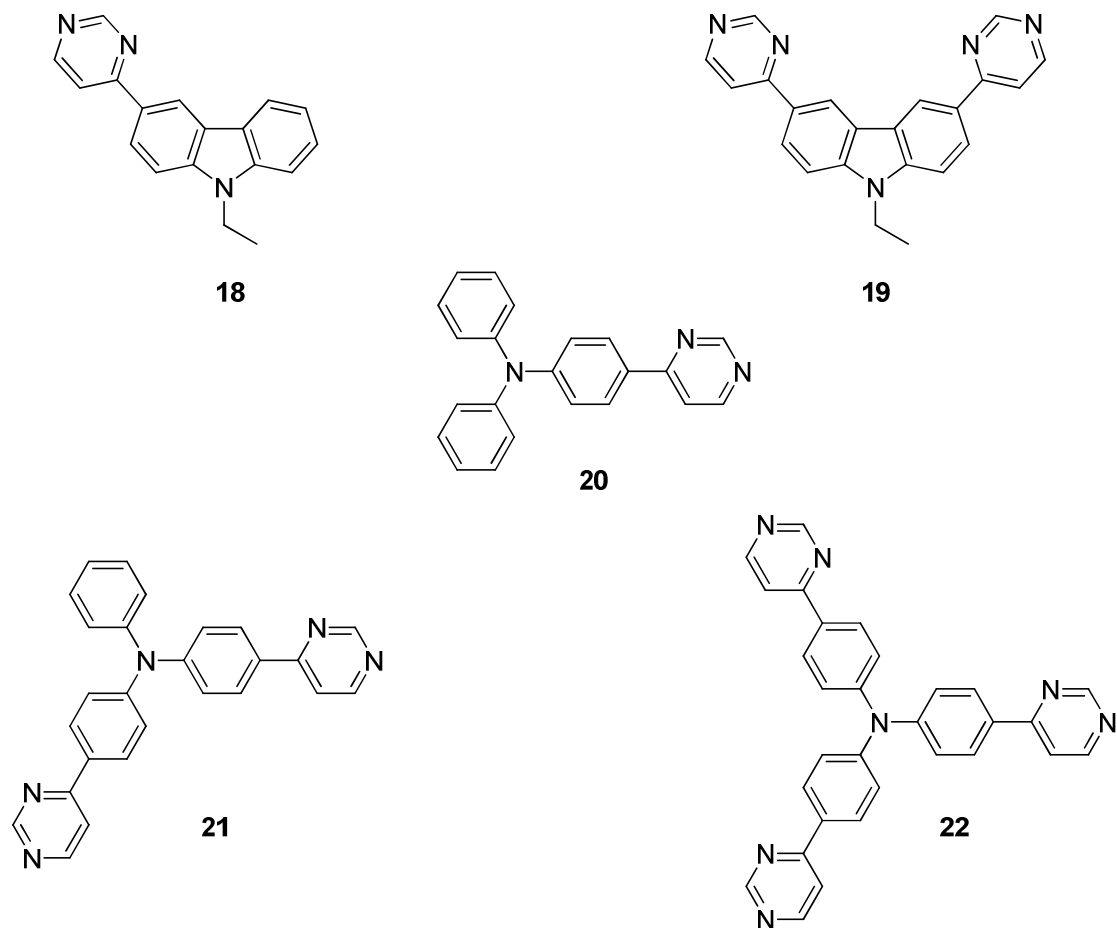
A series of pyrimidine derivatives bearing spirofluorene substituents **13–17** was synthesized by Shi *et al.* (Scheme 2).²² These compounds exhibit intense blue light emission either in dichloromethane solution ($\lambda_{em}=399\text{--}406$ nm, $\Phi_F=0.37\text{--}0.63$) or as solid ($\lambda_{em}=416\text{--}443$ nm).



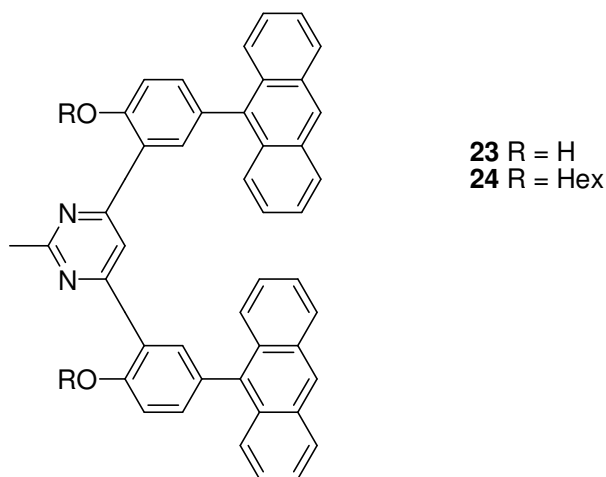
Scheme 2

Weng *et al.* described a series of push-pull pyrimidine materials bearing carbazole (**18** and **19**) or triphenylamine (**20–22**) as donors (Scheme 3).²³ These 4-monosubstituted pyrimidine compounds exhibit bright fluorescence with excellent quantum yields ($\Phi_F=0.53\text{--}0.93$) in the blue region in dichloromethane solution ($\lambda_{em}=397\text{--}472$ nm) as well as in solid film ($\lambda_{em}=423\text{--}473$ nm).

Suzaki and co-workers studied di(hydroxyphenyl)pyrimidine with two anthracenyl substituents **23** (Scheme 4).²⁴ Whereas this compound is not emissive, hexylation of the OH groups (compound **24**) leads to a strong emission in CHCl₃ solution from the anthracenyl group ($\lambda_{em}=410$ nm, $\Phi_F=0.39$). Fluorescence quenching in case of compound **23** was explained by a photo-induced electron-transfer (PET) process.



Scheme 3

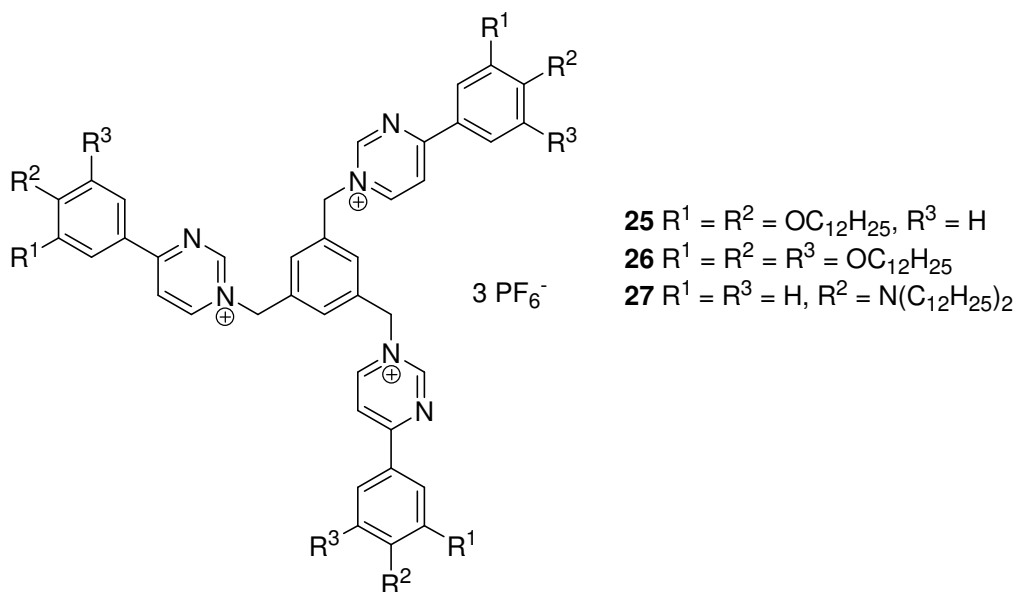


Scheme 4

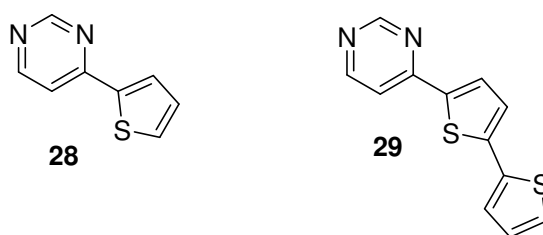
Tanabe and co-workers designed color-tunable luminescent ionic liquid crystals **25–27** (Scheme 5).²⁵ To achieve tuning of emission colors, ICT character was incorporated into tripodal molecules. Pyrimidinium part was incorporated as electron-accepting moieties and alkoxybenzene (**25** and **26**) as well as alkylaminobenzene (**27**) as electron-donating parts. Photoluminescent emissions of these tripodal molecules were observed in the visible region both in the self-assembled condensed state ($\lambda_{em}=560\text{--}586$ nm, $\Phi_F=0.01\text{--}0.09$) and in CH_2Cl_2 solution ($\lambda_{em}=524\text{--}535$ nm, $\Phi_F=0.02\text{--}0.06$).

Bolduc *et al.* designed D-A derivatives **28** and **29** incorporating thiophene/bithiophene moieties as donors and pyrimidine as acceptor (Scheme 6).²⁶ The biaryls were spectroscopically confirmed to be highly

conjugated. The bithiophene derivative **29** exhibits a large fluorescence quantum yield ($\lambda_{em}=433$ nm, $\Phi_F=0.66$ in dichloromethane) while the thiophene derivative **28** does not fluoresce. The quenched fluorescence observed for the thiophene derivative **28** was attributed to its higher triplet energy resulting in efficient intersystem crossing to the triplet state with $\Phi_{ISC} \geq 0.8$.

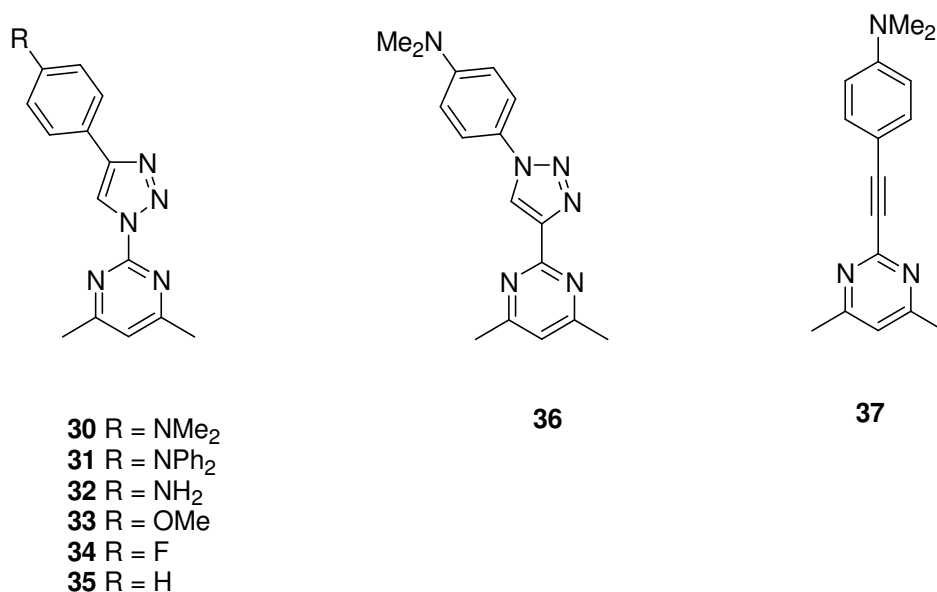


Scheme 5



Scheme 6

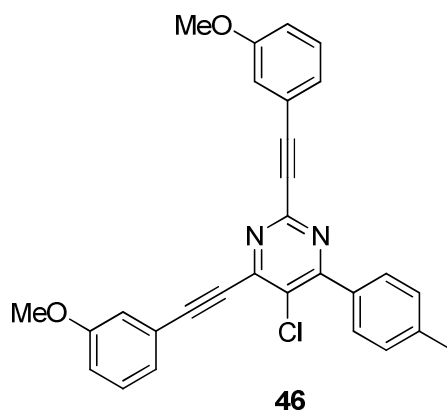
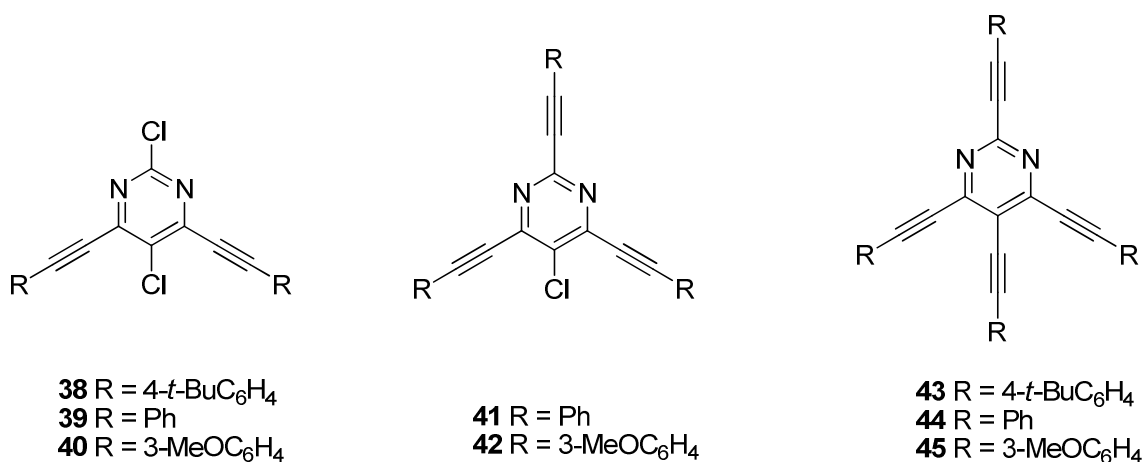
A series of A- π -D compounds **30–37** containing a pyrimidine moiety as π -acceptor (A) and various *para*-substituted benzene rings as donors (D) was designed and synthesized (Scheme 7).²⁷



Scheme 7

The influence of the π -conjugated linker (triazole rings and triple bond) was studied. Compounds bearing a triazole ring and substituted by strong amino-groups (**30–32**, **36**) exhibit strong fluorescence ($\lambda_{em}=434\text{--}486\text{ nm}$, $\Phi_F>0.3$). Triazolo-isomers **30** and **36** show similar photophysical properties in terms of both quantum yields and Stokes shifts; however hypsochromic shifts were observed in the absorption and emission wavelengths for **36**. Replacement of the triazole ring in **30** by an ethynyl linker in compound **37** results in a dramatic decrease of the quantum yield ($\Phi_F=0.04$).

Starting from tetrachloropyrimidine, Malik *et al.* synthesized by Sonogashira cross-coupling reactions a series of di-, tri- and tetraalkynyl-pyrimidines **38–46** (Scheme 8).²⁸ The products exhibit emission in the 395–470 nm range in CHCl_3 solution.

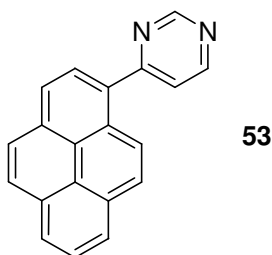


Scheme 8

The π -conjugated polymers **47–49** (Scheme 9) composed of alternating 4,6-diethynylpyrimidine electron-attracting moiety and benzene or 2,5-dialkoxybenzene electron-donating part were designed by Mamtimin *et al.*²⁹ These macromolecules ($M_n=4089\text{--}5951\text{ g mol}^{-1}$), soluble in common organic solvents, emit green light in solid state ($\lambda_{em}=445\text{--}501\text{ nm}$) and in CHCl_3 solution ($\lambda_{em}=465\text{--}495\text{ nm}$, $\Phi_F=0.07\text{--}0.12$). In the presence of acid ($\text{CH}_3\text{SO}_3\text{H}$), a bathochromic shift in emission is observed due to the formation of strong electron-accepting pyrimidinium salt.

A nitrogen-linked carbazole-containing fluorescent polymer **50** (Scheme 10) incorporating pyrimidine rings was also designed by Takagi and co-workers.³⁰ This macromolecule ($M_n=5600\text{ g mol}^{-1}$) is blue emissive in solution (in CH_2Cl_2 : $\lambda_{em}=410\text{ nm}$, $\Phi_F=0.17$). An important positive solvatochromism is observed

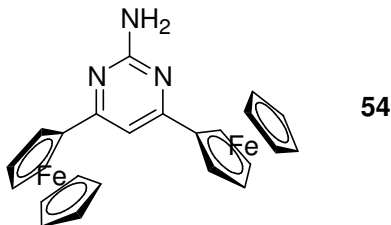
$\Phi_F=1.00$) to green ($\lambda_{em}=545$ nm) is observed only in case of addition of Hg^{2+} . Similar fluorescence change was also observed with Hg^{2+} in the presence of others ions. The photophysical properties of **53** confirmed a 2:1 (**53**, Hg^{2+}) binding model and the spectral response toward Hg^{2+} proved to be reversible.



Scheme 12

c) NLO materials

Zou and co-workers synthesized a donor-acceptor-donor biferrocenyl derivative with a pyrimidine central core **54** (Scheme 13).³⁵ This compound exhibits 3rd order NLO properties measured by Z-scan technique. A remarkable value is obtained for the 3rd order NLO susceptibility: $\chi^{(3)}=1.75 \times 10^{-8}$ esu. One consequence of the high value is the optical limiting property of **54**, measured by energy-dependent optical transmission at the focus. At lower energy, the optical response obeyed Beer's law very well. When the input energy reached about 4.92×10^{-8} μJ , the transmitted energy started to deviate from the normal line and exhibited a typical limiting effect. The threshold was 6.02×10^{-8} μJ , comparable to that of C_{60} which is considered as one of the best optical limiting material.³⁶

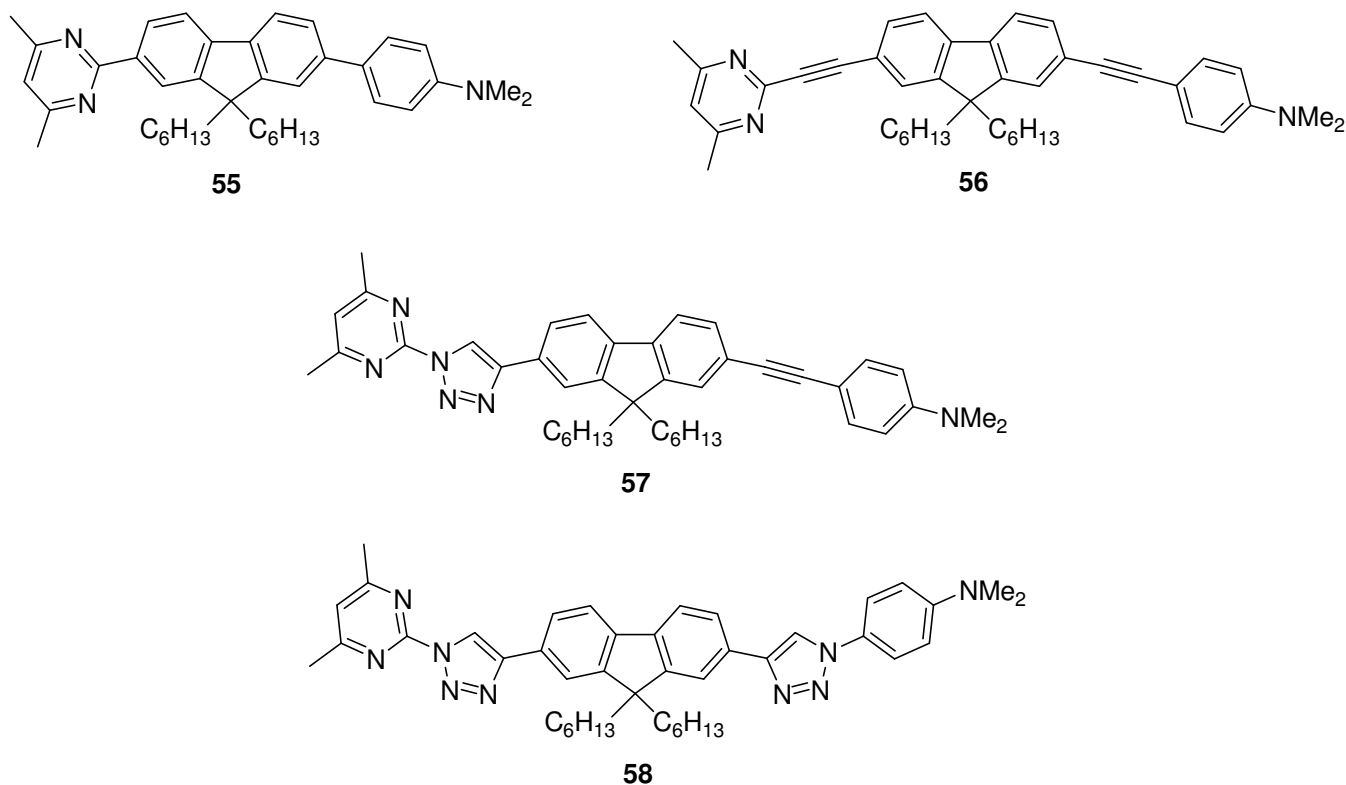


Scheme 13

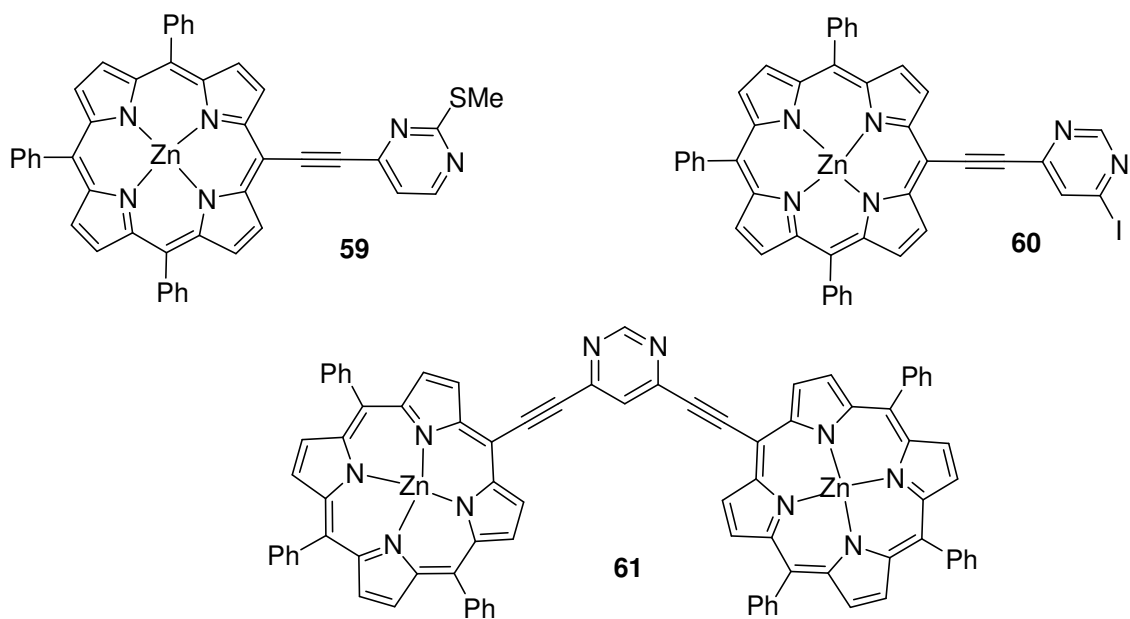
In our laboratories, we synthesized four push-pull pyrimidine derivatives **55–58** that contain fluorene as a central core, various π -conjugated linkers and the (dimethylamino)phenyl electron-donating group (Scheme 14).³⁷ All the compounds are strongly emissive in CH_2Cl_2 solution ($\lambda_{em}=422$ – 515 nm, $\Phi_F=0.47$ – 0.71). The more red-shifted derivative is compound **56** with two ethynyl linkers. Incorporation of one or two triazole rings as π -conjugated linkers (**57** and **58**) leads to a hypsochromic shift in emission. The TPA properties of these compounds were studied by two-photon excited fluorescence technique and cross-sections comprised between 32 GM (**58**) and 148 GM (**57**) were measured.

A series of zinc porphyrins conjugated with pyrimidine derivatives **59–61** was reported (Scheme 15).³⁸ All the compounds are fluorescent in CH_2Cl_2 solution ($\lambda_{em}=630$ – 648 nm, $\Phi_F=0.11$ – 0.18). ICT into the V-shaped porphyrin dimer **61** was highlighted by emission solvatochromic studies. This compound exhibits also TPA ($\delta=120$ GM at $\lambda=930$ nm) measured by two-photon excited fluorescence technique.

Four pyrimidine-based dipolar and quadrupolar dyes **62–65** (Scheme 16) bearing pro-aromatic methylenepyran donor groups were synthesized.³⁹ These derivatives are slightly emissive ($\lambda_{em}=495$ – 614 nm; $\Phi_F<0.01$) and are described as potential NLO materials.



Scheme 14

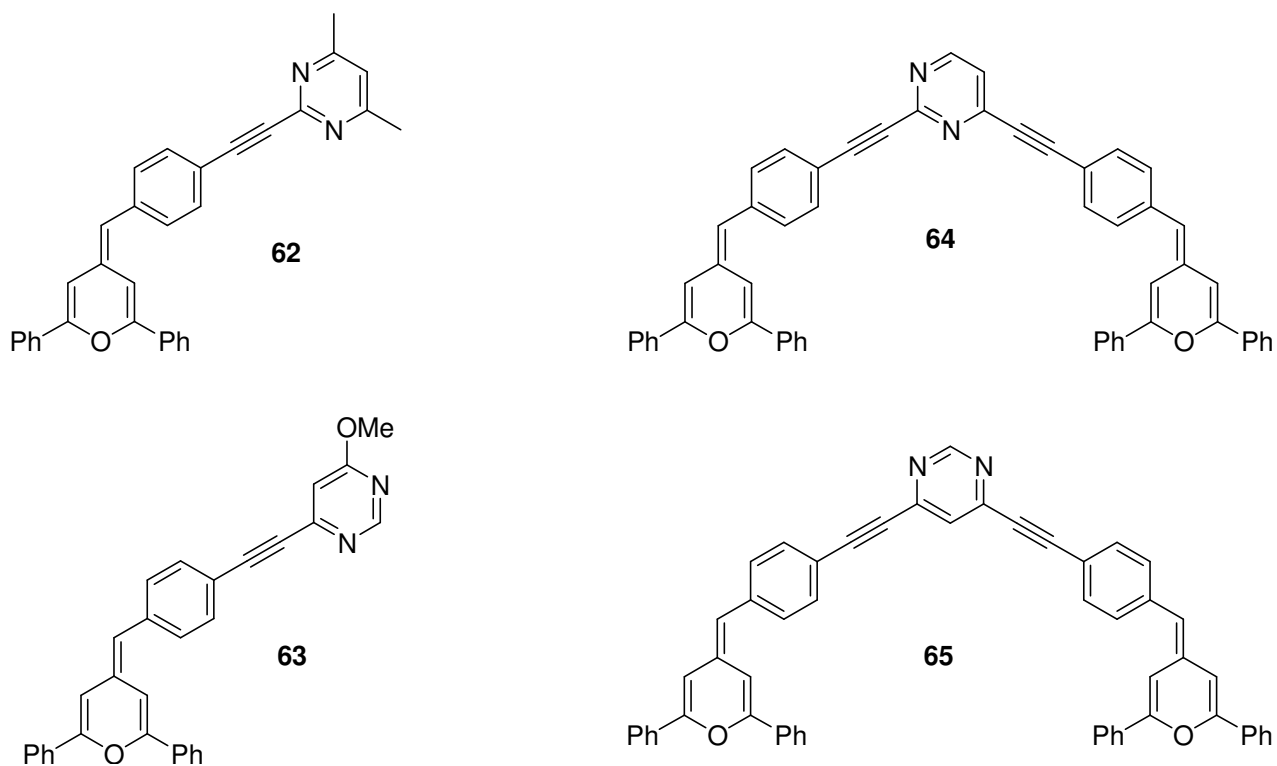


Scheme 15

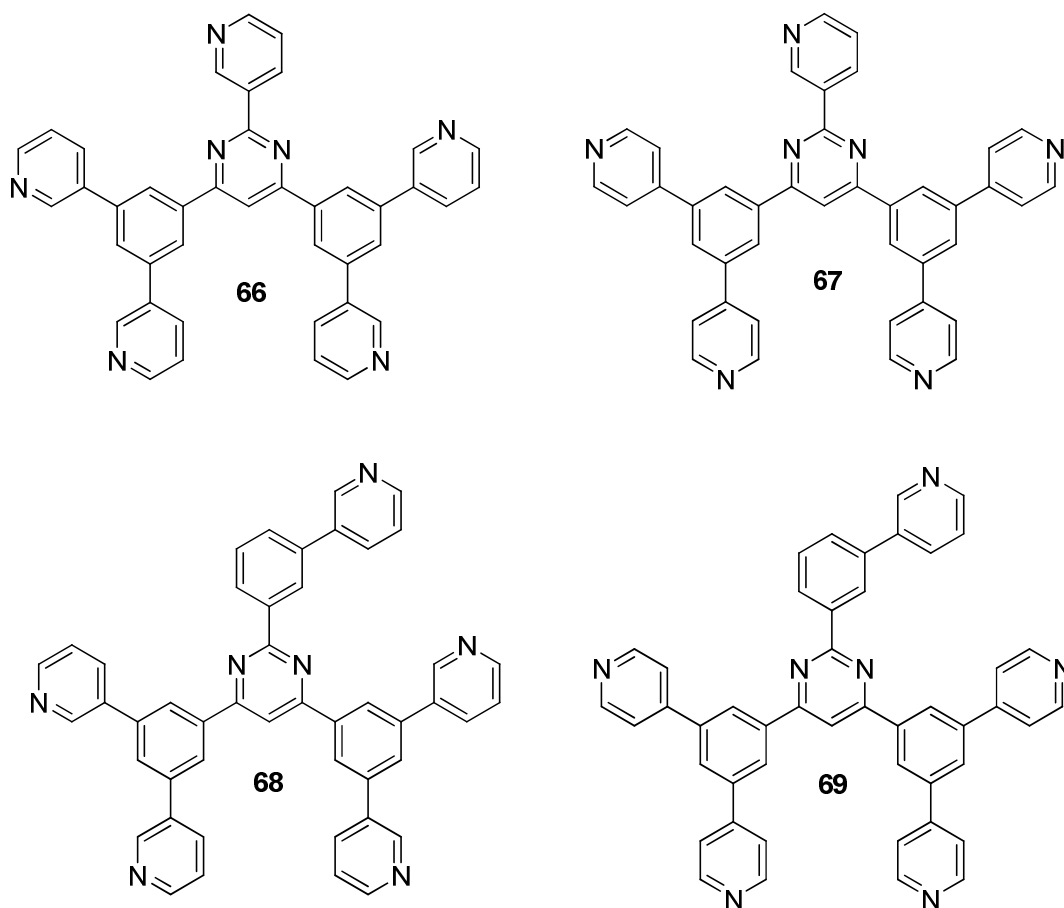
d) Materials for OLEDs

A series of pyrimidine-containing electron-transport materials with different pyridine substitution **66–69** was designed by Liu and co-workers (Scheme 17).⁴⁰ Extremely low turn-on voltages (V_{on}) of 2.1 V for electroluminescence, which are 0.2–0.3 V lower than the minimum value of the emitted photon energy ($h\nu$)/e, were experimentally achieved by utilizing the developed pyrimidine derivative **69** as an electron-transport and hole/exciton-block layer for the classical *fac*-tris(2-phenylpyridine) iridium ($\text{Ir}(\text{PPy})_3$)-based green phosphorescent OLEDs. In addition, hitherto the lowest operating voltages of 2.39, 2.72 and 3.88 V for 100, 1000 and 10 000 cd m^{-2} were achieved with simultaneously improved external quantum efficiency

(η_{ext}) to give a high power efficiency and the operating voltage for 100 cd m^{-2} is already corresponding to the value of $h\nu/e$.

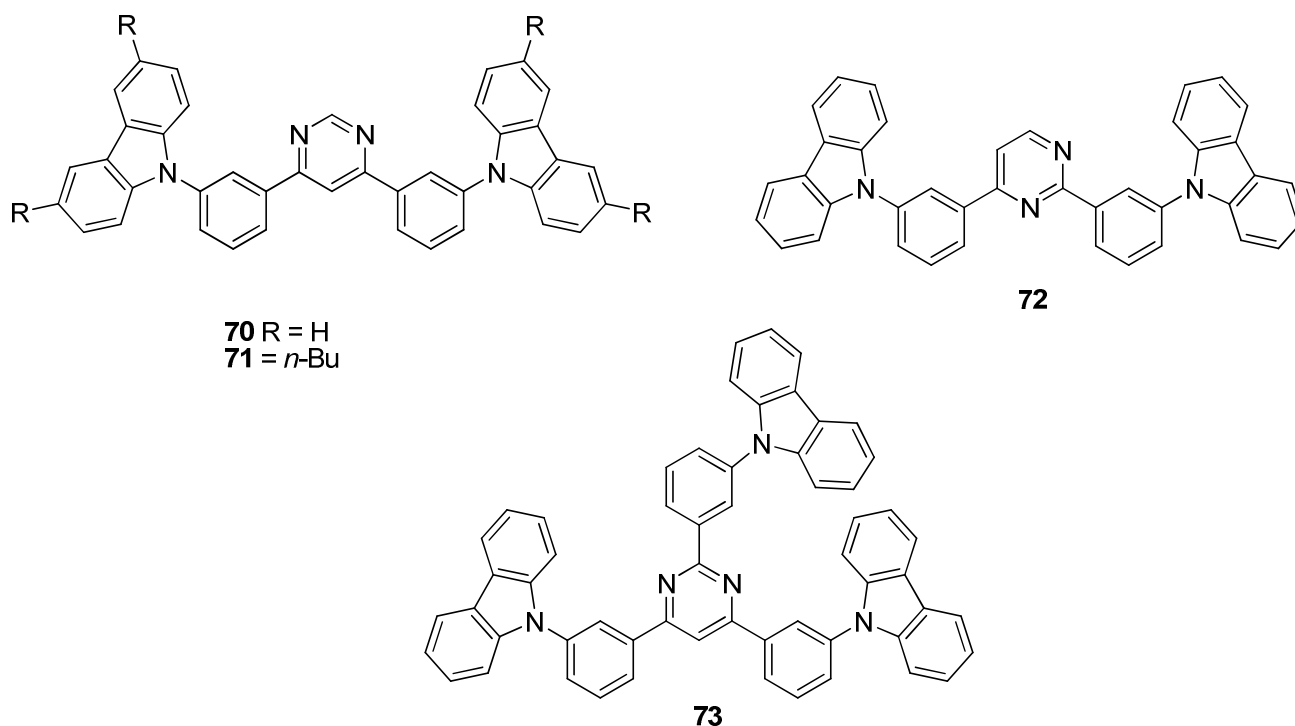


Scheme 16



Scheme 17

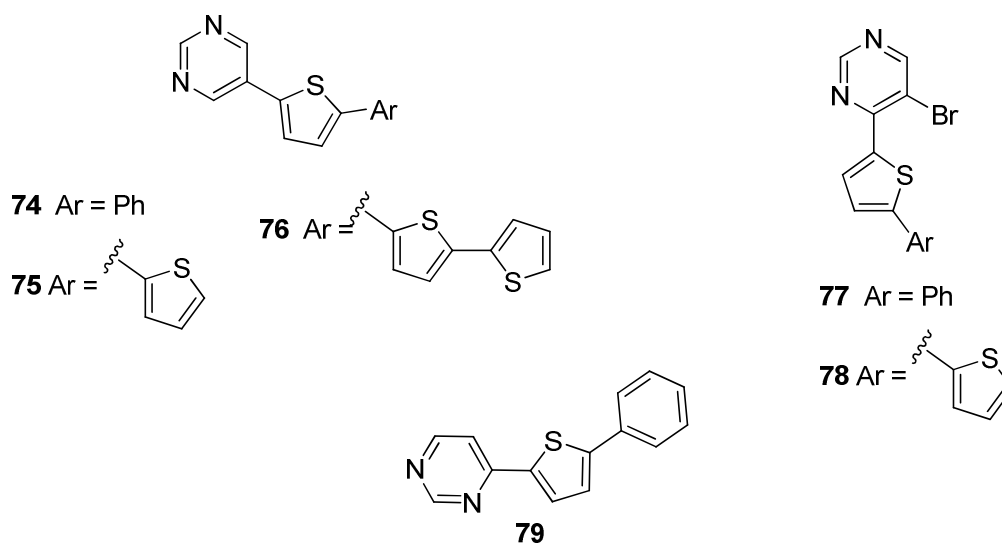
Su and co-workers also designed host materials **70–73** containing a pyrimidine core as part of iridium-based Red Green Blue phosphorescent OLEDs (Scheme 18).⁴¹ High efficiency (9.5 and 8.5% at 100 cd m⁻²) was achieved with **70** for the green phosphorescent *fac*-tris(2-phenylpyridine) iridium and for the red phosphorescent tris(1-phenylisoquinolinolato-C²,N) iridium-based OLED, which can be attributed to the low-lying LUMO level of **70**. The two nitrogen atoms in the central pyrimidine ring have a profound effect on the photoluminescence properties and the electron-accepting capability.



Scheme 18

e) Dyes for photovoltaic

Only a few examples of pyrimidine-based dyes were designed for photovoltaic applications. Verbitskiy and co-workers synthesized a series of 4- and 5-thiophenyl-substituted pyrimidines **74–79** (Scheme 19).⁴²



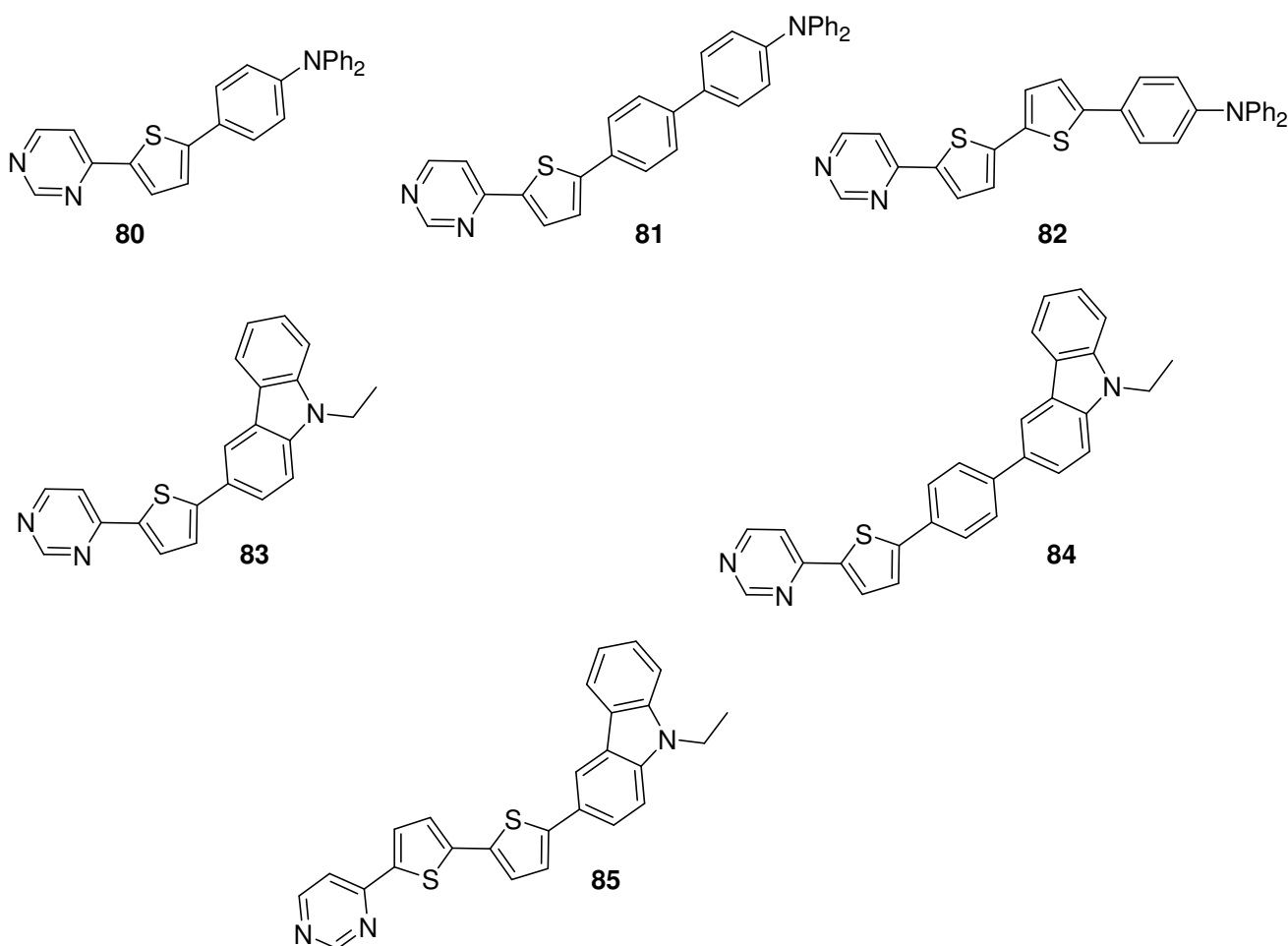
Scheme 19

These compounds exhibit blue fluorescence ($\lambda_{em}=394\text{--}472\text{ nm}$). The quantum yield observed are much higher for 4-substituted pyrimidines **77–79** ($\Phi_F=0.82\text{--}1.00$) than for 5-substituted pyrimidines **74–76** ($\Phi_F=0.06\text{--}0.11$). The authors claim that these structures can be potentially used for DSSC application.

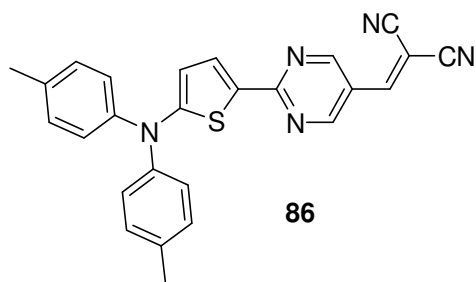
The same team designed six other push-pull structures **80–85** bearing pyrimidine attracting group and thiophene rings as π -conjugated linkers (Scheme 20).⁴³ All the compounds are highly emissive in toluene ($\lambda_{em}=444\text{--}504\text{ nm}$, $\Phi_F=0.32\text{--}0.63$). As expected for push-pull derivatives, the emission is red shifted and the quantum yield lower in more polar MeCN. The infrared spectra of which dyes adsorbed on TiO_2 indicate the formation of coordinative bonds between the pyrimidine ring of dyes and the Lewis acid sites (exposed Ti^{IV} cations) of the TiO_2 surface. This work demonstrates that the pyrimidine ring of dye sensitizers that form a coordinate bond with the Lewis acid site of a TiO_2 surface are promising candidates as the electron-withdrawing anchoring group. The data from quantum calculations show that all of the dyes are potentially good photosensitizers for dye-sensitized solar cells.

In 2012, Chiu and co-workers designed a D-A-A type pyrimidine derivative **86** (Scheme 21).⁴⁴ A vacuum-deposited planar-mixed heterojunction solar cell has been built with C_{70} as the acceptor, giving a power conversion as high as 6.4%.

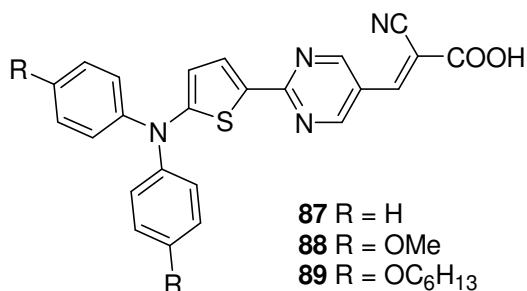
Similar structures **87–89** with classical cyanoacetic acid anchoring group for TiO_2 surface were also designed by Lin *et al.* (Scheme 22).⁴⁵ Through the introduction of two hexyloxy chains on the diphenylthienylamine donor, the DSSC employing dye **89** exhibited high power conversion efficiency up to 7.64% under AM1.5G irradiation.



Scheme 20



Scheme 21



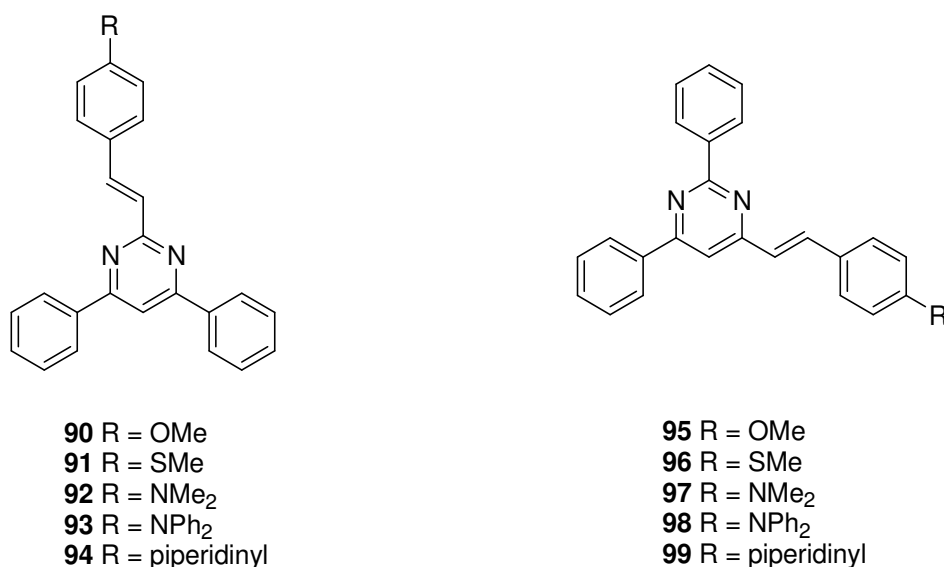
Scheme 22

2.2. Arylvinylpyrimidines

Among pyrimidine materials with luminescent and NLO properties, arylvinylpyrimidines are probably the class that have been extensively studied. In particular, since their first syntheses^{17a} and the demonstration of their TPA properties,⁴⁶ 4,6-di(arylvinyl)pyrimidines have become well established NLO dyes.

a) Luminescent materials

In order to study the influence of the substituted position on the pyrimidine ring, two series of arylvinylpyrimidines **90–99** were synthesized (Scheme 23).⁴⁷

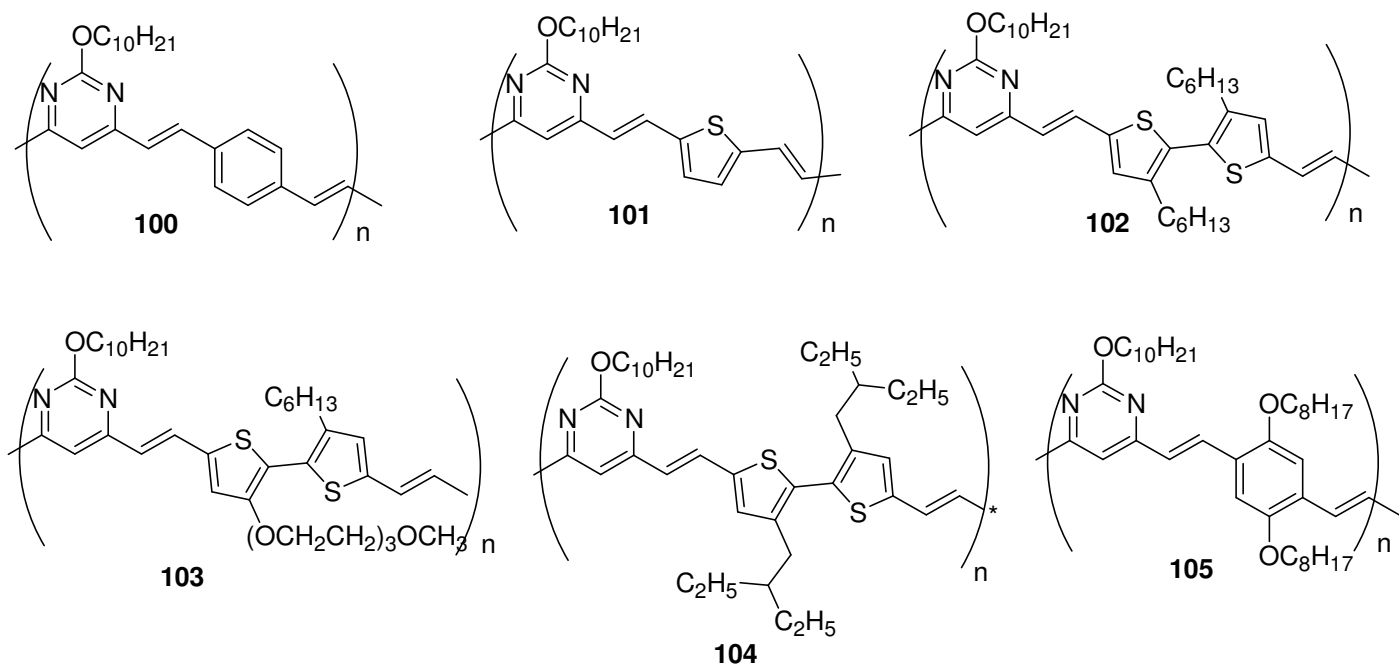


Scheme 23

Whereas highly emissive 4-arylvinylpyrimidine derivatives were already known, this was the first example of fluorescent 2-arylvinylpyrimidine compounds. The optical properties in CH₂Cl₂ solution of the two families were thoroughly compared. Whereas the series derived from 2-methylpyrimidine (**90–94**)

exhibits a blue shift in absorption and emission ($\lambda_{\text{abs}}=326\text{--}395$ nm, $\lambda_{\text{em}}=426\text{--}524$ nm) in comparison with 4-aryl-vinylpyrimidine **95–99** ($\lambda_{\text{abs}}=351\text{--}411$ nm, $\lambda_{\text{em}}=430\text{--}525$ nm), the influence of the position is less predictable on the fluorescence quantum yield (Φ_{F} up to 0.71 for **93**). An emission solvatochromism study has shown that a higher ICT seems to occur in 2-arylvinylpyrimidines **90–94** than in 4-arylvinylpyrimidines **95–99**.

A series of π -conjugated polymers **100–105** alternating 4,6-divinylpyrimidine and various aromatic rings was synthesized by Gunathilake *et al.* (Scheme 24).⁴⁸ These macromolecules (M_n comprised between 5000 and 12000 g mol^{-1}) exhibits strong fluorescence in chloroform solution ($\lambda_{\text{em}}=417\text{--}548$ nm, Φ_{F} up to 0.83 for **100**).



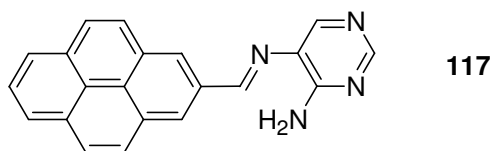
Scheme 24

b) Fluorescent probes

Pyridine-substituted 4-arylvinylpyrimidines **106–116** (Scheme 25) were also synthesized from 2,4-dichloro-6-methylpyrimidine by a double Stille cross coupling reaction followed by an aldol condensation with a series of aromatic aldehydes substituted with electron-donor, electron-acceptor, dendritic and water-soluble groups.⁴⁹ As for unfunctionalized 4-arylvinylpyrimidines the compounds exhibit strong fluorescence in CH_2Cl_2 solution ($\lambda_{\text{em}}=407\text{--}544\text{nm}$, Φ_{F} up to 0.52 for **110**), important emission solvatochromism (studied in term of solvent polarity but also in term of hydrogen bonding parameters of the solvent), and halochromism. An extensive qualitative study of the complexation properties of 4-arylvinyl-2,6-di(pyridin-2-yl)pyrimidines was performed by UV-vis and fluorescence spectroscopy.⁵⁰ All of the materials coordinate with a wide variety of metal ions, leading to noteworthy bathochromic shifts in the absorption spectra and diverse responses in the emission spectra (*i.e.* fluorescence quenching or increase in the fluorescence intensity) depending on the arylvinyl moiety and the cation. Quantitative studies demonstrated that **106–115** coordinate Zn^{2+} and Sn^{2+} with a 1:1 stoichiometry and with remarkably high binding constants although poor selectivity for Zn^{2+} over other competitive metal ions such as Ca^{2+} . A simple spot-test was developed to detect Zn^{2+} , Sn^{2+} and Ca^{2+} in aqueous media making **106–116** attractive

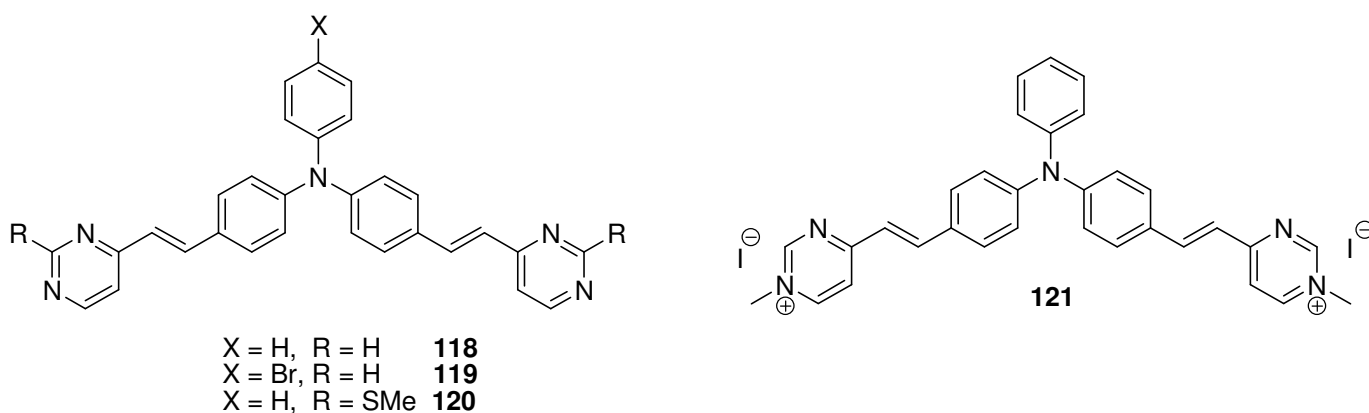
These probes exhibit a fast and fully reversible solvatochromic behaviour from yellow to purple when decreasing the pH solution. The nanoparticle can be also used to detect Zn^{2+} in aqueous solutions.

Das and co-workers designed an aryliminepyrimidine derivative **117** (Scheme 26) that can act as an Al^{3+} selective ratiometric fluorescent probe.⁵² The compound **117** exhibits an emission at $\lambda_{em}=368$ nm in DMSO- H_2O (4:1 v/v). In the presence of Al^{3+} , an excimer emission at $\lambda_{em}=445$ nm is observed along with the decrease of the ligand emission band. The lowest detection limit for Al^{3+} is 0.24 μM . Furthermore, it has been demonstrated that the ligand **117** can permeate through the cell membrane and detects intracellular Al^{3+} ions under a fluorescence microscope.

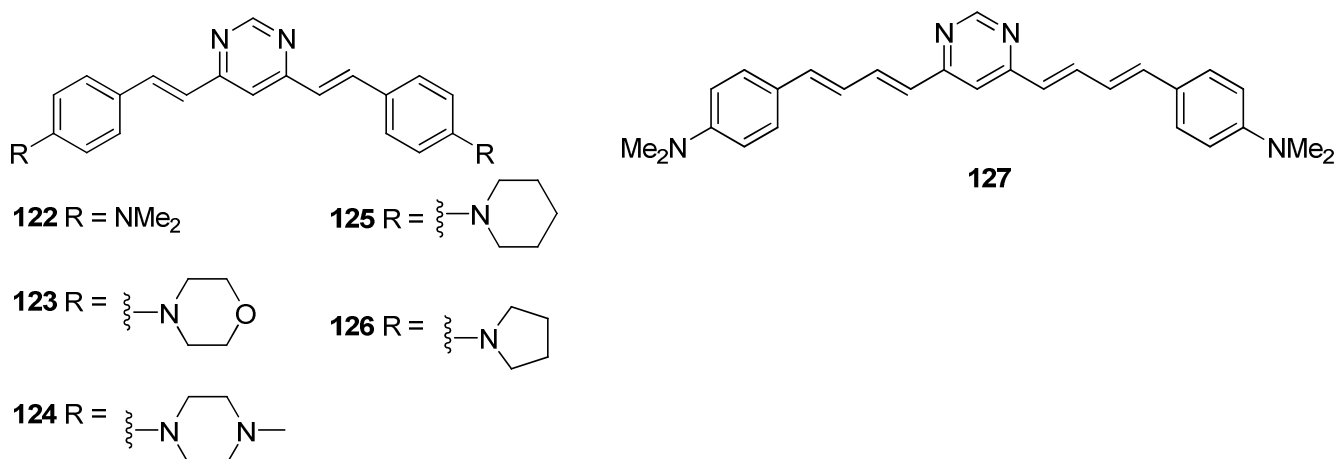


Scheme 26

Aranda *et al.* synthesized three quadrupolar dyes **118–120** with a triphenylamine core and pyrimidine fragments at the periphery (Scheme 27).⁵³ These derivatives exhibit a green-yellow fluorescence in dichloromethane (λ_{em} 540–550 nm) with high quantum yield ($\Phi_F=0.60–0.73$). Halochromism as well as important emission solvatochromism was also observed. Regioselective *N*-methylation of compound **118** provided the cationic dye **121** that exhibits affinity for double-stranded DNA. Binding to the biopolymer results in a strong bathochromic shift and increase of the emission intensity.



Scheme 27

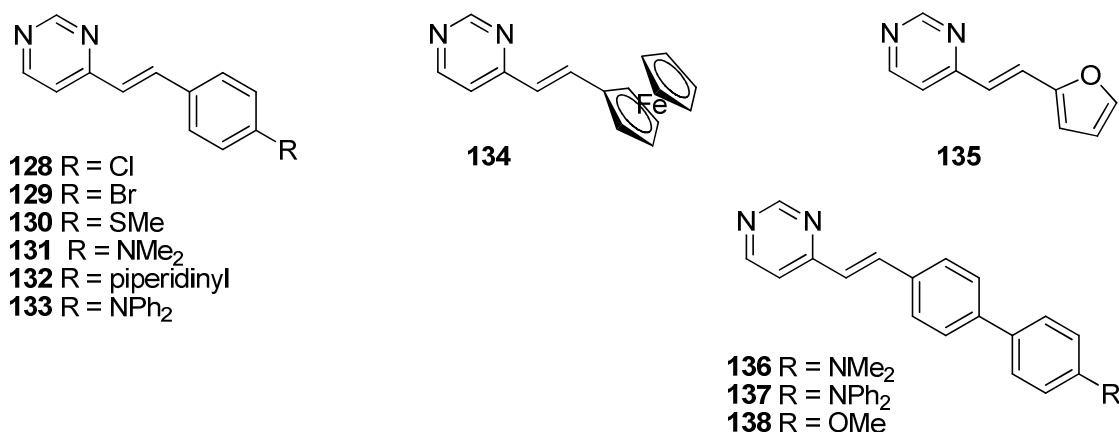


Scheme 28

Boländer and co-workers studied six 4,6-di(arylvinyl)pyrimidine derivatives **122–127** (Scheme 28) for *in vivo* diagnosis of Alzheimer's disease by tau protein fluorescence detection.⁵⁴ All of these derivatives exhibit fluorescence emission in the 538–587 nm range in methanol. Two of these compounds (**122** and **126**) even show a remarkably higher selectivity for aggregated tau, which qualifies them for further tau-selective imaging techniques with respect to an early-onset diagnosis of Alzheimer's disease. The ability of **122** to pass the blood-brain barrier was demonstrated in a transgenic mouse model.

c) NLO materials

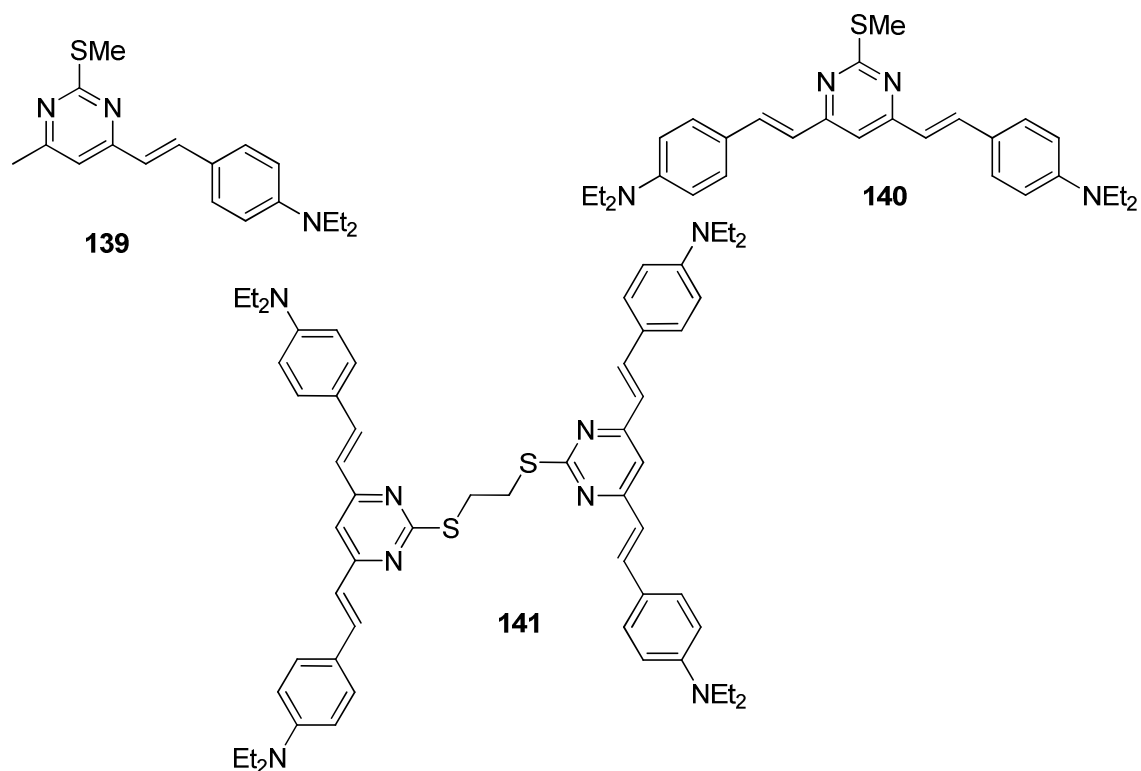
A series of push-pull 4-arylvinylpyrimidines **128–138** (Scheme 29) was described by us in 2012.⁵⁵ These molecules were obtained by aldol condensation from 4-methylpyrimidine and various aldehydes. Some of these compounds exhibit strong fluorescence properties in CH₂Cl₂ solution (λ_{em} =401–614 nm, Φ_F up to 0.66 for **136**). An important emission solvatochromism is observed with some of these compounds indicating a strong internal charge transfer upon excitation into these structures. These molecules also exhibit halochromic properties and are potential colorimetric and luminescence pH sensors. The second-order nonlinear properties have been investigated by EFISH method in CH₂Cl₂ solution for some of the compounds and large and positive $\mu\beta$ are obtained ($\mu\beta$ up to 470 10⁻⁴⁸ esu for **136**).



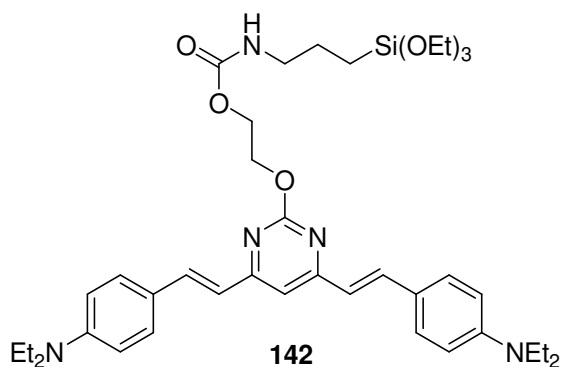
Scheme 29

Zhang and co-workers studied the application of already described TPA dye **139** (Scheme 30)⁵⁶ as NLO biological copper probe.⁵⁷ ¹H-NMR and theoretical computation have proven the binding interaction between the probe and copper ion, which support the functions of the molecule as a fluorescence signaling unit showing strong fluorescence quenching upon copper ion binding. The interaction of **139** with a variety of metal ions revealed that, contrary to 4,6-di(arylvinyl)pyrimidine equivalent molecules **140** and **141**, only Cu²⁺ ions changed the absorption behaviour significantly. On the other hand, the two-photon absorption cross-section of the novel copper probe increased from 275 to 591 GM (λ_{ex} =830 nm, measured by two-photon excited fluorescence technique) after interacting with copper ion. It was further demonstrated that the NLO response for copper (II) ion probe could be used for biological copper detection in live cells.

Silica based nanoparticles incorporating 4,6-di(arylvinyl)pyrimidine **142** (Scheme 31) were synthesized.⁵⁸ Free dye and dye-concentrated nanoparticles (DCNs) exhibit similar fluorescence emission at λ_{em} =540 nm in DMF. Whereas the TPA cross section of the free dye in DMF is negligible, DCNs exhibit a strongly enhanced TPA cross-section (δ =284 GM) measured by two-photon-excited fluorescence method.

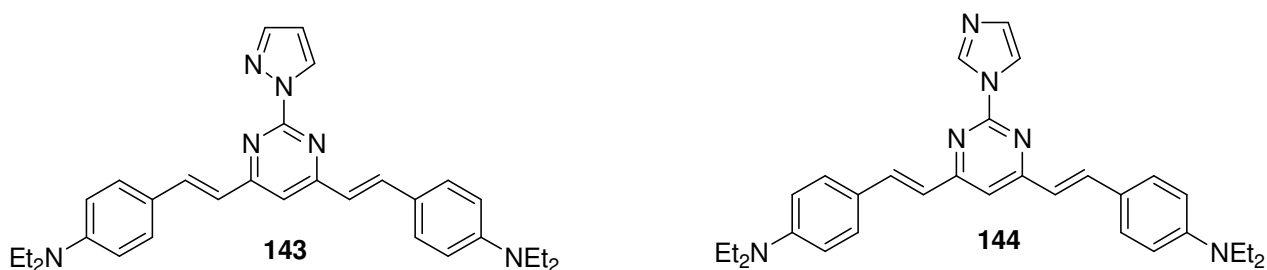


Scheme 30



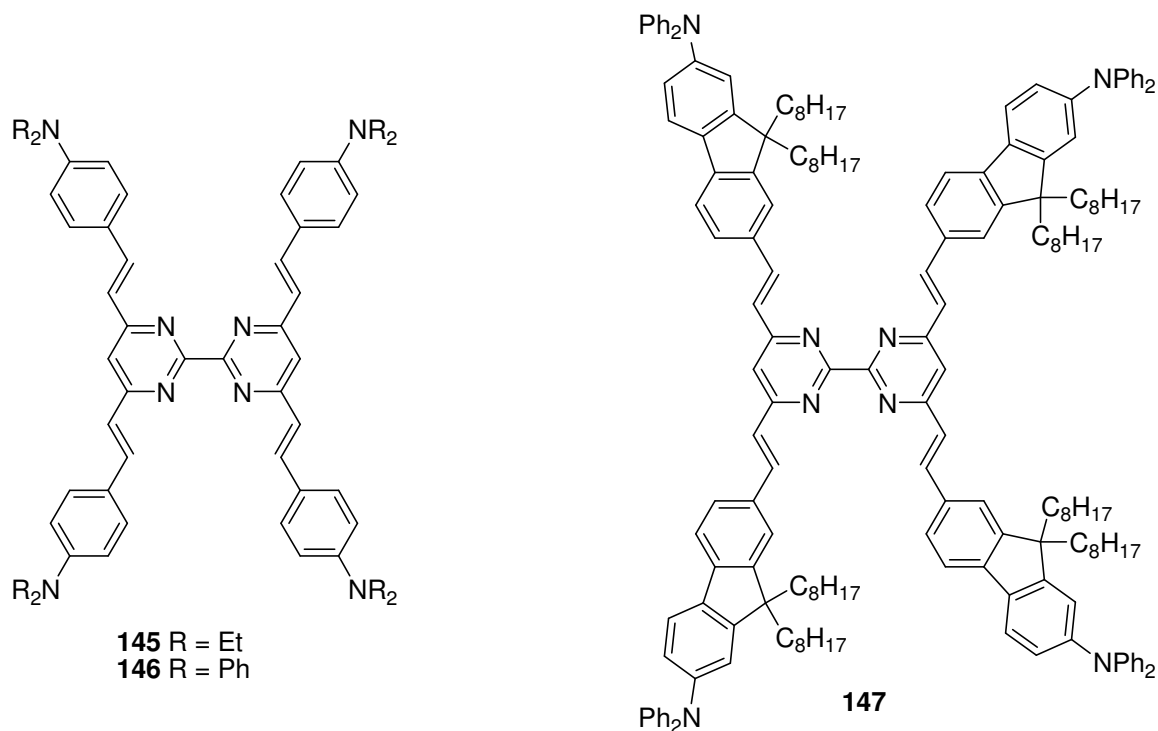
Scheme 31

Tang and co-workers also designed two 4,6-di(arylvinyl)pyrimidines **143** and **144** bearing a pyrazolyl and an imidazolyl group, respectively, in position two of the pyrimidine ring (Scheme 32).⁵⁹ These dyes are strongly fluorescent in dichloromethane (**143**: $\lambda_{em}=542$ nm, $\Phi_F=0.91$, **144**: $\lambda_{em}=546$ nm, $\Phi_F=0.37$) and exhibit important emission solvatochromism. The two chromophores have large two-photon absorption cross-sections in the near-infrared range (measured by two-photon excited fluorescence technique). Additionally, two-photon microscopy fluorescent imaging of BEL-7402 cells labeled with **143** and **144** revealed their potential application as a biological fluorescent probe.



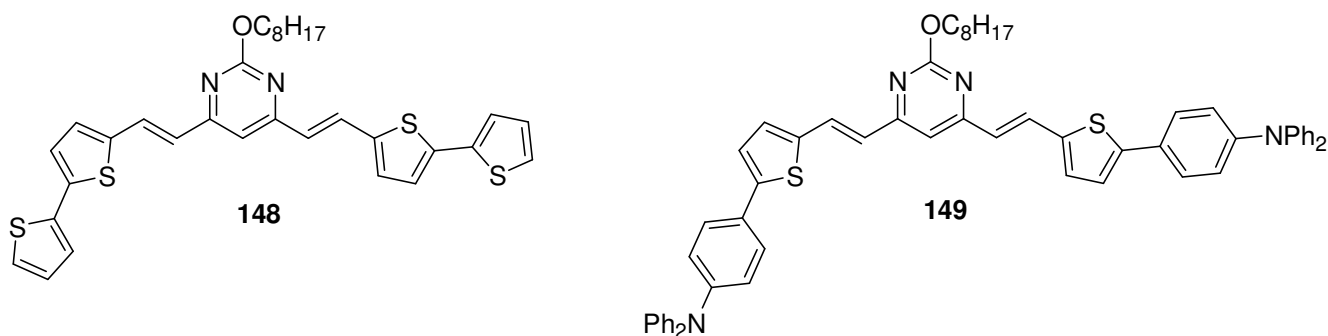
Scheme 32

Savel *et al.* reported the synthesis, the photophysical and the TPA properties of a series of octupolar bipyrimidine-based ligands incorporating *N*-substituted amines as terminal donors groups **145–147** (Scheme 33).⁶⁰ The compounds exhibit green-yellow fluorescence in dichloromethane ($\lambda_{em}=540\text{--}597$ nm, $\Phi_F=0.45\text{--}0.69$), as well as typical ICT emission solvatochromism. Compounds **145**, **146** and **147** exhibit also strong TPA properties (measured by two-photon excited fluorescence technique) with $\delta=530$ GM (at 775 nm), 460 GM (at 790 nm) and 1022 GM (at 790 nm), respectively. Zinc complexation of **147** promotes a strong enhancement of the TPA cross section ($\delta=1996$ GM at 870 nm).



Scheme 33

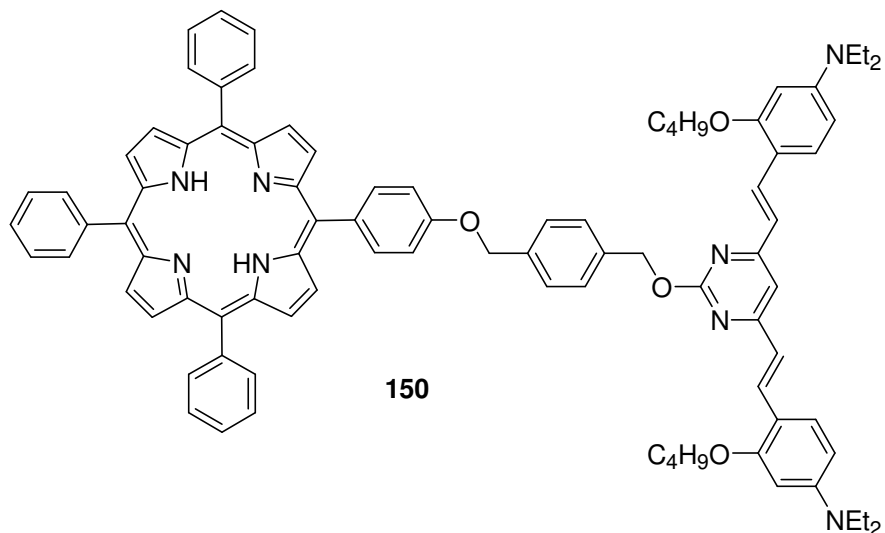
Chen and co-workers designed two new 4,6-bis(arylvinyl)pyrimidine derivatives **148** and **149** by incorporating thiophene ring in the π -conjugated scaffold (Scheme 34).⁶¹ Both compounds are fluorescent in chloroform ($\lambda_{em}=507$ nm and $\Phi_F=0.10$ for **148** and $\lambda_{em}=579$ nm and $\Phi_F=0.50$ for **149**). Both derivatives exhibit also large TPA cross section values in chloroform of 1702 GM (at $\lambda_{em}=810$ nm) and 1879 GM (at $\lambda_{em}=810$ nm) respectively for **148** and **149** (measured by two-photon excited fluorescence technique).



Scheme 34

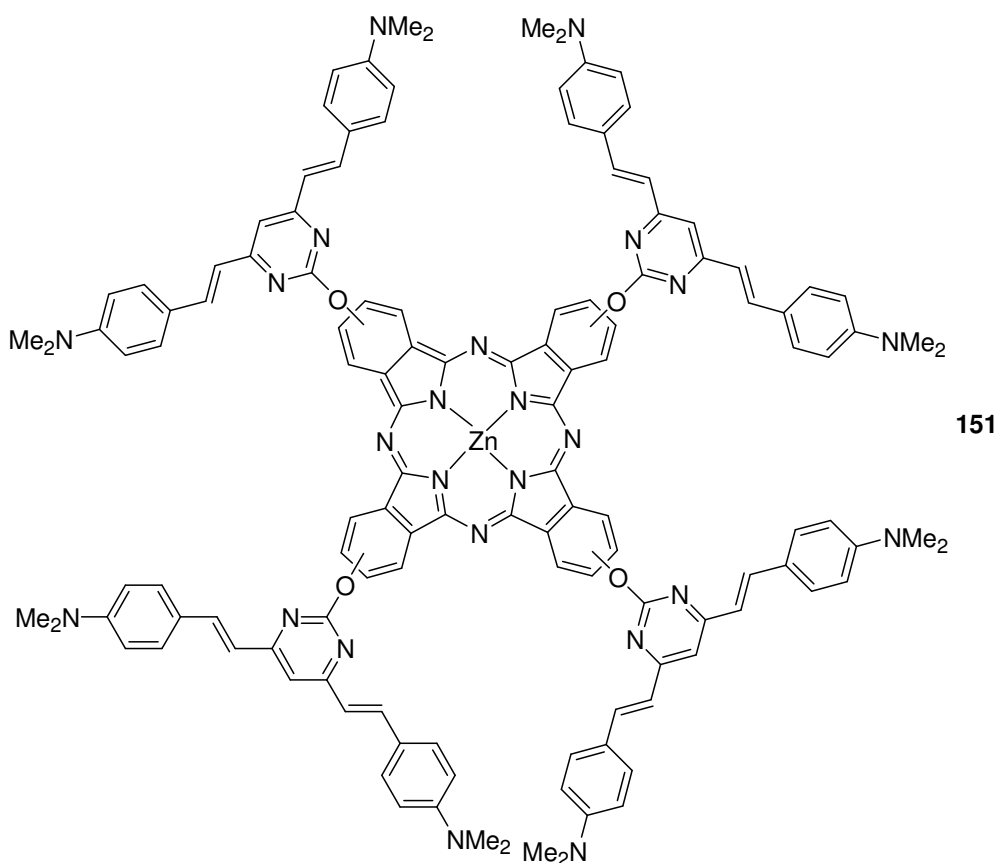
A porphyrin derivative **150** (Scheme 35) with one 4,6-di(arylvinyl)pyrimidine chromophore at the periphery was synthesized and its photophysical properties studied.⁶² A strong FRET from the pyrimidine

chromophore to the porphyrin is observed according to the emission spectra. The NLO properties and optical limiting performance, studied by Z-scan technique at 532 nm have demonstrated that **150** exhibits enhanced NLO absorption refraction and optical limiting response when compared with a simple tetraphenylporphyrin derivative. In this example, the pyrimidine chromophore strongly improves the potential for application optical limiting of porphyrin derivatives.



Scheme 35

The same strategy was employed with the phthalocyanine derivative **151** (Scheme 36) for two-photon absorption photodynamic therapy.⁶³ A strong energy transfer from peripheral chromophores to the phthalocyanine core was observed.

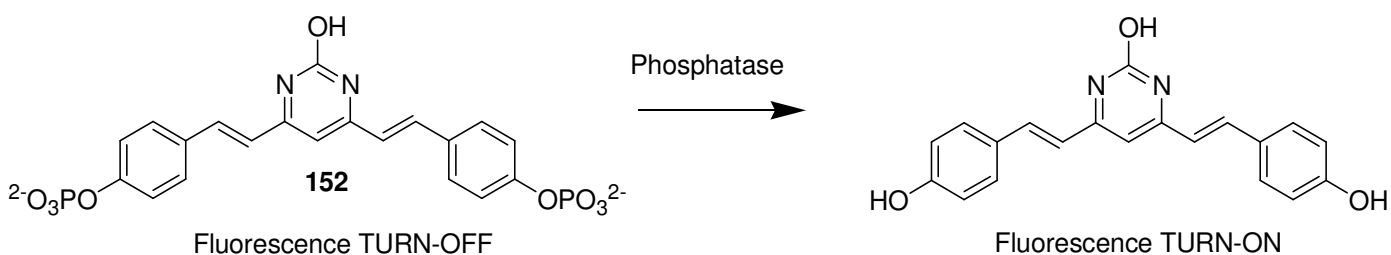


Scheme 36

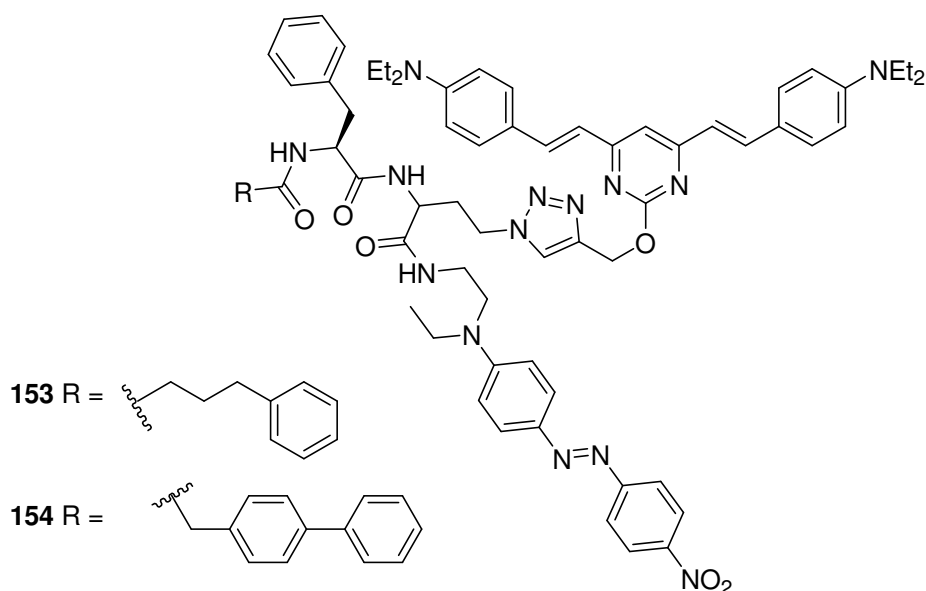
The compound exhibited strong two-photon absorption responses with a two-photon absorption cross-section up to 1153 GM in DMF when irradiated with a picosecond laser in the wavelength range of 800–870 nm (Z-scan technique), and gave good singlet oxygen generation.

Li *et al.* reported for the first time an enzyme reporting two-photon fluorescence bioimaging system. Indeed the authors have designed a TPA dye (**152**) capable of imaging endogenous phosphatase activities in both mammalian cells and *Drosophila* brains (Scheme 37).⁶⁴ This system is based on a 4,6-di(arylvinyl)pyrimidine **152** that become fluorescent upon phosphatase activity. By conjugation of this system to different cell-penetrating peptides by click chemistry, the authors were able to achieve organelle- and tumor cell-specific imaging of phosphatase activities with good spatial and temporal resolution.

Na and co-workers used the TPA properties of 4,6-diarylvinylpyrimidines into cell permeable small molecules probes **153** and **154** (Scheme 38) for live-cell imaging of cysteinyl cathepsin activities from cell lysates or live mammalian cells of HepG2 cancer cells.⁶⁵ The probes contain also Disperse Red 1 as fluorescence quencher. In the absence of a cysteinyl cathepsin, the intrinsic fluorescence is quenched due to the intramolecular FRET effect between 4,6-diarylvinylpyrimidine and Disperse Red 1. Upon binding to active enzyme, a successful proteolytic cleavage of the probes and release of the quencher occurs, leading to fluorescence ($\lambda_{em}=522$ nm) upon TPA excitation.



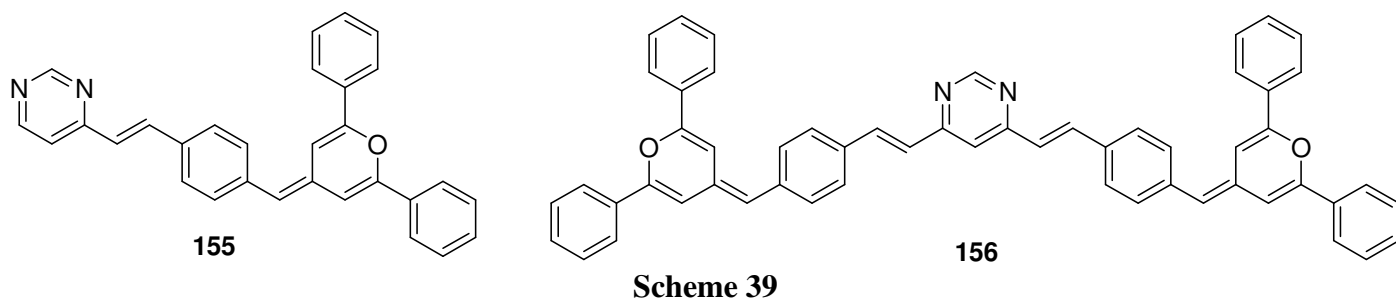
Scheme 37



Scheme 38

4-Arylvinylpyrimidine **155** and 4,6-di(arylvinyl)pyrimidine **156** (Scheme 39) bearing γ -methylene-pyrane fragments as pro-aromatic electron-donating groups were synthesized and their photophysical properties thoroughly investigated.⁶⁶ Both dipolar and quadrupolar branching strategies were explored and rationalized on the basis of the Frenkel exciton model. Even though a cooperative effect is clearly observed

if the dimensionality is increased, the nonlinear optical (NLO) response of this series is moderate if one considers the nature of the D/A couple and the size of the chromophores (as measured by the number of π electrons). The measured $\mu\beta$ values (EFISH method) are respectively equal to $400 \cdot 10^{-48}$ and $770 \cdot 10^{-48}$ esu for **155** and **156** and the TPA cross sections (measure by Z-scan method) are equal to 86 GM (at 880 nm) for **155** and 271 GM (at 900 nm) for **156**. This effect was attributed to a disruption in the electronic conjugation within the dyes scaffold for which the geometry deviates from planarity owing to a noticeable twisting of the pyranilidene end-groups. This latter structural parameter has also a strong influence on the excited state dynamics, which leads to a very efficient fluorescence quenching.

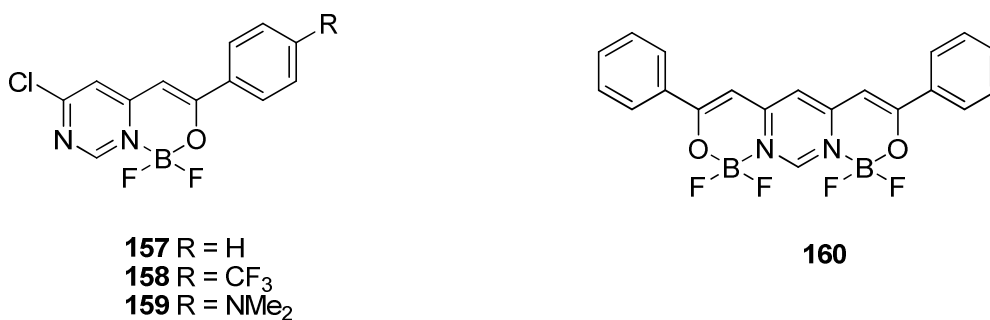


2.3. Organometallic and coordinated pyrimidine derivatives

The pyrimidine ring is known for its excellent complexation properties: indeed due to the lone pair on the two nitrogen atoms, a metal ion-ligand association can be easily established. Some pyrimidine complexes exhibit interesting luminescence properties. In particular, iridium pyrimidine complexes have found promising OLEDs applications.

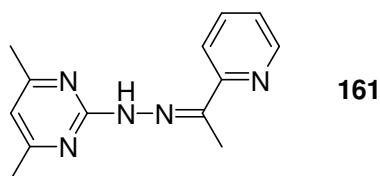
a) Luminescent materials

Kubota and co-workers designed fluorescent mono- and bis-boron complexes based on pyrimidine β -iminoenolate **157–160** (Scheme 40).⁶⁷ Compounds **157** and **158** exhibit higher fluorescence quantum yields in solid state (**157**: $\lambda_{em}=525$ nm, $\Phi_F=0.13$, **158**: $\lambda_{em}=488$ nm, $\Phi_F=0.15$) than in CH_2Cl_2 solution (**157**: $\lambda_{em}=429$ nm, $\Phi_F=0.02$, **158**: $\lambda_{em}=426$ nm, $\Phi_F=0.01$). A positive solvatochromism is observed for dimethylamino derivative **159** ($\lambda_{em}=529$ nm, $\Phi_F=0.78$ in CH_2Cl_2 solution), indicating an ICT excited state. The bisboron complex **160** shows a red shifted emission and a higher quantum yield in CH_2Cl_2 solution ($\lambda_{em}=517$ nm, $\Phi_F=0.55$), in comparison with the corresponding monoboron derivative **157**.



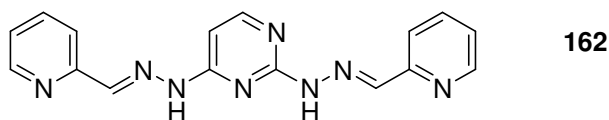
Ray *et al.* designed a new pseudohalide bridged dinuclear Zn(II) complex of pyrimidine derived Schiff base **161** where the Zn centres are held by $\mu_{1,1}$ azide ions (Scheme 41).⁶⁸ The ligand **161** is not emissive but the Zn complex shows a strong chelation-induced enhanced fluorescence (in MeOH, $\lambda_{em}=505$ nm,

$\Phi_F=6.26 \cdot 10^{-3}$). The fluorescence silent behaviour of **161** is attributed to the presence of several non-bonding electron pairs on the nitrogen donors. These electrons are involved in coordinate bond formation with metal ions during complexation. A less intense enhanced fluorescence is also observed with a similar Cd(II) complex.



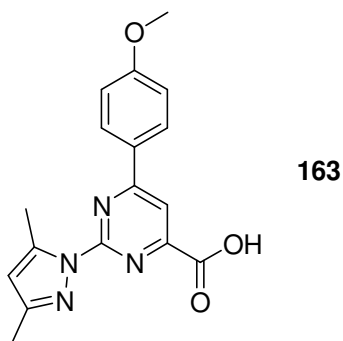
Scheme 41

Similar results were obtained with N_6 donor hexadentate Schiff base 2,4-bis [2-(pyridine-2-ylmethylidene) hydrazinyl] pyrimidine ligand **162** (Scheme 42).⁶⁹ Whereas the free ligand and the $[Cd(\mathbf{162})(H_2O)_2](ClO_4)_2$ complex are fluorescent silent, the $[Zn_3(\mathbf{162})_2Cl_6]$ complex exhibits UV fluorescence at $\lambda_{em}=330$ nm in aqueous methanol solution at room temperature. The fluorescence of the Zn complex is attributed to an intraligand ($\pi^* \rightarrow \pi$) transition.



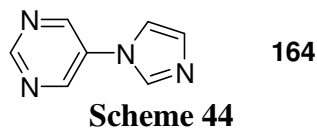
Scheme 42

Bushuev and co-workers designed **163**, another ligand for Zn(II) and Cd(II) (Scheme 43).⁷⁰ **163**, $Zn(\mathbf{163})_2 \cdot 0.5H_2O$ and $Cd(\mathbf{163})_2 \cdot 1.5H_2O$ manifest bright blue photoluminescence ($\lambda_{em}=420$ nm). The origin of luminescence of **163**, having an extended conjugated π -system, is attributed to $\pi^* \rightarrow \pi$ transitions. The luminescence mechanism for the complexes can be attributed to intra-ligand transitions as usual for Zn(II) and Cd(II) complexes.

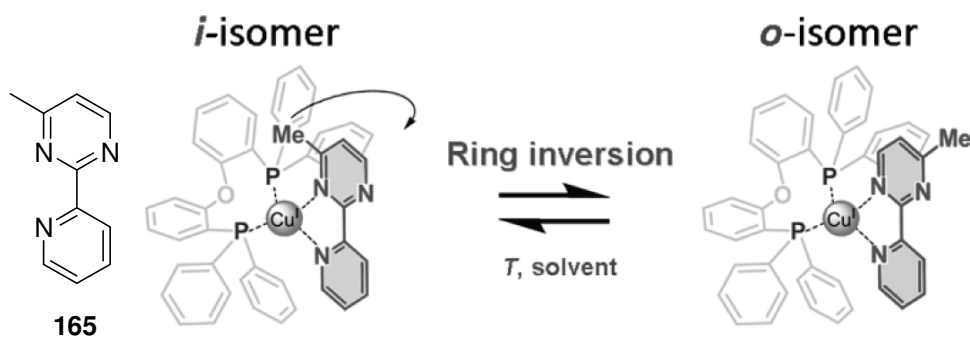


Scheme 43

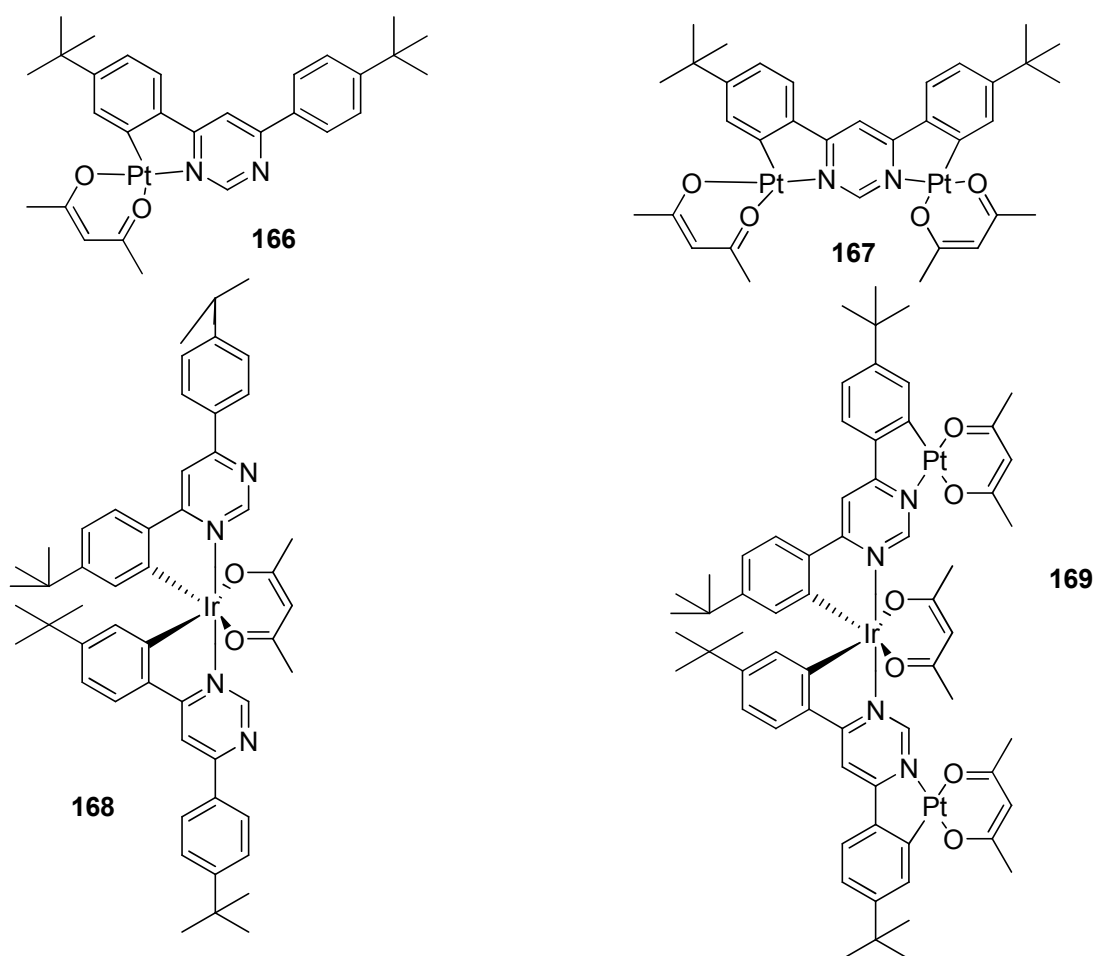
Hou and co-workers synthesized three complexes of 5-(1-imadazolyl)pyrimidine ligand **164** (Scheme 44): $(\mathbf{164})_2CdI_2$, $(\mathbf{164})_2Zn(NO_3)_2$ and $(\mathbf{164})_2Cd(NO_3)_2 \cdot (CH_3CN)_2$.⁷¹ In the solid state, the emission color of the free ligand **164** at 441 nm was significantly affected by its incorporation into the metal-containing complexes, as evidenced by the large blue shift to 412 nm for $(\mathbf{164})_2CdI_2$, and 413 nm for $(\mathbf{164})_2Zn(NO_3)_2$ and red shift to 496 nm for $(\mathbf{164})_2Cd(NO_3)_2 \cdot (CH_3CN)_2$ in the emission, respectively.



Nishikawa *et al.* developed a new convertible copper(I) complex using 2-pyridyl-4-methylpyrimidine **165** (Scheme 45) and diphosphine as ligands.⁷² This complex exhibits mechanical bistability based on the inversion motion of the pyrimidine ring, leading to dual luminescence behaviour (Scheme 45). The inversion dynamics was strongly dependent on temperature and solvent. The complex exhibited characteristic CT absorption ($\lambda_{\text{abs}}=378$ nm) and emission bands ($\lambda_{\text{em}}=635$ nm) in acetone solution. Emission lifetime measurements demonstrated that the emission could be deconvoluted into two components. The fast and slow components were assigned to the two isomers, the excited states of which were characterized by different structural relaxation process and/or additional solvent coordination properties.



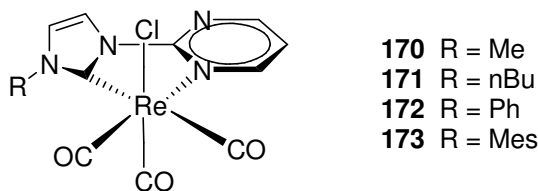
Scheme 45⁷³



Scheme 46

Kozhevnikov and co-workers synthesized four pyrimidine based mixed-metal Pt(II)/Ir(II) complexes **166–169** (Scheme 46).⁷⁴ The complexes are all highly luminescent ($\lambda_{em}=513–626$ nm), with quantum yields around 0.5 in CH_2Cl_2 solution at room temperature. The introduction of the additional metal centres is found to lead to a substantial redshift in absorption and emission, with λ_{max} in the order **166<167<168<169**.

Wang and co-workers synthesized rhenium(I) carbonyl complexes **170–173** containing pyrimidine-functionalized *N*-heterocyclic carbenes.⁷⁵ In both degassed CH_2Cl_2 solutions and solid state at room temperature, complexes **170–173** exhibit the emission at 515–570 nm (in solution Φ_F is around 0.05).



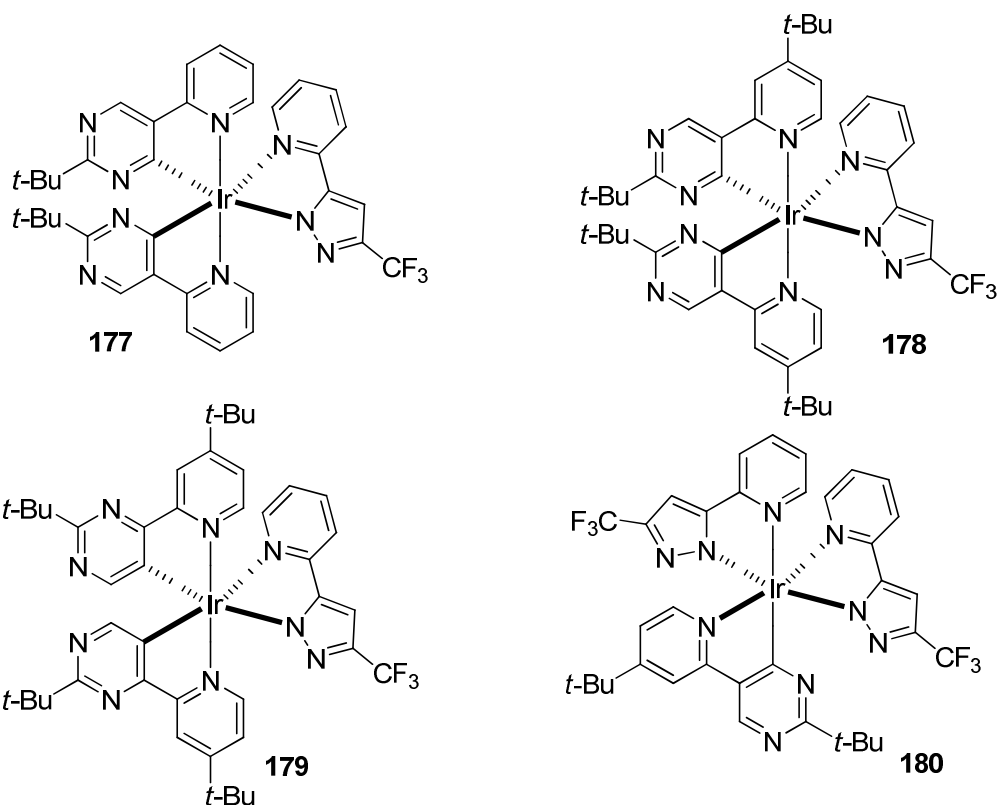
Scheme 47

b) Materials for OLEDs

Three pyrimidine chelates **174–176** with the pyridin-2-yl group residing at either the 5- or 4-positions were synthesized by Chang and co-workers (Scheme 48).⁷⁶



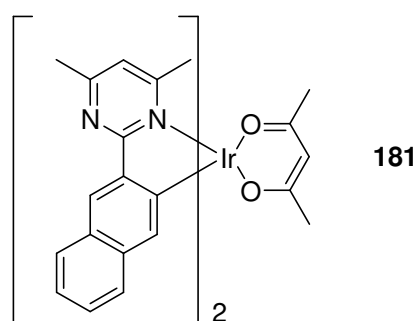
Scheme 48



Scheme 49

These chelates were utilized in synthesizing of a new class of heteroleptic Ir(III) metal complexes **177–180** (Scheme 49). The 5-substituted pyrimidine complexes **177**, **178** and **180** exhibit the first emission peak wavelength (λ_{max}) located in the range 452–457 nm with high quantum yields, whereas the emission of **179** with 4-substituted pyrimidine was red-shifted substantially to longer wavelength with $\lambda_{\text{max}}=535$ nm. Organic light-emitting diodes (OLEDs) were also fabricated using **178** and **180** as dopants, attaining the peak external quantum, luminance, and power efficiencies of 17.9% (38.0 cd/A and 35.8 lm/W) and 15.8% (30.6 cd/A and 24.8 lm/W), respectively. The blue emitting complex **178** was combined with a red emitting complex to obtain a phosphorescent white OLED with pure white emission.

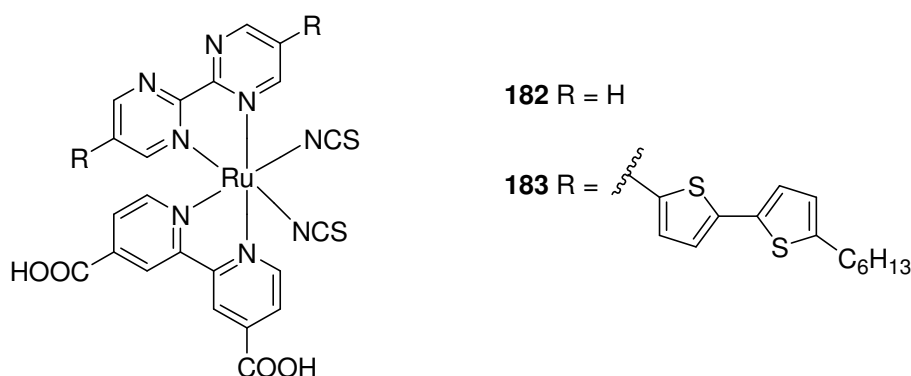
Wang *et al.* synthesized another iridium(III) pyrimidine complex **181** (Scheme 50).⁷⁷ A yellow emission at 560 nm in CH₂Cl₂ solution is observed and the author claimed that **181** is a promising phosphorescent material for OLEDs.



Scheme 50

c) Dyes for photovoltaic

Ozawa *et al.* designed two ruthenium sensitizers **182** and **183** with 2,2'-bipyrimidine derivatives for application in DSSCs (Scheme 51).⁷⁸ However, the DSSCs containing **182** ($\eta=2.04\%$) and **183** ($\eta=0.23\%$) showed much lower conversion efficiency than those with well-known pyridine based ruthenium sensitizers *cis*-[Ru(dcbpy)(bpy)(NCS)₂] ($\eta=8.32\%$) and N719 ($\eta=8.44\%$). The results of DFT calculations indicated that both, unfavourable populations of LUMO and LUMO+1, and the lower energy level of LUMO+1, contribute to the much poorer solar cell performances of **182** and **183**.



182 R = H

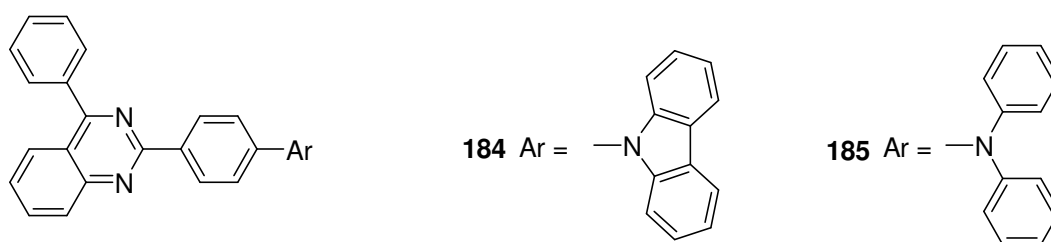
183 R =

Scheme 51

3. Quinazolines

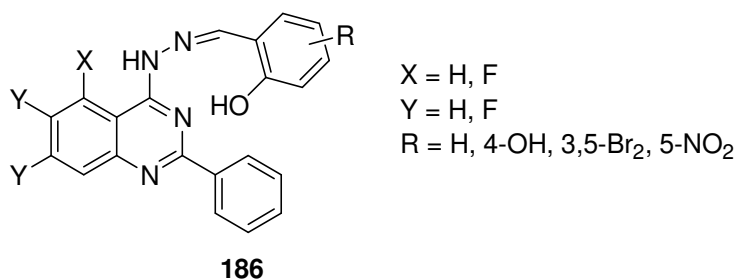
Whereas the pyrimidine derivatives have been fully investigated for their optical properties, the quinazoline derivatives remain up to now relatively unexplored.

Liu *et al.* synthesized two A- π -D blue emissive fluorophores **184** and **185** (Scheme 52) leading to solid-state white photoluminescence and electroluminescence emissions by controlled acid-protonation.⁷⁹ These fluorophores incorporating the quinazoline moiety as electron-withdrawing part (λ_{em} =487 and 539 nm in CH₂Cl₂ for **184** and **185**, respectively), showed strong emission solvatochromism while only slight change was observed in absorption which is characteristic of ICT in excited states. The electron-withdrawing character was enhanced upon protonation resulting in red-shifted emission in solution. The fluorescence color change in the solid phase was also observed under acidic conditions leading to orange emissive moieties. When the thin film incorporating compound **184** was treated with camphorsulfonic acid (0.1wt%–0.5wt%), white photoluminescence was observed which suggests that such compounds have potential for applications in fabricating white OLEDs.



Scheme 52

A series of 2-hydroxybenzaldehyde (2-phenylquinazolin-4-yl)hydrazones **186** (Scheme 53) and their Zn^{II} complexes were prepared and their photophysical properties were investigated.⁸⁰ Hydrazone derivatives **186** and their complexes absorb in the range of 370–495 nm and emit in dark blue to green light (λ_{em} =465–549 nm) in acetonitrile solution. The formation of the complexes from the hydrazone derivatives **186** results in hypsochromic shifts of the emission peaks, a strong decrease of the Stokes shift and better quantum yields (Φ_F complexes=0.002–0.29 vs Φ_F hydrazones=0.001–0.004) which can be due to the increased rigidity of the system. The quinazoline-containing hydrazones are promising ligand systems for the design of fluorescent complexes with other metals.

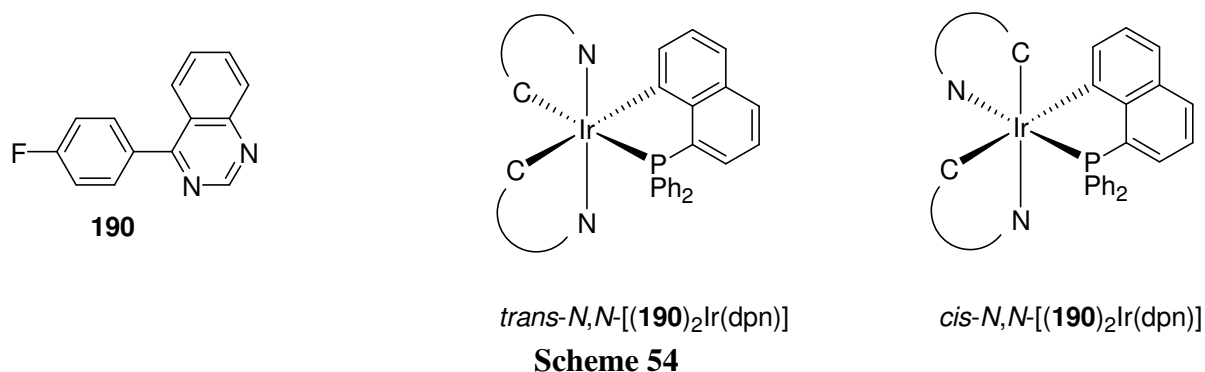


Scheme 53

Machura and co-workers prepared cadmium(II) complexes based on quinazoline and pseudohalide (N_3^- , NCS^- and $N(CN)_2^-$) ligands: $[Cd(Qnz)_2(SCN)_2]_n$ (**187**), $[Cd(Qnz)_2(dca)_2]_n$ (**188**), $[Cd(Qnz)_2(N_3)_2]_n$ (**189**).⁸¹ The fluorescence properties of these coordination compounds were studied in the solid state and compared with the quinazoline. The quinazoline ligand displays a broad and intense emission at 397 and a weaker band at 295 nm. The solid emission spectra of complexes **187–189** are very similar to the emissions of the free ligand. High similarity in the locations and profiles of emission peaks of free quinazoline and compounds **187–189** allows to attribute the emission in these complexes to intraligand (π - π^*) transition

within the heterocyclic ligand. In comparison with free quinazoline ligand, the enhancement of the luminescence emission maxima in complexes **187–189** is attributed to the enhancement of the rigidity of the quinazoline leading to the reduction of the non-radiative intraligand ($\pi-\pi^*$) excited state.

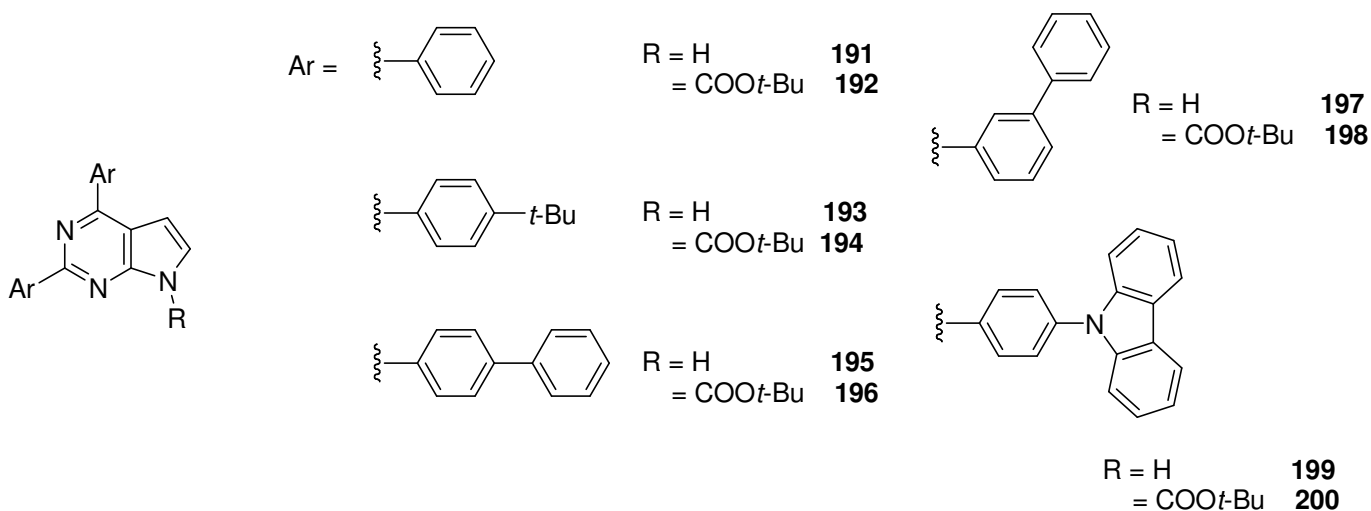
Du and co-workers developed cyclometalated Ir(III) complexes *trans*-*N,N*-[(**190**)₂Ir(dpn)] and *cis*-*N,N*-[(**190**)₂Ir(dpn)] (Scheme 54).⁸² The photophysical properties of these complexes were measured in CH₂Cl₂ solution exhibiting a weak and broad emission at ~630 nm. A blue shift in emission (λ_{em} =628 vs 638 nm) as well as a better quantum yield (Φ_F =0.11 vs 0.016) were observed for the complex *cis*-*N,N*-[(**202**)₂Ir(dpn)] in comparison with the *trans*-isomer. OLED was fabricated using red phosphorescent *cis*-*N,N*-[(**190**)₂Ir(dpn)] as dopant. At the practical brightness of 500 cd m⁻², decent external quantum efficiency of 10.6% could be reached for this complex.



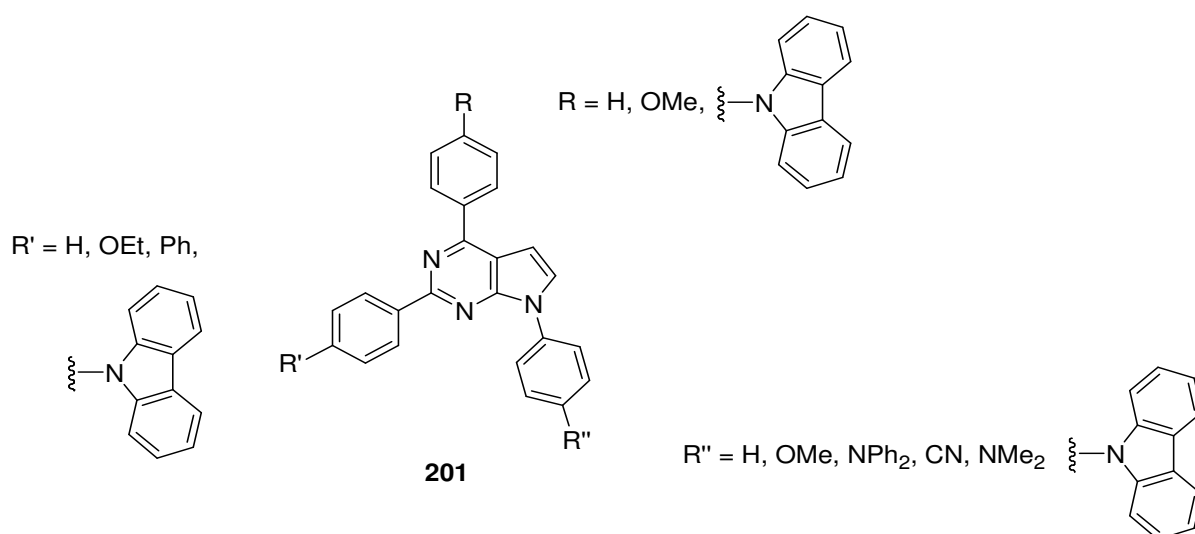
4. Pyrrolo[2,3-d]pyrimidines

This class of molecules has been extensively studied by the group of Tumkevičius.

This group described the synthesis and photophysical properties of pyrrolo[2,3-*d*]pyrimidine derivatives **191–200** incorporating various peripheral chromophoric units (Scheme 55).⁸³ These fluorophores exhibit strong absorption and blue-UV fluorescence ranging from 380 nm to 440 nm with emission quantum yields up to 0.67 in THF. Slight modifications in terms of emission maxima and quantum yield were observed by varying aryl branches. However, introduction of an electron-withdrawing *t*-BuOCO group attached to the pyrrole ring was found to have a dramatic quench on the fluorescence properties of the pyrrolopyrimidines except for the compound **200** which exhibits an increased fluorescence quantum yield compared to **199** (0.67 vs 0.13).



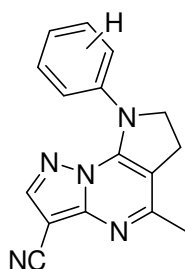
The same group designed similar triarylpyrrolo[2,3-*d*]pyrimidine derivatives **201** incorporating various aryl and heteroaryl in positions 2, 4 and 7 (Scheme 56).⁸⁴ The photophysical properties of the synthesized 2,4,7-triarylpyrrolo[2,3-*d*]pyrimidines were evaluated in THF. These compounds exhibit strong absorption ($\lambda_{\text{abs}}=256\text{--}342\text{ nm}$) and fluorescence ($\lambda_{\text{em}}=403\text{--}549\text{ nm}$, Φ_{F} up to 40%). The fluorescence lifetimes were estimated ranging from 2.6 ns to 12.2 ns. The authors compared the photophysical properties of the 2,4-diaryl and the 2,4,7-triarylpyrrolopyrimidine derivatives showing an enhancement of the absorption when an aryl group is introduced in position 7 whereas the quantum yield decreases. The influence of the *para* substituent borne by the phenyl ring in position 7 was evaluated resulting in a red shift when an electron-donating group was introduced whereas a blue shift was observed in presence of an electron-withdrawing group. The formation of nanoaggregates *via* reprecipitation method of some of compounds **201** in aqueous method was also demonstrated.^{79c} The aggregation induced emission with a maximal 20-fold emission efficiency enhancement was obtained.



Scheme 56

5. Other fused pyrimidines

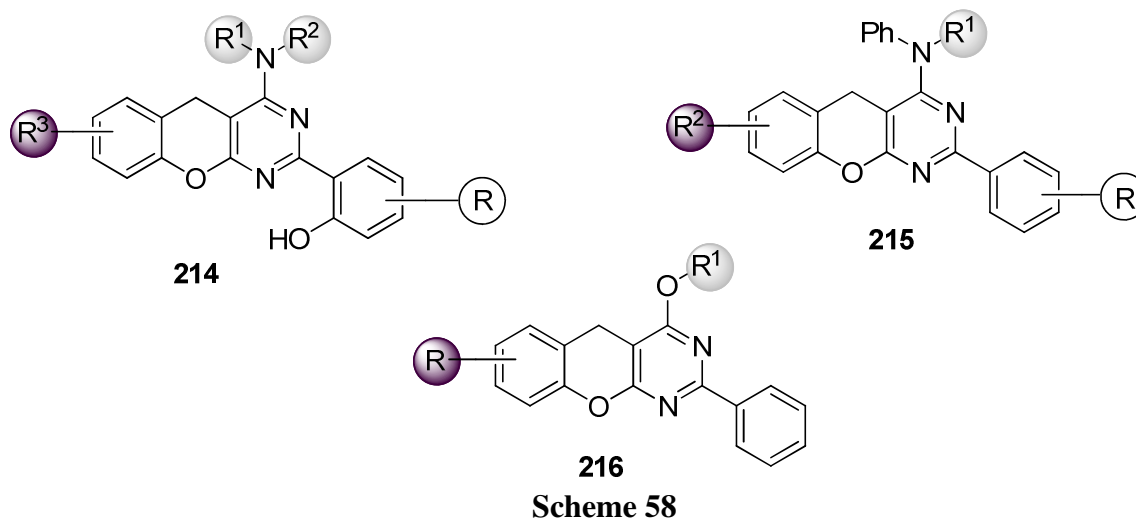
A series of pyrazolo-pyrrolo-pyrimidines **202–213** bearing different substituent in *ortho*, *meta* or *para* position on the phenyl ring was prepared by Rote *et al.* (Scheme 57).⁸⁵ All these compounds are fluorescent ($\lambda_{\text{em}}=383\text{--}457\text{ nm}$, $\Phi_{\text{F}}=0.15\text{--}0.30$ in DMF). Both the position and the effect of substituents were studied on their photophysical properties. A bathochromic shift was observed when an electron-donating effect is present on the phenyl ring and the highest quantum yield was obtained with the methoxy group in *para*-position. Similarly, the lowest quantum yield was achieved with the *para*-nitro substituent, an electron-withdrawing group and a hypsochromic shift was also observed. The authors claim that these structures are promising for applications in OLEDs and for opto-electronic applications.



- 202** R = H
203 R = *p*-NO₂
204 R = *p*-OCH₃
205, 206, 207 R = *p*-CH₃, *m*-CH₃, *o*-CH₃
208, 209 R = *p*-F, *m*-F
210, 211 R = *p*-Br, *m*-Br
212, 213 R = *p*-Cl, *m*-Cl

Scheme 57

A library of 22 chromenopyrimidine derivatives **214**, **215** and **216** was described by Zonouzi and co-workers (Scheme 58).⁸⁶ The three series of molecules exhibit blue to green fluorescence upon excitation at 290 nm.



6. Conclusions

The research efforts in the field of synthesis and use of optical materials have strongly increased within the last few years. The considerable interest for these compounds is due to their wide range of applications in various fields. They can be used as fluorescent sensors (polarity, pH, metal cations or more particularly to detect explosives), as stain for microscopy and diagnostic in medicine, for lighting in OLEDs and photovoltaic in DSSCs and NLO materials.

As shown in this review, the number of molecules incorporating pyrimidine ring in their scaffold and designed for their optical properties was dramatically increased during the last three years. Indeed, due to their π -deficient character, incorporation of *N*-heterocycles such as pyrimidine in the backbone of luminescent molecules leads to significant modifications of the photophysical properties of π -conjugated materials. The electron-deficiency of the pyrimidine ring can be used as a dipolar moiety, which favours the internal charge transfer. As largely illustrated in this review, this kind of molecules exhibits important fluorescence solvatochromism, good NLO properties and can be used as dyes for solar cells. Quadrupolar (D- π -A- π -D) structures with a pyrimidine central core is now a well-established design of 3rd order NLO chromophores and exhibit TPA properties with high cross-sections.

Moreover, the presence of nitrogen atoms with lone electron pairs allows the pyrimidine ring to act as effective and stable complexing agents making of them good cation sensors. For the same reasons, pyrimidine derivatives can be protonated exhibiting halochromism; it has been illustrated by numerous examples given in this review. Specific interactions of some pyrimidine compounds with particular forms of DNA and specific proteins lead to anticipate their use as promising tools for medical diagnosis of diseases such as cancer or Alzheimer disease.

Another aspect of the luminescence of pyrimidine is the electroluminescence properties leading to OLEDs. Some examples are detailed along the review.

This review emphasizes the great interest to incorporate pyrimidine moieties in π -extended conjugated systems, owing to their applications in various fields. The elaboration of new efficient structures with such a target is always topical and constitutes an interesting challenge.

References

1. Barlin, G. B. In *Chemistry of Heterocyclic Compounds*; John Wiley and Sons: New York, 1982; Vol. 41.
2. Brown, J. In *Chemistry of Heterocyclic Compounds*; John Wiley and Sons: New York, 1962; Vol. 16.
3. Castle, R. N. In *Chemistry of Heterocyclic Compounds*; John Wiley and Sons: New York, 1962; Vol. 23.
4. Lagoja, I. M. *Chem. Biodiv.* **2005**, 2, 1.
5. See, for example: (a) Darbyshire, J.; Foulkes, M.; Peto, R.; Duncan, W.; Babiker, A.; Collins, R.; Hughes, M.; Peto, T.; Walker, A. In *The Cochrane Library*; John Wiley & Sons: Chichester, 2004; Issue 2. (b) Petersen, E.; Schmidt, D. R. *Expert Rev. Anticancer Ther.* **2003**, 1, 175. (c) Joffe, A. M.; Farley, J. D.; Linden, D.; Goldsand, G. *Am. J. Med.* **1989**, 87, 332. (d) Rosemeyer, H. *Chem. Biodiv.* **2004**, 1, 361.
6. (a) Zhang, C. Z.; Lu, C. G.; Zhu, J.; Lu, G. Y.; Wang, X.; Shi, Z. W.; Liu, F.; Cui, Y. P. *Chem. Mater.* **2006**, 18, 6091. (b) Luo, J. D.; Hua, J. L.; Qin, J. G.; Cheng, J. Q.; Shen, Y. C.; Lu, Z. H.; Wang, P.; Ye, C. *Chem. Commun.* **2001**, 171. (c) Verbiest, T.; Houbrechts, S.; Kauranen, M.; Clays, K.; Persoons, A. *J. Mater. Chem.* **1997**, 7, 2175. (d) Wang, C.; Zhang, T.; Lin, W. *Chem. Rev.* **2012**, 112, 1084. (e) Kim, H. M.; Cho, B. R. *Chem. Commun.* **2009**, 153.
7. (a) Taniuchi, T.; Okada, S.; Nakanishi, H. *Appl. Phys. Lett.* **2004**, 95, 5984. (b) Taniuchi, T.; Ikeda, S.; Okada, S.; Nakanishi, H. *Jpn. J. Appl. Phys.* **2005**, 44, L652. (c) Schneider, A.; Neis, M.; Stillhart, M.; Ruiz, B.; Khan, R. U. A.; Günter, P. *J. Opt. Soc. Am. B* **2006**, 23, 1822. (d) Schneider, A.; Stillhart, M.; Günter, P. *Opt. Express* **2006**, 14, 5376. (e) Yang, Z.; Mutter, L.; Stillhart, M.; Ruiz, B.; Aravazhi, S.; Jazbinšek, M.; Schneider, A.; Gramlich, V.; Günter, P. *Adv. Funct. Mater.* **2007**, 17, 2018.
8. (a) Li, Z.; Li, Q.; Qin, J. *Polym. Chem.* **2011**, 2, 2723. (b) He, G. S.; Tan, L. S.; Zheng, Q.; Prasad, P. N. *Chem. Rev.* **2008**, 108, 1245. (c) Kim, H. N.; Guo, Z.; Zhu, W.; Yoon, J.; Tian, H. *Chem. Soc. Rev.* **2011**, 40, 79. (d) Xia, R. J.; Malval, J. P.; Jin, M.; Spangenberg, A.; Wan, D. C.; H. T. Pu, H. T.; Vergote, T.; Morlet-Savary, F.; Chaumeil, H.; P. Baldeck, P.; Poizat, O.; Soppera, O. *Chem. Mater.* **2012**, 24, 237.
9. (a) Petrov, V. P. *Mol. Cryst. Liq. Cryst.* **2006**, 457, 121. (b) Lin, Y.-C.; Lai, C. K.; Chang, Y.-C.; Liu, K.-T. *Liq. Cryst.* **2002**, 29, 237.
10. Littke, A. F.; Fu, G. C. *Angew. Chem. Int. Ed.* **2002**, 41, 4176.
11. (a) Schomaker, J. M.; Delia, T. J. *J. Org. Chem.* **2001**, 66, 7125. (b) Achelle, S.; Ramondenc, Y.; Marsais, F.; Plé, N. *Eur. J. Org. Chem.* **2008**, 3129. (c) Rossi, R.; Bellina, F.; Lessi, M. *Adv. Synth. Catal.* **2012**, 354, 1181. (d) Hussain, M.; Hung, N. T.; Khera, R. A.; Malik, I.; Zinad, D. S.; Langer, P. *Adv. Synth. Catal.* **2010**, 352, 1429. (e) Verbitskiy, E. V.; Cheprakova, E. M.; Slepukhin, P. A.; Kodess, M. I.; Ezhikova, M. A.; Pervova, M. G.; Rusinov, G. L.; Chupzkhin, O. N.; Charushin, V. N. *Tetrahedron* **2012**, 68, 5445.
12. (a) Gazivoda, T.; Kristafor, S.; Cetina, M.; Nagl, A.; Raic-Malic, S. *Struct. Chem.* **2008**, 19, 441. (b) Farahat, A.; Boykin, D. W. *Synthesis* **2012**, 44, 120.
13. (a) Stanetty, P.; Hattinger, G.; Schnuerch, M.; Mihovilovic, M. D. *J. Org. Chem.* **2005**, 70, 5215. (b) Stanetty, P.; Roehrling, J.; Schnuerch, M.; Mihovilovic, M. D. *Tetrahedron* **2006**, 62, 2380. (c) Achelle, S.; Ramondenc, Y.; Dupas, G.; Plé, N. *Tetrahedron* **2008**, 64, 2783.
14. (a) Benderitter, P.; de Araujo, J. X., Jr.; Schmitt, M.; Bourguignon, J.-J. *Tetrahedron*, **2007**, 63, 12465. (b) Ibrahim, N.; Chevot, F.; Legraverend, M. *Tetrahedron Lett.* **2011**, 52, 305.
15. Tobram, T.; Dvorak, D. *Eur. J. Org. Chem.* **2008**, 2923.
16. (a) Fürstner, A.; Letner, A.; Méndez, M.; Krause, H. *J. Am. Chem. Soc.* **2002**, 124, 13856. (b) Bouilly, L.; Darabantu, M.; Turck, A.; Plé, N. *J. Heterocycl. Chem.* **2005**, 42, 1423.
17. Tumkevičius, S.; Dodonova, J. *Chem. Heterocycl. Compd.* **2012**, 48, 258.
18. (a) Vanden Eynde, J.-J.; Pascal, L.; Van Haverbeke, Y.; Dubois, P. *Synth. Commun.* **2001**, 32, 3167. (b) Lipunova, G. N.; Nosova, E. V.; Trashakhova, T. V.; Charushin, V. N. *Russ. Chem. Rev.* **2011**, 80, 1115.
19. (a) Achelle, S.; Plé, N. *Curr. Org. Synth.* **2012**, 9, 161. (b) Achelle, S.; Plé, N.; Turck, A. *RSC Adv.* **2011**, 1, 364. (c) Achelle, S.; Baudequin, C.; Plé, N. *Dyes Pigm.* **2013**, 98, 575.

20. (a) Itami, K.; Yamazaki, D.; Yoshida, J. *J. Am. Chem. Soc.* **2004**, *126*, 15396. (b) Bagley, M. C.; Lin, Z.; Pope, S. J. A. *Tetrahedron Lett.* **2009**, *49*, 6818. (c) Achelle, S.; Ramondenc, Y.; Dupas, G.; Plé, N. *Tetrahedron* **2008**, *64*, 2783.
21. Tumkevičius, S.; Voitechovičius, A.; Adomėnas, P. *Chemija* **2012**, *23*, 61.
22. Shi, Y.; Liu, Q.; Tang, J. *Monatsh. Chem.* **2011**, *142*, 907.
23. Weng, J.; Mei, Q.; Fan, Q.; Ling, Q.; Tong, B.; Huang, W. *RSC Adv.* **2013** doi: 10.1039/c3ra43631d.
24. Suzaki, Y.; Tsuchido, Y.; Osakada, K. *Tetrahedron Lett.* **2011**, *52*, 3883.
25. Tanabe, K.; Suzui, Y.; Hasegawa, M.; Kato, T. *J. Am. Chem. Soc.* **2012**, *134*, 5662.
26. Bolduc, A.; Dufresne, S.; Hanan, G. S.; Skene, W. G. *Can. J. Chem.* **2010**, *88*, 236.
27. Cornec, A.-S.; Baudequin, C.; Fiol-Petit, C.; Plé, N.; Dupas, G.; Ramondenc, Y. *Eur. J. Org. Chem.* **2013**, 1908.
28. Malik, I.; Ahmed, Z.; Reimann, S.; Ali, I.; Villinger, A.; Langer, P. *Eur. J. Org. Chem.* **2011**, 2088.
29. Mamtimin, X.; Matsidik, R.; Nurulla, I. *Polymer* **2010**, *51*, 437.
30. Takagi, K.; Takao, H.; Nakagawa, T. *J. Polym. Sci. Polym. Chem.* **2010**, *48*, 3729.
31. See, for example: (a) Katan, C.; Terenziani, F.; Mongin, O.; Werts, M. H. W.; Porres, L.; Pons, T.; Mertz, J.; Tretiak, S.; Blanchard-Desce, M. *J. Phys. Chem. A* **2005**, *109*, 3024. (b) Lartia, R.; Allain, C.; Bordeau, G.; Schmidt, F.; Fiorini-Debuischert, C.; Charra, F.; Teulade-Fichou, M.-P. *J. Org. Chem.* **2008**, *73*, 1732. (c) Panthi, K.; Adhikari, R. M.; Kinstle, T. H. *J. Phys. Chem. A* **2010**, *114*, 4542.
32. Suryawanshi, V. D.; Gore, A. H.; Walekar, L. S.; Anbhule, P. V.; Patil, S. R.; Kolekar, G. B. *J. Mol. Liq.* **2013**, *184*, 4.
33. Suryawanshi, V. D.; Gore, A. H.; Dongare, P. R.; Anbhule, P. V.; Patil, S. R.; Kolekar, G. B. *Spectrochim. Acta A* **2013**, *114*, 681.
34. Weng, J.; Mei, Q.; Ling, Q.; Fan, Q.; Huang, W. *Tetrahedron* **2012**, *68*, 3129.
35. Zou, Y.; Zhang, Q.; Hossain, A. M. S.; Li, S.-L.; Wu, J.-Y.; Ke, W.-Z.; Jin, B.-K.; Yang, J.-X.; Zhang, S.-Y.; Tian, Y.-P. *J. Organomet. Chem.* **2012**, *720*, 66.
36. McLean, D. G.; Sutherland, R. L.; Brant, M. L.; Brandelik, D. M.; Pottenger, T. *Opt. Lett.* **1993**, *18*, 858.
37. Denneval, C.; Moldovan, O.; Baudequin, C.; Achelle, S.; Baldeck, P.; Plé, N.; Darabantu, M.; Ramondenc, Y. *Eur. J. Org. Chem.* **2013**, 5591.
38. Achelle, S.; Saettel, N.; Baldeck, P.; Teulade-Fichou, M.-P.; Maillard, P. *J. Porphyrins Phthalocyanines* **2010**, *14*, 877.
39. Gauthier, S.; Vologdin, N.; Achelle, S.; Barsella, A.; Caro, B.; Robin-le Guen, F. *Tetrahedron* **2013**, *69*, 8392.
40. Liu, M.; Su, S.-J.; Jung, M.-C.; Qi, Y.; Zhao, W.-M.; Kido, J. *Chem. Mater.* **2012**, *24*, 3817.
41. (a) Su, S.-J.; Cai, C.; Kido, J. *Chem. Mater.* **2011**, *23*, 274. (b) Cai, C.; Su, S.-J.; Chiba, T.; Sasabe, H.; Pu, Y.-J.; Nakayama, K.; Kido, J. *Org. Electron.* **2011**, *12*, 843. (c) Aizawa, N.; Pu, Y.-J.; Sasabe, H.; Kido, J. *Org. Electron.* **2012**, *13*, 2235. (d) Su, S.-J.; Cai, C.; Kido, J. *J. Mater. Chem.* **2012**, *22*, 3447.
42. Verbitskiy, E. V.; Cheprakova, E. M.; Zhilina, E. F.; Kodess, M. I.; Ezhikova, M. A.; Pervova, M. G.; Slepukhin, P. A.; Subbotina, J. O.; Schepochkin, A. V.; Rusinov, G. L.; Chupakhin, O. N.; Charushin, V. N. *Tetrahedron* **2013**, *69*, 5164.
43. Verbitskiy, E. V.; Cheprakova, E. M.; Subbotina, J. O.; Schepochkin, A. V.; Slepukhin, P. A.; Rusinov, G. L.; Charushin, V. N.; Chupakhin, O. N.; Makarova, N. I.; Metelitsa, A. V.; Minkin, V. I. *Dyes Pigm.* **2014**, *100*, 201.
44. Chiu, S.-W.; Lin, L.-Y.; Lin, H.-W.; Chen, Y.-H.; Huang, Z.-Y.; Lin, Y.-T.; Lin, F.; Liu, Y.-H.; Wong, K.-T. *Chem. Commun.* **2012**, *48*, 1857.
45. Lin, L.-Y.; Tsai, C.-H.; Wong, K.-T.; Huang, T.-W.; Wu, C.-C.; Chou, S.-H.; Lin, F.; Chen, S.-H.; Tsai, A.-I. *J. Mater. Chem.* **2011**, *21*, 5950.
46. Liu, B.; Hu, X.-L.; Liu, J.; Zhao, Y.-D.; Huang, Z.-L. *Tetrahedron Lett.* **2007**, *48*, 5958.
47. Achelle, S.; Robin-le Guen, F. *Tetrahedron Lett.* **2013**, *54*, 4491.
48. Gunathilake, S. S.; Magurudeniya, H. D.; Huang, P.; Nguyen, H.; Rainbolt, E. A.; Stefan, M. C.; Biewer, M. C. *Polym. Chem.* **2013**, *4*, 5216.
49. Hadad, C.; Achelle, S.; García-Martínez, J. C.; Rodríguez-López J. *J. Org. Chem.* **2011**, *76*, 3837.

50. Hadad, C.; Achelle, S.; López-Solera, I.; García-Martínez, J. C.; Rodríguez-López, J. *Dyes Pigm.* **2013**, *97*, 230.
51. Vurth, L.; Hadad, C.; Achelle, S.; García-Martínez, J. C.; Rodríguez-López, J.; Stéphan, O. *Colloid Polym. Sci.* **2012**, *290*, 1353.
52. Das, S.; Sahana, A.; Banerjee, A.; Lohar, S.; Safin, D. A.; Babashkina, M. G.; Bolte, M.; Garcia, Y.; Hauli, I.; Mukhopadhyay, S. K.; Das, D. *Dalton Trans.* **2013**, *42*, 4757.
53. Aranda, A. I.; Achelle, S.; Hammerer, F.; Mahuteau-Betzer, F.; Teulade-Fichou, M.-P. *Dyes Pigm.* **2012**, *95*, 400.
54. Gravitz, L. *Nature* **2011**, *475*, S5.
55. Achelle, S.; Barsella, A.; Baudequin, C.; Caro, B.; Robin-le Guen, F. *J. Org. Chem.* **2012**, *77*, 4087.
56. Li, L.; Tian, Y.-P.; Yang, J.-X.; Sun, P.-P.; Wu, J.-Y.; Zhou, H.-P.; Zhang, S.-Y.; Jin, B.-K.; Xing, X.-J.; Wang, C.-K.; Li, M.; Cheng, G.-H.; Tang, H.-H.; Huang, W.-H.; Tao, X.-T.; Jiang, M.-H. *Chem. Asian J.* **2009**, *4*, 668.
57. Zhang, Q.; Li, L.; Zhang, M.; Liu, Z.; Wu, J.; Zhou, H.; Yang, J.; Zhang, S.; Tian, Y. *Dalton Trans.* **2013**, *43*, 8848.
58. Li, L.; Tian, Y.; Yang, J.; Sun, P.; Kong, L.; Wu, J.; Zhou, H.; Zhang, S.; Jin, B.; Tao, X.; Jiang, M. *Chem. Commun.* **2010**, *46*, 1673.
59. Tang, C.; Zhang, Q.; Li, D.; Zhang, J.; Shi, P.; Li, S.; Wu, J. *Dyes Pigm.* **2013**, *99*, 20.
60. Savel, P.; Akdas-Kilig, H.; Malval, J.-P.; Spangenberg, A.; Roisnel, T.; Fillaut, J.-L. *J. Mater. Chem. C* **2014**, *2*, 295.
61. Chen, D.; Zhong, C.; Dong, X.; Liu, Z.; Qin, J. *J. Mater. Chem.* **2012**, *22*, 4343.
62. Wang, A.; Long, L.; Meng, S.; Li, X.; Zhao, W.; Song, Y.; Cifuentes, M. P.; Humphrey, M. G.; Zhang, C. *Org. Biomol. Chem.* **2013**, *11*, 4250.
63. Liu, Z.; Xiong, X.; Li, Y.; Li, S.; Qin, J. *Photochem. Photobiol. Sci.* **2011**, *10*, 1804.
64. Li, L.; Ge, J.; Wu, H.; Xu, Q.-H.; Yao, S. Q. *J. Am. Chem. Soc.* **2012**, *134*, 12157.
65. Na, Z.; Li, L.; Uttachandani, M.; Yao, S. Q. *Chem. Commun.* **2012**, *48*, 7304.
66. Achelle, S.; Malval, J.-P.; Aloise, S.; Barsella, A.; Spangenberg, A.; Mager, L.; Akdas-Kilig, H.; Fillaut, J.-L.; Caro, B.; Robin-le Guen F. *ChemPhysChem* **2013**, *14*, 2725.
67. Kubota, Y.; Ozaki, Y.; Funabiki, K.; Matsui, M. *J. Org. Chem.* **2013**, *78*, 7058.
68. Ray, S.; Konar, S.; Jana, A.; Jana, S.; Patra, A.; Chatterjee, S.; Golen, J. A.; Rheingold, A. L.; Mandal, S. S.; Kar, S. K. *Polyhedron* **2012**, *33*, 82.
69. Das, K.; Jana, A.; Konar, S.; Chatterjee, S.; Mondal, T. K.; Barik, A. K.; Kar, S. K. *J. Mol. Struct.* **2013**, *1048*, 98.
70. Bushuev, M. B.; Krivopalov, V. P.; Nikolaenkova, E. B.; Pervukhina, N. V.; Naumov, D. Y.; Rakhmanova, M. I. *Inorg. Chem. Commun.* **2011**, *14*, 749.
71. Hou, G.-G.; Sun, J.-F.; Wang, C.-H.; Zhao, F.; Dai, X.-P.; Li, H.-J.; Han, J.-T. *J. Mol. Struct.* **2013**, *1048*, 295.
72. Nishikawa, M.; Nomoto, K.; Kume, S.; Inoue, K.; Sakai, M.; Fujii, M.; Nishihara, H. *J. Am. Chem. Soc.* **2010**, *132*, 9579.
73. Adapted with permission from reference 68. Copyright 2010 American Chemical Society.
74. Kozhevnikov, V. N.; Durrant, M. C.; Williams, J. A. G. *Inorg. Chem.* **2011**, *50*, 6304.
75. Wang, G.-F.; Liu, Y.-Z.; Chen, X.-T.; Zheng, Y.-X.; Xue, Z.-L. *Inorg. Chim. Acta* **2013**, *394*, 488.
76. Chang, C.-H.; Wu, Z.-J.; Chiu, C.-H.; Liang, Y.-H.; Tsai, Y.-S.; Liao, J.-L.; Chi, Y.; Hsieh, H.-Y.; Kuo, T.-Y.; Lee, G.-H.; Pan, H.-A.; Chou, P.-T.; Lin, J.-S.; Tseng, M.-R. *ACS Appl. Mater. Interfaces* **2013**, *5*, 7341.
77. Wang, Z.-Q.; Xu, C.; Dong, X.-M.; Zhang, Y.-P.; Hao, X.-Q.; Gong, J.-F.; Song, M.-P.; Ji, B.-M. *Inorg. Chem. Commun.* **2011**, *14*, 316.
78. Ozawa, H.; Kawagushi, H.; Okuyama, Y.; Arakawa, H. *Eur. J. Inorg. Chem.* **2013** doi: 10.1002/ejic.201300345.
79. Liu, D.; Zhang, Z.; Zhang, H.; Wang, Y. *Chem. Commun.* **2013**, *49*, 10001.
80. Trashakhova, T. V.; Nosova, E. V.; Slepukhin, P. A.; Valova, M. S.; Lipunova, G. N.; Charushin, V. N. *Russ. Chem. Bull. Int. Ed.* **2011**, *60*, 2347.
81. Machura, B.; Nawrot, I.; Kruszynski, R.; Dulski, M. *Polyhedron* **2013**, *54*, 272.

82. Du, B.-S.; Lin, C.-H.; Chi, Y.; Hung, J.-Y.; Chung, M.-W.; Lin, T.-Y.; Lee, G.-H.; Wong, K.-T.; Chou, P.-T.; Hung, W.-Y.; Chiu, H.-C. *Inorg. Chem.* **2010**, *49*, 8713.
83. Tumkevičius, S.; Dodonova, J.; Kazlauskas, K.; Masevicius, V.; Skardžiūte, L.; Juršėnas, S. *Tetrahedron Lett.* **2010**, *51*, 3902.
84. (a) Tumkevičius, S.; Dodonova, J. *Synlett* **2011**, *12*, 1705. (b) Dodonova, J.; Skardžiūte, L.; Kazlauskas, K.; Juršėnas, S.; Tumkevičius, S. *Tetrahedron* **2012**, *68*, 329. (c) Skardžiūte, L.; Kazlauskas, K.; Dodonova, J.; Bucevičius, J.; Tumkevičius, S.; Juršėnas, S. *Tetrahedron* **2013**, *69*, 9566.
85. Rote, R. V.; Shelar, D. P.; Patil, S. R.; Shinde, S. S.; Toche, R. B.; Jachak, M. N. *J. Fluoresc.* **2011**, *21*, 453.
86. Zonouzi, A.; Hosseinzadeh, F.; Karimi, N.; Mirzazadeh, R.; Weng, Ng S. *ACS Comb. Sci.* **2013**, *15*, 240.

A UNIFIED STRATEGY FOR THE SYNTHESIS OF BRIDGED INDOLE ALKALOIDS AND THEIR CLOSE ANALOGUES

M.-Lluïsa Bennasar

Laboratory of Organic Chemistry, Faculty of Pharmacy, and Institut de Biomedicina (IBUB), University of Barcelona, Barcelona E-08028, Spain (e-mail: bennasar@ub.edu)

Abstract. *A general strategy for the assembly of the bridged tetracyclic topography of some indole alkaloids, taking advantage of a combination of a ring-closing metathesis (RCM) and a vinyl halide Heck cyclization, is described. The approach has enabled the construction of the ervitsine and 5-nor cleavamine ring systems as well as the accomplishment of the total synthesis of apparicine and cleavamines.*

Contents

1. Introduction
2. Construction of the ervitsine ring system
3. First total synthesis of apparicine
 - 3.1. Initial studies
 - 3.2. Completion of the total synthesis
4. Synthesis of cleavamine-type indole alkaloids and their 5-nor derivatives
 - 4.1. Construction of the 5-nor cleavamine skeleton
 - 4.2. Total synthesis of cleavamines

5. Conclusion

Acknowledgments

References

1. Introduction

The indole nucleus is commonly found in the core structure of many biologically active compounds and occupies an important position in medicinally relevant heterocyclic systems.¹ Consequently, the synthesis of diversely substituted and functionalized indole derivatives has long been a research target, leading to a variety of well-established methods.² In particular, the monoterpene indole alkaloids, a large class of natural products with highly diverse and often challengingly complex structures, have called for the development of novel synthetic strategies.³

Over the course of our long-standing interest in this field, we have exploited the rich chemistry of pyridinium salts and dihydropyridines to elaborate advanced intermediates for the synthesis of a number of indole alkaloids,⁴ including ervitsine and ervatamines,⁵ akagerine,⁶ as well as the pharmacologically relevant pyrroloquinoline alkaloid camptothecin.⁷ More recently, we have discovered that 2-indolylacyl radicals efficiently participate in cyclizations upon alkenes and heteroaromatic rings,⁸ giving access to a wide range of 2-acylindolic structures including ellipticine quinones,⁹ calothrixin B¹⁰ and uleine alkaloids.¹¹

Several indole alkaloids belonging to different biogenetic families (*e.g.*, apparicine, cleavamine or pericine, Figure 1) structurally feature bridged tetracyclic frameworks consisting of an indolo-fused medium-sized ring and a 3-substituted piperidine moiety.

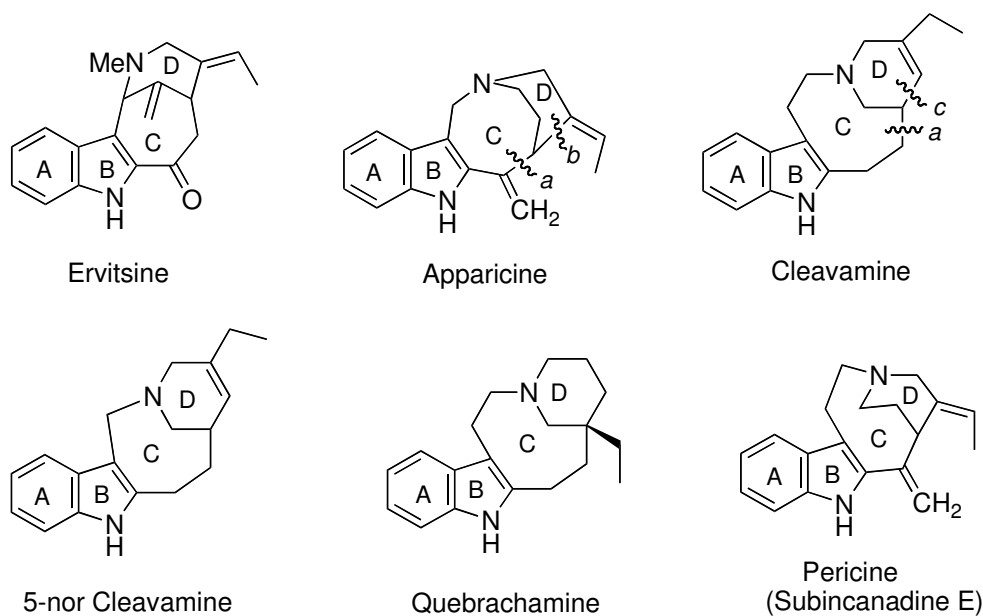


Figure 1

We envisaged these arrangements to be accessible by a unified strategy wherein a combination of two well-established C–C bond-forming reactions, a ring-closing metathesis (RCM)¹² and a Heck cyclization¹³ plays a crucial role. Thus, the metathetic ring closure from different indole-containing dienes would serve to build the tricyclic ABC substructures of the alkaloids, forming bond *a* as depicted in apparicine and cleavamine structures. Subsequently, an *exocyclic* or *endocyclic* vinyl halide Heck cyclization upon the double bond left by the previous RCM step (forming bond *b* or *c*) would complete the bridged carbon skeletons and at the same time install the requisite *E*-ethylidene or ethyl appendages.

It is widely assumed that medium-sized rings are difficult to access by direct cyclization reactions due to entropic factors and transannular interactions in the transition state. RCM techniques have emerged as a powerful tool to address this issue and several reviews covering this specific topic are available.¹⁴ On the other hand, Heck couplings, involving vinyl halides and elaborated cyclohexenes, have proved to be useful for the assembly of the bridged core of indole alkaloids, including pentacyclic *Strychnos* alkaloids,¹⁵ strychnine,¹⁶ minfiensine¹⁷ and aspidophylline A.¹⁸ However, Heck cyclizations upon medium-sized rings to produce strained bridged systems are rare,¹⁹ most reported examples dealing with cyclizations from more robust aryl halides.^{20,21}

This account will focus on the development of the above annulation chemistry in the context of the synthesis of ervitsine, apparicine, 5-nor cleavamine and cleavamine.

2. Construction of the ervitsine ring system

Ervitsine²² is a minor indole alkaloid isolated in 1977 from *Pandaca boiteau* (*Apocynaceae*)²³ with a unique tetracyclic skeleton comprising a 2-azabicyclo[4.3.1]decane system fused to the indole ring and two exocyclic alkylidene (16-methylene and 20*E*-ethylidene) substituents (Figure 2). This particular structure inspired several research groups in the eighties and early nineties to initiate synthetic studies, resulting in different approaches to the core structure^{24,25} and a total synthesis based on biomimetic considerations.^{5a,26} Despite the variety of strategies used, all routes converge in the formation of the central carbocyclic ring in the last synthetic steps, either by cyclization of an iminium-type ion upon the indole 3-position or by Friedel-Crafts acylation of the indole 2-position.

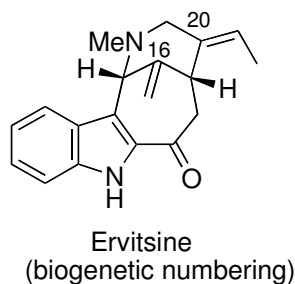
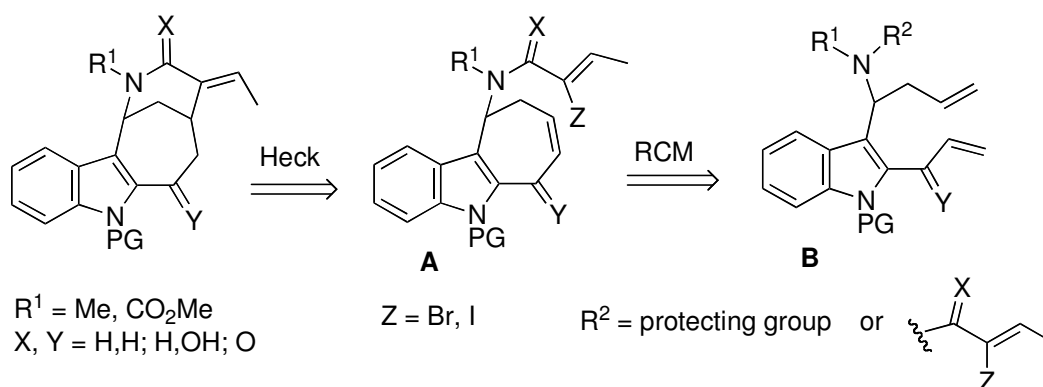


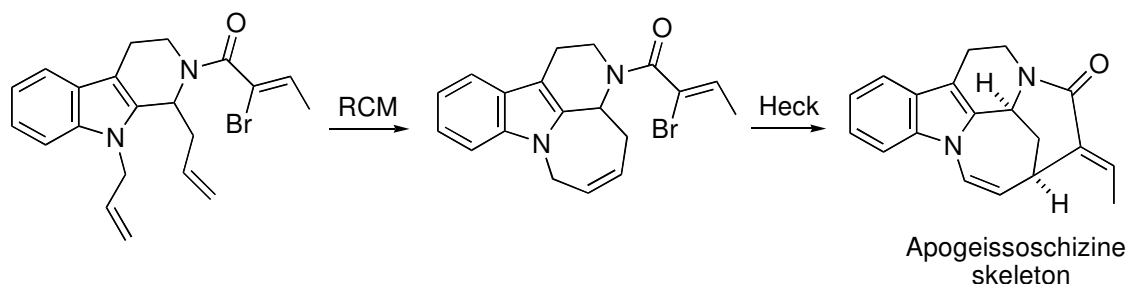
Figure 2

Following our plan, the application of the RCM-Heck annulation strategy resulted in a completely different synthetic approach to the ervitsine ring system.²⁷ As depicted in Scheme 1, RCM of 2,3-dialkenylindoles of general structure **B** would produce the central medium-sized ring²⁸ (*i.e.*, cyclohepta[*b*]indoles **A**), with the appropriate double bond functionality for the subsequent intramolecular Heck reaction with the amino-tethered vinyl halide.



Scheme 1

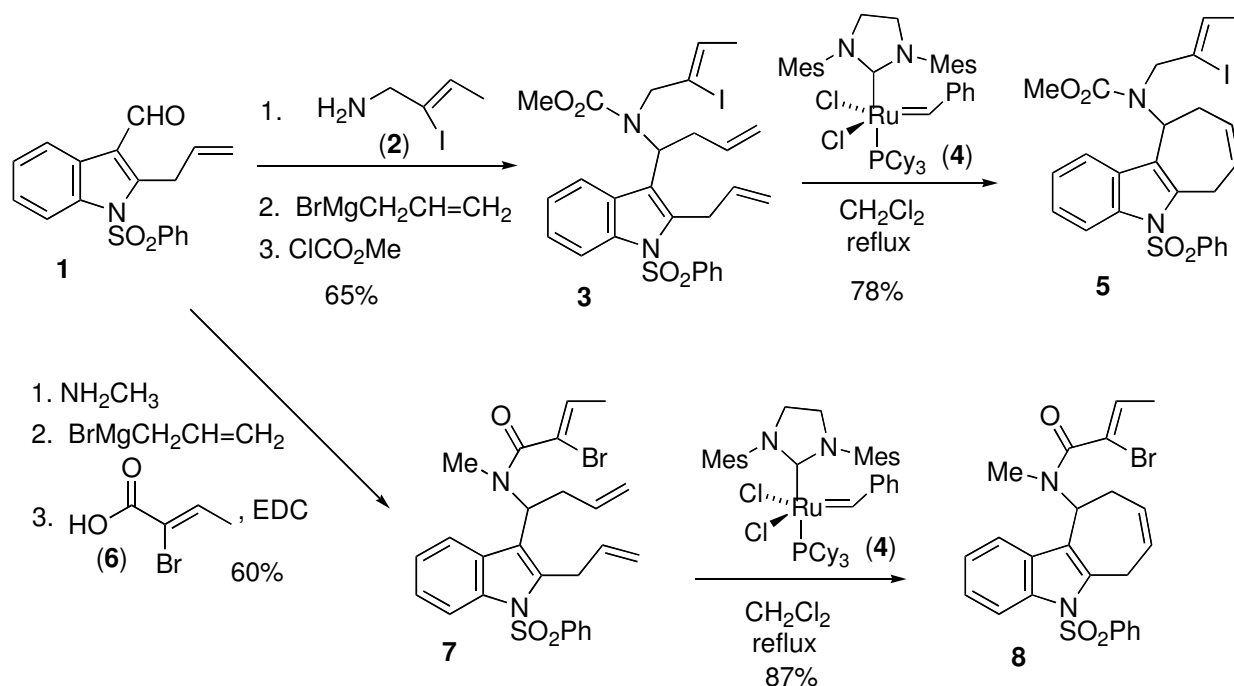
In a pioneering approach developed by Rawal,¹⁹ the apogeissoschizine skeleton had been assembled in a similar manner, taking advantage of a RCM reaction of a tetrahydro- β -carboline diene and a Heck coupling upon the resulting azepine ring (Scheme 2).



Scheme 2

We designed intermediates unfunctionalized at the benzylic indole 2-position, knowing that this methylene group could be oxidized at a later stage of the synthesis.²⁹ Thus, we targeted the cyclohepta[*b*]indoles **5** and **8** as substrates for the key Heck reaction, bearing a carbamate or amide exocyclic function and a strong electron-withdrawing phenylsulfonyl group at the indole nitrogen to stabilize the 3-(aminomethyl)indole (gramine) moiety (Scheme 3). The synthetic route began with 2-allyl-3-indolecarbaldehyde **1**, from which the homoallylic amine required for the RCM step was installed by means of an

amination–imine allylation sequence. To avoid the use of additional protecting groups, we chose a direct route and incorporated the haloalkenyl appendage either at the amination step (for **5**) or at the final acylation step (for **8**), with the hope that it would be sufficiently inert under the RCM conditions. Reaction of aldehyde **1** with (*Z*)-2-iodo-2-butenylamine (**2**), followed by alkylation of the resulting imine with allylmagnesium bromide led to an unstable secondary amine (not isolated), which was subsequently acylated with ClCO₂Me to give carbamate **3** in 65% overall yield. On the other hand, reaction of aldehyde **1** with methylamine and allylation of the resulting imine as above, followed by acylation with (*Z*)-2-bromo-2-butenic acid (**6**) in the presence of 1-ethyl-3-(3-dimethylaminopropyl)carbodiimide (EDC) gave amide **7** in 60% overall yield.

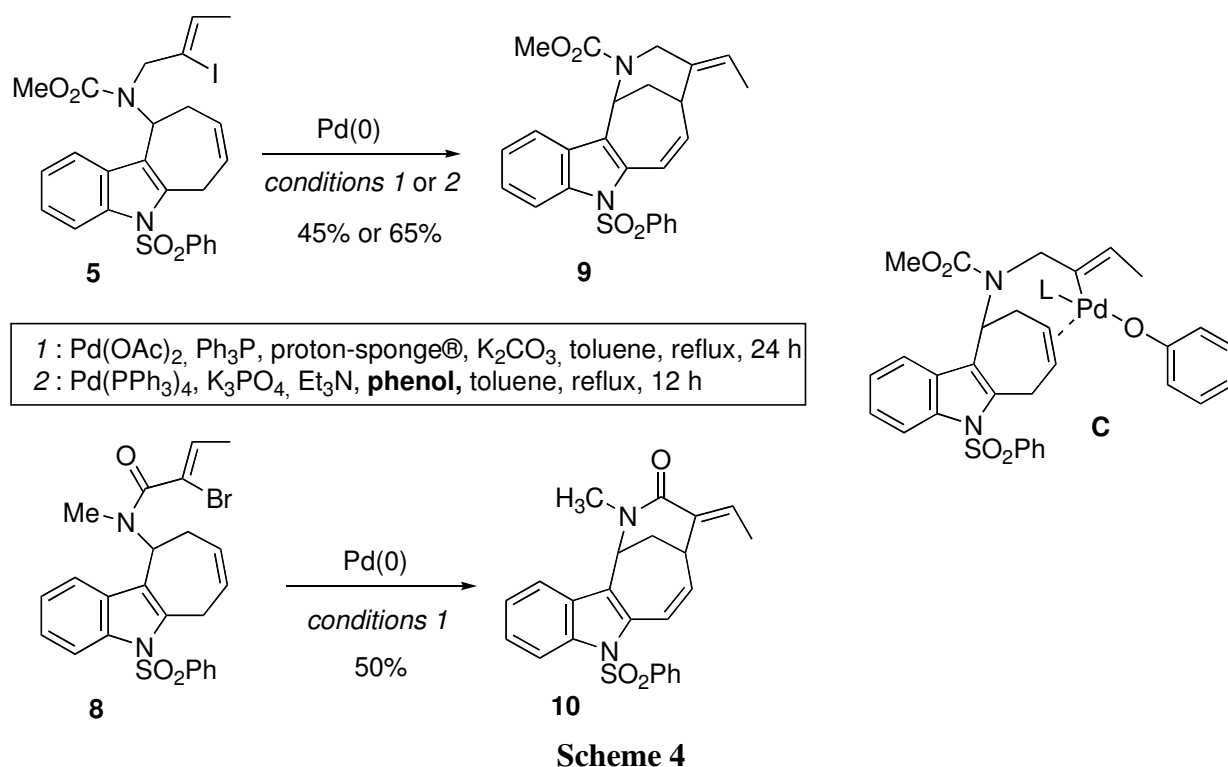


Scheme 3

At this point, we proceeded to study the RCM reaction. As expected, considering the different substitution and electronic nature of the double bonds in the trienic substrates **3** and **7**, the preferred RCM event was the indole-templated cyclization, leading to the desired cycloheptenes **5** and **8** as the only products (78% and 87% yield) on exposure to the second-generation Grubbs catalyst (**4**). It should be mentioned that the extension of the chemistry outlined above to the elaboration of functionalized tricyclic erivitsine substructures (**A**, Y=H, OH or O, Scheme 1) met with failure.^{27b}

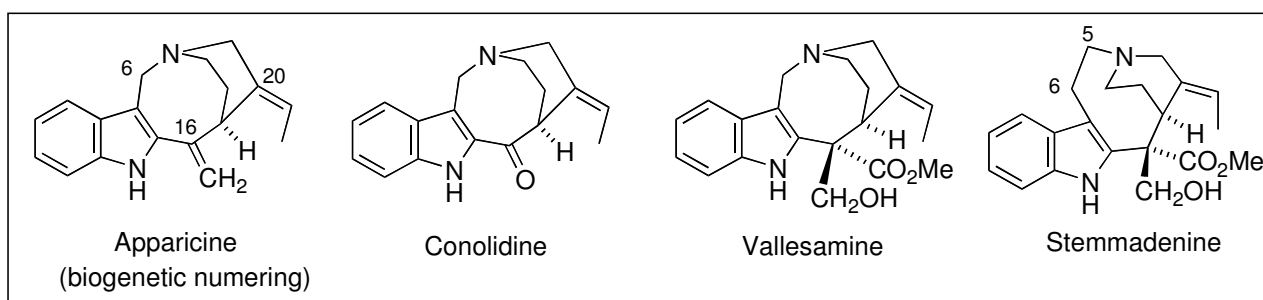
We turned our attention to the intramolecular Heck reaction to complete the erivitsine ring system. Satisfactorily, the desired cyclization took place, although in moderate yields, upon treatment of vinyl halides **5** and **8** under the non-polar protocol referred to as *conditions 1* in Scheme 4. The resulting tetracycles **9** and **10**, embodying the 4*E*-ethylidene-2-azabicyclo[4.3.1]decane bridged core of erivitsine, were isolated in 45% and 50%, respectively. After some experimentation, we found that the addition of phenol (*conditions 2*) resulted in a more efficient cyclization of **5**, giving the erivitsine tetracycle **9** in a higher yield (65%). As far as we know, the use of phenol as a catalytic additive in the Heck reaction is unprecedented, although its positive role in some palladium-catalyzed arylations of ketone enolates has been previously observed.^{30,31} According to these reports,³⁰ the intermediacy of a palladium phenoxide (*e.g.*, **C**),

which would stabilize an otherwise unstable intermediate, could account for the beneficial effect of the added phenol.



3. First total synthesis of apparicine

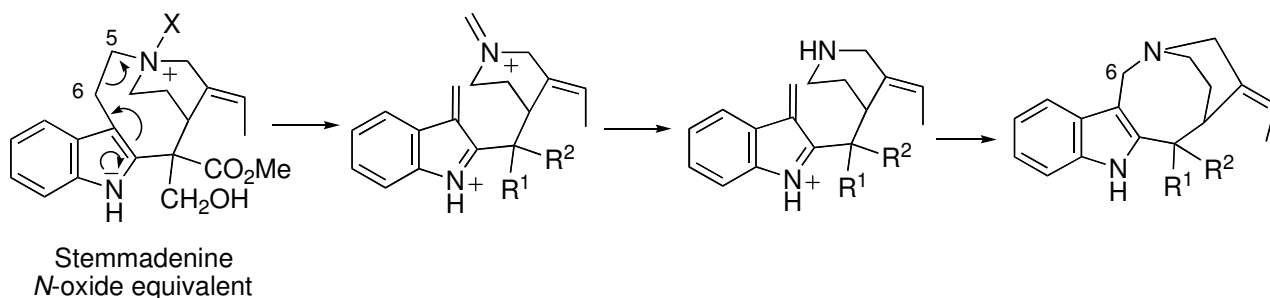
First isolated from *Aspidosperma dasycarpon* more than forty years ago,^{32,33} apparicine is the main representative of a small group of alkaloids, also including vallesamine or conolidine, which are structurally defined by the presence of only one carbon (C-6) connecting the indole 3-position with the aliphatic nitrogen (Figure 3).³⁴



This structural arrangement, featuring a strained 1-azabicyclo[4.2.2]decane framework fused to the indole ring, is the biogenetic result of the C-5 excision from the original two-carbon tryptamine bridge of the alkaloid stemmadenine. The fragmentation–iminium hydrolysis–recyclization sequence depicted in Scheme 5, which involves the participation of a stemmadenine *N*-oxide equivalent, has been proposed to rationalize this biogenetic relationship.³⁵

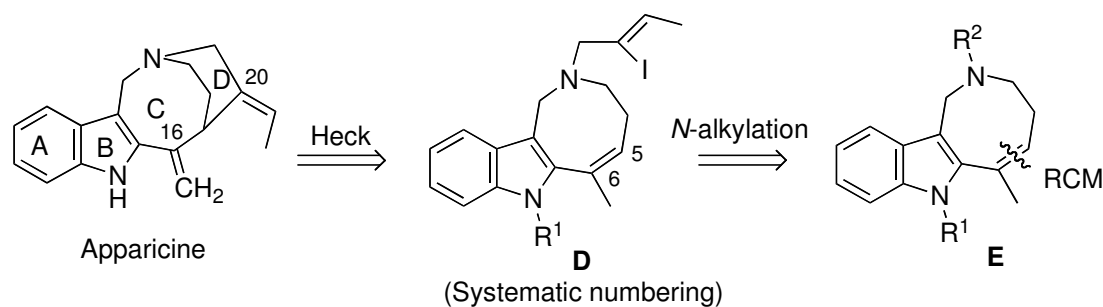
The compact architecture of apparicine alkaloids make them challenging targets for synthesis. However, when we undertook the synthetic journey that would ultimately lead to the first total synthesis of

apparicine,³⁶ very little progress had been made in this area. An approach developed by Joule's group in the late seventies³⁷ allowed the construction of the ring skeleton of apparicine but proved unsuitable for the total synthesis of the alkaloid. Some partial biomimetic transformations had also been reported.^{38,39}



Scheme 5

We planned to carry out the synthesis of apparicine by first of all constructing tricyclic ABC substructures containing the central eight-membered ring (*e.g.*, azocino[4,3-*b*]indoles **E**, Scheme 6)⁴⁰ by RCM from a suitable indolic diene. The assembly of the bridged carbon skeleton would then be concluded by inserting an ethylideneethano unit between the aliphatic nitrogen and C-5. Thus, we envisaged that after *N*-alkylation with the appropriate haloalkenyl halide or tosylate, an intramolecular Heck coupling upon the vinylindole moiety would lead not only to the closure of the 3*E*-ethylidenepiperidine ring but also to the concomitant placement of the exocyclic 16-methylene appendage.



Scheme 6

3.1. Initial studies

Installing an eight-membered ring on an indole nucleus represents an attractive synthetic operation,⁴¹ as the resulting units have been found in several natural products. In particular, some indole alkaloids, such as deoxyisoaustamide, balasubramide and lundurines (Figure 4), embody a nitrogen-containing azocine ring 5,4-*b* fused to the indole nucleus.

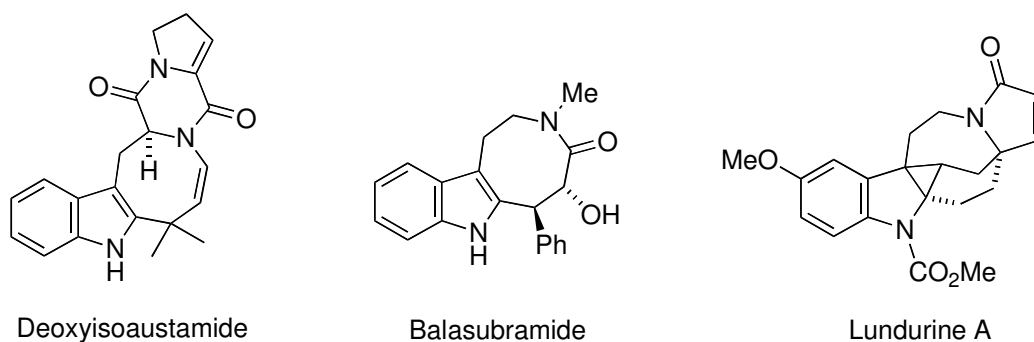
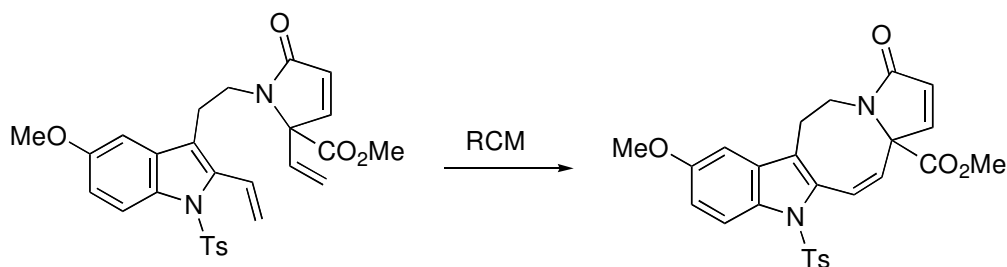


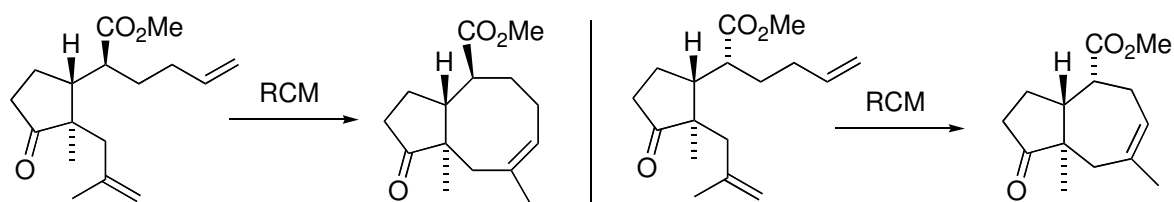
Figure 4

As stated in the *Introduction*, RCM is particularly useful for the assembly of eight-membered rings^{14c,d,e} and has been applied, for instance, in the construction of advanced intermediates for the synthesis of lundurine A (Scheme 7).⁴²



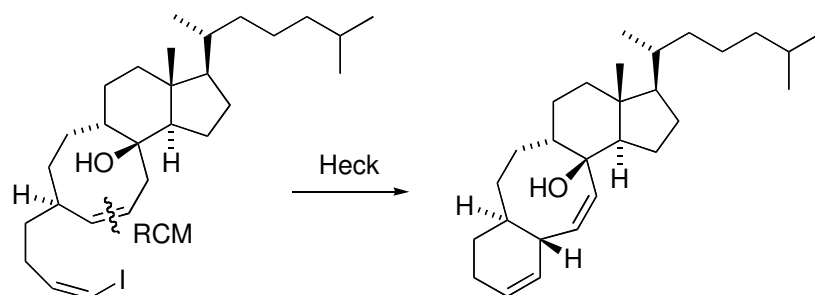
Scheme 7

As a general rule, RCM leading to cyclooctenes benefits from conformational constraints, such as preexisting rings or stereoelectronic effects in the substrate, but is less predictable when it involves the generation of trisubstituted double bonds.⁴³ For example, the metathesis reaction of the epimeric dienic substrates depicted in Scheme 8 produced different results: the expected cyclopentacyclooctene or the corresponding ring-contracted product, the latter arising from the competitive isomerization of the monosubstituted terminal double bond, followed by cyclization with liberation of propene.⁴⁴



Scheme 8

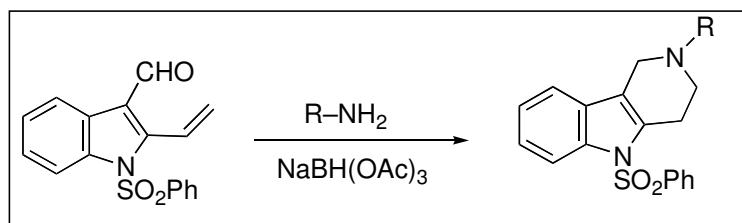
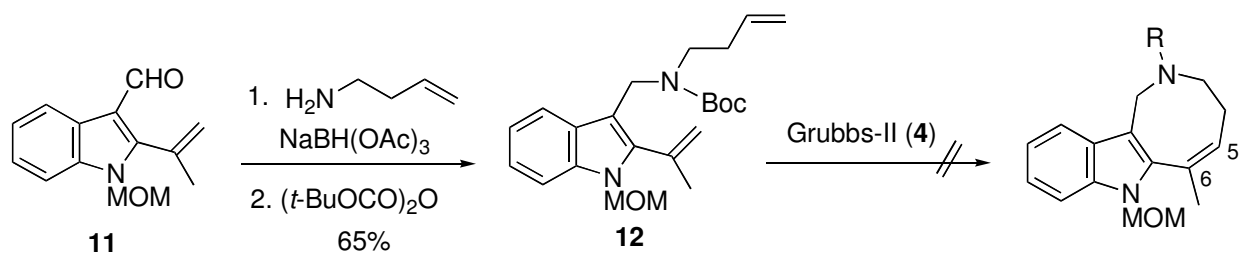
In a similar context, the combination of a RCM leading to a cyclooctene ring and a vinyl halide Heck cyclization upon the resulting double bond has been used to assemble 8-6 fused carbocyclic rings included in polycyclic steroid-like systems (Scheme 9).⁴⁵



Scheme 9

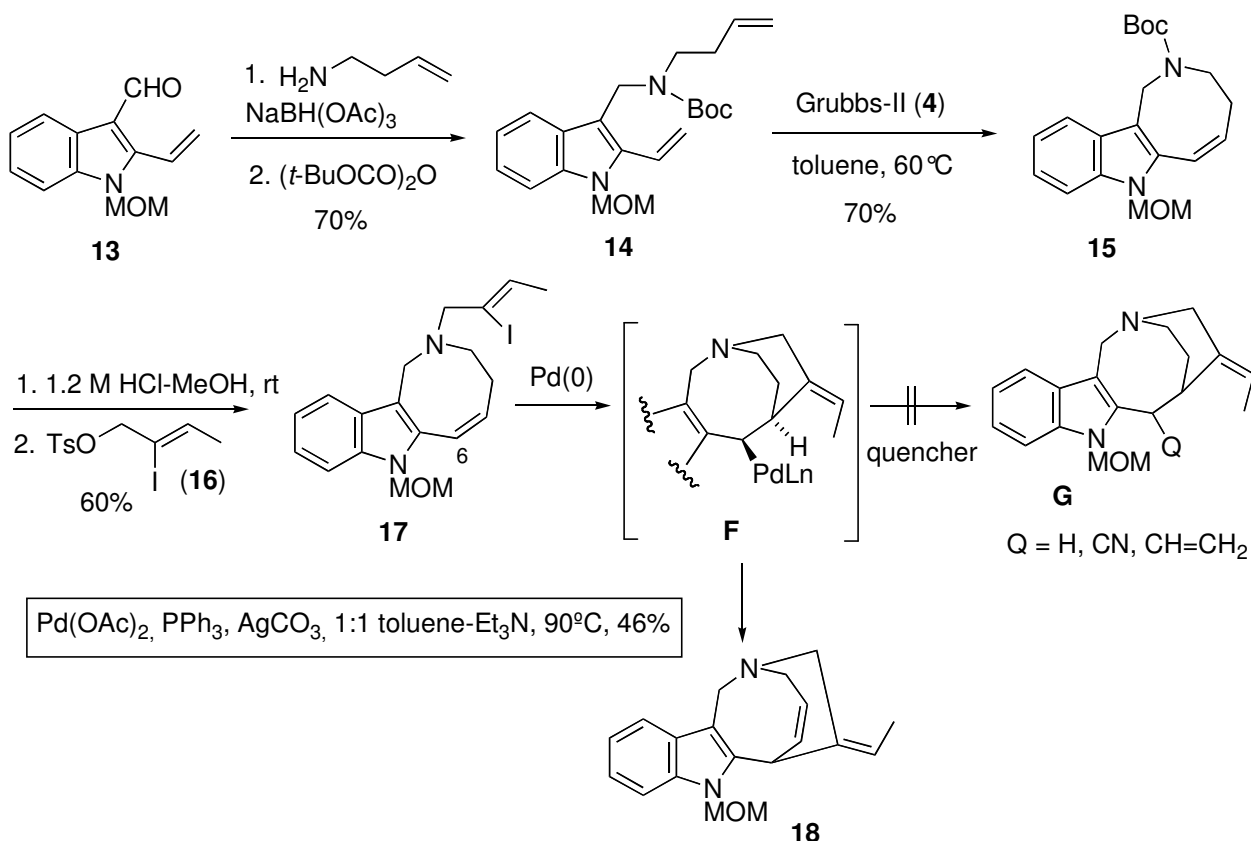
With these precedents in mind, we set out to study the indole-templated RCM en route to apurinic, directly targeting 6-methylazocino[4,3-*b*]indoles, with the trisubstituted 5,6-double bond required for the Heck coupling (Scheme 10).

2-Isopropenylindole **12**, equipped with a robust methoxymethyl (MOM) group at the indole nitrogen, was efficiently prepared by reductive amination of aldehyde **11** with 3-butenylamine and acylation of the resulting secondary amine with di-*tert*-butyl dicarbonate.



Scheme 10

It is worth mentioning that we now deliberately avoided protecting the indole nitrogen as benzene-sulfonamide, as in the above ervitsine series, since this electron-withdrawing group has proven to be incompatible with the reductive amination of 2-vinyl-3-indolecarbaldehydes. On the contrary, it favours the exclusive generation of tetrahydro- β -carbolines through an annulation process initiated by addition of the primary amine to the conjugated double bond and concluded by intramolecular reductive amination.⁴⁶



Scheme 11

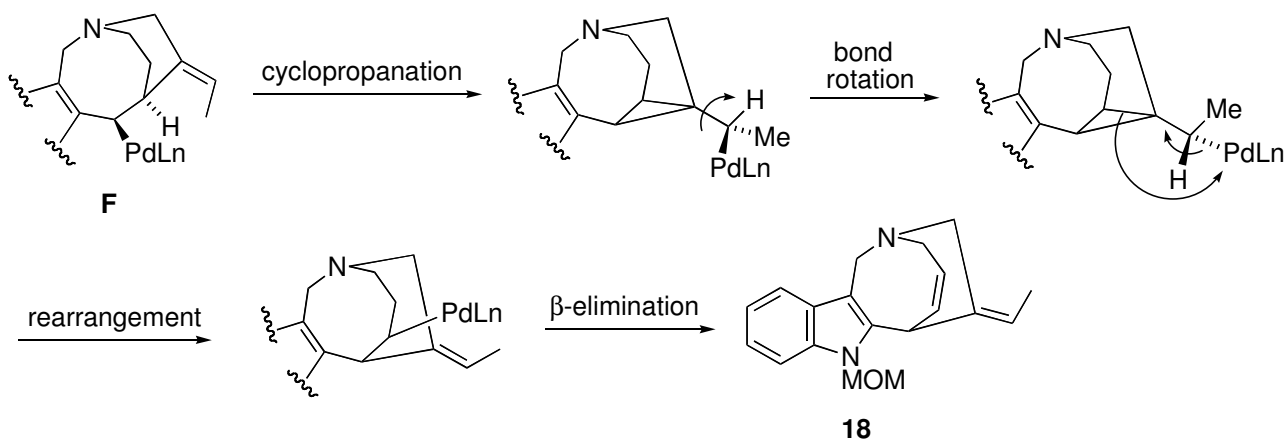
Unfortunately, all attempts to promote RCM of diene **12** failed to produce the required azocinoindole. Instead, **12** underwent intermolecular metathesis reactions leading to dimeric products on exposure to the second-generation Grubbs catalyst (**4**) in CH_2Cl_2 or toluene, even when working under high dilution conditions (0.007 M). The use of other metathesis catalysts, either based on ruthenium (first-generation

Grubbs or second-generation Hoveyda-Grubbs catalysts) or molybdenum (Schrock's catalyst) did not bring about to any improvement.

Attributing this result to the difficulty of forming a conjugated trisubstituted double bond included in the azocine ring, we turned our attention to a 6-demethyl tricyclic substructure, thinking that such a model substrate would also serve as a precursor for assembling the bridged skeleton of apparicine. In fact, we hoped to take advantage of a reductive Heck cyclization or a tandem Heck cyclization-capture, which could also allow the introduction of the remaining carbon atom. The development of this new chemistry is depicted in Scheme 11. The required diene **14** was uneventfully prepared as in the above isopropenyl series, by reductive amination of aldehyde **13** with 3-butenylamine followed by *N*-acylation. As anticipated, cyclization of **14**, involving two terminal monosubstituted alkene units, took place with the second-generation Grubbs catalyst (**4**) under standard conditions (0.01 M, toluene, 60 °C) to give azocinoindole **15** in acceptable yield (70%).⁴⁷ With this key intermediate in hand, the preparation of the more advanced synthetic intermediate **17** proceeded without difficulty as it only required the manipulation of the aliphatic nitrogen of **15** to introduce the iodoalkenyl chain. Exposure to a mild acidic protocol (1.2 M HCl in MeOH at rt) accomplished the removal of the Boc group and the resulting secondary amine was directly subjected to alkylation with (*Z*)-2-iodo-2-butenyl tosylate (**16**) to give **17** in 60% isolated yield over the two steps.

We next studied the key formation of the piperidine ring by Pd-catalyzed cyclization of the vinyl iodide upon the 2-vinylindole moiety. We expected that the initially formed alkylpalladium intermediate **F**, in which no β -hydrogen is available for elimination, would be stable enough to be reduced or trapped with a suitable quencher. However, when **17** was subjected to a number of standard conditions for reductive Heck cyclizations or Heck cyclization-capture in the presence of KCN, $K_4[Fe(CN)_6]$, TMSiCN or tributylvinylstannane as trapping agents, the desired tetracyclic system **G** was never detected. In all cases, the only isolated product was tetracycle **18**, arising from an apparent 7-*endo* cyclization with inversion of the ethylidene configuration. The best yield of this unexpected product (46%) was obtained under cationic conditions, in the presence of Ag_2CO_3 as the additive.

The formation of unusual Heck cyclization products like **18** has been previously observed⁴⁸ and rationalized⁴⁹ by considering that the initial 6-*exo* cyclization leading to the alkylpalladium intermediate **F** is followed by an intramolecular carbopalladation on the exocyclic alkene. The resulting cyclopropane intermediate would undergo rearrangement, with concomitant inversion of the alkene geometry, and final β -hydride elimination (Scheme 12).



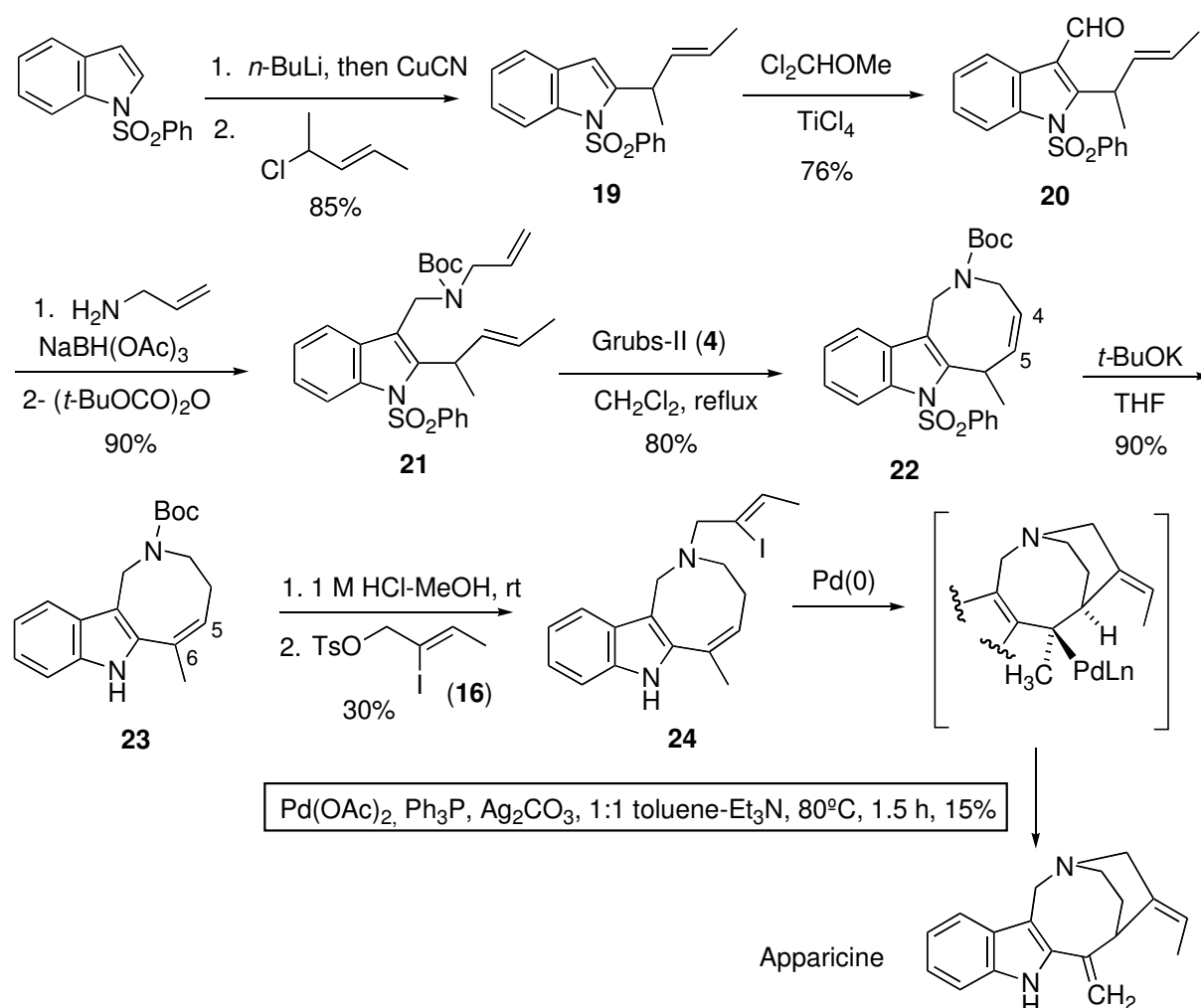
Scheme 12

In our case, this cyclopropanation–rearrangement route would be fast enough to prevent the quenchers from intercepting the initially formed alkylpalladium intermediate **F**.

It became apparent that the presence of a 6-methyl group in the Heck cyclization substrate was critical for the assembly of the bridged framework of apparicine as it would guarantee the β -elimination of the alkylpalladium intermediate resulting from cyclization, thus avoiding the undesired route. We therefore sought another synthetic plan to access 6-methylazocino[4,3-*b*]indoles by RCM.

3.2. Completion of the total synthesis

Since we were unable to directly form the trisubstituted double bond included in the azocine ring by RCM, we decided to change the cyclization site from the 5,6-position to the less crowded 4,5-position by using a 3-(allylaminomethyl)-2-allylindole such as **21** as the diene (Scheme 13). Consequently, the synthesis of the Heck precursor would now require an additional step to isomerize the resulting double bond.



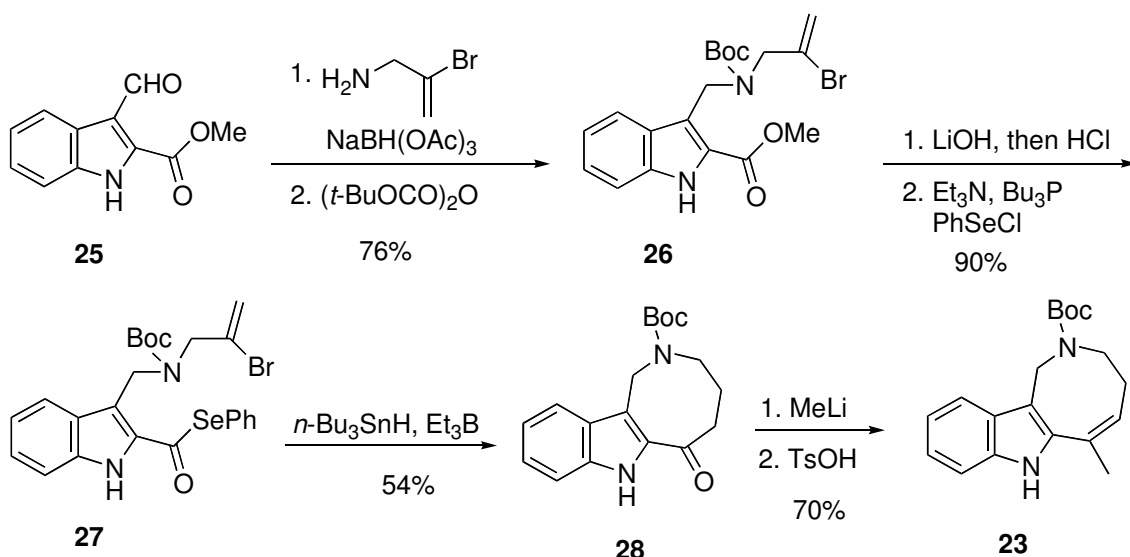
Scheme 13

To install the α -methyl substituted allyl-type chain at the indole 2-position, 1-(phenylsulfonyl)indole was allowed to react with *n*-BuLi and CuCN and the intermediate organocopper derivative was treated with (*E*)-4-chloro-2-pentene. The resulting indole **19** was then converted into the RCM precursor **21** by Friedel-Crafts formylation, reductive amination of aldehyde **20** with allylamine and the subsequent protection of the aliphatic nitrogen with a Boc group. The overall yield of the four steps was 58%. Satisfactorily, ring closure

of diene **21** took place with the second-generation Grubbs catalyst (**4**) under standard conditions (0.07 M, CH₂Cl₂, reflux) to give the desired 6-methylazocinoindole **22** in 80% yield.

With facile access to **22**, we focused our attention on the isomerization step. After much experimentation using ruthenium-based reagents, we fortuitously discovered that the double bond of azocinoindole **22** moved into conjugation with the aromatic ring under the basic conditions used to remove the phenylsulfonyl group. Thus, long exposure to *t*-BuOK in refluxing THF brought about the anticipated indole deprotection along with alkene isomerization, affording **23** in 90% yield. By using shorter reaction times, we found that the migration of the double bond took place after the initial indole *N*-deprotection step, which suggests that the base-induced isomerization is only compatible with the presence of a free indole NH group.

The above RCM-isomerization route allows the efficient synthesis of the key intermediate **23** in 41% overall yield from 1-(phenylsulfonyl)indole by way of four isolated intermediates. In the course of our work, we explored an alternative approach based on an 8-*endo* cyclization of a 2-indolylacyl radical upon an amino tethered alkene (Scheme 14).^{8,50} The new synthesis required the preparation of the radical precursor, *i.e.*, selenoester **27**, bearing a bromovinyl chain to increase the efficiency and the *endo* regioselectivity of the ring closure.⁵⁰ It was accomplished by reductive amination of aldehyde **25** with 2-bromo-2-propenylamine, followed by protection with a Boc group and phenylselenation of the resulting ester **26** via the corresponding carboxylic acid. The radical cyclization was promoted by treatment of selenoester **27** with *n*-Bu₃SnH as the radical mediator and Et₃B as the initiator to give ketone **28** in a moderate yield (50%). Finally, reaction of **28** with methyl-lithium, followed by dehydration of the resulting tertiary alcohol under mild acid conditions, provided the target alkene **23**. This alternative route took place in 26% overall yield by way of only three isolated intermediates.



Scheme 14

Having secured azocinoindole **23**, we next sought to install the haloalkenyl chain on the aliphatic nitrogen for the subsequent Heck reaction as in the above 6-demethyl series. Removal of the *N*-Boc group of **23** required a mild acid protocol to avoid decomposition of the resulting secondary amine, which proved to be highly sensitive and was directly alkylated with tosylate **16**. Even after considerable experimentation, amine **24** could be isolated only in a moderate 30% isolated yield over the two steps.⁵¹

We were now ready to construct the full carbon skeleton of apparicine by intramolecular coupling of the vinyl iodide and the trisubstituted alkene. Extensive studies were carried out but only the starting material or decomposition products were recovered. However, it was found that closure of the strained 1-azabicyclo[4.2.2]decane framework with concomitant incorporation of the exocyclic alkylidene substituents took place under cationic conditions, although loss of material was still considerable. When vinyl iodide **24** was subjected to the specific protocol depicted in Scheme 13, racemic apparicine was obtained in a consistent, reproducible 15% isolated yield. The spectroscopic data of synthetic apparicine matched those described in the literature for the natural product.

4. Synthesis of cleavamine-type indole alkaloids and their 5-nor derivatives

The *Iboga* family of indole alkaloids has long attracted the attention of synthetic organic chemists owing to the intricate architecture of its members as well as their diverse and important biological activities.⁵² Most of these alkaloids, exemplified by catharanthine (Figure 5), are structurally characterized by a pentacyclic skeleton with indole and isoquinolidine rings fused by a seven-membered C ring.

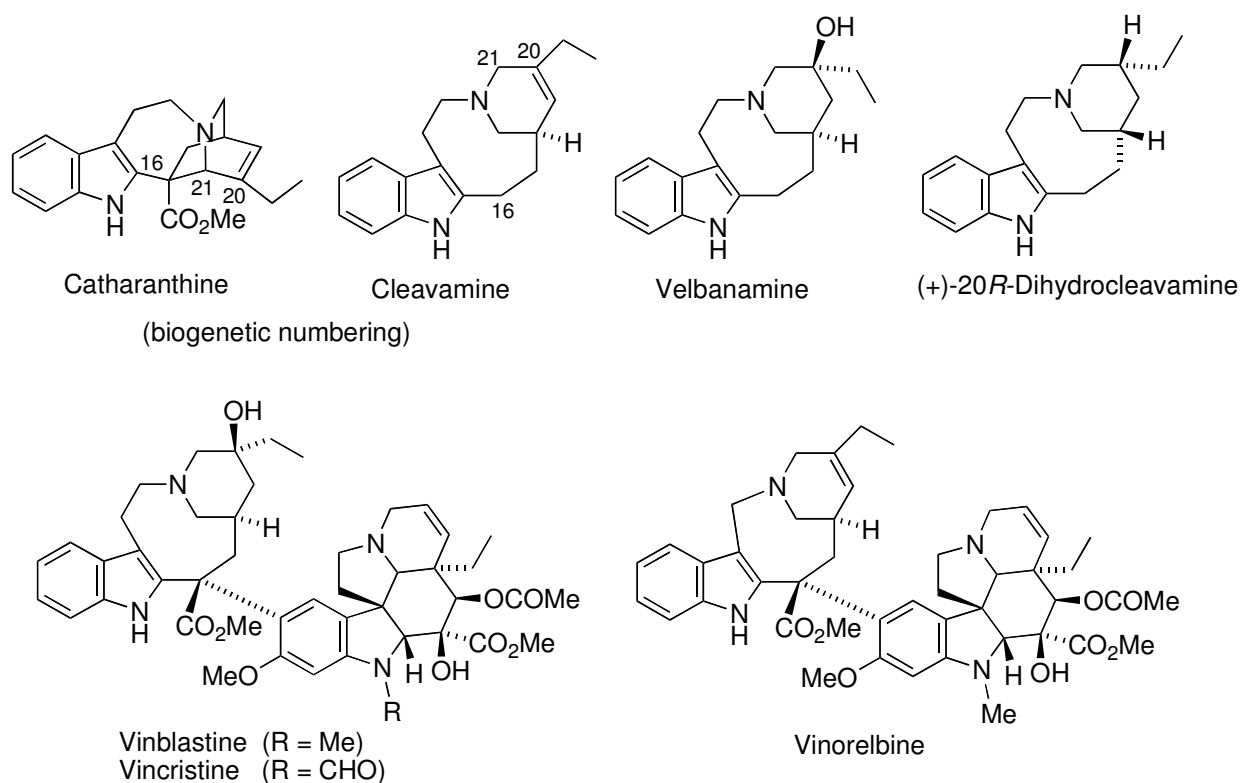
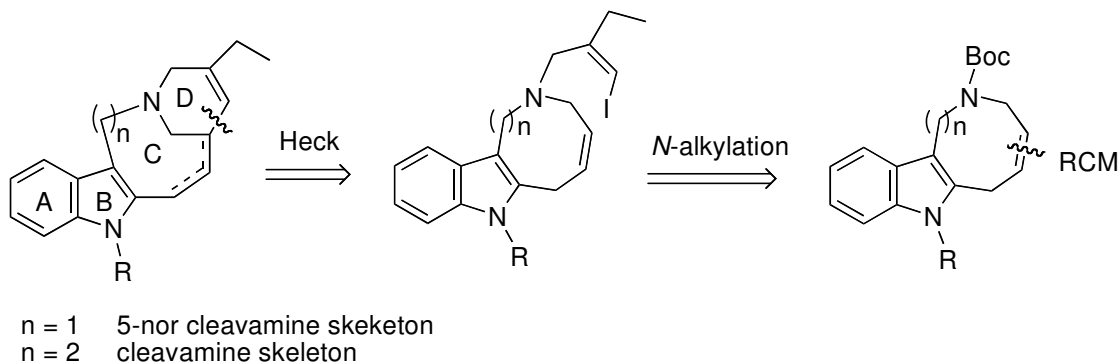


Figure 5

However, there is a small subgroup of natural bases (cleavamine, velbanamine or (+)-20R-dihydrocleavamine) that exhibit a 16,21-*seco* structure and, consequently, incorporate a central nine-membered ring and a bridged piperidine ring, featuring a 1-azabicyclo[6.3.1]dodecane framework. Cleavamines are of particular interest not only because they have provided key synthetic intermediates for pentacyclic *Iboga* derivatives⁵³ but also because they constitute the indole *upper half* of the antitumoral bisindole *Catharanthus* alkaloids vinblastine and vincristine.⁵⁴ Also used in cancer chemotherapy,⁵⁵ vinorelbine^{54,56} is a semisynthetic bisindole compound formally derived from anhydrovinblastine by C-ring contraction.^{56,57} As a consequence, the vinorelbine indole *upper-half* embodies a 5-nor cleavamine skeleton, containing an eight-membered ring included in a 1-azabicyclo[5.3.1]undecane bridged system.

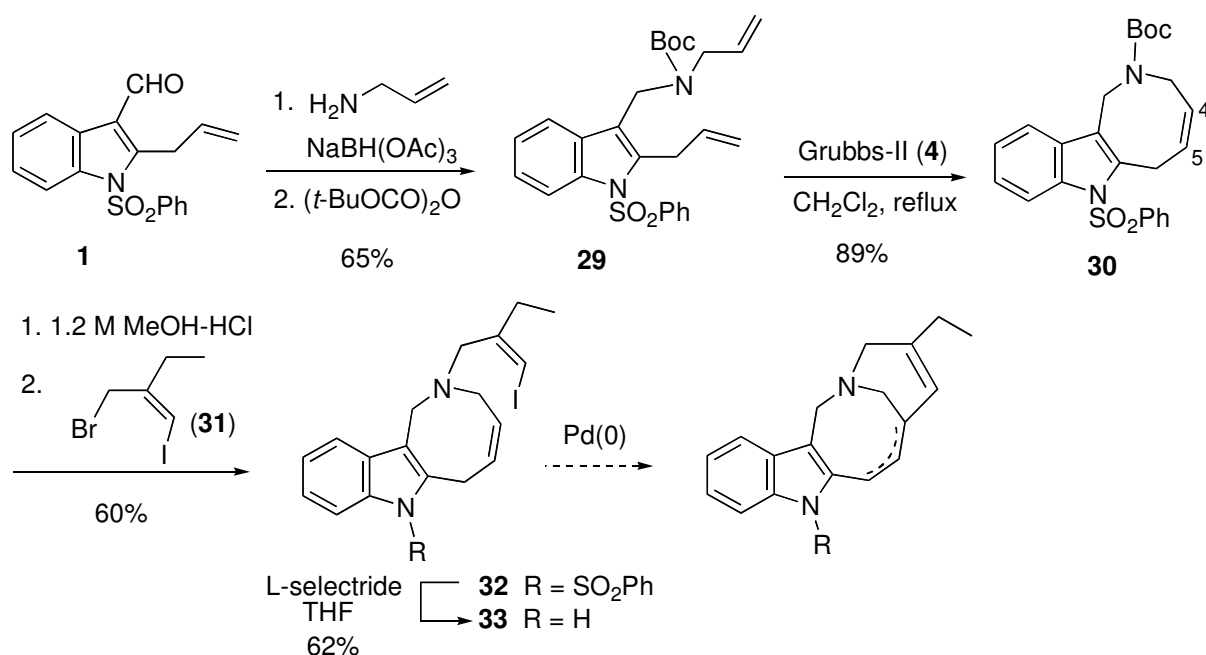
Our synthetic approach to the bridged arrangements of cleavamines and their 5-nor derivatives relied on a RCM to build up the tricyclic ABC substructures containing the central medium-sized ring. The carbon skeleton would then be completed by stitching a 2-ethylpropeno unit between the aliphatic nitrogen and the appropriate alkene, using a challenging *endocyclic* vinyl halide Heck cyclization in the last step (Scheme 15).⁵⁸



Scheme 15

4.1. Construction of the 5-nor cleavamine skeleton

Access to the 1-azabicyclo[5.3.1]undecane bridged system, which defines the indole *upper-half* of vinorelbine, first required the synthesis of azocino[4,3-*b*]indole **30**⁵⁹ (Scheme 16), with the 4,5-double bond functionality needed for the subsequent Heck coupling.

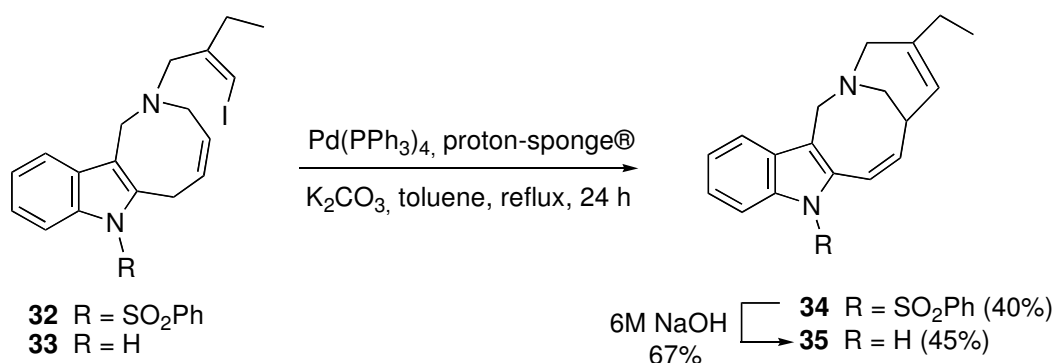


Scheme 16

With this aim, 2-allyl-3-indolecarbaldehyde **1** was subjected to reductive amination with allylamine and the resulting secondary amine was protected with a Boc group. The resulting carbamate **29** smoothly underwent RCM in the presence of the second-generation Grubbs catalyst (**4**) to give azocinoindole **30** in 58% overall yield. En route to the Heck cyclization substrates, the *N*-Boc group of **30** was cleaved under a mild acid protocol and the resulting secondary amine was subsequently alkylated with allylic bromide **31** to give **32**, bearing the 3-iodo-3-propenyl chain that would serve for the piperidine ring closure. We also

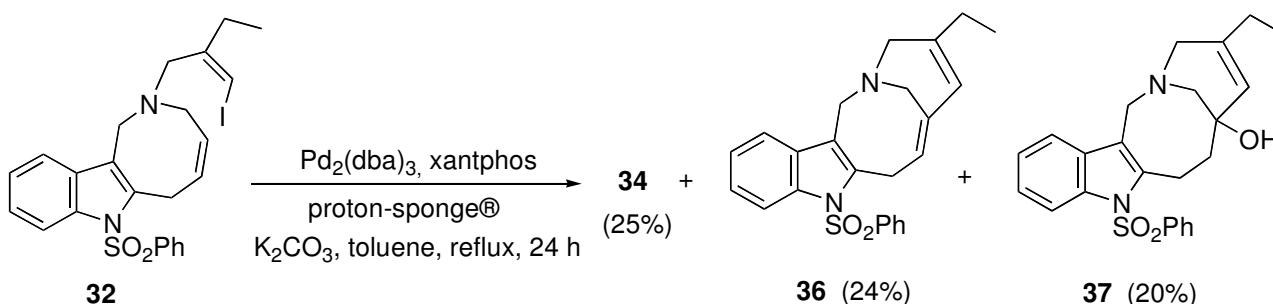
considered it would be interesting to prepare the respective indole-protected substrate **33**, which was achieved by treatment of **32** with L-selectride in refluxing THF (62% yield). This reductive protocol was chosen to minimize both the previsible isomerization of the double bond to its indole-conjugated counterpart (see the above synthesis of apparicine) and elimination of the haloalkenyl chain under basic conditions.

We then undertook an exhaustive investigation into the Heck reaction using tetracycle **32** as the main substrate. Having examined a variety of conditions to promote the closure of the 1-azabicyclo[5.3.1]undecane system, we found that tetracycle **34**, arising from the expected *exo* cyclization with generation of a disubstituted indole-conjugated double bond, could be isolated in a moderate 40% yield using Pd(PPh₃)₄ as the precatalyst and proton-sponge® as the additive. This protocol was also found to be convenient for promoting cyclization of substrate **33**, which cleanly led to tetracycle **35** in 45% yield (Scheme 17). This compound could be alternatively obtained in 67% yield by removal of the *N*-phenylsulfonyl group of tetracycle **34** under standard basic conditions. It is worth mentioning that all attempts to selectively remove the disubstituted double bond of **34** by catalytic hydrogenation met with failure. However, from the synthetic point of view this double bond could prove useful for the synthesis of “dimeric” vinorelbine.



Scheme 17

On the other hand, the cyclization of vinyl iodide **32** followed a different course in the presence of Pd₂(dba)₃ and the bidentate ligand xantphos, as a nearly equimolecular mixture of **34**, its double bond isomer **36**, and carbinol **37** was obtained in a higher cyclization yield (70%, Scheme 18). Carbinol **37** is produced by hydration of the strained bridgehead double bond of **36**, which is probably the result of a direct β-hydride elimination from the initially formed σ-alkyl palladium intermediate rather than an isomerization process from **34**. The different regioselectivity in the β-elimination step in the presence of xantphos proved to be crucial for our successful Heck cyclization in the higher homologous cleavamine series (see below).

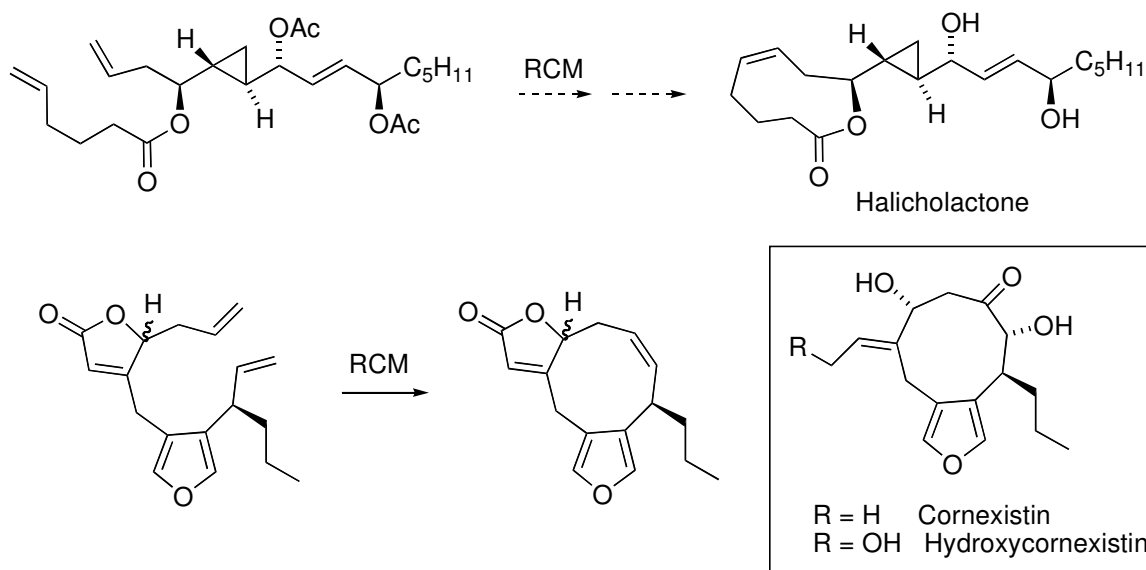


Scheme 18

4.2. Total synthesis of cleavamines

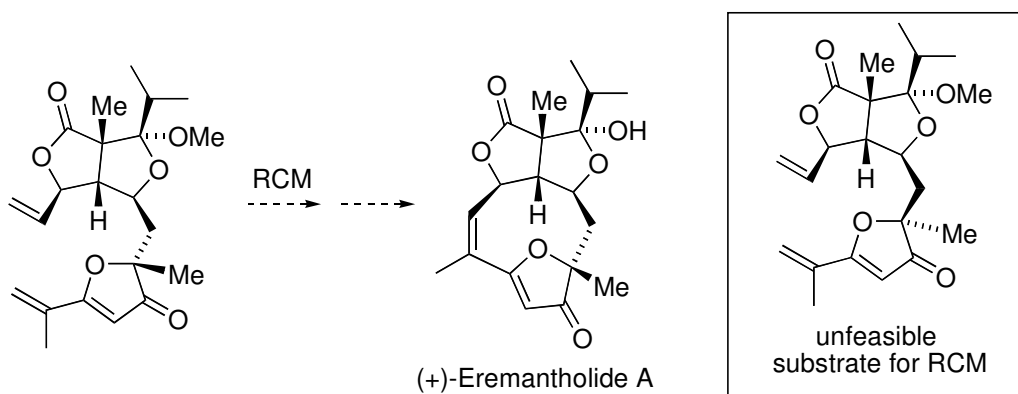
As stated before, the application of the RCM-Heck cyclization strategy to assemble the bridged tetracyclic framework of the cleavamine alkaloids would start with the construction of a suitable indolo-fused nine-membered ring and end with the formation of the 3-ethylpiperidine ring (Scheme 15, $n=2$).^{58,60}

RCM is far less frequently used to form nine-membered rings than their smaller-sized counterparts, most reported successful cyclizations benefiting from some conformational constraints. Particularly noteworthy in this area are the syntheses of halicholactone⁶¹ and cornexistins,⁶² which both involve the generation of a disubstituted double bond embedded in the formed ring (Scheme 19).



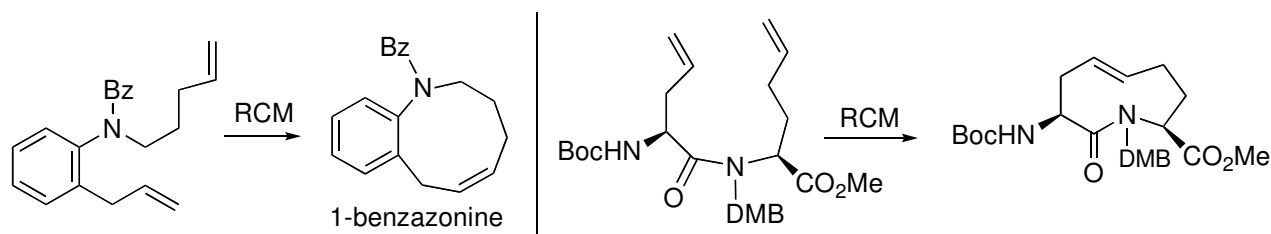
Scheme 19

RCM leading to cyclononenes with formation of a trisubstituted double bond is also possible, as illustrated by the synthesis of (+)-eremantholide A depicted in Scheme 20.⁶³ Again, the feasibility of the process depended on subtle structural factors: only one of the available epimeric substrates underwent cyclization.⁶⁴



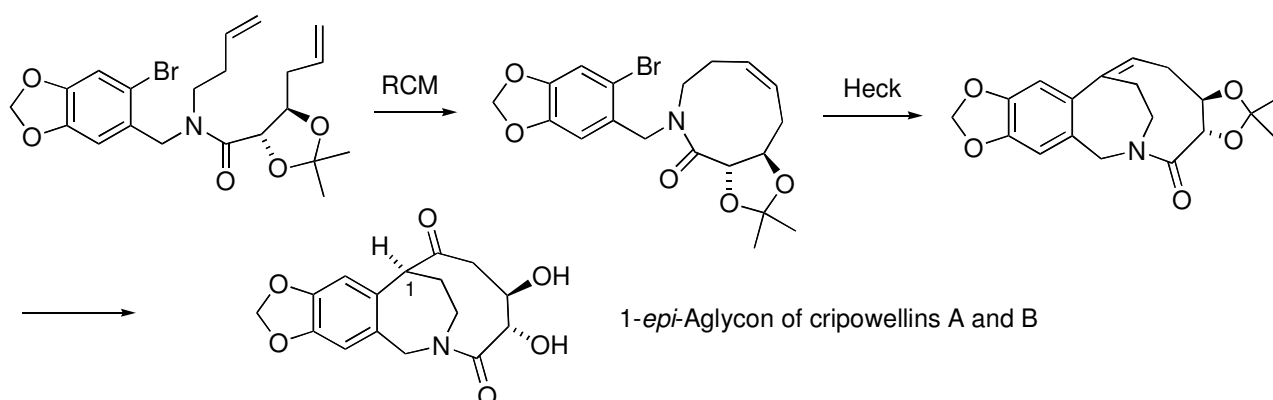
Scheme 20

Access to the nitrogen-containing azonine ring⁶⁵ by RCM is exemplified in Scheme 21 by the closure of a 1-benzazonine ring⁶⁶ and a dipeptide lactam incorporating an *E*-configured double bond.⁶⁷

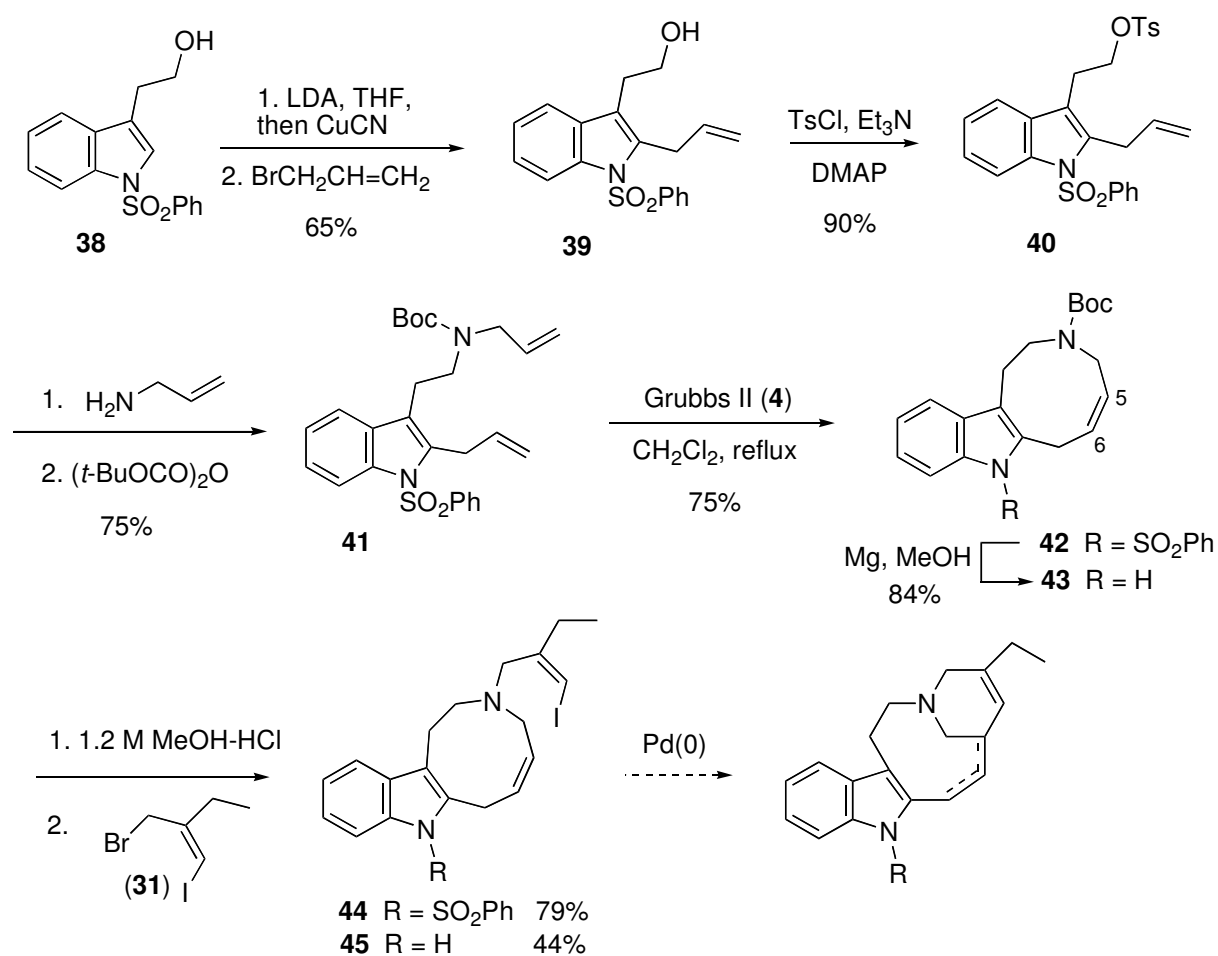


Scheme 21

It is worth mentioning that the synthesis of a nine-membered lactam by RCM, followed by an aryl halide Heck cyclization upon the resulting disubstituted *Z*-configured double bond, has been used to build up the 1-azabicyclo[5.3.2]dodecane core of the 1-*epi*-aglycon of cripowellins A and B (Scheme 22).²¹



Scheme 22



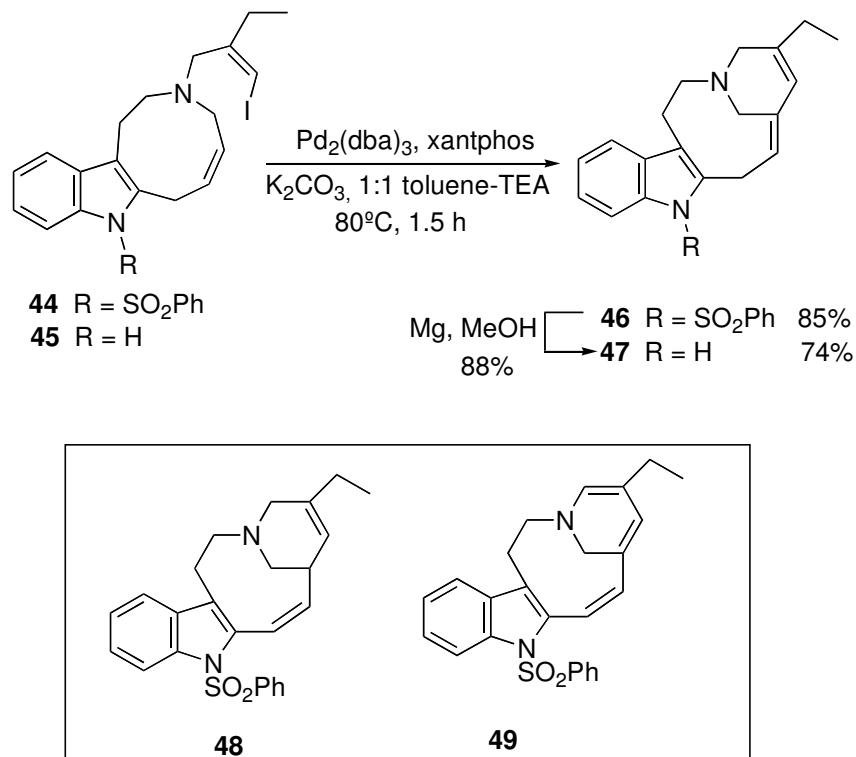
Scheme 23

With this background, we undertook the assembly of the 1-azabicyclo[6.3.1]dodecane bridged framework of cleavamines, first tacking the RCM synthesis of azonino[5,4-*b*]indole **42**,⁶⁸ which incorporates a double bond at the 5,6 position (Scheme 23).

Diene **41** was prepared in 44% overall yield from tryptophol **38** by successively installing the required alkenyl appendages. Thus, exposure to excess LDA and CuCN followed by reaction of the intermediate organocopper with allyl bromide led to 2-allylindole **39**, which was uneventfully converted into diene **41** by treatment of the corresponding tosylate **40** with allylamine and subsequent protection of the resulting secondary amine. Satisfactorily, RCM of diene **41** proceeded smoothly in the presence of the second-generation Grubbs catalyst (**4**) in refluxing CH₂Cl₂. The reaction was completed in a short reaction time (2.5 hours) and azoninoindole **42**, with the *Z* configuration of the double bond, was isolated in 75% yield.

Our next task was to install the haloalkenyl chain required for the subsequent Heck reaction. To this end, the *N*-Boc group of **42** was removed under the usual acid protocol and the resulting secondary amine was alkylated with bromide **31** to give the tertiary amine **44** in a higher (79%) overall yield than in the above series. In turn, the respective indole-protected amine **45** was prepared from carbamate **42** by reductive removal of the phenylsulfonyl group (84%) and derivatization of the aliphatic nitrogen of the resulting compound **43** (44%).

The ready availability of substrate **44** allowed us to examine in detail the intramolecular coupling of the vinyl iodide and the disubstituted double bond included in the azonine ring to complete the bridged tetracyclic framework of cleavamines (Scheme 24). In fact, we expected tetracycle **48** to be preferentially formed as a result of an *exo* cyclization and the subsequent generation of an indole-conjugated double bond.



Scheme 24

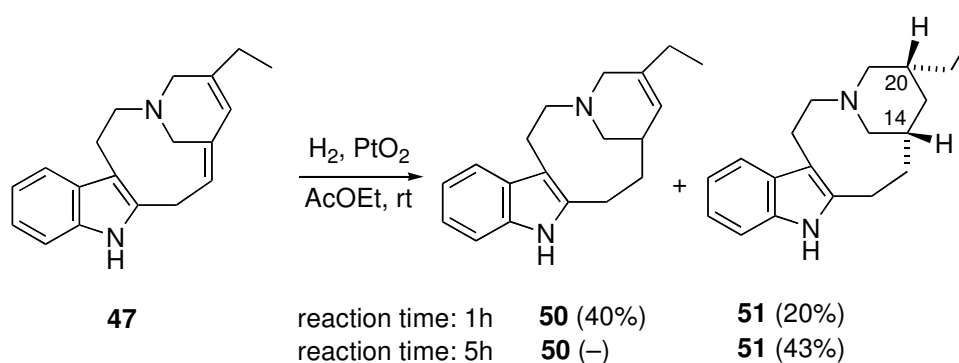
However, under a variety of conditions, including different palladium precatalysts [Pd(PPh₃)₄, Pd₂dba₃], ligands (BINAP, dppe) and additives (proton-sponge®, Et₃N, diisopropylethylamine) in refluxing toluene, we only obtained mixtures of the starting material and variable amounts of tetracycle **49**, which

presumably arose from **48** by oxidation. Although we were able to isolate **48** using shorter reaction times or lower temperatures, it proved to be highly unstable, slowly being converted into **49** under the extractive workup or column chromatography.

We then examined the Heck cyclization in the presence of the phosphine xantphos, expecting a different regioselectivity in the elimination step, as in our previous synthesis of 5-nor cleavamines, which would avoid the undesirable formation of **49**. Fortunately, the outcome of the cyclization changed completely on exposure of vinyl iodide **44** to Pd₂dba₃/xantphos and K₂CO₃ in toluene–Et₃N at 80 °C within a short reaction time (1.5 hours). Tetracycle **46**, embodying a trisubstituted bridgehead double bond, was isolated in a yield as high as 85%. In contrast to its regioisomer **48**, tetracycle **46** showed no tendency to undergo oxidation.

On the other hand, the application of this cyclization protocol to the indole-protected substrate **45** led to tetracycle **47** in a slightly lower yield (74%). As this key cleavamine precursor could be also obtained in 88% yield by desulfonylation of tetracycle **46** under reductive conditions, the synthetic route from **42** was clearly more efficient by way of intermediates **44**→**46** (59% overall yield) than through intermediates **43**→**45** (27% overall yield).

With tetracycle **47** in hand, all that remained to conclude the synthesis of (±)-cleavamine (**50**) was the selective reduction of the bridgehead double bond, which was achieved in 40% yield by catalytic hydrogenation under PtO₂ for a short reaction time (Scheme 25). The corresponding 3,5-*cis*-disubstituted piperidine **51**, *i.e.*, the racemic form of the alkaloid (+)-20*R*-dihydrocleavamine, was also formed in minor amounts. As expected, longer reaction times (5 hours) gave **51** as the only product. Synthetic cleavamines displayed spectroscopic data identical to those reported for the natural products.



Scheme 25

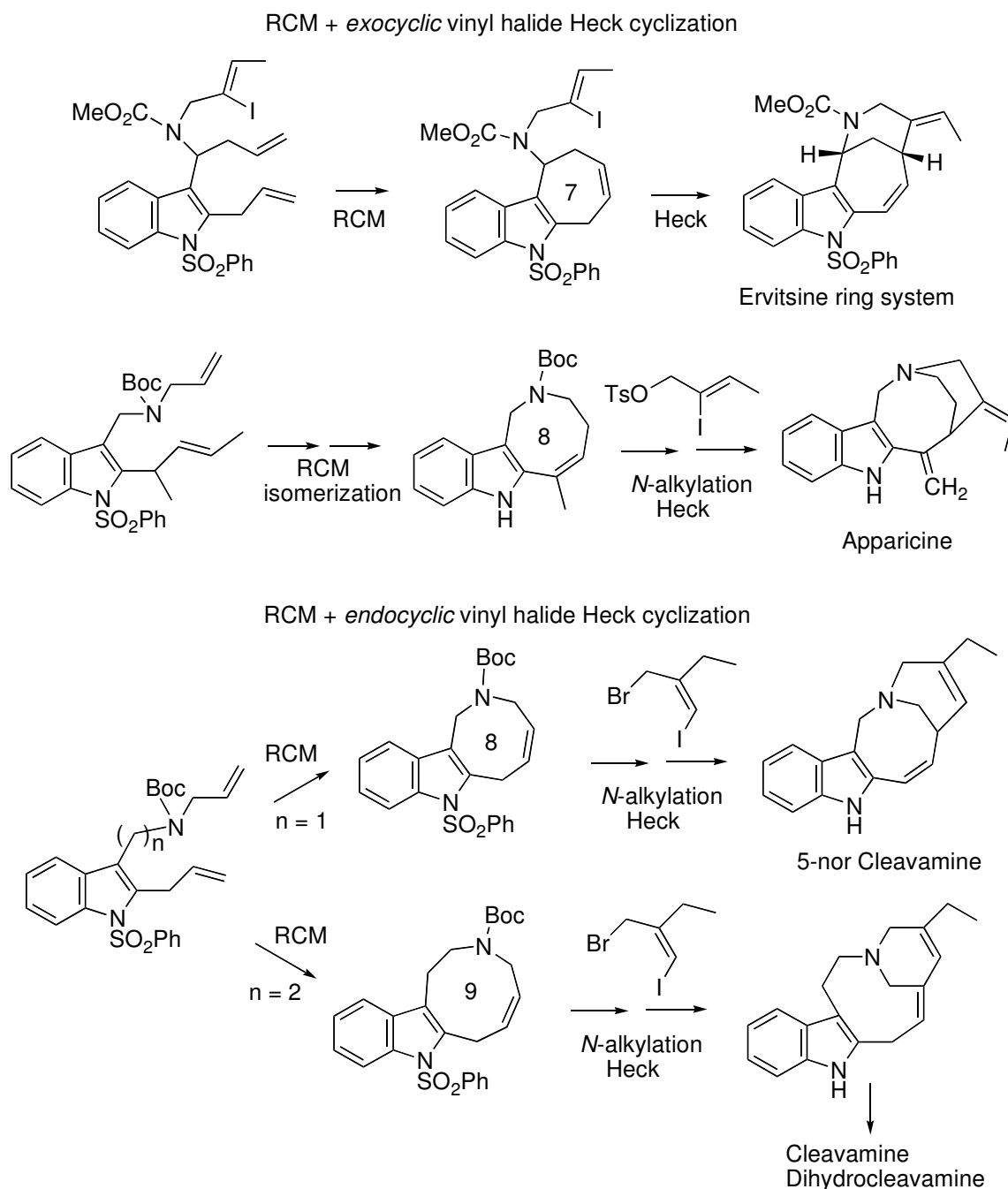
5. Conclusion

The sequential use of indole-templated RCM and intramolecular vinyl halide Heck reactions has demonstrated to be an innovative and effective strategy for rapidly assembling four types of indolo-fused bridged frameworks: 2-azabicyclo[4.3.1]decane, 1-azabicyclo[4.2.2]decane, 1-azabicyclo[5.3.1]undecane and 1-azabicyclo[6.3.1]dodecane. By appropriate selection of precursors and intermediates, this approach has enabled concise total syntheses of the indole alkaloids apparicine and cleavamines as well as providing easy access to ervitsine and 5-nor cleavamine tetracycles, which illustrates its utility for the construction of complex molecules. The synthetic routes are summarized in Scheme 26.

Whereas the RCM step smoothly generates the carbocyclic seven-membered ring of ervitsine, the eight-membered azocine rings of apparicine and 5-nor cleavamine and the nine-membered azonine ring of

cleavamines, the strained carbon skeleton of the alkaloids is completed by the subsequent *exocyclic* or *endocyclic* vinyl halide Heck cyclization upon the alkene moiety left by the metathetic ring closure, directly or after an isomerization step (apparicine). Worthy of mention is the high yield of the Heck cyclization step in the cleavamine series.

The expansion of the RCM-Heck double annulation to the straightforward construction of other bridged indole alkaloids such as pericine (subincanadine E) or quebrachamine (Figure 1) is currently under investigation in our laboratory.



Acknowledgments

The author would like to thank all past and present co-workers for their enthusiastic dedication. Financial support by the Spanish Ministry of Economy and Competitiveness (MINECO), through projects CTQ2006-00500/BQU, CTQ2009-07175 and CTQ2012-31391 is gratefully acknowledged.

References

1. (a) Sundberg, R. J. *Indoles*; Academic Press: New York, 1996. (b) Joule, J. A. In *Science of Synthesis (Houben-Weyl, Methods of Molecular Transformations)*; Georg Thieme Verlag: Stuttgart, 2000; Vol. 10, p. 361.
2. (a) Sundberg, R. J. In *Comprehensive Heterocyclic Chemistry*; Katritzky, A. R.; Rees, C. W., Eds.; Pergamon: Oxford, U.K., 1984; Vol. 4, p. 313. (b) Cacchi, S.; Fabrizi, G. *Chem. Rev.* **2011**, *111*, PR215.
3. Ishikura, M.; Abe, T.; Choshi, T.; Hibino, S. *Nat. Prod. Rep.* **2013**, *30*, 694, and previous reviews in this series.
4. For reviews, see: (a) Bosch, J.; Bannasar, M.-L. *Synlett* **1995**, 587. (b) Bosch, J.; Bannasar, M.-L.; Amat, M. *Pure Appl. Chem.* **1996**, *68*, 557.
5. (a) Bannasar, M.-L.; Vidal, B.; Bosch, J. *J. Org. Chem.* **1997**, *62*, 3597. (b) Bannasar, M.-L.; Vidal, B.; Kumar, R.; Lázaro, A.; Bosch, J. *Eur. J. Org. Chem.* **2000**, 3919.
6. Bannasar, M.-L.; Jiménez, J.-M.; Vidal, B.; Sufi, B. A.; Bosch, J. *J. Org. Chem.* **1999**, *64*, 9605.
7. Bannasar, M.-L.; Zulaica, E.; Juan, C.; Alonso, Y.; Bosch, J. *J. Org. Chem.* **2002**, *67*, 7465.
8. For a review, see: Bannasar, M.-L.; Roca, T. In *Progress in Heterocyclic Chemistry*; Gribble, G. W.; Joule, J. A., Eds.; Elsevier: Amsterdam, The Netherlands, 2008; Vol. 20, Chapt. 1.
9. Bannasar, M.-L.; Roca, T.; Ferrando, F. *J. Org. Chem.* **2005**, *70*, 9077.
10. Bannasar, M.-L.; Roca, T.; Ferrando, F. *Org. Lett.* **2006**, *8*, 561.
11. Bannasar, M.-L.; Roca, T.; García-Díaz, D. *J. Org. Chem.* **2008**, *73*, 9033.
12. For general reviews, see: (a) *Handbook of Metathesis*; Grubbs, R. H., Ed.; Wiley-VCH: Weinheim, 2003; Vol. 2. (b) Deiters, A.; Martin, S. F. *Chem. Rev.* **2004**, *104*, 2199. (c) Nicolau, K. C.; Bulger, P. C.; Sarlah, D. *Angew. Chem. Int. Ed.* **2005**, *44*, 4490. (d) Prunet, J. *Eur. J. Org. Chem.* **2011**, 3634.
13. For general reviews, see: (a) Bräse, S.; de Meijere, A. In *Metal-Catalyzed Cross-Coupling Reactions*; de Meijere, A.; Diederich, F., Eds.; Wiley-WCH: New York, 2004; p. 217. (b) Zeni, G.; Larock, R. C. *Chem. Rev.* **2006**, *106*, 4644.
14. See, for instance: (a) Maier, M. E. *Angew. Chem. Int. Ed.* **2000**, *39*, 2073. (b) Yet, L. *Chem. Rev.* **2000**, *100*, 2963. (c) Michaut, A.; Rodriguez, J. *Angew. Chem. Int. Ed.* **2006**, *45*, 5740. (d) Blanchard, N.; Eustache, J. In *Metathesis in Natural Product Synthesis: Strategies, Substrates and Catalysts*; Cossy, J.; Arseniyadis, S.; Meyer, C., Eds.; Wiley-VCH: Weinheim, 2010; p. 1. (e) Tori, M.; Mizutani, R. *Molecules* **2010**, *15*, 4242.
15. (a) Rawal, V. H.; Michoud, C. *Tetrahedron Lett.* **1991**, *32*, 1695. (b) Rawal, V. H.; Michoud, C.; Monestel, R. F. *J. Am. Chem. Soc.* **1993**, *115*, 3030. (c) Martin, D. B. C.; Vanderwal, C. D. *J. Am. Chem. Soc.* **2009**, *131*, 3472.
16. (a) Rawal, V. H.; Iwasa, S. *J. Org. Chem.* **1994**, *59*, 2685. (b) Solé, D.; Bonjoch, J.; García-Rubio, S.; Peidró, E.; Bosch, J. *Chem.–Eur. J.* **2000**, *6*, 655. (c) Eichberg, M. J.; Dorta, R. L.; Grotjahn, D. B.; Lamottke, K.; Schmidt, M.; Vollhardt, K. P. C. *J. Am. Chem. Soc.* **2001**, *123*, 9324. (d) Mori, M.; Nakanishi, M.; Kahishima, D.; Sato, Y. *J. Am. Chem. Soc.* **2003**, *125*, 9801. (e) Martin, D. B. C.; Nguyen, L. Q.; Vanderwal, C. D. *J. Org. Chem.* **2012**, *77*, 17.
17. Dounay, A. B.; Humphreys, P. G.; Overman, L. E.; Wroblewski, A. D. *J. Am. Chem. Soc.* **2008**, *130*, 5368.
18. Zu, L.; Boal, B. W.; Garg, N. K. *J. Am. Chem. Soc.* **2011**, *133*, 8877.
19. Birman, V. B.; Rawal, V. H. *J. Org. Chem.* **1998**, *63*, 9146.
20. For example, see: (a) Grigg, R.; Sridharan, V.; York, M. *Tetrahedron Lett.* **1998**, *39*, 4139. (b) Ribelin, T. P.; Judd, A. S.; Akritopoulou-Zanze, I.; Henry, R. F.; Cross, J. L.; Whittern, D. N.; Djuric, S. W. *Org. Lett.* **2007**, *9*, 5119.
21. (a) Enders, D.; Lenzen, A.; Raabe, G. *Angew. Chem. Int. Ed.* **2005**, *44*, 3766. (b) Enders, D.; Lenzen, A.; Backes, M.; Janeck, C.; Catlin, K.; Lannou, M.-I.; Runsink, J.; Raabe, G. *J. Org. Chem.* **2005**, *70*, 10538.
22. Joule, J. A. In *Indoles, The Monoterpenoid Indole Alkaloids*; Saxton, J. E., Ed.; Wiley: New York, 1983; Vol. 25, p. 232.
23. Andriantsiferana, M.; Besselièvre, R.; Riche, C.; Husson, H.-P. *Tetrahedron Lett.* **1977**, 2587.

24. (a) Grierson, D. S.; Harris, M.; Husson, H.-P. *Tetrahedron* **1983**, *39*, 3683. (b) Bosch, J.; Rubiralta, M.; Domingo, A.; Bolós, J.; Linares, A.; Minguillón, C.; Amat, M.; Bonjoch, J. *J. Org. Chem.* **1985**, *50*, 1516. (c) Bosch, J.; Rubiralta, M.; Bolós, J. *Tetrahedron* **1987**, *43*, 391. (d) Salas, M.; Joule, J. A. *J. Chem. Res. (M)* **1990**, 664. (e) Rubiralta, M.; Marco, M.-P.; Bolós, J.; Trapé, J. *Tetrahedron* **1991**, *47*, 5585.
25. For a more recent approach, see: Amat, M.; Checa, B.; Llor, N.; Pérez, M.; Bosch, J. *Eur. J. Org. Chem.* **2011**, 898.
26. (a) Bennasar, M.-L.; Vidal, B.; Bosch, J. *J. Am. Chem. Soc.* **1993**, *115*, 5340. (b) For the enantioselective version, see: Bennasar, M.-L.; Zulaica, E.; Alonso, Y.; Bosch, J. *Tetrahedron: Asymmetry* **2003**, *14*, 469.
27. (a) Bennasar, M.-L.; Zulaica, E.; Solé, D.; Alonso, S. *Synlett* **2008**, 667. (b) Bennasar, M.-L.; Zulaica, E.; Solé, D.; Alonso, S. *Tetrahedron* **2012**, *68*, 4641.
28. For a review on general strategies to access seven-membered carbocycles, see: Nguyen, T. V.; Hartmann, J. M.; Enders, D. *Synthesis* **2013**, *45*, 845.
29. For instance, see: (a) Ban, Y.; Yoshida, K.; Goto, J.; Oishi, T.; Takeda, E. *Tetrahedron* **1983**, *39*, 3657. (b) Gràcia, J.; Casamitjana, N.; Bonjoch, J.; Bosch, J. *J. Org. Chem.* **1994**, *59*, 3939. (c) Saito, M.; Kawamura, M.; Hiroya, K.; Ogasawara, K. *J. Chem. Commun.* **1997**, 765.
30. Rutherford, J. L.; Rainka, M. P.; Buchwald, S. L. *J. Am. Chem. Soc.* **2002**, *124*, 15618.
31. See also: (a) Solé, D.; Urbaneja, X.; Bonjoch, J. *Tetrahedron Lett.* **2004**, *45*, 3131. (b) Solé, D.; Urbaneja, X.; Bonjoch, J. *Adv. Synth. Catal.* **2004**, *346*, 1646.
32. Gilbert, B.; Duarte, A. P.; Nakagawa, Y.; Joule, J. A.; Flores, S. E.; Brissolèse, J. A.; Campello, J.; Carrazzoni, E. P.; Owellen, R. J.; Blossey, E. C.; Brown, K. S., Jr.; Djerassi, C. *Tetrahedron* **1965**, *21*, 1141.
33. Joule, J. A.; Monteiro, H.; Durham, L. J.; Gilbert, B.; Djerassi, C. *J. Chem. Soc.* **1965**, 4773.
34. For a review, see: Alvarez, M.; Joule, J. A. In *The Alkaloids*; Cordell, G. A., Ed.; Academic Press: New York, 2001; Vol. 57, Chapt. 4.
35. Ahond, A.; Cavé, A.; Kan-Fan, C.; Langlois, Y.; Potier, P. *J. Chem. Soc., Chem. Commun.* **1970**, 517.
36. (a) Bennasar, M.-L.; Zulaica, E.; Solé, D.; Alonso, S. *Chem. Commun.* **2009**, 3372. (b) Bennasar, M.-L.; Zulaica, E.; Solé, D.; Roca, T.; García-Díaz, D.; Alonso, S. *J. Org. Chem.* **2009**, *74*, 8359.
37. (a) Scopes, D. I. C.; Allen, M. S.; Hignett, G. J.; Wilson, N. D. V.; Harris, M.; Joule, J. A. *J. Chem. Soc., Perkin Trans. 1* **1977**, 2376. (b) Joule, J. A.; Allen, M. S.; Bishop, D. I.; Harris, M.; Hignett, G. J.; Scopes, D. I. C.; Wilson, N. D. V. *Indole and Biogenetically Related Alkaloids*; Phillipson, J. D.; Zenk, M. H., Eds.; Academic Press: London, 1980; p. 229.
38. (a) Scott, A. I.; Yeh, C.-L.; Greenslade, D. *J. Chem. Soc., Chem. Commun.* **1978**, 947. (b) Lim, K.-H.; Low, Y.-Y.; Kam, T.-S. *Tetrahedron Lett.* **2006**, *47*, 5037.
39. For more recent syntheses of apparicine alkaloids, see: (a) Tarselli, M. A.; Raehal, K. M.; Brasher, A. K.; Streicher, J. M.; Groer, C. E.; Cameron, M. D.; Bohn, L. M.; Micalizio, G. C. *Nat. Chem.* **2011**, *13*, 449. (b) Noguchi, Y.; Hirose, T.; Furuya, Y.; Ishiyama, A.; Otoguro, K.; Omura, S.; Sunazuka, T. *Tetrahedron Lett.* **2012**, *53*, 1802.
40. For a different previous approach to apparicine ABC substructures, see: (a) Street, J. D.; Harris, M.; Bishop, D. I.; Heatley, F.; Beddoes, R. L.; Mills, O. S.; Joule, J. A. *J. Chem. Soc., Perkin Trans. 1* **1987**, 1599. (b) See also reference 37b.
41. For instance, see: (a) Ferrer, C.; Amijs, C. H. M.; Echavarren, A. M. *Chem. Eur. J.* **2007**, *13*, 1358. (b) Donets, P. A.; Van Hecke, K.; Van Meervelt, L.; Van der Eycken, E. V. *Org. Lett.* **2009**, *11*, 3618. (c) Zhu, C.; Zhang, X.; Lian, X.; Ma, S. *Angew. Chem. Int. Ed.* **2012**, *51*, 1.
42. Orr, S. T. M.; Tian, J.; Niggemann, M.; Martin, S. F. *Org. Lett.* **2011**, *13*, 5104.
43. For examples of successful RCM producing a trisubstituted double bond included in a cyclooctane ring, see: (a) Codesido, E. M.; Castedo, L.; Granja, J. R. *Org. Lett.* **2001**, *3*, 1483. (b) Nickel, A. Maruyama, T.; Tang, H.; Murphy, P. D.; Greene, B.; Yusuff, N.; Wood, J. L. *J. Am. Chem. Soc.* **2004**, *126*, 16300.
44. (a) Michalak, K.; Michalak, M.; Wicha, J. *Tetrahedron Lett.* **2005**, *46*, 1149. (b) Michalak, K.; Michalak, M.; Wicha, J. *Molecules* **2005**, *10*, 1084.

45. (a) Codesido, E. M.; Rodríguez, J. R.; Castedo, L.; Granja, J. R. *Org. Lett.* **2002**, *4*, 1651. (b) García-Fandiño, R.; Aldegunde, M. J.; Codesido, E. M.; Castedo, L.; Granja, J. R. *J. Org. Chem.* **2005**, *70*, 8281.
46. Bennasar, M.-L.; Zulaica, E.; Alonso, S. *Tetrahedron Lett.* **2005**, *46*, 7881.
47. The synthesis of a closely related azocino[4,3-*b*]indole by RCM appeared later in the literature: Zaimoku, H.; Taniguchi, T.; Ishibashi, H. *Org. Lett.* **2012**, *14*, 1656.
48. (a) Rawal, V. H.; Michoud, C. *J. Org. Chem.* **1993**, *58*, 5583. (b) Feutren, S.; McAlonan, H.; Montgomery, D.; Stevenson, P. J. *J. Chem. Soc., Perkin Trans 1* **2000**, 1129.
49. Owczarczyk, Z.; Lamaty, F.; Vawter, E. J.; Negishi, E. *J. Am. Chem. Soc.* **1992**, *114*, 10091.
50. Bennasar, M.-L.; Roca, T.; García-Díaz, D. *J. Org. Chem.* **2007**, *72*, 4562.
51. For an alternative synthesis of amine **24**, ultimately resulting in a formal synthesis of apparicine, see: Kettle, J. G.; Roberts, D.; Joule, J. A. *Heterocycles* **2010**, *82*, 349.
52. For reviews, see: (a) Cordell, G. A. In *Indoles, The Monoterpenoid Indole Alkaloids*; Saxton, J. E., Ed.; Wiley: New York, 1983; Vol. 25, Part 4, Chapt. 10. (b) Saxton, J. E. In *Monoterpenoid Indole Alkaloids*; Saxton, J. E., Ed.; Wiley: Chichester, 1994; Supplement to Vol. 25, Part 4, Chapt. 10.
53. Sundberg, R. J.; Smith, S. Q. In *The Alkaloids*; Cordell, G. A., Ed.; Academic Press: Amsterdam, 2002; Vol. 59, Chapt. 2.
54. *The Alkaloids*; Brossi, A.; Suffness, M., Eds; Academic Press: San Diego, 1990; Vol. 37.
55. Fahy, J. *Curr. Pharm. Design.* **2001**, *7*, 1181.
56. Mangeney, P.; Andriamialisoa, R. Z.; Lallemand, J.-Y.; Langlois, N.; Langlois, Y.; Potier, P. *Tetrahedron* **1979**, *35*, 2175.
57. In fact, vinorelbine is prepared by ring contraction of anhydrovinblastine: (a) Mangeney, P.; Andriamialisoa, R. Z.; Langlois, N.; Langlois, Y.; Potier, P. *J. Org. Chem.* **1979**, *44*, 3765. (b) Andriamialisoa, R. Z.; Langlois, N.; Langlois, Y.; Potier, P. *Tetrahedron* **1980**, *36*, 3053. See also: (c) Magnus, P.; Thurston, L. S.; *J. Org. Chem.* **1991**, *56*, 1166.
58. Bennasar, M.-L.; Solé, D.; Zulaica, E.; Alonso, S. *Tetrahedron* **2013**, *69*, 2534.
59. Bennasar, M.-L.; Zulaica, E.; Solé, D.; Alonso, S. *Tetrahedron* **2007**, *63*, 861.
60. Bennasar, M.-L.; Solé, D.; Zulaica, E.; Alonso, S. *Org. Lett.* **2011**, *13*, 2042.
61. (a) Baba, Y.; Saha, G.; Nakao, S.; Iwata, C.; Tanaka, T.; Ibuka, T.; Ohishi, H.; Takemoto, Y. *J. Org. Chem.* **2001**, *66*, 81. (b) Takahashi, T.; Watanabe, H.; Kitahara, T. *Heterocycles* **2002**, *58*, 99.
62. (a) Clark, J. S.; Marlin, F.; Nay, B.; Wilson, C. *Org. Lett.* **2003**, *5*, 89. (b) Clark, J. S.; Northall, J. M.; Marlin, F.; Nay, B.; Wilson, C.; Blake, A. J.; Waring, M. J. *Org. Biomol. Chem.* **2008**, *6*, 4012.
63. Li, Y.; Hale, K. *J. Org. Lett.* **2007**, *9*, 1267.
64. For an unsuccessful attempt to produce a trisubstituted double bond included in a cyclononane ring, see: Paquette, L. A.; Dong, S.; Parker, G. D. *J. Org. Chem.* **2007**, *72*, 7135.
65. For a review on the synthesis of azonine derivatives, see: Fadda, A. A.; Afsah, E. M.; Bondock, S.; Hammouda, M. M. *Tetrahedron* **2012**, *68*, 2081.
66. Qadir, M.; Cobb, J.; Shelldrake, P. W.; Whittall, N.; White, A. J. P.; Hii, K. K.; Horton, P. N.; Hursthouse, M. B. *J. Org. Chem.* **2005**, *70*, 1552.
67. Kaul, R.; Surprenant, S.; Lubell, W. D. *J. Org. Chem.* **2005**, *70*, 3838.
68. For previous syntheses of azonino[5,4-*b*]indoles, see: (a) Kuehne, M. E.; Matson, P. A.; Bornmann, W. G. *J. Org. Chem.* **1991**, *56*, 513. (b) Bornmann, W. G.; Kuehne, M. E. *J. Org. Chem.* **1992**, *57*, 1752. (c) Fokas, D.; Hamzik, J. A. *Synlett* **2009**, 581. (d) Hoefgen, B.; Decker, M.; Mohr, P.; Schramm, A. M.; Rostom, S. A. F.; El-Subbagh, H.; Schweikert, P. M.; Rudolf, D. R.; Kassack, M. U. *Lehmann, J. J. Med. Chem.* **2006**, *49*, 760. (e) Fokas, D.; Kaselj, M.; Isome, Y.; Wang, Z. *ACS Comb. Sci.* **2013**, *15*, 49.

RECENT ADVANCES IN THE SYNTHESIS OF SELECTED INDOLIZIDINE AND QUINOLIZIDINE ALKALOIDS

Sunil V. Pansare* and Rakesh G. Thorat

Department of Chemistry, Memorial University, St. John's, Newfoundland, Canada A1B 3X7

(e-mail: spansare@mun.ca)

Abstract. Advances in synthetic methodology for the construction of indolizidine and quinolizidine ring systems, in the context of the total synthesis of selected alkaloids featuring these heterocyclic motifs, are reviewed.

Contents

1. Introduction
 2. Scope and organization of the review
 3. Synthetic strategies for selected indolizidine and quinolizidine alkaloids
 - 3.1. Ring formation *via* nucleophilic displacement or addition reactions
 - 3.1.1. Nitrogen-carbon cyclizations with preformed azacycles as starting materials
 - 3.1.2. Nitrogen-carbon cyclizations with open chain precursors
 - 3.1.3. Carbon-carbon cyclizations with preformed azacycles as starting materials
 - 3.1.4. Carbon-carbon cyclizations *via* azacyclic intermediates
 - 3.2. Syntheses employing ring closing metathesis as a key transformation
 - 3.3. Asymmetric cycloaddition-based strategies
 - 3.4. Iminium ion-based approaches
 - 3.5. Syntheses involving organocatalysis
 4. Closing remarks
- Acknowledgments
- References

1. Introduction

The indolizidine and quinolizidine alkaloids constitute a prominent group of biologically relevant structural motifs. These alkaloids exhibit a wide array of biological activities¹ and the synthesis of indolizidines and quinolizidines, naturally occurring or non-natural, is therefore an enterprise that has engaged organic chemists for decades. A large number of studies have addressed the synthesis of indolizidine and quinolizidine alkaloids and the field continues to be intensely investigated.² The structural diversity of these alkaloids arises from substitution of the heterocyclic core and the alkaloids selected for this review are shown in Figure 1.

2. Scope and organization of the review

The focus of this review is on methodologies reported during the period 2008–2013 and the majority of these reports have appeared after the most recent, general reviews on indolizidine and quinolizidine systems.^{2a,e} Strategies that have achieved a total synthesis, or have culminated in a formal synthesis, of a naturally occurring alkaloid or its closely related isomer are included in this review.

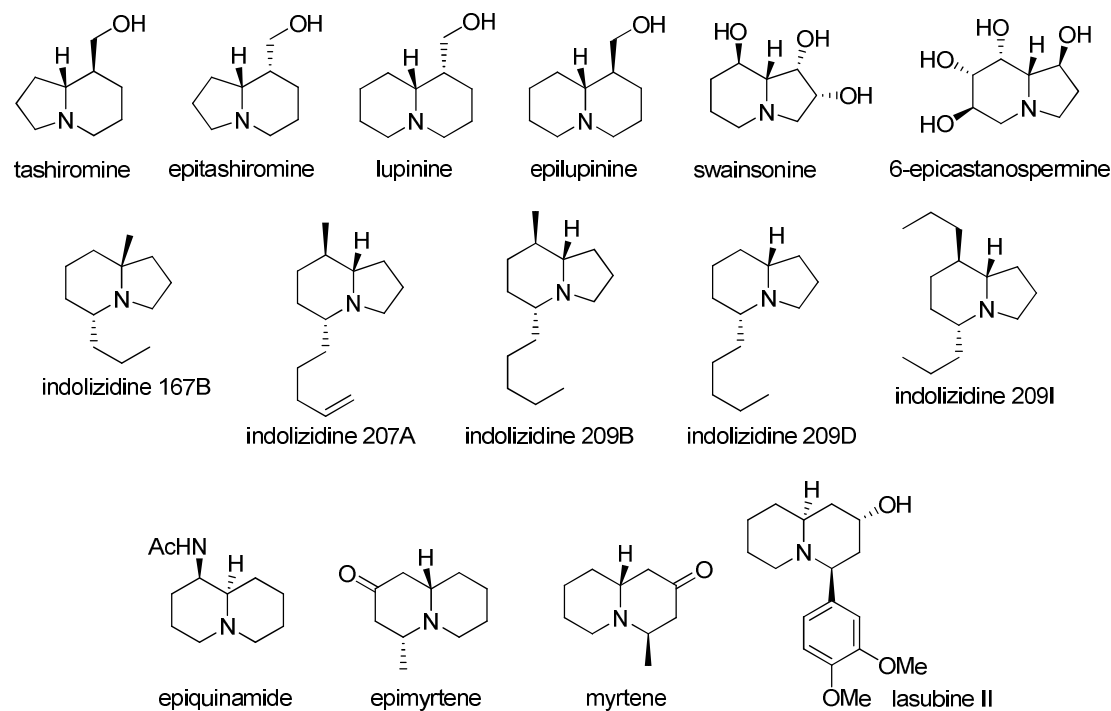


Figure 1. Indolizidine and quinolizidine alkaloids selected for this review (only relative stereochemistry is shown).

These include enantioselective syntheses as well as the preparation of racemates. General approaches to the title ring systems are not included. The organization of this review is based on synthetic strategies, irrespective of the alkaloid targets. Often, individual studies have addressed the total synthesis of selected alkaloids, but the synthetic strategy is, in principle, also applicable to analogs or congeners of the natural product. Hence, a synthetic tactic-based analysis is presented. Accordingly, the following strategies were identified and these will be elaborated upon in the ensuing sections: a) cyclization *via* nucleophilic displacement or electrophilic addition reactions; these include syntheses employing preformed azacycles and syntheses from acyclic precursors, b) syntheses employing ring closing metathesis, c) asymmetric cycloaddition-based strategies, d) iminium ion-based approaches and e) syntheses involving organocatalysis.

3. Synthetic strategies for selected indolizidine or quinolizidine alkaloids

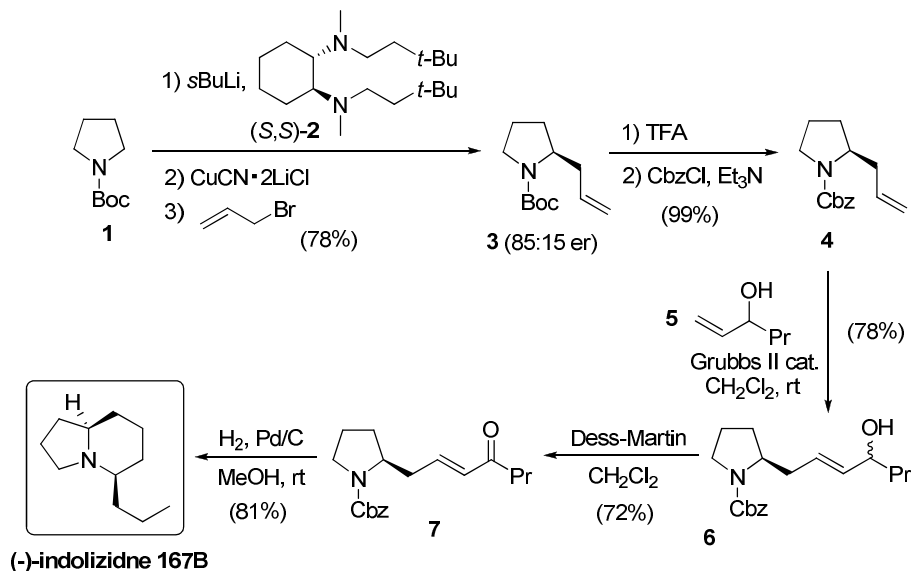
3.1. Ring formation *via* nucleophilic displacement or addition reactions

3.1.1. Nitrogen-carbon cyclizations with preformed azacycles as starting materials

Operationally, the inclusion of preformed heterocycles as building blocks for the synthesis of bicyclic alkaloid motifs offers obvious advantages and hence this approach has been quite popular. Recently, the O'Brien group reported³ a synthesis of (–)-indolizidine 167B that was based on the asymmetric functionalization of *N*-Boc pyrrolidine. The strategy is an extension of the (–)-sparteine-based asymmetric deprotonation methodology by Hoppe^{4a} and Beak.^{4b} The synthesis begins with the deprotonation of *N*-Boc pyrrolidine (**1**) with *s*-BuLi in the presence of the chiral diamine **2**, followed by cyanocuprate formation and alkylation with allylbromide. This provides the allyl pyrrolidine **3** with moderate enantioselectivity (85:15 er, Scheme 1). This step sets the ring-junction stereocentre in the target.

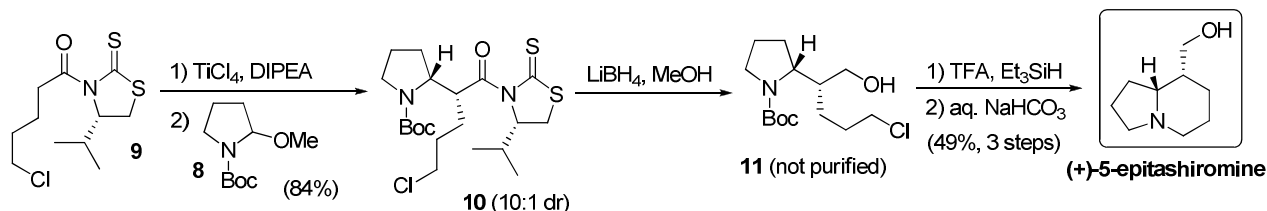
Subsequent transformations required a protecting group change in **3** which was achieved by removal of the Boc protecting group and re-protection with CbzCl to provide **4**. Cross metathesis of **4** with the allylic

alcohol **5** provided **6** which was oxidized to the key enone **7**, a known intermediate⁵ to the target. Conversion of **7** to (-)-indolizidine 167B was achieved in one step by hydrogenation which effected *N*-deprotection, reduction of the enone and subsequent reduction of the iminium ion produced by cyclization of the amino ketone. Despite the moderate enantioselectivity (85:15 er), this synthesis is attractive for its brevity and efficiency.



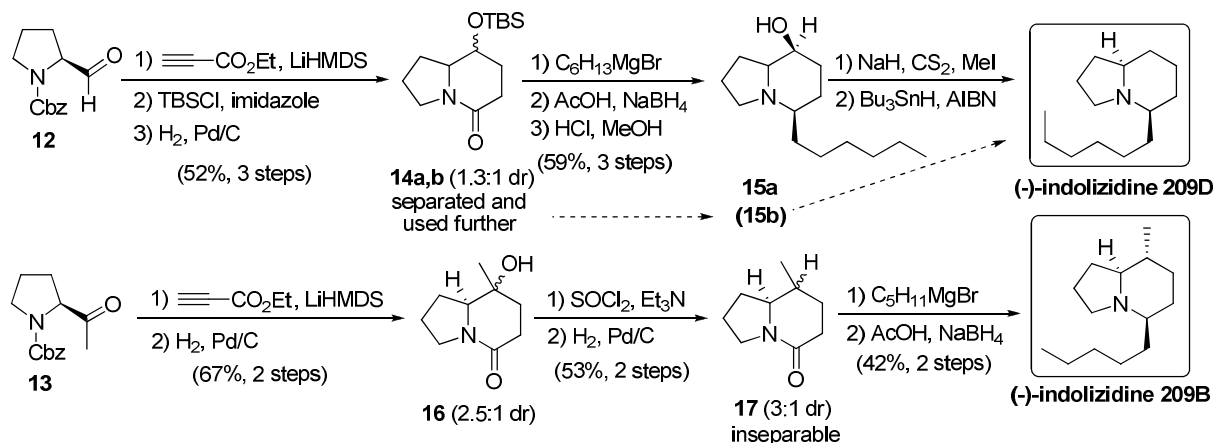
Scheme 1. Synthesis of (-)-indolizidine 167B via asymmetric alkylation of Boc-pyrrolidine.

Complementary to the above strategy, Pilli has reported⁶ a concise synthesis of (+)-5-epitashiromine utilizing a stereoselective nucleophilic functionalization of *N*-Boc-2-methoxypyrrolidine (**8**) as the key step (Scheme 2). The synthesis uses a chiral thiazolidinone derived nucleophile for the key transformation and begins with the *N*-chloropentanoyl-1,3-thiazolidin-2-thione **9**. Generation of the titanium enolate of **9** and subsequent reaction with **8** provides the key intermediate **10** with moderate diastereoselectivity (10:1 dr). Reduction of **10** with lithium borohydride provided a mixture of **11** and the thiazolidinone auxiliary. This mixture was directly treated with acid and the deprotected amine in **11** was cyclized to provide, after purification, (+)-epitashiromine. The strategy was also applied in the synthesis of (+)-isoretronecanol by employing an analog of **9** bearing an *N*-chlorobutyl group.



Scheme 2. Synthesis of (+)-5-*epi*-tashiromine by nucleophilic alkylation of *N*-Boc-2-methoxypyrrolidine.

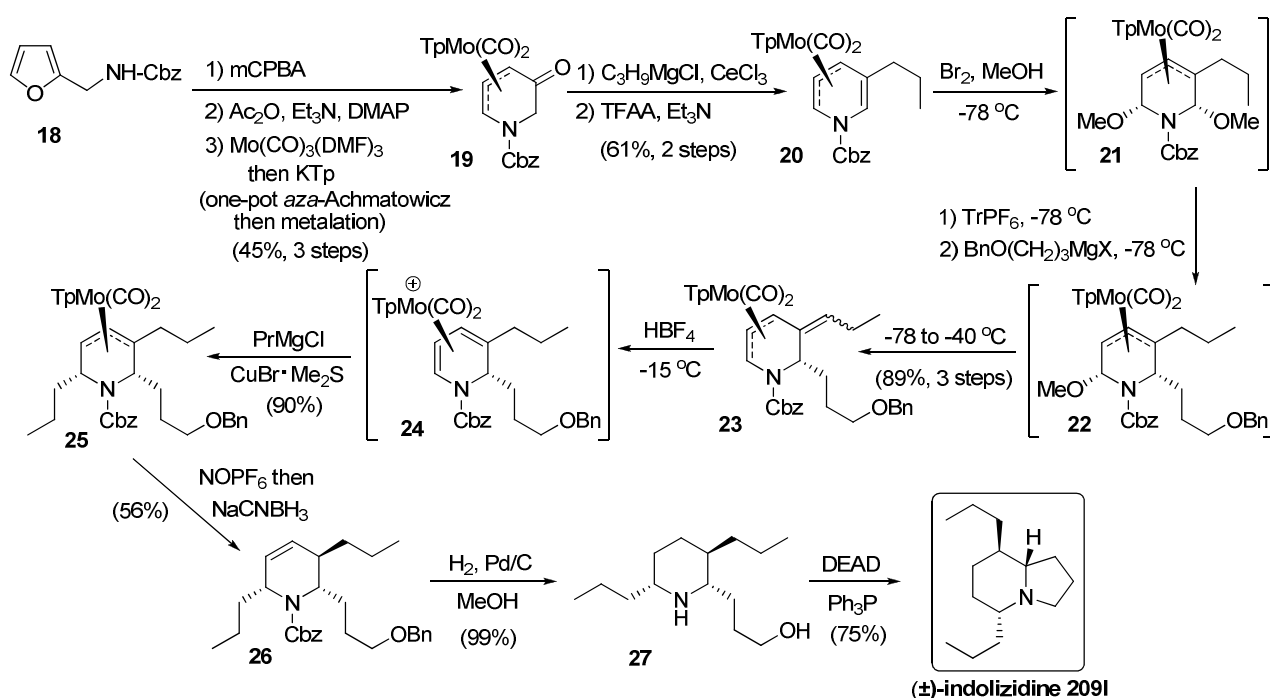
A *S*-proline-based synthesis of the indolizidines (-)-209D and (-)-209B was developed by Zhao and co-workers (Scheme 3).⁷ This approach uses the existing stereocentre in proline to control two new stereocentres that are constructed in the course of the synthesis. The synthesis of (-)-indolizidine 209B begins with (2*S*)-*N*-Cbz-pyrrolidine-2-carboxaldehyde (**12**) and that of (-)-indolizidine 209D uses the proline-derived methyl ketone, (*S*)-benzyl 2-acetylpyrrolidine-1-carboxylate (**13**).



Scheme 3. S-Proline-based syntheses of the indolizidines (-)-209D and (-)-209B.

The approach utilized in both syntheses relied on construction of the indolizidine motif by adding a three carbon fragment, in the form of ethyl propargylate, to the proline core and subsequent cyclization of the pyrrolidine nitrogen and the ester. Thus **12** was converted to the hydroxyamides **14a,b** (1.3:1 dr) that were separated and carried further. The hexyl substituent in 209D was introduced by addition of hexylmagnesium bromide to the amide in **14a** to generate the hemiaminal which was reduced *in situ*, via the iminium ion, to the tertiary amine. Deoxygenation of the secondary alcohol provided the target (-)-indolizidine 209D. An identical series of transformations on **14b** also provided (-)-indolizidine 209D. Similarly, the hydroxyamide **16** was obtained from the methyl ketone **13**. Dehydration of the tertiary alcohol in **16** and reduction of the alkene provided **17** (3:1 dr). Addition of pentylmagnesium bromide and *in situ* reduction generated the target (-)-indolizidine 209B (42%). Conversion of a diastereomeric mixture (**17**) to the diastereomerically pure target 209B suggests loss of one of the diastereomers of **17** either during the reaction or during isolation of the product.

A versatile tactic for the synthesis of piperidines and indolizidine and quinolizidine alkaloids, employing the concept of organometallic scaffolding, was recently reported by Liebeskind.⁸

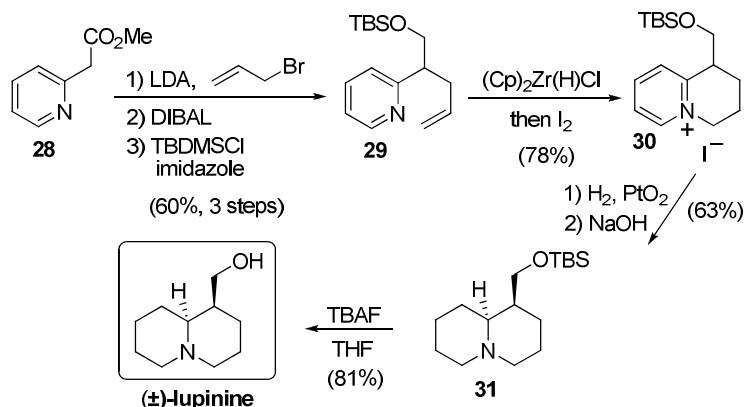


Scheme 4. Synthesis of (±)-indolizidine 209I by functionalization of a 5-oxo-dihydropiperidyl scaffold.

The key feature of this approach is the chemoselective tri-functionalization of a 5-oxodihydropiperidinyll scaffold which allows the stereoselective construction of three stereocentres in the product piperidine. Nitrogen to carbon cyclization in the piperidine provides the target alkaloids. The synthesis of (\pm)-indolizidine 209I is illustrative (Scheme 4).

The synthesis begins with *N*-Cbz furfurylamine (**18**) which is converted to the key starting material, a 5-oxo-dihydropiperidine complex **19**, via an *aza*-Achmatowicz oxidative ring expansion. Subsequent metallation of the resulting acetoxy dihydropiperidinone with Mo(CO)₃(DMF)₃, followed by ligand exchange with potassium hydrido tris(1-pyrazolyl)borate (KTp), provided **19**. Addition of PrMgCl to **19** and dehydration of the obtained tertiary alcohol provided **20**. Oxidative di-functionalization of **20** was achieved by treatment with bromine in methanol to provide the 3-propyl-2,6-dimethoxy- η^3 -dihydropyridinyl complex **21** in which the 2 and 6 positions are functionalized *anti* to the molybdenum. Treatment of **21** with triphenyl carbenium hexafluorophosphate *in situ* resulted in a highly regioselective abstraction of the methoxy group adjacent to the propyl group. The resulting iminium ion was reacted with an appropriately functionalized Grignard reagent to provide **22** which, upon warming, underwent an elimination of the second methoxy group to provide **23** as a mixture of *E* and *Z* isomers. Protonation of the exocyclic double bond in **23** generated the cationic η^4 -diene intermediate **24** which was reacted *in situ* with the cuprate derived from propyl magnesium chloride to generate **25**. Decomplexation of **25** was achieved by a CO/NO⁺ ligand exchange. Subsequent reduction of the cationic intermediate proceeded *anti* to the TpMo(CO)(NO⁺) moiety to provide **26** as a single diastereomer. Hydrogenation of **26** provided the piperidine **27** which was cyclized to (\pm)-indolizidine 209I under Mitsunobu conditions. An asymmetric version of this general strategy was also developed by using a chiral analog of **21** with a carbamate protecting group derived from (*S*)-1-phenyl-1-butanol. Indolizidine (\pm)-8-*epi*-219F and quinolizidine (–)-251AA were also prepared in this study.

Vasse and co-workers have developed a simple route to quinolizidines that utilizes a suitably functionalized pyridine as the starting material.⁹ The pivotal step in this approach involves cyclization of the pyridine nitrogen onto a pendant alkene via a hydrozirconation of the alkene. The syntheses of (\pm)-lupinine and (–)-epiquinamide demonstrate the utility of this approach. The lupinine synthesis begins with the pyridinyl acetate **28** which was converted into the hydrozirconation substrate **29** by alkylation of the benzylic position with allylbromide and reduction of the ester (Scheme 5).

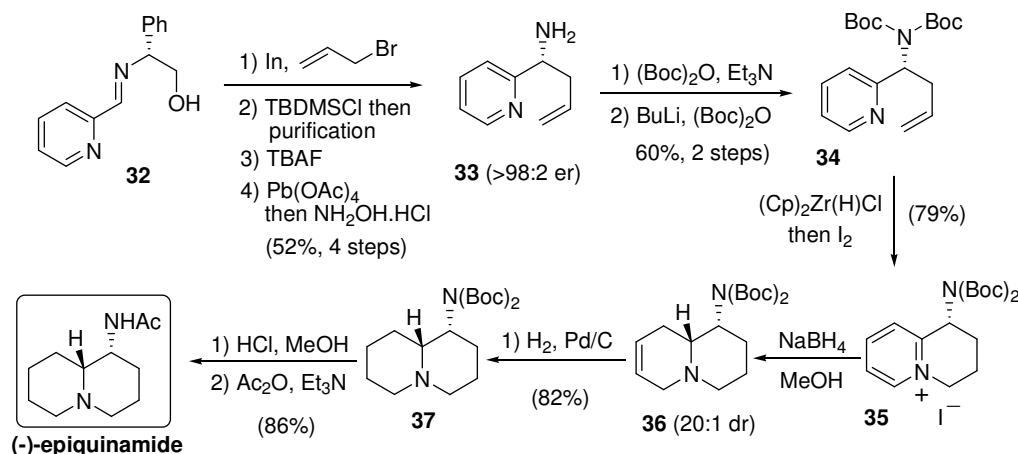


Scheme 5. Synthesis of (\pm)-lupinine employing a hydrozirconative cyclization.

Treatment of **29** with the Schwartz reagent, followed by the addition of iodine, generated a primary iodide from the alkene. *In situ*, intramolecular *N*-alkylation of the pyridine by the iodide generated the

bicyclic salt **30**. Hydrogenation of the pyridinium ring in **30** generated a mixture of diastereomeric reduction products (5.5:1 dr). The major diastereomer **31**, which presumably results from hydrogenation *anti* to the CH₂OTBS side-chain, was separated by chromatography and converted into (±)-lupinine.

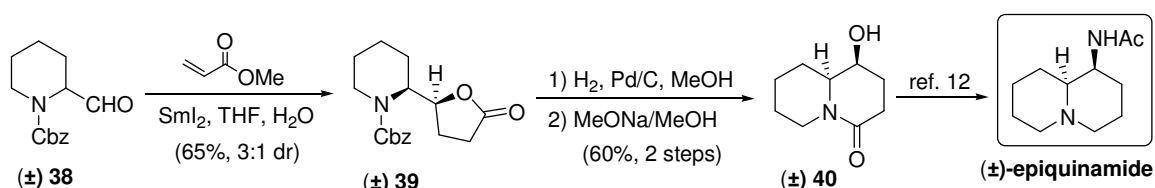
A similar strategy was applied in the synthesis of (–)-epiquinamide which began with the diastereoselective allylation of the imine **32** (derived from pyridine-2-carboxaldehyde and (*R*)-phenylglycinol) according to the reported procedure¹⁰ to provide, after deprotection, the key homoallylic amine **33** (>98:2 er, Scheme 6).



Scheme 6. Synthesis of (–)-epiquinamide employing a hydrozirconative cyclization.

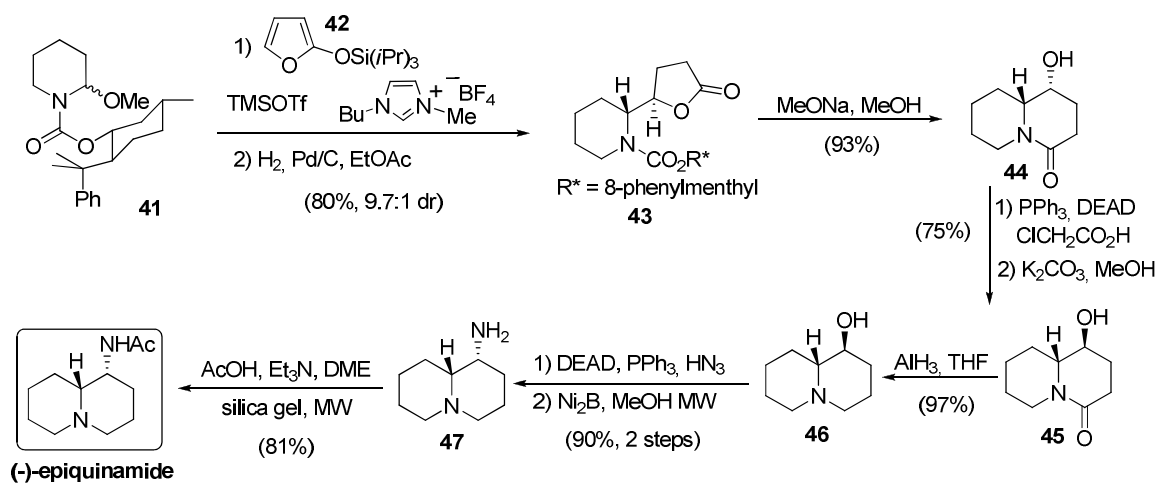
Protection of the amine as the di-Boc derivative **34** was necessary to limit the amount of Schwartz reagent used in the hydrozirconation step (1.2 equivalents) and also to facilitate the isolation of the salt **35**. Diastereoselective reduction of **35** with NaBH₄ provided the *syn* diastereomer **36** (*syn* orientation of C(1)H and C(9a)H, 20:1 dr) which was hydrogenated to the aminoquinolizidine derivative **37**. Deprotection of **37**, followed by acetylation of the primary amine, provided (–)-epiquinamide. The above strategy was also utilized for the synthesis of other C-1 substituted quinolizidines. Overall, this pyridine-quaternization strategy for constructing the quinolizidine framework is notable for its novelty and efficiency in the key N–C bond construction step.

Recently, Burtoloso and co-workers developed an efficient protocol for the construction of piperidine, indolizidine and quinolizidine systems.¹¹ The strategy, which involves samarium iodide-mediated coupling of α -amino acid derivatives with methyl acrylate, was employed in a formal synthesis of (±)-epiquinamide (Scheme 7). Reductive coupling of the 2-formyl piperidine derivative **38** with methyl acrylate generated **39** with moderate diastereoselectivity (3:1 dr). Deprotection of the major (*syn*) diastereomer, followed by intramolecular acylation of the secondary amine with the butyrolactone moiety, provided **40** which is a known intermediate to epiquinamide.¹² This strategy was also employed in a synthesis of (–)-pumiliotoxin 251D.



Scheme 7. Synthesis of (±)-epiquinamide employing a stereoselective coupling reaction of an α -aminoaldehyde.

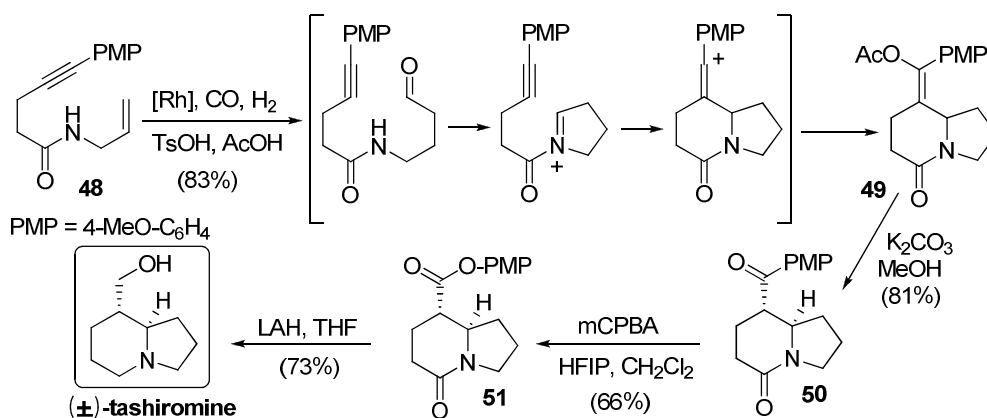
An asymmetric vinylogous Mannich reaction was employed by Santos in a synthesis of (–)-epiquinamide (Scheme 8).¹³ Treatment of the 2-methoxypiperidine derivative **41** with the silyloxyfuran **42** in the presence of trimethylsilyl triflate provides the corresponding Mannich product (9.7:1 dr), hydrogenation of which generates **43**. Notably, the use of 1-butyl-3-methylimidazolium tetrafluoroborate (BMI·BF₄) as an additive is necessary for good diastereoselectivity in the Mannich reaction. Treatment of **43** with sodium methoxide effected deprotection of the piperidine and also the subsequent intramolecular acylation of the piperidine with the butyrolactone moiety to provide **44**. Mitsunobu inversion of the secondary alcohol in **44** provided **45** which was reduced to **46** with alane. The primary amine in the target was now introduced by azidation with hydrazoic acid under Mitsunobu conditions and reduction of the azide to provide **47**. Acetylation of **47** provided (–)-epiquinamide. The asymmetric vinylogous Mannich reaction strategy was also employed in a synthesis of (–)-lupinine.



Scheme 8. Synthesis of (–)-epiquinamide employing a chiral carbamate-protected methoxypiperidine as the starting material.

3.1.2. Nitrogen-carbon cyclizations with open chain precursors

Syntheses based on this strategy outnumber the N–C cyclization approaches starting with azacycles. This is probably due to the greater number of options available for designing suitably functionalized open chain precursors of indolizidines and quinolizidines. Recently, Chiou and co-workers reported an alkyne-mediated, domino hydroformylation/double cyclization approach to the indolizidine motif with an application in the synthesis of (±)-tashiromine.¹⁴ The procedure utilizes a suitable *N*-allyl-alkynamide **48** as the starting material (Scheme 9).

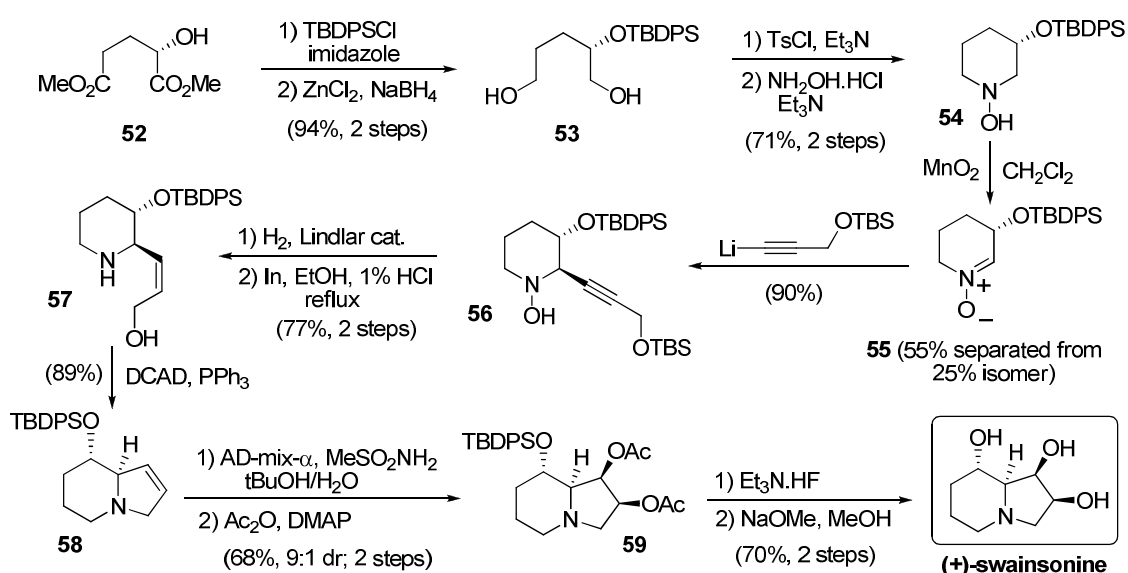


Scheme 9. Synthesis of (±)-tashiromine by alkyne-mediated domino hydroformylation/double cyclization.

Hydroformylation of the allyl group in **48** generates an aldehyde which provides an acyl iminium species by *in situ* reaction with the amide nitrogen. This is captured by the alkyne to produce the enol acetate **49** which was methanolized to the ketone **50**. Bayer-Villiger oxidation of **50** to the ester **51**, followed by reduction, provided (±)-tashiromine (33% overall yield from **48**).

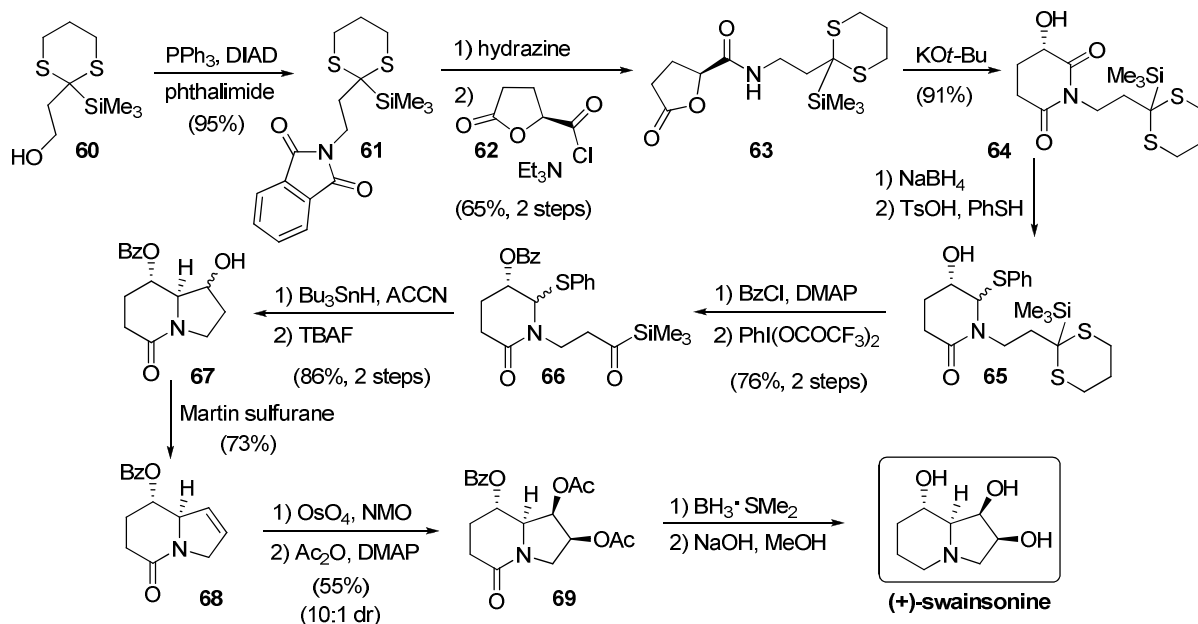
An important aspect of this synthesis is the highly diastereoselective protonation of the enolate (or enol) generated by methanolysis of the enolacetate **49** to produce **50** as a single diastereomer. While this diastereoselectivity is high for **49**, a limitation of the methodology is the lack of selectivity for substituted indolizidinones related to **49** and also for the related pyrroloazepine ring systems. Methanolysis of analogs of **49** obtained from these ring systems leads to the formation of diastereomeric mixtures. Nonetheless, the strategy is notable for simplicity.

A glutamic acid-based synthesis of the indolizidine alkaloid (–)-swainsonine was recently reported by Barker, Caprio and co-workers.¹⁵ The synthesis was initiated with the glutamic acid-derived hydroxy diester **52** which was first protected and then reduced to provide the triol derivative **53** (Scheme 10). Activation of the primary alcohols in **53**, followed by treatment with hydroxylamine, provided the *N*-hydroxy piperidine **54** which was oxidized to the key nitron intermediate **55** and its isomeric nitron (N–C(6) double bond). The required nitron **55** was separated and elaborated to **56** by stereoselective *anti* (to the OTBDPS group) addition of a propargyl alcohol-derived alkenyllithium reagent that incorporates all of the remaining carbon atoms required for construction of the target indolizidine. The conversion of **56** to **57** was best achieved by first reducing the alkyne to the *cis*-alkene and then reducing the N–O bond in the hydroxylamine. Reversal of this reaction sequence invariably provided low yields of the required alkene. Cyclization of **57** under Mitsunobu conditions provided **58** which was subjected to stereoselective dihydroxylation (9:1 dr for the required diastereomer) and acetylation to provide **59**. Finally, global deprotection of **59** provided (+)-swainsonine.



Scheme 10. Synthesis of (+)-swainsonine from glutamic acid.

A synthesis of (+)-swainsonine based on a radical cyclization of an acylsilane as the pivotal ring-forming step, and also utilizing a glutamic acid derived synthon, was developed by Chan and Tsai.¹⁶ The synthesis begins with the dithiane **60** (a masked acylsilane, Scheme 11) which was prepared by a stepwise silylation and alkylation of 1,3-dithiane.



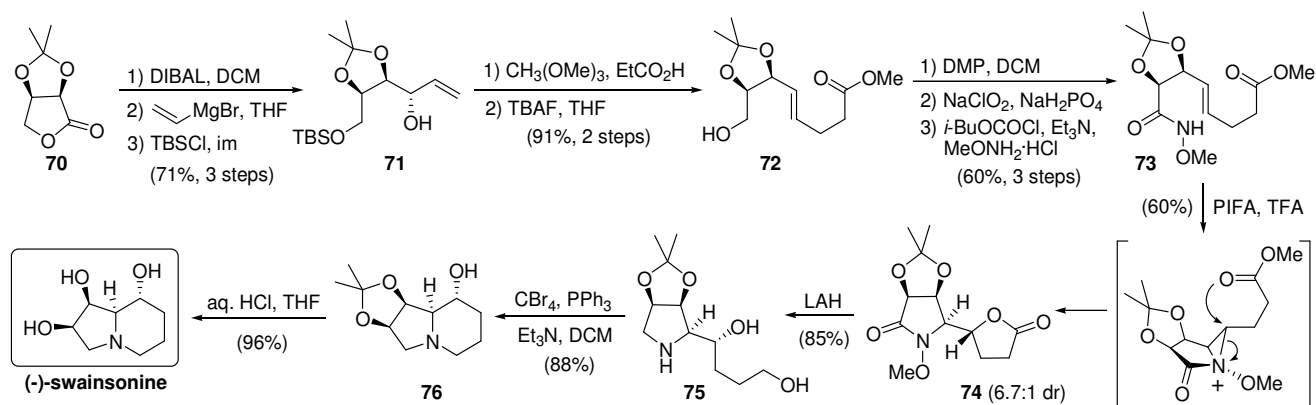
Scheme 11. Synthesis of (+)-swainsonine based on a radical cyclization of an acylsilane.

Conversion of the alcohol in **60** into a primary amine was achieved *via* the phthalimido derivative **61** which was deprotected and acylated *in situ*, with the glutamic acid-derived lactone chloride **62**, to provide **63**. A base-induced rearrangement of the lactone in **63** to a glutarimide moiety provided **64**. Chemoselective reduction of the more reactive carbonyl group in **64** provided the corresponding hemiaminal which was converted into the sulfide **65**. Oxidative removal of the dithiane with $\text{PhI}(\text{OCOCF}_3)_2$ [phenyliodine(III) bis(trifluoroacetate)] provided the key acylsilane **66**. Radical formation from the sulfide and subsequent cyclization onto the acylsilane in **66** was achieved by treatment with Bu_3SnH and 1,1'-azobis-(cyclohexane carbonitrile). This step generated the silyl ethers of **67** (mixture of diastereomers at the newly formed stereocentre) which were converted into the alcohols by exposure to TBAF. Further functionalization of the five-membered ring was achieved by dehydration of **67** to **68** and dihydroxylation of the alkene in **68** to provide **69** after protection of the diol as the diacetate. Moderate diastereoselectivity was observed for the dihydroxylation reaction (10:1 dr for **69**) and this mixture was carried further. Borane reduction of the amide in **69** and basic hydrolysis of the acetates provided the target (+)-swainsonine. Presumably, the minor diastereomer of **69** is lost, either during the two step conversion to, or during the purification of, (+)-swainsonine. This radical cyclization strategy was also employed in the synthesis of (–)-epiquinamide.¹⁶

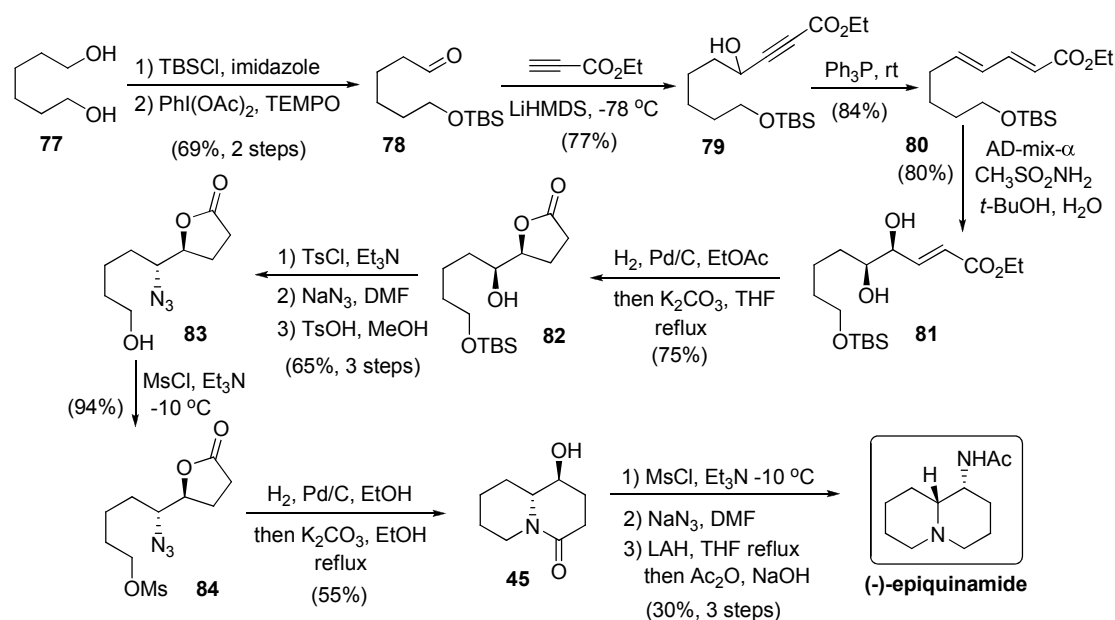
A nitrenium ion-mediated diastereoselective cyclization-based strategy was recently applied in the synthesis of (–)-swainsonine by Wardrop and co-workers (Scheme 12).¹⁷ The synthesis begins with the D-erythrone lactone derivative **70** which was converted into **71** by reduction of the lactol, followed by a diastereoselective addition of vinyl magnesium bromide. A Johnson-Claisen rearrangement of **71** employing propanoic acid generated **72** which was elaborated into the key *O*-alkyl hydroxamate **73** by conventional oxidation to the acid and amidation. Treatment of **73** with $\text{PhI}(\text{OCOCF}_3)_2$ generated the corresponding nitrenium ion which reacted with the pendant alkene to generate an aziridinium ion which provided the pyrrolidinyl lactone **74** *via* an intramolecular ring-opening involving the ester in **73**. Reduction of **74** led to **75** which was converted to **76** and ultimately to (–)-swainsonine.

A synthesis of epiquinamide that relies on a propargyl alcohol to dienophile rearrangement and the Sharpless asymmetric dihydroxylation as the key transforms was reported by Chandrasekhar and

co-workers.¹⁸ 1,6-Hexane diol (**77**) was converted to the protected hydroxy aldehyde **78** which provided the propargyl alcohol **79** upon addition of the acetylide anion derived from ethyl propargylate (Scheme 13).



Scheme 12. Synthesis of (-)-swainsonine employing a diastereoselective nitrenium ion-alkene addition as the pivotal step.

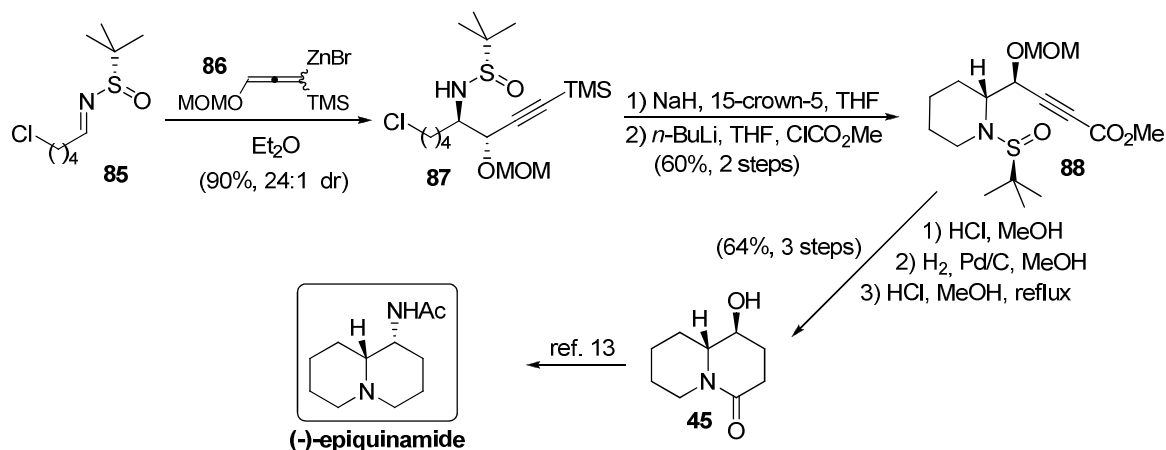


Scheme 13. Synthesis of (-)-epiquinamide employing a propargyl alcohol to dienophile rearrangement.

Treatment of **79** with triphenylphosphine induced a rearrangement to the dienophile **80** (presumably *via* the corresponding allene).¹⁹ Sharpless asymmetric dihydroxylation of the more reactive alkene in **80** with AD-mix- α provided **81** which was converted to the butyrolactone **82** by hydrogenation and subsequent lactonization. Invertive azidation of **82** provided **83** which was converted to the key azidomesylate **84**. Reduction of the azide in **84** proceeded with concomitant piperidine ring formation by displacement of the mesylate by the primary amine and lactamization of the resulting piperidine. This double cyclization provided **45** with the quinolizidine scaffold of epiquinamide. A second invertive azidation and simultaneous reduction of the lactam and the azide generated 9-aminoquinolizidine which was acetylated *in situ* to provide (-)-epiquinamide. Notably, the use of AD-mix- β in the reaction of **80** provided *ent*-**81** which can potentially be converted to (+)-epiquinamide and the authors therefore describe their approach as being stereoflexible. A limitation of this approach is the modest yields for the last four steps in the synthesis.

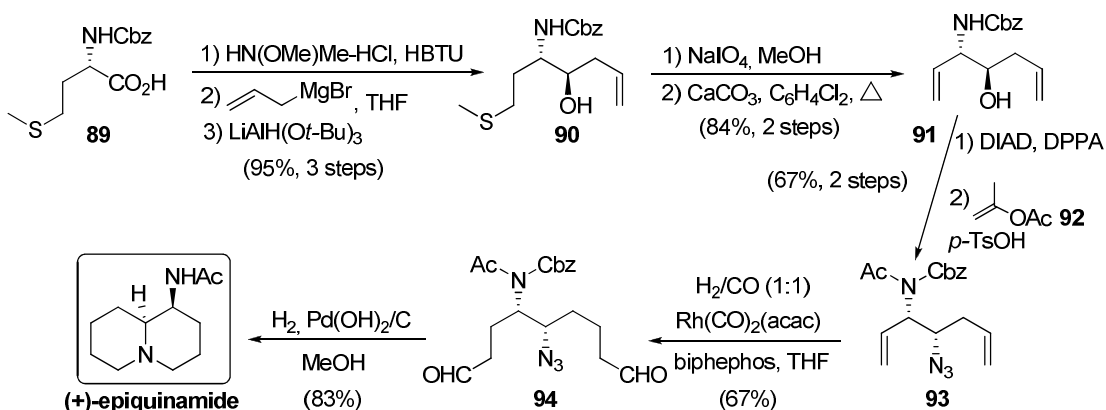
The diastereoselective addition of a racemic allenylzinc reagent to a chiral imine was employed as the key reaction in a formal synthesis of (-)-epiquinamide by Chemla and co-workers.²⁰ Readily available

5-chloropentanal was converted into the chiral sulfenimine **85** by reaction with commercially available (*S*_s)-*N*-*tert*-butanesulfenamide. Reaction of **85** with the racemic allenylzinc **86** provided **87** with high diastereoselectivity. Treatment of **87** with sodium hydride effected cyclization of the sulfenamide and the chlorobutyl group to provide the piperidine with concomitant desilylation of the acetylene. Further functionalization of the terminal acetylenic carbon was achieved by lithiation and acylation with methyl chloroformate to provide **88**. Removal of the *N*-*tert*-butanesulfinyl moiety, hydrogenation of the acetylene and deprotection of the secondary alcohol provided **45** which is a known intermediate to (–)-epiquinamide (see Scheme 8).¹³ This strategy was also employed in a synthesis of (–)-homopumiliotoxin 223G.



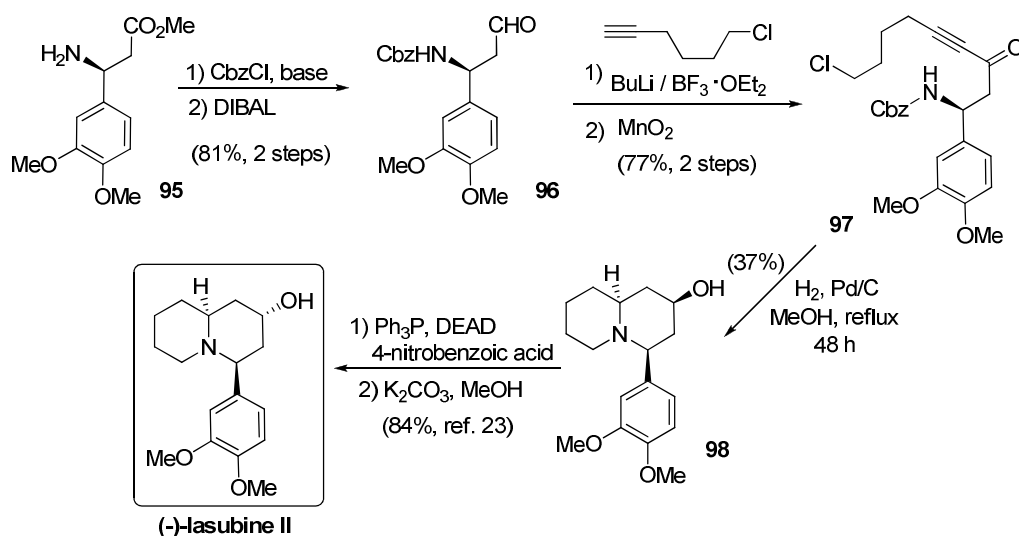
Scheme 14. Chiral *N*-sulfenimine-based strategy for the synthesis of (–)-epiquinamide.

A double hydroformylation strategy was used as the pivotal step by Bret, Mann and co-workers in their synthesis of (+)-epiquinamide.²¹ The synthesis begins with Cbz-*L*-methionine (**89**). Conversion of **89** to the corresponding Weinreb amide, reaction of the amide with allylmagnesium bromide to provide the amino ketone and stereoselective reduction of the amino ketone provided the *anti*-amino alcohol derivative **90**. Oxidation of the sulfide in **90** to the sulfoxide and subsequent thermal elimination provided the bis-homoallylic alcohol **91**. Invertive azidation of the secondary alcohol in **91** provided the corresponding azide which was *N*-acetylated with isopropenylacetate (**92**) to provide the key intermediate **93**. Double hydroformylation of **93** gave the azido dialdehyde **94** which was hydrogenated in the presence of Pearlman's catalyst (Scheme 15). This resulted in four reactions in one pot: 1) conversion of the azide to the primary amine, 2) two reductive aminations to generate the quinolizidine ring system and 3) removal of the Cbz protecting group to provide (+)-epiquinamide. This strategy was also employed in a synthesis of (+)-lupinine.



Scheme 15. A double hydroformylation-based strategy for the synthesis of (+)-epiquinamide.

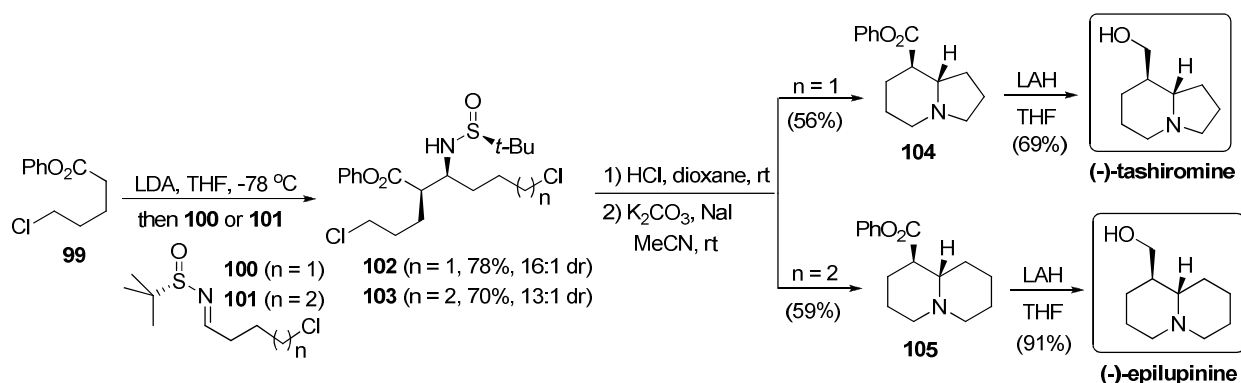
A formal synthesis of (–)-lasubine II from the known, enantiomerically enriched β -amino ester **95** was reported by Lim and Kim (Scheme 16).²² As in synthetic strategies discussed earlier (Scheme 10 and Scheme 13), the addition of a functionalized acetylide was used to introduce the requisite number of carbon atoms.



Scheme 16. Synthesis of (–)-lasubine II from an enantiomerically enriched β -amino ester.

Thus, **95** was converted to the aldehyde **96** which was elaborated to the key intermediate **97** via addition of a 6-chlorohexyne-derived acetylide and subsequent oxidation of the obtained alcohol to the ketone. Hydrogenation of **97** resulted in several transformations: 1) deprotection of the primary amine, 2) cyclization of the amine onto the ynone to provide the cyclic enone (which can be isolated), 3) reduction of the enone and finally 4) cyclization of the secondary amine and the primary chloride to provide **98**, which has been previously converted into (–)-lasubine II by Mitsunobu inversion of the secondary alcohol.²³ Although the yield of **98** is only modest (37%), the synthesis is notable for the multiple bond formations achieved in a single hydrogenation step.

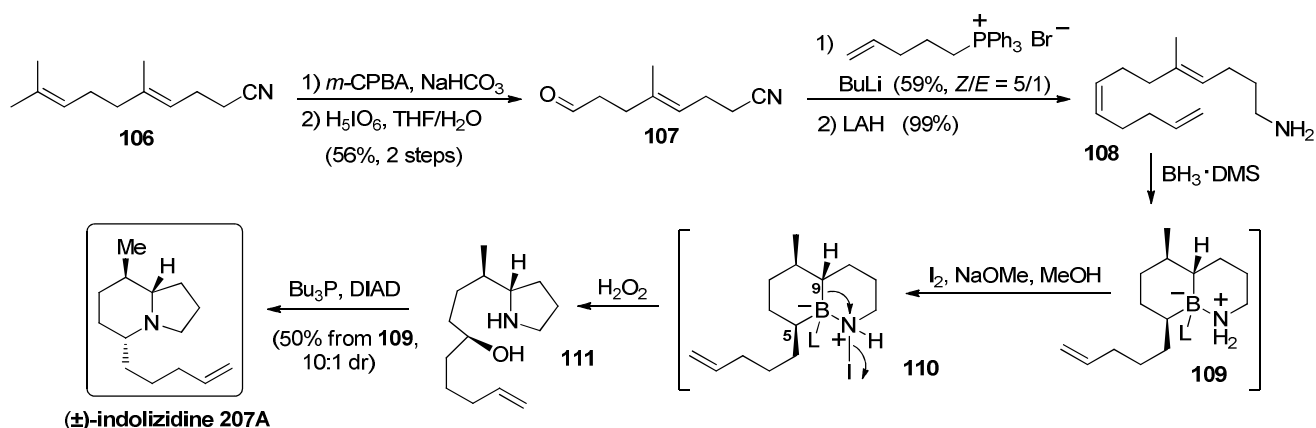
An efficient variant of the above ‘sequential cyclization’ strategy was described recently by Brown and co-workers in their synthesis of (–)-epilupinine and (–)-tashiromine.²⁴ This approach uses a stereoselective imino-aldol reaction of (*S*)-*tert*-butylsulfinyl imines of suitably functionalized aldehydes with the enolate of phenyl 5-chloropentanoate. Thus, the *syn* imino-aldol products **102** and **103** were obtained in good yield and high diastereoselectivity (Scheme 17).



Scheme 17. Stereoselective imino-aldol strategy for the synthesis of (–)-tashiromine and (–)-epilupinine.

Acid-catalyzed removal of the *tert*-butylsulfinyl protection and a double cyclization of the primary amine provided the indolizidine **104** and the quinolizidine **105** from **102** and **103**, respectively. These were converted into (–)-tashiromine and (–)-epilupinine by reduction of the phenyl ester to a primary alcohol. While the simplicity of this synthesis makes it particularly attractive, exploring the scope of the imino-aldol reaction with substituted imines, as a route to ring-substituted alkaloid motifs, would be worthwhile.

A conceptually novel synthesis of polysubstituted indolizidines was recently reported by Shenvi.²⁵ This strategy relies on the intramolecular hydroamination of aminoalkenes that proceeds in a formal *anti*-Markovnikov manner. This unusual transformation is achieved indirectly; initial hydroboration of the alkenes generates an aminoborate resulting from complexation of the amine with the boron. This is followed by an oxidation of the nitrogen which induces a migration of the newly formed C–B bond to the nitrogen. Application of this methodology in the stereoselective synthesis of (±)-indolizidine 207A is illustrative (Scheme 18).

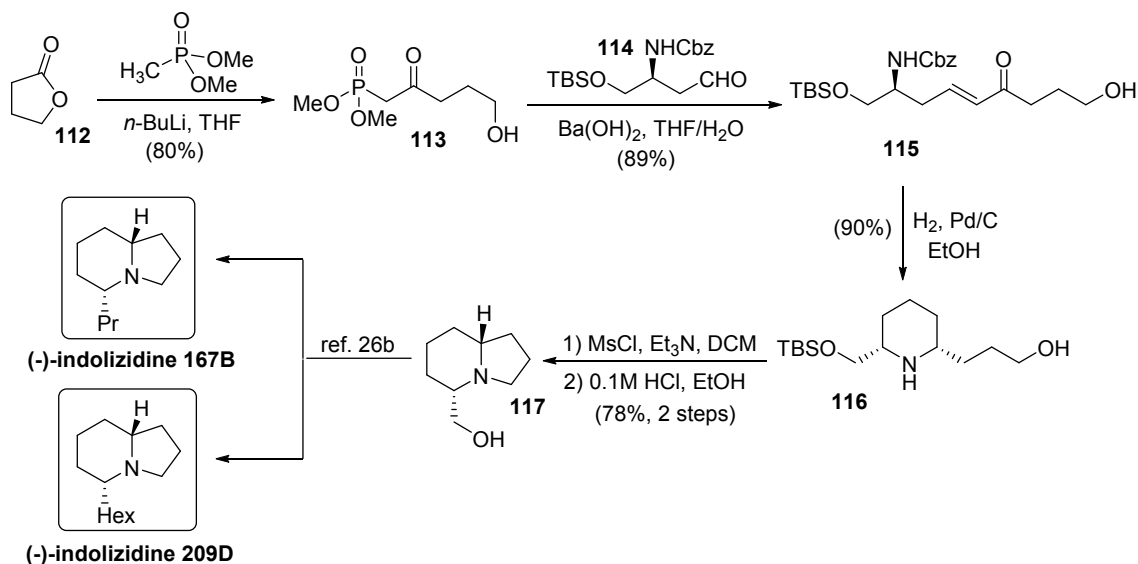


Scheme 18. Intramolecular hydroamination-based synthesis of (±)-indolizidine 207A.

Geranyl acetonitrile (**106**) was converted into the aldehyde **107** by oxidative cleavage of its terminal alkene. Wittig reaction of **107** with the 5-bromopentene derived phosphorane and subsequent reduction of the nitrile provided the key aminotriene **108**. Hydroboration of the tri- and disubstituted alkenes in **108** lead to the aminoborate **109** which was directly treated with iodine and NaOMe to provide the *N*-iodoborate **110**. A selective migration of C-9 from boron to nitrogen generated a pyrrolidine ring. This is followed by oxidation of the organoborane to an alcohol to finally provide the pyrrolidinyllithium alcohol **111**. The authors state that the selective migration of C-9, but not C-5, in **110** is surprising. In the last step, an invertive ring closure in **111**, under Mitsunobu conditions, provided (±)-indolizidine 207A (10:1 dr, 50% from **109**).

Recently, formal syntheses of (–)-indolizidine 167B and 209D from a common intermediate were reported by Reddy and co-workers.²⁶ Acylation of the anion derived from dimethyl methylphosphonate with γ -butyrolactone (**112**) provided the β -ketophosphonate **113** which was employed in a Horner-Wadsworth-Emmons olefination with the aspartic acid-derived synthon **114** to provide **115** (Scheme 19).

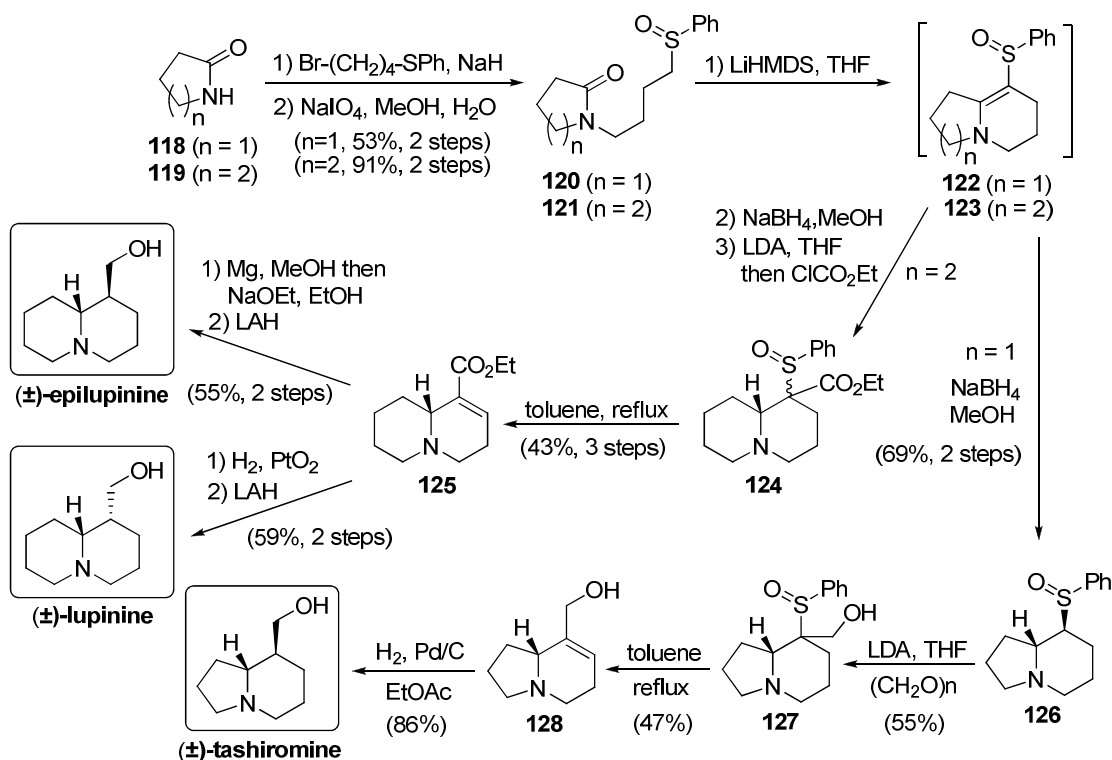
Hydrogenation of **115** effected deprotection of the amine and reduction of the alkene. The resulting ketone underwent intramolecular reductive amination to directly provide the 2,6-disubstituted piperidine **116** as a single diastereomer. Cyclization of **116** to the indolizidine motif was achieved by mesylation of the primary alcohol. Subsequent desilylation provided the hydroxymethyl indolizidine **117** which has previously been converted to (–)-indolizidine 167B and (–)-indolizidine 209D.^{26b}



Scheme 19. Syntheses of (–)-indolizidine 167B and 209D employing an aspartic acid-derived synthon.

3.1.3. Carbon-carbon cyclizations with preformed azacycles as starting materials

The use of α -sulfinyl carbanions for intramolecular carbon-carbon bond forming reactions has been applied to the synthesis of several indolizidine and quinolizidine alkaloids by Pohmakotr, Reutrakul and co-workers.²⁷ This relatively simple, but versatile, tactic relies on the susceptibility of cyclic amides to nucleophilic addition of α -sulfinyl carbanions. Conceptually, this approach is closely related to the addition of π -nucleophiles to activated amides developed by Belang r,²⁸ but it avoids the amide activation reagent required in the earlier study. Syntheses of (\pm)-tashiromine, (\pm)-lupinine and (\pm)-epilupinine were achieved *via* the current approach and these are summarized in Scheme 20.



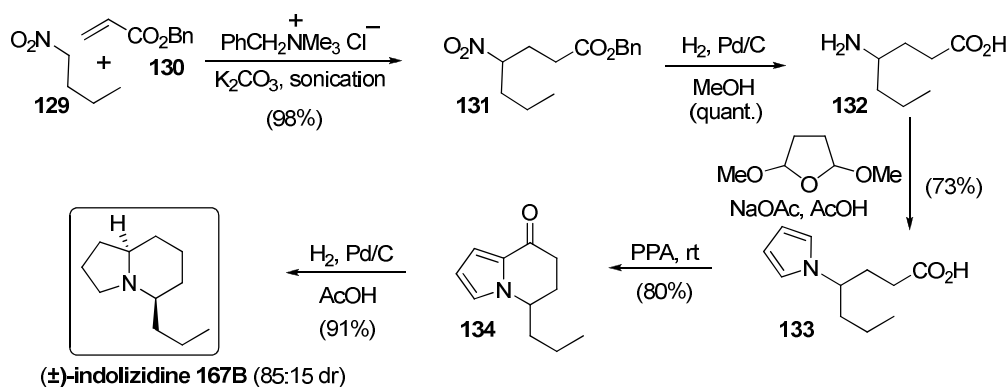
Scheme 20. Sulfinyl-carbanion cyclization-based approaches to (\pm)-tashiromine, (\pm)-lupinine and (\pm)-epilupinine.

N-Alkylation of 2-pyrrolidinone (**118**) and 2-piperidinone (**119**) with 4-bromobutylphenylsulfane and oxidation provided the sulfoxides **120** and **121**, respectively. Deprotonation of these sulfoxides resulted in cyclization onto the amide to provide **122** and **123** which could be isolated but were not purified. Reduction of **123** provided the corresponding sulfonyl quinolizidine which was acylated in the α position to the sulfoxide to provide **124** as a mixture of diastereomers. This was converted into **125** *via* sulfoxide elimination. Interestingly, hydrogenation of **125** was highly diastereoselective and the resulting ester was reduced with LAH to provide (\pm)-lupinine as a single diastereomer. Alternatively, a stereorandom reduction of **125** (Mg in MeOH), followed by epimerization of the ester under thermodynamic control (NaOEt/EtOH) and reduction (LAH), provided (\pm)-epilupinine as a single diastereomer. This stereodivergence is an attractive feature of these syntheses.

As with **123**, the reduction of **122** provided **126** which was subjected to an aldol-type process with paraformaldehyde to generate the hydroxymethyl indolizidine **127** as a diastereomeric mixture. Pyrolysis of **127** generated **128** which was hydrogenated to provide diastereomerically pure (\pm)-tashiromine (Scheme 16). This strategy was also applied to the syntheses of (\pm)-indolizidines 167B and 209D and their epimers. The generality of the above strategy was further demonstrated by application in a synthesis of (+)-swainsonine employing an enantiomerically enriched α -hydroxy glutarimide as the starting material.²⁹

3.1.4. Carbon-carbon cyclizations *via* azacyclic intermediates

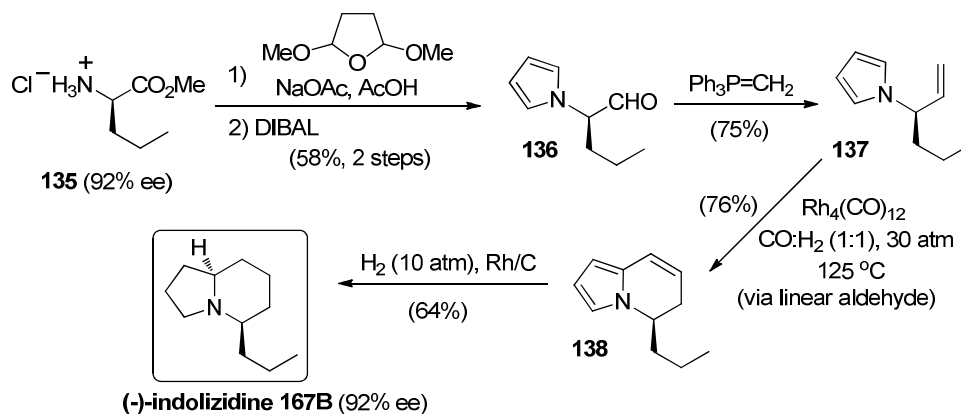
A synthesis of (\pm)-indolizidine 167B that utilizes an intramolecular electrophilic aromatic substitution on a pyrrole intermediate was reported by Pellet-Rostaing and Lemaire.³⁰ The first stage of the synthesis involves the construction of a suitably functionalized pyrrole which is then converted into the target (Scheme 21).



Scheme 21. Synthesis of (\pm)-indolizidine 167B employing an intramolecular Friedel-Crafts reaction.

The synthesis begins with the conjugate addition of 1-nitrobutane (**129**) to benzyl acrylate (**130**) under phase transfer conditions to provide the 4-nitroheptanoate **131** which was reduced to the γ -amino acid **132**. Conversion of **132** to the key pyrrole intermediate **133** was achieved by reaction with 2,5-dimethoxytetrahydrofuran. Intramolecular Friedel-Crafts type acylation of the pyrrole in **133** was achieved by exposure to polyphosphoric acid to provide **134**. Finally, catalytic reduction of the pyrrole as well as the ketone in **134** provided (\pm)-indolizidine 167B with moderate diastereoselectivity (85:15 dr).

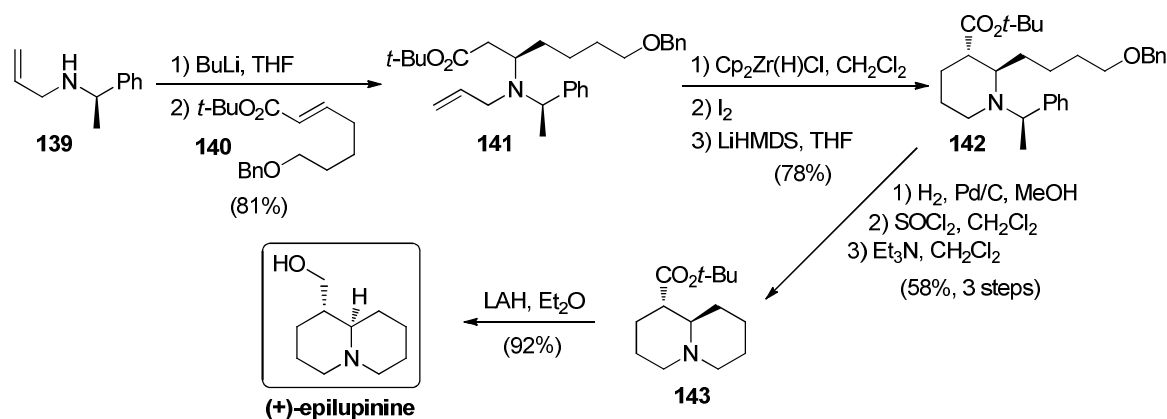
A related, but enantioselective, synthesis of (–)-indolizidine 167B was developed by Settambolo.³¹ This notably concise synthesis relies on the amino ester **135**, obtained from the unnatural amino acid D-norvaline (92% ee), as the starting material (Scheme 22).



Scheme 22. A domino hydroformylation/cyclization-based synthesis of (–)-indolizidine 167B.

Elaboration of the amine in **135** into the pyrrole by treatment with 2,5-dimethoxytetrahydrofuran (as in the conversion of **132** to **133**, Scheme 21), followed by a controlled reduction of the ester, provided the aldehyde **136** which was converted into the terminal alkene **137** by a conventional Wittig reaction. A regioselective, rhodium-catalyzed hydroformylation of the alkene in **137** provided the corresponding linear aldehyde as the major product which reacted further under the reaction conditions to provide **138** (via electrophilic aromatic substitution on the pyrrole and dehydration of the resulting alcohol). Complete hydrogenation of **138** provided (–)-indolizidine 167B (92% ee). The authors point out that the absence of racemization of **136** under the hydroformylation conditions and isomerization of the branched alkyl rhodium (obtained at lower reaction temperatures) to the linear species to provide the linear aldehyde are notable features of this synthesis. The marked difference in the diastereoselectivity of the reduction of **134** (85:15 dr, Scheme 21) and that of **138** (completely diastereoselective, Scheme 22) to provide indolizidine 167B is also noteworthy.

A synthesis of (+)-epilupinine that hinges on a hydrozirconation/iodination/cyclization strategy was described by Szymoniak.³² Conceptually, this approach closely parallels the synthesis of (±)-lupinine, from the same group, employing a hydrozirconative cyclization of a primary alkyl iodide (see Scheme 5). In the present approach, the cyclization step involves a carbon-carbon bond formation and the synthesis is rendered enantioselective by incorporation of an enantiomerically enriched amine as the starting material (Scheme 23).



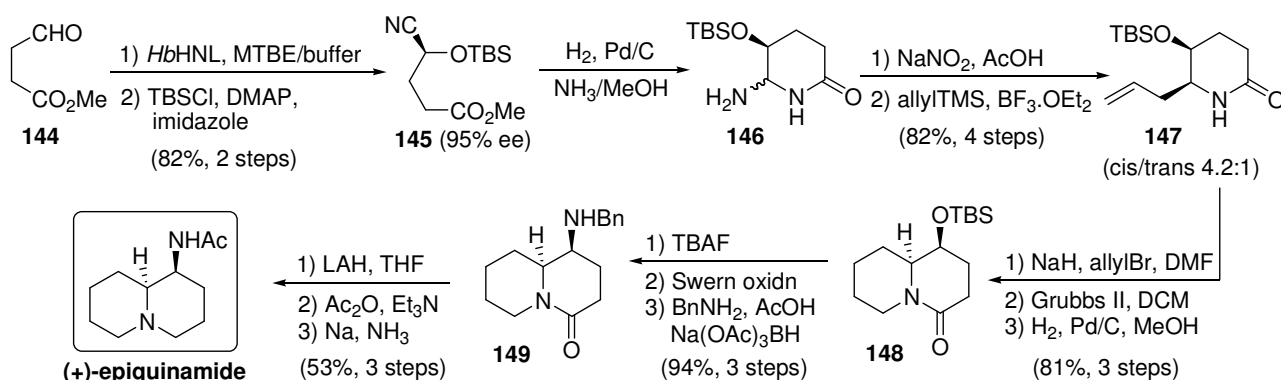
Scheme 23. A hydrozirconation/iodination/cyclization approach to (+)-epilupinine.

The synthesis begins with a conjugate addition of the lithium salt of (*R*)-*N*-allyl- α -(methylbenzylamine) **139** to the enoate **140** providing the β -amino ester derivative **141** as a single diastereomer.

Subjection of **141** to hydrozirconation with the Schwartz reagent, iodination and LiHMDS-mediated cyclization provided the piperidine derivative **142**. Hydrogenolysis of **142** to the amino alcohol and subsequent conversion of the alcohol to the chloride, followed by cyclization, generated **143** which was reduced to provide (+)-epilupinine. Other *trans*-2,3-disubstituted piperidines were also prepared in this study.

3.2. Syntheses employing ring closing metathesis as a key transformation

For the targets and the time period identified for this review, relatively few investigations have relied on ring closing metathesis (RCM) as the pivotal step in a total synthesis of indolizidine or quinolizidine alkaloids. The majority of these studies have addressed the synthesis of (+)-epiquinamide. Rutjes and co-workers have disclosed a RCM-based synthesis of (+)-epiquinamide which employs a biocatalytic cyanohydrin synthesis to establish a key stereocentre in their starting material (Scheme 24).¹²

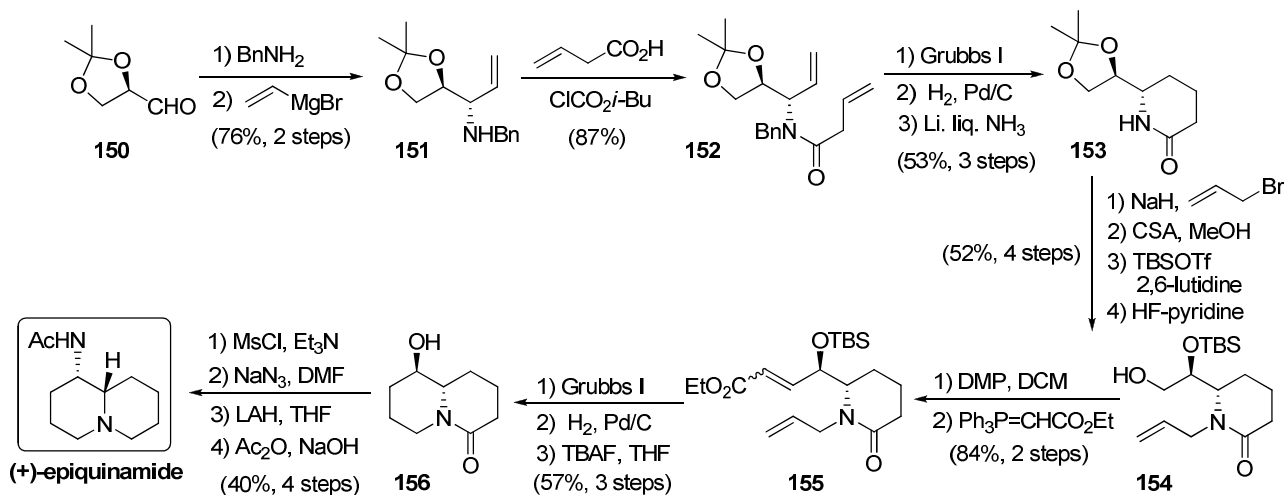


Scheme 24. Synthesis of (+)-epiquinamide employing asymmetric hydrocyanation and ring closing metathesis.

Treatment of succinic semialdehyde (**144**) with HCN in the presence of the hydroxynitrile lyase enzyme from *Hevea brasiliensis* (*HbHNL*) at pH 4.5 provided the (*S*)-cyanohydrin (95% ee) which was protected to provide **145**. Hydrogenation of the nitrile in the presence of ammonia directly provided the *N,N*-acetal **146**. This was converted into **147** by diazotization of the amine to generate an acyliminium ion, followed by a moderately diastereoselective allylation of the iminium ion. Although **147** is obtained as a mixture of diastereomers, these can be separated by chromatography. The requisite RCM substrate was prepared from *cis*-**147** by *N*-allylation. Conversion to **148** was then achieved by a Grubbs II catalyst mediated RCM, followed by hydrogenation of the product cycloalkene. This step establishes the bicyclic motif of the target alkaloid. Functional group transformations, involving conversion of an alcohol to an amine, in **148** provided the aminolactam **149** which was converted into (+)-epiquinamide *via* a lactam reduction, *N*-acetylation and debenzoylation protocol. This study also established that (+)-epiquinamide is the natural product by chiral GC comparison.

Two RCM reactions were employed for the construction of the bicyclic motif of (+)-epiquinamide in a synthesis by Ghosh and Shashidhar (Scheme 25).³³ This approach is initiated with the (*R*)-glyceraldehyde derivative **150** (obtained from D-mannitol). The relative stereochemistry of the two stereocentres in the target was set early in the synthesis by diastereoselective addition of vinyl magnesium bromide to the *N*-benzyl imine derived from **150** to provide **151** according to the literature procedure.^{33b}

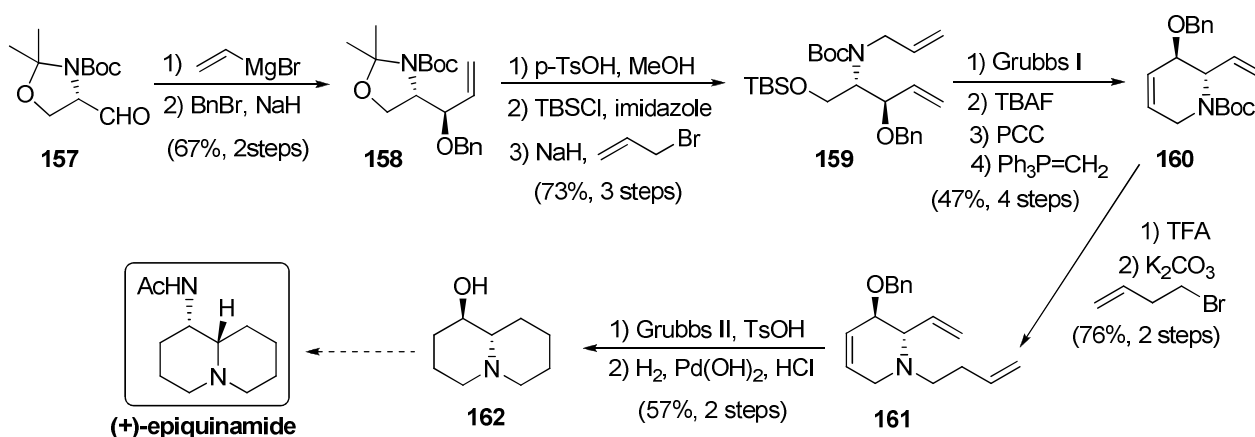
N-acylation of **151** with 3-butenic acid provided **152** which upon ring closing metathesis, cycloalkene reduction and debenzoylation gave **153**.



Scheme 25. A synthesis of (+)-epiquinamide featuring two RCM transformations.

Further transformations of **153** were designed to provide the second RCM substrate. To this effect, the diol acetonide in **153** was deprotected and then converted into **154** using a conventional protection/deprotection strategy. Oxidation of **154** to the aldehyde and subsequent reaction with a stabilized phosphorane yielded **155**. Ring closing metathesis of **155** provided access to the bicycle **156** after reduction of the RCM product. Conversion of the secondary alcohol in **156** into the secondary acetamide was achieved *via* invertive azidation, reduction and *N*-acetylation to provide (+)-epiquinamide.

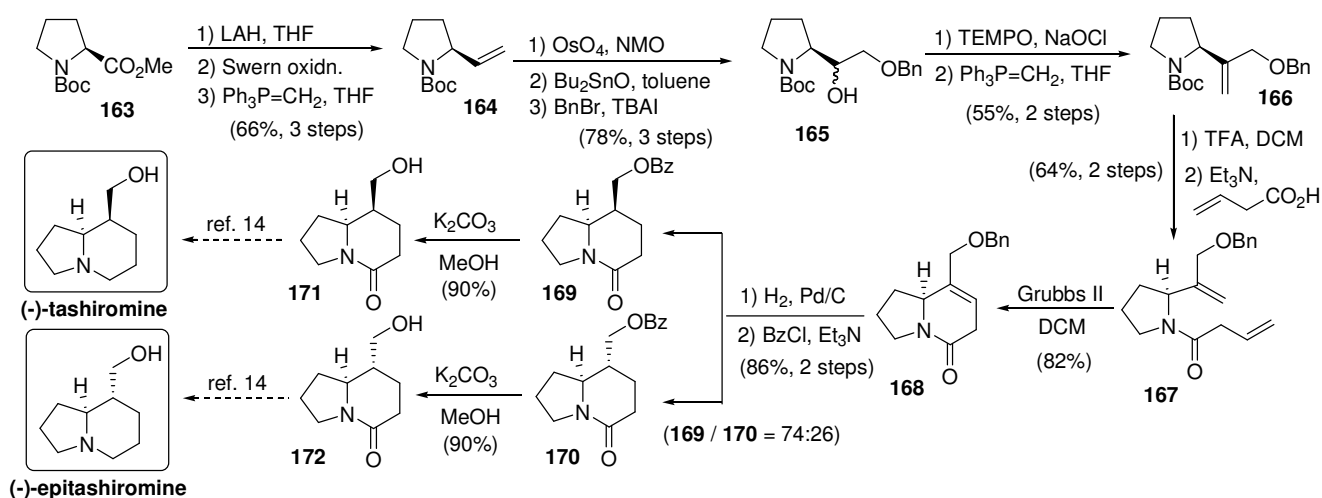
A conceptually similar, but formal, synthesis of (+)-epiquinamide that starts with the Garner aldehyde (**157**) was developed by Panda and co-workers (Scheme 26).³⁴



Scheme 26. Synthesis of (+)-epiquinamide from the Garner aldehyde.

Diastereoselective addition of vinylmagnesium bromide to **157** provided **158** which was elaborated into the RCM substrate by conversion of the oxazolidine in **158** to the protected amino alcohol, followed by *N*-alkylation to provide the diene **159**. Ring closure in **159** was achieved with the Grubbs I catalyst. The protected hydroxymethyl group in the cyclohexene derivative thus obtained was first liberated and then oxidized to the aldehyde, methylenation of which provided **160**. The substrate for the second RCM reaction was prepared by removal of the Boc protection in **160** and alkylation of the obtained amine with 4-bromobutene. Ring closing metathesis of **161** was best achieved by prior conversion to its tosylate salt. Reduction and debenzoylation of the RCM product was effected by hydrogenation over Pd(OH)₂ in acidic medium to provide **162** which can be converted to (+)-epiquinamide by invertive azidation, reduction and acetylation as described in Scheme 25.

(*S*)-Proline-based formal syntheses of the indolizidine alkaloids (–)-tashiromine and (–)-epitashiromine involving RCM to construct the bicyclic heterocycle motif were developed by Rao and co-workers (Scheme 27).³⁵ Their approach begins with Boc methylprolinate (**163**) which functions as a source of chirality and also as a component of the target indolizidine motif. Conversion of **163** to the vinyl pyrrolidine **164** was achieved *via* the corresponding aldehyde. Dihydroxylation and chemoselective protection of the diol provided **165** which was converted to **166** by oxidation to the ketone and Wittig methylenation. An appropriate *N*-acyl group was then introduced to provide **167** which upon RCM with the Grubbs II catalyst efficiently provided **168**. Conversion of **168** to the targets was straightforward and involved reduction and benzylation to provide **169** and **170** which were separated. Debzylation provided the indolizidinones **171** and **172** which are potential intermediates to (–)-tashiromine and (–)-epitashiromine, respectively, by reduction of the amide (*cf.* the reduction of **51** to (±)-tashiromine, Scheme 9 and of **156** to (+)-epiquinamide, Scheme 25).

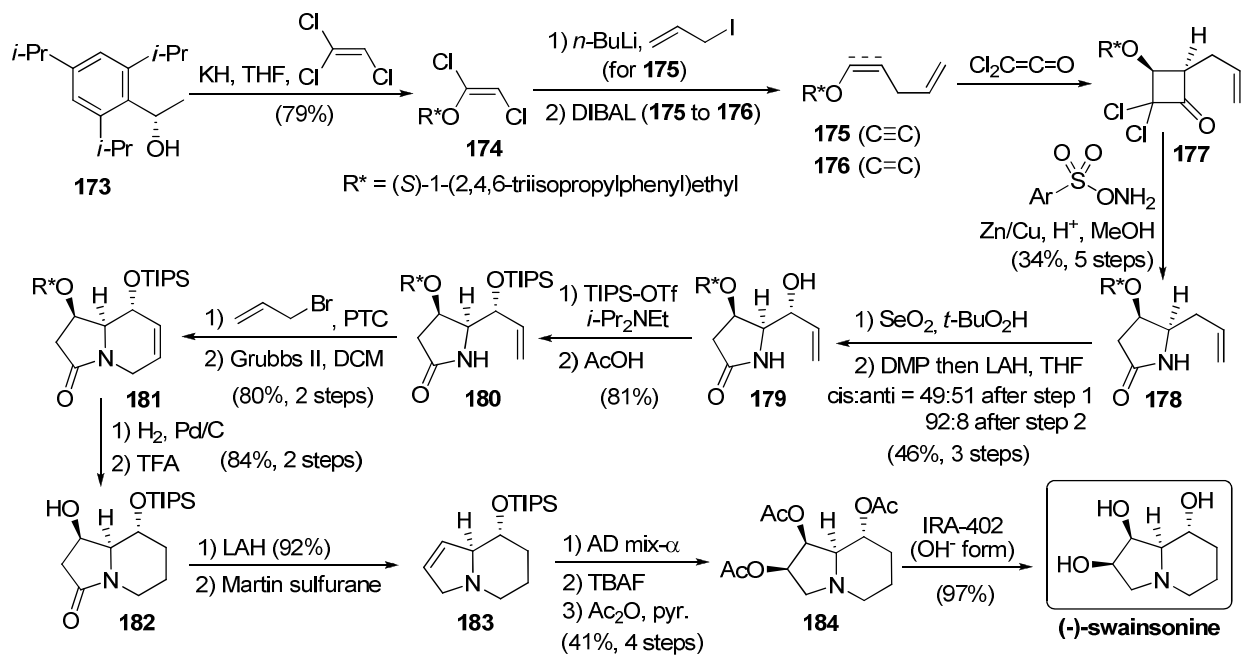


Scheme 27. (*S*)-Proline-based approach to (–)-tashiromine and (–)-epitashiromine involving RCM.

A limitation of this synthesis is the lack of diastereoselectivity in the reduction of **168** (**169/170**=74:26) which is in contrast to the highly diastereoselective reduction of **125** to (±)-lupinine and of **128** to (±)-tashiromine (Scheme 20). Presumably, the indolizidinone ring system in **168** is conformationally more flexible despite the presence of an amide.

3.3. Asymmetric cycloaddition-based strategies

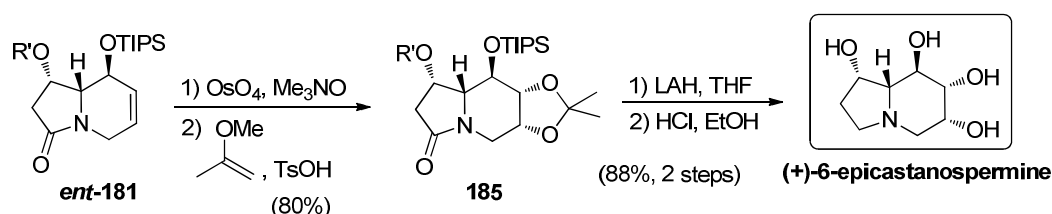
Asymmetric cycloaddition reactions are attractive transformations for the stereoselective construction of multiple stereocentres. Not surprisingly, this approach has been utilized in the enantioselective synthesis of a number of quinolizidines and indolizidines. Most of the syntheses in this category also incorporate reactions that are highlighted in previous sections of the review (*e.g.*, RCM reactions, N–C cyclizations). However, the major difference in strategy is the use of a cycloaddition reaction as an element of stereocontrol and hence these syntheses are considered separately. Poission and co-workers have reported a diastereoselective [2+2] cycloaddition of a chiral enol ether as the pivotal reaction for setting two contiguous stereocentres in their synthesis of (–)-swainsonine (Scheme 28).³⁶ The requisite enol ether was prepared by the *O*-alkylation of (*S*)-1-(2,4,6-triisopropylphenyl)ethanol (**173**) with trichloroethylene to furnish the dichloroenol ether **174** which was elaborated into the 1-alkoxydiene **176** (Scheme 24). In the key step, **176** was reacted with dichloroketene to provide **177** with high diastereoselectivity (97:3 dr).



Scheme 28. Synthesis of (–)-swainsonine based on an asymmetric [2+2] cycloaddition reaction.

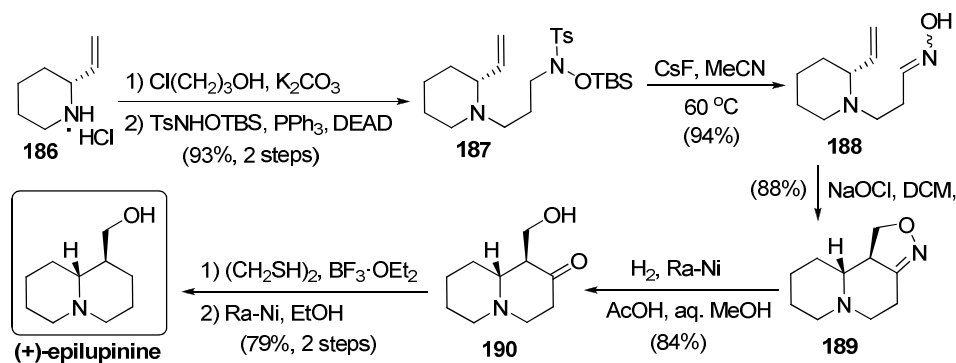
A highly regioselective Beckmann rearrangement of **177** was achieved *via* the activated oxime prepared with Tamura's reagent (mesitylenesulfonyl hydroxylamine). Dechlorination of the product oxazolidinone provided the pivotal intermediate **178**. Allylic hydroxylation of **178**, under the Sharpless conditions, did provide **179** but with low diastereoselectivity (1:1 dr). This difficulty was overcome *via* oxidation to the enone, followed by a diastereoselective reduction, which provided **179** with good diastereoselectivity (92:8 dr) for the required diastereomer. Bis-silylation of **179**, followed by hydrolysis of the silyl imidate, yielded **180** which was *N*-allylated to provide the diene substrate for the ensuing RCM which yielded the indolizinone **181**. Hydrogenation of **181** and acid-catalyzed removal of the chiral auxiliary provided **182** which, upon reduction of the lactam and dehydration of the secondary alcohol, yielded indolizine **183**. The remaining functionality and the stereocentres in the target were installed by an asymmetric dihydroxylation reaction. Conversion of the monoprotected triol so obtained to the triacetate **184** was necessary to enable purification. Deacetylation on a basic ion exchange resin provided (–)-swainsonine.

The same strategy was used, but with (*R*)-1-(2,4,6-triisopropylphenyl)ethanol as the chiral auxiliary, to prepare *ent*-**181**. This was dihydroxylated and protected as the acetonide to provide **185**. Reduction of the amide in **185**, followed by acid-catalyzed global deprotection, provided (+)-epicastanospermine (Scheme 29).



Scheme 29. Synthesis of (+)-epicastanospermine from *ent*-**181**.

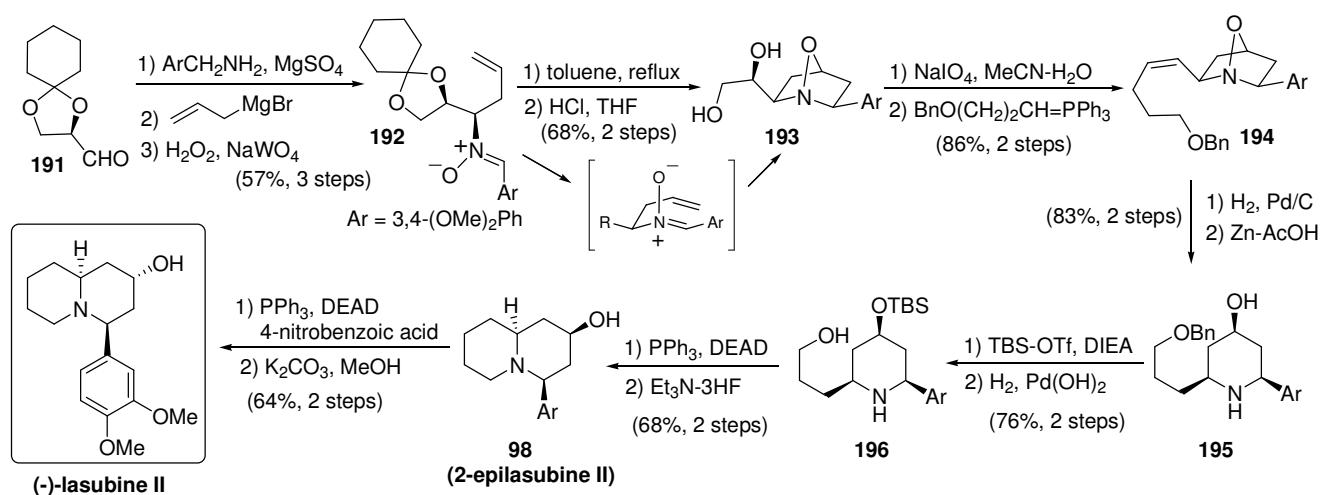
A synthesis of (+)-epilupinine that starts with the enantiomerically enriched 2-vinyl piperidine **186** was reported by Wang, Hu and co-workers.³⁷ The piperidine **186** was prepared from a known, enantiomerically enriched Betti base derivative.^{37b} This synthesis relies on an intramolecular nitrile oxide cycloaddition reaction (Scheme 30).



Scheme 30. Synthesis of (+)-epilupinine *via* an intramolecular nitrile oxide cycloaddition reaction.

The cycloaddition substrate was prepared from **186** by the Fukuyama procedure³⁸ which involves *N*-alkylation with 3-chloropropanol, elaboration of the alcohol into the *N*-tosyl-*O*-TBS hydroxylamine derivative **187** and generation of the oxime **188** by exposure of **187** to CsF. Oxidation of the oxime with NaOCl generated the nitrile oxide which underwent an intramolecular [3+2] cycloaddition to provide the isoxazoline **189** as a single diastereomer. Cleavage of the N–O bond in **189** and hydrolysis provided **190** which was deoxygenated, by reduction of the corresponding dithiolane, to provide (+)-epilupinine.

An intramolecular nitron cycloaddition strategy was employed in the synthesis of (–)-lasubine by Chattopadhyay (Scheme 31).³⁹ The requisite chiral nitron was prepared from the (*R*)-glyceraldehyde derivative **191**. Addition of allylmagnesium bromide to the (3,4-dimethoxybenzyl)imine of **191** proceeded with moderate diastereoselectivity (82:18 dr) and the major *syn* diastereomer of the secondary amine product was separated and carried further. Interestingly, this low diastereoselectivity is in contrast to the highly selective *anti* addition of a vinyl Grignard reagent to the *N*-benzyl imine of the (*R*)-glyceraldehyde acetonide **150** (see the conversion of **150** to **151**, Scheme 25). Clearly, small changes in the structure of the imine have a significant influence on the diastereoselectivity of nucleophilic additions.

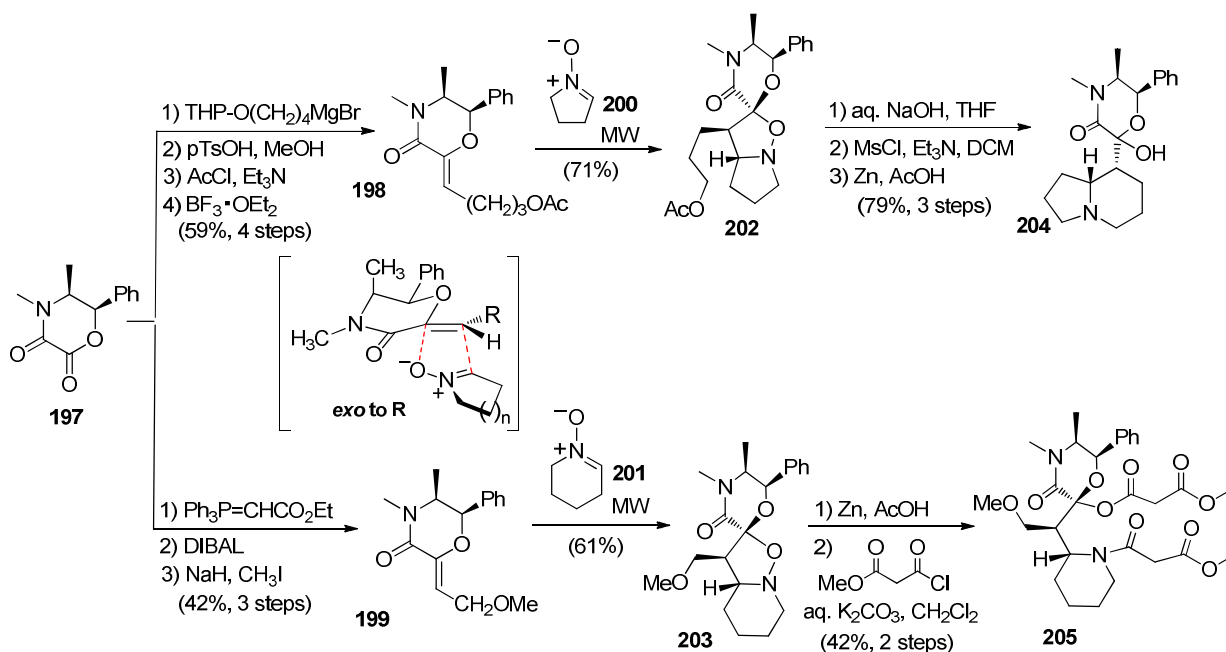


Scheme 31. Intramolecular [3+2] cycloaddition strategy for the synthesis of (–)-lasubine.

Oxidation of the secondary amine provided exclusively the *Z*-nitron **192** which, after intramolecular [3+2] cycloaddition (presumably *via* the transition state assembly shown in Scheme 31) and hydrolysis of the ketal, provided **193** (~11:1 dr). Oxidative cleavage of the diol in **193** to the aldehyde and an ensuing Wittig olefination provided **194**. A two step reduction of **194** provided **195** with retention of the benzyl ether. This was converted into the monoprotected aminodiols **196** which provided the quinolizidine **98** (see Scheme

16) by Mitsunobu cyclization and removal of the TBS protection. Finally, inversion of the secondary alcohol in **98** provided (–)-lasubine II (as in Scheme 16). The authors note that this methodology can also be applied to the synthesis of (+)-lasubine II, since the addition of an allylzinc reagent to **191** provides the diastereomer of **192**.

Recently, Pansare and Thorat developed a general strategy for the synthesis of 1-hydroxymethyl-quinolizidine and 8-hydroxymethylindolizidine stereoisomers.⁴⁰ This approach relies on a regio- and stereoselective 1,3-dipolar cycloaddition of achiral nitrones with ephedrine-derived alkylidene morpholinones. The intermediate isoxazolidines are converted into either an indolizidine or a quinolizidine depending on the nitron and the substituent on the chiral alkene. The methodology was applied to the synthesis of (+)-epitashiromine and in formal syntheses of (+)-epilupinine and (+)-tashiromine (Schemes 32 and 33). The synthesis begins with the morpholinone **197** which was converted into the alkylidene morpholinones **198** and **199** either by addition of a carbon nucleophile to the lactone carbonyl, followed by dehydration (as for **198**) or by a Wittig reaction of the lactone carbonyl (as for **199**, Scheme 32).

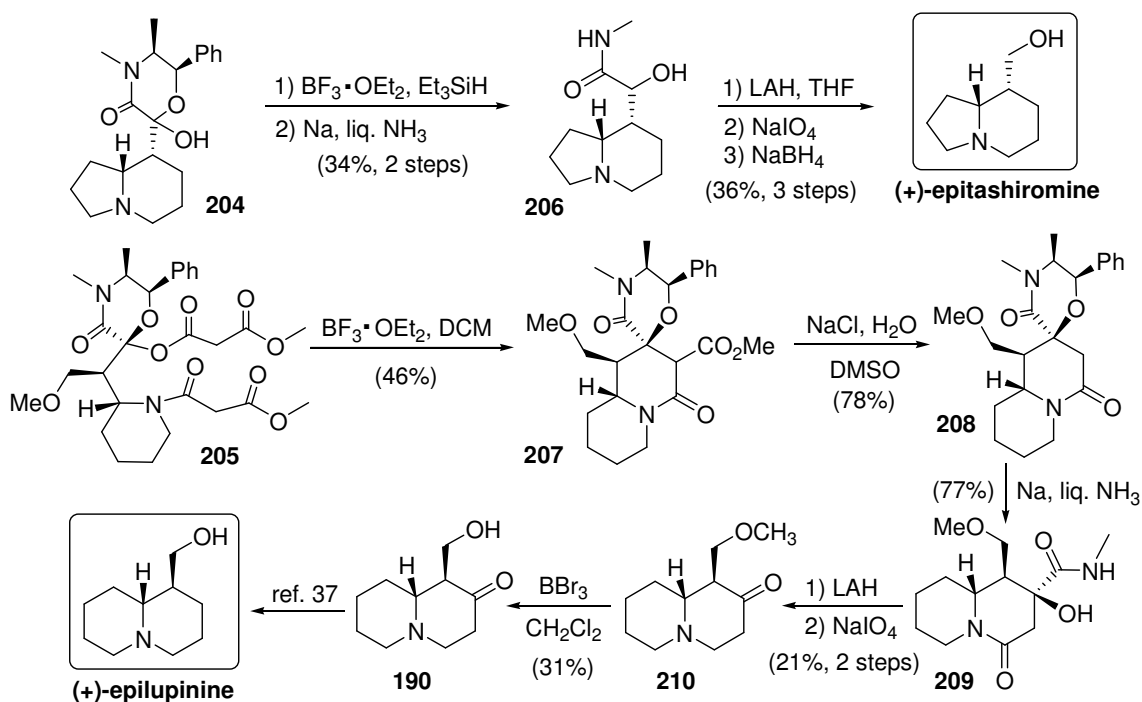


Scheme 32. Regio- and diastereoselective [3+2] cycloadditions of chiral alkylidene morpholinones.

Cycloaddition reactions of **198** and **199** were conducted under microwave irradiation. The reaction of **198** with nitron **200** and of **199** with nitron **201** provided the spiro isoxazolidines **202** and **203**, respectively, both as single diastereomers. The strategy for converting **202** into the indolizidine motif involved a ring formation of the nitron-derived pyrrolidine ring with the alkyl group on the dipolarophile and hence, the side chain in **202** was first activated as a mesylate. Reductive cleavage of the isoxazolidine ring in **202** liberated the secondary amine which cyclized *in situ* to provide the functionalized indolizidine **204**. Conversely, the tactic for building the quinolizidine core from **203** involved a ring formation with the morpholinone section. In this approach, the methoxymethyl group from the dipolarophile would eventually become a substituent in the target. Accordingly, **203** was first reduced and then bis-acylated to provide **205**. The conversion of **204** and **205** into the targets is summarized in Scheme 33.

Reduction of the hemiacetal in **204**, followed by a reductive removal of the ephedrine portion, provided **206**. Conversion of the hydroxy amide side chain into a hydroxymethyl group was achieved by

reduction to the amino alcohol, oxidative cleavage to the aldehyde and reduction to the alcohol. This three step procedure provided (+)-epitashiromine from **206**. In the other synthetic route, generation of an oxonium ion from the activated hemiacetal in **205** and its intramolecular capture provided **207** which was decarboxylated to **208**. Reductive removal of the ephedrine portion and oxidative removal of the hydroxy amide functionality provided **209** which was converted to the ketone **190**, a known precursor^{37a} of (+)-epilupinine (see Scheme 30). This constitutes a formal synthesis of (+)-epilupinine. Notably, this is the only synthetic strategy that provides access to either isomer (*syn* or *anti*) of the hydroxymethyl-substituted indolizidines and quinolizidines.



Scheme 33. Synthesis of (+)-epitashiromine and (+)-epilupinine from **204** and **205**, respectively.

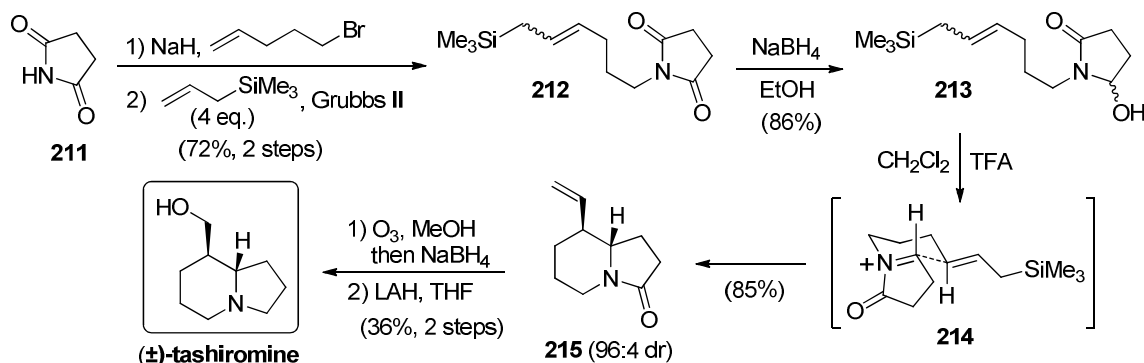
3.4. Iminium ion-based approaches

The applications of *N*-acyliminium ions in the synthesis of piperidine ring-containing alkaloids have been recently reviewed by Remuson^{2e} and hence only those iminium ion-based strategies reported after this review are included in this section. The unique feature of all of these studies is the rapid assembly of the heterocyclic core of the targets from acyclic precursors and they are among the most concise syntheses reported for the targets covered in this review.

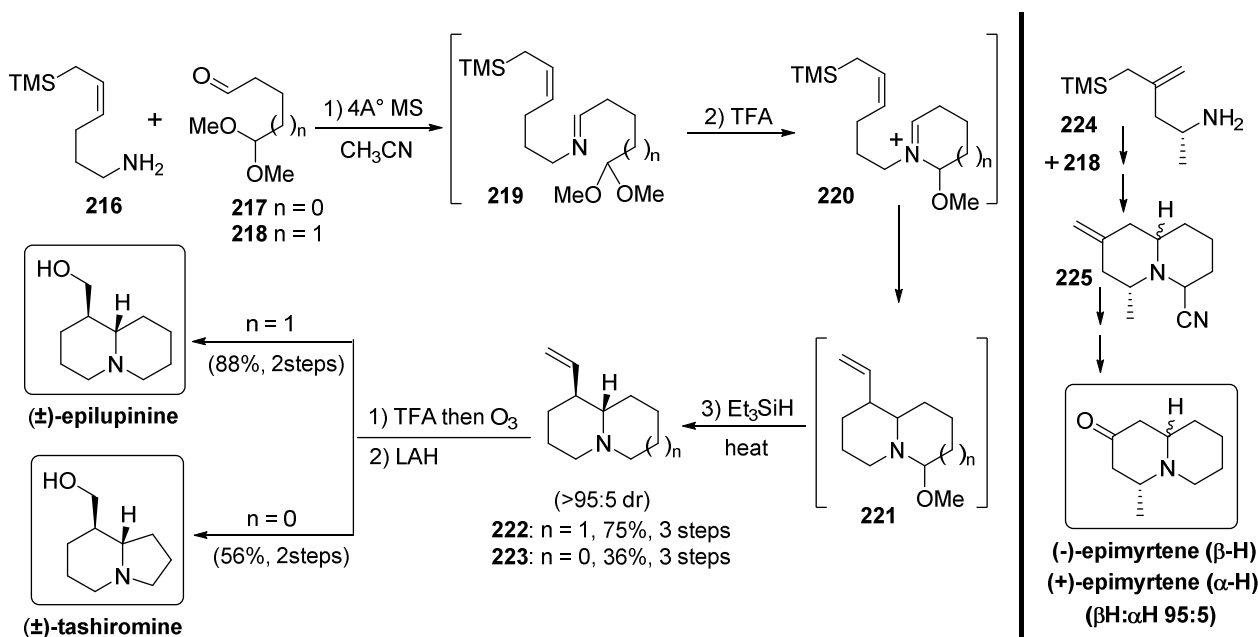
A simple *N*-acyliminium ion-based strategy for synthesis of (\pm)-tashiromine was reported by Marsden and McElhinney.⁴¹ The requisite iminium ion precursor was prepared from succinimide (**211**, Scheme 34). *N*-alkylation of **211** with 5-bromopentene and cross metathesis of the alkenyl succinimide with allyltrimethyl silane provided **212** which was partially reduced to the hydroxy lactam **213**. Treatment of **213** with trifluoroacetic acid smoothly effected its conversion to the indolizidinone **215** via the intermediacy of **214**. The authors suggest that the intramolecular capture of the iminium ion proceeds via a chair-like transition state assembly (**214**) to provide **215** with the shown stereochemistry. Reductive ozonolysis of **215** and subsequent reduction provided (\pm)-tashiromine.

Employing a closely related iminium ion allylation strategy, Martin and co-workers⁴² have developed syntheses of (\pm)-epilupinine, (\pm)-tashiromine and (–)-epimyrtene (Scheme 35). Their approach relies on the

protonation and intramolecular allylation of a preformed imine. Thus, condensation of the aminosilane **216** with the monoprotected dialdehyde **217** or **218** provided the corresponding imine **219** which, upon protonation to the iminium ion **220**, underwent a facile intramolecular allylation to provide the bicyclic *N,O*-acetal **221**. Further, ionization of **221** *in situ* provided the corresponding iminium ion which was reduced with triethylsilane to provide either **222** or **223** depending on the aldehyde used. Presumably, the key cyclization step proceeds through a chair-like transition state assembly similar to **214** (Scheme 34). The conversion of **222** to (±)-epilupinine and of **223** to (±)-tashiromine was achieved by ozonolysis of the vinyl group and reduction of the product aldehyde.



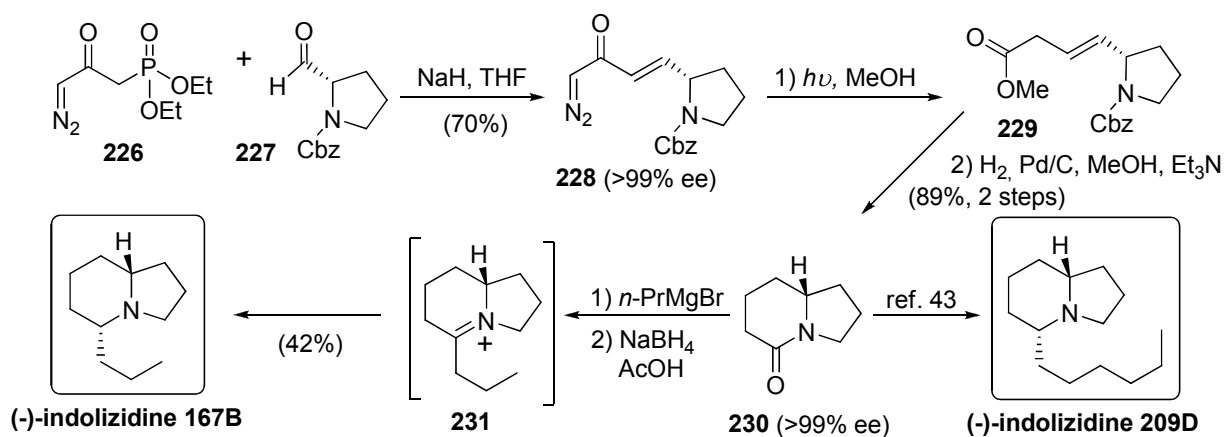
Scheme 34. Stereoselective, intramolecular *N*-acyliminium ion capture in the synthesis of (±)-tashiromine.



Scheme 35. Intramolecular, iminium ion silylation strategy for (±)-epilupinine, (±)-tashiromine and (-)-epimyrtene.

Employing a similar strategy, but starting with the enantiomerically enriched aminosilane **224** and the aldehyde **218**, the quinolizidine **225** was obtained (NaCN capture of iminium ion instead of reduction). This was converted to (-)-epimyrtene (95:5 dr) which was obtained as an inseparable mixture with (+)-myrtene.

The stereoselective reduction of an indolizidinone-derived iminium ion⁴³ was employed as a pivotal step in the synthesis of (-)-indolizidine 167B reported by Pinho and Burtoloso.⁴⁴ This synthesis relies on the Wolff rearrangement of an α -diazo- α' , β' -unsaturated ketone to the corresponding β,γ -unsaturated ester, for the construction of the indolizidinone precursor (Scheme 36).



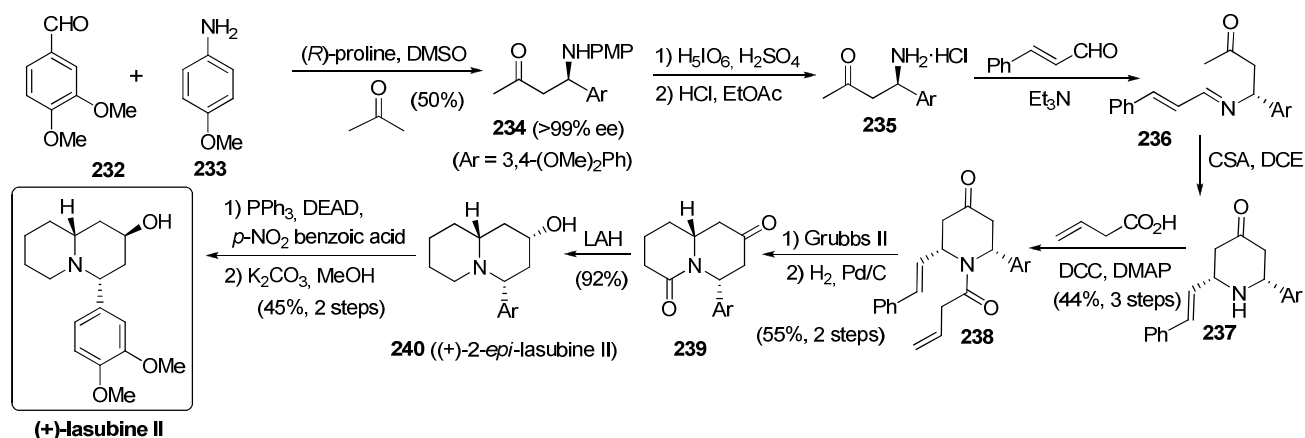
Scheme 36. A Wolff rearrangement/iminium ion reduction strategy for (–)-indolizidine 167B.

Reaction of diethyl 3-diazo-2-oxopropylphosphonate (**226**) with the (*S*)-*N*-Cbz-prolinal (**227**) provided the unsaturated α -diazo ketone **228**. A photochemically initiated Wolff rearrangement of **228** provided the ester **229** which cyclized to the indolizidinone **230** upon hydrogenation. Addition of propylmagnesium bromide presumably generated the corresponding indolizidinol which is converted to the iminium ion **231** with acetic acid. Stereoselective reduction of **231** with sodium borohydride provided (–)-indolizidine 167B. The indolizidinone **230** is also a known intermediate³⁹ to (–)-indolizidine 209D.

3.5. Syntheses involving organocatalysis

In keeping with the current interest in organocatalysis,⁴⁵ applications of carbon-carbon bond forming organocatalytic reactions have been investigated for the synthesis of indolizidine and quinolizidine alkaloids. These studies have relied on an organocatalytic reaction for the construction of a single stereocentre, which in turn is employed in a subsequent diastereoselective process for establishing additional stereocentres in the target alkaloids.

Rutjes and co-workers have utilized two organocatalytic Mannich reactions as key steps in their synthesis of (+)-lasubine II.⁴⁶ In the first Mannich reaction the imine, generated *in situ* from 3,4-dimethoxybenzaldehyde (**232**) and *p*-anisidine (**233**), reacted enantioselectively with a (*R*)-proline and acetone derived enamine to provide the β -aminoketone **234** (>99% ee, Scheme 37).

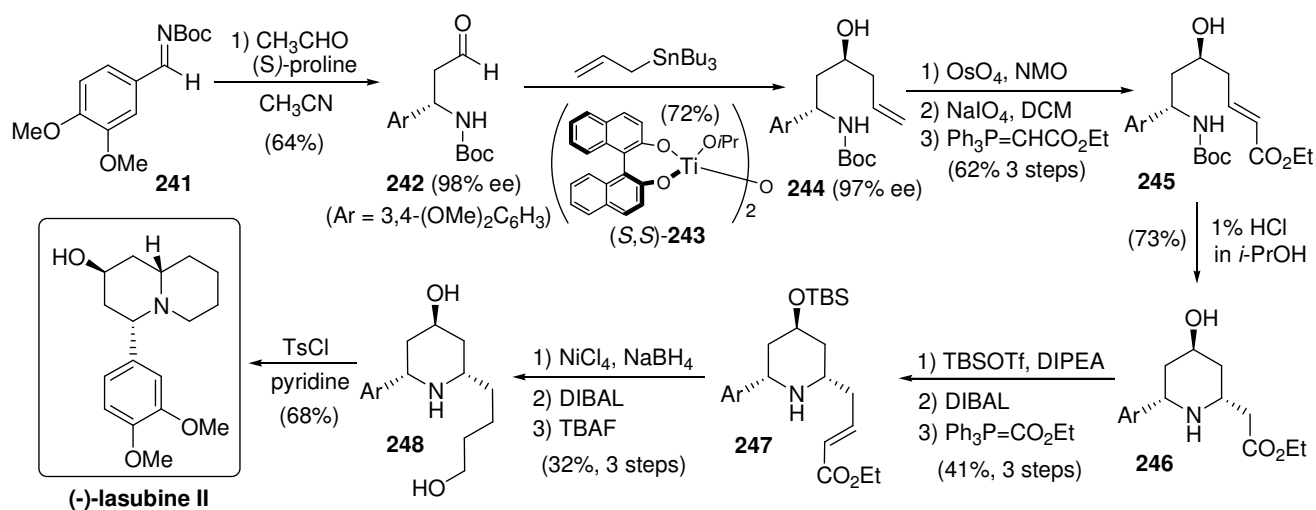


Scheme 37. Inter- and intramolecular organocatalytic Mannich reactions in the synthesis of (+)-lasubine II.

Deprotection of **234**, followed by condensation with *trans*-cinnamaldehyde, provided the imine **236**. In the second, organic acid-catalyzed, intramolecular Mannich reaction **236** was cyclized to the key piperidine

intermediate **237**. Notably, **237** is obtained as single diastereomer, presumably the outcome of a *cis*-diequatorial orientation of the two substituents during formation of the six-membered ring. The piperidine was elaborated into the diene **238** which was subjected to a RCM reaction to provide the indolizidine dione **239** which, upon complete reduction, provided 2-*epi*-lasubine **240**. Finally, Mitsunobu inversion of the secondary alcohol in **240** provided (+)-lasubine II.

The enantioselective organocatalytic Mannich reaction of a pre-formed, *N*-Boc imine was used as the key step by Chandrasekhar and co-workers in their synthesis of (–)-lasubine II.⁴⁷ This synthesis begins with the imine **241** which was used in an enantioselective, (*S*)-proline-catalyzed aldol reaction with acetaldehyde to provide the β-aminoaldehyde **242** (97% ee, Scheme 38). Alkylation of this aldehyde in the presence of a chiral titanium catalyst **243**⁴⁸ provided the amino alcohol **244** which incorporates two of the three stereocentres in the target. The allyl group in **244** was then elaborated further *via* an oxidative cleavage-Wittig olefination protocol to provide the unsaturated ester **245**. Deprotection of **245** and intramolecular *aza*-Michael addition of the resulting amino ester provided **246** as a single diastereomer (2,6-diequatorial isomer, similar to **237**, Scheme 37).



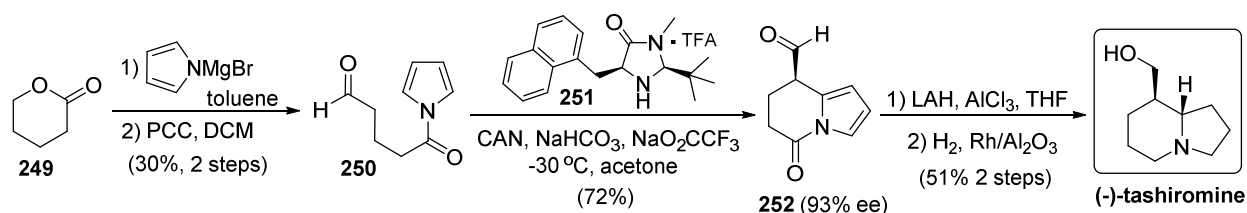
Scheme 38. Intermolecular organocatalytic Mannich and intermolecular *aza*-Michael reactions in the synthesis of (–)-lasubine II.

Elaboration of **246** into the target was fairly straightforward. Protection of the alcohol and side-chain extension by reduction of the ester to the aldehyde and Wittig olefination provided **247**. Conjugate reduction of the double bond in **247** with nickel boride, followed by reduction of the obtained saturated ester with DIBAL, provided the primary alcohol. Subsequent deprotection of the secondary alcohol provided **248**. Selective tosylation of the primary alcohol in **248** resulted in cyclization to provide (–)-lasubine II.

A remarkably short, organo-SOMO catalysis-based, synthesis of (–)-tashiromine was reported by MacMillan and co-workers.⁴⁹ This strategy relies on the enantioselective α-arylation of aldehydes, a reaction that is achieved by catalytic iminium ion formation of the aldehyde component in the presence of an inorganic oxidant and a suitable aromatic nucleophile. The intramolecular version of this tactic was applied in the synthesis (–)-tashiromine (Scheme 39).

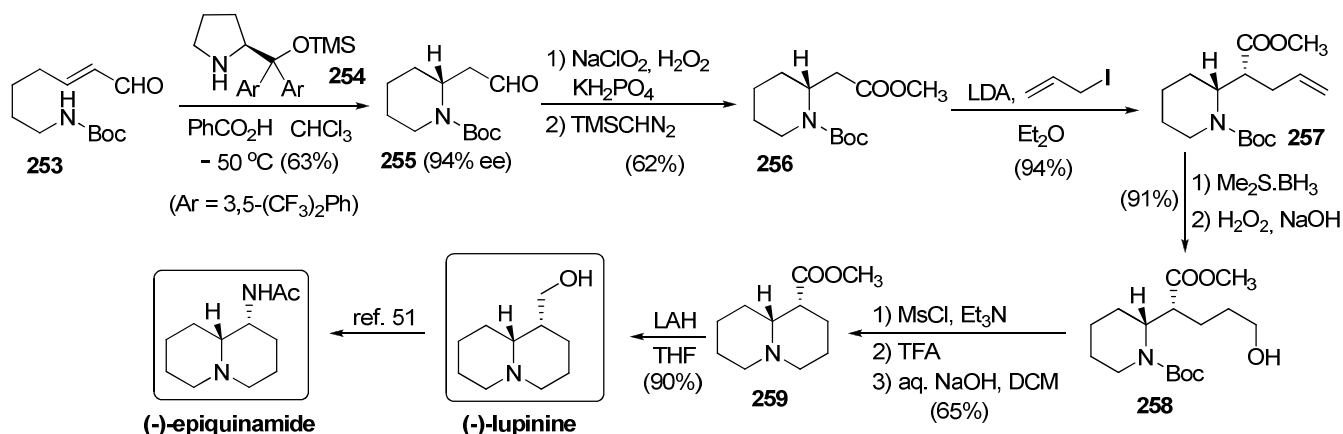
The required arylaldehyde was prepared from the lactone **249** by treatment with the magnesium salt of pyrrole (prepared *in situ* by deprotonation of pyrrole with MeMgBr) and oxidation of the alcohol product to provide aldehyde **250**. In the key step, the aldehyde was converted into the corresponding iminium ion by

exposure to a catalytic amount of the imidazolidinone salt **251** and oxidation of the transient iminium ion with ceric ammonium nitrate. This resulted in an enantioselective, intramolecular α -arylation reaction to ultimately provide the tetrahydroindolizinone **252** (93% ee). Reduction of the aldehyde and the lactam in **252**, followed by hydrogenation of the pyrrole portion, provided (–)-tashiromine.



Scheme 39. Enantioselective intramolecular aldehyde α -arylation-based synthesis of (–)-tashiromine.

An enantimerically enriched piperidine derivative was used as the key starting material by Fustero, del Pozo and co-workers in their syntheses of (–)-lupinine, (+)-myrtene and a formal synthesis of (–)-epiquinamide.⁵⁰ The requisite starting material was prepared by an iminium ion catalyzed intramolecular *aza*-Michael reaction of the *N*-Boc amino enal **253**^{50b} (Scheme 40).



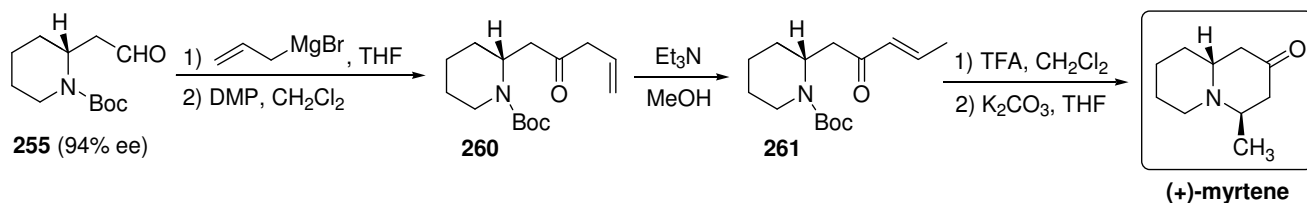
Scheme 40. Synthesis of (–)-lupinine relying on an organocatalytic intramolecular *aza*-Michael reaction.

Treatment of **253** with a catalytic amount of the (*S*)-diarylprolinol derivative **254** provided the 2-(2-oxoethyl)piperidine derivative **255** which was readily converted into the ester **256**. A highly diastereoselective allylation of **256** provided **257** which incorporates both of the required stereocentres in the target. Elaboration of the terminal alkene in **257** into a primary alcohol **258** and subsequent activation and cyclization provided the quinolizidine **259**. This was reduced to provide (–)-lupinine.

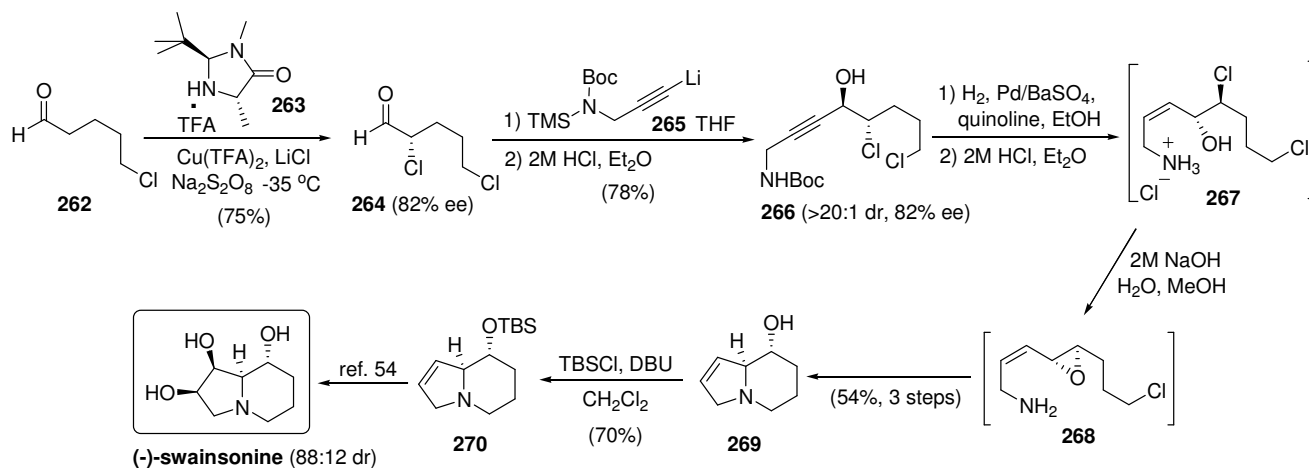
The conversion of (–)-lupinine to (–)-epiquinamide *via* oxidation of the primary alcohol, Curtius rearrangement of the obtained acid to the primary amine and acetylation to provide (–)-epiquinamide was reported recently.⁵¹ Hence the above synthetic route also constitutes a formal synthesis of (–)-epiquinamide.

The pyrrolidine **255** was also used in a short synthesis of (+)-myrtene (Scheme 41). Conversion of the aldehyde in **255** to the allyl ketone **260** was readily achieved by addition of allylmagnesium bromide and oxidation of the obtained secondary alcohol. Base-catalyzed conjugative isomerization of **260** provided **261**. Deprotection of the amine in **261** and cyclization onto the enone side chain provided (+)-myrtene as a single diastereomer. An organocatalysis-based, formal synthesis of (–)-swainsonine was recently reported by Britton and co-workers.⁵² In the initial organocatalytic step, 5-chloropropanal (**262**) was subjected to

MacMillan's SOMO-activated aldehyde α -chlorination procedure.⁵³ Notably, the use of imidazolidinone **263** and conducting the reaction at low temperature is necessary to avoid racemization of the α -chloroaldehyde product **264** (82% ee, Scheme 42).



Scheme 41. Synthesis of (+)-myrtene from the pyrrolidine **237**.



Scheme 42. Organocatalysis based formal synthesis of (–)-swainsonine.

Addition of the protected propargylamine derived anion **265** to the aldehyde **264** proceeded with high diastereoselectivity to provide the *anti*-chlorohydrin **266**. Partial hydrogenation of **266** to the *cis*-alkene and deprotection of the amine provided **267**. Treatment of **267** with sodium hydroxide effected the critical cyclization steps in the synthesis. Presumably, the chlorohydrin cyclized to provide the epoxide **268** which, upon a double cyclization, provided the hydroxyindolizine **269**. Protection of **269** as the TBS ether provided **270** which is a known intermediate to (–)-swainsonine.⁵⁴

4. Closing remarks

The syntheses presented in the foregoing sections are testament to the continuing interest in the indolizidine and quinolizidine ring systems. It is also evident that the indolizidine and quinolizidine alkaloids are deceptively simple synthetic targets which demand a high level of synthetic creativity and sophistication. Most of the asymmetric syntheses have relied on enantiomerically enriched starting materials. Interestingly, some of the most concise strategies have, so far, examined the synthesis of only racemic products. Asymmetric modifications of these approaches will certainly be the next challenge. It is notable that, of the syntheses described above, only a few have utilized a metal-based asymmetric catalyst for a pivotal, stereochemistry-determining step. In this context, the recent organocatalysis-based synthetic strategies are noteworthy. These represent a notable advance in the area of indolizidine and quinolizidine synthesis. There is no doubt that, as a prominent group of structurally diverse alkaloids, the indolizidines and quinolizidines will continue to engage present and future generations of synthetic chemists.

Acknowledgement

Financial support from the Natural Sciences and Engineering Research Council of Canada is gratefully acknowledged.

References

- (a) Daly, J. W.; Spande, T. F.; Garrafo, H. M. *J. Nat. Prod.* **2005**, *68*, 1556. (b) Lourenco, A. M.; Maximo, P.; Ferreira, L. M.; Pereira, M. M. A. *Studies in Nat. Prods. Chem.* **2002**, *27 (Part H)*, 233. (c) Liljefors, T.; Boegesoe, K. P.; Hyttel, J.; Wikstroem, H.; Svensson, K.; Carlsson, A. *J. Med. Chem.* **1990**, *33*, 1015. (d) Tsuneki, H.; You, Y.; Naoki, T.; Kagawa, S.; Kobayashi, S.; Sasaoka, T.; Nemoto, H.; Kimura, I.; Dani, J. A. *Mol. Pharmacol.* **2004**, *66*, 1061. (e) King, F. D.; Hadley, M. S.; McClelland, C. M. *J. Med. Chem.* **1988**, *31*, 1708. (f) Bogeso, K. P.; Arnt, J.; Lundmark, M.; Sundell, S. *J. Med. Chem.* **1987**, *30*, 142. (g) Gomez, L.; Garrabou, X.; Joglar, J.; Bujons, J.; Parella, T.; Vilaplana, C.; Cardona, P. J.; Clapes, P. *Org. Biomol. Chem.* **2012**, *10*, 6309.
- Recent reviews: (a) Michael, J. P. *Nat. Prod. Rep.* **2008**, *25*, 139. (b) Honda, T. *Heterocycles* **2011**, *83*, 1. (c) Perreault, S.; Rovis, T. *Chem. Soc. Rev.* **2009**, *38*, 3149. (d) Michael, J. P. *Beil. J. Org. Chem.* **2007**, *3*, No. 10, doi: 10.1186/1860-5397-3-27. (e) Remuson, R.; Gelas-Mialhe, Y. *Mini-Rev. Org. Chem.* **2008**, *5*, 193.
- Stead, D.; O'Brien, P.; Sanderson, A. *Org. Lett.* **2008**, *10*, 1409.
- (a) Hoppe, D.; Hintze, F.; Tebben, P. *Angew. Chem., Int. Ed. Engl.* **1990**, *29*, 1422. (b) Beak, P.; Kerrick, S. T.; Wu, S.; Chu, J. *J. Am. Chem. Soc.* **1994**, *116*, 3231.
- Fleurant, A.; Celerier, J. P.; Lhommet, G. *Tetrahedron: Asymmetry* **1992**, *3*, 695.
- Pereira, E.; Alves, C. F.; Bockelmann, M. A.; Pilli, R. A. *Quim. Nova* **2008**, *31*, 771.
- Wu, H.; Yu, M.; Zhang, Y.; Zhao, G. *Chin. J. Chem.* **2009**, *27*, 183.
- Wong, H.; Garnier-Amblard, E. C.; Liebeskind, L. S. *J. Am. Chem. Soc.* **2011**, *133*, 7517.
- Hajri, M.; Blondelle, C.; Martinez, A.; Vasse, J.-L.; Szymoniak, J. *Tetrahedron Lett.* **2013**, *54*, 1029.
- Vilaivan, T.; Winotapan, C.; Banphavichit, V.; Shinada, T.; Ohfune, Y. *J. Org. Chem.* **2005**, *70*, 3464.
- Pinho, V. D.; Procter, D. J.; Burtoloso, A. C. B. *Org. Lett.* **2013**, *15*, 2434.
- Wijdeven, M. A.; Wijtmans, R.; van den Berg, R. J. F.; Noorduyn, W.; Schoemaker, H. E.; Sonke, T.; van Delft, F. L.; Blaauw, R. H.; Fitch, R. W.; Spande, T. F.; Daly, J. W.; Rutjes, F. P. J. *Org. Lett.* **2008**, *10*, 4001.
- Santos, L. S.; Mirabal-Gallardo, Y.; Shankariah, N.; Simirgiotis, M. J. *Synthesis* **2011**, 51.
- Chiou, W.-H.; Lin, Y.-H.; Chen, G.-T.; Gao, Y.-K.; Tseng, Y.-C.; Kao, C.-L.; Tsai, J.-C. *Chem. Commun.* **2011**, *47*, 3562.
- Archibald, G.; Lin, P.-C.; Boyd, P.; Barker, D.; Caprio, V. *J. Org. Chem.* **2005**, *77*, 7968.
- Chen, M.-J.; Tsai, Y.-M. *Tetrahedron* **2011**, *67*, 1564.
- Wardrop, D. J.; Bowen, E. G. *Org. Lett.* **2011**, *13*, 2379.
- Chandrasekhar, S.; Parida, B. B.; Rambabu, C. *Tetrahedron Lett.* **2009**, *50*, 3294.
- Guo, C.; Lu, X. *J. Chem. Soc., Chem. Commun.* **1993**, 394.
- Voituriez, A.; Ferreira, F.; Pérez-Luna, A.; Chemla, F. *Org. Lett.* **2007**, *9*, 4705.
- Airiau, E.; Spangenberg, T.; Girard, N.; Breit, B.; Mann, A. *Org. Lett.* **2010**, *12*, 528.
- (a) Lim, J.; Kim, G. *Tetrahedron Lett.* **2008**, *50*, 88. (b) For the synthesis of amino ester **95**, see: Chalard, P.; Remuson, R.; Gelas-Mialhe, Y.; Gramain, J.-C. *Tetrahedron: Asymmetry* **1998**, *9*, 4391.
- Ma, D.; Zhu, W. *Org. Lett.* **2001**, *3*, 3927.
- Cutter, A. C.; Miller, I. R.; Kelly, J. F.; Bellingham, R. K.; Light, M. E.; Brown, R. C. *Org. Lett.* **2011**, *15*, 3988.
- Pronin, S. V.; Tabor, M. G.; Jansen, D. J.; Shenvi, R. A. *J. Am. Chem. Soc.* **2012**, *134*, 2012.
- (a) Reddy, C. R.; Latha, B.; Rao, N. N. *Tetrahedron* **2012**, *68*, 145. (b) Reddy, P. G.; Baskaran, S. *J. Org. Chem.* **2004**, *69*, 3093.
- (a) Pohmakotr, M.; Seubsai, A.; Numechai, P.; Tuchinda, P. *Synthesis* **2008**, 1733. (b) Pohmakotr, M.; Prateptongkum, S.; Chooprayoon, S.; Tuchinda, P.; Reutrakul, V. *Tetrahedron* **2008**, *64*, 2339.
- Belangér, G.; Larouche-Gauthier, R.; Ménard, F.; Nantel, M.; Barabé, F. *J. Org. Chem.* **2006**, *71*, 704.

29. Chooprayoon, S.; Kuhakarn, C.; Tuchinda, P.; Reutrakul, V.; Pohmakotr, M. *Org. Biomol. Chem.* **2011**, *9*, 531.
30. Gracia, S.; Jerpan, R.; Pellet-Rostaing, S.; Popowycz, F.; Lemaire, M. *Tetrahedron Lett.* **2010**, *51*, 6290.
31. Guazzelli, G.; Lazzaroni, R.; Settambolo, R. *Beil. J. Org. Chem.* **2008**, *4*, No. 2, doi:10.1186/1860-5397-4-2.
32. Ahari, M.; Perez, A.; Manant, C.; Vasse, J.-L.; Szymoniak, J. *Org. Lett.* **2008**, *10*, 2473.
33. (a) Ghosh, S.; Shashidhar, J. *Tetrahedron Lett.* **2009**, *50*, 1177. (b) Badorrey, R.; Cativiela, C.; Díaz-de-Villegaz, M. D.; Gálvez, J. A. *Synthesis* **1997**, 747.
34. Srivastava, A. K.; Das, S. K.; Panda, G. *Tetrahedron* **2009**, *65*, 5322.
35. Reddy, K. K. S.; Rao, B. V.; Raju, S. S. *Tetrahedron: Asymmetry* **2011**, *22*, 662.
36. Ceccon, J.; Greene, A. E.; Poisson, J.-F. *Org. Lett.* **2006**, *8*, 4739.
37. (a) Su, D.; Wang, X.; Shao, C.; Xu, J.; Zhu, R.; Hu, Y. *J. Org. Chem.* **2011**, *76*, 188. (b) Wang, X.; Dong, Y.; Sun, J.; Li, R.; Xu, X.; Hu, Y. *J. Org. Chem.* **2005**, *70*, 1897.
38. Kitahara, K.; Toma, T.; Shimokawa, J.; Fukuyama, T. *Org. Lett.* **2008**, *10*, 2259.
39. Saha, N.; Biswas, T.; Chattopadhyay, S. K. *Org. Lett.* **2011**, *13*, 5128.
40. Thorat, R. G.; Pansare, S. V. *Eur. J. Org. Chem.* **2013**, 7282.
41. Marsden, S. P.; McElhinney, A. D. *Beil. J. Org. Chem.* **2008**, *4*, No. 8, doi:10.1186/1860-5397-4-8.
42. (a) Amorde, S. M.; Jewett, I. T.; Martin, S. F. *Tetrahedron* **2009**, *65*, 3222. (b) Martin, S. F. *Pure Appl. Chem.* **2009**, *81*, 195.
43. Nukui, S.; Sodeoka, M.; Sasai, H.; Shibasaki, M. *J. Org. Chem.* **1995**, *60*, 398.
44. Pinho, V. D.; Burtoloso, A. C. B. *Tetrahedron Lett.* **2012**, *53*, 876.
45. Selected recent reviews: (a) Alemán, J.; Cabrera, S. *Chem. Soc. Rev.* **2013**, *42*, 774. (b) Marson, C. M. *Chem. Soc. Rev.* **2012**, *41*, 7712. (c) Jensen, K. L.; Dickmeiss, G.; Jiang, H.; Albrecht, L.; Jørgensen, K. A. *Acc. Chem. Res.* **2012**, *45*, 248, and references therein.
46. Verkade, J. M. M.; van der Pijl, F.; Willems, M. M. J. H. P.; Quaedflieg, P. J. L. M.; van Delft, F. L.; Rutjes, F. P. J. T. *J. Org. Chem.* **2009**, *74*, 3207.
47. Chandrasekhar, S.; Murali, R. V. N. S.; Raji Reddy, C. *Tetrahedron Lett.* **2009**, *50*, 5686.
48. Hanawa, H.; Hashimoto, T.; Maruoka, K. *J. Am. Chem. Soc.* **2003**, *125*, 1708.
49. Conrad, J. C.; Kong, J.; Laforteza, B. N.; MacMillan, D. W. C. *J. Am. Chem. Soc.* **2009**, *131*, 11640.
50. (a) Fustero, S.; Moscardó, J.; Sánchez-Roselló, M.; Flores, S.; Guerola, M.; del Pozo, C. *Tetrahedron* **2011**, *67*, 7412. (b) Fustero, S.; Jiménez, D.; Moscardó, J.; Catalán, S.; del Pozo, C. *Org. Lett.* **2007**, *9*, 5283.
51. Fitch, R. W.; Sturgeon, G. D.; Patel, S. R.; Spande, T. F.; Garraffo, H. M.; Daly, J. W.; Blaauw, R. H. *J. Nat. Prod.* **2009**, *72*, 243.
52. Dhand, V.; Draper, J. A.; Moore, J.; Britton, R. *Org. Lett.* **2013**, *15*, 1914.
53. Amatore, M.; Beeson, T. D.; Brown, S. P.; MacMillan, D. W. C. *Angew. Chem. Int. Ed.* **2009**, *48*, 5121.
54. Mukai, C.; Sugimoto, Y.; Miyazawa, K.; Yamaguchi, S.; Hanaoka, M. *J. Org. Chem.* **1998**, *63*, 6281.

THIAZOLO[5,4-*d*]THIAZOLE-BASED COMPOUNDS: EMERGING TARGETS IN MATERIALS SCIENCE, ORGANIC ELECTRONICS AND PHOTOVOLTAICS

Lorenzo Zani,^{a,b} Massimo Calamante,^a Alessandro Mordini^a and Gianna Reginato^{*a}

^a*Istituto di Chimica dei Composti Organometallici (CNR-ICCOM), Via Madonna del Piano 10, I-50019 Sesto Fiorentino, Italy (e-mail: gianna.reginato@iccom.cnr.it)*

^b*Istituto per la Sintesi Organica e la Fotoreattività (CNR-ISOF), Via Piero Gobetti 101, I-40129 Bologna, Italy*

Abstract. *Thiazolo[5,4-*d*]thiazoles are fused bicyclic heteroaromatic compounds characterized by a rigid planar backbone and an extended π -conjugated electronic structure. Although they have been known for many decades, interest in their properties and applications has increased only recently, following their incorporation into a series of active materials used in the field of organic electronics. Despite the growing attention surrounding these heterocycles, the synthetic chemistry of thiazolo[5,4-*d*]thiazoles is not yet fully developed: improvements in both their preparation and subsequent elaboration are still required in order to extend the materials scope and optimize their properties. This review will present an overview of the currently available synthetic methods, the properties of the compounds prepared to date and their main applications, focusing in particular on organic (opto)electronics and new generation photovoltaics.*

Contents

1. Introduction
 2. Synthesis, elaboration and characterization of thiazolo[5,4-*d*]thiazoles and related materials
 - 2.1. Synthesis and functionalization of thiazolo[5,4-*d*]thiazoles
 - 2.2. Thiazolothiazole-based polymers
 - 2.3. Structural, photophysical and spectroscopic properties
 3. Applications of thiazolo[5,4-*d*]thiazole-based materials
 - 3.1. Biological activity
 - 3.2. Preparation of metal complexes and crystal engineering
 - 3.3. Non-linear optics and fluorescent sensors/emitters
 - 3.4. Organic light-emitting diodes
 - 3.5. Organic field-effect transistors
 - 3.6. Organic and polymeric solar cells
 - 3.7. Dye-sensitized solar cells
 4. Conclusions
- Acknowledgments
References

1. Introduction

Thiazolo[5,4-*d*]thiazole (TzTz) is one of the possible regioisomeric heterocycles formally derived from the [3.3.0] fusion of two thiazole rings (Figure 1). Thiazolo[5,4-*d*]thiazoles, and especially those in which the central bicyclic core is flanked by (hetero)aromatic rings, usually display a rigid and planar backbone

and are characterized by an extended π -conjugated electronic structure. Such properties lead to the possibility of strong π - π stacking and efficient intermolecular charge transfer in the solid state. In addition, compared to similar bicyclic thiophene derivatives, the thiazolothiazole ring is more electron-deficient due to the presence of the additional nitrogen atoms and therefore shows superior oxidative stability.¹ While such features are potentially useful in the field of materials and semiconductors science (see Section 3), they are often accompanied by limited solubility in organic solvents, sometimes resulting in difficult purification, derivatization and handling. Such problem is usually addressed by appropriate molecular design, introducing suitable solubilizing moieties on the heterocyclic scaffold.

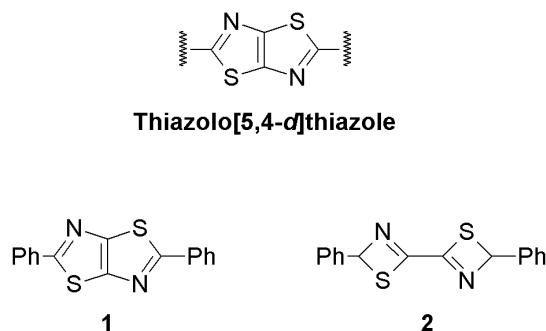


Figure 1

The first compound of this class, 2,5-diphenylthiazolo[5,4-*d*]thiazole (**1**, Figure 1), was probably prepared already in 1891 by Ephraim, who carried out the condensation of benzaldehyde with dithiooxamide (also known as rubeanic acid).² However, in that occasion the wrong molecular formula ($C_{16}H_{12}N_2S_2$) was assigned to the product and, consequently, it was proposed to have a rather unusual bithiazethine structure (**2**). It was only almost seventy years later that Johnson and Ketcham established the real nature of the condensation product based on extensive spectroscopic studies of a series of analogues, which showed a symmetric structure devoid of aliphatic C–H bonds.³

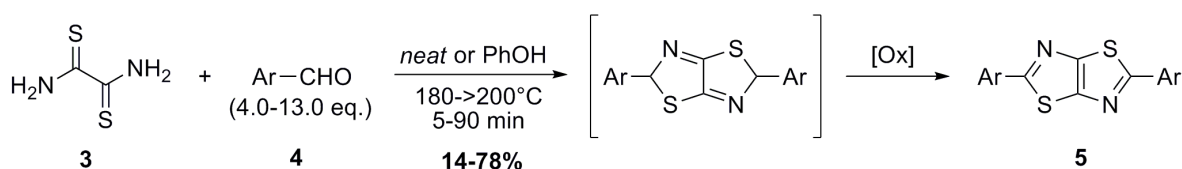
For several years after its discovery, the thiazolo[5,4-*d*]thiazole ring system attracted relatively small attention from the scientific community and consequently reports dealing with its synthesis and elaboration, as well as its properties and applications, remained somewhat scarce. In the last decade, however, interest in this class of compounds grew dramatically, especially thanks to some early studies concerning their application in organic electronics, in particular in light-emitting diodes (OLEDs)⁴ and organic field-effect transistors (OFETs).^{5,6} Following these initial reports, an ever increasing number of small molecules and polymeric materials incorporating the thiazolo[5,4-*d*]thiazole unit has been described in the literature and employment in various fields, including organic electronics, crystal engineering, non-linear optics and photovoltaics, has been investigated.¹

Despite the remarkable increase in the number of publications witnessed in recent years, the chemistry of thiazolo[5,4-*d*]thiazoles remains underdeveloped compared to that of other classes of heterocyclic compounds; therefore, it appears that significant improvements are still possible, both in terms of synthetic methods efficiency as well as materials scope and properties. This review will review the currently available synthetic methods, the physico-chemical properties of the resulting compounds and their main applications, with the aim of stimulating further research in this promising area of heterocyclic chemistry.

2. Synthesis, elaboration and characterization of thiazolo[5,4-*d*]thiazoles and related materials

2.1. Synthesis and functionalization of thiazolo[5,4-*d*]thiazoles

As mentioned above, after the initial studies of Ephraim,² the actual structure of thiazolo[5,4-*d*]thiazoles was determined by Johnson and Ketcham, who were also the first to prepare a wide range of diaryl-substituted derivatives.³ The reactions were carried out by refluxing dithiooxamide (**3**) with a moderate to large excess of an aromatic aldehyde **4** (4.0–13.0 eq.), either in solvent-free conditions or in the presence of phenol as a high boiling point solvent (Scheme 1); notably, the intermediate stemming from the condensation of two molecules of aldehyde with dithiooxamide underwent spontaneous dehydrogenation to give final product **5**. Usually the products were insoluble solids which were recovered from the reaction mixture by simple filtration. In general, yields were moderate but in a few cases they exceeded 60%; however, the reaction conditions were quite harsh and temperatures above 180 °C had to be applied for the transformations to proceed. Finally, the reaction was reported to be unsuccessful for the conversion of aliphatic substrates.



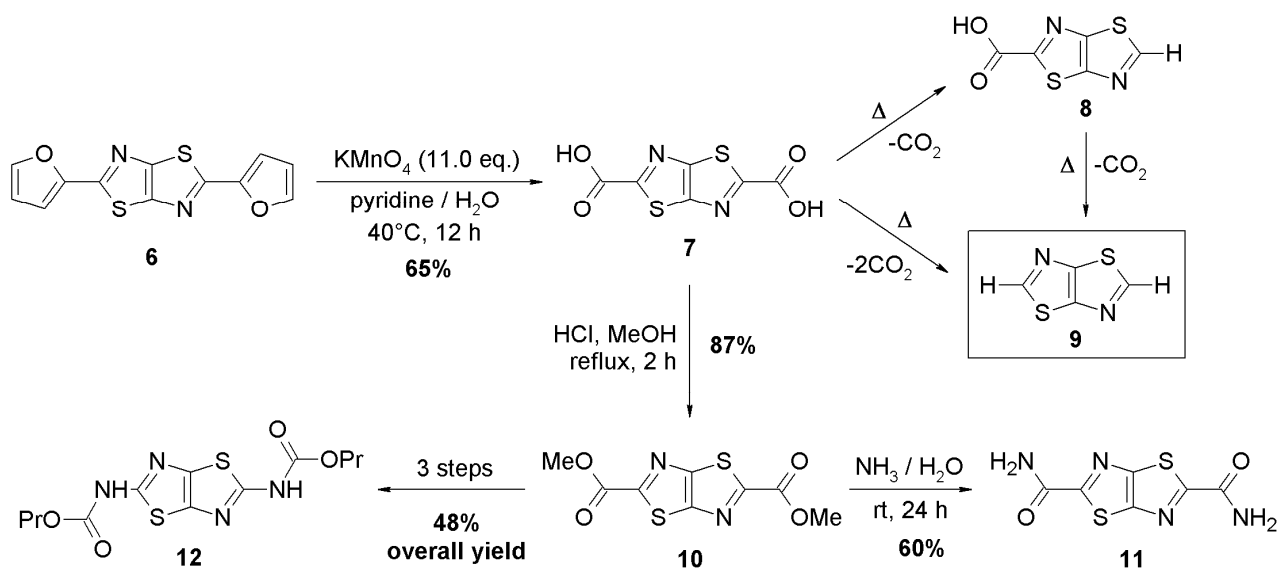
Scheme 1

Following the above report, some improvements of the same protocol were later described, mostly based on simple modifications of the reaction conditions. Preston suggested the employment of *N,N*-dimethylacetamide as the solvent,⁷ while Thomas used *N,N*-dimethylformamide:⁸ this resulted in more controlled reactions, allowing to increase the yields and reduce the amount of aldehyde used in the process. More recently, it was shown that slightly milder reaction conditions could be applied by using nitrobenzene as the solvent: in this case, conversion of a small library of aromatic and heteroaromatic aldehydes took place in one day at 130 °C under strictly stoichiometric conditions, affording products in 37–79% yield.⁹

The synthesis of the parent heterocycle, namely thiazolo[5,4-*d*]thiazole (**9**), was reported by Ketcham and co-workers only a decade after their first study and was based upon the ingenious manipulation of 2,5-*bis*-2-furylthiazolo[5,4-*d*]thiazole (**6**), in turn obtained from furfural.¹¹ Oxidation of compound **6** by means of potassium permanganate afforded 2,5-thiazolothiazolecarboxylic acid (**7**), which underwent decarboxylation upon melting to give initially 2-thiazolothiazolecarboxylic acid (**8**) and, after loss of a further equivalent of carbon dioxide, thiazolo[5,4-*d*]thiazole itself (**9**, Scheme 2). Compound **9** showed the properties of a stable aromatic system and was found to have a strong electrophilic character; accordingly, reactions typical of nucleophilic aromatic compounds, such as nitrations, direct brominations and Friedel-Crafts acylations were unsuccessful. Elaboration of acids **7** and **8** gave access to a large array of derivatives, including esters, amides and protected amines (*via* Curtius rearrangement): some of the corresponding reactions are displayed in Scheme 2.

Improved conditions for the preparation of dicarboxylic acid **7** starting from *bis*-furan derivative **6** were described in 2008 and involved the use of a 1:1 mixture of *t*-BuOH and H₂O as the solvent, as well as a simplified work-up, resulting in a higher yield of the product.¹² In the same work, it was shown that, despite

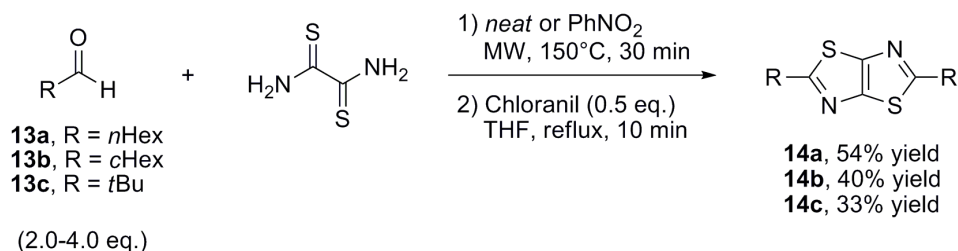
its purported inertness toward electrophiles, thiazolo[5,4-*d*]thiazole could be halogenated by treatment with suitable electrophilic halogen donors: thus, both 2-bromo- and 2,5-dibromothiazolo[5,4-*d*]thiazoles were formed upon reaction with an increasing excess of elemental bromine in the presence of pyridine, while the corresponding mono- and dichloro-compounds were obtained by employment of trichloroisocyanuric acid in refluxing CCl₄.



Scheme 2

Surprisingly, but also significantly, the original synthetic procedure³ is still the most popular approach to the synthesis of the thiazolothiazole ring system. While the possibility to obtain the desired product in a single step from simple starting materials is certainly valuable, the protocol is still affected by considerable drawbacks such as moderate yields, formation of insoluble by-products and harsh reaction conditions.

In search of improvements to the current methodology, the possibility to carry out the reaction under microwave heating was investigated, resulting in a cleaner and more efficient transformation. Furthermore, it was observed that addition of a mild oxidant (such as DDQ or Chloranil) at the end of the microwave-assisted reaction enhanced the yields and allowed using a smaller excess of aldehyde compared to literature precedents, probably by accelerating the oxidation of partially hydrogenated intermediates (see Scheme 1). Remarkably, these conditions allowed also the conversion of difficult substrates, such as unfunctionalized aliphatic aldehydes, with the corresponding thiazolothiazoles being formed in moderate yields (Scheme 3).¹³

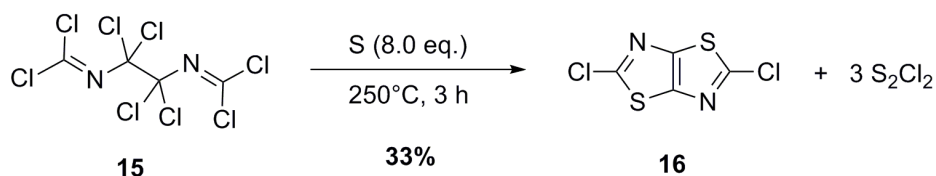


Scheme 3

Over time, a few alternative approaches to the synthesis of the thiazolo[5,4-*d*]thiazole core have been proposed, but so far they have found only limited use compared to the original procedure by Johnson and

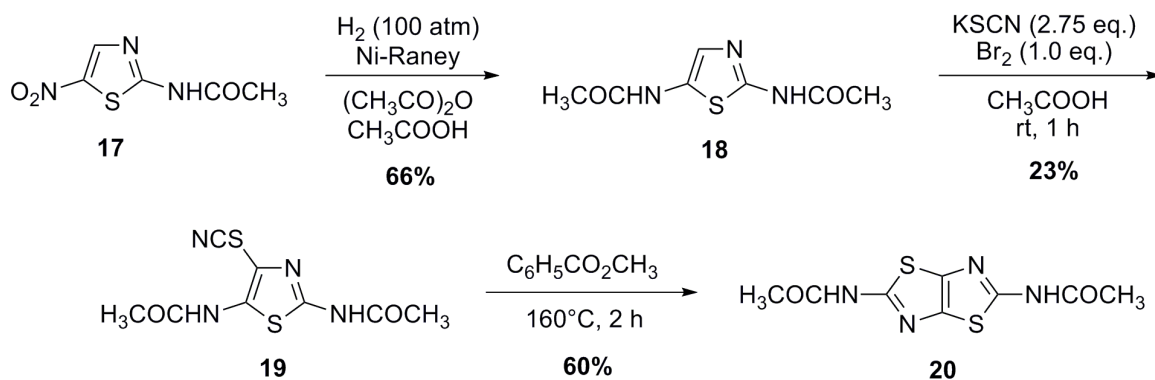
Ketcham,³ probably due to the fact that most of them consist of two or more synthetic steps and require the use of non-commercially available starting materials.

Direct access to 2,5-dichlorothiazolo[5,4-*d*]thiazole (**16**) was demonstrated by reaction of tetrachloroethylene-1,2-*bis*-isocyanide-dichloride (**15**) with an excess of elemental sulfur, thus representing an alternative to chlorination of thiazolo[5,4-*d*]thiazole (**9**).¹⁴ Use of a stoichiometric quantity of sulfur resulted in an incomplete reaction, but even under optimized conditions the yield did not exceed 33% (Scheme 4).¹⁵



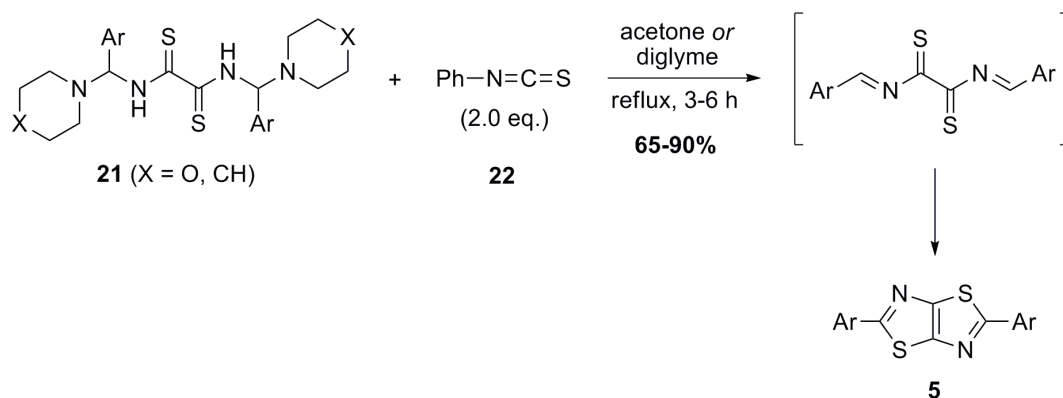
Scheme 4

The first direct synthesis of a 2,5-diaminothiazolo[5,4-*d*]thiazole derivative (not relying on the lengthy synthetic sequence shown in Scheme 2) was reported in 1979 by Seybold and Eilingsfeld, who employed 2-acetylthiazole-5-nitro (**17**) as the starting material. Reduction of compound **17** in the presence of acetic anhydride gave *bis*-acetylthiazole species **18**, which was converted to 3-isothiocyanate derivative **19** by reaction with potassium thiocyanate and bromine. Finally, dissolution in methyl benzoate and heating of the reaction mixture at 160 °C caused the ring closing to form the desired product (**20**, Scheme 5).¹⁶



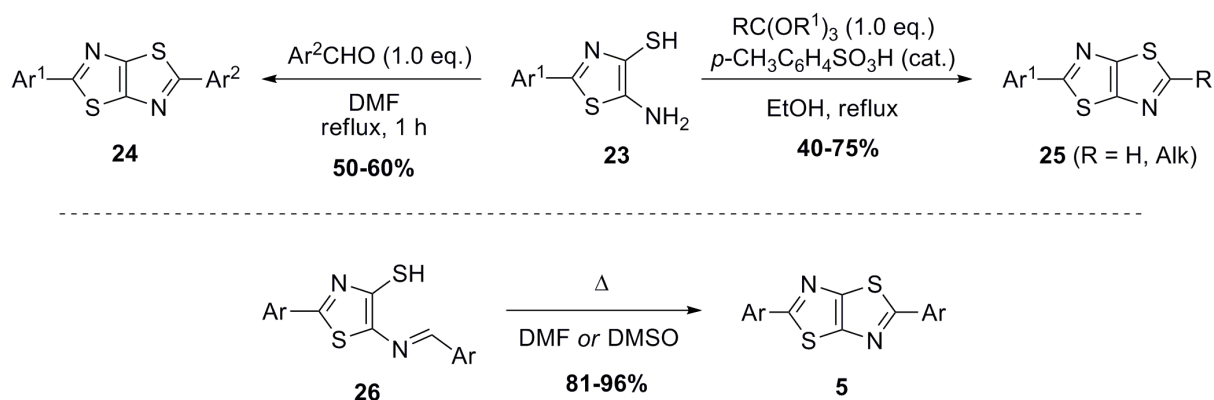
Scheme 5

The preparation of 2,5-diaryl-thiazolothiazoles was described starting from the corresponding *N,N'*-*bis*-(1-dialkylaminobenzyl)dithiooxamide (**21**), which in turn had to be accessed from rubeanic acid. Piperidino- and morpholino-derivatives were found to be the best starting materials; the heating of these species in refluxing acetone or diglyme in the presence of phenylisothiocyanate (**22**) provided the desired thiazolothiazoles in good to high yield (65–90%), probably through the intermediacy of the corresponding *N,N'*-*bis*-benzylidenedithiooxamides (Scheme 6).¹⁷ Although the yields obtained in this work were among the best ever reported for 2,5-diarylthiazolo[5,4-*d*]thiazoles, this method has never been applied by other researchers: this could be due to the necessity of preparing compounds **21**, which would make the one-step procedure of Johnson and Ketcham³ more attractive, despite the lower efficiency of the ring-forming reaction.



Scheme 6

In 1984, three consecutive patents described procedures for the synthesis of 2,5-disubstituted thiazolothiazoles starting from functionalized thiazoles. In a first report, it was claimed that reaction of 5-amino-2-aryl-4-mercaptothiazole **23** with an aromatic aldehyde in a high boiling point solvent (toluene, DMF) under reflux could give the desired thiazolothiazole in 50–60% yield after crystallization; the reaction could proceed both in the presence and in absence of a catalytic amount of *p*-toulenesulfonic acid, depending on the conditions employed. Remarkably, the possibility to obtain unsymmetrical products was also declared (Scheme 7, left).¹⁸ Later, a similar reaction was described, in which the same starting material **23** was treated with an orthoester in the presence of *p*-toulenesulfonic acid. The reaction could be carried out in solvent-free conditions or in refluxing alcohols and gave rise to unsymmetrical thiazolothiazoles in which the substituent in position 5 could be either a hydrogen atom or an alkyl group: thus, it was the first procedure to describe the preparation of a 2-aryl-5-alkylthiazolo[5,4-*d*]thiazole (Scheme 7, right).¹⁹ Finally, the third patent described the synthesis in high yields of symmetrical 2,5-diarylthiazolo[5,4-*d*]thiazoles from the corresponding 2-aryl-5-benzylidenamino-4-mercaptothiazoles **26**; such species are likely intermediates of the two previous reactions, but here it was claimed that they could be independently obtained by heating the appropriate *N,N'*-bis-aminoalkyl-dithiooxamide for a short time in a high boiling point nonpolar solvent.²⁰

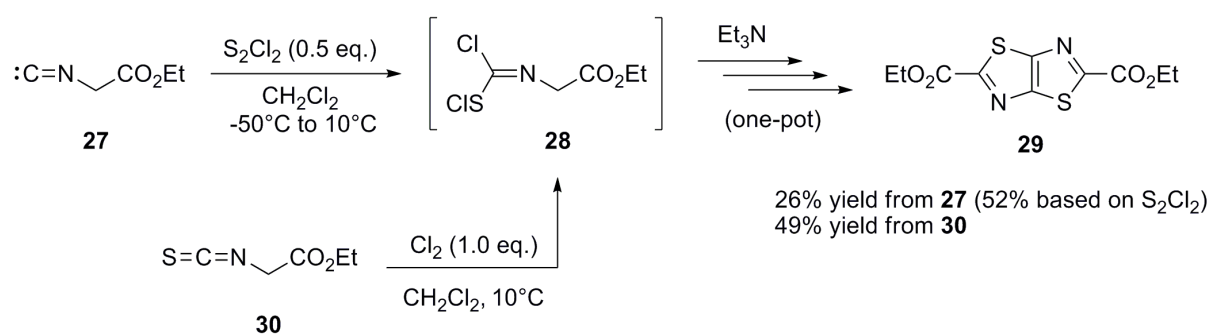


Scheme 7

An interesting, single-pot procedure for the preparation of diethylthiazolo[5,4-*d*]thiazole-2,5-dicarboxylate (**29**) starting from an alkyl isocyanacetate was serendipitously discovered by Marcaccini and co-workers during their studies on the synthesis of oxazolyl disulfates. It was found that the treatment of

ethyl isocyanoacetate (**27**) with dichlorodisulfane, S₂Cl₂, in the presence of triethylamine did not afford the desired product, but rather led to the formation of bicycle **29** in 52% yield based on S₂Cl₂ (Scheme 8).²¹ The reaction was suggested to proceed through a complicated series of steps (only key intermediate **28** is shown in Scheme 8), but ultimately provided the product in a single synthetic operation, thus representing an efficient alternative to the lengthy procedure previously described for the preparation of thiazolothiazole-2,5-dicarboxylates (see Scheme 2).¹¹

Later, Rössler and Boldt re-examined the synthetic methodology proposed by Marcaccini *et al.* and found out that intermediate **28** could be more efficiently accessed by treatment of ethyl isothiocyanoacetate (**30**) with elemental chlorine; subsequent addition of triethylamine to the reaction mixture would lead to product formation with an improved yield compared to the previous protocol (Scheme 8).²²



Scheme 8

As can be seen from the previous examples, several attempts have been made to discover easier and more efficient synthetic routes towards thiazolo[5,4-*d*]thiazoles but, unfortunately, most of those efforts have only been the subject of isolated studies and systematic investigations of their scope and limitations have not yet been carried out. Some of the alternative procedures, however, appear very promising since they proceed under mild conditions and do not require the use of excess reagents: accordingly, if studied in more detail and properly optimized, they could serve as ideal starting points for the development of improved synthetic strategies.

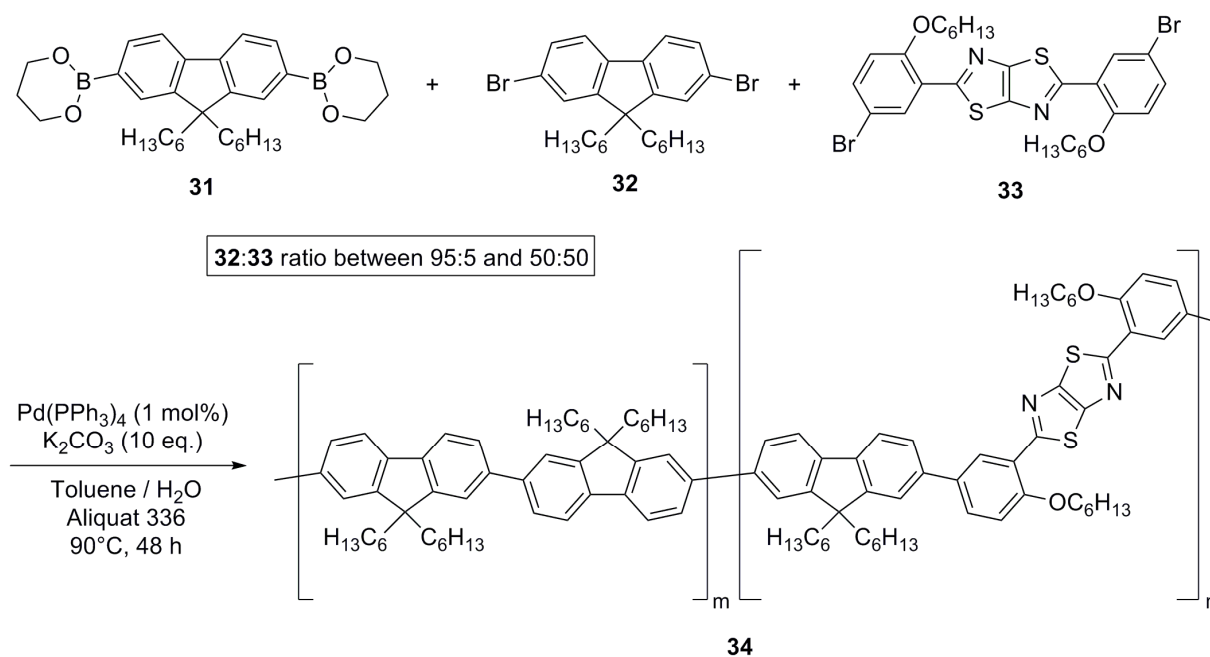
2.2. Thiazolothiazole-based polymers

In recent years, several examples of polymeric materials containing the thiazolo[5,4-*d*]thiazole unit have been described in the literature. As discussed in detail in the following paragraphs (see Section 3), such compounds have found applications in various areas of research, including non-linear optics,²³ organic (opto)electronics^{4,6} and, more recently, photovoltaics.²⁴ In this Section, a brief overview of the main synthetic methods employed to access these species will be provided.

The main strategy applied so far for the synthesis of thiazolothiazole-containing co-polymers is represented by the formation of carbon-carbon bonds *via* palladium-catalyzed transformations, in particular Suzuki and Stille cross-coupling reactions. In this approach, the preliminary preparation of two different, symmetrical co-monomers is required, one featuring aryl- or heteroaryl halides as end groups, the other having either boronic acid/boronate or stannane functionalities in terminal positions, depending on the particular transformation chosen: clearly, the possibility to easily access such species in high purity is crucial

for the success of this strategy. Often, after complete consumption of the starting materials, the reactions are ended by addition of suitable capping agents (usually bromobenzene and benzenboronic acid, or the corresponding thiophene species) which react on the terminal positions of the polymer chain, thus placing stable aryl or heteroaryl groups at both ends.

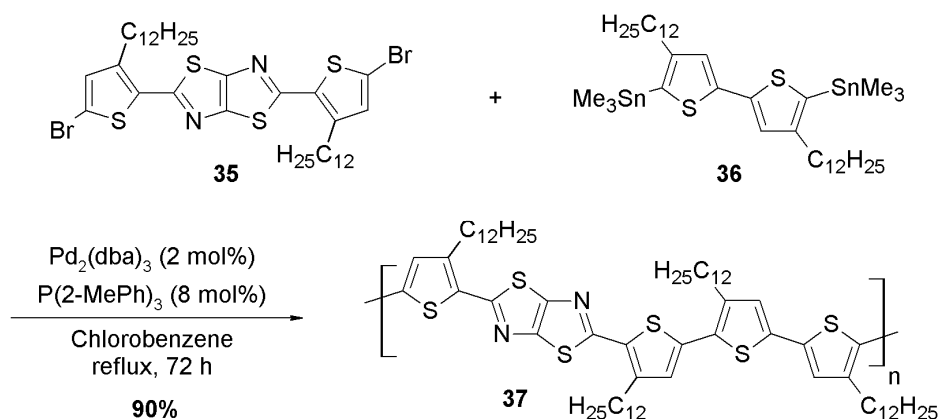
The first example of a thiazolothiazole co-polymer prepared *via* Suzuki coupling was reported in 2005 by Kang and co-workers, who employed 9,9-dihexylfluorene-2,7-bis(trimethylene boronate) (**31**) as one monomer, in combination with a mixture of two different dibromides **32** and **33** (Scheme 9): variation of the relative ratio of the latter two species gave rise to a series of co-polymers **34** with different compositions (average molecular weights ranging from 8.8 to 32.2 KDa, polydispersities between 1.44 and 2.17), whose electroluminescent properties were studied.⁴ The catalyst was simple Pd(PPh₃)₄ and the reaction was run in a toluene/water mixture using K₂CO₃ as the base.



Scheme 9

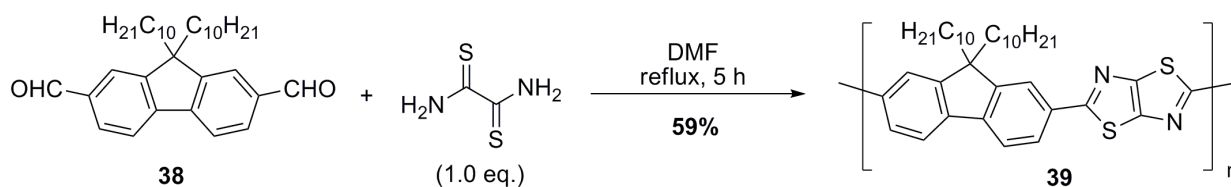
A similar approach, based on a Stille cross-coupling reaction instead of a Suzuki one, was employed by McCullough *et al.*, who used it to prepare some polymers to be used in semiconductor layers of organic field-effect transistors.⁶ In this case, the preferred catalyst was generated by mixing Pd₂(dba)₃ with tris-*o*-tolylphosphine and the reaction was carried out in refluxing chlorobenzene, giving the products in 78–90% yield (Scheme 10).

Although the preparation of thiazolothiazole-based polymers by means of cross-coupling reactions appears quite straightforward, some drawbacks have been underlined in the literature. First of all, the polymers generated in this way are sometimes characterized by a low to average molecular weight and relatively large polydispersity: this has been attributed to an insufficient purity of the starting materials²⁵ and a thorough purification procedure has been demonstrated to increase the molecular weight.²⁶ Secondly, an optimization of the reaction conditions would often be too time-consuming, resulting in the use of non-optimal catalysts which in turn can lead to moderate yields. Finally, a simple change in the reaction conditions can deeply affect the outcome, giving rise to polymers with very different properties: this can be advantageous in terms of versatility, but, in some cases, limits the reproducibility of the process.

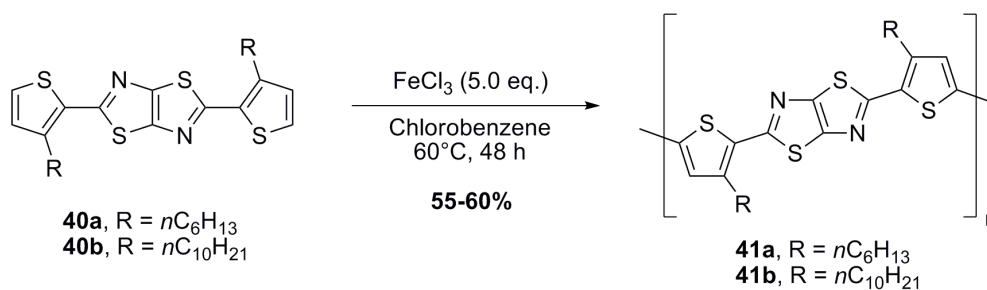


Scheme 10

Consequently, a few alternative procedures have been proposed for the synthesis of the polymers, but so far they have only been the subject of single studies from individual research groups and therefore their general utility has yet to be demonstrated. In 2005, Belfied and co-workers reported a polycondensation reaction involving dithiooxamide and *bis*-aldehyde **38**, in turn obtained in a few steps from fluorene.²³ The reaction took place in refluxing DMF for 5 hours and afforded polymer **39** in 59% yield (Scheme 11); unfortunately, no information regarding the product molecular weight and polydispersity was provided by the authors. More recently, an original protocol for the synthesis of thiophene-thiazolothiazole co-polymers was described by Naraso and Wudl: after preparation of monomers **40a,b** *via* the usual procedure, the latter were subjected to oxidative polymerization in the presence of FeCl₃ to give polymers **41a,b**, having moderate MWs of 2082–2305 g·mol⁻¹ and polydispersities in the 1.08–1.29 range, as determined by GPC (Scheme 12).²⁷



Scheme 11



Scheme 12

2.3. Structural, photophysical and spectroscopic properties

It took almost twenty years after the initial synthesis of Ketcham *et al.*¹¹ for the first crystal structure of parent thiazolo[5,4-*d*]thiazole (**9**) to be described by Porzio and co-workers.²⁸ As expected, the structure consisted of planar molecules located on inversion centres; a slight decrease of aromaticity was observed due

to the elongation of some bonds, which was attributed to resonance delocalization and a few short lateral contacts between heteroatoms were found to define intramolecular packing. Crystal structures of similar species carrying simple substituents were also described by Marcaccini *et al.* for compound **29** (Scheme 8)²¹ and by Benin *et al.* for 2-bromo- and 2,5-dibromothiazolo[5,4-*d*]thiazole,¹² respectively. In this latter case, the presence of several short contacts with distances less than the sum of the van der Waals radii was confirmed and the molecules were arranged in columnar structures, with strongly manifested π -stacking and a slight offset between the rings of consecutive layers.

When the π -conjugated system of the compounds was extended, as in 2,5-*bis*(2-thienyl)thiazolo[5,4-*d*]thiazole, the molecules in the solid state were still found to lie on the centre of symmetry of the crystals. The rings were all planar and a very small dihedral angle of 1.68° was measured between the thiazolothiazole and thiophene units. Bond lengths were similar to those found for compound **9**, which indicated also in this case the presence of resonance delocalization.²⁹

The first detailed spectroscopic study of parent thiazolo[5,4-*d*]thiazole (**9**) was reported in 1983 by Zanirato *et al.*, who examined its UV spectrum both in gas phase and in solution. In both cases, compound **9** displayed two main absorption bands in the 240–270 nm region, which were interpreted in terms of two overlapping $\pi \rightarrow \pi^*$ transitions.³⁰

More recently, Atvars and co-workers carried out a combined computational and experimental investigation of the photophysical properties of 2,5-diphenyl-thiazolo[5,4-*d*]thiazole (**1**), which was found to exhibit a red-shifted absorption maximum compared to the parent structure, no doubt because of its more extended conjugation. In particular, compound **1** presented its main absorption bands in the 353–362 nm region in a series of different solvents: highly polar solvents, such as DMSO, stabilized the electronic ground state, resulting in a blue-shifted absorption; conversely, protic solvents such as MeOH exerted the opposite effect, causing a bathochromic shift. The spectroscopic characteristics of **1** in acid solution were also assessed, and at high acid concentration a red-shift was observed for the absorption, accompanied by a broader fluorescence spectrum and a larger Stokes shift, which was attributed to protonation of the ring nitrogens. Overall, the experimental observations all pointed to the conclusion that electronic $\pi \rightarrow \pi^*$ transitions were mostly involved in the excitation process for molecule **1**.³¹ Similar considerations have later been reported for various aromatic polycyclic TzTz derivatives.

The physical, spectroscopic and electrochemical features of the simple thiazolothiazole-based polymers **41a,b** (Scheme 12) were discussed by Naraso and Wudl.²⁷ The polymers were found to be very thermally stable and exhibited red-shifted and broadened absorption and emission bands compared to the corresponding monomers (*ca.* 100 nm), once again due to their additional conjugation; interestingly, while the absorption spectra were featureless, in both cases the emissions presented two main bands and a red-shifted shoulder. Finally, electrochemical measurements showed that compounds **41a,b** had LUMO levels around 4.00–4.02 eV, which was deemed promising in view of their possible employment as *n*-type FET materials (see Section 3.4.). It should also be mentioned that thiazolothiazole-based co-polymers, prepared using benzotriazole co-monomers, have been shown to possess electrochromic properties, that is, their absorption spectrum was altered upon application of a voltage within a photoelectrochemical cell. Interestingly, different applied potentials caused a progressive spectral variation, which was deemed important in view of possible practical applications of these species.³² As far as NMR spectroscopy is concerned, a thorough investigation of the ¹H- and ¹³C-NMR spectra of a series of thiazolothiazole

derivatives (**40a** and **42–47**, Figure 2) was recently conducted, with the aim of providing a full assignment of their resonance peaks.

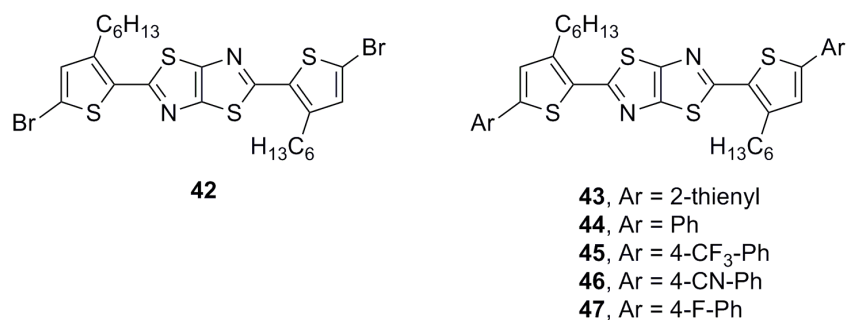


Figure 2

After having synthesized the desired compounds, for each of them the authors carried out a full set of mono- and bi-dimensional NMR experiments and compared the observed spectra with those predicted by means of DFT calculations, thus allowing a complete elucidation of the new compounds chemical structures.^{33,34} In addition, the gathered chemical shift data provided useful input for chemical shift prediction software, since very limited experimental data were previously available for thiazolothiazoles. Such knowledge could become valuable given the spectacular increase in the application of TzTz-containing semiconductor materials currently observed.

3. Applications of thiazolo[5,4-*d*]thiazole-based materials

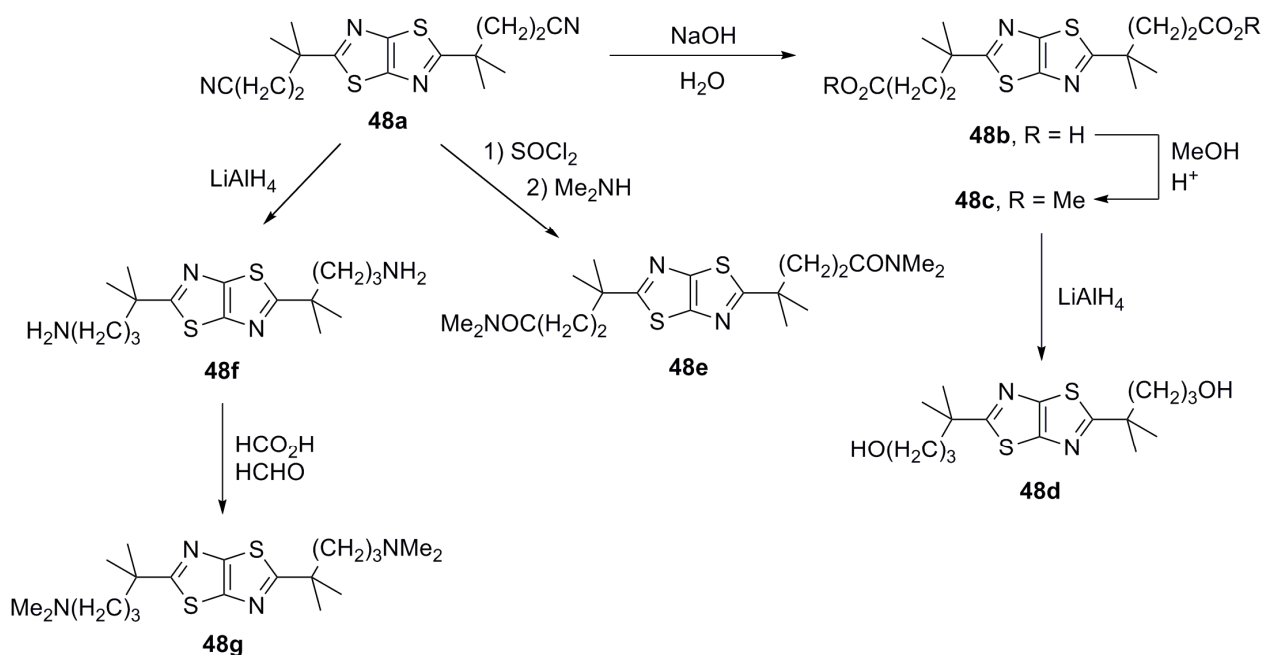
Soon after the initial report on the synthesis of thiazolothiazole derivatives,³ the first examples of practical applications started to appear, especially in patent literature. For instance, already in the early 60's, a patent application was filed by Geigy Chemical Corporation concerning the use of thiazolo[5,4-*d*]thiazoles as stabilizers for polymeric materials, in particular polypropylene.³⁵ In the same period, Eastman Kodak examined the possibility to use this class of compounds as additives for photographic films, in particular as UV filters³⁶ and, thanks to their fluorescence properties, brightening agents.³⁷

As already pointed out, over the years the interest in thiazolothiazole-based materials has been steadily growing, especially in the last decade. In the following paragraphs, the main fields of application of these heterocycles will be presented with the aid of relevant examples from the chemical literature.

3.1. Biological activity

Some of the early studies concerning thiazolothiazoles focused on the evaluation of their potential biological activity. Despite this initial interest, however, work in this area has not witnessed significant developments in recent years.

In 1962, Fikrat and Oneto prepared $\gamma,\gamma,\gamma',\gamma'$ -tetramethylthiazolo[5,4-*d*]thiazole-2,5-dibutyronitrile (**48a**, Scheme 13), a rare example of *bis*-alkyl derivative, and found that, although the new compound had negligible antiviral and antimicrobial activity, it could act as a central nervous system (CNS) depressant, mostly by induction of sleep in rodents.³⁸ This study was later expanded by Ketcham and Mah, who, starting from **48a**, synthesized a series of analogues (some of which are depicted in Scheme 13) and carried out the relevant biological testing.



Scheme 13

The authors observed that thiazolothiazoles were characterized by a relatively low toxicity ($LD_{50} > 0.5 \text{ g/Kg}$ in mice) and were often able to protract the sleeping time induced by barbiturate anesthetics, with bisamide **48e** being particularly potent.³⁹ A further TzTz derivative was reported to have a similar activity, but the details of biological screening experiments were not provided.⁴⁰

Interestingly, it was found that 2,5-diphenyl-thiazolo[5,4-*d*]thiazole (**1**) inhibited metastasis of the human epidermoid carcinoma in a standard ovo test, where the tumour was grown on the chorioallantoic membrane of embryonated chicken eggs;⁴¹ unfortunately, however, extension of these studies to other animal models or to the treatment of human patients has not been reported. Finally, 2,5-dichlorothiazolo[5,4-*d*]thiazole (**16**) was reported to have insecticidal properties, as demonstrated by standard laboratory tests against some known plant parasites.¹⁴

3.2. Preparation of metal complexes and crystal engineering

Due to the presence of Lewis basic nitrogen and sulfur atoms within a rigid bicyclic structure, thiazolothiazoles have also found use as ligands for transition as well as main-group metals, both for the preparation of discrete complexes and metal-organic polymers.

Curiously, one of the first reports concerning TzTz-metal complexes described their application as colour formers in imaging systems. More precisely, it was claimed that formation of coloured coordination compounds between thiazolothiazoles and metal cations could be exploited in the manufacture and use of pressure sensitive transfer papers for preparing carbonless copies. When an appropriate nickel(II) salt was reacted with 2,5-*bis*(2-hydroxyphenyl)thiazolo[5,4-*d*]thiazole, the formation of a yellow-green coordination polymer of the generic formula **49** was invoked (Figure 3a), whose colour could be also altered by employment of specific additives.⁴²

In 2004, Steel and co-workers described the preparation of binuclear metal complexes of pyridine-containing ligand **50** (Figure 3b).⁴³ Reaction of the latter with a methanolic solution of $\text{Cu}(\text{NO}_3)_2$ led to formation of symmetrical complex **51** as dark green plates: the thiazolothiazole acted as a planar bridging ligand and the two copper atoms were pentacoordinated, displaying a distorted square pyramidal geometry

(Figure 3c). On the other hand, treatment of **50** with $[\text{Ru}(\text{bpy})_2\text{Cl}_2]$ yielded a binuclear ruthenium complex, which was isolated as its hexafluorophosphate salt: NMR analysis showed that this was indeed a mixture of two different diastereomers, *meso*-**52** and *rac*-**52**, in a 2:1 ratio. Fortunately, the two diastereomers could be separated by column chromatography on a cation exchange resin and their structures could be independently assessed by X-ray diffraction analysis. Intriguingly, while in the *meso*-complex **52** the ligand presented a planar structure, in the case of *rac*-**52** it assumed a clearly bowed shape in order to facilitate π - π stacking interactions between two different pyridine rings (Figure 3d). More recently, the same group described the synthesis of a further TzTz-based ligand bearing additional pyridine rings, whose introduction formed two tridentate binding domains:⁴⁴ however, the preparation of the corresponding metal complexes has not yet been reported. Complex formation between 2,5-diphenylthiazolo[5,4-*d*]thiazole (**1**) and Ag^+ ions was also recently described: the resulting complex was shown to have a relative 1:2 stoichiometry, with silver ions coordinated in a bidentate fashion by the S and N atoms of the central heterocyclic unit.⁴⁵

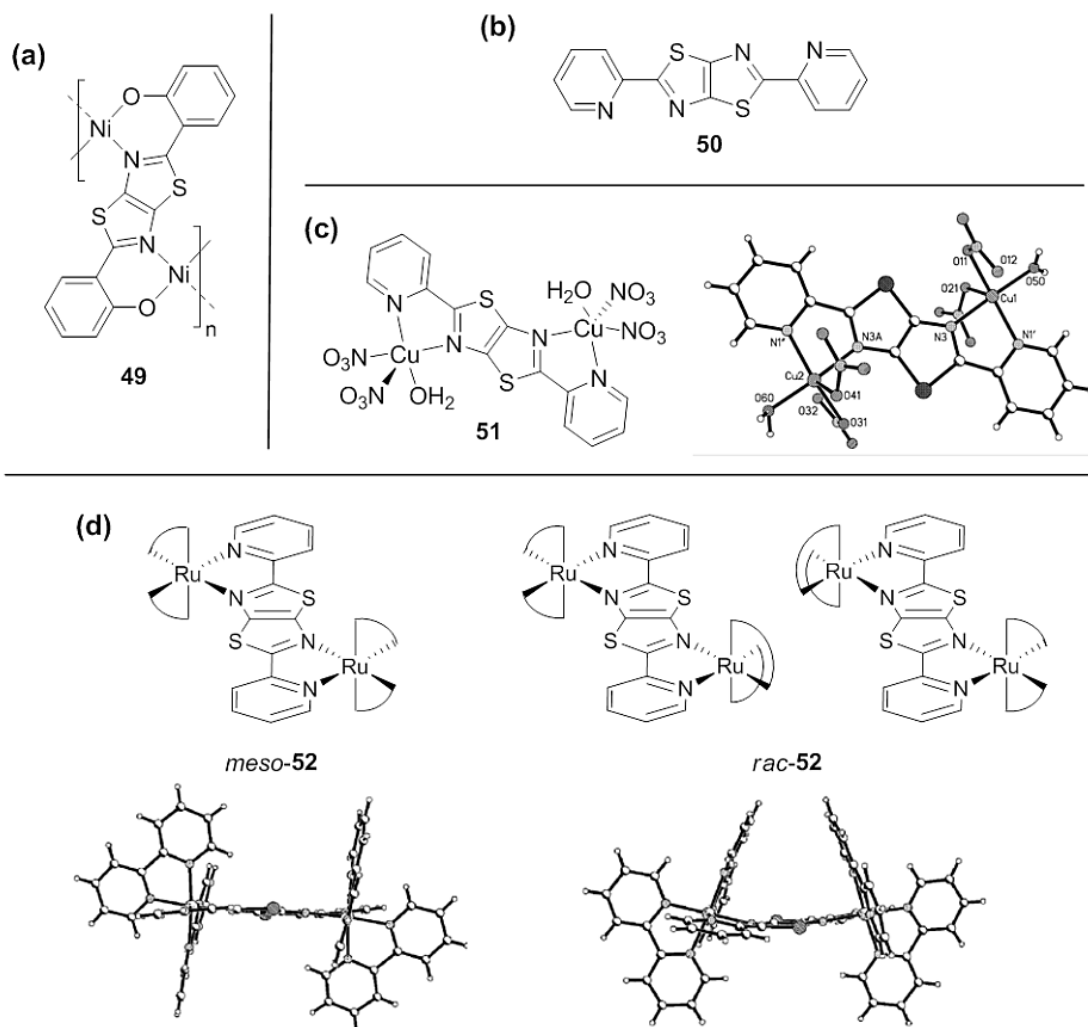


Figure 3. (Crystal structures in (c) and (d) reproduced by permission from ref. 43, © 2004 Royal Society of Chemistry).

In 2008, Cheetam and co-workers investigated the possibility to use dicarboxylic acid **7** (see Scheme 2) in combination with various alkaline earth cations to form organic-inorganic frameworks. The authors found that, after deprotonation of the ligand and mixing with salts of Mg, Ca, Sr and Ba, coordination

polymers of different structures and connectivities were formed depending on the metal employed. In particular, it was observed that an increase in the cation size and coordination requirements (in the order $Mg < Ca < Sr < Ba$) was directly related to an increase in the inorganic connectivity of the resulting metal-organic framework. Thus, while the coordination polymer obtained with Mg contained isolated octahedra (with the metal at their centre), the one made with Ca featured polyhedra dimers (with bridging water molecules), which became an infinite 1-D inorganic chain in the case of Sr (where nitrogen also participated to binding) and, finally, a continuous 2-D layer in the one featuring Ba (Figure 4).⁴⁶

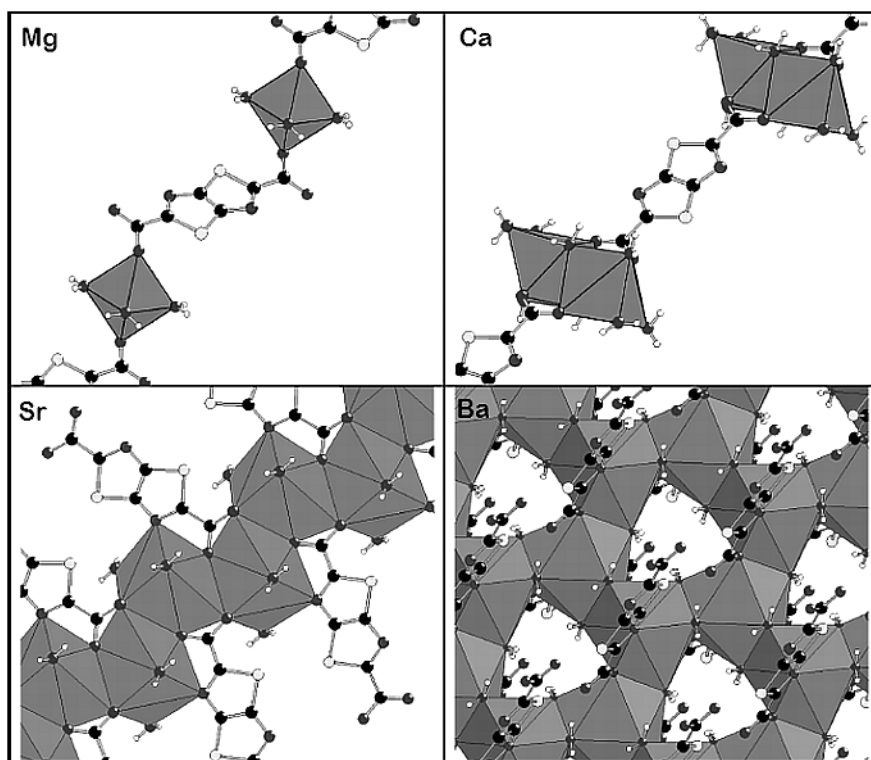


Figure 4. (Reproduced by permission from ref. 46, © 2008 American Chemical Society).

A few years later, the same ligand was once again used for the preparation of coordination networks, this time in combination with a series of transition metals such as Mn, Co, Cu, Zn and Ag. The new coordination polymers were fully characterized by analytical and thermal methods and their crystalline structures were assessed by means of *ab initio* X-ray powder diffraction (XRPD). Interestingly, it was found that with first-row transition metals the expected *O,O'*-coordination mode was neglected in favour of *N,O*-chelation, resulting in the formation of 1-D ribbons (elongating in different directions depending on the particular metal present). Only in the case of Ag, the contemporary presence of μ_2 -bridging carboxylates and monocoordinated nitrogen atoms allowed the formation of a densely packed 3-D coordination network, unable to host small molecules (Figure 5).⁴⁷ Very recently,⁴⁸ the same group reported the preparation of another thiazolothiazole-based ligand, featuring pyrazole groups in terminal positions rather than carboxylic acid moieties; application of such ligand for the preparation of organic-inorganic frameworks is currently in progress, but the authors already found that it could give rise to extended 2-D structures in the solid state, which makes it promising for the construction of higher-porosity materials.

Finally, it was demonstrated that thiazolo[5,4-*d*]thiazoles could be employed to form tridimensional coordination networks even in the absence of metal ions, exploiting the formation of hydrogen bonds with

appropriate building blocks. Thus, combination of *N,N'*-dimethyl-*N,N'*-diphenylureadicarboxylic acid (**53**) as a U-shaped structural element with 2,5-*bis*(4-pyridyl)thiazolo[5,4-*d*]thiazole (**54**) afforded a zig-zag type tridimensional structure with different layers stacked upon the *a* axis (Figure 6a and 6b, respectively).⁴⁹

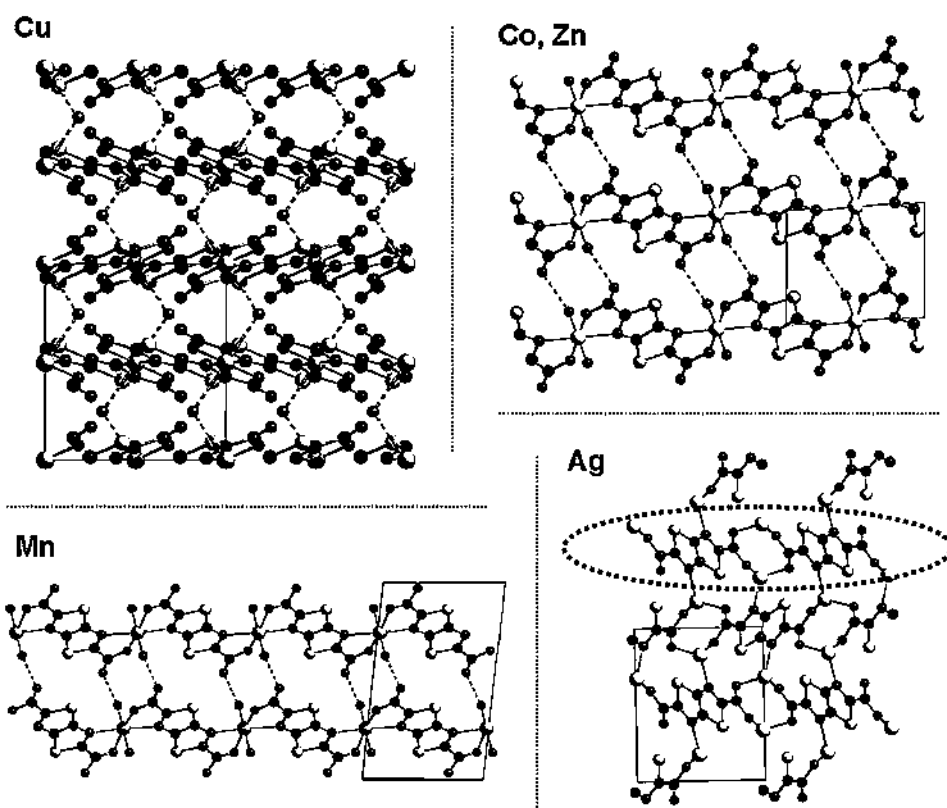


Figure 5. (Crystal structures reproduced by permission from ref. 47, © 2010 Elsevier).

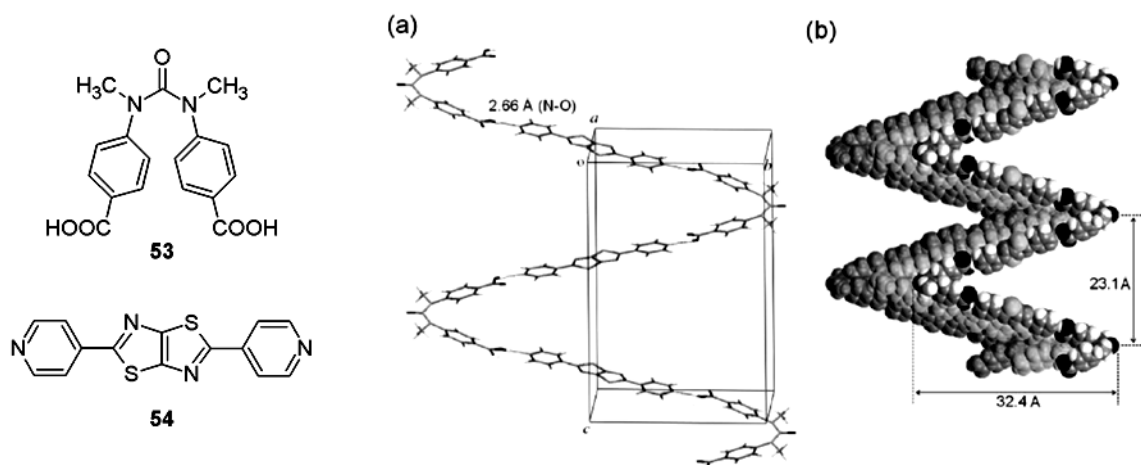


Figure 6. (Crystal structures reproduced by permission from ref. 49, © 2011 American Chemical Society).

3.3. Non-linear optics and fluorescent sensors/emitters

Thiazolo[5,4-*d*]thiazoles and derived polymers have found application in the field of non-linear optics (NLO), where they have been shown to participate in two-photon-absorption (TPA) processes. TPA, first discovered in 1931, takes place through the simultaneous absorption of two photons *via* virtual states within

an absorption medium;⁵⁰ remarkably, the probability of TPA is proportional to the square of incident light intensity, making it a non-linear process most easily observed employing laser sources. Two-photon-adsorbing materials often present very interesting properties, such as upconverted emission (for example from IR to visible) and highly localized excitation, which render them potentially useful for applications ranging from fluorescence imaging to data storage and photodynamic therapy.

In 2002, a highly extended symmetric thiazolothiazole, named **AF-389** (Figure 7), designed to have a “D- π -core- π -D” structure, has been prepared and evaluated as a two-photon chromophore. The compound displayed one-photon absorption in the visible region around 435 nm; when excited by a IR laser beam of wavelength around 800 nm, **AF-389** was found to be a strong two-photon adsorber in that region, with a higher TPA cross section compared to those of materials based on the same architecture. Considering the blue shift of the TPA peak compared to the one-photon absorption peak (relative to the energy of the incoming photons), the authors concluded that the excited state generated by the two-photon process was different from that generated by the single-photon excitation.⁵¹ An analog of **AF-389** possessing two carbazole moieties instead of triphenylamines (**AF-387**, Figure 7) was later reported to have similar characteristics, although with a much smaller TPA cross-section (61.2 GM vs. 584 GM for **AF-389**).⁵²

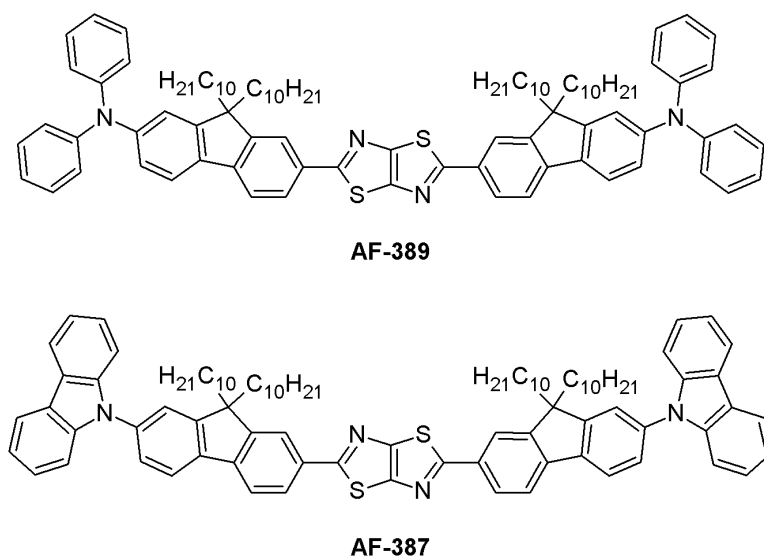


Figure 7

Shortly after, Belfield and co-workers examined the TPA properties of polymer **39** (see Scheme 11). The compound was found to display a one-photon absorption at around 440 nm; when irradiated with a Ti:sapphire-based laser source, it showed good TPA in the 700–800 nm range, with a maximum cross section of approximately 420 GM at 710 nm. The latter value was inferior to that measured for a monomeric model compound, which, according to the authors, was due to polymer aggregation induced by strong interchain π - π interactions.²³

The photophysical properties of TzTz-based materials have also been exploited in the field of fluorescent sensors and emitters. 2,5-Bis-aryl derivatives **55** and **56**, bearing ethylene oxide side chains, have been shown to undergo large fluorescent enhancements when complexed to certain metal ions: in particular, in CH₃CN solution, **55** acted as a sensor for both Cr³⁺ and Al³⁺, while **56** displayed a significant fluorescent change selectively with Cr³⁺ only (Figure 8).⁵³ Remarkably, fluorescence intensity increased with the

amount of Cr^{3+} present in solution and a 1:1 complex stoichiometry was determined by means of a Job plot (Figure 8, inset).

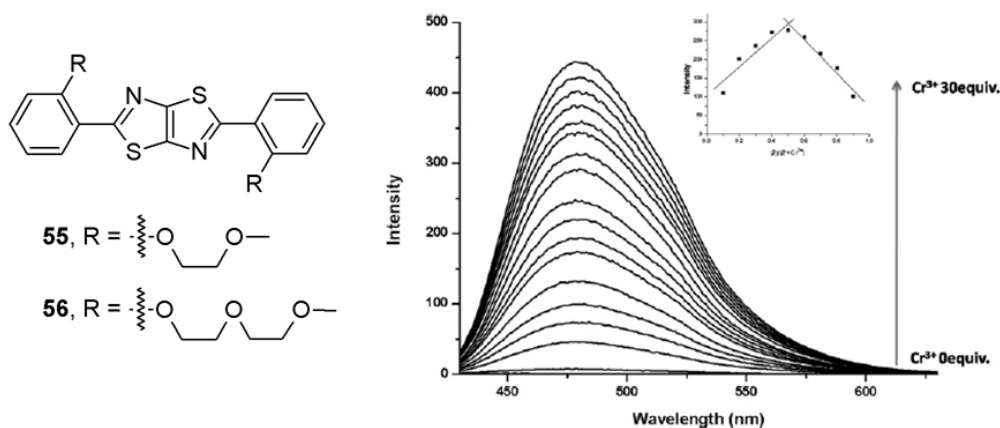


Figure 8. (Fluorescence and Job plots reproduced by permission from ref. 53, © 2012 Elsevier).

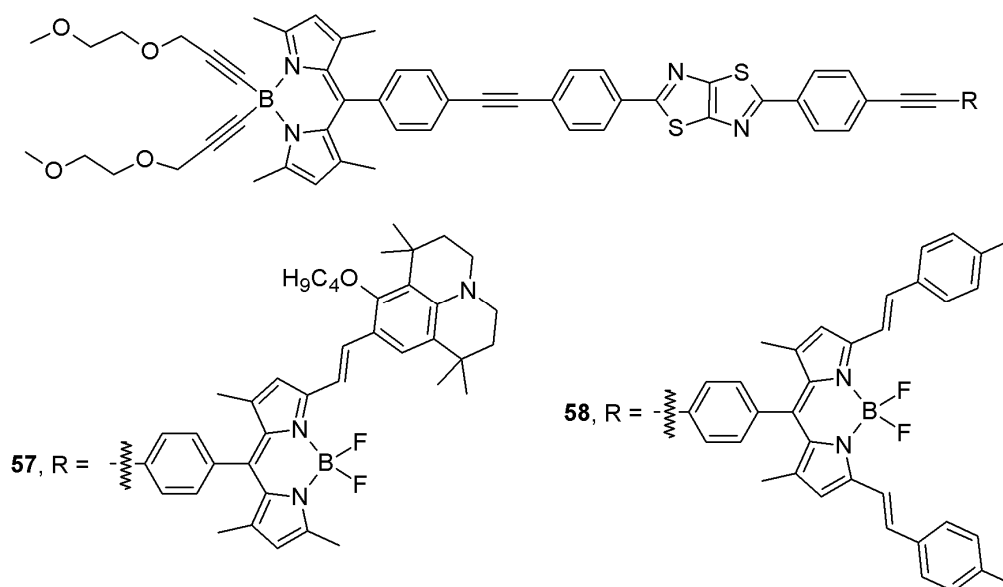


Figure 9

A different class of emitters has been investigated by Ziessel and co-workers, who employed the thiazolo[5,4-*d*]thiazole moiety as a central core in donor-acceptor fluorescent compounds. In such species (see, for example, structures **57** and **58**, Figure 9), the heterocyclic unit played the role of a conjugated bridge and energy input centre able to promote cascade intramolecular energy transfer to bodipy energy acceptors: such process was made possible by the excellent spectroscopic overlap between the thiazolothiazole group emission and the bodipy group absorption (Förster mechanism). Remarkably, in compounds **57** and **58**, no residual emission was observed for the thiazolothiazole core, indicating efficient energy transfer to the acceptors.⁵⁴

3.4. Organic light-emitting diodes

Over time, thiazolothiazole derivatives have found extensive application in the field of optoelectronics. In a few cases, they have been used in the active layer of organic light-emitting diodes (OLEDs), where they acted as electroluminescent materials, generating visible light in response to an electric current.⁵⁵

Traditionally, polyfluorenes (PFO) have been a very important class of organic materials for light-emitting applications, due to their excellent photo- (PL) and electro-luminescence (EL) properties, their good processability and chemical stability and their facile colour tunability.⁵⁶ PFO, however, are hole-transport-dominated materials, in which hole mobility is much higher than electron mobility: this characteristic limits the efficient recombination of holes and electrons in the active layer, lowering electroluminescence efficiency. As a possible solution to this problem, Kang and co-workers proposed the use of fluorene-thiazolothiazole co-polymers **34** (see Scheme 9), incorporating the more electron-withdrawing TzTz unit alongside the electron-rich fluorene moiety.⁴ A total of four new polymers were prepared (with varying monomers ratios, ranging from 95:5 to 50:50) and their photo- and electro-chemical properties were tested. In thin film, the new compounds showed both red-shifted absorption and emission compared to solution, possibly due to the formation of aggregates in the solid state or the increase in the effective conjugation length due to chain planarization, as a consequence of tight molecular packing (both effects being known to enhance charge mobility); devices built with polymers **34** displayed a bright blue emission and showed similar turn-on voltages, higher luminances and superior EL efficiencies compared to those containing pure PFO, especially at higher TzTz content (above 25%). Thus, introduction of the new heterocyclic unit appeared to have a positive impact on materials properties.

A similar study was conducted a few years later by Shim *et al.*, who synthesized a fluorene-thiazolothiazole co-polymer featuring alkylated thiophenes as spacers between these two ring systems (**PF-TTZZT**, Figure 10). The polymer exhibited high molecular weight and good thermal stability; its absorption characteristics in solution were similar to those in thin film, although in the latter case a bathochromic shift was observed for the emission, probably due to tighter intermolecular packing and a more planar structure. Electroluminescent devices built with **PF-TTZZT** showed a yellow-orange emission and were characterized by a higher luminance than those previously reported by Kang,⁴ although their EL quantum efficiency was lower. Finally, it should be pointed out that a similar polymer, featuring a head-to-head bithiazole unit instead of the thiazolo[5,4-*d*]thiazole, presented better quantum efficiency and luminance compared to **PF-TTZZT**.⁵⁷ In search for new materials displaying good oxidative stability and narrow electronic band-gap, Patri's group investigated the synthesis and application of co-polymers incorporating electron-rich thieno[3,2-*b*]thiophene units together with electron-deficient thiazolo[5,4-*d*]thiazoles (**59a-c**, Figure 10). Interestingly, the synthesis of polymers **59a-c** was carried out by means of a Stille coupling-polymerization (see Section 2.2.) in the presence of CuO as an additive, which was found to increase the products molecular weight.⁵⁸

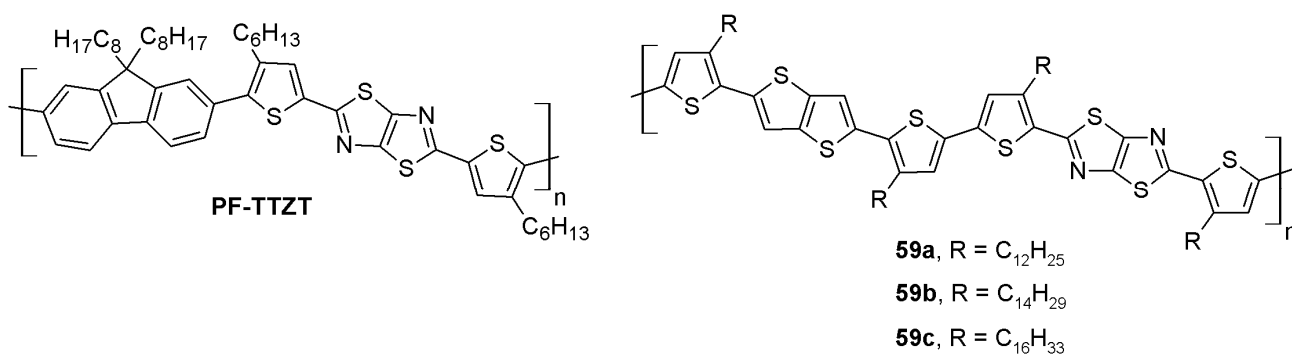


Figure 10

The new polymers presented some favourable properties, such as good thermal stability and relatively high oxidation potentials, making handling under inert atmosphere unnecessary; furthermore, they displayed red-shifted absorption and emission spectra, indicating the occurrence of intramolecular charge transfer during the excitation process and a small HOMO-LUMO gap. OLEDs built with compounds **59a–c** showed a bright red emission with a relatively low turn-on voltage (approximately 4.0 V); on the other hand, luminances were only average and EL efficiencies were low, which the authors explained with the presence of strong intramolecular interactions and aggregate formation quenching fluorescence in the solid state.⁵⁸

In conclusion of this Section, it is important to mention that OLED fabrication has been carried out also using thiazolothiazole-based small molecules, such as the boron-bridged conjugate structures reported by Zhang and co-workers, characterized by a ladder-type skeleton. Based on previous work on compounds **60a–d** (Figure 11), which were shown to be efficient fluorescent emitters in the visible region,⁵⁹ the authors prepared derivatives **61a–d**, possessing an extra oxygen atom in the boron-containing ring (Figure 11). The new species adsorbed light in the 442–481 nm region and displayed yellow-green fluorescence both in solution and in the solid state, with the latter being significantly red-shifted (2–29 nm, depending on the compound) due to the presence of C–H $\cdot\pi$ or C–F $\cdot\pi$ intramolecular interactions, as demonstrated by crystal structures. The highest fluorescence quantum yields were obtained with compounds **61a,b**, which were therefore selected for the preparation of electroluminescent devices. OLEDs built with **61a,b** showed green emission, with very good brightness values between 10340 and 18060 cd/m² (depending on device architecture), high EL efficiency and low turn-on voltages. In general, such devices presented higher brightness and efficiency than those of similar OLEDs fabricated using other boron-containing emitter materials.⁶⁰

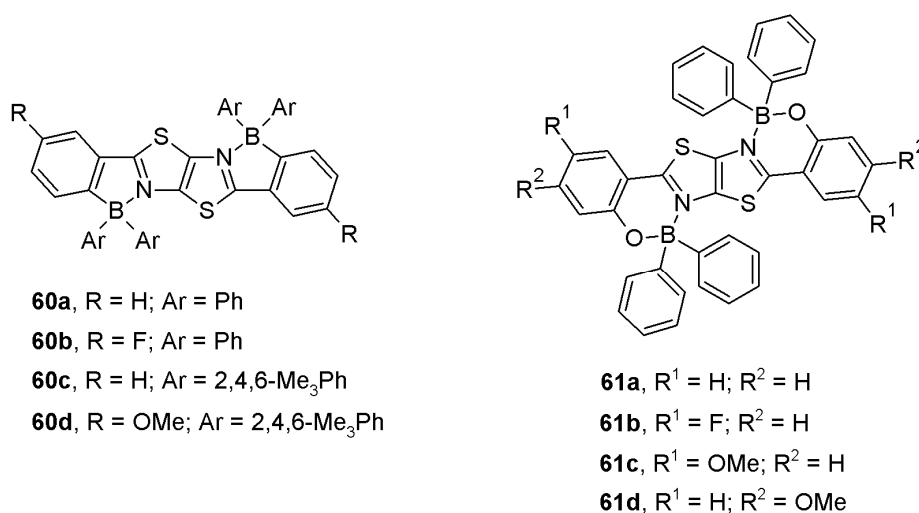


Figure 11

3.5. Organic field-effect transistors

As mentioned in the Introduction, the main reason for the rapid increase in the number of studies dealing with thiazolo[5,4-*d*]thiazoles has been their employment in the field of organic electronics. In this context, one of their main applications has been as active layer components in organic field-effect transistors (OFETs), a class of organic thin-film transistors (OTFTs).⁶¹

OFETs are usually composed of an organic semiconductor layer (acting as the conducting channel), an insulating layer (usually constituted by SiO₂) and three electrodes (source, drain and gate). The source and drain electrodes are placed at the two ends of the conducting channel, while the gate electrode is placed on the bottom of it (and separated by the insulator): application of a voltage between the gate and the source electrodes will induce charges in the conducting channel; then, if a voltage is applied between source and drain electrodes, an electric current will be generated. Most commonly, holes will be generated in the semiconductor film (due to the high hole mobilities often observed in organic semiconductors) giving rise to *p*-type devices (Figure 12); alternatively, if electrons are generated in the semiconductor, an *n*-type device will be obtained.⁶²

The magnitude of the electric current will depend both on the gate potential (V_G) and the source-drain potential difference (V_{SD}). In particular, it is observed that V_G must be larger than a certain value (called the “threshold voltage”, V_T) for the channel to significantly conduct electricity: for a given V_{SD} value, when $V_G > V_T$ the channel is “switched on” and an electric current can flow; the ratio between the current flowing when the channel is “on” and the current flowing when the channel is “off” is called “on/off ratio” and usually amounts to several orders of magnitude.⁶² For this reason, OFETs have found application in several classes of devices, such as sensors and actuators, switches and, recently, large-area flexible displays.

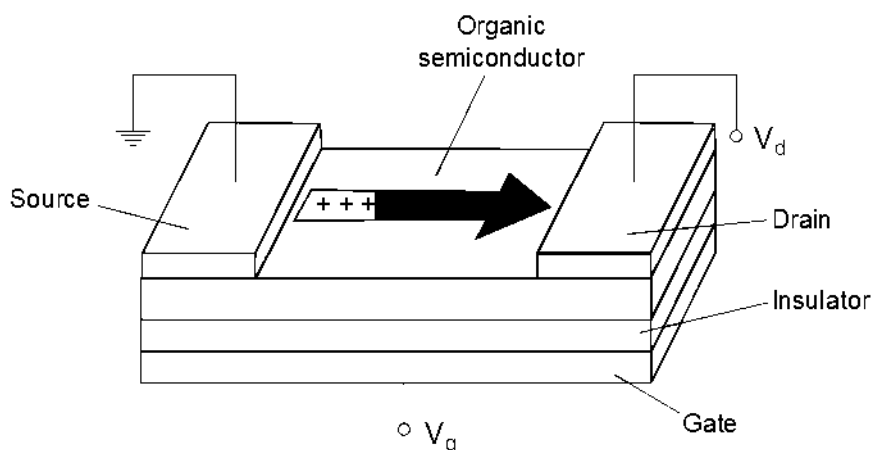


Figure 12

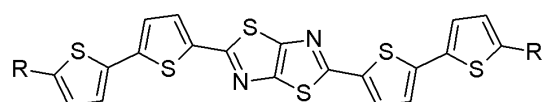
Historically, the first TzTz-based compounds used as semiconductors in OFETs have been small *bis*-aryl and heteroaryl derivatives. Their properties have been initially investigated by Yamashita and co-workers, who succeeded in preparing both *p*-channel^{5,63} and *n*-channel devices.⁶⁴ Later, a few other examples have also appeared in the literature,^{65,66} a couple of which in patents.^{67,68} The structures of the most interesting compounds are presented in Figure 13 while their OFET characteristics are summarized in Table 1 and 2 (*p*-channel and *n*-channel devices, respectively).

As it can be seen in Table 1, TzTz derivatives showed in most cases acceptable *p*-type semiconductor properties, although the nature of the substituents flanking the central heteroaromatic unit clearly had a major impact on device performances, probably due to differences in the crystal packing of the corresponding compounds. The highest values for charge mobility and on/off ratio were observed for compound **64**, whose performances could be even improved by treatment of the substrate/insulator layer with hexamethyldisilazane (HMDS) prior to semiconductor deposition.^{63c} Furthermore, it was observed that

deposition temperature had a strong influence on OFET properties: with the aid of AFM measurements, the authors concluded that the same compound deposited at different temperatures presented a different morphology (small/large grains, smooth/rough surface) which affected intramolecular charge transfer and therefore mobility.⁶³ An increase in the size and structural complexity of the semiconductor did not necessarily result in better performances, as demonstrated by compound **66**, which showed modest charge transfer characteristics.⁶⁶

More interestingly, TzTz-based compounds displayed excellent *n*-type semiconductor characteristics (Table 2), which was in part due to the presence of the electron-withdrawing thiazolothiazole moiety.

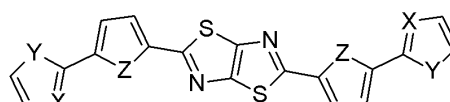
p-Channel OFETs



TTFZTT, R = H

DH-TTFZTT, R = C₆H₁₃

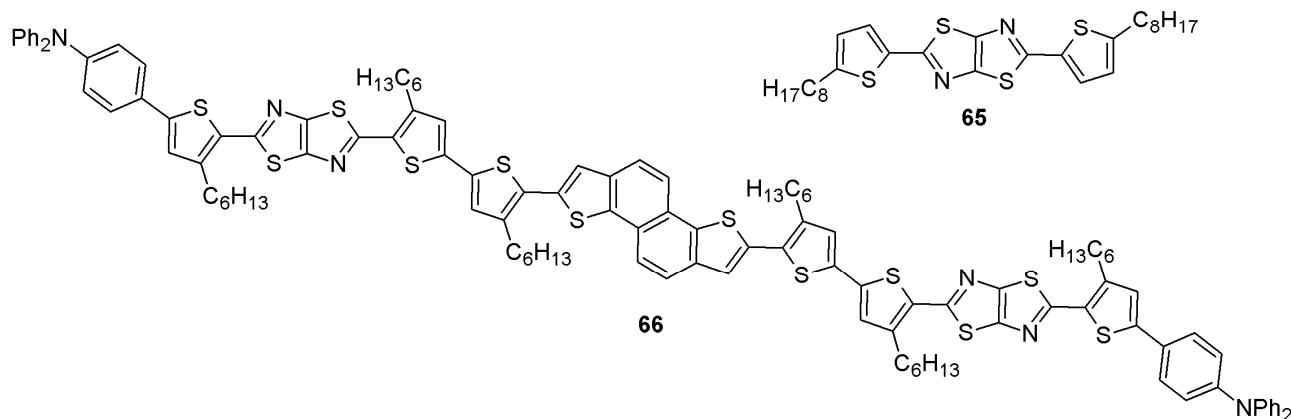
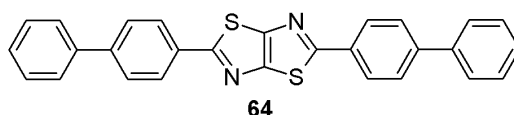
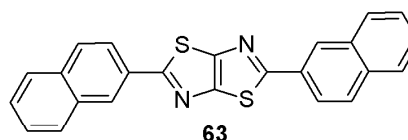
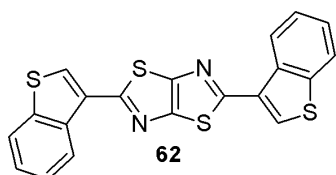
10TT-ZZ-TT10, R = C₁₀H₂₁



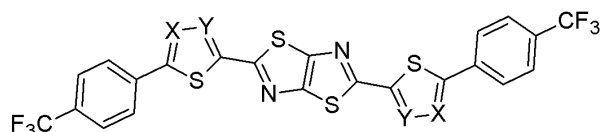
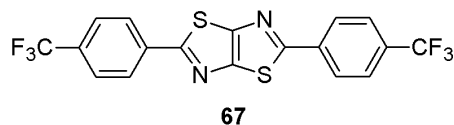
ZTFZTZ, X = N, Y, Z = S

FTFZTF, X = CH, Y = O, Z = S

FFFZFF, X = CH, Y, Z = O



n-Channel OFETs



68a, X, Y = CH

68b, X = N, Y = CH

68c, X = CH, Y = N

Figure 13

In particular, compound **68a**, despite a relatively high threshold voltage, yielded an electron mobility of $1.2 \text{ cm}^2 \text{ V}^{-1} \text{ s}^{-1}$ and an on/off ratio of 10^7 , among the best values ever reported for *n*-type OFETs at the time the study was published.^{64b} Such performance was obtained by treatment of the insulator with octadecyltrichlorosilane (OTCS) prior to deposition of **68a**, which also allowed to carry out the fabrication procedure at room temperature. The observed improvement was explained by formation of a self-assembled monolayer of long alkyl chains, which efficiently suppressed the influence of electron trap sites on SiO₂ surface, thus enhancing electron mobility. Remarkably, compound **67**,^{64a} having similar end groups to **68a**, did not show any OFET property, which once again underlines the importance of good solid state packing to obtain efficient devices.

Table 1. *p*-Type OFET characteristics of thiazolo[5,4-*d*]thiazole-based semiconductors.

Compound	T sub (°C)	Hole mobility (cm ² /V·s)	on/off ratio	V _T (V)	ref.
TTFZTT	50	2×10^{-2}	10 ⁴	-7	5
DH-TTFZTT	20	3×10^{-3}	10 ³	-2	5
10-TTZZTT-10	60	1.7×10^{-3}	10 ⁴	n. r. ^a	67
ZTFZTZ	20	1×10^{-7}	10 ³	n. r. ^a	63a
FTFZTF	70	1×10^{-3}	10 ³	n. r. ^a	63a
FFFZFF	50	4×10^{-4}	10 ³	n. r. ^a	63a
62	20	6×10^{-9}	10 ²	n. r. ^a	63b
63	70	4.2×10^{-2}	10 ⁴	-51	63c
64	70	8.2×10^{-2}	10 ⁵	-59	63c
64	70 ^b	0.12	10 ⁶	-58	63c
43	25	1.6×10^{-3}	10 ⁵	+1.4	65
45	25	2×10^{-6}	10 ³	-2.2	65
47	25	1×10^{-5}	10 ⁴	-3.4	65
65	60	1.8×10^{-2}	10 ⁵	n.r. ^a	67
66	25	2×10^{-6}	10 ²	n.r. ^a	66

^aNot reported. ^bThe SiO₂ substrate/insulator was treated with hexamethyldisilazane (HMDS) prior to semiconductor deposition.

Despite the interesting results obtained with thiazolothiazole-containing small molecules, in recent years most of the research related to organic field-effect transistors has been conducted using polymeric materials. After the initial studies of McCullough and co-workers,⁶ several co-polymers have been reported in which the thiazolothiazole unit was present together with different heteroaromatic moieties,⁶⁹ such as thiophene,^{70,71} cyclopentadithiophene,^{24,72} benzodithiophene,^{73,74} carbazole,⁷⁵ dibenzo-⁷⁶ and dithienosilole,^{77,78} phenanthrocarbazole,⁷⁹ isothianaphthene,²⁵ diketopyrrolopyrrole^{80,81} and indacenodithienothiophene,⁸² as well as a peculiar ethynyleneplatinum spacer.⁸³ Importantly, all the reported materials displayed only *p*-channel semiconductivity and to date no *n*-type OFET has been built using TzTz-based polymers.

Table 2. *n*-Type OFET characteristics of thiazolo[5,4-*d*]thiazole-based semiconductors.

Compound	T sub (°C)	El. mobility (cm ² /V·s)	on/off ratio	V _T (V)	ref.
67	25	Not observed			64a
68a	50	0.30	10 ⁶	60	64a
68a	25 ^a	1.2	10 ⁷	67	64b
68b	80 ^a	0.64	10 ⁶	24	64c
68c	20 ^b	3 × 10 ⁻⁴	10 ⁶	64	64c

^aThe SiO₂ substrate/insulator was treated with octadecyltrichlorosilane (OTCS) prior to semiconductor deposition. ^bThe SiO₂ substrate/insulator was treated with hexamethyldisilazane (HMDS) prior to semiconductor deposition.

The most efficient and newest compounds are shown in Figure 14 and the OFET properties of the corresponding devices are reported in Table 3. For all other polymers, an excellent discussion can be found in the recent overview by Maes and co-workers.¹

The results presented in Table 3 indicate that thiazolothiazole-containing polymers were on average better semiconductors than the corresponding small molecules, with good to high hole mobility values. The presence of electron-deficient thiazole rings lowered their HOMO energies, improving their air-stability in comparison with other polymers (such as polythiophenes), thus simplifying device fabrication. In many cases, it was observed that annealing of the organic material at a temperature between 120 and 200 °C enhanced the electric properties of the device. Moreover, performances were also enhanced by pre-treatment of the inorganic substrate with a long-chain alkyl silane (most often OTCS), as seen above for small organic semiconductors. Notably, even simple thiazolothiazole-thiophene co-polymers **37**, **69** and **70** exhibited hole mobilities up to 0.30 cm² V⁻¹ s⁻¹, which the authors attributed to the highly ordered three-dimensional structure possessed by these materials.⁷⁰ Interestingly, hole mobilities increased with the increasing length of alkyl side chains in the order **69**<**37**<**70**: based on X-ray scattering measurements, this phenomenon was attributed to the higher lamellar ordering induced by the long alkyl chains.^{70a}

The best results reported to date were obtained with thiazolothiazole-diketopyrrolopyrrole co-polymers **PDPTTOx**⁸⁰ and **PDPPTzBT**,⁸¹ which yielded devices characterized by 1.2–3.4 cm² V⁻¹ s⁻¹ hole mobilities accompanied by on/off ratios in the 10⁶/10⁷ range: these values were among the best ever reported for polymeric organic semiconductors. In addition, it is remarkable that **PDPPTzBT** required annealing under relatively mild conditions (100–120 °C for 5 minutes) compared to those required by the other materials and this fact is favourable in terms of device processability. The high charge mobilities observed were thought to derive from strong intermolecular interactions between polymer chains, due to the enhanced π -stacking of the fused heterocyclic moieties and the short interchain π - π distances observed in the crystal structures, providing efficient channels for hole transmission.

While in some cases the introduction of highly conjugated co-monomers afforded efficient devices (as in the case of **PPTT**),⁷⁹ this strategy was not always successful: indeed, OFETs built with **PIDTT-TzTz-TT** displayed only moderate charge mobilities and on/off ratios.⁸² Finally, introduction of metal atoms in the polymer structure was demonstrated in the case of compounds **71** and **72**, which gave hole mobility values in the 10⁻² range, superior to those previously observed with different metallopolynes.⁸³

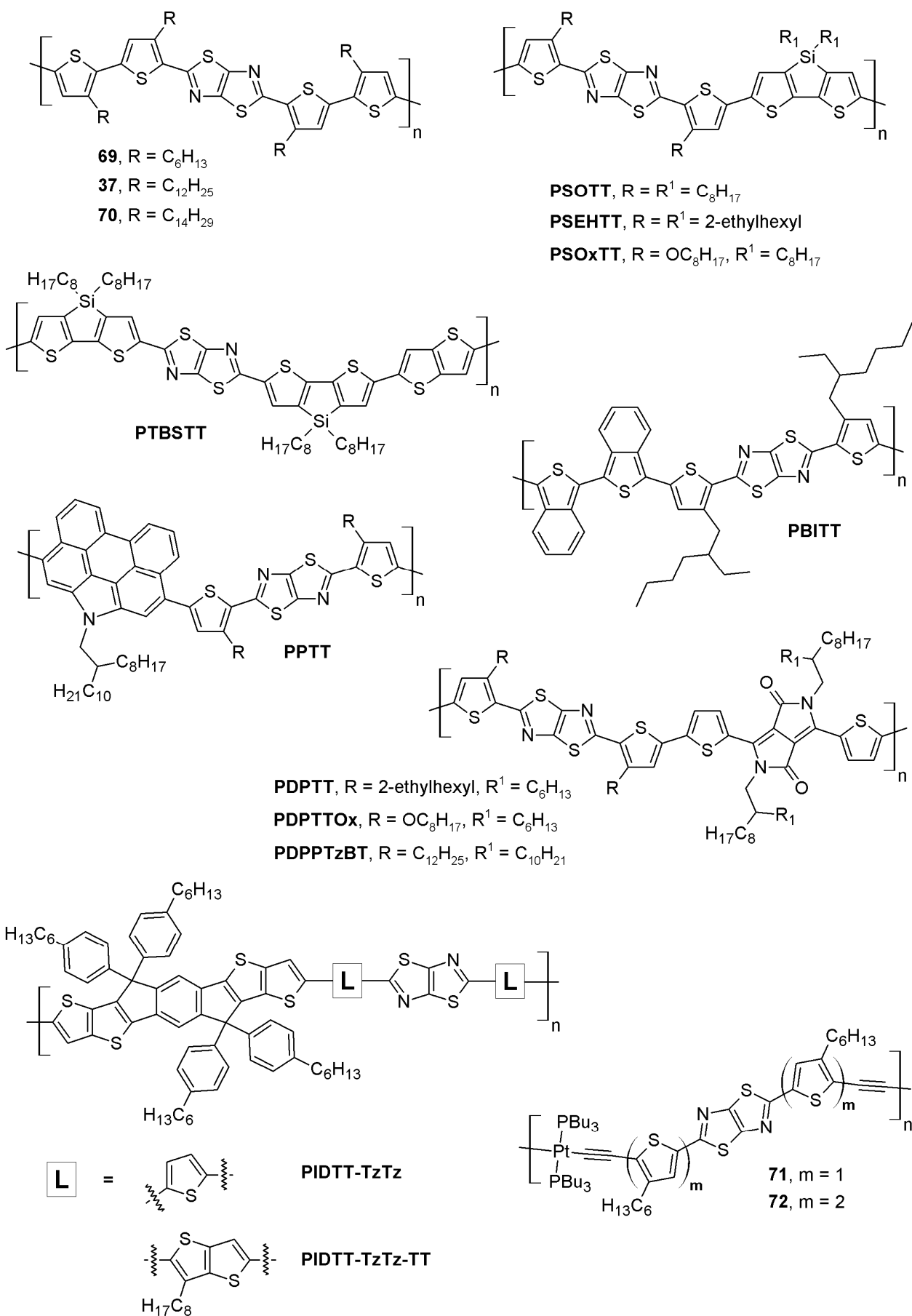


Figure 14

Table 3. *p*-Type OFET characteristics of polymeric thiazolo[5,4-*d*]thiazole-based semiconductors.

Compound	T ann (°C) ^a	Hole mobility (cm ² /V·s)	on/off ratio	V _T (V)	ref.
69	150	5 × 10 ⁻²	10 ⁷	-17	70
37	150	0.23	10 ⁷	-22	6
70	150	0.30	10 ⁷	-23	70
PSOTT	200	1 × 10 ⁻²	10 ⁵ /10 ⁶	n.r. ^b	77
PSEHTT	200	3 × 10 ⁻²	10 ⁵ /10 ⁶	n.r. ^b	77
PSOxTT	200	0.12	10 ⁵ /10 ⁶	n.r. ^b	77
PTBSTT	200	4.2 × 10 ⁻²	10 ⁵	-10.7	78
PPTT	200	0.13	10 ⁷	n.r. ^b	79
PBITT	240 ^c	2.2 × 10 ⁻⁴	10 ²	-18	25
PDPTT	200	0.5	10 ⁵ /10 ⁶	-29.3	80
PDPTTOx	200	1.2	10 ⁵ /10 ⁶	-23.8	80
PDPPTzBT	120	3.4	10 ⁷	n.r. ^b	81
PIDTT-TzTz	- ^d	1.5 × 10 ⁻⁴	10 ⁴	-29.6	82
PIDTT-TzTz-TT	- ^d	7 × 10 ⁻⁴	10 ⁴	-19.8	82
71	120	2.1 × 10 ⁻²	10 ⁵	n.r. ^b	83
72	120	2.8 × 10 ⁻²	10 ⁵	n.r. ^b	83

^aAnnealing temperature (after semiconductor deposition). ^bNot reported. ^cNo surface treatment of the substrate was described. ^dThe SiO₂ substrate was treated with divinyltetramethyldisiloxane-bis(benzocyclobutene) (BCB) prior to semiconductor deposition.

3.6. Organic and polymeric solar cells

The economic and environmental concerns related to the use of classic, nonrenewable energy sources, such as fossil fuels, have been a powerful driving force towards the discovery of alternative methods for energy production. In this context, direct conversion of sunlight into electricity by means of photovoltaic devices has long been the subject of intense research. Among the various technologies currently available, organic photovoltaics (OPV) is characterized by the employment of organic semiconductor materials to perform solar light harvesting as well as charge separation and transfer.⁸⁴ In recent years, the field of OPV has witnessed a very rapid development and several thiazole-based materials (both polymers and small molecules) have been employed in the fabrication of organic photovoltaic devices.⁸⁵ The most common device architecture found in OPV is the so-called “bulk-heterojunction solar cell” (BHJ, Figure 15), featuring few simple components: (a) a transparent electrode, usually made of glass layered with conductive indium-tin oxide (ITO); (b) a photoactive layer constituted by a blend of two organic substances, acting as electron-donor and acceptor, respectively; (c) a hole-conducting layer (usually made of PEDOT:PSS); (d) a metal cathode able to accept electrons from the active layer.⁸⁶

When the sunlight hits the active layer, the donor material adsorbs one photon and promotes one of its electrons from the HOMO to the LUMO, attaining an excited state (the so-called “exciton”). At this stage,

charge separation takes place: the donor transfers the electron to the acceptor, from which it moves to the metal contact; meanwhile, a hole is transferred to the front electrode through the PEDOT:PSS layer. Finally, the electron travels through the external circuit to recombine with the hole, generating an electric current.

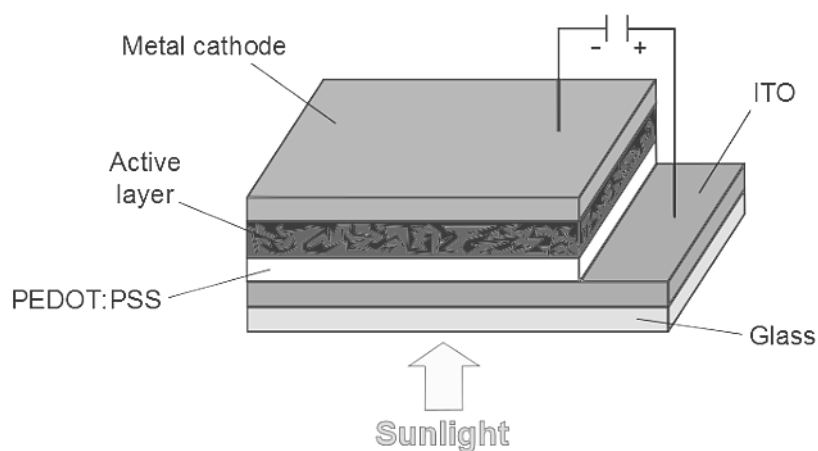


Figure 15

From the brief description above, it is clear that efficient light absorption is crucial for the good functioning of the device, as it is a perfect alignment of the energy levels of all the components involved.⁸⁷ Furthermore, the donor and acceptor materials should form an interpenetrating network with defined nanosized domains and large interface area (from which the term “bulk-heterojunction”): such requirement arises from the fact that excitons have typically short diffusion lengths (10–20 nm) and they need to reach the donor-acceptor interface for charge separation to occur before unproductive recombination takes place. Donor substances have traditionally been polythiophenes (such as poly-3-hexylthiophene), but later more sophisticated co-polymers have appeared,⁸⁸ followed by small molecule-based materials.⁸⁹ As for the acceptors, at present they are almost exclusively constituted by fullerene derivatives, although suitable alternatives are currently being pursued.

Starting from 2010,²⁴ various thiazolothiazole derivatives have been used in BHJ solar cells and their photovoltaic properties have been discussed in a copious amount of papers:¹ contrary to what was observed in the case of OFETs (see Section 3.5.), polymeric compounds have been studied before small molecules. Most of them have been employed as light-harvesting/donor materials, but studies concerning their use as alternative acceptors,⁹⁰ as well as their employment in combination with quantum dots,⁹¹ have also been published. Several of these compounds (Figure 15) were also reported in studies concerning organic transistors,^{24,25,72–80,82} underlining the connections between these two research areas. In addition to those cited above, the OPV co-polymers described to date combine the thiazolothiazole moiety with such diverse (hetero)cyclic units as benzo[1,2-*b*:4,5-*b'*]dithiophene^{92,93} (also with furan rings in the main chain⁹⁴), benzo[1,2-*b*:4,3-*b'*]dithiophene,⁹⁵ naphthalene,⁹⁶ indacenodibenzothiophene,⁹⁷ dithienosilole,^{98–101} dithienogermole,¹⁰² indacenodithiophene,¹⁰³ indenofluorene and indolocarbazole,¹⁰⁴ thiophene,²⁶ diindeno-pyrazine¹⁰⁵ and thiophenylmethylene-9*H*-fluorene.¹⁰⁶ Some of the most efficient and recent structures are presented in Figure 16 and the relevant photovoltaic performances are summarized in Table 4.

In various instances, TzTz-based compounds gave solar cells with high power conversion efficiencies (PCE, defined as the ratio between the electrical power produced by the cell and the power of incident light)

in the 5.0–5.9% range. For each donor, several devices had to be produced with different polymer/acceptor ratios in order to find the ideal stoichiometry, highlighting the importance of this parameter.

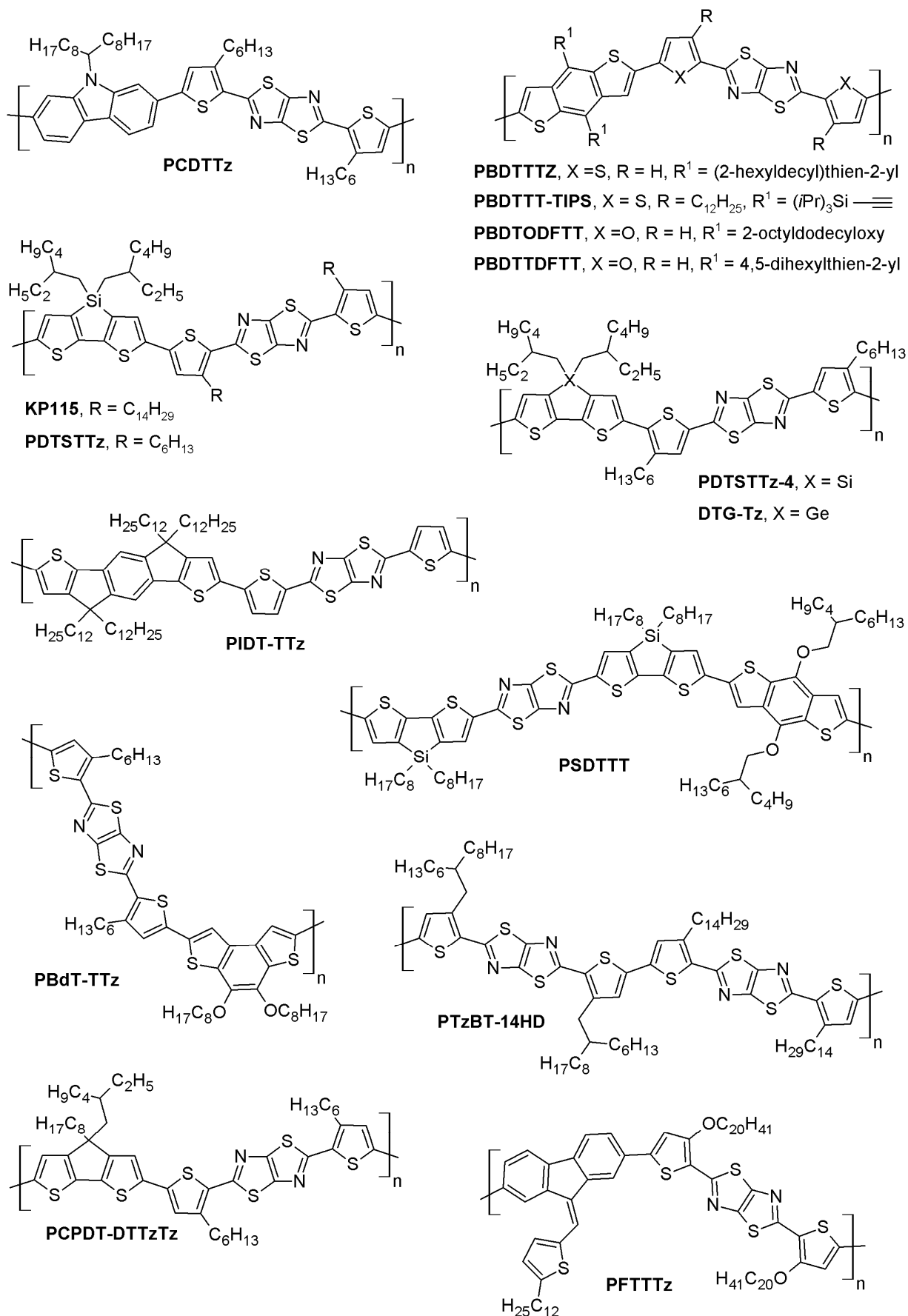


Figure 16

In addition, as exemplified in the case of compound **PSEHTT** (Figure 15), the nature of the acceptor was also crucial.

Among fullerene derivatives, changing from PC₆₁BM to its C₇₀-analog PC₇₁BM caused a substantial increase in PCE, which was then further enhanced using indene-C₆₀ bisadduct ICBA (5.36%, Table 4).^{77,101} In this latter case, the good performance was mostly due to a high open-circuit voltage (V_{oc}), reflecting the larger energy difference between the donor HOMO and the acceptor LUMO. Jenekhe and co-workers explored also the possibility to build an all-polymer solar cell, using **PSEHTT** as the donor and three different naphthalene diimide co-polymers as acceptors: the best performance was obtained with selenium-containing PNDIS-HD, which gave a PCE similar to that observed with classic acceptor PC₆₁BM (3.26% vs. 3.61%).¹⁰⁷ The highest short-circuit current (J_{sc}) was obtained with indacenodithiophene-containing polymer **PIDT-TTz**, which reflected both the excellent light-harvesting ability of this compound (λ_{max} = 590 nm in thin film) and its good intermolecular charge transfer properties. However, the overall solar cell performance was limited by the relatively low fill factor (FF), probably indicating some problems in the charge transfer process between the active layer and the electrodes.¹⁰³

The two best PCEs, both around 5.90%, were obtained with compounds **PDTSTTz-4**¹⁰⁰ and **PIDTT-TzTz** (Figure 16).⁸² Both polymers exhibited hole mobilities in the 10^{-3} – 10^{-4} range, much lower than those observed for the best-performing OFETs (see Section 3.5.), underlining that other properties, such as the energy level alignment and the crystalline packing of the donor-acceptor blend, are more important than charge mobility to define solar cell performance. In agreement with this observation, a simple shift of the alkyl side chain from the 3-position of the thiophene ring (as in **PDTSTTz**⁹⁹) to the 4-position (as in **PDTSTTz-4**¹⁰⁰) was found to improve PCE. The importance of side-chain engineering and ideal donor/acceptor blending was also confirmed by thiazolothiazole-thiophene co-polymer **PTzBT-14HD**, which attained an high efficiency of 5.7% despite the absence of complex poly(hetero)cyclic moieties in the main chain.²⁶ In this case, it was also found that different polymerization conditions, leading to products with the same composition but different MW, profoundly affected device performance, with PCE variations larger than 2.0%.

In the last two years, a small number of studies have been published, which dealt with BHJ solar cells having thiazolothiazole-containing small molecules as light absorbing/donor materials. In most cases, such compounds present a symmetric structure with a central electron-deficient TzTz moiety flanked by conjugated chains ending with electron-rich units, most often triphenylamines. Such arrangement induces a red-shift of the absorption spectra of the resulting compounds, so maxima of that absorption in solution are usually found in the visible region between 400 and 500 nm; in addition, a further bathochromic shift is often observed in the solid state, probably as a result of strong intermolecular stacking.

Small molecules have a series of potential advantages compared to polymers, such as simple and reproducible synthesis (no issues with average chain length and molecular weight), higher purity and easy solution processing. On the other hand, at least in the case of thiazolothiazoles, photovoltaic efficiencies measured to date are still lower than those recorded with polymers (Table 4). In particular, photocurrent and fill factor values still need to be improved, indicating deficiencies both in the light-harvesting ability and in the donor-acceptor solid state organization, which should be addressed by changes in the molecular design. Compounds structures are reported in Figure 17 and their relevant PV parameters are summarized in Table 5.

Table 4. Photovoltaic properties of polymeric thiazolo[5,4-*d*]thiazole-based semiconductors.

Compound	Acceptor ^a	J_{sc} (mA cm ⁻²)	V_{oc} (V)	FF	PCE (%)	Ref.
PCDTTz	PC ₇₁ BM (1:3)	9.15	0.86	0.62	4.88	75
KP115	PC ₆₁ BM (1:2)	11.8	0.60	0.66	4.70	98a
PDTSTTz	PC ₇₁ BM (1:1)	11.9	0.77	0.61	5.59	99
PSEHTT	PC ₆₁ BM (1:2)	8.94	0.65	0.62	3.61	101a
PSEHTT	PC ₇₁ BM (1:2)	12.6	0.65	0.61	5.00	77
PSEHTT	ICBA (1:2)	10.1	0.92	0.58	5.36	101a
PSEHTT	PNDIS-HD (1:1)	7.78	0.76	0.55	3.26	107
PDTSTTz-4	PC ₇₁ BM (1:1.3)	11.25	0.73	0.72	5.88	100
DTG-Tz	PC ₇₁ BM (1:3.6)	6.31	0.58	0.65	2.38	102
PIDT-TTz	PC ₇₁ BM (1:2)	13.3	0.89	0.49	5.79	103
PSDTT	PC ₇₁ BM (1:1.5)	11.6	0.69	0.66	5.30	78
PBdT-TTZ	PC ₇₁ BM (1:3)	5.50	0.90	0.69	3.40	95
PBDTTTz	PC ₇₁ BM (1:3)	10.4	0.85	0.59	5.22	93
PBDTTT-TIPS	PC ₇₁ BM (1:1)	9.77	0.89	0.50	4.33	74
PPTT	PC ₇₁ BM (1:2)	8.16	0.80	0.49	3.20	79
PTzBT-14HD	PC ₆₁ BM (1:2)	10.6	0.84	0.64	5.70	26
PDPTT	PC ₇₁ BM (1:2) ^b	8.03	0.70	0.60	3.27	80
PCPDT-DTTzTz	PC ₇₁ BM (1:3)	11.13	0.67	0.54	4.03	72
PBDTODFTT	PC ₆₁ BM (1:1) ^b	5.20	0.75	0.48	1.87	94
PBDTTDFTT	PC ₆₁ BM (1:1) ^b	7.67	0.83	0.48	3.06	94
PIDTT-TzTz	PC ₇₁ BM (1:3) ^c	10.99	0.90	0.59	5.90	82
PFTTTz	PC ₇₁ BM (1:2)	2.48 ^d	0.70	0.62	2.21	106

^aPolymer/acceptor ratio in parentheses. ^b1,8-Diiodooctane (DIO) was used as an additive in the polymer/acceptor blend. ^cInverted device architecture. ^dIncident light intensity was 49 mW cm⁻² instead of 100 mW cm⁻².

The first example was reported by Li, Zhan and co-workers, who prepared and applied compound **TT-TTPA**. The molecule was decorated with long alkyl chains to improve solubility and facilitate device fabrication and featured a relatively low-lying HOMO, which was considered useful to generate a high open-circuit potential in the solar cell. Indeed, the best performing device had a remarkable V_{oc} of 0.91 V, which was accompanied by a good photocurrent: unfortunately, the low fill factor limited the overall efficiency to 3.73%.¹⁰⁸ A compound very similar to **TT-TTPA**, differing only in the length of the linear alkyl chains (**73**, Figure 17), was independently described by Lee *et al.*, who reported a maximum efficiency of only 2.39% for the corresponding solar cells, mostly due to a lower J_{sc} and poor fill factor. Clearly, the higher annealing

temperature and polymer/acceptor ratios influenced device performance, highlighting the importance of all manufacturing parameters to obtain highly efficient cells.¹⁰⁹

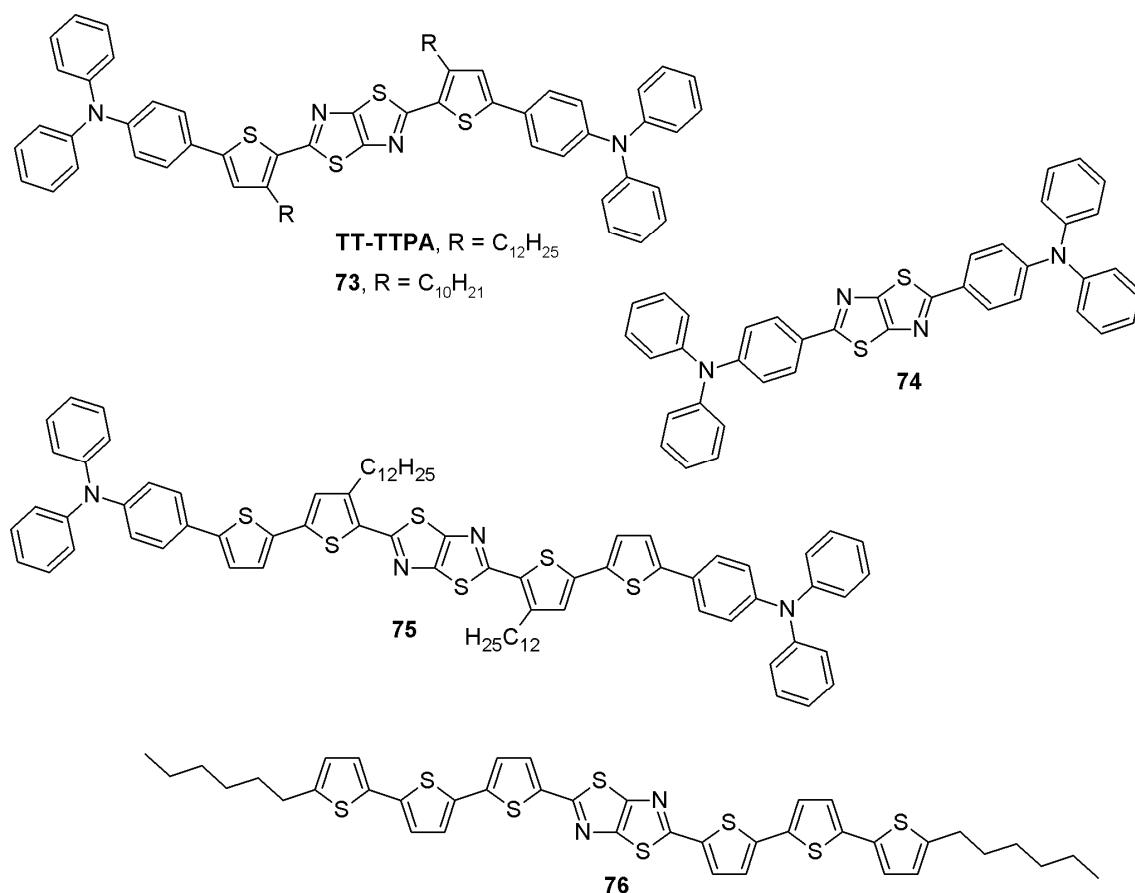


Figure 17

Table 5. Photovoltaic properties of thiazolo[5,4-*d*]thiazole-based molecular semiconductors.

Compound	Acceptor ^a	J_{sc} (mA cm ⁻²)	V_{oc} (V)	FF	PCE (%)	Ref.
TT-TTPA	PC ₇₁ BM (1:4) ^a	9.39	0.91	0.44	3.73	108
73	PC ₇₁ BM (1:3) ^b	6.49	0.94	0.39	2.39	109
74	PC ₇₁ BM (1:4) ^a	6.08	0.86	0.42	2.19	110
75	PC ₇₁ BM (1:4) ^c	9.74	0.85	0.47	4.05	110
66	PC ₇₁ BM (1:2)	5.10	0.75	0.38	1.44	66
76	PC ₆₁ BM (1:1)	7.85	0.65	0.31	1.57	111

^aAnnealing at 110 °C. ^bAnnealing at 140 °C. ^cAnnealing at 120 °C.

In a subsequent study, the performance obtained with **TT-TTPA** was compared with those registered using compounds **74** and **75** (Figure 17). The latter exhibited a red-shifted and intense light absorption due to its superior conjugation length, which was reflected in a slightly higher J_{sc} ; in addition, the balanced hole and electron mobilities helped improving the fill factor, thus yielding a device with 4.05% PCE. In general, it was observed that thermal annealing of the organic films at 110–120 °C resulted in improved charge mobilities, in turn yielding more efficient devices.¹¹⁰

Finally, worse performances were registered with both compound **66**⁶⁶ (Figure 13) and **76**,¹¹¹ showing that, while an extended conjugation length and the presence of terminal donor groups were beneficial to device performance, application of a very elaborated structure could also be unproductive due to issues with molecular planarity, low hole mobility and donor-acceptor crystal packing.

3.7. Dye-sensitized solar cells

The research area in which thiazolo[5,4-*d*]thiazoles have been most recently applied concerns the synthesis and application of new organic photosensitizers for dye-sensitized solar cells (commonly abbreviated as DSSCs).¹¹² Although DSSCs share some of the features of organic solar cells (Section 3.6.), their working principle is much different and it is inspired to natural photosynthesis. DSSCs are made of few simple components (Figure 18): (a) a photoanode, constituted by a layer of an inorganic semiconductor (typically nanocrystalline TiO₂) deposited on conductive ITO-glass. A light-absorbing dye (sensitizer) is adsorbed on the surface of the semiconductor nanoparticles to harvest light; (b) a suitable electrolyte, which can be either a liquid solution or a gel containing a redox couple (most often the I⁻/I₃⁻ couple) or a solid hole-conducting material; (c) a metal cathode (usually made of platinum) able to efficiently catalyze the reduction of the electrolyte.

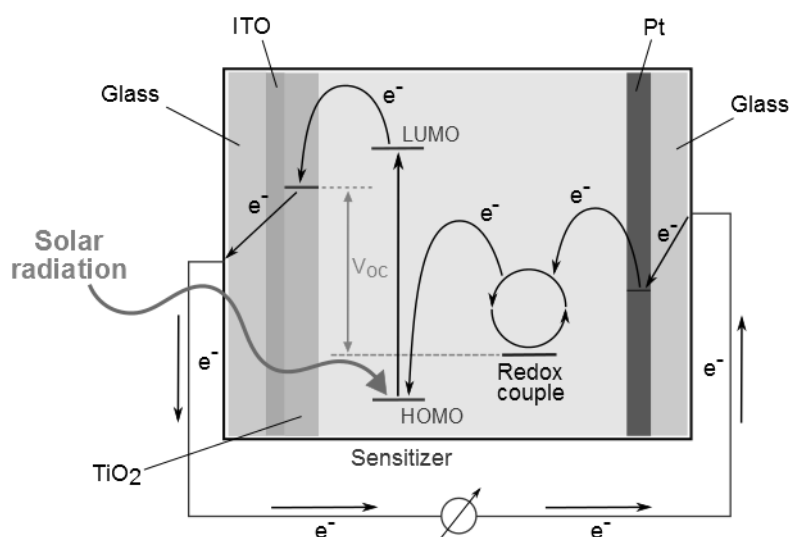


Figure 18

When sunlight hits the front electrode, an electron is promoted from the sensitizer HOMO to its LUMO and from there it is transferred to the conduction band of nc-TiO₂ (a process called “injection”). The resulting positive charge on the sensitizer (hole) is then transferred to the redox mediator, which is thus converted in its oxidized form. Meanwhile, the electron travels through the external circuit (generating an electric current) and is collected at the cathode, where the reduction of the oxidized redox mediator takes place, closing the circuit. Despite the various redox processes described above, no permanent chemical transformation occurs within the cell.¹¹³

The light-harvesting dye is surely one of the most important components of a DSSC, being involved both in the light absorption and charge separation processes. Usually, organic compounds acting as sensitizers present a D- π -A architecture, in which an electron-rich donor group (usually a triarylamine) is connected to an electron-deficient acceptor (also functioning as anchoring group to TiO₂) through a

π -conjugated spacer.¹¹⁴ As shown in Figure 19, the TzTz moiety was inserted into this latter section of the molecule, due to its already-mentioned properties of high planarity, good electronic conductivity and oxidative stability.

At the beginning of 2013, two different research groups independently reported the synthesis and application of very similar thiazolothiazole-thiophene-based dyes **FNE71-74**¹¹⁵ and **TTZ1-2**,¹¹⁶ whose scaffolds differed only for the length of the π -conjugated system and the relative positioning of the alkyl chains on the thiophene rings flanking the central TzTz moiety; due to the electron-poor nature of the latter, such structures could also be described as “D- π -A π -A” sensitizers. The dyes were prepared following similar pathways comprising electrophilic halogenation reactions, Suzuki cross-couplings and (only in the first case) a Vilsmeier-Haack formylation; in both cases, the terminal cyanoacrylic moiety was introduced by means of a Knoevenagel condensation between intermediate aldehyde **80** or **83** and cyanoacetic acid (Scheme 14).

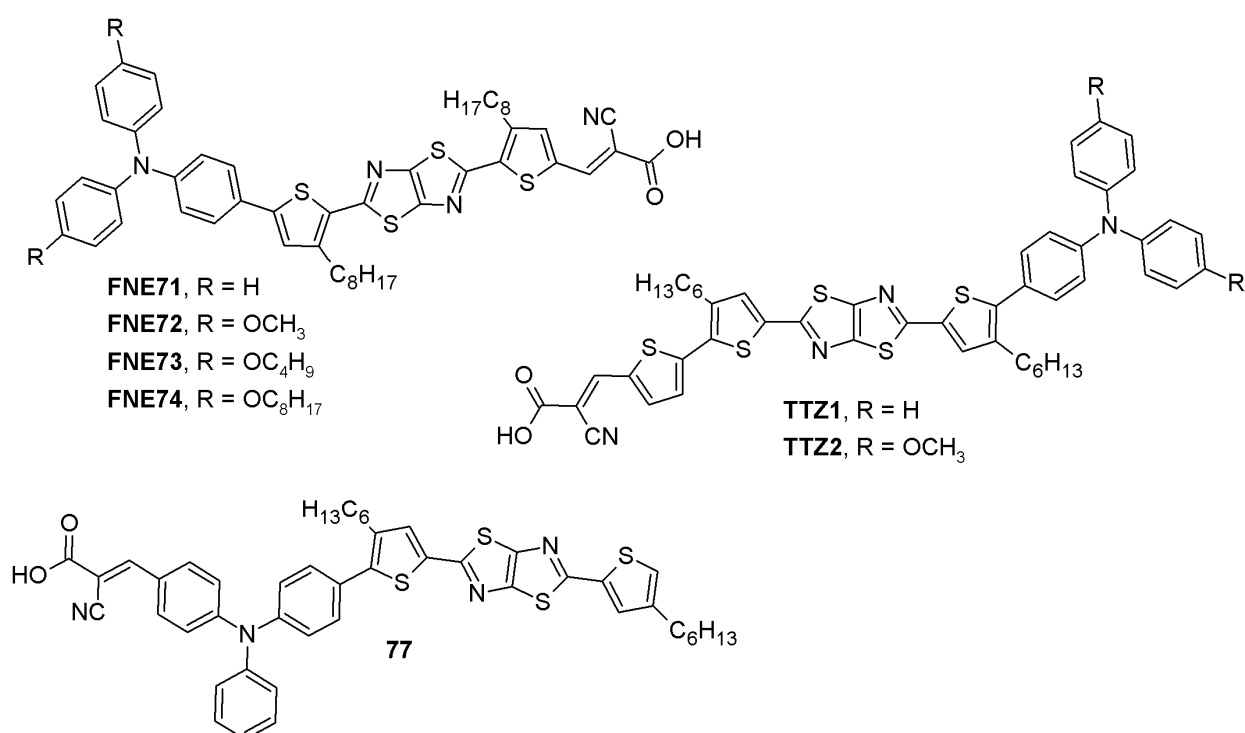
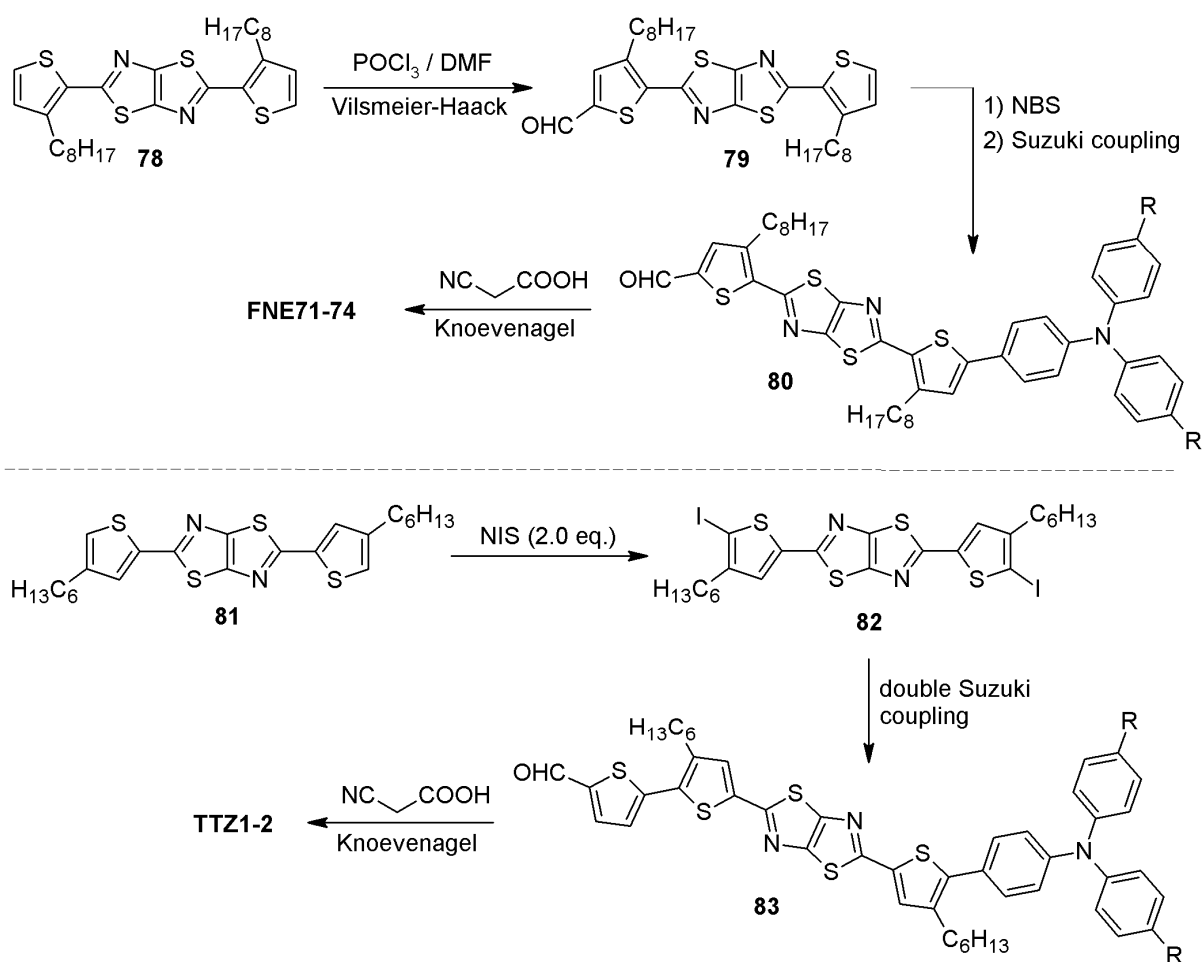


Figure 19

The two series of compounds had very similar chemical and photophysical properties, with absorption maxima in the 470–490 nm range and optical bandgaps between 2.02 and 2.33 eV. Unfortunately, due to the different fabrication procedures employed, the photovoltaic performances of the resulting DSSCs cannot be directly compared. Despite that, it can be observed that compound **FNE74**, featuring long alkyl chains on the donor moiety, was the best-performing sensitizer among its series, giving a maximum PCE of 5.10% in the presence of a quasi-solid state Γ/I_3^- electrolyte: such good performance was obtained after careful electrolyte optimization and was mainly due to a remarkable J_{sc} value of 14.5 mA·cm⁻².¹¹⁵ On the other hand, **TTZ1**, bearing unsubstituted phenyl rings, performed better than the corresponding methoxy-substituted analogue **TTZ2**, giving a maximum PCE of 3.53% with a liquid electrolyte; in this case, despite good V_{oc} and FF values, a relatively low photocurrent (6.9 mA·cm⁻²) limited the overall efficiency of the device.¹¹⁶



Finally, a different thiazolothiazole-containing sensitizer was also reported, which was based on a rather unconventional π -D-A architecture (**77**, Figure 19). Compound **77** was prepared following a procedure similar to **FNE71-74**, but with inversion of the Vilsmeier-Haack formylation and bromination/Suzuki coupling steps: the resulting structure presents a heteroaromatic conjugated unit placed in terminal position rather than between the donor and the acceptor moieties. Remarkably, such compound presented a red-shifted absorption compared to a similar molecule lacking the heteroaromatic section, indicating that the latter was capable to enhance light harvesting in the visible region. In addition, DSSCs built using dye **77** showed a good V_{oc} value of 0.712 V and yielded a power conversion efficiency of 2.55%. Although this value was lower than those observed for **FNE71-74** and **TTZ1-2**, the result was still significant, since it demonstrated that also dyes based on uncommon structural designs could be employed to fabricate working dye-sensitized solar cells.¹¹⁷

4. Conclusions

In this review, the most important aspects of the chemistry of thiazolo[5,4-*d*]thiazoles have been reviewed, including the main methods available for their synthesis and elaboration, their structural, spectroscopic and photophysical characterization as well as their applications in a range of different research areas, extending from pharmaceuticals to materials science and organic electronics.

As shown above, while the thiazolo[5,4-*d*]thiazole ring system was already identified at the beginning of the 1960s³ (and has a long history of industrial interest, as demonstrated by patent literature), it received

relatively scarce attention from the scientific community until the use of thiazolothiazole-containing materials in light-emitting diodes⁴ and organic transistors^{5,6} was demonstrated in the years 2004–2007. From then on, the number of publications concerning the synthesis and employment of TzTz-based materials has been rapidly growing and several new potential fields of application have been investigated.¹ Among them, the use of thiazolothiazoles in organic photovoltaics, and more precisely bulk-heterojunction solar cells, has been at the centre of intense research efforts from many academic and industrial groups and very promising results in terms of device efficiency and ease of fabrication have already been described.⁸⁵

Despite such achievements, the relatively late development of thiazolothiazole chemistry means that in several areas there is still room for considerable improvement. First of all, synthetic methods appear still underdeveloped: while a few alternative procedures have been introduced over the years, the vast majority of TzTz-based compounds are still prepared using the traditional methodology by Johnson and Ketcham.³ In addition, virtually all polymers are obtained by transition metal-catalyzed cross-coupling polymerization processes.^{4,6} Although these methods are able to provide the desired compounds in useful quantities for the subsequent applicative studies, improvements are clearly desirable: in this context, the use of non-conventional heating conditions¹³ or different reaction mechanisms^{14–22} has already been documented and should be investigated further. Secondly, application of thiazolothiazoles in various technological fields is still in its infancy, as exemplified by their use as sensitizers for dye-sensitized solar cells:^{115–117} developments in this area could have a significant impact on the future large-scale application of such devices.

The thiazolo[5,4-*d*]thiazole ring system is now a well-established scaffold in heterocyclic chemistry. In view of its favourable structural and electronic properties, its employment in materials science and organic electronics is expected to further increase in the future, making it a privileged building block for the preparation of various organic functional materials.

Acknowledgments

The authors thank Regione Toscana (“FOTOSENSORG” project, POR FSE 2007–2013) and Ente Cassa di Risparmio di Firenze (“IRIS” project) for financial support.

References

1. Bevk, D.; Marin, L.; Lutsen, L.; Vanderzande, D.; Maes, W. *RSC Adv.* **2013**, *3*, 11418.
2. Ephraim, J. *Ber. Dtsch. Chem. Ges.* **1891**, *24*, 1026.
3. Johnson, J. R.; Ketcham, R. *J. Am. Chem. Soc.* **1960**, *82*, 2719.
4. Peng, Q.; Peng, J.-B.; Kang, E. T.; Neoh, K. G.; Cao, Y. *Macromolecules* **2005**, *38*, 7292.
5. Ando, S.; Nishida, J.-i.; Inoue, Y.; Tokito, S.; Yamashita, Y. *J. Mater. Chem.* **2004**, *14*, 1787.
6. Osaka, I.; Sauv e, G.; Zhang, R.; Kowalewski, T.; McCullough, R. D. *Adv. Mater.* **2007**, *19*, 4160.
7. Preston, J. J. *Heterocycl. Chem.* **1965**, *2*, 441.
8. Thomas, D. A. *J. Heterocycl. Chem.* **1970**, *7*, 457.
9. Knighton, R. C.; Hallet, A. J.; Kariuki, B. M.; Pope, S. J. A. *Tetrahedron Lett.* **2010**, *51*, 5419.
10. In addition to reports concerning the synthesis of the thiazolothiazole core, the homologation of a 2,5-diaryl derivative (Ar=4-Me-Ph in Scheme 1) to access a *bis*-stilbene-substituted species was also described: Siegrist, A. E. *Helv. Chim. Acta* **1967**, *50*, 906.
11. Johnson, J. R.; Rotenberg, D. H.; Ketcham, R. *J. Am. Chem. Soc.* **1970**, *92*, 4046.
12. Benin, V.; Yeates, A. T.; Dudis, D. *J. Heterocycl. Chem.* **2008**, *45*, 811.
13. Dessi, A.; Calamante, M.; Mordini, A.; Zani, L.; Taddei, M.; Reginato, G. *RSC Adv.* **2014**, *4*, 1322.

14. Beck, G.; Holtschmidt, H. DE2214610 (1972).
15. Beck, G.; Heitzer, H.; Holtschmidt, H. *Synthesis* **1985**, 586.
16. Seybold, G.; Eilingsfeld, H. *Liebigs Ann. Chem.* **1979**, 1271.
17. Hansen, P.; Liebich, W. DD154978 (1982).
18. Roethling, T.; Schroeder, A.; Kibbel, H.; Kochmann, W.; Naumann, K. DD208354 (1984).
19. Roethling, T.; Schroeder, A.; Kibbel, H.; Kochmann, W.; Naumann, K. DD210457 (1984).
20. Roethling, T.; Polanek, M.; Hansen, P.; Kibbel, H.; Neumann, K.; Thust, U. DD216241 (1984).
21. Bossio, R.; Marcaccini, S.; Pepino, R.; Torroba, T.; Valle, G. *Synthesis* **1987**, 1138.
22. Rössler, A.; Boldt, P. *J. Chem. Soc., Perkin Trans. I* **1998**, 685.
23. Belfield, K. D.; Yao, S.; Morales, A. R.; Hales, J. M.; Hagan, D. J.; Van Stryland, E. W.; Chapela, V. M.; Percino, J. *Polym. Adv. Technol.* **2005**, *16*, 150.
24. Jung, I. H.; Yu, J.; Jeong, E.; Kim, J.; Kwon, S.; Kong, H.; Lee, K.; Woo, H. Y.; Shim, H.-K. *Chem. Eur. J.* **2010**, *16*, 3743.
25. Umeyama, T.; Hirose, K.; Noda, K.; Matsushighe, K.; Shishido, T.; Saarenpää, H.; Tkachenko, N. V.; Lemmetyinen, H.; Ono, N.; Imahori, H. *J. Phys. Chem. C* **2012**, *116*, 17414.
26. Osaka, I.; Saito, M.; Mori, H.; Koganezawa, T.; Takimiya, K. *Adv. Mater.* **2012**, *24*, 425.
27. Naraso, N.; Wudl, F. *Macromolecules* **2008**, *41*, 3169.
28. Bolognesi, A.; Catellani, M.; Destri, S.; Porzio W. *Acta Cryst. Sect. C: Cryst. Struct. Commun.* **1987**, *C43*, 2106.
29. Wagner, P.; Kubicki, M. *Acta Cryst. Sect. C: Cryst. Struct. Commun.* **2003**, *C59*, 91.
30. Brillante, A.; Samorì, B.; Stremmenos, C.; Zanirato, P. *Mol. Cryst. Liq. Cryst.* **1983**, *100*, 263.
31. Pinto, M. R.; Takahata, Y.; Atvars, T. D. *Z. J. Photochem. Photobiol. A: Chem.* **2001**, *143*, 119.
32. Akpinar, H. Z.; Udum, Y. A.; Toppare, L. *J. Polym. Sci. Polym. Chem.* **2013**, *51*, 3901.
33. Van Mierloo, S.; Chambon, S.; Boyukbayram, A. E.; Adriaensens, P.; Lutsen, L.; Cleij, T. J.; Vanderzande, D. *Magn. Reson. Chem.* **2010**, *48*, 362.
34. Van Mierloo, S.; Liégeois, V.; Kudrjasova, J.; Botek, E.; Lutsen, L.; Champagne, B.; Vanderzande, D.; Adriaensens, P.; Maes, W. *Magn. Reson. Chem.* **2012**, *50*, 379.
35. Spivack, J. D.; Steinberg, D. H.; Dexter, M. US3316209 (1967).
36. Sawdey, G. W. US3250617 (1966).
37. Dear, K. M.; Jeffreys, R. A.; Thomas, D. A. US3630738 (1971).
38. Fikrat, H. T.; Oneto, J. F. *J. Pharm. Sci.* **1962**, *51*, 527.
39. Ketcham, R.; Mah, S. *J. Med. Chem.* **1971**, *14*, 743.
40. Moffett, R. B. *J. Heterocycl. Chem.* **1980**, *17*, 753.
41. Gitterman, C. O. US3988463 (1976).
42. Jubran, N. US5350857 (1994).
43. Zampese, J. A.; Keene, F. R.; Steel, P. J. *Dalton Trans.* **2004**, 4124.
44. Slater, J. W.; Steel, P. J. *Tetrahedron Lett.* **2006**, *47*, 6941.
45. Olgun, U.; Gülfen, M. *Dyes Pigm.* **2013**, *99*, 1004.
46. Falcão, E. H. L.; Naraso; Feller, R. K.; Wu, G.; Wudl, F.; Cheetam, A. K. *Inorg. Chem.* **2008**, *47*, 8336.
47. Aprea, A.; Colombo, V.; Galli, S.; Masciocchi, N.; Maspero, A.; Palmisano, G. *Solid State Sci.* **2010**, *12*, 795.
48. Maspero, A.; Cernuto, G.; Galli, S.; Palmisano, G.; Tollari, S.; Masciocchi, N. *Solid State Sci.* **2013**, *22*, 43.
49. Hisamatsu, S.; Masu, H.; Azumaya, I.; Takahashi, M.; Kishikawa, K.; Kohmoto, S. *Cryst. Growth Des.* **2011**, *11*, 5387.
50. Goeppert-Mayer, M. *Ann. Physik* **1931**, *9*, 273.
51. He, G. S.; Lin, T.-C.; Prasad, P. N.; Kannan, R.; Vaia, R. A.; Tan, L.-S. *J. Phys. Chem. B* **2002**, *106*, 11081.
52. Kannan, R.; Tan, L.-S.; Reinhardt, B. A.; Vaia, R. A. US6730793 B1 (2004).
53. Jung, J. Y.; Han, S. J.; Chun, J.; Lee, C.; Yoon, J. *Dyes Pigm.* **2012**, *94*, 423.
54. Ziessel, R.; Nano, A.; Heyer, E.; Bura, T.; Retailleau, P. *Chem. Eur. J.* **2013**, *19*, 2582.
55. Tang, C. W.; Van Slyke, S. A. *Appl. Phys. Lett.* **1987**, *51*, 913.

56. Bernius, M.; Inbasekaran, M.; O'Brien, J.; Wu, W. *Adv. Mater.* **2000**, *12*, 1737.
57. Jung, I. H.; Jung, Y. K.; Lee, J.; Park, J.-H.; Woo, H. Y.; Lee, J.-I.; Chu, H. Y.; Shim, H.-K. *J. Polym. Sci. Polym. Chem.* **2008**, *46*, 7148.
58. Mishra, S. P.; Palai, A. K.; Kumar, A.; Srivastava, R.; Kamalasanan, M. N.; Patri, M. *Macromol. Chem. Phys.* **2010**, *211*, 1890.
59. Li, D.; Zhang, Z.; Zhao, S.; Wang, Y.; Zhang, H. *Dalton Trans.* **2011**, *40*, 1279.
60. Li, D.; Yuan, Y.; Bi, H.; Yao, D.; Zhao, X.; Tian, W.; Wang, Y.; Zhang, H. *Inorg. Chem.* **2011**, *50*, 4825.
61. Wen, Y.; Liu, Y.; Guo, Y.; Yu, G.; Hu, W. *Chem. Rev.* **2011**, *111*, 3358.
62. Wang, C.; Jiang, L.; Hu, W. *Organic/Polymeric Field-Effect Transistors In Organic Optoelectronics*; Hu, W., Ed.; Wiley-VCH: Weinheim, 2013.
63. (a) Ando, S.; Nishida, J.-i.; Fujiwara, E.; Tada, H.; Inoue, Y.; Tokito, S.; Yamashita, Y. *Chem. Lett.* **2004**, *33*, 1170. (b) Ando, S.; Nishida, J.-i.; Fujiwara, E.; Tada, H.; Inoue, Y.; Tokito, S.; Yamashita, Y. *Synth. Met.* **2006**, *156*, 327. (c) Ando, S.; Kumaki, D.; Nishida, J.-i.; Tada, H.; Inoue, Y.; Tokito, S.; Yamashita, Y. *J. Mater. Chem.* **2007**, *17*, 553.
64. (a) Ando, S.; Nishida, J.-i.; Tada, H.; Inoue, Y.; Tokito, S.; Yamashita, Y. *J. Am. Chem. Soc.* **2005**, *127*, 5336. (b) Kumaki, D.; Ando, S.; Shimono, S.; Yamashita, Y.; Umeda, T.; Tokito, S. *Appl. Phys. Lett.* **2007**, *90*, 53506. (c) Mamada, M.; Nishida, J.-i.; Kumaki, D.; Tokito, S.; Yamashita, Y. *Chem. Mater.* **2007**, *19*, 5404. (d) Fujisaki, Y.; Mamada, M.; Kumaki, D.; Tokito, S.; Yamashita, Y. *Jpn. J. Appl. Phys.* **2009**, *48*, 111504.
65. Van Mierloo, S.; Vasseur, K.; Van den Brande, N.; Boyukbayram, A. E.; Ruttens, B.; Rodriguez, S. D.; Botek, E.; Liégeois, V.; D'Haen, J.; Adriaensens, P. J.; Heremans, P.; Champagne, B.; Van Assche, G.; Lutsen, L.; Vanderzande, D. J.; Maes, W. *ChemPlusChem* **2012**, *77*, 923.
66. Dutta, P.; Park, H.; Lee, W.-H.; Kang, I.-N.; Lee, S.-H. *Org. Electron.* **2012**, *13*, 3183.
67. Tomino, K.; Sugawara, S.; Maeda, H.; Matsuoka, M. US2007/0128764 A1 (2007).
68. Kim, D.-Y.; Lim, B.; Baeg, K.-J.; Jeong, H.-G.; Oh, S.-H.; Park, H.-J. EP2065389 A1 (2009).
69. Kiselev, R.; Yoon, S.-H.; Choi, H.; Lee, J.-M. US2010/0236631 A1 (2010).
70. (a) Osaka, I.; Zhang, R.; Sauv e, G.; Smilgies, D.-M.; Kowalewski, T.; McCullough, R. D. *J. Am. Chem. Soc.* **2009**, *131*, 2521. (b) Osaka, I.; Zhang, R.; Liu, J.; Smilgies, D.-M.; Kowalewski, T.; McCullough, R. D. *Chem. Mater.* **2010**, *22*, 4191.
71. Shi, Q.; Fan, H.; Liu, Y.; Chen, J.; Shuai, Z.; Hu, W.; Li, Y.; Zhan, X. *J. Polym. Sci. Polym. Chem.* **2011**, *49*, 4875.
72. Van Mierloo, S.; Hadipour, A.; Spijkman, M.-J.; Van den Brande, N.; Ruttens, B.; Kesters, J.; D'Haen, J.; Van Assche, G.; de Leew, D. M.; Aernouts, T.; Manca, J.; Lutsen, L.; Vanderzande, D. J.; Maes, W. *Chem. Mater.* **2012**, *24*, 587.
73. Shi, Q.; Fan, H.; Liu, Y.; Hu, W.; Li, Y.; Zhan, X. *J. Phys. Chem. C* **2010**, *114*, 16843.
74. Shi, Q.; Fan, H.; Liu, Y.; Hu, W.; Li, Y.; Zhan, X. *Macromolecules* **2011**, *44*, 9173.
75. Lee, S. K.; Cho, J. M.; Goo, Y.; Shin, W. S.; Lee, J.-C.; Lee, W.-H.; Kang, I.-N.; Shim, H.-K.; Moon, S.-J. *Chem. Commun.* **2011**, *47*, 1791.
76. Lee, S. K.; Kang, I.-N.; Lee, J.-C.; Shin, W. S.; So, W.-W.; Moon, S.-J. *J. Polym. Sci. Polym. Chem.* **2011**, *49*, 3129.
77. Subramaniyan, S.; Xin, H.; Kim, F. S.; Shoaee, S.; Durrant, J. D.; Jenekhe, S. A. *Adv. Energy Mater.* **2011**, *1*, 854.
78. Subramaniyan, S.; Xin, H.; Kim, F. S.; Jenekhe, S. A. *Macromolecules* **2011**, *44*, 6245.
79. Chen, H.; He, C.; Yu, G.; Zhao, Y.; Huang, J.; Zhu, M.; Liu, H.; Guo, Y.; Li, Y.; Liu, Y. *J. Mater. Chem.* **2012**, *22*, 3696.
80. Subramaniyan, S.; Kim, F. S.; Ren, G.; Li, H.; Jenekhe, S. A. *Macromolecules* **2012**, *45*, 9029.
81. Cheng, C.; Yu, C.; Guo, Y.; Chen, H.; Fang, Y.; Yu, G.; Liu, Y. *Chem. Commun.* **2013**, *49*, 1998.
82. Xu, Y.-X.; Chueh, C.-C.; Yip, H.-L.; Chang, C.-Y.; Liang, P.-W.; Intemann, J. J.; Chen, W.-C.; Jen, A. K.-Y. *Polym. Chem.* **2013**, *4*, 5220.
83. Yan, L.; Zhao, Y.; Wang, X.; Wang, X.-Z.; Wong, W.-Y.; Liu, Y.; Wu, W.; Xiao, Q.; Wang, G.; Zhou, X.; Zeng, W.; Li, C.; Wang, X.; Wu, H. *Macromol. Rapid Commun.* **2012**, *33*, 603.

84. *Organic Photovoltaics: Materials, Device Physics, and Manufacturing Technologies*; Brabec, C.; Dyakonov, V.; Scherf, U., Eds.; Wiley-VCH: Weinheim, 2008.
85. Lin, Y.; Fan, H.; Li, Y.; Zhan, X. *Adv. Mater.* **2012**, *24*, 3087.
86. For a detailed description of the working mechanism of a bulk-heterojunction solar cell, see: Po, R.; Maggini, M.; Camaioni, N. *J. Phys. Chem. C* **2010**, *114*, 695.
87. Li, Y. *Acc. Chem. Res.* **2012**, *45*, 723.
88. Kularatne, R. S.; Magurudeniya, H. D.; Sista, P.; Biewer, M. C.; Stefan, M. C. *J. Polym. Sci. Polym. Chem.* **2013**, *51*, 743.
89. (a) Lin, Y.; Li, Y.; Zhan, X. *Chem. Soc. Rev.* **2012**, *41*, 4245. (b) Mishra, A.; Bäuerle, P. *Angew. Chem. Int. Ed.* **2012**, *51*, 2020.
90. Nevil, N.; Ling, Y.; Van Mierloo, S.; Kesters, J.; Piersimoni, F.; Adriaensens; Lutsen, L.; Vanderzande, D.; Manca, J.; Maes, W.; Van Doorslaer, S.; Goovaerts, E. *Phys. Chem. Chem. Phys.* **2012**, *14*, 15774.
91. Strein, E.; Colbert, A.; Subramaniyan, S.; Nagaoka, H.; Schlenker, C. W.; Janke, E.; Jenekhe, S. A.; Ginger, D. S. *Energy Environ. Sci.* **2013**, *6*, 769.
92. Yang, M.; Peng, B.; Liu, B.; Zou, Y.; Zhou, K.; He, Y.; Pan, C.; Li, Y. *J. Phys. Chem. C* **2010**, *114*, 17989.
93. Huo, L.; Guo, X.; Zhang, S.; Li, Y.; Hou, J. *Macromolecules* **2011**, *44*, 4035.
94. Hu, C.; Wu, Z.; Cao, K.; Sun, B.; Zhang, Q. *Polymer* **2013**, *54*, 1098.
95. Zhang, M.; Sun, Y.; Guo, X.; Cui, C.; He, Y.; Li, Y. *Macromolecules* **2011**, *44*, 7625.
96. Dutta, P.; Yang, W.; Park, H.; Baek, M.-j.; Lee, Y.-S.; Lee, S.-H. *Synth. Met.* **2011**, *161*, 1582.
97. Lee, T. W.; Kang, N. S.; Yu, J. W.; Hoang, M. H.; Kim, K. H.; Jin, J.-I.; Choi, D. H. *J. Polym. Sci. Polym. Chem.* **2010**, *48*, 5921.
98. (a) Peet, J.; Wen, L.; Byrne, P.; Rodman, S.; Forberich, K.; Shao, Y.; Drolet, N.; Gaudiana, R.; Dennler, G.; Waller, D. *Appl. Phys. Lett.* **2011**, *98*, 043301. (b) Clarke, T. M.; Rodovsky, D. B.; Herzog, A. A.; Peet, J.; Dennler, G.; DeLongchamp, D.; Lugenschmied, C.; Mozer, A. J. *Adv. Energy Mater.* **2011**, *1*, 1062. (c) Clarke, T. M.; Peet, J.; Denk, P.; Dennler, G.; Lugenschmied, C.; Mozer, A. J. *Energy Environ. Sci.* **2012**, *5*, 5241.
99. Zhang, M.; Guo, X.; Li, Y. *Adv. Energy Mater.* **2011**, *1*, 557.
100. Zhang, Z.-G.; Min, J.; Zhang, S.; Zhang, J.; Zhang, M.; Li, Y. *Chem. Commun.* **2011**, *47*, 9474.
101. (a) Xin, H.; Subramaniyan, S.; Kwon, T.-W.; Shoaee, S.; Durrant, J. R.; Jenekhe, S. A. *Chem. Mater.* **2012**, *24*, 1995. (b) Shoaee, S.; Subramaniyan, S.; Xin, H.; Keiderling, C.; Tuladhar, P. S.; Jamieson, F.; Jenekhe, S. A.; Durrant, J. R. *Adv. Funct. Mater.* **2013**, *23*, 3286.
102. Hwang, Y.-M.; Ohshita, J.; Harima, Y.; Mizumo, T.; Ooyama, Y.; Morhara, Y.; Izawa, T.; Sugioka, T.; Fujita, A. *Polymer* **2011**, *52*, 3912.
103. Zhang, M.; Guo, X.; Wang, X.; Wang, H.; Li, Y. *Chem. Mater.* **2011**, *23*, 4264.
104. Jeong, E.; Kim, G.; Jung, I. H.; Jeong, P.; Kim, J. Y.; Woo, H. Y. *Curr. Appl. Phys.* **2012**, *12*, 11.
105. Shen, P.; Liu, X.; Tang, P.; Zhao, B.; Wang, L.; Weng, C.; Cao, J.; Wu, Y.; Chen, Y.; Tan, S. *Macromol. Chem. Phys.* **2013**, *214*, 1147.
106. Hai, J.; Zhao, B.; Zhang, F.; Sheng, C.-X.; Yin, L.; Li, Y.; Zhu, E.; Bian, L.; Wu, H.; Tang, W. *Polymer* **2013**, *54*, 4930.
107. Earmme, T.; Hwang, Y.-J.; Murari, N. M.; Subramaniyan, S.; Jenekhe, S. A. *J. Am. Chem. Soc.* **2013**, *135*, 14960.
108. Shi, Q.; Cheng, P.; Li, Y.; Zhan, X. *Adv. Energy Mater.* **2012**, *2*, 63.
109. Dutta, P.; Yang, W.; Eom, S. H.; Lee, S.-H. *Org. Electron.* **2012**, *14*, 273.
110. Cheng, P.; Shi, Q.; Lin, Y.; Li, Y.; Zhan, X. *Org. Electron.* **2012**, *14*, 599.
111. Nazim, M.; Ameen, S.; Akhtar, M. S.; Lee, Y.-S.; Shin, H.-S. *Chem. Phys. Lett.* **2013**, *574*, 89.
112. *Dye-sensitized solar cells*; Kalyanasundaram, K., Ed.; EPFL Press: Lausanne, 2010.
113. Hagfeldt, A.; Boschloo, G.; Sun, L.; Kloo, L.; Pettersson, H. *Chem. Rev.* **2010**, *110*, 6595.
114. Ooyama, Y.; Harima, Y. *ChemPhysChem* **2012**, *13*, 4032, and references cited therein.
115. Zhang, W.; Feng, Q.; Wang, Z.-S.; Zhou, G. *Chem. Asian J.* **2013**, *8*, 939.

116. Dessì, A.; Barozzino Consiglio, G.; Calamante, M.; Reginato, G.; Mordini, A.; Peruzzini, M.; Taddei, M.; Sinicropi, A.; Parisi, M. L.; Fabrizi de Biani, F.; Basosi, R.; Mori, R.; Spatola, M.; Bruzzi, M.; Zani, L. *Eur. J. Org. Chem.* **2013**, 1916.
117. Zani, L.; Reginato, G.; Mordini, A.; Calamante, M.; Peruzzini, M.; Taddei, M.; Sinicropi, A.; Parisi, M. L.; Fabrizi de Biani, F.; Basosi, R.; Cavallaro, A.; Bruzzi, M. *Tetrahedron Lett.* **2013**, *54*, 3944.

SYNTHESIS AND PHOTOPHYSICAL PROPERTIES OF THE GREEN FLUORESCENT PROTEIN CHROMOPHORE AND ANALOGUES

David Martínez-López and Diego Sampedro*

*Departamento de Química, Centro de Investigación en Síntesis Química (CISQ),
Madre de Dios 51, E-26006, Logroño, Spain (e-mail: diego.sampedro@unirioja.es)*

Abstract. *In this contribution, we will review the synthesis, photophysical properties and applications of several families of compounds based on the green fluorescent protein (GFP) chromophore. Different synthetic routes leading to diverse modifications of the GFP chromophore will be presented. Then, the analysis of their photophysical and photochemical properties, including photoswitching and emission, will be performed. Finally, some selected applications in medicine, biology and chemistry of these families of compounds will be discussed.*

Contents

1. Introduction
 2. Synthesis of GFP chromophore analogues
 - 2.1. Synthesis of oxazolones
 - 2.2. Synthesis of imidazolinones
 - 2.3. Synthesis of other derivatives
 3. Photophysical properties of GFP and GFP derivatives
 - 3.1. Absorption
 - 3.1.1. Oxazolones
 - 3.1.2. Imidazolinones
 - 3.2. Fluorescence
 - 3.2.1. Oxazolones
 - 3.2.2. Imidazolinones
 - 3.3. Photoisomerisation
 - 3.4. Photophysical properties of other derivatives
 4. Applications
 5. Conclusions
- Acknowledgments
- References

1. Introduction

Since its discovery, the green fluorescent protein (GFP) has shown an impressive potential in many different scientific fields from organic chemistry to biological imaging, from photophysics to materials science. Proof of this huge success is the Nobel Prize in Chemistry awarded in 2008 to Martin Chalfie, Osamu Shimomura and Roger Y. Tsien “for their discovery and development of the green fluorescent protein”.¹ The GFP was first isolated from the jellyfish *Aequorea Victoria* and it is the best known and most used of a family of fluorescent proteins that have been isolated from natural sources and used in many different applications.² Following this success, many artificial mutants have been also designed, synthesized

and studied trying to tune the properties of these proteins. The chromophore of the GFP is the 4-(*p*-hydroxybenzylidene)imidazolidin-5-one (Figure 1) which is covalently bound to the protein structure.

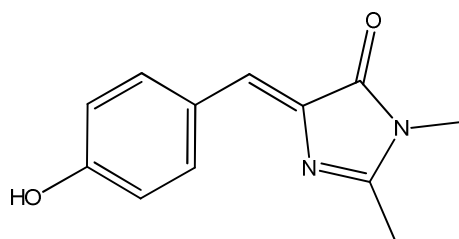


Figure 1

Interestingly, the photophysical properties of the wild-type GFP and the chromophore in solution are quite different. While the GFP is strongly fluorescent, the fluorescence is lost when the chromophore is not linked to the protein. Also, the fluorescence can be recovered after denaturalization by cooling at 77 K.

Soon after its first uses in molecular and cell biology, the potential for many different uses of the GFP prompted the researchers to design and engineer different modifications with increased fluorescence, higher photostability or tuned properties. From single point mutations, in which only one amino acid in the protein is changed, to bigger changes causing colour mutants (blue, cyan, red, yellow fluorescent proteins) many GFP derivatives have been reported. In addition, different versions of the GFP with properties as pH- or redox-sensitive proteins have been also prepared.³

This variety of properties, uses and mechanisms turns the GFP and derivatives into an extremely active research field. In this contribution, we will focus on the synthesis, properties and applications of some of the GFP chromophore analogues reported to date. Although some applications of the fluorescent proteins will be presented, we will focus on the relevant features of the chromophores responsible for the photophysics and photochemistry.

2. Synthesis of GFP chromophore analogues

2.1. Synthesis of oxazolones

The synthesis and photophysical behaviour of arylidene oxazolones is very similar to the GFP chromophore. In fact, the preparation of several derivatives of the GFP chromophore uses oxazolones as intermediates. This makes relevant to study their synthesis and photophysical properties. Arylidene oxazolones have the general structure shown below in Figure 2. The main difference between them and the GFP chromophore is that oxazolones feature a lactone as the five-membered ring instead of a lactam (Figure 2).

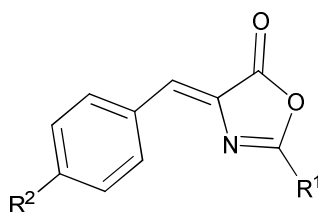
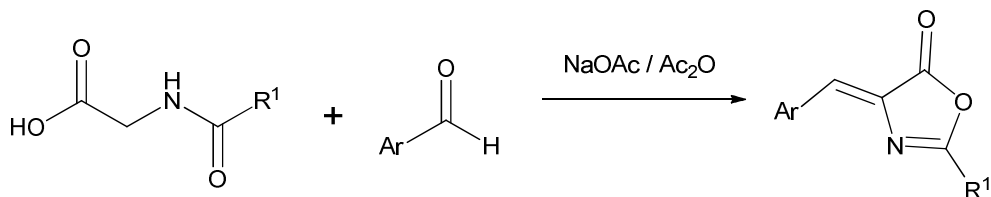


Figure 2

Many different oxazolones derivatives have been reported.⁴ In first place, the substituent R^1 present in the iminic bond can be modified by several groups with different electronic properties, such as aromatic

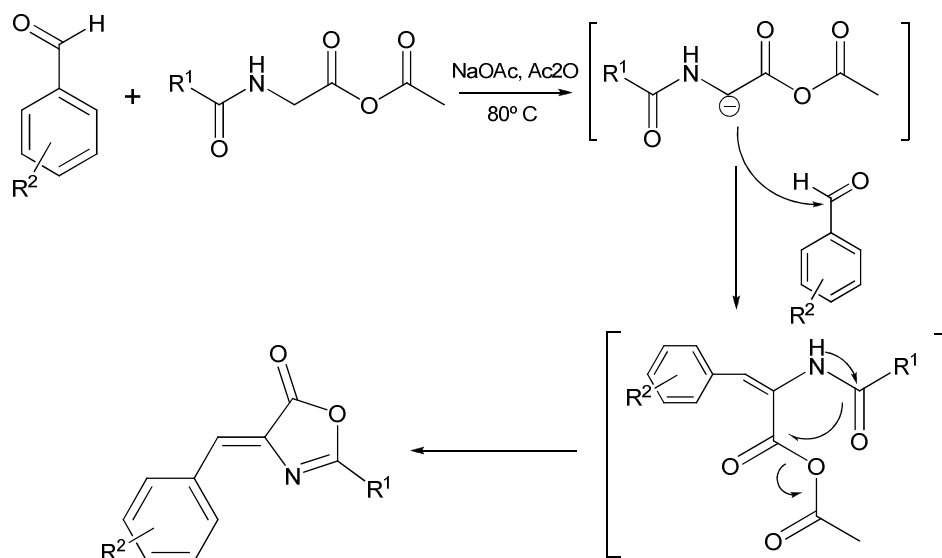
rings or alkyl groups. In the same way, it is possible to change the R² group in the aromatic ring by an electron-donating or an electron-withdrawing substituent.

The general procedure to synthesise these compounds in one step is shown in Scheme 1.



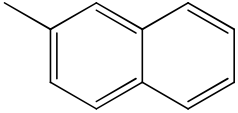
Scheme 1

To a solution of *N*-acylglycine in acetic anhydride, a solution of sodium acetate and aryl aldehyde is added to give the target oxazolone. The mechanism of the reaction is very simple. First, *N*-acylglycine is deprotonated by the sodium acetate solution to perform the aldol condensation. Subsequent intramolecular cyclization yields the oxazolone as final product⁴ (Scheme 2).



Scheme 2

Table 1

R ¹	R ²	Yield (%)
Ph	Ph	85%
Ph	<i>p</i> -MeOPh	60%
Ph	<i>p</i> -BrPh	72%
Me	<i>o</i> -MeOPh	82%
Me	Ph	80%
Me	<i>p</i> -NO ₂ Ph	60%
Me		91%

This synthetic route allows for the preparation of different oxazolones with a wide range of substitution. Besides, both the simple reaction conditions and the high yields make this pathway a good entry door for the synthesis of a good number of derivatives, as shown in Table 1.

Although this reaction works well with many different aldehydes, the use of certain compounds with electron-withdrawing groups such as 2-carboxy- or 2-cyanobenzaldehyde is prevented.⁵

Other derivatives of glycine have been also successfully used in the preparation of oxazolones. For instance, *N*-crotonylglycine, prepared from crotonic acyl chloride and glycine under basic conditions and the analogue of hexadienoic acid were used to prepare models of the red fluorescent protein chromophore through a similar methodology.⁶

2.2. Synthesis of imidazolinones

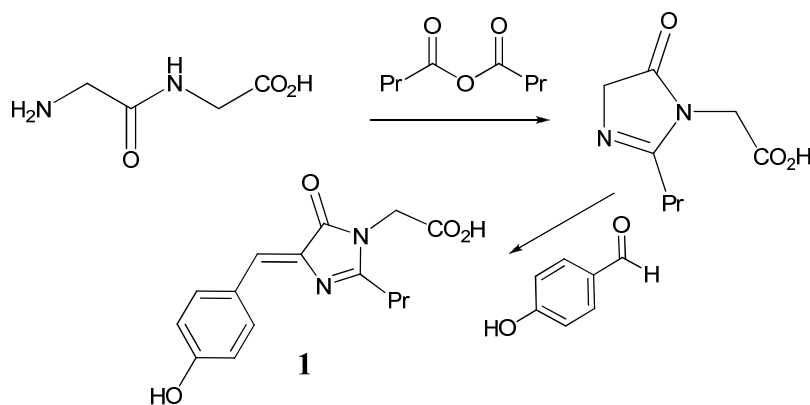
As explained before, the chromophore *p*-hydroxybenzylideneimidazolidinone is the responsible for the green fluorescence of the GFP. In order to tune the photophysical properties of the GFP, several imidazolinone derivatives have been also synthesised to alter the optical properties (Figure 1).

There are three groups in the structure of imidazolinones that could be modified by several substituents with different chemical properties. Modification of these substituents has been achieved by diverse routes.

✓ Route A

The basic synthesis of this kind of compounds was reported by Shimomura in 1979.⁷ The synthesis took place by reaction of glycyglycine and butyric anhydride and subsequent reaction of the intermediate with an aromatic aldehyde (Scheme 3).

The products synthesized with this reaction were obtained in very low yields as compound **1** and more complex products cannot be synthesized this way. Thus, this reaction is not a good, general method for the synthesis of imidazolinones.



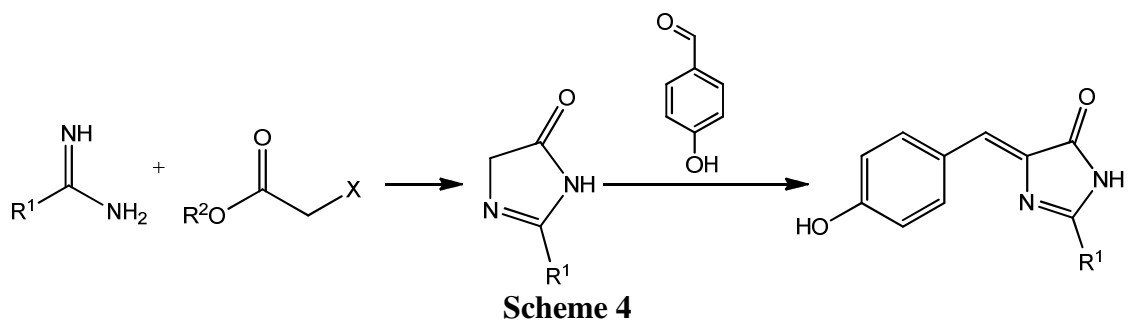
Scheme 3

✓ Route B

A related synthetic route was reported later. First, the preparation of 3,5-dihydro-4*H*-imidazol-4-one through the treatment of amidine with esters of chloro- or bromo-acetic acids to get the five membered ring is performed followed by the reaction with an aromatic aldehyde⁸ (Scheme 4).

To date, only the simplest 2-substituted chromophore has been synthesized by this approach, so this reaction only works properly if the aromatic aldehyde is *p*-hydroxybenzaldehyde. In addition, the use of

alkylamidines produced an extreme decrease in the reaction yield.⁹ Therefore, this reaction features many drawbacks to be considered a good approach to get this type of compounds.



✓ Route C

Another approach to get these compounds is based on the direct condensation of oxazolones described in Section 2.1. The reaction consists of the treatment of the suitable oxazolone with primary amines in the presence of a base, as shown in Scheme 5.¹⁰

Several imidazolinones have been synthesized with these reaction conditions as shown in Table 2.

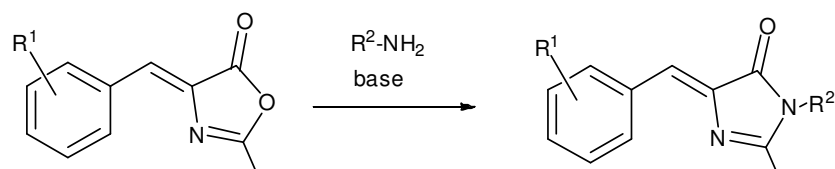


Table 2

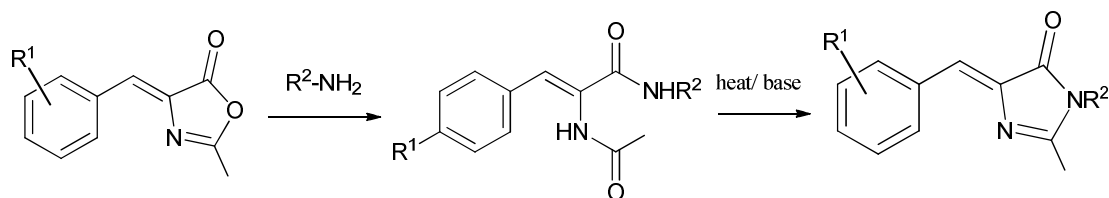
R¹	R²	Yield (%)
<i>p</i> -MeO	Bn	44%
<i>p</i> -NH ₂	Bn	41%
<i>p</i> -Cl	Bn	13%
<i>p</i> -Br	Bn	14%

These compounds were obtained with low yields, especially when R¹ is an electron-withdrawing group. This is due to the decreased electrophilicity of the oxazolone which makes the nucleophilic attack by the amine less efficient. Thus, this synthetic procedure has also a serious drawback.

✓ Route D

A small modification of route C allowed for the preparation of these compounds with higher yields. In this case, the synthesis consists of two steps that involve an oxazolone as in the previous route. The reaction is based on a nucleophilic ring opening of the oxazolone to get the *N*-acyl amides and subsequent thermal or base-catalysed cyclization (Scheme 6).

The reaction in two steps leads to improved yields¹⁰ and it is much faster. Many compounds were synthesized through this methodology using pyridine as base (Table 3).



Scheme 6

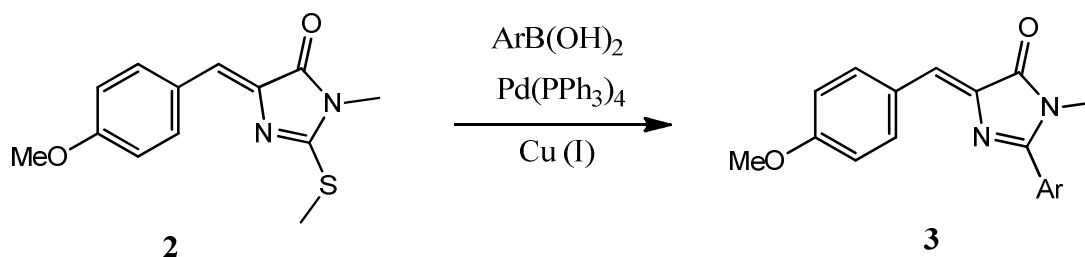
Table 3

R^1	R^2	Yield (%)
<i>p</i> -MeO	Me	86%
<i>p</i> -NH ₂	Me	72%
<i>p</i> -Cl	Me	92%
<i>p</i> -Br	Me	98%

✓ Route E

Finally, a different route is based on the cross-coupling strategy using boronic acids. Several studies describing this type of functionalization of heterocycles have appeared.¹¹ For this purpose, the reaction between boronic acids and heteroaromatic thioethers in the presence of Pd(PPh₃)₄ and a source of Cu (I) is performed (Scheme 7).

Once synthesized **2**, it reacts with a boronic acid and the cross-coupling reaction takes place so that the formation of the C_{sp2}-C_{sp2} bond occurs under several reaction conditions to give **3**.¹²



Scheme 7

2.3. Synthesis of other derivatives

Although the most used GFP chromophore derivatives are those shown in the previous Sections, many other structures related with or based on the GFP chromophore have been reported. For instance, other derivatives which have been also studied are the butenolides and pyrrolinones with structures are based on the presence of a five-membered heteroaromatic ring (Figure 3).

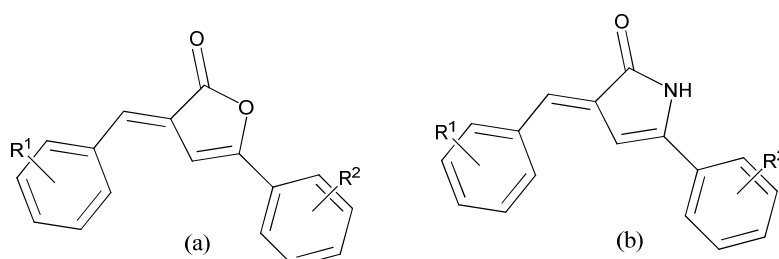
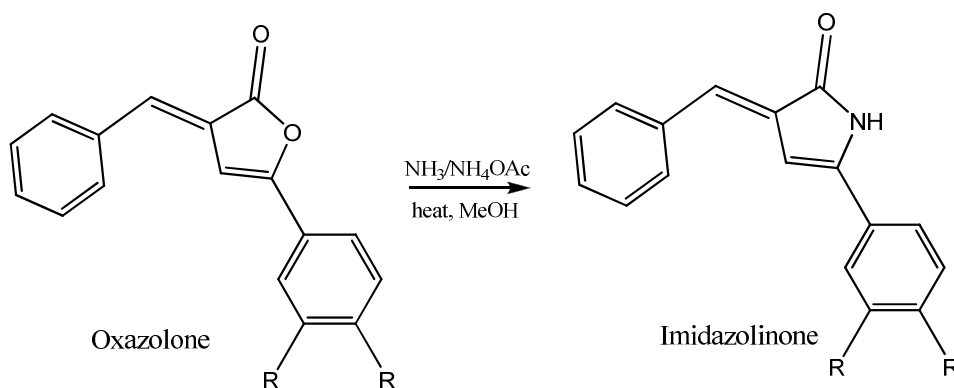


Figure 3. (a) Butenolide; (b) Pyrrolinone.

Butenolides are synthesized by cyclization of 3-benzoylpropionic acid upon reaction with an aldehyde, under the same reaction conditions as in synthesis of oxazolones described in Section 2.1. The synthesis of pyrrolinones is performed from the butenolide analogues by reaction with ammonia or primary amines in solution and glacial acetic acid in refluxing methanol (Scheme 8). In the case of primary amines, the target pyrrolinone was obtained in low yields (<30%).^{13,14} Pure products were easily obtained by filtration, although the yield was only moderate.



Scheme 8

Table 4

Structure	R	Yield (%)
Oxazolone	H	51
	OMe	46
Imidazolinone	H	31
	OMe	50

3. Photophysical properties of the GFP chromophore and derivatives

GFP and related fluorescent proteins have found ubiquitous applications in life sciences. Protein-protein interactions, fluorescence imaging, dynamics at the single-molecule level, among other uses, have been developed. However, it is now well known the dependence of the photophysical and photochemical behaviour on different aspects such as the protein environment, the chemical structure of the chromophore and the solvent used. The control of these applications and the development of new ones rely on the detailed knowledge of the molecular mechanisms in play. Some important factors for any optical application of the GFP, its mutants and GFP chromophore derivatives are the absorption and emission parameters. In some cases, a certain wavelength is required to promote the reactivity or offers an improved sensitivity in molecular imaging. Also, increased emission quantum yields are necessary for better signal/noise ratios. In this Section, we will review some of the aspects that affect the photophysics of the GFP chromophore and analogues.

3.1. Absorption

One of the interactions between matter and light is the absorption of one or more photons, generating excited molecules. The energy of the photon can be used to induce several processes as photochemical

reactions. The part of the molecule responsible for the absorption of a photon is known as chromophore, so the modification of the chromophore's structure can directly affect the absorption properties as the wavelength of absorption or the molar extinction coefficient. In the next Section, we will deal with these changes in the structure and the effect on the properties.

3.1.1. Oxazolones

The arylidene oxazolones feature an extended chromophore composed by the aryl group, the central double bond and the oxazolone ring. Also, the substituents can increase the conjugation depending on their nature. These substituents can modify the absorption band maximum. Thus, changes in these positions could be helpful to tune the spectral properties of the compounds. In the oxazolone structure (Figure 2), there are two substituents that can be easily modified in order to adjust the wavelength of absorption.¹⁵ This parameter could be critical depending on the final application. For instance, longer, low-energy wavelengths are generally needed for biological applications. Thus, it is possible to tune its UV/Vis absorption spectrum by modifying the substituents present in the structure (Table 5).

Table 5

Compound	R ¹	R ²	λ_{\max} (nm) in CH ₃ CN/ ϵ (M ⁻¹ cm ⁻¹)
4	Ph	Ph	360/81673
5	Me		327/26633
6	Ph	<i>p</i> -MeOPh	403/32821
7	Me		355/28261
8	Ph	<i>p</i> -NO ₂ Ph	376/47450
9	Me		350/24769

A bathochromic shift of the lowest energy band of absorption takes place when R¹ is changed from a methyl to a phenyl group due to the extended conjugation present in the aryl-substituted molecules. Besides, stronger absorptions are found in **4**, **6** and **8** since R¹=Ph, as shown by the extinction coefficients.

When R¹ is a methyl group (compounds from **10** to **12**) and R² changes from a phenyl group to phenyl substituted by another functional groups presenting different electronic properties as *p*-MeOPh or *p*-NO₂Ph, the absorption band is also displaced (Table 6).

Table 6

Compound	R ¹	R ²	λ_{\max} (nm) in CH ₃ CN
10	Me	Ph	327
11	Me	<i>p</i> -MeOPh	355
12	Me	<i>p</i> -NO ₂ Ph	350

This bathochromic shift occurs as we include an electron-donating or an electron-withdrawing substituent and it is due to the increased conjugation and higher π -charge delocalization in the excited state.

3.1.2. Imidazolinones

There are many imidazolones (Figure 4) synthesized with different substituents to mimic the GFP chromophore structure whose photophysical properties have been studied.^{6,10} These substituents have also a huge importance in the fluorescence of these derivatives as it will be discussed in the next Section.

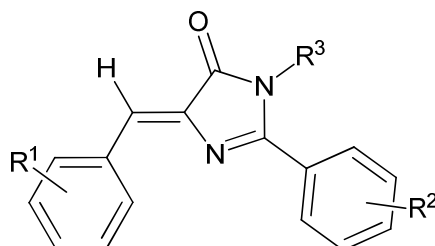


Figure 4

The absorption spectra of imidazolones feature two main bands centred at *ca.* 395 and 475 nm.¹⁶ These absorption wavelengths can be changed depending on a wide range of substituents in R^1 , R^2 and R^3 (Table 7).¹⁰

Table 7

Compound	R^1	R^2	R^3	λ_{\max} (nm) in $\text{CH}_3\text{CN}/\epsilon(\text{M}^{-1}\text{cm}^{-1})$
13	H	H	H	384/13100
14	CO_2Me	H	H	394/28800
15	CO_2Me	<i>p</i> - NO_2	H	405/25300
16	CN	H	H	393/24800

Thus, imidazolones **14**, **15** and **16** show a bathochromic shift as there is an electron-withdrawing group in the aromatic ring (R^1) that increases the π conjugation of the system.

3.2. Fluorescence

The fluorescence is a photophysical process typical of some molecules. This process takes place when a compound absorbs a photon of light with a determinate wavelength generating an excited state. The molecule then returns to the ground state by emission of a photon of light with a longer wavelength and therefore lower energy than the absorbed radiation. All of these processes are represented in the Jablonsky diagram (Figure 5).¹⁷

There are a number of molecules in Nature that show this photoprocess. In fact, the main feature of GFP is its green emission. The use of the emission of the GFP in a wide range of contexts and applications has driven the research of diverse GFP mutants and GFP chromophore derivatives, including oxazolones and imidazolinones.

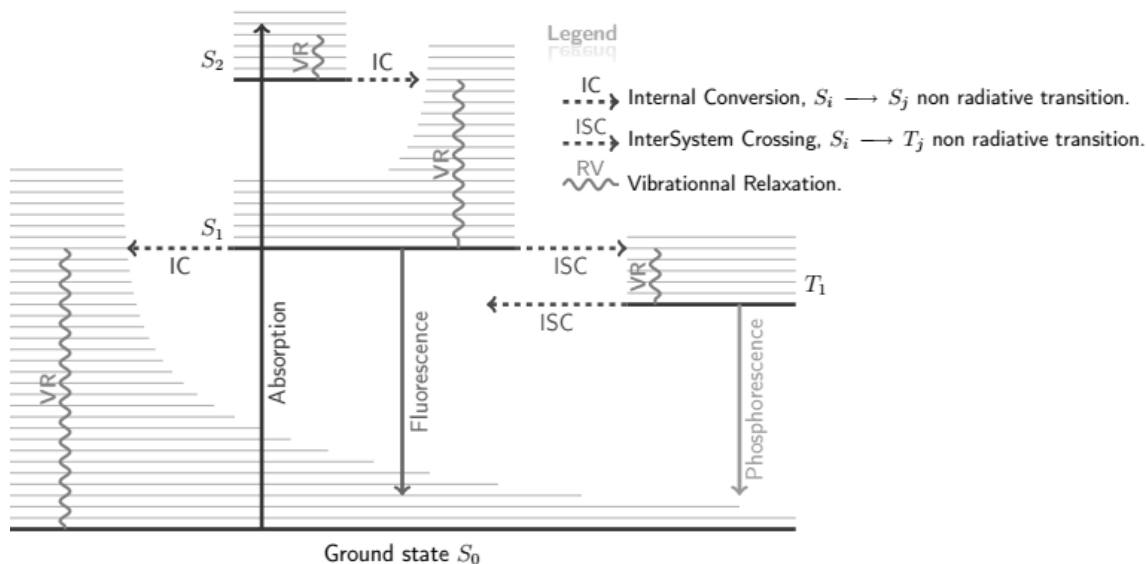


Figure 5

In this Section, we will describe photophysical properties as emission wavelength and quantum yield of fluorescence. Both are very important in the research of different applications for these compounds since if the quantum yield of fluorescence is very low, these compounds will not be able to be used as emissive displays or fluorescent markers. However, if the value of quantum yield is high, it will not act as a molecular switch since most energy will be spent on light emission.

3.2.1. Oxazolones

The emission of different oxazolone derivatives has been widely explored. In this Section, several features of the emission of oxazolones including the dependence on the substituents present on the basic structure will be reviewed.

As discussed before, two main possibilities to fine tune the photophysical properties of arylidene oxazolones are the modification of the substituents in R^1 and R^2 (Figure 6). Changes in R^1 while keeping $R^2=H$ produce the effects shown in Table 8.¹⁸

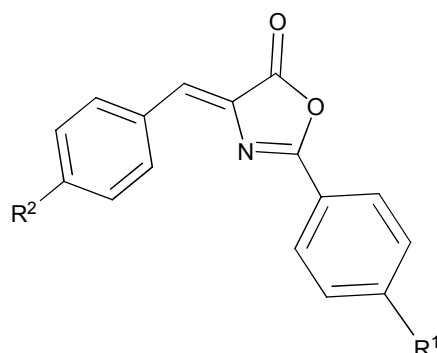


Figure 6

In compounds in which the R^1 group is an electron-withdrawing group as **18** and **19**, there is a charge delocalization from the phenyl group to the acceptor group at R^1 . In the case of **20**, as R^1 is dimethylamine, the charge density is transferred from the amine to the acceptor group placed at R^2 . This substituent affects

directly to the deactivation energy mechanism since the intersystem crossing to the triplet state does not compete with emission from S₁.

Table 8. Photophysical properties measured in THF.

Compound	R ¹	λ _{absorption}	λ _{emission}	Φ _{emission}
4	H	360	416	0.0009
18	<i>p</i> -NO ₂	383	450	0.0055
19	<i>p</i> -CN	374	440	0.0020
20	<i>p</i> -N(CH ₃) ₂	432	532	0.75

Also, excited state surfaces have been studied to determine the predominant energy relaxation process.¹⁸ From the data of the absorption spectra, it is found that the energy gap between the ground state (S₀) and the first excited state (S₁) depends on the electronic properties of R¹. The derivative **20** with the shortest energy gap has an electron-donating group as R¹. This compound presents the highest emission quantum yield due to the presence of dimethylamine in the aromatic ring. The low emission quantum yield of the other compounds has been associated with an intersystem crossing (ISC) into non-emissive triplets or reversible ring opening.¹⁸ The existence of non-radiative processes implies that not all the radiation absorbed is emitted. In addition, the emitted photon is less energetic than the absorbed one. This fact is known as Stokes shift and it measures the energy difference between the absorption and emission between two states.

3.2.2. Imidazolinones

Many of the imidazolinones (Figure 4) with different groups synthesized as described in previous Sections have been prepared to mimic the GFP chromophore's structure and photophysical properties. Again, the main interest is to tune the emission wavelength and their fluorescence quantum yield (Φ, Table 9).¹⁹

Table 9. Photophysical properties measured in dioxane.

Compound	R ¹	R ²	R ³	λ _{emission}	Φ _{emission}
21	MeO	H	H	464	0.0002
22	N(Me) ₂	H	H	520	0.0020
23	CN	H	H	464	0.158
24	CO ₂ Me	3,4-diMeOPh	H	478	0.295

As in the case of oxazolones, several reports have appeared in literature¹⁶ which support that the presence of an electron-donating group could be responsible for some fluorescence properties of the anionic form of the chromophore. In Table 9, it is shown the influence on the photophysical properties of the substituents present in diverse derivatives. When a donor group is present in R¹ as in **21** and **22**, no influence in the fluorescence is detected, with very low quantum yields. On the other hand, when other substituents

with different electronic properties as $-\text{CN}$ or $-\text{COOMe}$ are present in **23** and **24**, respectively, an increase in the emission quantum yield is found.

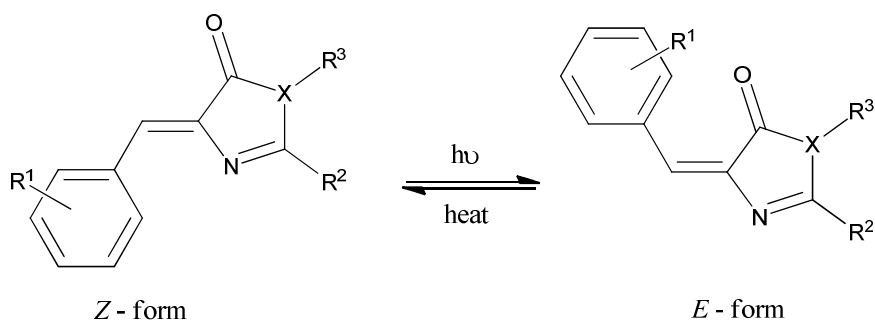
3.3. Photoisomerisation of GFP chromophore

For this type of compounds there are several competitive deactivation processes available. Therefore, usually a high quantum yield of fluorescence implies that the photoisomerisation process will not take place efficiently. In contrast, both processes can take place at the same time with low quantum yields.²⁰

Considering the values in Table 9, the low quantum yield obtained for synthetic derivatives of the GFP chromophore is the main difference between them and the natural chromophore.²¹ This chromophore is the responsible for the fluorescence of this protein *in vivo* when it undergoes excited-state proton transfer, resulting in very intense anion fluorescence. However, a very low fluorescence quantum yield is obtained for the GFP chromophore in solution. This is in agreement with the existence of different nonradiative processes upon irradiation. For instance, a competitive *Z/E* photoisomerisation can take place contributing to a reduced luminescence quantum yield.²²

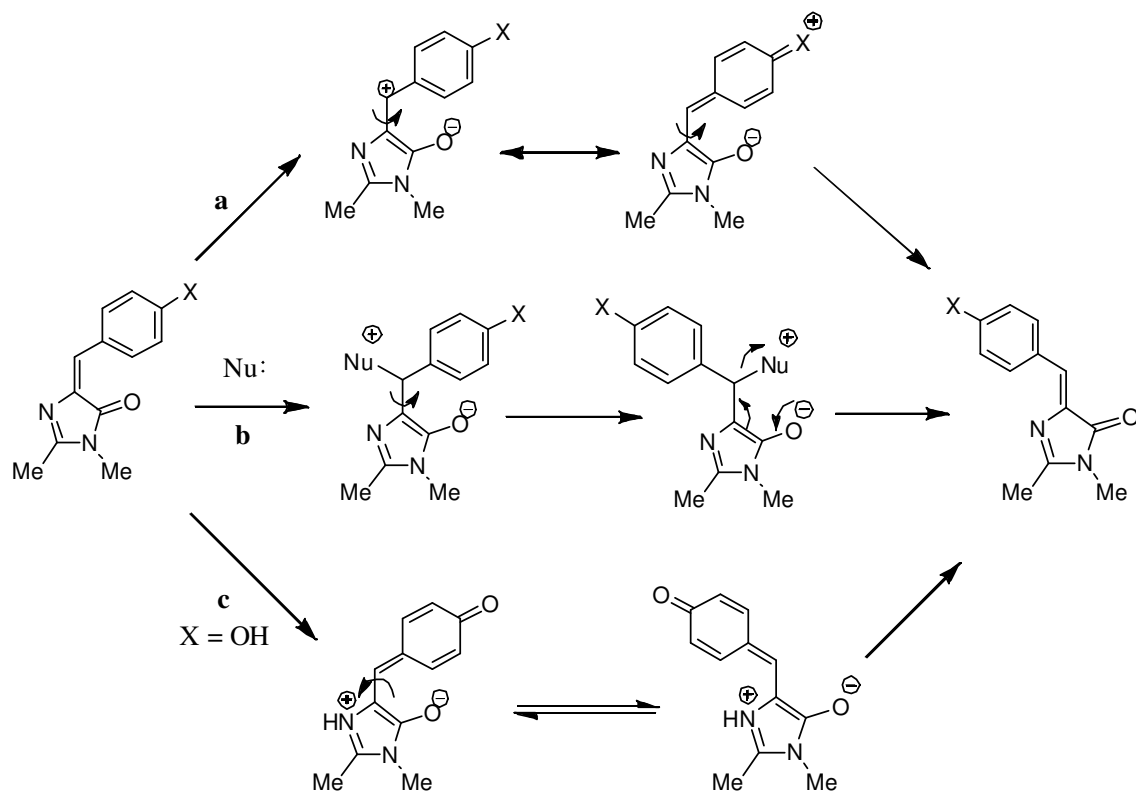
Photoisomerisation takes place when a molecule is excited and it decays to the ground state by a rapid internal conversion with a *Z/E* isomerisation of the molecule. In the case of the GFP chromophore, photoisomerisation occurs around the exocyclic double bond.

In the natural GFP chromophore, photoisomerisation affects also the protein fluorescence.²³ This molecule suffers a *Z/E* photoisomerisation between the fluorescent (thermally stable *Z* form) and the dark form (*E* isomer). Since the *Z* form is fluorescent and the *E* isomer is not, photoisomerisation can be used to switch the emission on and off. The photoisomerisation process of the GFP chromophore is shown in Scheme 9.



There are many studies dealing with the *Z/E* isomerisation of the GFP chromophore and other derivatives.^{24,25} In addition, the thermal back-isomerisation has also several possible mechanisms as shown in Scheme 10.²⁶

Other GFP derivatives also show a similar behaviour. This property has been exploited to build molecular devices. Specifically, compounds that can photoisomerise in a controllable fashion could act as molecular switches. Therefore, a molecular switch is a molecular device that can be reversibly interchanged between two different states, in this case the *Z/E* isomers.²⁷ These two states can be interchanged by an external stimulus, as for example light or heat. In this case, these devices work with light energy, which presents several advantages over the chemical or electrochemical inputs: light can be easily switched on/off, has a high spatial and temporal resolution and can be tuned to be absorbed only by the photoswitch.²⁸



Scheme 10. Pathways for the GFP chromophore isomerisation: (a) direct; (b) addition/elimination; (c) isomerisation by tautomerisation.

Both types of GFP derivatives described before, imidazolinones and oxazolones can be used as molecular switches. When solutions of these compounds are irradiated with different light sources, the photoisomerisation of the molecule takes place. This process can be followed by $^1\text{H-NMR}$, since *Z* and *E* isomers have distinctive $^1\text{H-NMR}$ signals and UV-Vis absorption bands. Irradiation proceeds until the photostationary state (PSS) is reached. The PSS of a reversible photochemical reaction is the equilibrium chemical composition under a specific kind of external stimulus, usually visible or UV light.

In the case of oxazolones (Figure 2), different derivatives were irradiated in a 125 W medium-pressure Hg lamp to yield different PSSs (Table 10). It should be noted that the PSS does not depend on external factors as the power of the lamp used or the irradiation time but can be affected by substitution, solvent or irradiation wavelength. Thus, it can be tuned to obtain improved results depending on the specific applications.

Table 10

Compound	R ¹	R ²	PSS (% Z/E)
4	Ph	Ph	75/25
6	Ph	<i>p</i> -MeOPh	83/17
7	Me	<i>o</i> -MeOPh	64/36
5	Me	Ph	80/20

As explained before, the substituents present in the structure of each compound are decisive to determine their photophysical properties. In this case, the PSS depends on several factors:

- Absorption bands of each compound.
- Relative absorption between both isomers (*Z/E*) at a given wavelength.
- The topology of the excited state near the crossing point between surfaces.

The three factors related before depend directly on the structure of each compound. Thus, a simple structure modification can alter and tune the properties of the molecular switches in order to match the specific necessities of a given application.

3.4. Photophysical properties of other derivatives

The photophysical and photochemical properties of pyrrolinones and butenolides have been also studied.¹³ These compounds share some features with oxazolones and imidazolones discussed before. Thus, we will focus only in several aspects which are relevant enough to be highlighted. The photophysical properties of some analogues of the GFP chromophore are shown in Table 11.

Table 11

Compound	R ¹	R ²	R ³	λ_{abs}	λ_{em}	Φ_{emission}
25	H	H	H	422	539	0.012
26	<i>p</i> -CN	H	^{<i>i</i>} Bu	440	598	0.153
27	<i>p</i> -CN	H	H	438	569	0.294
28	H	H	-	442	493	0.007
29	<i>p</i> -CN	H	-	400	494	0.027
30	<i>p</i> -NO ₂	<i>p</i> -OMe	-	401	495	0.043

Considering the values showed in Table 11, a significant change in the emission properties can be noticed. Specially, in the case of the pyrrolinone **26** in which R²=H and R³=^{*i*}Bu the emission wavelength suffers a clear bathochromic effect but the steric hindrance of the nitrogen atom produce a decrease in the quantum yield compared with the compound with R³=H.

These compounds were irradiated producing the *E/Z* photoisomerisation with quantum yield with values between 0.1 and 0.4. These values confirm that the structures studied act as quite efficient molecular switches.¹⁴

4. Applications

The discovery of fluorescent proteins in Nature has been a total revolution in cellular biology.²⁹ Among them, the green fluorescent protein coming from *Aequorea Victoria* jellyfish is the most important as shown by the Nobel Prize in Chemistry awarded.¹ This discovery had a great impact when it was observed that the fluorescent properties found in the jellyfish were preserved in other living organisms.³⁰ The GFP protein is considered as a cell marker since it does not affect the cell physiologic behaviour. This fact allows to follow different processes without affecting them such as illuminating growing cancer tumours and showing the development of brain diseases.

The most important medical application of GFP is its use in the study of cancer. Nowadays, this disease is the most aggressive in the occidental world, so it is interesting to know their behaviour in a living

organism. Most cancer deaths are due to cancer that has spread from its primary site to other organs, so the first step in the fight against this disease is the primary detection.

In this way, the GFP has been used to study subcellular processes such as gene expression and protein localization.³¹ For instance, GFP-labelled cells were injected into mice, where, by 7 days, they formed brilliantly fluorescing metastatic colonies on mouse lung. Tumour progression was then continuously visualized by GFP fluorescence over a 52-day period, during which the tumours spread throughout the lung.³² In the case that a fluorescent protein as GFP is linked to another protein in which the fluorescence depends on the medium conditions, it could be used as a sensor of different processes as changes in pH *in vivo*³³ or in the concentration of different ions as calcium³⁴ or copper.³⁵

The uses and applications of the GFP have been extensively reviewed and the interested readers are pointed to some of the references indicated before. Instead, we will focus on the applications of the different GFP chromophore analogues described in previous sections. Only a selection of the most recent applications will be discussed.

✓ *Fluorescent proteins*

Since the discovery of the interesting properties of the GFP, much effort has been devoted to the development of new engineered variations of the natural protein. These new GFP mutants show modified photophysical properties, increased brightness and photostability and higher emission quantum yields. The photocontrol of these new proteins allow for the tuning of the features even at the molecular level and have been designed to act as data storage and optical memories. The biological techniques and details of these modified proteins are well beyond the scope of this contribution, although some relevant contributions will be indicated.

It has been shown³⁶ that a minor modification in only one aminoacid in the protein sequence (threonin 203) allows for the photocontrol of the switching between the states of the protein down to the molecular level. Photochromic behaviour of single molecules was detected and controlled by light with two different wavelengths. The emissive and dark states of the GFP mutant could be easily controlled which, in turn, could be used for different imaging processes.

The impulse in the research of diverse modifications of the GFP has allowed to produce mutants with carefully designed properties. For instance, Dronpa³⁷ is a reversibly photoswitchable fluorescent protein. This protein can be interchanged by absorption at 488 nm between a bright fluorescent state with emission at 518 nm and a dim state. The emissive state can be easily recovered by absorption of light of 405 nm. The switching process takes place at the single molecule level in milliseconds and it is fully reversible for many cycles. This new protein has also found extensive use in the study of signalling proteins in single cells.

It is worth noting that the photophysical and photochemical behaviour of the GFP protein and the GFP chromophore in solution is very different. This is usually the same with other engineered proteins and their corresponding chromophores. For instance, in the wild-type protein, the fluorescence emission is the main deactivation channel, while the isolated chromophore shows a very efficient radiationless decay.³⁸ In the first case, a proton transfer between the chromophore and the protein backbone seems to be responsible for the photophysics. Also, in different GFP mutants with diverse photophysical properties, a variety of deactivation mechanisms could be involved. This diversity is at the heart of the wide applicability of the GFP, their mutants and the isolated chromophores.

✓ *Photoswitches*

Among the many different molecular devices prepared, molecular switches have been widely studied. Many different applications have been developed to make use of the switching ability of certain molecules with two or more stable states. As described before, the GFP chromophore and different analogues show a prominent *Z-E* photoisomerisation capability. If embedded in the protein (wild-type or modified), this photoisomerisation can be used to alter the behaviour of the whole protein or even a complex between this and other biomolecules. If the chromophore is in solution, a precise design, photochemical study and fine-tuning of the optical properties can be performed in order to obtain very efficient molecular switches. For instance, simple chemical modification allowed for the preparation of analogues of the GFP chromophore to yield new structures with interesting properties as molecular photoswitches, namely, the cyan fluorescent protein (CFP) chromophore and the blue fluorescent protein (BFP) chromophore.²² In these cases, the *Z-E* photoisomerisation seems to be a general decay mechanism of the excited state. Thus, it is the protein environment the main factor in the control of the efficiency of the photoisomerisation *versus* the emission.

Beyond the protein environment, other external factors seem to play also a major role in the photoisomerisation mechanism and, therefore, also in the emission process. For instance, the use of protic solvents causes a dramatic decrease in the quantum yields of both emission and photoisomerisation for the GFP chromophore and several imidazolinone analogues.³⁹ This result suggests the importance of the chromophore-solvent hydrogen bonding and its effect in the deactivation pathways of the excited states. As both types of quantum yields decrease, it seems that a new, different decay channel may be operating in protic solvents. In addition, the photoisomerisation is affected in the solid state and it is also influenced by the substituents in the chromophore or the wavelength of irradiation.⁴⁰

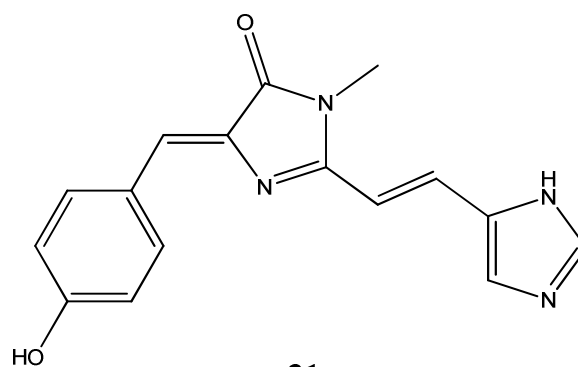
Also, the excited-state dynamics of several imidazolones have been tuned by different substituents and experimental conditions.⁴¹ The nature and positions of the substituents, the viscosity and polarity of different solvents and the presence of a rigid medium allowed for the modification of the available deactivation channels. Although the photoisomerisation appeared as the main reactive path, other possibilities arise dependent on the solvent and substituents, such as inter- and intramolecular hydrogen bonding assisted deactivation. Alternatively, the presence of strong hydrogen bonding prevents the photoisomerisation from taking place. For instance, the *o*-hydroxy imidazolinone ring is capable of suppressing the rotation. Therefore, the emission quantum yield is 0.2 in solution and up to 0.9 in solid state. Further tuning of the wavelength of emission between 560 and 670 nm can be achieved through substituent modification.

Arylidene-oxazolones have been also used in the development of new and efficient molecular switches.⁴³ These compounds feature an easy and versatile synthesis and the photoisomerisation can take place using a wide variety of experimental conditions. Also, high thermal and photochemical stabilities, adequate photoisomerisation quantum yields and lack of fluorescence turn these compounds into quite efficient switches.

✓ *Solar cells*

Nowadays, it is important to produce electricity from different kinds of energy and much attention has been paid to the development of photovoltaic energy. This type of energy is based on the production of electricity from light. Thus, a solar cell is an electrical device that converts the energy of light directly into electricity by the photovoltaic effect.

The study of the GFP chromophore potential as dye in solar cells has been explored. Also, different derivatives of the GFP chromophore have been synthesized and studied in this context (Figure 7).



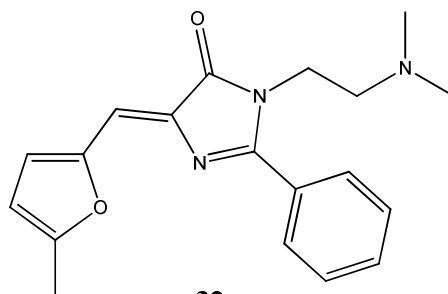
31

Figure 7

The emission quantum yield of **31** has been measured to be 0.13. This value is different from other imidazolinone compounds described before (Section 3.2.). This result suggests that the bulky imidazole group hinders the exocyclic C=C bond rotation. Using this chromophore as photosensitizer, a dye sensitized nanocrystalline TiO₂ solar cell produces a 3.04% solar light to electricity conversion efficiency.⁴⁴ The use of this compound to produce electricity from solar energy opens huge opportunities in the renewable energy field.

✓ *pH sensors*

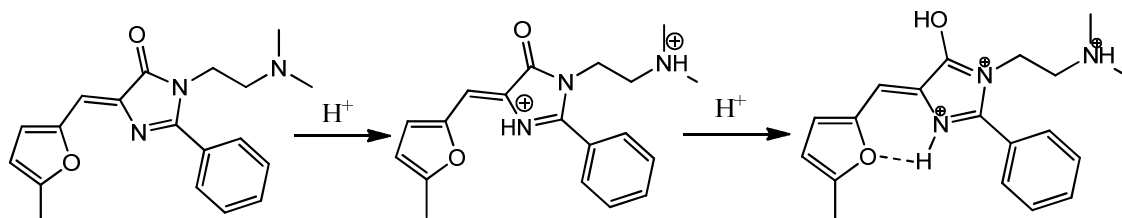
As we said before, the GFP is established as a fluorescent marker in different biological processes. The isolated GFP chromophore, as other imidazolinones, shows low fluorescence due to the photoisomerisation of the double bond C=C. In related species, it was also found that the fluorescence depends on the pH of the solution. Thus, the variation of the emission can be used to follow the changes in the pH of the solution. Doing so, different GFP chromophore analogues could be used as pH sensors, detecting the pH of the solution and providing different optical outputs depending on it. A representative example is shown in Figure 8.



32

Figure 8

When **32** is placed in solutions at different pH values, different species are predominant depending on the acid-base equilibria. Consecutive protonation processes take place depending on the pH values (Scheme 11).



Scheme 11

As it is shown in Scheme 11, the structure of the predominant species depends on the pH. As the photophysical properties of these species are different, the optical properties of the solution will depend on the pH value and these properties could be used to measure the pH change. For this purpose, the emission spectra were recorded over the pH range 1–7, as it is shown in Figure 9.⁴⁵

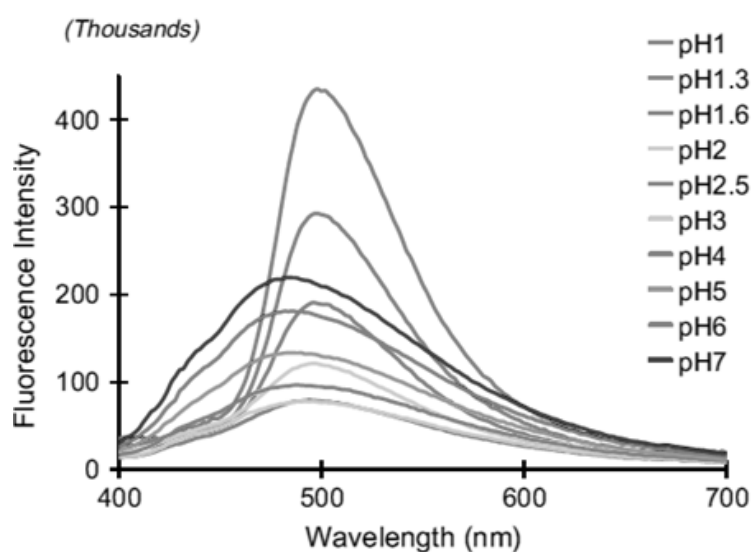


Figure 9. Reproduced with permission from reference 41.

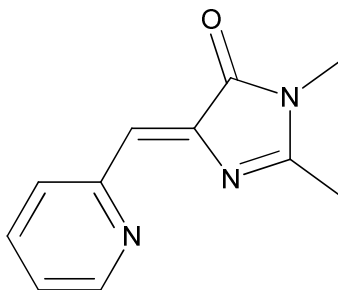
The results shown in Figure 9 reflect that the emission spectra below pH 2.5 produces a significant intensity increase in the fluorescence band centred at 500 nm. The protonation of the nitrogen atom of the imidazolinone ring and H-bonding with the furyl oxygen enforces the planarity, increasing the conjugation of the compound. Thus, a change in the fluorescence wavelength and enhancement in the intensity is produced (see Figure 9). Thus, this and related compounds act as a pH sensors due to the change of its fluorescence depending on the proton concentration.

✓ *Metal sensors*

This type of compounds also presents another way to act as a sensor. In this case, this property is based on the change of fluorescence emission when the process which produces a low emission is blocked.

As explained in Section 3.2., some compounds based on the chromophore of GFP have a low emission because their energy in the excited state produces a photoisomerisation process instead of emitting light. If the photoisomerisation process could be blocked, the emission quantum yield could be increased. Different alternatives to block this photoisomerisation have been explored, but the best results were obtained using metals. Thus, several compounds based on the GFP chromophore have been studied as metal sensors. In the

presence of metals, a new species is formed with the GFP chromophore acting as a ligand. In this new species, the photoisomerisation is no longer possible. Thus, after irradiation of the sample, only the emission path is available. This implies an increase in the emission quantum yield. Therefore, the presence of metals in solution can be detected through the changes in the optical properties of the ligand. Good results were obtained with **33** (Figure 10).⁴⁶



33

Figure 10

The study of the luminescence properties in presence of several metals was performed. In the case of Zn^{2+} ion, it turns on the intensity emission when the concentration of Zn^{2+} increases. The presence of Zn^{2+} blocks the photoisomerisation process since an octahedral compound is formed with Zn^{2+} as the metallic centre. Thus, in this case, the presence of Zn^{2+} in solution can be related with changes in the optical properties of the GFP chromophore and this compound can be used as a metallic sensor.

Oxazolones have been also used as metal sensors both in solution and in polyvinyl chloride (PVC) matrix.⁴⁷ In this case, Fe^{3+} can be detected and quantified through fluorescence emission. These sensors are reversible and feature a reasonably dynamic response. Also, the effect of the change in pH within the range of 4–11 is small. Therefore, variations of the concentration of acid do not hamper the functioning of the sensor.

✓ Biosensors

The sensing capabilities of different analogues of the GFP chromophore have been also employed to detect and quantify complex molecules. For instance, oxazolone derivatives have been used⁴⁸ as optical sensors for different biomolecules. Specifically, compounds **34–36** shown in Figure 11, in which the oxazolone is linked to an azacrown moiety, can be used to detect neurotransmitters such as acetylcholine and acetylcholinesterase inhibitor *Donezepil*.

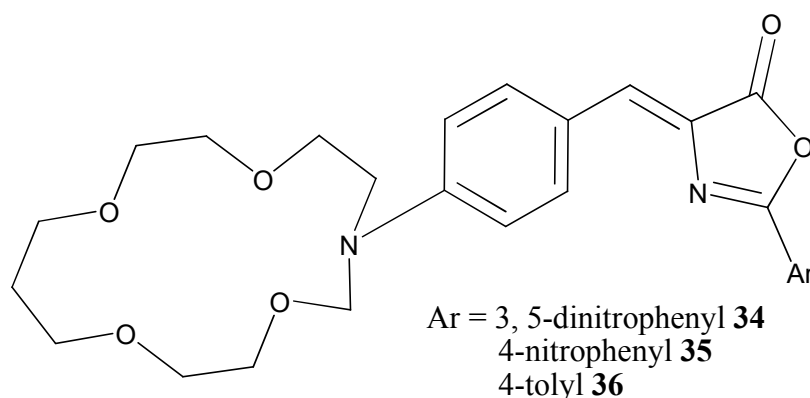


Figure 11

Once incorporated in PVC films, these compounds generate sensor films fully reversible and reproducible for the detection of the abovementioned molecules though the changes in absorption and fluorescent measurements.

✓ *Nonlinear optical properties*

Due to the extended π -systems that some arylidene-oxazolones feature, these materials have been also considered as promising candidates for the development of materials with applications in photonics and electronics due to their nonlinear optical properties.⁴⁹ It is the large π -system the main reason behind the nonlinearity of these compounds. Interestingly, oxazolones show this behaviour both in solution and in solid state which implies a further advantage for technological applications. Some report⁵⁰ on the structure-properties relationship of different oxazolones show a strong influence of the substituents on the second-order harmonic generation values, although the maximum absorption wavelengths, absorption coefficients, maximum emission wavelengths and second-order nonlinear polarization values remain quite similar. In the solid state, the reason for this change in the nonlinear is the different crystal packaging induced by the substituents behaviour.

5. Conclusions

GFP, as the better known and probably most used of the whole family of the fluorescent proteins, has shown an impressive potential in many different applications. In this contribution we have shown how minor changes in the chromophore chemical structure or the experimental conditions can be used to adjust a wide range of photochemical properties. This allows for the design of complex applications in biology, biochemistry, chemistry, physics and materials science. Although many things are already known on the behaviour of the GFP, its mutants and the analogues of the chromophore in many different contexts, it is clear that much more is yet to be done. Mechanistic details on the dynamics of the system in both the ground and the excited state, control of the diverse deactivation channels, modification of the conditions to achieve the complete participation of only one reaction path and, of course, the design, synthesis and exploration of new, different analogues of the chromophore and protein mutants. Research in this field is far from been exhausted and new and exciting discoveries will appear in the next years.

Acknowledgments

The support from the Spanish Ministerio de Ciencia e Innovación (MICINN) / Fondos Europeos para el Desarrollo Regional (FEDER) (CTQ2011-24800) is gratefully acknowledged.

References

1. (a) Shimomura, O. (Nobel lecture) *Angew. Chem. Int. Ed.* **2009**, 48, 5590. (b) Chalfie, M. (Nobel lecture) *Angew. Chem. Int. Ed.* **2009**, 48, 5603. (c) Tsien, R. Y. (Nobel lecture) *Angew. Chem. Int. Ed.* **2009**, 48, 5612.
2. Heim, R.; Prasher, D. C.; Tsien, R. Y. *Proc. Natl. Acad. Sci. U.S.A.* **1994**, 91, 12501.
3. Chalfie, M. *Green Fluorescent Proteins, Properties, Applications and Protocols*; Wiley-Liss: New York, 1998.
4. Audia, J. E.; Droste, J. J.; Nissen, J. S.; Murdoch, G. L.; Evrard, D. A. *J. Org. Chem.* **1996**, 61, 7937.
5. Blanco-Lomas, M.; Campos, P. J.; Sampredo, D. *Org. Lett.* **2012**, 14, 4334.
6. He, X.; Bell, A. F.; Tonge, P. J. *Org. Lett.* **2002**, 4, 1523.

7. Shimomura, O. *FEBS Lett.* **1979**, *104*, 220.
8. Devasia, G. M.; Shafi, M. *Indian J. Chem.* **1981**, *20B*, 526.
9. (a) Ivashkin, P. E.; Yampolsky, I. V.; Lukyanov, K. A. *Russ. J. Bioorg. Chem.* **2009**, *35*, 652. (b) Baldrige, A.; Kowalik, J.; Tolbert, L. M. *Synthesis* **2010**, *14*, 2424.
10. Lee, C.-Y.; Chen, Y.-C.; Lin, H.-C.; Jhong, Y.; Chang, C.-W.; Tsai, C.-H.; Kao, C.-L.; Chien, T.-C. *Tetrahedron* **2012**, *68*, 5898.
11. Lisbeskind, L. S.; Srogl, L. *Org. Lett.* **2002**, *4*, 979.
12. Oumouch, S.; Bourotte, M.; Schmitt, M.; Bourguignon, J.-J. *Synthesis* **2005**, 25.
13. Bourotte, M.; Schmitt, M.; Follenius-Wund, A.; Pigault, C.; Haiech, J.; Bourguignon, J.-J. *Tetrahedron Lett.* **2004**, *45*, 6343.
14. Abbandonato, G.; Signore, G.; Nifosì, R.; Voliani, V.; Bizzarri, R.; Beltram, F. *J. Eur. Biophys.* **2011**, *40*, 1205.
15. Blanco-Lomas, M.; Funes-Ardoiz, I.; Campos, P. J.; Sampedro, D. *Eur. J. Org. Chem.* **2013**, 6611.
16. Bell, A. F.; He, X.; Wachter, R. M.; Tonge, P. J. *Biochemistry* **2000**, *39*, 4423.
17. <http://www.texample.net/tikz/examples/the-perrin-jablonski-diagram/>
18. Rodrigues, C. A. B.; Mariz, I. F. A.; Maçôas, E. M. S.; Afonso, C. A. M.; Martinho, J. M. G. *Dyes Pigm.* **2013**, *99*, 642.
19. Follenius-Wund, A.; Bourotte, A.; Schmitt, M.; Iyice, F.; Lami, H.; Bourguignon, J.-J.; Haiech, J.; Pigault, C. *Biophys. J.* **2003**, *85*, 1839.
20. Addison, K.; Conyard, J.; Dixon, T.; Bulman Page, P. C.; Solntsev, K. M.; Meech, S. R. *J. Phys. Chem. Lett.* **2012**, *3*, 2298.
21. Niwa, H.; Inouye, S.; Hirano, T.; Matsuno, T.; Kojima, S.; Kubota, M.; Ohashi, M.; Tsuji, F. *Proc. Natl. Acad. Sci. USA* **1996**, *93*, 13617.
22. Voliani, V.; Bizzarri, R.; Nifosì, R.; Abbruzzetti, S.; Grandi, E.; Viappani, C.; Beltram, F. *J. Phys. Chem. B* **2008**, *112*, 10714.
23. Luin, S.; Voliani, V.; Lanza, G.; Bizzarri, R.; Nifosì, R.; Amat, P.; Tozzini, V.; Serresi, M.; Beltram, F. *J. Am. Chem. Soc.* **2009**, *131*, 96.
24. Martin, M. E.; Negri, F.; Olivucci, M. *J. Am. Chem. Soc.* **2004**, *126*, 5452.
25. Toniolo, A.; Olsen, S.; Manohar, L.; Martínez, T. *J. Faraday Discuss.* **2004**, *127*, 149.
26. Dong, J.; Abulwerdi, F.; Baldrige, A.; Kowalik, J.; Solntsev, K. M.; Tolbert, L. M. *J. Am. Chem. Soc.* **2008**, *130*, 14096.
27. García-Iriepa, C.; Marazzi, M.; Frutos, L. M.; Sampedro, D. *RSC Advances* **2013**, *3*, 6241.
28. Balzani, V.; Credi, A.; Venturi, M. *Molecular Devices and Machines: Concepts and Perspectives for the Nanoworld*; Wiley-VCH: Verlag, Germany, Weinheim, Germany, 2008.
29. Chalfie, M.; Kain, S. R. *Methods of Biochemical Analysis, Green Fluorescent Protein: Properties, Applications and Protocols*; Wiley: Liss, 1998.
30. Shaner, N.; Patterson, G.; Davidson, M. W. *J. Cell Sci.* **2007**, *120*, 4247.
31. Kain, S. R.; Adams, M.; Kondepudi, A.; Yang, T. T.; Ward, W. W.; Kitts, P. *BioTechniques* **1995**, *19*, 650.
32. Chishima, T.; Meng, Y.; Miyagi, Y.; Li, L.; Tan, Y.; Baranov, E.; Shimada, H.; Moossa, A. R.; Penman, S.; Hoffman, R. M. *Proc. Natl. Acad. Sci. USA* **1997**, *94*, 11573.
33. Robey, R. B.; Ruiz, O.; Santos, A. V. P.; Ma, J. F.; Kear, F.; Wang, L. J.; Li, C. J.; Bernardo, A. A.; Arruda, J. A. L. *Biochemistry* **1998**, *37*, 9894.
34. Vysotsky, E. S.; Lee, J. *Acc. Chem. Res.* **2004**, *37*, 40.
35. Isarankura-Na-Ayudhya, C.; Tantimongcolwat, T.; Galla, H.-J. *Biol. Trace Elem. Res.* **2010**, *134*, 352.
36. Cinelli, R.; Pellegrini, V.; Ferrari, A.; Faraci, P.; Nifosì, R.; Tyagi, M.; Giacca, M.; Beltram, F. *App. Phys. Lett.* **2001**, *79*, 3353.
37. Ando, R.; Mizuno, H.; Miyawaki, A. *Science* **2004**, *306*, 1370.
38. Tonge, P. J.; Meech, S. R. *J. Photochem. Photobiol. A* **2009**, *205*, 1.
39. Yang, J.-S.; Huang, G.-J.; Liu, Y.-H.; Peng, S.-M. *Chem. Commun.* **2008**, 1344.
40. Naumov, P.; Kowalik, J.; Solntsev, K. M.; Baldrige, A.; Moon, J.-S.; Kranz, C.; Tolbert, L. *J. Am. Chem. Soc.* **2010**, *132*, 5845.

41. Petkova, I.; Dobrikov, G.; Banerji, N.; Duvanel, G.; Perez, R.; Dimitrov, V.; Nikolov, P.; Vauthey, E. *J. Phys Chem. A* **2010**, *114*, 10.
42. Chuang, W.-T.; Hsieh, C.-C.; Lai, C.-H.; Lai, C.-H.; Shih, C.-W.; Chen, K.-Y.; Hung, W.-Y.; Hsu, Y.-H.; Chou, P.-T. *J. Org. Chem.* **2011**, *76*, 8189.
43. Funes-Ardoiz, I.; Blanco-Lomas, M.; Campos, P. J.; Sampedro, D. *Tetrahedron* **2013**, *69*, 9766.
44. Chung, W. T.; Chen, B. S.; Chen, K. Y. *Chem. Commun.* **2009**, 6982.
45. Katritzky, A. R.; Yoshioka-Tarver, M.; El-Gendy, B. E.-D. M.; Hall, C. D. *Tetrahedron Lett.* **2011**, *52*, 2224.
46. Baldrige, A.; Solntsev, K. M.; Song, C.; Tanioka, T.; Kowalik, J.; Hardcastle, K.; Tolbert, L. M. *Chem. Commun.* **2010**, *46*, 5686.
47. Ozturk, G.; Alp, S.; Ertekin, K. *Dyes Pigm.* **2007**, *72*, 150.
48. Ozturk, G.; Alp, S.; Timur, S. *Dyes Pigm.* **2008**, *76*, 792.
49. Murthy, Y. L. N.; Christopher, V.; Prasad, U. V.; Bisht, P. B.; Ramanaih, D. V.; Kalanoor, B. S.; Ali, S. *A. Synth. Met.* **2010**, *160*, 535.
50. Song, H. C.; Wen, H.; Li, W. M. *Spectrochim. Acta Part A* **2004**, *60*, 1587.

SYNTHESIS, CHEMICAL AND BIOLOGICAL PROPERTIES OF TRIFLUOROMETHYLATED PYRIMIDIN-2-ONES(THIONES) AND THEIR FUSED ANALOGUES

Veronika M. Shoba, Viktor M. Tkachuk, Volodymyr A. Sukach and Mykhailo V. Vovk

*Institute of Organic Chemistry, National Academy of Science of Ukraine,
Murmans'ka str. 5, Kyiv UKR-02094, Ukraine, (e-mail: shoba.veronika@gmail.com)*

Abstract. *Development of new synthetic routes to 4-, 5- and 6-(trifluoromethyl)-pyrimidin-2-ones(thiones) and the investigation of their chemical and biological properties are a highly topical subject. These heterocycles are well-known as effective anti-cancer, antibacterial, cytotoxic, anti-inflammatory and antiviral agents. In particular, DPC082, DPC083, DPC961 and DPC963 played a prominent role in the development of drugs against the wild-type human immunodeficiency virus and its new strains. [NCN]+[CCC], [CCCN]+[CN] and [CNC]+[NCC] cyclocondensation schemes as well as the Biginelli reaction are the most common synthetic approaches to the trifluoromethylated pyrimidine nucleus. Nucleophilic addition reactions and photochemical processes involving free radicals represent the major strategies to modify pyrimidin-2-ones(thiones) and to synthesize their optically active derivatives and fused analogues.*

Contents

1. Introduction
 2. Synthesis of trifluoromethylated pyrimidin-2-ones(thiones)
 - 2.1. Biginelli reaction
 - 2.2. [NCN]+[CCC] cyclization
 - 2.3. [CCCN]+[CN] cyclization
 - 2.4. [CNC]+[NCC] cyclization
 3. Chemical properties of trifluoromethylated pyrimidin-2-ones(thiones)
 - 3.1. Nucleophilic addition reactions
 - 3.2. Photochemical reactions and processes involving free radicals
 4. Biological properties of trifluoromethylated pyrimidin-2-ones(thiones)
 5. Conclusions
- References

1. Introduction

Trifluoromethylpyrimidin-2-ones(thiones) and their fused analogues are currently receiving increasing attention from biological and pharmaceutical chemists. First of all, their core nucleus, pyrimidine, belongs to the most important vital heterocycles and enters into the structure of nucleic acids, vitamin B and a variety of other natural compounds.¹ Pyrimidine derivatives exhibit anticancer, antibacterial, cytotoxic, anti-inflammatory and antiviral activities; they are also known as efficient calcium channel blockers and antagonists for a number of receptors.² Based on various pyrimidine derivatives, the analogues of natural nucleotides have been synthesized which are of great use in biological studies.³

Another important feature of this type of heterocycles is the presence of the trifluoromethyl functional group which is known to significantly improve drug pharmacokinetic properties due to its strong electron-withdrawing character, lipophilicity and metabolic stability. These remarkable properties have been widely exploited in the design of novel targets for pharmaceutical, agrochemical and material science industries.⁴⁻⁶ Among trifluoromethylated pyrimidin-2-ones(thiones), effective herbicides,⁷⁻⁹ insecticides, acaricides¹⁰ as well as promising anticancer,¹¹ antimycobacterial¹² and antiviral agents^{13,14} were found. The trifluoromethylated pyrimidin-2-one moiety is contained in compounds antagonistic to metabotropic glutamate (MGIUR2),¹⁵ dopamine D3¹⁶ and gonadotropin-releasing hormone receptors¹⁷ and also to the viral polymerase N85B.¹⁸ This activity could be used for the treatment and prevention of acute and chronic neurological disorders, sex-hormone related diseases and HCV infections. An abundance of new data on the synthesis, biological and chemical properties of trifluoromethylated pyrimidin-2-ones(thiones) is reported each year thus requiring further detailed study for rationalization and systematization.

2. Synthesis of trifluoromethylated pyrimidin-2-ones(thiones)

A large number of synthetic routes to trifluoromethylated pyrimidin-2-ones(thiones) have been described and this area is still under active development. There are two fundamentally different approaches to the target systems, namely direct introduction of the CF₃ group into the heterocycle and cyclocondensations using fluorinated building blocks. Among the reported syntheses of 4-, 5- and 6-(trifluoromethyl)-pyrimidin-2-ones(thiones), only few are concerned with the trifluoromethylation of pyrimidine core at position 5 including the most recent scheme with the use of CF₃-radical sources.¹⁹⁻²² Most of the methods are based on the cyclization of two (three in the case of the Biginelli reaction) components, at least one of them containing the trifluoromethyl group. Almost all known cyclocondensations leading to the key heterocycle can be classified with one of the following four methods:

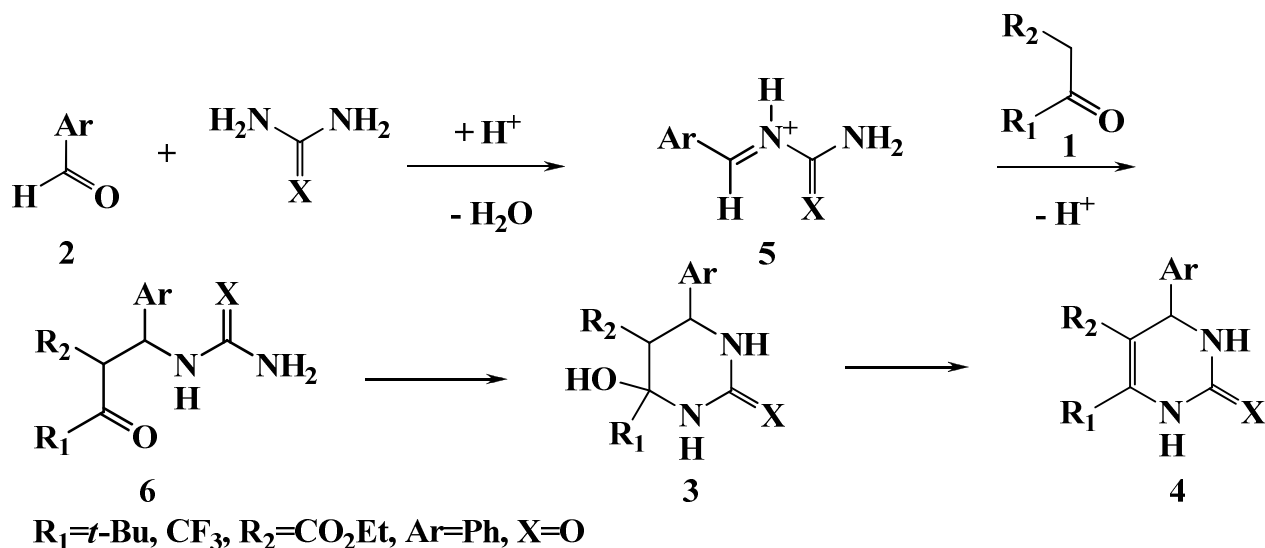
1. Biginelli reaction
2. [NCN]+[CCC] cyclization
3. [CCCN]+[CN] cyclization
4. [CNC]+[NCC] cyclization

The Biginelli reaction involves three structural units: an aromatic aldehyde, (thio)urea and a trifluoromethylated carbonyl compound (ketone, diketone, oxoalkylphosphonate, ketoester, etc.). As a result, condensation products contain the CF₃ and Ar groups in respective positions 4 and 6 of pyrimidin-2-one. Usually hydrogenated pyrimidones with the 4- and 6-hydroxy groups are obtained. Dehydration leading to desired products proceeds only under extremely severe conditions (on heating in a strongly acidic medium) what is probably attributed to the electron-withdrawing effect of the trifluoromethyl substituent.

The 1,3-binucleophilic [NCN] and 1,3-bielectrophilic [CCC] synthons can be cyclocondensed by the [NCN]+[CCC] scheme allowing a variety of 4-6 substituents to be introduced. In contrast to other cyclization types, the reaction provides an access to 5-CF₃ substituted derivatives.

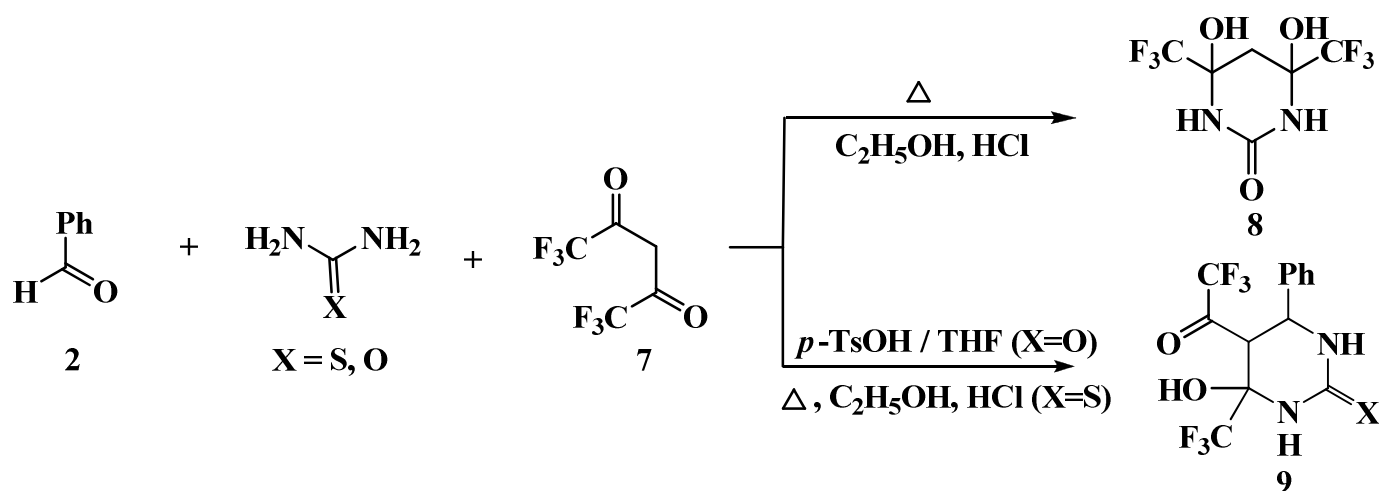
The [CCCN]+[CN] cyclocondensation of 1,4-nucleophilic-electrophilic reagents with cyanates, isocyanates and their thio analogues is another interesting and widely used route to construct the pyrimidine nucleus. 4-(Trifluoromethyl)-pyrimidin-2-ones can be prepared using CF₃-containing enaminones and β -aminoketones as a source of the [CCCN] synthon, whereas their benzo homologues, quinazolones, result from the analogous reaction of 2-trifluoromethylacylanilines.

the C=N double bond and intermediate (thio)urea **6** undergoes intramolecular cyclization by the nucleophilic attack of the amino group on the carbonyl group (Scheme 2).²⁷ As demonstrated later,^{12,25,28,29} the multi-component Biginelli reaction in acid medium is a general method to synthesize fluorine-containing di- and tetrahydropyrimidin-2-ones(thiones) from various carbonyl compounds **1** such as ketones, 1,3-diketones and ketoesters (Scheme 1). With unsymmetrical 1,3-diketones, the reaction proceeds selectively through the cyclization at the fluoroalkyl-bound carbonyl group.^{30,31}



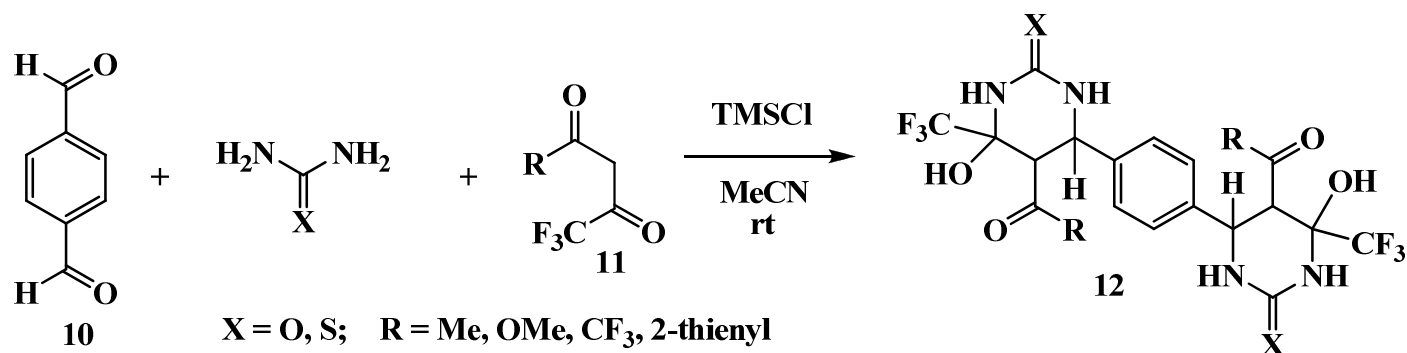
Scheme 2

Unlike the reactions of 1,3-dicarbonyl compounds considered above, hexafluoroacetylacetone **7** enters into the Biginelli reaction with benzaldehyde **2** and urea (in boiling ethanol with hydrochloric acid as catalyst) to yield substituted hexahydropyrimidin-2-one **8** (Scheme 3). The latter compound probably results from a reaction competing with the Biginelli condensation in which hexafluoroacetylacetone cyclocondenses at both its carbonyl groups with the urea amino group by the [CCC]+[NCN] scheme (to be discussed in the next section), while benzaldehyde does not react at all. If carried out under anhydrous conditions in an aprotic solvent (tetrahydrofuran) in the presence of catalytic amounts of *p*-toluenesulfonic acid, the same reaction affords product **9** (X=O) (Scheme 3). Likewise, thiourea reacts with hexafluoroacetylacetone under the classical Biginelli reaction conditions to expectedly produce analogous thione **9** (X=S).³¹



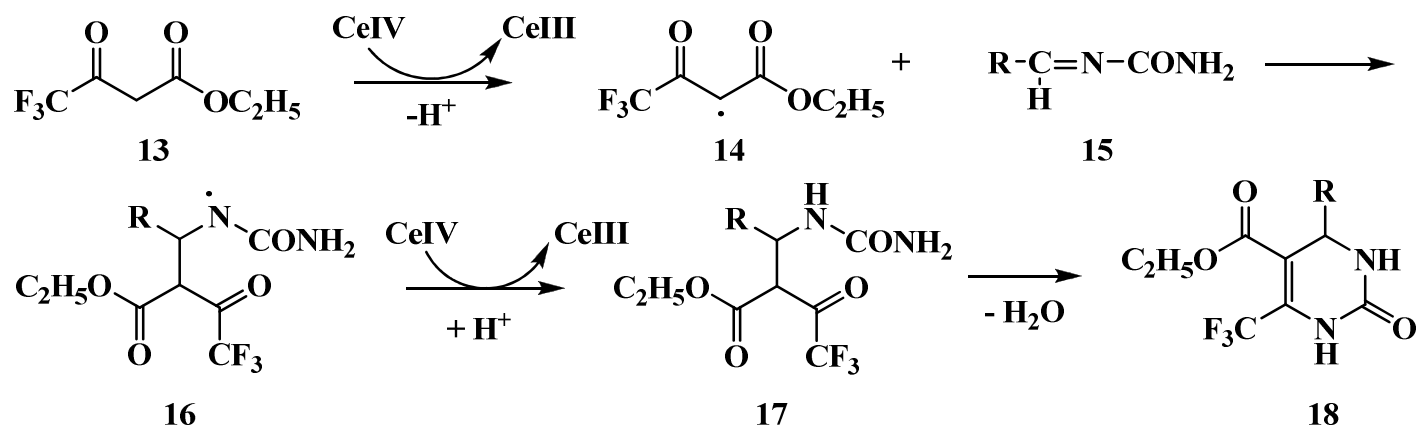
Scheme 3

A facile one-pot procedure was developed for the three-component condensation of terephthalic aldehyde **10** with urea and fluorinated 1,3-dicarbonyl derivatives **11** using catalytic quantities of chlorotrimethylsilane (TMSCl) in acetonitrile at room temperature.^{32,33} TMSCl remarkably accelerates the reaction. Experiments showed that 10 mol% quantities of the catalyst were enough for the reaction to complete in less than 1 hour, while the conversion without catalyst was only 10% after 24 hours. With *meta*- and *para*-phthalic aldehyde **10**, the reaction runs smoothly with the formation of fluorine-containing 1,4-bis(2-oxo(thioxo)tetrahydropyrimidyl-4)benzenes **12** (Scheme 4); in contrast, *ortho*-phthalic aldehyde gave rise to a mixture of condensation products.³²



Scheme 4

In the syntheses of trifluoromethylated di- and tetrahydropyrimidin-2-ones(thiones) by the Biginelli reaction, there were used also catalysts as boron trifluoride diethyl etherate with and without copper (I) oxide,²⁸ zirconium tetrachloride,^{34,35} bismuth triflate,³⁶ a mixture of tin(II) and lithium chlorides³⁷ and polyphosphate esters³⁸ as well as manganese triacetate, Oxone and ceric ammonium nitrate under sonication.³⁹ In the last-mentioned study,³⁹ the ultrasound-accelerated synthesis of 3,4-dihydropyrimidin-2-ones was carried out in neutral medium thus allowing the use of acid-sensitive aldehydes like 2-furaldehyde and phenylacetaldehyde (they worked well without the formation of side products which are generally observed under strongly protic or Lewis acidic conditions).



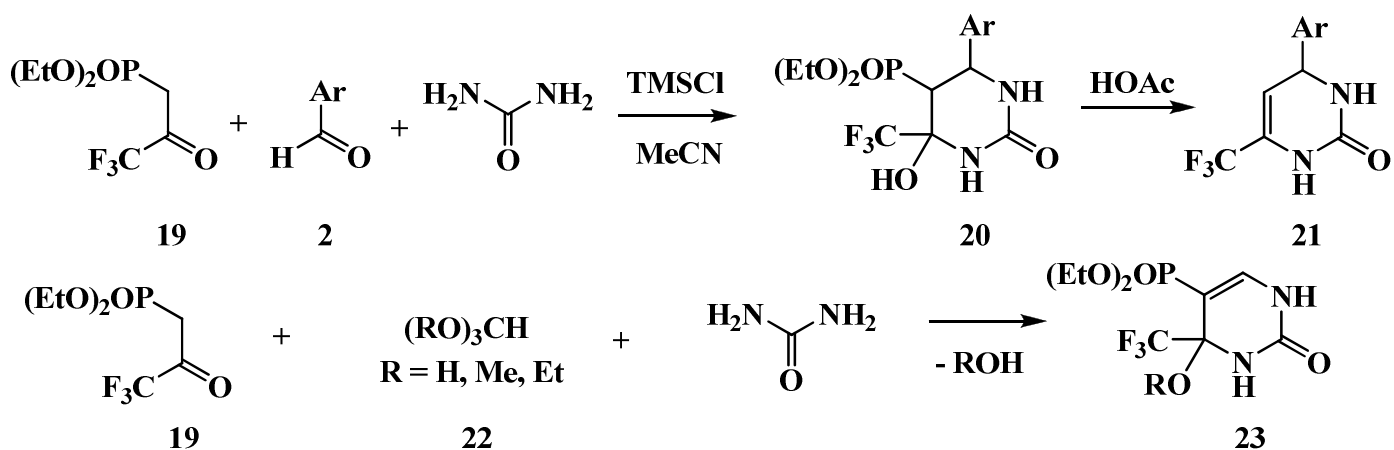
R = MeC₆H₄, MeOC₆H₄, 3,4-methylenedioxyphenyl

Scheme 5

Another important feature of this procedure is the survival of a variety of functional groups such as olefins, ethers, esters, nitro groups and halides during the reaction. In addition to its simplicity and mild

reaction conditions, this method is even effective with aliphatic and α,β -unsaturated aldehydes, which normally produce poor yields because of their decomposition or polymerization under strongly acidic conditions. The Biginelli reaction performed with cerium nitrate, manganese triacetate, iron (III) chloride and other oxidative catalysts is most likely to start with a single-electron transfer giving rise to β -ketoester radical **14** which then adds to the imine intermediate **15** to form radical **16** (Scheme 5). The latter adds another electron and a proton to produce urea **17** which provides target product **18** as a result of intramolecular cyclization.³⁹

Diethyl 2-oxo-3,3,3-trifluoropropylphosphonate **19** reacted with aryl aldehydes **2** and urea under the Biginelli reaction conditions to give, as unstable products, diethyl (6-aryl-4-hydroxy-2-oxo-4-trifluoromethylhexahydropyrimidin-5-yl)phosphonates **20**. On heating them in acetic acid, dephosphorylation occurred and 4-aryl-6-trifluoromethyl-3,4-dihydropyrimidin-2-ones **21** were formed in good yields (Scheme 6).⁴⁰ To obtain phosphorylated pyrimidones **23**, orthoformates **22** instead of aryl aldehydes **2** were reacted (Scheme 6).⁴⁰

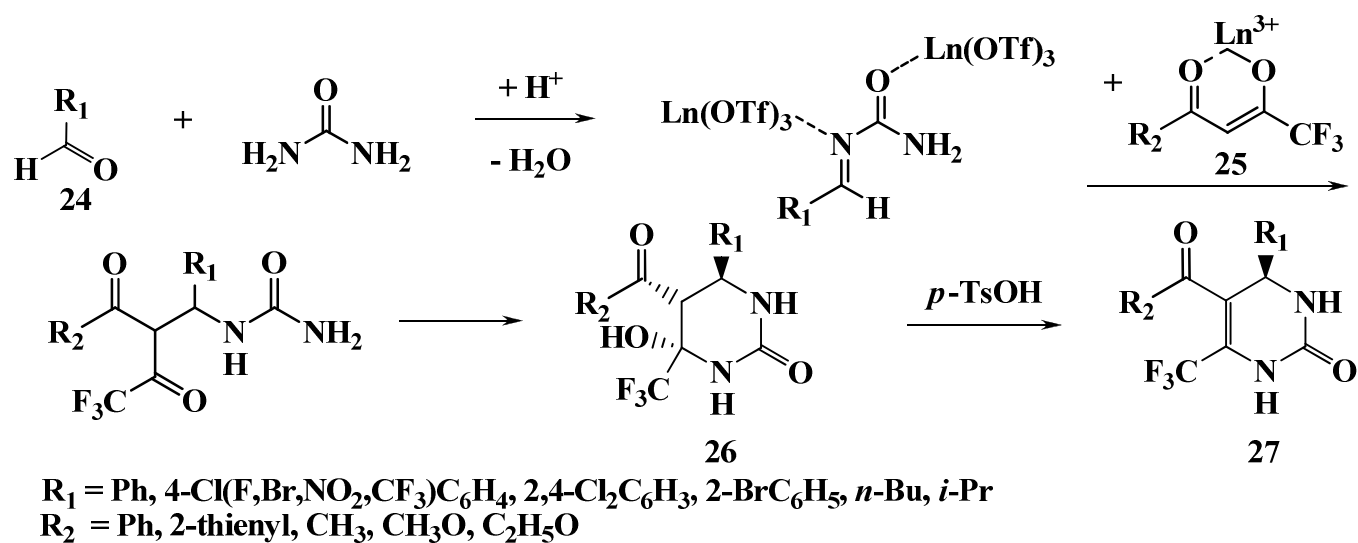


For the sake of both substrate-tolerance and operational simplicity, heterogeneous catalysis was applied to the Biginelli reaction. The condensation was shown to proceed in high yields (~ 90%) for a range of aromatic aldehydes, irrespective of their acid sensitivity and electron nature of substituents, at 80 °C in acetonitrile in the presence of 10% bioglycerol-based sulfonic acid functionalized carbon catalyst. The salient features of the protocol used were easy work-up, recyclability of the bioglycerol-based carbon catalyst and good yields.⁴¹

Chinese researchers developed a solvent-free lanthanide triflate-catalyzed version of the Biginelli reaction. Compared to the classical Biginelli method, an important feature of the novel protocol is the ability to tolerate the variation in all the three components. A variety of β -ketoesters, carboaromatic and heterocyclic β -diketones **25** were examined and not only aromatic but also aliphatic *n*-valeric and isobutyric aldehydes **24** were successfully reacted. With β -diketones **25**, the condensation was completed in 20 minutes to afford tetrahydropyrimidones **26** which were converted to dihydro derivatives **27** by heating in toluene in the presence of strong *p*-toluenesulfonic acid (Scheme 7).⁴² The reaction products were obtained in high diastereomeric purity (99%); one of compounds **27** ($R_1=2$ -thienyl, $R_2=Ph$) was structurally determined by X-ray diffraction analysis. By using $Yb(OTf)_3$ as a catalyst under solvent-free reaction conditions, the yields of the one-pot Biginelli process can be increased from 20–50% to 81–99%, while the reaction times can be

shortened from 18–48 hours to 20 minutes. In addition, the catalyst can be easily recovered and reused. Thus, the approach developed not only leads to economical automation but also reduces hazardous pollution to achieve environmentally friendly processes.⁴²

Recently, it has been shown that tri- and tetra-alkylammonium, 1,3-dialkylimidazolium and 1,2,3-trialkylimidazolium salts with BF_4^- , PF_6^- , AlCl_4^- , Al_2Cl_7^- ⁴³ and TaBr_5 ⁴⁴ as counterions also effectively catalyze the Biginelli reaction on heating the reagents in the absence of a solvent. Moreover, the synthesis of 1,4-bis-(2-oxo(thioxo)tetrahydropyrimidyl-4)benzenes **12** described in Scheme 4 can be performed within 10 minutes under solvent-free conditions, if assisted by microwave irradiation and catalyzed by TMSCl ⁴⁵ or nanosilica.⁴⁶



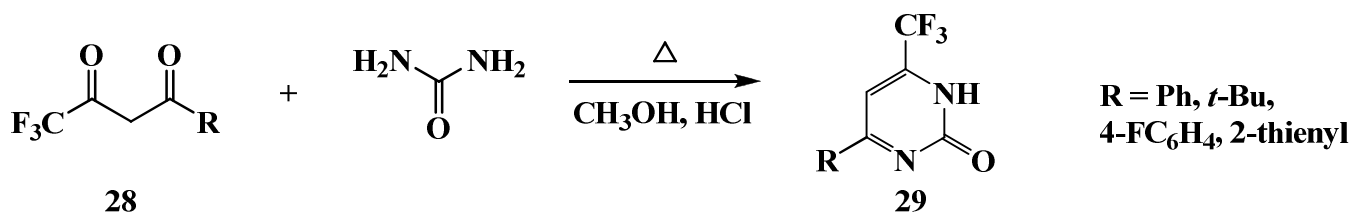
Scheme 7

Generally, the Biginelli reaction is a powerful strategy to obtain trifluoromethylated pyrimidin-2-ones(thiones) and their di- and tetrahydro derivatives (despite the last difficult dehydration step). This method is remarkable for its tolerance to wide-range variations in reaction components. Additional optimization of reaction conditions and catalysts enables the process to be carried out solvent-free within a short time and in high yield.

2.2. [NCN]+[CCC] cyclization

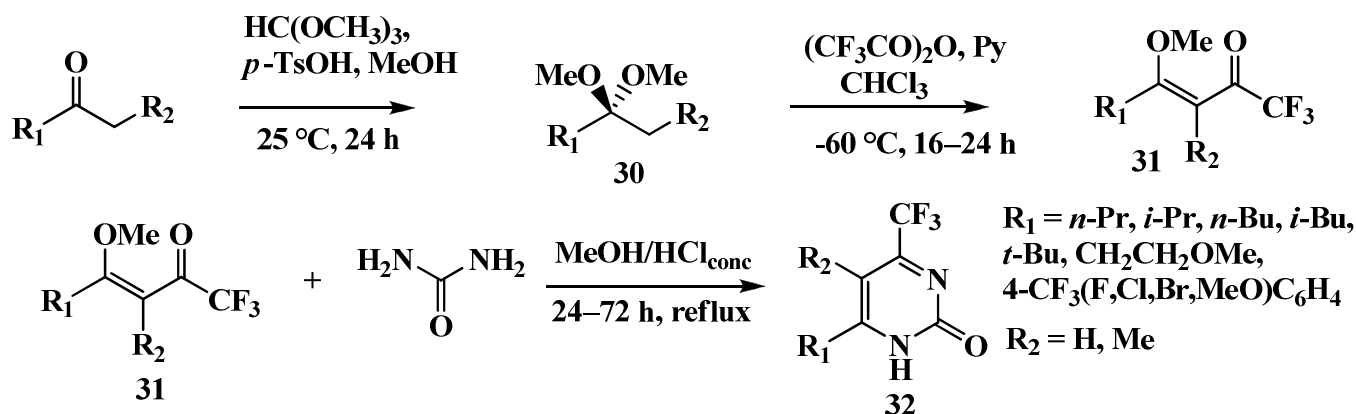
[NCN]+[CCC] cyclization is the most widely employed synthetic route to pyrimidones and their trifluoromethylated analogues. In the first half of the 20th century, uracil was synthesized by the condensation of thiourea with β -diketones or ketoesters followed by the replacement of sulfur by oxygen.⁴⁷ At the same time, 6-trifluoromethyl(thio)uracil was obtained by boiling of (thio)urea with ethyl trifluoroacetoacetate in the presence of sodium ethoxide.^{48–50} In spite of the fact that urea reacts with fluorinated 3-oxoesters more readily than with fluorinated β -diketones, the synthesis of 4,6-di(trifluoromethyl)pyrimidin-2-one involved the condensation of hexafluoroacetylacetone **7** with urea to product **8**, followed by its dehydration in the presence of *p*-toluenesulfonic acid (Scheme 3).³¹

In 1978, 6-trifluoromethylpyrimidin-2-ones **29** were reported to be formed as by-products in the synthesis of chromium (III) chelates by heating unsymmetrical β -diketones **28** in aqueous ethanol in the presence of urea (Scheme 8).⁵¹



Scheme 8

Brazilian researchers have greatly expanded the potentialities of [NCN] + [CCC] cyclization by broadening the range of substituents on the [CCC] synthon. In particular, long alkyl chains and various aromatic residues were introduced at position 6 of the pyrimidone ring. Based on the trifluoromethylation of acetals **30**, a facile method was developed to prepare β -aryl(alkyl)- β -methoxyvinyl ketones **31** which furnished, as a result of the condensation with urea in methanol, a range of 6-aryl(alkyl)-substituted 4-trifluoromethylpyrimidin-2-ones **32** (Scheme 9).⁵²⁻⁵⁴



Scheme 9

Later, this approach was successfully applied to synthesize cyclic β -methoxyvinyl ketones **33**, condensation of which with (thio)urea or guanidine produced 4-CF₃ substituted (thio, amino)pyrimidones **34**, with the heterocyclic moiety fused to 5-, 6-, 7-, 8- and 12-membered cycloalkane rings (Scheme 10). Notably, the yields of the thus obtained thio compounds **34** are significantly higher than those obtained starting from the corresponding β -diketones⁵⁵ and the reaction efficiency can be increased even more with boron trifluoride diethyl etherate used as a catalyst.^{56,57}

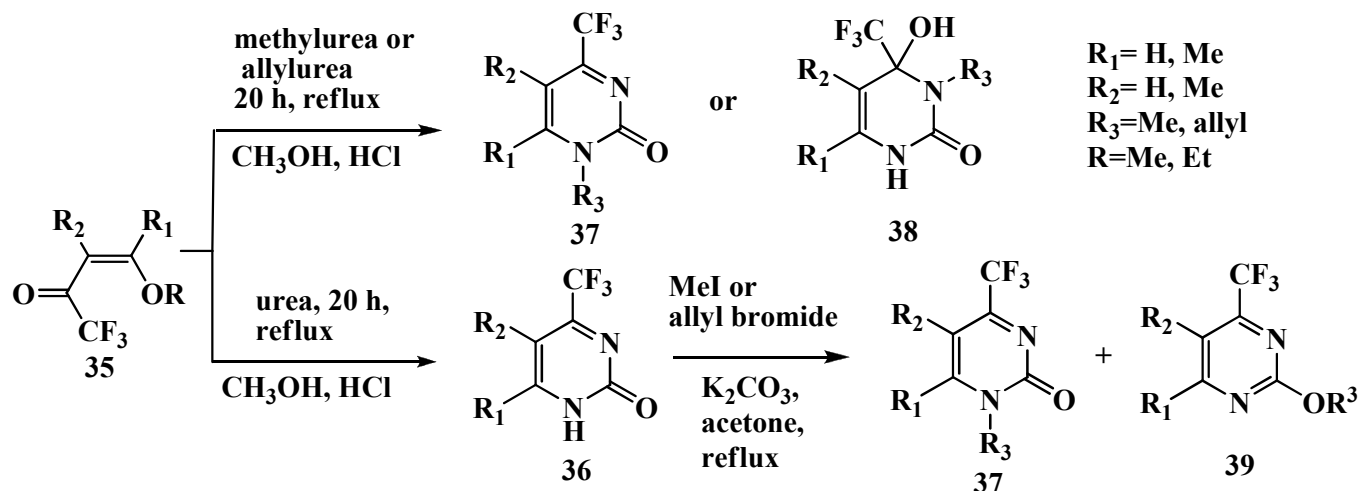


Scheme 10

In view of the low nucleophilicity of urea and also taking into account the possible formation of N1- and N3-alkylated product mixture in the condensation of unsymmetrical ureas with 1,3-dicarbonyl compounds, mono *N*-substituted pyrimidones are preferably prepared by alkylation of *N*-unsubstituted

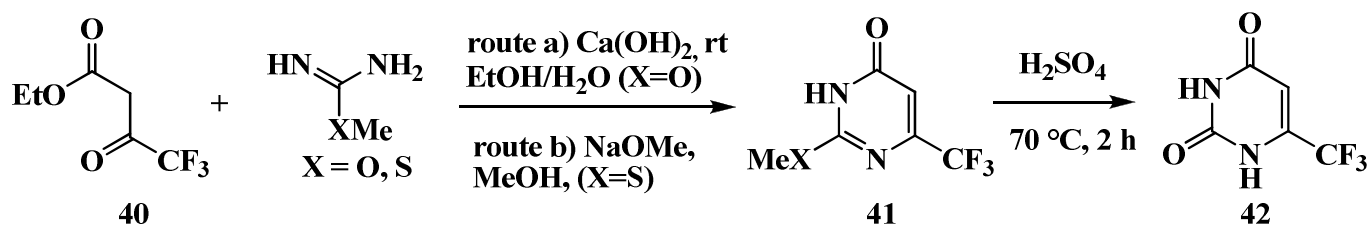
heterocycles. Zanatta *et al.*⁵⁸ reported a comparative study of the chemoselectivity and yields between two synthetic ways to *N*-alkyl-4-(trifluoromethyl)-1*H*-pyrimidin-2-ones, one based on the cyclocondensation of 4-alkoxy-1,1,1-trifluoro-3-alken-2-ones **35** ($R_1=Me$, $R_2=H$) with methyl- and allylureas and the other involving the *N*-alkylation of 4-(trifluoromethyl)-1*H*-pyrimidin-2-ones **36** with methyl iodide and allyl bromide. This study has demonstrated that the cyclocondensation reactions give better yields and furnish either *N1*- or *N3*-alkylated products (**37** or **38**, respectively) depending on both the reaction conditions and the substituents on the enones, whereas the alkylation of pyrimidin-2-ones gives lower total yields and either leads to a mixture of *N1*- and *O*-alkylated products **37** and **39** (as with 6-methylated pyrimidin-2-ones **36**, $R_1=Me$, $R_2=H$) or smoothly affords an *N1*-alkylated product (with all other substrates) (see Scheme 11). For instance, *N3*-alkylated product **38** ($R_1=H$, $R_2=Me$) can be selectively obtained by the cyclocondensation when sufficiently dilute HCl is used. Overall, of the two methods compared, the cyclocondensation appears to be more advantageous being a one-step process (in contrast to the alkylation requiring the pre-synthesis of pyrimidones) which additionally allows for controllable regioselectivity and higher yields of the target products.

The same [NCN]+[CCC] cyclization scheme was employed under analogous conditions to prepare *N1*-methyl-4-(trifluoromethyl)pyrimidin-2-thiones⁵⁹ as well as 5- and 6-substituted 2-methylthio-4-trifluoromethylpyrimidines.⁶⁰



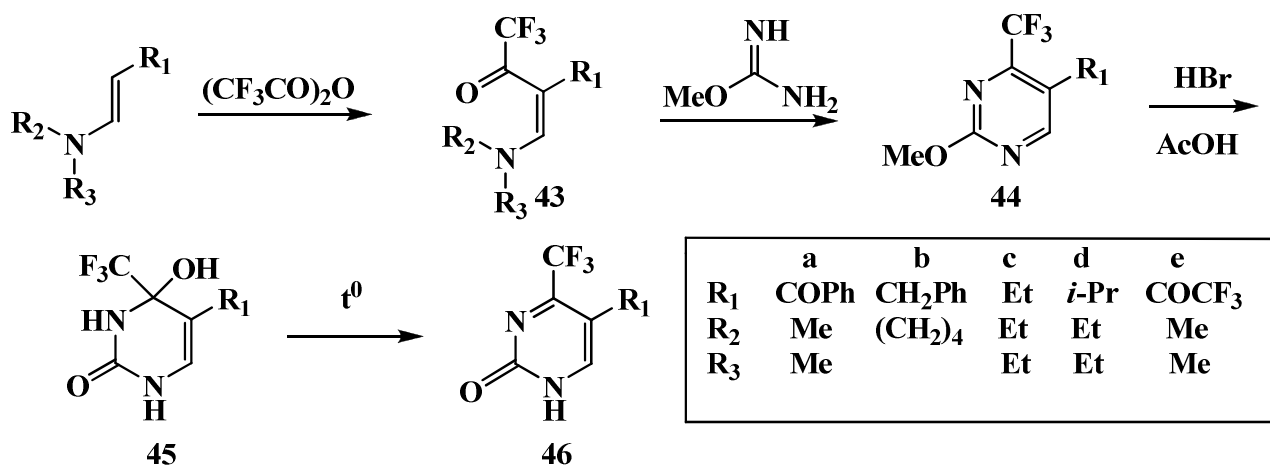
Scheme 11

6-Trifluoromethyluracil **42** and its derivatives can be obtained by the $Ca(OH)_2$ -catalyzed condensation of β -ketoester **40** with *O*-methylisourea in aqueous alcohol at room temperature⁶¹ or by the analogous reaction of **40** with *S*-methylthiourea in the presence of catalytic amounts of sodium methylate,¹⁰ followed by acid hydrolysis of condensation products **41** (Scheme 12).



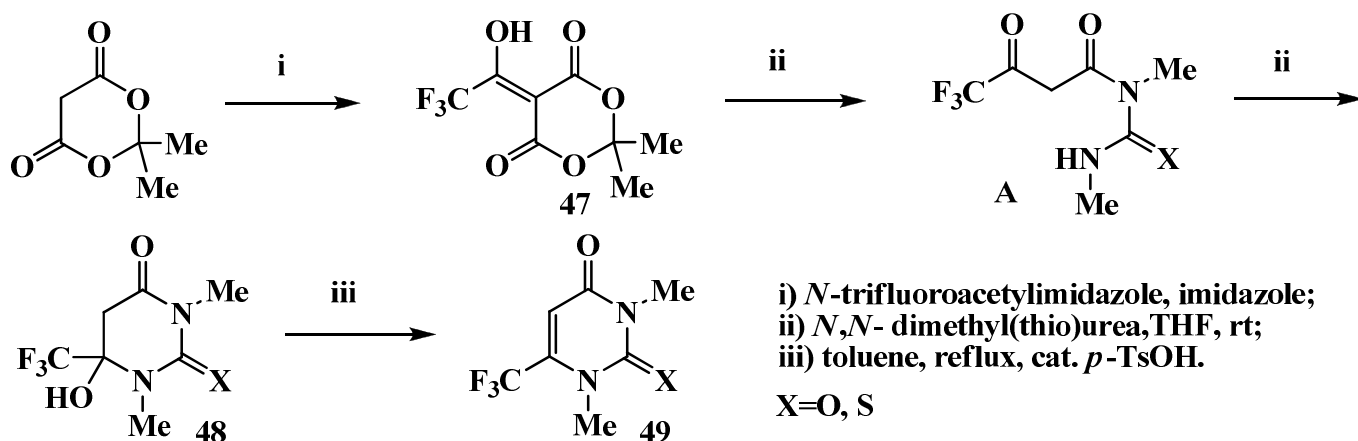
Scheme 12

An important synthetic strategy to trifluoromethylated pyrimidones is the reaction of *O*-methylisourea with trifluoroacetylated enaminoketones **43** which yields 2-methoxypyrimidines **44**. A mixture of aqueous hydrobromic and acetic acids hydrolyzes **44** to dihydropyrimidones **45**. On boiling compounds **45b–d**, their dehydrated derivatives **46b–d** are formed, whereas **45a** and **45e** resisted to the dehydration (Scheme 13).^{62–64}



Scheme 13

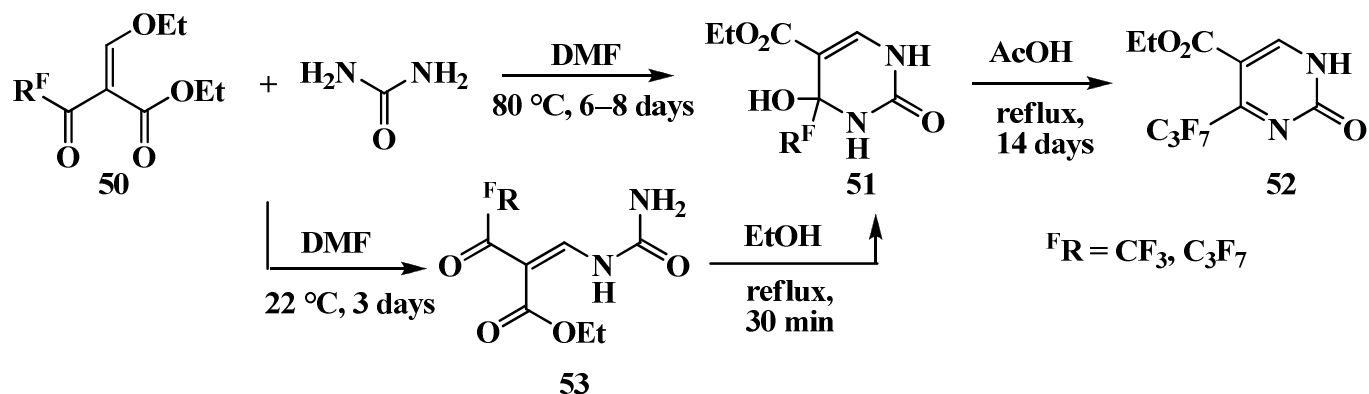
A convenient preparation of trifluoroacetylated Meldrum's acid **47** and its use as an effective building block for trifluoromethylated pyrimidines was reported (Scheme 14).⁶⁵ The reaction of **47** with 1,3-dimethyl-(thio)urea in THF at room temperature proceeds *via* trifluoroacetoacetyl intermediate **A** to give dihydro-uracil derivatives **48**. These products can be dehydrated to 1,3-dimethyl-6-trifluoromethyl(thio)uracils **49** in 80% yield by heating under reflux in toluene with a catalytic amount of *p*-toluenesulfonic acid.



Scheme 14

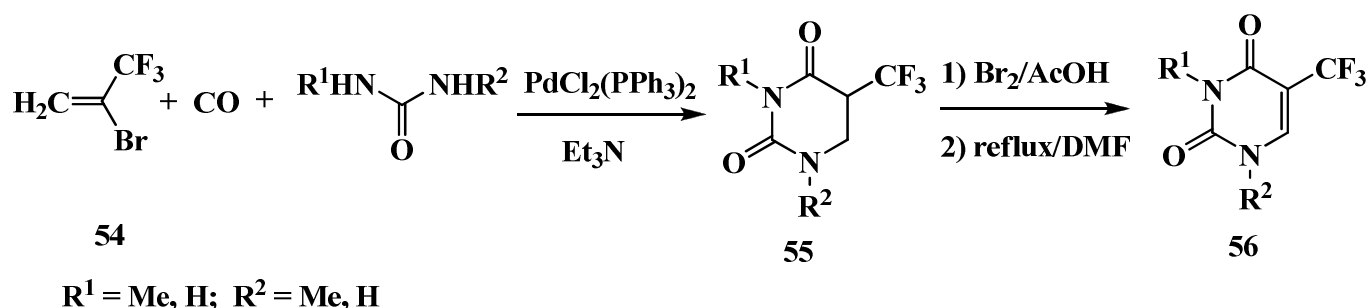
Functionalized pyrimidines are conveniently synthesized from 1,3-dicarbonyl compounds containing various 2-substituents: along with the 1,3-dicarbonyl moiety, reactive groups at position 2 can be involved in the construction of the pyrimidine nucleus. To exemplify, ethyl 2-ethoxymethylidene-3-oxoalkanoates **50** are suitable synthons for the preparation of 5-carboxylpyrimidines. On prolonged heating in DMF at 80 °C, compounds **50** enter into cyclocondensation with urea to afford tetrahydropyrimidines **51**; the reaction proceeds as a cycloaddition of the binucleophile to the ethoxymethylidene fluoroacyl moiety accompanied by elimination of an ethanol molecule. However, if carried out at room temperature, the process stops at the

stage of monocondensation of the ethoxymethylidene substituent so that esters **53** result (Scheme 15). These products can be isolated from the reaction mixture and easily converted to **51** by boiling in methanol for 30 minutes. Like compounds **45a** and **45e**, 4-trifluoromethyl dihydropyrimidone **51** ($R^F = \text{CF}_3$) fails to be dehydrated (probably due to the electron-withdrawing effect of the 5-carboxyl group) and only its 4-heptafluoropropyl substituted analogue eliminates a water molecule to yield **52**.^{66,67}



Scheme 15

The [NCN]+[CCC] cyclization strategy opens a simple and efficient way not only to 4- and 6- but also to 5-trifluoromethylated pyrimidones. In 1962 Heidelberger *et al.* obtained 5-trifluoromethyluracil through the condensation of β -bromo- α -trifluoromethyl propionamide with an excess of urea.⁶⁸ Later, in 1982, it was shown that palladium complex-catalyzed carbonylation of 2-bromo-3,3,3-trifluoropropene **54** with ureas afforded 5-trifluoromethyl-5,6-dihydrouracils **55** in moderate to good yields. Compounds **55** were almost quantitatively converted into 5-trifluoromethyluracils **56** by boiling in DMF with a mixture of bromine and acetic acid (Scheme 16).⁶⁹

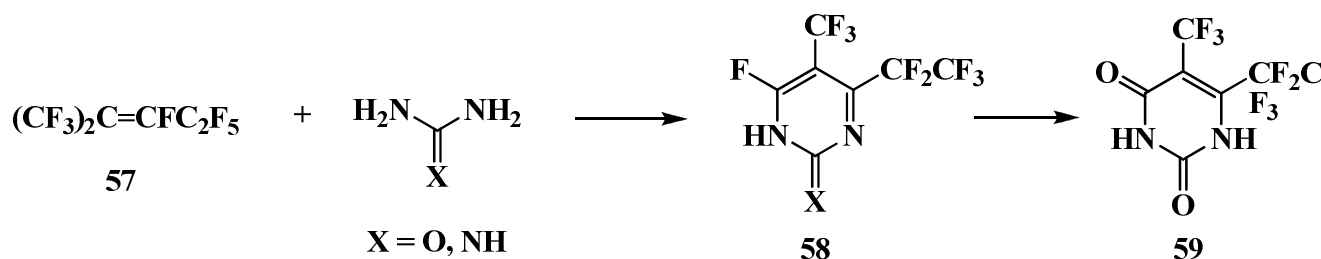


Scheme 16

A synthesis of trifluoromethyl pyrimidine was described, in which perfluoro-2-methylpent-2-ene **57** acted as a [CCC] bielelectrophilic building block. It was reacted with urea or guanidine in the presence of triethylamine to effectively produce 6-fluoro-4-pentafluoroethyl-5-trifluoromethyl-1*H*-pyrimidin-2-one **58** ($X=O$) and its 2-imino analogue ($X=NH$). The reactive fluorine atom at the double bond in **58** ($X=O$) is readily hydrolyzed leading to uracil **59** (Scheme 17).⁷⁰

Compensating the low nucleophilicity of urea, the electron-withdrawing effect of the CF_3 group in dicarbonyl compounds enhances their electrophilicity to a degree sufficient for the [NCN]+[CCC] cyclization to proceed quite efficiently and actively. It can thus be regarded as a convenient method to

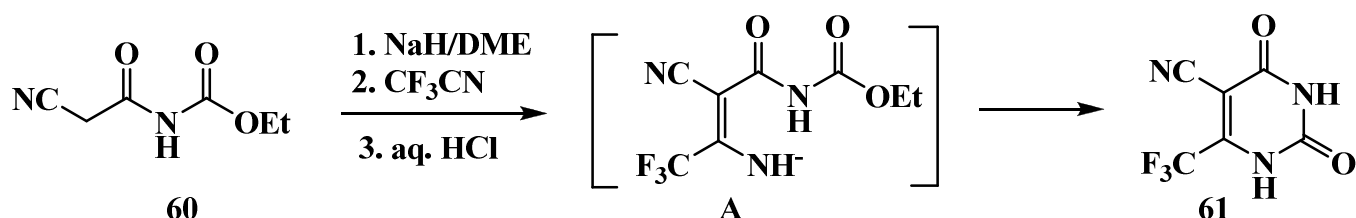
prepare multisubstituted trifluoromethylated pyrimidones exhibiting a wide range of biological properties.^{15-17,68,71} The above-discussed approach is remarkable for its structural flexibility stemming from a great variety of starting synthons: 1,3-bielectrophilic [CCC] components include CF₃-substituted diketones,^{31,51} β-methoxyvinyl ketones,^{53,54,56,57} ketoesters,^{10,61} α,β-unsaturated ketones,⁷² enamino ketones,⁶²⁻⁶⁴ Meldrum's acid,⁶⁵ perfluoroalkenes⁷⁰ and α,β-unsaturated acids with their derivatives,⁷³ whereas 1,3-binucleophilic [NCN] components are represented by (thio)urea with its mono- and di-substituted derivatives, methyliso(thio)urea and guanidine.



Scheme 17

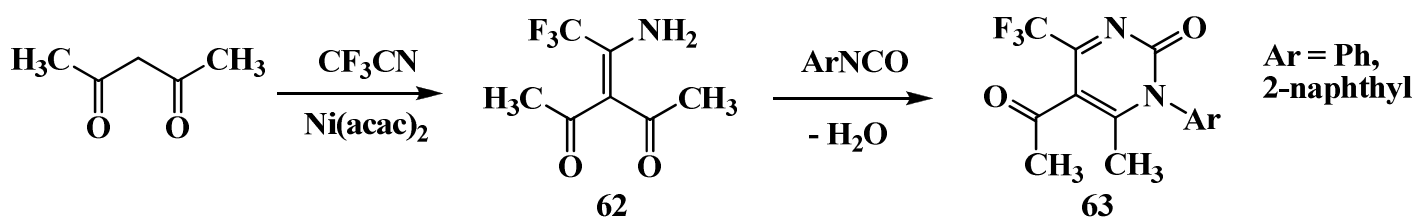
2.3. [CCCN]+[CN] cyclization

[CCCN]+[CN] cyclization involves various 1,4-nucleophilic-electrophilic [CCCN]-synthons and electrophilic [CN] components mostly contained in cyanates, isocyanates and their thio analogues. Based on this approach, 5-cyano-6-trifluoromethyluracil **61** was obtained by cyclocondensation of *N*-(cyanoacetyl)urethane **60** and trifluoroacetonitrile in the presence of sodium hydride. Notably, the reaction pathway proceeds *via* intermediate A which is an intramolecular combination of the [CCCN] and [CN] components. Resulting compound **61** is used as a convenient substrate in the synthesis of 5-substituted uracils (Scheme 18).⁷⁴



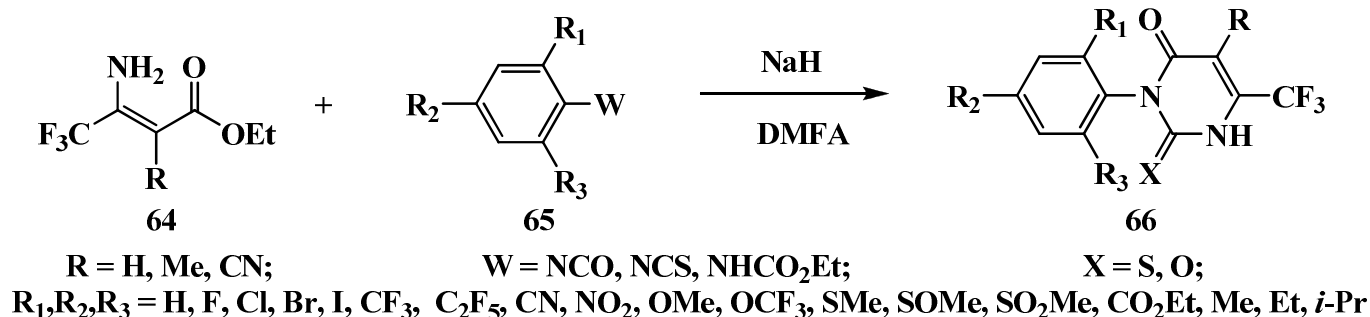
Scheme 18

Later a facile synthetic route to trifluoromethyl enaminone **62** was described which involved the addition of trifluoroacetonitrile to acetylacetone in the presence of catalytic amounts of nickel acetylacetonate. Condensation of **62** with aryl isocyanates furnishes 4-trifluoromethyl-1*H*-pyrimidin-2-ones **63** (Scheme 19).⁷⁵



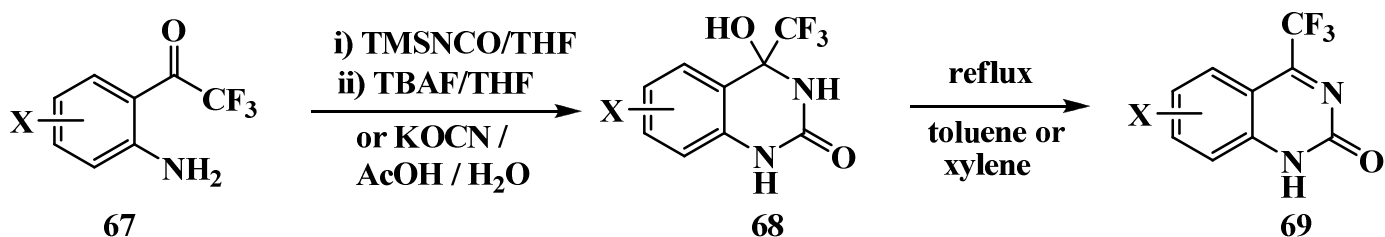
Scheme 19

The reaction of β -enamino esters **64** with aryl iso(thio)cyanates or carbamates **65** in the presence of sodium hydride in DMF produced 3-aryl-6-trifluoromethyl-2-(thio)uracils **66**, known to be effective insecticides¹⁰ and herbicides⁹ (Scheme 20). Ethyl 3-amino-4,4,4-trifluorocrotonate **64** (R=H) was also reacted with methyl isocyanate to give, in three steps, 3-methylated analogue of **66**, a structural building block for potent antagonists to α_4 , $\alpha_4\beta_1$, and $\alpha_4\beta_7$ integrins.⁷⁶



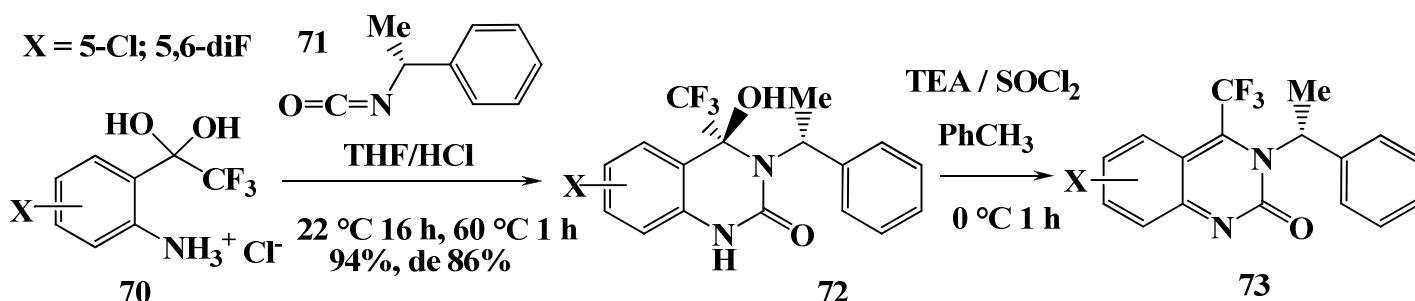
Scheme 20

The [CCCN]+[CN] cyclization scheme was likewise applied in the synthesis of 4-trifluoromethyl-2(1*H*)-quinazolinones **69**, the key compounds in the preparation of **DPC961** and **DPC082** (to be described below).^{13,14,77,78} To this end, halogenated amino ketones **67** were reacted with trimethylsilyl isocyanate (TMSNCO), followed by the treatment with tetrabutylammonium fluoride (TBAF)^{13,14} or potassium cyanate in aqueous acetic acid. Resulting hemiaminals **68**, when heated with 4Å molecular sieves in toluene or xylene under reflux, underwent dehydration to desired ketimines **69** (Scheme 21).



X = 5-F; 5-Cl; 5,6-diF; 6-Cl; 5-Cl, 6-F; 6-F; 6-MeO; 5-F, 6-Cl; 5,6-diCl

Scheme 21

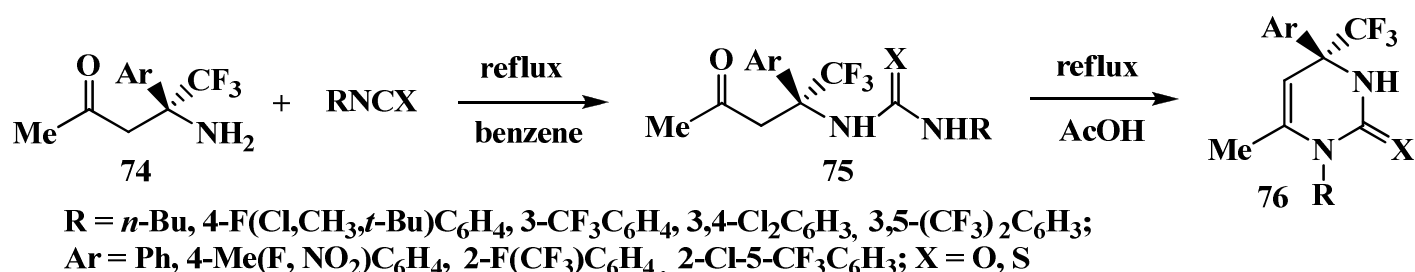


Scheme 22

Hydrated ketoanilines **70** reacted with (*R*)-(+)-methylbenzyl isocyanate **71** in THF containing 1N HCl to provide a 93:7 mixture of diastereomeric hemiaminals **72**. A cooled to 0 °C solution of **72** in a toluene-triethylamine (TEA) mixture was treated with 1 equivalent of thionyl chloride to generate quinazolines **73**

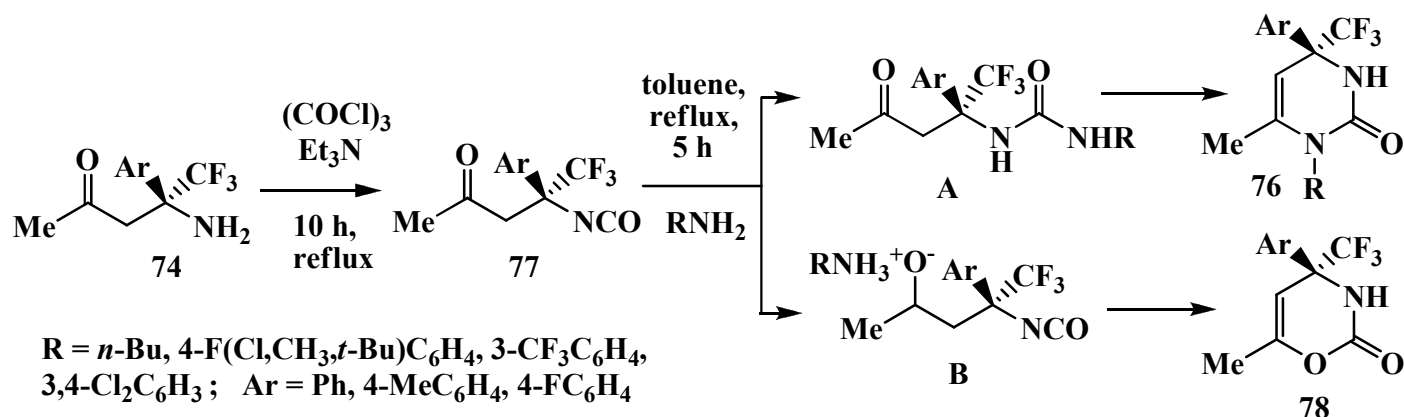
(Scheme 22),^{78,79} the substrates for the enantiopure **DPC961** synthesis by nucleophilic substitution (for details, see the next section).

The recently reported condensation of optically active 4-amino-4-aryl-5,5,5-trifluoropentan-2-ones **74** with aryl iso(thio)cyanates produces disubstituted (thio)ureas **75** which, on boiling in acetic acid, afford cyclization products **76** (Scheme 23).^{80–82}



Scheme 23

β -Amino ketones **74** were converted to corresponding isocyanates **77** in 85–90% yields by the reaction with triphosgene in inert solvents in the presence of basic catalysts. Heating crude products **77** with primary aliphatic amines in dry toluene furnishes mixtures of 1-alkyl-substituted dihydropyrimidones **76** and dihydrooxazinones **78** in the ratios 2:1 to 3:1. The two heterocycles obtained are likely to result from the intramolecular cyclocondensation of the corresponding intermediates, ureas **A** or enolates **B** (Scheme 24).⁸¹

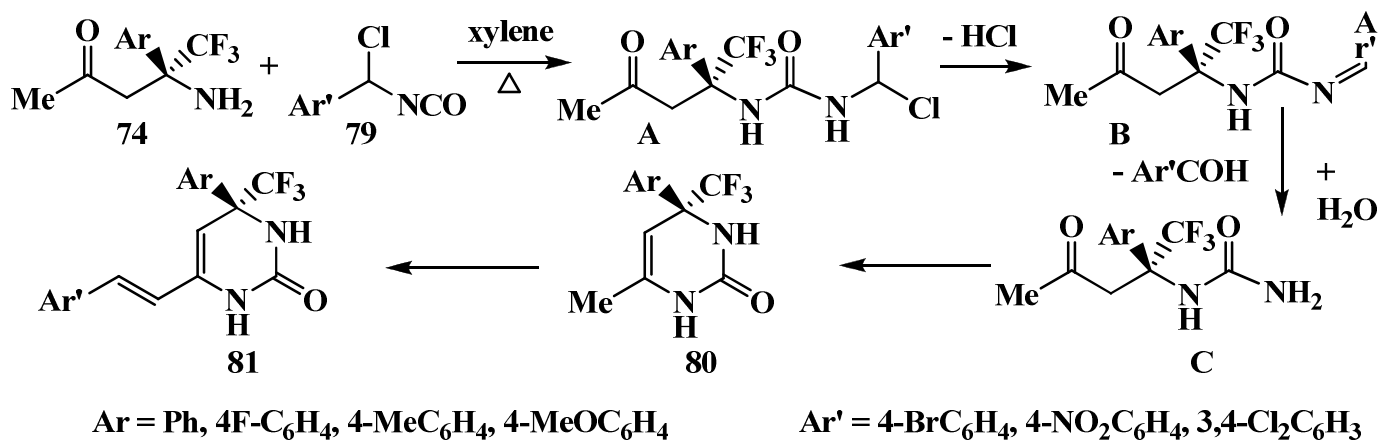


Scheme 24

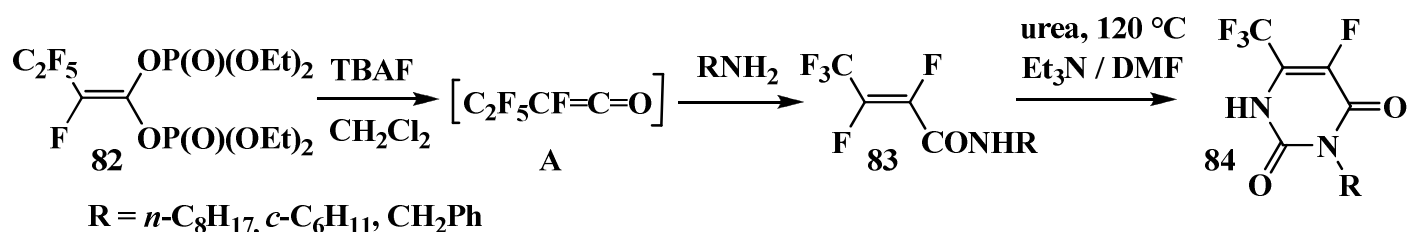
On heating β -amino ketones **74** with α -chlorobenzyl isocyanates **79** in boiling xylene over a period of 8 hours, (*S*)-(+)-4-aryl-6-(2-arylethenyl)-4-trifluoromethyl-3,4-dihydropyrimidin-2(1*H*)-ones **81** were formed. Presumably, the reaction pathway starts with the carbamylation of the amino group in **74** with **79** leading to *N*-(α -chlorobenzyl)ureido ketone **A** which loses hydrogen chloride at elevated temperatures to yield ureido ketone **B**. The double C=N bond in the latter is activated by the adjacent carbonyl group and is readily hydrolyzed by traces of water in the reaction mixture to produce ureido ketone **C** and aromatic aldehyde Ar'CHO. Acid-unstable intermediate **C** rapidly cyclizes to dihydropyrimidone **80** with elimination of water thus giving rise to the next hydrolysis cycle. Finally, Me group in **80** reacts with the released aromatic aldehyde to furnish 6-styryldihydropyrimidone **81** (Scheme 25).⁸³

Another example of [CCCN]⁺[CN]⁻ cyclization is the formation of polyfluorinated pyrimidone **84** in the reaction of fluorinated α,β -unsaturated amide **83** with urea in the presence of triethylamine in DMF at

120 °C. To obtain starting amide **83**, amines are reacted with ketene **A** generated *in situ* from 1,1-alkenediyl tetraethyl bis-phosphate **82** by the addition of tetrabutylammonium fluoride or any other fluoride ion source (Scheme 26).⁸⁴



Scheme 25



Scheme 26

Thus, the [CCCN]+[CN] methodology offers a practical synthetic route to the pyrimidine nucleus. It is a convenient alternative to the Biginelli reaction and [CCC]+[NCN] scheme and, moreover, it quite often provides the only feasible way to obtain pyrimidines. For instance, the attempted reaction of ethyl trifluoroacetoacetate with urea failed to produce 6-trifluoromethyluracils, whereas the condensation of trifluoromethylated aminocrotonates with isocyanates was found to most efficiently afford the desired products.⁸⁵ As another strength of [CCCN]+[CN] reactions, they can be performed with optically active enamines and β -amino ketones thus yielding enantiopure trifluoromethylated dihydropyrimidones, which is of great relevance to the development of potential drugs.

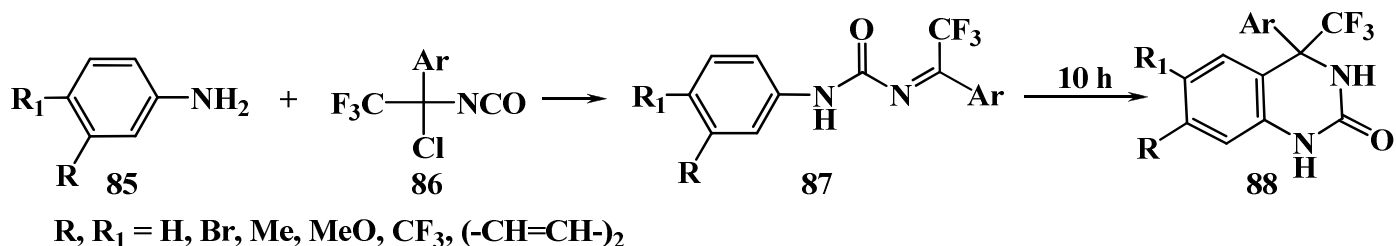
2.4. [CNC]+[NCC] cyclization

[CNC]+[NCC] cyclization is a new, promising and rapidly developing method to construct the trifluoromethylated pyrimidone moiety. Strong bielelectrophiles such as CF_3 -substituted 1-chloroalkyl isocyanates, 1,1-dichloroalkyl isocyanates, 1-chloroalkylcarbodiimides, 1-chloroalkylideneureas (carbamates), etc. can be used as effective [CNC] components.

It has been found that the reaction between 1-chloroalkyl isocyanates **86** and aniline **85** gives, as initial products, *N*-alkylideneureas **87** which undergo intramolecular cyclization to quinazolin-2-ones **88** on prolonged heating (10 hours) in toluene (Scheme 27).^{86,87}

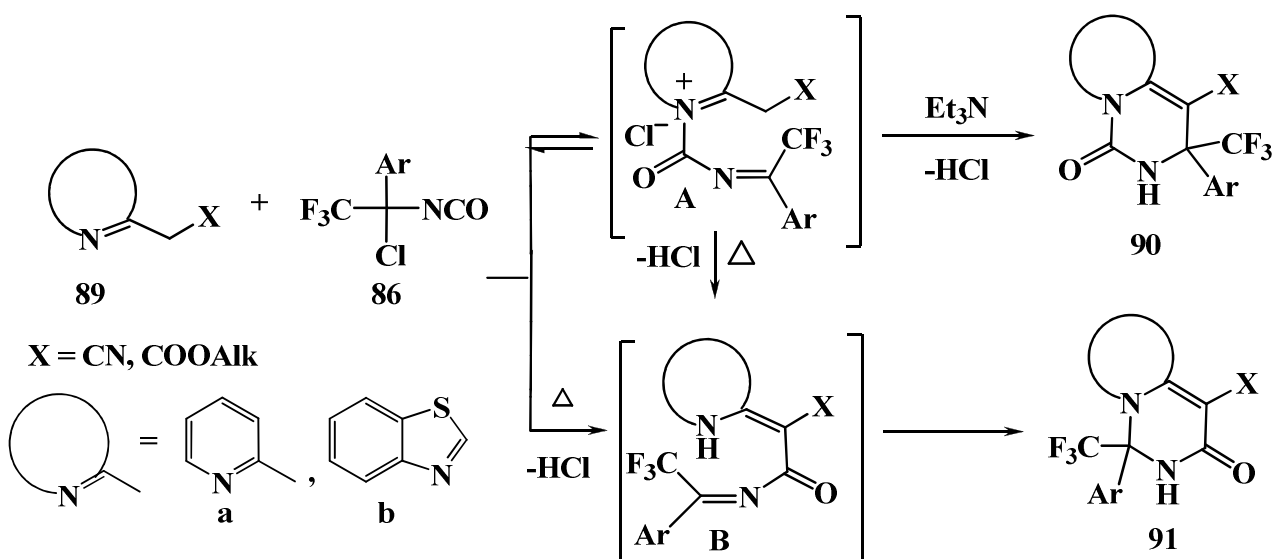
A number of *N*-heterocyclic derivatives with an activated methylene group including substituted pyridines **89a**,⁸⁸ benzothiazoles **89b**⁸⁹ and benzimidazoles **89c**⁹⁰ were tested as [NCC] components.

Importantly, variation of the reaction conditions allows the heterocyclization to proceed regioselectively via one of the two alternative pathways leading to products **90** or **91** (Scheme 28).



Scheme 27

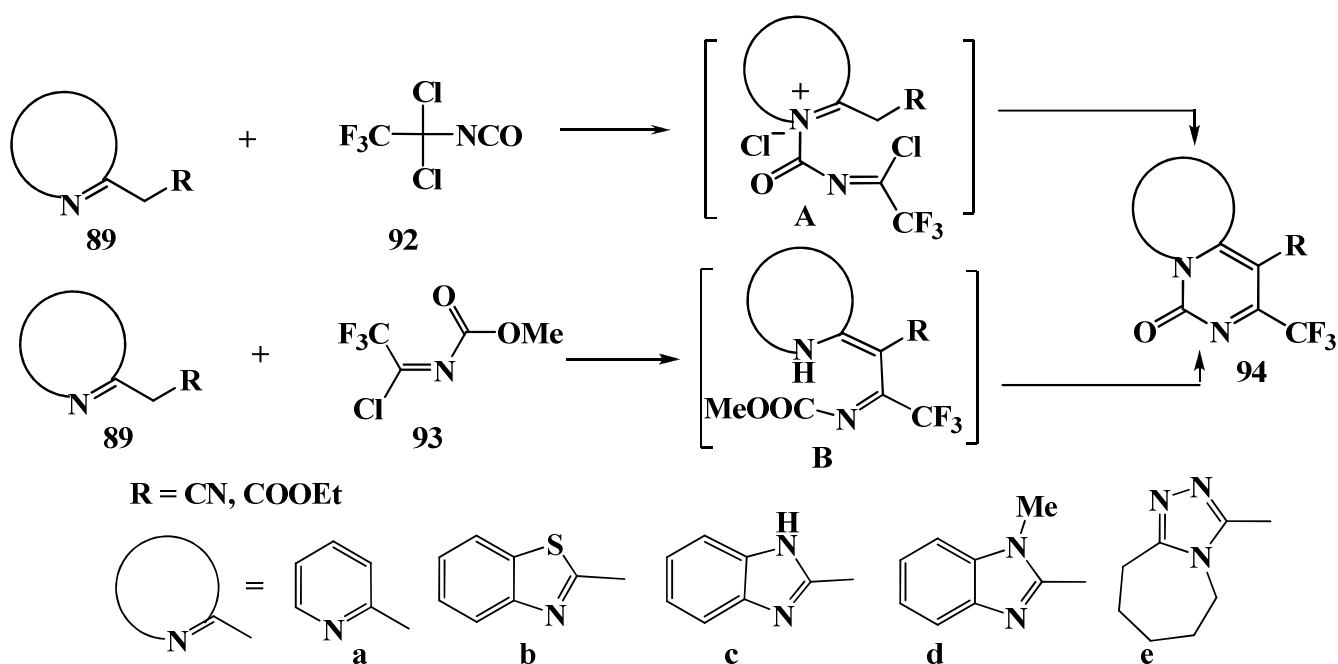
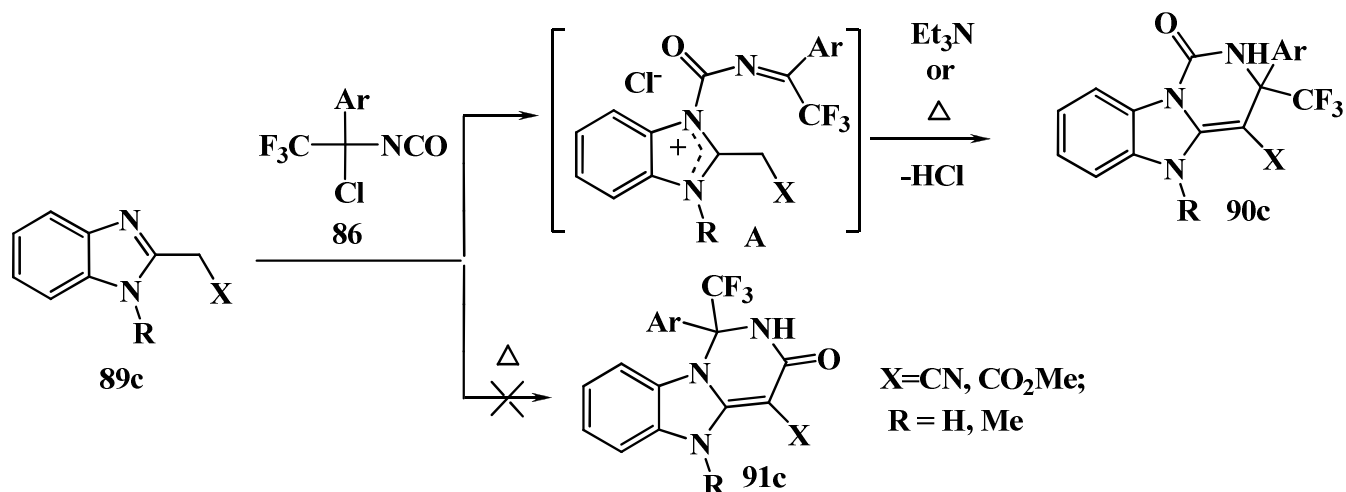
To exemplify, if the reaction is carried out in benzene at room temperature in the presence of triethylamine, then electrophiles **86** attack the *N*-nucleophilic centre of [NCC] synthons **89a,b**, followed by the formation of intermediates **A** and their cyclization to target compounds **90**. In contrast, heating reagents **89a,b** and **86** in toluene without bases results in the initial electrophilic attack of **86** on the methylene group of **89a,b** and, accordingly, formation of intermediates **B** which then cyclize to products **91a,b**. The thus controlled regioselectivity of the reaction enables the directed construction of isomeric dihydropyrimidones fused to pyridine and benzothiazole nuclei.^{88,89}



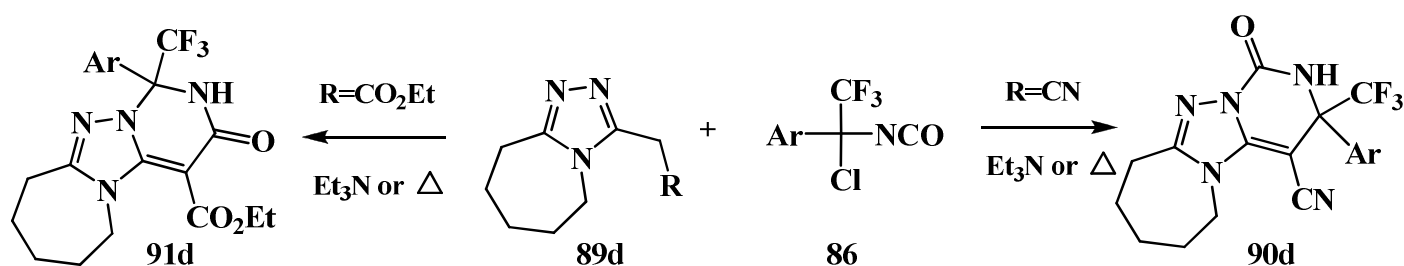
Scheme 28

However, the condensation of isocyanates **86** with 2-benzimidazole **89c** provides only tetrahydropyrimido[1,6-*a*]benzimidazol-1(2*H*)-ones **90c**, irrespective of the reaction conditions (Scheme 29). This effect is probably due to the higher nucleophilicity of the benzoimidazole nucleus as compared with benzothiazole and pyrimidine, which accounts for the predominance of the reaction pathway via intermediate **A**.⁹⁰

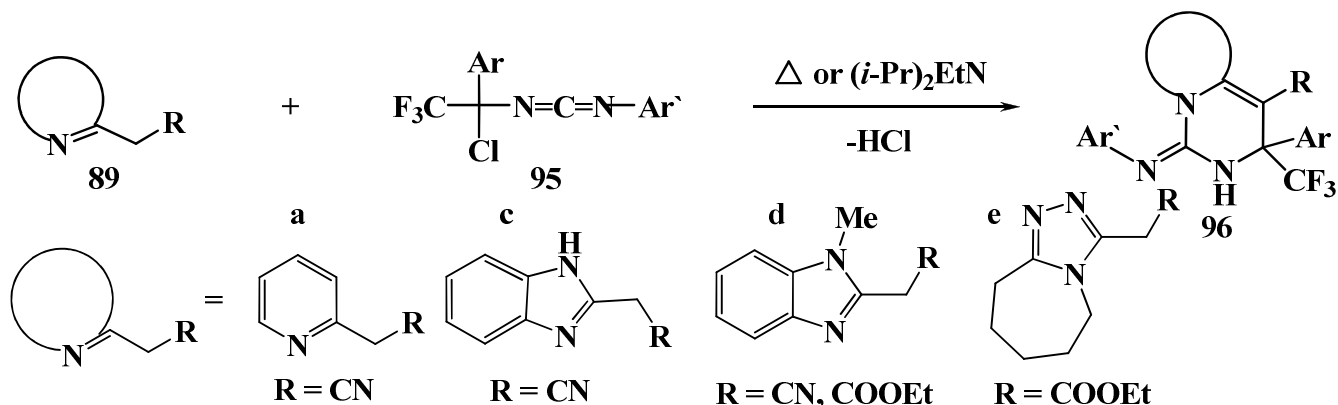
To obtain dehydro analogues of **90**, heterocycles **89** were introduced into the reactions with 1,1-dichloro-2,2,2-trifluoroethyl isocyanate **92** and methyl *N*-(1-chloro-2,2,2-trifluoroethylidene)carbamate **93**. In both cases, the reaction follows a single pathway via relatively stable intermediate **A** (or **B**) which eliminates, under base treatment or heating, HCl (or MeOH) to give fused systems **94** (Scheme 30).^{30–32}



It is notable that the course of the reaction between 1-chloroalkyl isocyanates **86** and 3-(1,2,4-triazolyl) acetic acid derivatives **89d** is governed by the nature of the substituent R in the NCC component. With triazolylacetonitrile (R=CN), polycyclic systems **90d** are formed, whereas the corresponding acetate (R=COOEt) gives rise to isomeric products **91d** (Scheme 31).⁹¹ Evidently, the electron-withdrawing strength of the substituent R affects the competition between the N and C nucleophilic reaction centres and hence determines the cyclization direction.

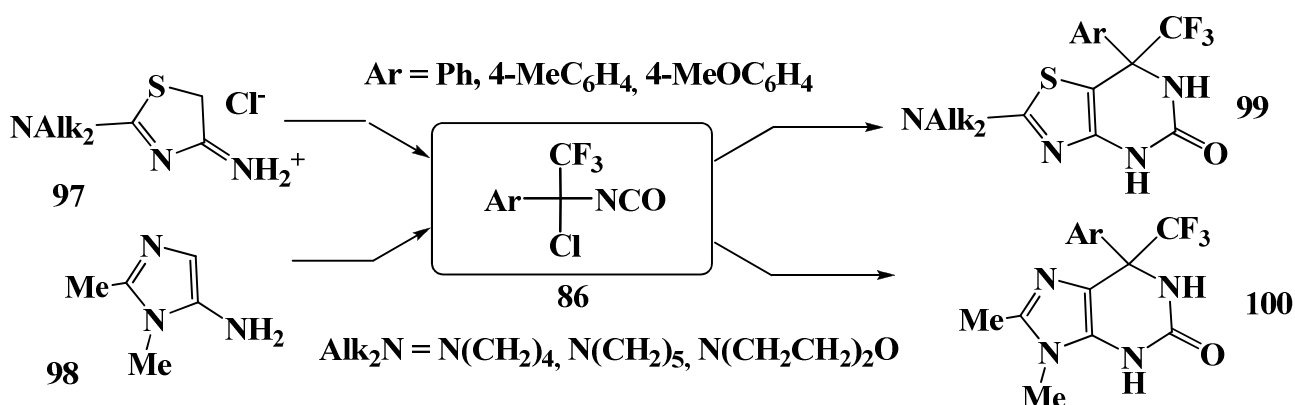


The reaction between azahetarylacetic acid derivatives **89** and fluorinated 1-chloroalkylcarbodiimides **95** which proceeds on heating in benzene or at room temperature in the presence of *N*-ethyl-*N,N*-diisopropylamine yields heterofused 1-(*N*-arylimino)dihydropyrimidines **96** (Scheme 32).^{88,90,91}



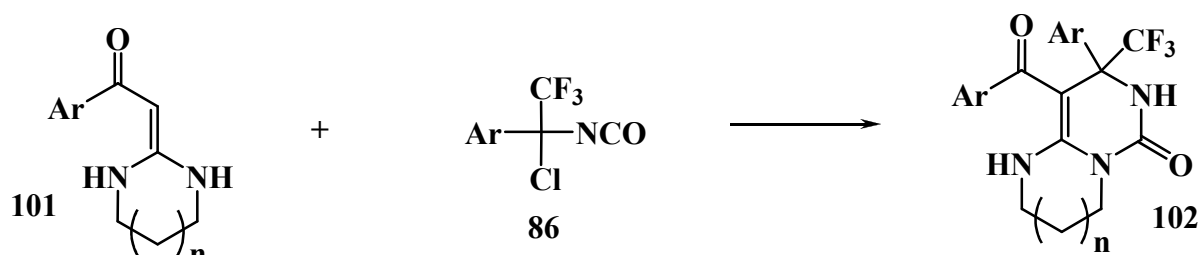
Scheme 32

The reactions of 2-(dialkylamino)-1,3-thiazol-4-amines **97** and 1,2-dimethyl-1*H*-imidazol-5-amine **98** with 1-chloroalkyl isocyanates **86** furnish, respectively, thiopurines **99** and purines **100** with the trifluoromethylated pyrimidine ring (Scheme 33).⁹²



Scheme 33

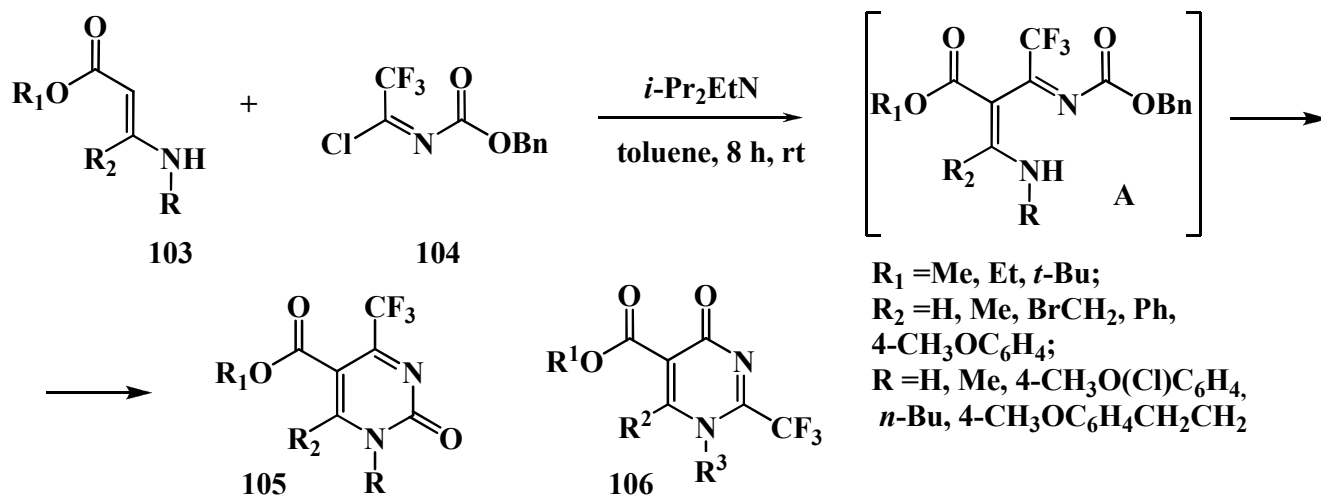
Condensation of cyclic α -aroyl-*N,N*-ketenaminals **101** with 1-chloroalkyl isocyanates **86** is a facile method to prepare imidazo[1,2-*c*]pyrimidin-5(1*H*)-ones and pyrimido[1,6-*c*]pyrimidin-6(1*H*)-ones **102** (Scheme 34).^{93,94}



Scheme 34

Recently, a novel synthetic strategy to 4-trifluoromethyl substituted 2-oxo-1,2-dihydropyrimidine-5-carboxylates has been developed based on the cyclocondensation of β -enaminoesters **103** with *N*-(1-chloro-

2,2,2-trifluoroethylidene)carbamates **104**. It has been established that the reaction is highly regioselective and leads to pyrimidin-2-ones **105** rather than to isomeric pyrimidin-4-ones **106**. The most likely initial step is the imidoylation of the nucleophilic β -carbon atom in the enamine moiety of compounds **103**; the resulting intermediate **A** cyclizes at room temperature to compounds **105**. The product structure is supported by ^1H - and ^{13}C -NMR spectroscopy as well as by X-ray diffraction analysis (Scheme 35).⁹⁵

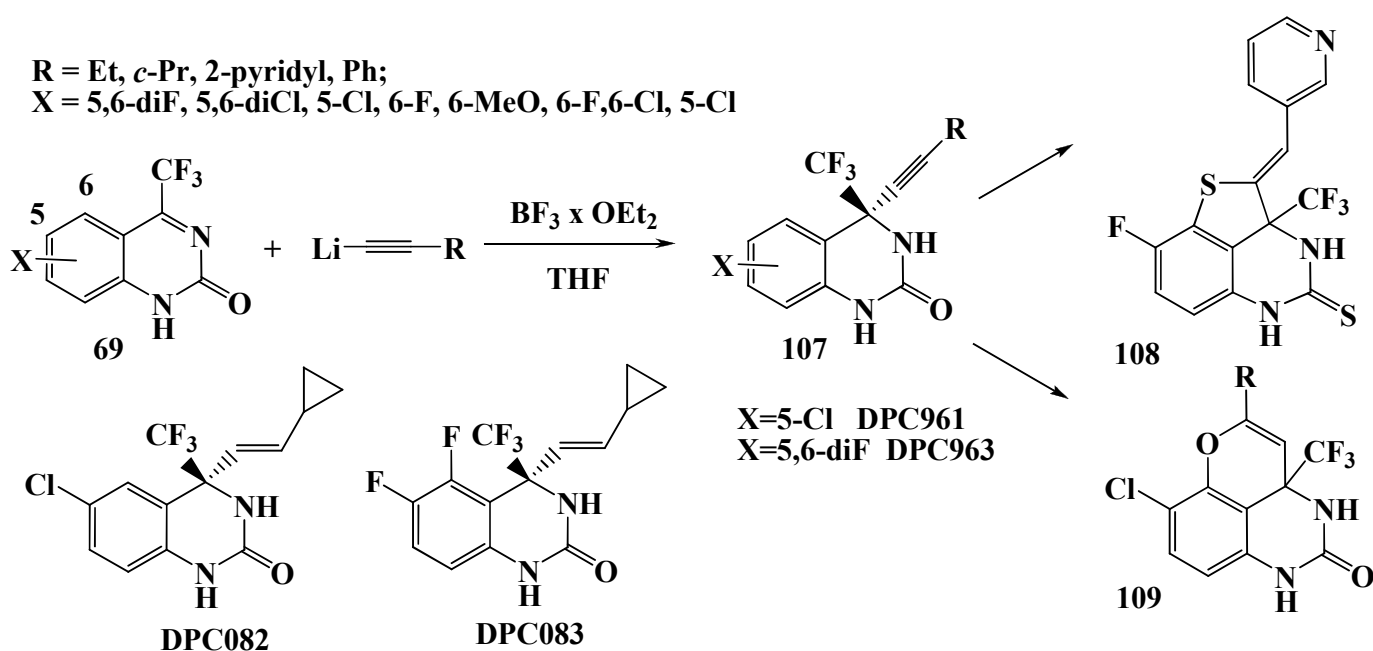


Scheme 35

3. Chemical properties of trifluoromethylated pyrimidin-2-ones(thiones)

3.1. Nucleophilic addition reactions

4-Trifluoromethylpyrimidin-2-ones(thiones) and their fused analogues are typical electrophilic systems which readily undergo nucleophilic additions by electron-rich compounds. This type of reactions provides a convenient toolkit not only to modify heterocyclic systems but also to create asymmetric centres in them. Addition at position 4 of the pyrimidine nucleus is of special significance as an access to promising anti-HIV agents (**DPC961**, **DPC082**).

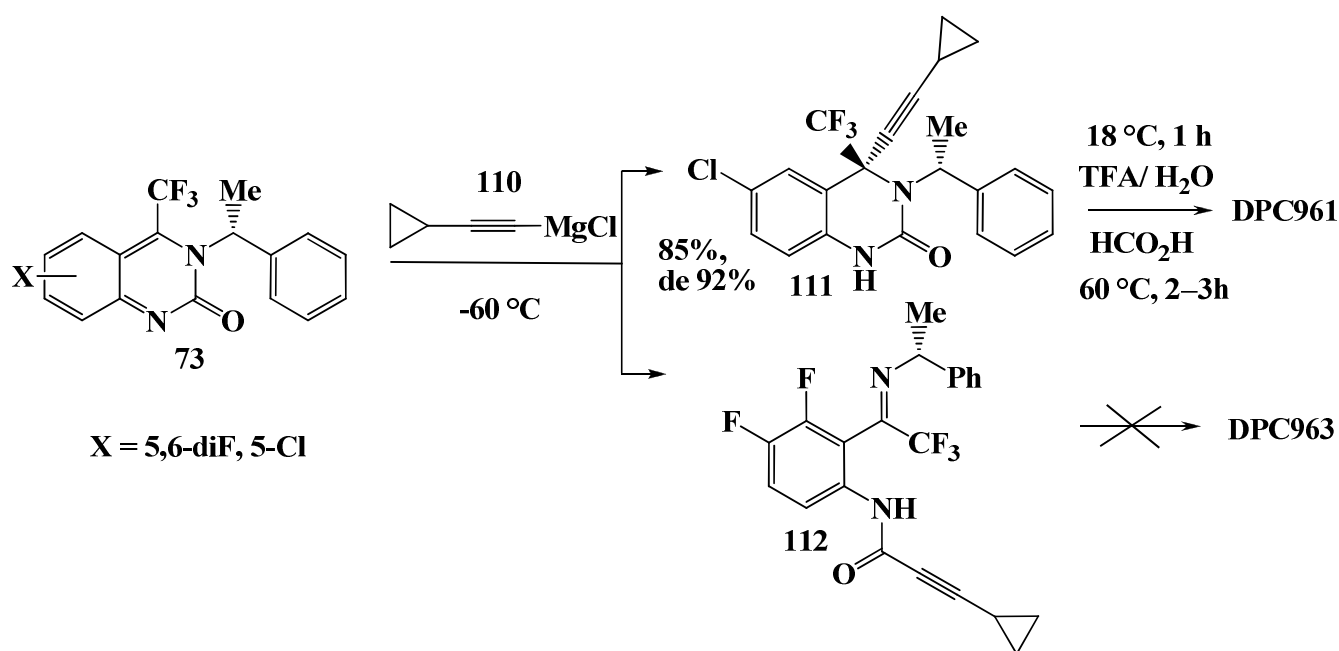


Scheme 36

In the first reported syntheses of **DPC961**, **DPC963**, **DPC082** and **DPC083**, desired quinazolones **107** were obtained as racemates by the alkylation of ketimines **69** with lithiated alkynes in THF in the presence of catalytic amounts of boron trifluoride etherate.^{13,14} In the course of these synthetic studies, an interesting cyclization was discovered to afford unique tricyclic structures **108** and **109** (Scheme 36).⁹⁶

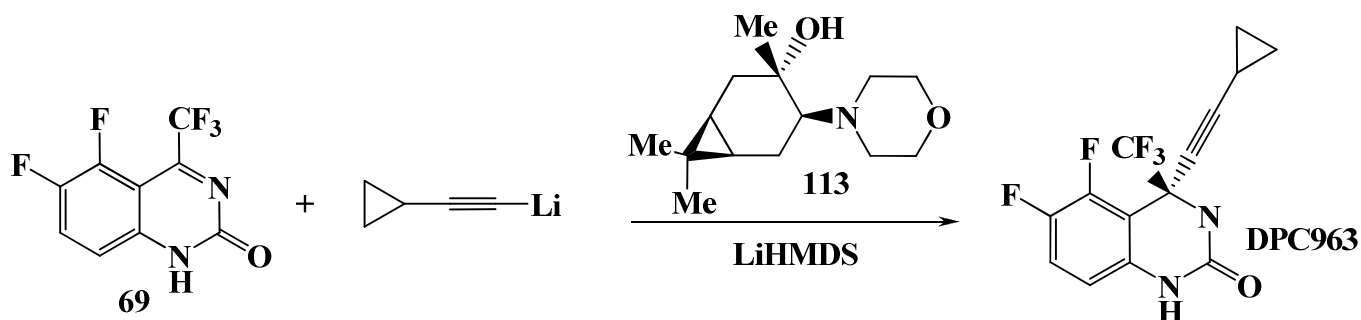
A nucleophilic addition to trifluoromethyl pyrimidin-2-ones gives rise to a new asymmetric centre and it is a challenging task for synthetic chemists to prepare enantiomerically pure compounds. Though vast majority of optical resolutions is done by fractional crystallization of diastereomers (obtained, *e.g.*, with camphoryl chloride)⁷⁸ and also by chiral chromatography.^{13,14} It is much more elegant and convenient to take advantage of direct asymmetric synthesis. Enantioselective nucleophilic addition can be carried out in several alternative ways, all involving a chiral factor (substrate, reagent, catalyst, ligand, etc.)

Obtained *in situ* enantiopure quinazolones **73** (for the synthesis, see Scheme 22) were treated with magnesium bromide cyclopropylacetylide **110** to afford the desired dihydroquinazolone **111** in high yield (85%) and diastereoselectivity (*de*=92%). Recrystallization from methanol gave pure diastereomer **111** which was converted to target **DPC961** by the action of trifluoroacetic or formic acid.^{77,78} Unfortunately, this chiral substrate-based approach failed to produce **DPC963**, since corresponding difluoro-substituted azatetraene **73**, when likewise reacted, underwent pyrimidine ring opening and the 1,2-addition of organometallic reagent **110** to give **112** as the only product (Scheme 37).⁷⁹



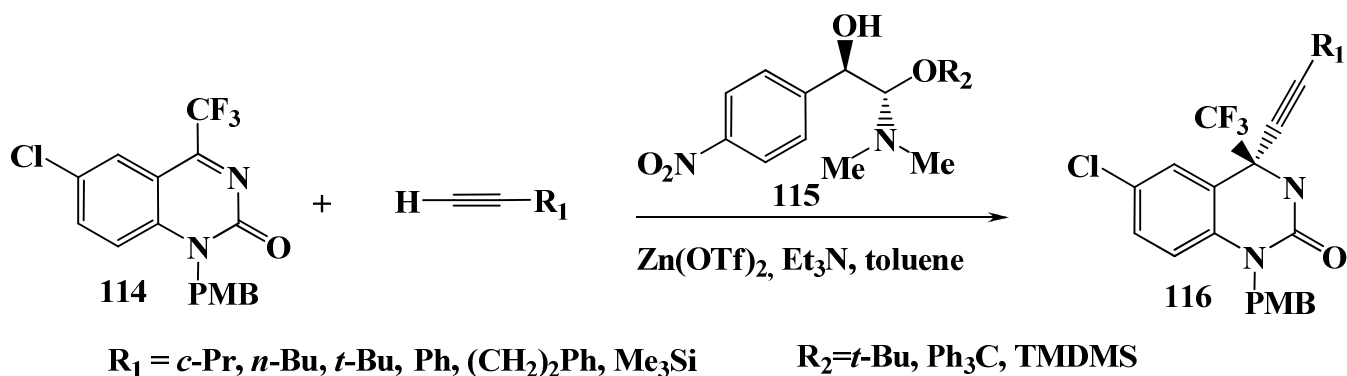
Chemists of DuPont Pharmaceuticals Company found an alternative chiral catalyst-based strategy to optically pure **DPC963** which involved the enantioselective addition of lithium cyclopropylacetylide to ketimine **69** (X=5,6-diF) in the presence of chiral amino alcohol **113**.⁷¹ Among forty chiral compounds screened, 4- β -morpholinocaran-3-ol **113** showed the best results in terms of asymmetric induction (*ee*=80%) (Scheme 38). Further optimization of the reaction conditions, namely the use of lithium bis(trimethylsilyl)amide LiHMDS as a strong base instead of butyl lithium,^{13,14} resulted in improved enantioselectivity, so that nucleophilic adduct **107** (X=5,6-diF) was isolated in 94% *ee*. Recrystallization from heptane afforded **DPC963** in 85% yield and 99.6% *ee*. One of the strengths of the method is that amino alcohol **113** can be

recovered in 92% yield by extraction with citric acid and the following extract basification.⁷⁹ To gain an insight into the mechanism of the asymmetric catalysis by the amino alcohol and LiHMDS, detailed structural and kinetic studies were conducted.^{97,98}



Scheme 38

Ephedrine derivatives **115** were also used as asymmetric catalysts of nucleophilic addition reactions. The PMB-protected trifluoromethylated cyclic *N*-acyl ketimine **114** was alkynylated with cyclopropylacetylene in toluene at room temperature in the presence of zinc triflate, amino alcohol **115** and triethylamine to provide adducts **116** in 98 to 99.5% ee (Scheme 39). Among the advantages of this approach are high enantioselectivity, the use of relatively small amounts of acetylene and standard reaction conditions as well as catalyst availability and recyclability.⁹⁹

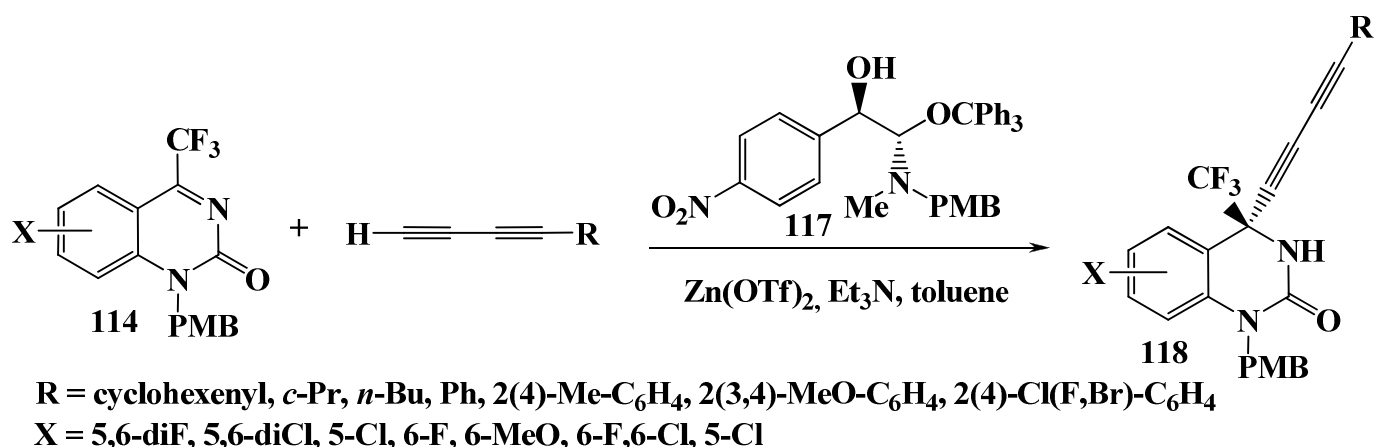


Scheme 39

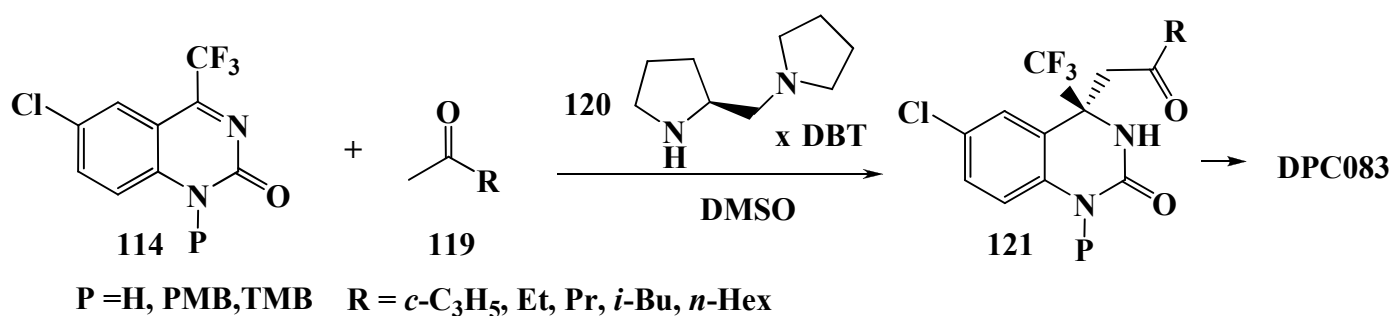
The principles of asymmetric synthesis developed for the nucleophilic additions of acetylenes were successfully extended to diynylation reactions. The same trifluoromethylated quinazolones **114** were reacted with diacetylenes in the presence of chiral additive **117** to furnish diynylated tertiary trifluoromethylcarbinamines **118** in high yields and ee of 70 to 90% (Scheme 40). Product enantiopurity can be improved up to 99% ee by recrystallization from a $\text{CH}_2\text{Cl}_2/\text{C}_6\text{H}_{12}$ mixture.¹⁰⁰

In the recent years, much chemical attention has been focused on organocatalytic methods of asymmetric synthesis. For instance, ketimine **114** ($\text{X}=\text{5-Cl}$) was reacted with ketone **119** ($\text{R}=c\text{-C}_3\text{H}_5$) in DMSO at room temperature in the presence of *L*-proline derived organocatalyst **120** and 0.5 equivalents of dibenzoyl *D*-tartaric acid (*D*-DBT) to form adduct **121** (ee=60–80%) which has recently been used as a key compound in the synthesis of the HIV reverse transcriptase inhibitor **DPC083**. Recrystallization of compounds **121** is remarkable for enantiomeric self-discrimination. This effect is due to the predominant formation of more stable heterochiral H-bonded dimers in the solid state. As a result, recrystallization leads

to an almost racemic crystal precipitate consisting of *R-S* dimers and a mother liquor enriched in the major enantiomer of **121** (Scheme 41).¹⁰¹



Scheme 40

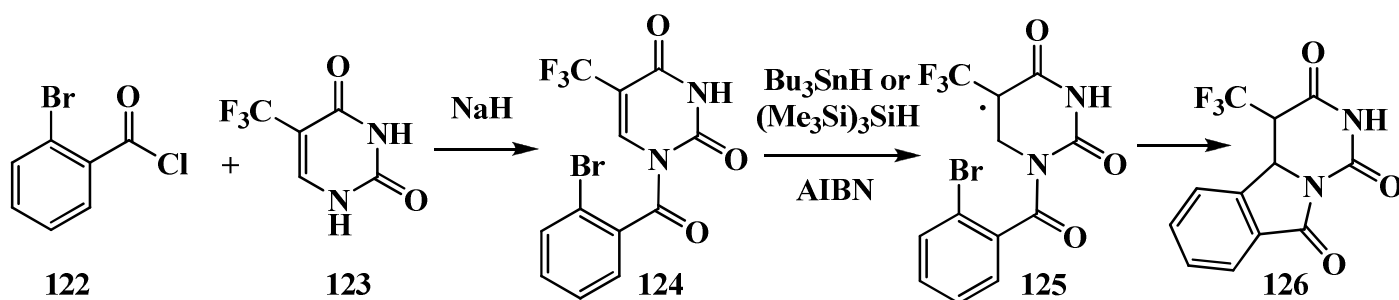


Scheme 41

Due to the high reactivity of the endocyclic ketimine moiety, substrates **114** were further exploited in the asymmetric nitro-Mannich,¹⁰² decarboxylative Mannich¹⁰³ and Strecker¹⁰⁴ reactions catalyzed by chiral functionalized thioureas and offering a variety of synthetic routes to the anti-HIV drug candidate **DPC083**.

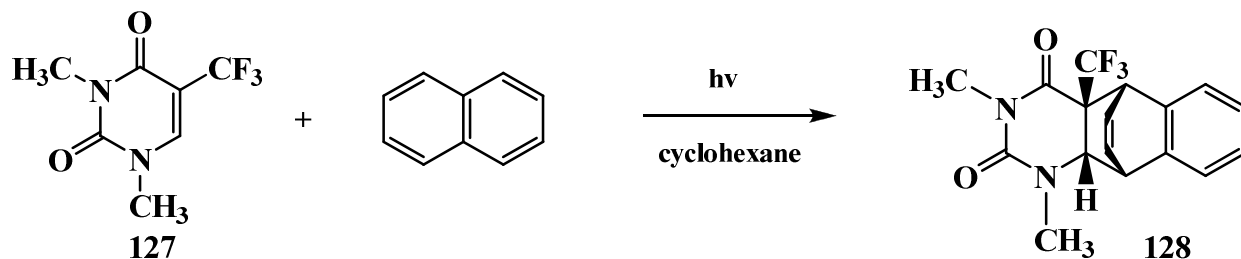
3.2. Photochemical reactions and processes involving free radicals

Photochemical reactions and processes involving free radicals allow for flexible structural modifications of trifluoromethylated pyrimidin-2-ones(thiones), *e.g.*, for the formation of their fused analogues. *N*-Acylation of pyrimidone **123** with 2-bromobenzoyl chloride **122** in the presence of NaH readily furnished free-radical precursor **124** which was treated with Bu₃SnH or (CH₃Si)₃SiH using catalytic amounts of the initiator AIBN to produce radical **125** and finally cyclization product **126** (Scheme 42).^{105,106}



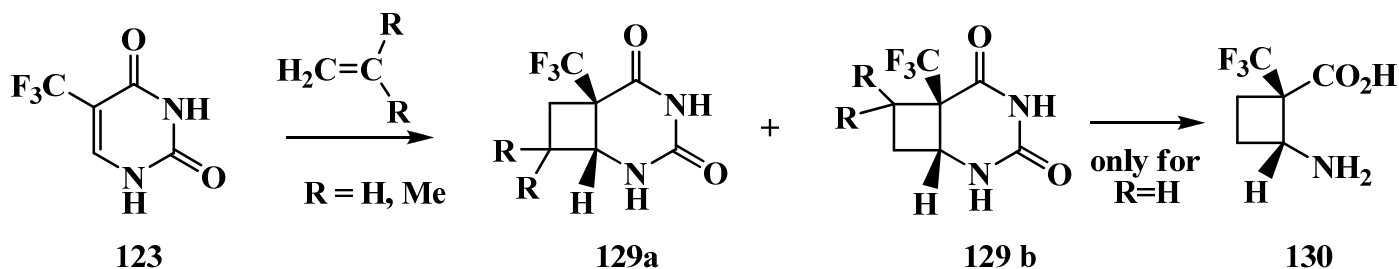
Scheme 42

UV-irradiation of an equivalent molar solution of 1,3-dimethyl-5-(trifluoromethyl)uracil **127** and naphthalene in cyclohexane for 15 hours at room temperature induced a [4+2] cycloaddition to give 4a-(trifluoromethyl)-5,10-ethenobenzo[*f*]-quinazolones **128** (Scheme 43).¹⁰⁷



Scheme 43

[2+2] Photochemical reactions of 5-trifluoromethyluracil **123** with ethylene¹⁰⁸ and isobutylene¹⁰⁹ were carried out. Resulting heterocycle **129** (R=H) underwent a two-step controlled degradation leading in high yields to trifluoromethyl-substituted *cis*-cyclobutane β -amino acid **130**.¹⁰⁸ With isobutylene, the [2+2] cyclocondensation provided regioisomer **129a** and a trace amount (3%) of **129b** (Scheme 44).¹⁰⁹



Scheme 44

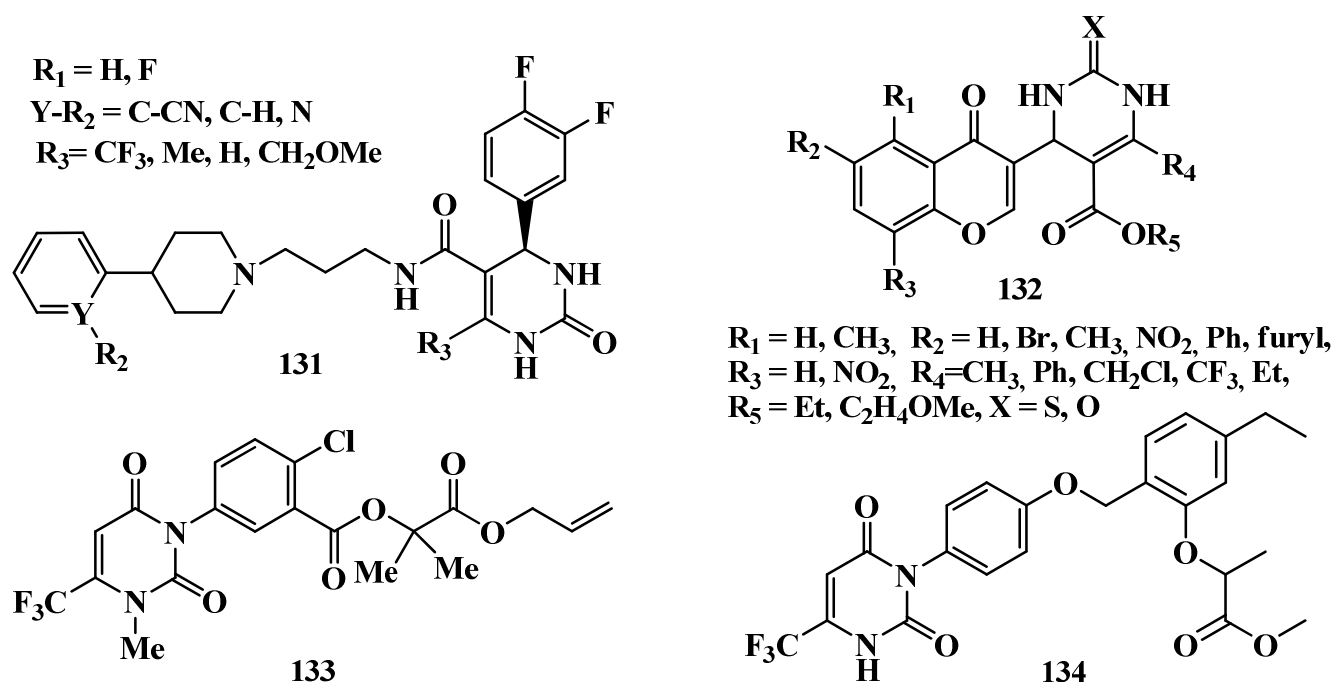
4. Biological properties of trifluoromethylated pyrimidin-2-ones(thiones)

Though trifluoromethyl-substituted pyrimidones and their analogues have been extensively utilized in pharmacology and agriculture for a long time, their biological activity is still far from being completely revealed and understood. The antiviral and cytotoxic properties of 5-trifluoromethyl-2'-deoxyuridine (trifluridine) prepared by Heidelberger⁶⁸ have been known as early as 1962. However, it was not until recently that trifluridine combined with the thymidine phosphorylase inhibitor tipiracil was reported to demonstrate profound anticancer activity.¹¹⁰ The corresponding drug TAS-102 manufactured by Taiho Pharmaceutical Co., Ltd. is currently in phase III clinical trials for the treatment of colorectal cancer.

Recently, it has been shown that 4-aryl-2-oxo-3,4-dihydropyrimidine-5-carboxamides **131** bearing the 3-(4-(het)arylpiperidyl-1)propyl substituents at the exocyclic amido group are excellent α_{1A} adrenoreceptor antagonists, which makes them a promising drug candidates for the treatment of benign prostatic hyperplasia.²⁸ 6-(4*H*-Chromenyl-3)-2-(thio)(oxo)-1,2,3,4-tetrahydropyrimidine-5-carboxylates **132** synthesized by the Biginelli reaction in 2011 proved to be potent antimycobacterial and anticancer agents.¹² A series of novel 3-aryltriazolones has been positively tested for herbicidal and insecticidal/acaricidal activity;^{9,10} in particular, butafenacil **133**⁷ and benzfendione **134**⁸ have been developed as commercial herbicides (Scheme 45).

However, the most recognized biological effect of trifluoromethylated pyrimidin-2-ones is probably related to their broad anti-HIV activity.^{13,14} In recent decades, due to the spread of HIV infection and the

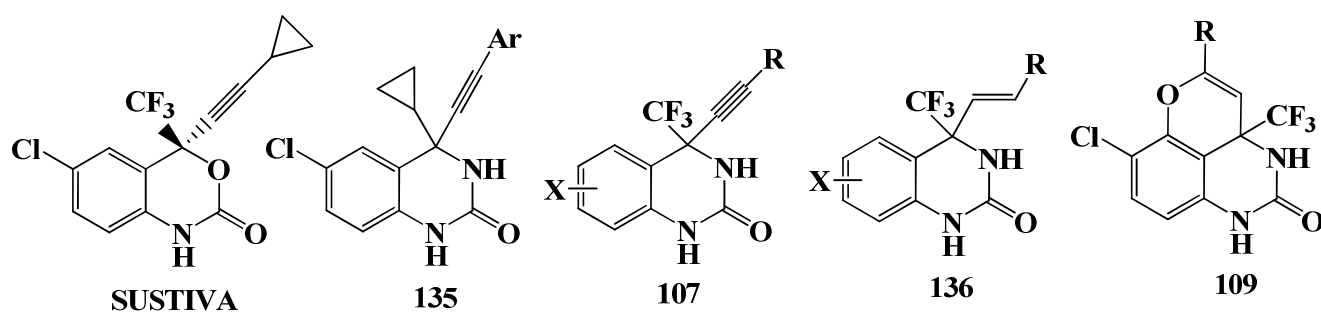
emergence of new mutant virus strains resistant to known drugs, it is of paramount importance to develop new wide-range agents with a long-term curative effect and high *in vivo* stability.



Scheme 45

Taking into consideration the therapeutic target, anti-HIV drugs are divided into three classes including HIV protease inhibitors, HIV integrase inhibitors and HIV reverse transcriptase inhibitors. The latter type drugs acting on the reverse transcriptase (RT), the enzyme responsible for the formation of proviral DNA from viral RNA, are classified into the nucleoside reverse transcriptase inhibitors (NRTIs) which bind to the ATP binding pocket and act as substrate decoys and chain terminators and the non-nucleoside reverse transcriptase inhibitors (NNRTIs) which bind to an allosteric site in the HIV-1 RT enzyme. Second-generation NNRTIs such as nevirapine, delavirdine and efavirenz (SustivaTM) are most frequently used to date.

In 1994, chemists of Merck Research Laboratories synthesized a range of NNRTIs of general structure **135**.¹¹ A comparison of structure-activity relationships between compounds **135** and efavirenz enabled synthetic scientists of DuPont Pharmaceuticals Company to develop a number of new NNRTIs on the basis of 4-alkenyl(alkynyl)-4-trifluoromethyl-3,4-dihydroquinazolin-2-ones **107** and **136** (Scheme 46).^{13,14}



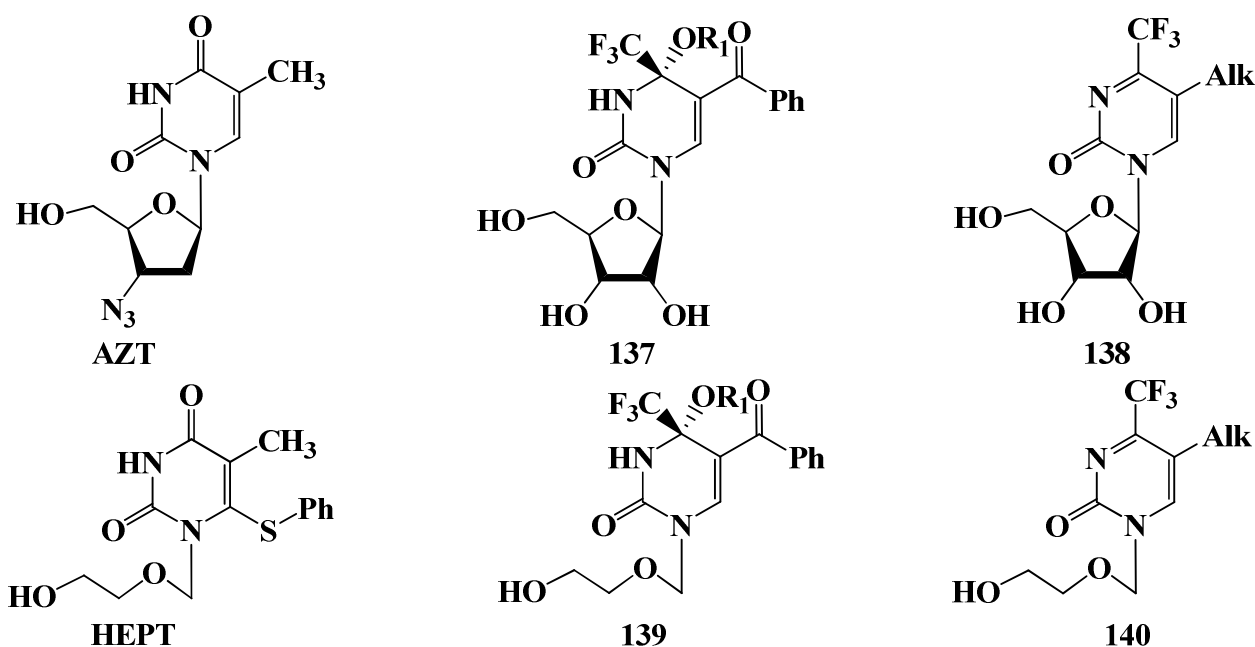
$X = 5\text{-F; 5-Cl; 5,6-diF; 6-Cl; 5-Cl, 6-F; 6-F; 6-MeO; 5-F, 6-Cl; 5,6-diCl}$

$R = \text{Et, } c\text{-Pr, } i\text{-Pr, Ph, 2-Pyridyl; Ar = 2-pyridyl, 3-pyridyl, 4-pyridyl, 2-pyrazinyl, 5-pyrimidinyl}$

Scheme 46

It is known that the main factor dictating the effective concentration of drugs in the body is their binding to plasma proteins. All quinazolones **107** and **136** tested by DuPont Pharmaceuticals Company showed 3–14 times less protein binding and a higher inhibitory potency against the wild-type HIV strains compared to nevirapine and efavirenz. It was also found that halogenation of the quinazolone nucleus at positions 5 and 6 resulted in enhanced inhibitory activity. As another feature, small alkyl substituents on the alkynyl moiety of quinazolone **107** (R=Et or *c*-Pr) caused greater activity than bulky groups. A series of biological studies on the inhibition of wild-type forms (K103N, V1081, P225H and L103N), protein binding degree and pharmacokinetic properties revealed four most promising drug candidates, **DPC961** and **DPC963** as well as their partially hydrogenated derivatives **DPC082** and **DPC083** (Scheme 36). The properties of alkynyl (**DPC961** and **DPC963**) and alkenyl (**DPC082** and **DPC083**) derivatives differ notably: alkynes are stronger inhibitors, whereas alkenes showed a lower degree of plasma protein binding. In general, new drugs exhibited better inhibition activity than efavirenz, nevirapine and delavirdine, especially toward viral strains with the single mutation K103N (most frequently occurring in AIDS treatment with efavirenz).^{13,14}

In the preparation of quinazolones **107** (Scheme 36), unexpected tricyclic systems **109** were obtained, with their activity against the K103N mutation higher than that of efavirenz but lower than those of **DPC083** and **DPC961**. As an example, $IC_{50}=46$ nM was found for **109** (R=Ph), whereas **DPC083**, **DPC961** and efavirenz demonstrated the respective IC_{50} values of 27, 10 and 64 nM. Interestingly, bulky substituents R deteriorated pharmacokinetics and inhibitory properties of compounds **107** and **136** but, *viceversa*, reduced the IC_{50} value of tricyclic derivatives **109**, especially against viruses carrying the double mutation K103N/L100I.



Scientists of DuPont Pharmaceuticals Company detected a difference in the metabolic mechanism between efavirenz and **DPC961**. The metabolism of the latter starts with the hydroxylation of the tertiary carbon atom in the cyclopropyl ring and, only after this event, glutathione adds to the triple bond. In contrast, the initial step of the **DPC961** metabolic pathway involves the direct oxidation of the triple bond to form the oxirene intermediate.¹¹²

4-Trifluoromethyl-2-pyrimidone moiety was also applied in the development of new NRTIs, AZT and HEPT analogues. Cyclic and acyclic nucleosides **137–140** proved, however, to be inactive against HIV-1 (Scheme 47).⁶²

Though **DPC** agents showed a number of positive results in biological tests, in 2003 the investigation of **DPC083** was halted because of unfavourable pharmacokinetic and safety profiles. Later it was found that **DPC961** provoked the development of suicidal thoughts in healthy volunteers. Since **DPC963** has a similar structure to **DPC961**, its safety is also questionable. As a result, compounds **DPC961**, **DPC963**, **DPC083** and **DPC082** are no longer being pharmacologically studied and developed.¹¹³

5. Conclusions

A versatile approach to the construction of 4(5,6)-trifluoromethylpyrimidin-2-ones(thiones) not only allows a wide variety of functional groups to be introduced in the pyrimidine system but also provides a way to modify the heterocyclic core. To exemplify, the Biginelli reaction is a classical method to obtain hydrogenated pyrimidin-2-ones bearing aromatic substituents at positions 4 and 6, while the [CNC]+[NCC] cyclization is the most convenient strategy for the synthetic excess to 5-functionalized analogues. If the goal is to obtain core-modified, *e.g.*, fused pyrimidine-2-ones(thiones), then, depending on whether a saturated cycle, a benzene ring or a heterocycle should be annelated to the pyrimidine moiety, the most suitable synthetic routes are represented by the following respective schemes: [NCN]+[CCC], [CCCN]+[CN] and [CNC]+[NCC]. Cyclization [CNC]+[NCC] is a novel method that provides an access to a number of hitherto unknown or difficult-to-obtain 4-trifluoromethylpyrimidin-2-one derivatives. Modifications of the trifluoromethylpyrimidin-2-one nucleus can also result from nucleophilic additions or photochemical and free-radical reactions. Nucleophilic additions performed with the use of a chiral factor (substrate, reagent, catalyst, ligand, etc.) afford optically active products which are of special relevance to biological and pharmacological applications. Finally, the development of new synthetic routes to trifluoromethylpyrimidin-2-ones(thiones) and their fused analogues remains a challenging and rewarding line of research both in terms of synthetic methodology development and from the pharmacological point of view, due to a broad manifold of outstanding biological activities of pyrimidines.

References

1. Lagoja, I. M. *Chem. Biodiversity* **2005**, *2*, 1.
2. Lednicer, D. *The Organic Chemistry of Drug Synthesis*; John Wiley & Sons, Inc.: Hoboken, New Jersey, 2008; Vol. 7, p. 121.
3. Galmarini, C. M.; Jordheim, L.; Dumontet, C. *Expert Rev. Anticancer Ther.* **2003**, *3*, 717.
4. Petrov, V. A. *Fluorinated Heterocyclic Compounds: Synthesis, Chemistry, and Applications*; John Wiley & Sons, Inc.: Hoboken, New Jersey, 2009.
5. Kirk, K. L. *J. Fluor. Chem.* **2006**, *127*, 1013.
6. Filler, R.; Saha, R. *Future Med. Chem.* **2009**, *1*, 777.
7. Sting, A. R.; Siegrist, U. E.; Baumeister, P. F. *Chem. Abstr.* **1998**, *128*, 243878.
8. Sehgel, S.; Theodoridis, G. In *Trip Report: The 30th Northeast Regional Meeting of the American Chemical Society*; Durham: New Hampshire, June 24–27, 2001.
9. Daoxin, W.; Jiong, S.; Dulin, Y.; Mingzhi, H.; Xiaoguang, W.; Yeguo, R.; Zhibing, H.; Lian, H.; Hongbon, M.; Hongwei, L. *Chinese J. Chem.* **2011**, *29*, 2401.
10. Yagi, K.; Akimoto, K.; Mimori, N.; Miyake, T.; Kudo, M.; Arai, K.; Ishii, S. *Pest Management Science* **2000**, *56*, 65.

11. Agbaje, O. C.; Fadeyi, O. O.; Fadeyi, S. A.; Myles, L. E.; Okoro, C. O. *Bioorg. Med. Chem. Lett.* **2011**, *21*, 989.
12. China, R. B.; Nageswara, R. R.; Suman, P.; Yogeewari, P.; Sriram, D.; Shaik, T. B.; Kalivendi, S. V. *Bioorg. Med. Chem. Lett.* **2011**, *21*, 2855.
13. Corbett, J. W. *Antimicrob. Agents Chemother.* **1999**, *43*, 2893.
14. Corbett, J. W. *J. Med. Chem.* **2000**, *43*, 2019.
15. McArthur, S. G.; Goetschi, E.; Wichmann, J.; Woltering, T. J. *US2007/2325832007 (A1)*, **2007**.
16. Abbott GmbH & Co. KG. *WO2004/80981 (A1)*, **2004**.
17. Neurocrine Biosciences, Inc. *WO2008/124610 (A1)*, **2008**.
18. Beaulieu, P.; Bonneau, P.; Coulombe, R.; Forgione, P.; Gillard, J.; Jakalia, A.; Rancourt, J.; Boehringer Ingelheim International GmbH, *WO2010/37210 (A1)*, **2010**.
19. Kobayashi, Y.; Yamamoto K.; Asai, T.; Nakano, M.; Kumadaki, I. *J. Chem. Soc., Perkin Trans. 1* **1980**, 2755.
20. Masakazu, N.; Shozo, F.; Hiroshi, K.; Yoshio, H.; Hideo, S.; Louis, A. C. *J. Fluor. Chem.* **1993**, *63*, 43.
21. Ji, Y.; Brueckl, T.; Baxter, D. R.; Fujiwara, Y.; Seiple, I. B.; Su, S.; Blackmond, D. G.; Baran, P. S. *Proc. Natl. Acad. Sci. USA* **2011**, *108*, 14411.
22. Montesarchio, D.; Musumeci, D.; Irace, C.; Santamaria, R. *Med. Chem. Commun.* **2013**, *4*, 1405.
23. Biginelli, P. G. *Chem. Ital.* **1893**, *23*, 360.
24. Rutter, H. A.; Gustafson, L. O. *Chem. Abstr.* **1955**, *49*, 14769i.
25. Kappe, C. O. *J. Org. Chem.* **1997**, *62*, 7201.
26. Sweet, F.; Fissekis, J. D. *J. Am. Chem. Soc.* **1973**, *95*, 7841.
27. Kappe, C. O.; Falsone, S. F.; Fabian, W. M. F. *Heterocycles* **1999**, *51*, 77.
28. Barrow, J. C.; Nantermet, P. G.; Selnick, H. G.; Glass, K. L.; Rittle, K. E.; Gilbert, K. F.; Steele, T. G.; Homnick, C. F.; Freidinger, R. M.; Ransom, R. W.; Kling, P. *et al. J. Med. Chem.* **2000**, *43*, 2703.
29. Bigdeli, M. A.; Gholami, G.; Sheikhhosseini, E. *Chinese Chem. Lett.* **2011**, *22*, 903.
30. Saloutin, V. I.; Burgart, Ya. V.; Kuzueva, O. G.; Kappe, C. O.; Chupakhin, O. N. *J. Fluor. Chem.* **2000**, *103*, 17.
31. Burgart, Ya. V.; Kuzueva, O. G.; Pryadeina, M. V.; Kappe, C. O.; Saloutin, V. I. *Russ. J. Org. Chem.* **2001**, *37*, 869.
32. Azizian, J. B.; Mirza, M. M.; Mojtahedi, M. S. A.; Sargordan M. *J. Fluor. Chem.* **2008**, *129*, 1083.
33. Lannou, M. I.; Helion, F.; Nami, J. L. *Synlett* **2008**, 105.
34. Reddy C. V.; Mahesh, M.; Raju, P. V. K.; Babu, T. R.; Reddy, V. V. N. *Tetrahedron Lett.* **2002**, *43*, 2657.
35. Suman, L. J.; Prasad, V. V. D. N.; Sain, B. *Catal. Commun.* **2008**, *9*, 499.
36. Ravi, V.; Mujahid, A. M.; Srinivas, R. A. *Synlett* **2003**, 67.
37. Shailaja, M.; Manjula, A.; Rao, B. V.; Parvathi, N. *Synth. Commun.* **2004**, *34*, 1559.
38. Kappe, C. O.; Falsone, S. F. *Synlett* **1998**, 718.
39. Yadav, J. S.; Reddy, B. V. S.; Reddy, K. B.; Raj, K. S.; Prasad, A. R. *J. Chem. Soc., Perkin Trans. 1* **2001**, 1939.
40. Timoshenko, V. M.; Markitanov, Yu. N.; Shermolovich, Yu. G. *Chem. Heterocycl. Compd.* **2011**, *47*, 977.
41. Konkala, K.; Sabbavarapu, N. M.; Katla, R.; Durga, N. Y. V.; Kumar, R. T. V.; Bethala, L. A.; Prabhavathi, D.; Rachapudi, B. N. P. *Tetrahedron Lett.* **2012**, *53*, 1968.
42. Ma, Y.; Qian, C.; Wang, L.; Yang, M. *J. Org. Chem.* **2000**, *65*, 3864.
43. Putilova, E. S.; Troitskii, N. A.; Zlotin, S. G.; Khudina, O. G.; Burgart, Ya. V.; Saloutin, V. I.; Chupakhin, O. N. *Russ. J. Org. Chem.* **2006**, *42*, 1392.
44. Ahmed, N.; van Lier, J. E. *Tetrahedron Lett.* **2007**, *48*, 5407.
45. Azizian, J.; Mohammadi, M. K.; Mirza, B.; Firuzi, O.; Miri, R. *Chem. Biol. Drug Des.* **2010**, *75*, 375.
46. Mirza, B.; Sargordan, M.; Fazaeli, R. *Asian J. Chem.* **2012**, *24*, 1421.
47. Roblin, R. O.; Lampen, J. O.; English, J. P.; Cole, Q. P.; Vaughan, J. R. *J. Am. Chem. Soc.* **1945**, *67*, 290.
48. Kaiser, C.; Burger, A. *J. Org. Chem.* **1959**, *24*, 113.

49. Miller, W. H.; Dessert, A. M.; Anderson, G. W. *J. Am. Chem. Soc.* **1948**, *70*, 500.
50. Giner-Sorolla, A.; Bendich, A. *J. Am. Chem. Soc.* **1958**, *80*, 5744.
51. Dilli, S.; Robards, K. *Aust. J. Chem.* **1978**, *31*, 1833.
52. Zanatta, N.; Pachoski, I. L.; Martins, M. A. P.; Blanco, I. *J. Braz. Chem. Soc.* **1991**, *2*, 118.
53. Bonacorso, H. G.; Lopes, I. S.; Wastowski, A. D.; Zanatta, N.; Martins, M. A. P. *J. Fluor. Chem.* **2003**, *120*, 29.
54. Bonacorso, H. G.; Martins, M. A. P.; Bittencourt, S. R. T.; Lourega, R. V.; Zanatta, N.; Flores, A. F. *C. J. Fluor. Chem.* **1999**, *99*, 177.
55. Sevenard, D. V.; Khomutov, O. G.; Koryakova, O. V.; Sattarova, V. V.; Kodess, M. I.; Stelten, J.; Loop, I.; Lork, E.; Pashkevich, K. I.; Roschenthaler, G.-V. *Synthesis* **2000**, 1738.
56. Bonacorso, H. G.; Costa, M. B.; Lopes, I. S.; Oliveira, M. R.; Drekenner, R. L.; Martins, M. A. P.; Zanatta, N.; Flores, A. F. *Synth. Commun.* **2005**, *35*, 3055.
57. Bonacorso, H. G.; Costa, M. B.; Cechinel, C. A.; Sehnem, R. C.; Martins, M. A. P.; Zanatta, N. *J. Heterocycl. Chem.* **2009**, *46*, 158.
58. Zanatta, N.; Faoro, D.; Fernandes, L. D. S.; Brondani, P. B.; Flores, D. C.; Flores, A. F. C.; Bonacorso, H. G.; Martins, M. A. P. *Eur. J. Org. Chem.* **2008**, 5832.
59. Zanatta, N.; Madruga, C. C.; Marisco, P. C.; Flores, D. C.; Bonacorso, H. G.; Martins, M. A. P. *J. Heterocycl. Chem.* **2000**, *37*, 1213.
60. Zanatta, N.; Madruga, C. C.; Clerici, E.; Martins, M. A. P. *J. Heterocycl. Chem.* **1995**, *32*, 735.
61. Felczak, K.; Drabikowska, A. K.; Vilpo, J. A.; Kulikowski, T.; Shugar, D. *J. Med. Chem.* **1996**, *39*, 1720.
62. Berber, H.; Soufyane, M.; Mirand, C.; Schmidt, S.; Aubertin, A. *Tetrahedron* **2001**, *57*, 7369.
63. Soufyane, M.; Broek, S. V. D.; Khamliche, L.; Mirand, C. *Heterocycles* **1999**, *51*, 2445.
64. Soufyane, M.; Mirand, C.; Levy, J. *Tetrahedron Lett.* **1993**, *34*, 7737.
65. Morita, Y.; Kamakura, R.; Takeda, M.; Yamamoto, Y. *Chem. Commun.* **1997**, 359.
66. Goryaeva, M. V.; Burgart, Ya. V.; Saloutin, V. I. *Russian Chem. Bull.* **2009**, *58*, 1259.
67. Palanki, M. S. S.; Erdman, P. E.; Gayo Fung, L. M.; Shevlin, G. I.; Sullivan, R. W.; Goldman, M. E.; Ransone, L. J.; Bennet, B. L.; Manning, A. M.; Suto, M. J. *J. Med. Chem.* **2000**, *43*, 3995.
68. Heidelberger, C.; Parsons, D.; Remy, D. C. *J. Am. Chem. Soc.* **1962**, *84*, 3597.
69. Fuchikami, T.; Ojima, I. *Tetrahedron Lett.* **1982**, *23*, 4099.
70. Chi, K.-W.; Furin, G. G.; Gatilov, Y. V.; Bagryanskaya, I. Yu.; Zhuzhgov, E. L. *J. Fluor. Chem.* **2000**, *103*, 105.
71. Neurocrine Biosciences, Inc. *WO2008/124614 (A1)*, **2008**.
72. Nenajdenko, V. G.; Sanin, A. V.; Kuzmin, V. S.; Balenkova, E. S. *Russ. J. Org. Chem.* **1996**, *32*, 1529.
73. Fuchikami, T.; Yamanouchi, A.; Ojima, I. *Synthesis* **1984**, 766.
74. Sing, Y. L.; Lee, L. F. *J. Org. Chem.* **1985**, *50*, 4642.
75. Dorokhov, V. A.; Komkov, A. V.; Vasilev, L. S.; Azarevich, O. G.; Gordeev, M. F. *Bull. Acad. Sci. USSR, Ch. (Engl. Transl.)* **1991**, *40*, 2311.
76. Sidduri, A.; Tilley, J. W.; Lou, J.; Tare, N.; Cavallo, G.; Frank, K.; Pamidimukkala, A.; Choi, D. S.; Gerber, L.; Railkar, A.; Renzetti, L. *Bioorg. Med. Chem. Lett.* **2013**, *23*, 1026.
77. Magnus, N. A.; Confalone, P. N.; Storace, L. *Tetrahedron Lett.* **2000**, *41*, 3015.
78. Magnus, N. A.; Confalone, P. N.; Storace, L.; Patel, M.; Wood, Ch. C.; Davis, W. P.; Parsons, R. L. *J. Org. Chem.* **2003**, *68*, 754.
79. Kauffman, G. S.; Harris, G. D.; Dorow, R.; Stone, B. R. P.; Parsons, R. L.; Pesti, J. A., Jr.; Magnus, N. A.; Fortunak, J. M.; Confalone, P. N.; Nugent, W. A. *Org. Lett.* **2000**, *2*, 3119.
80. Sukach, V. A.; Golovach, N. M.; Pirozhenko, V. V.; Rusanov, E. B.; Vovk, M. V. *Tetrahedron: Asymmetry* **2008**, *19*, 761.
81. Sukach, V. A.; Golovach, N. M.; Melnichenko, N. V.; Tsymbal, I. F.; Vovk, M. V. *J. Fluor. Chem.* **2008**, *129*, 1180.
82. Golovach, N. M.; Sukach, V. A.; Vovk, M. V. *Russ. J. Org. Chem.* **2012**, *48*, 430.
83. Golovach, N. M.; Sukach, V. A.; Vovk, M. V. *Russ. J. Org. Chem.* **2010**, *46*, 1571.
84. Ishihara, T.; Yamasaki, Y.; Ando, T. *Tetrahedron Lett.* **1986**, *27*, 2879.
85. Lutz, A. W.; Trotto, S. H. *J. Heterocycl. Chem.* **1972**, *9*, 513.

86. Dorokhov, V. I. *Russ. J. Org. Chem.* **1997**, *33*, 1666.
87. Vovk, M. V.; Bol'but, A. V. *Ukrainian Chem. J.* **1998**, *64*, 46.
88. Vovk, M. V.; Lebed', P. S.; Chernega, A. N.; Pirozhenko, V. V.; Boiko, V. I.; Tsymbal, I. F. *Chem. Heterocycl. Compd.* **2004**, *40*, 47.
89. Vovk, M. V.; Lebed', P. S.; Sukach, V. A.; Kornilov, M. Yu. *Russ. J. Org. Chem.* **2003**, *39*, 1781.
90. Vovk, M. V.; Lebed', P. S.; Pirozhenko, V. V.; Tsymbal, I. F. *Russ. J. Org. Chem.* **2004**, *40*, 1669.
91. Vovk, M. V.; Lebed, P. S.; Yepishev, V. I.; Pirozhenko, V. V. *Zh. Org. Pharm. Chem. (Ukraine)* **2004**, *2*, 20.
92. Iaroshenko, V. O.; Volochnyuk, D. M.; Yan, W.; Vovk, M. V.; Boiko, V. J.; Rusanov, E. B.; Groth, U. M.; Tolmachev, A. A. *Synthesis* **2007**, 3309.
93. Vovk, M. V.; Kushnir, O. V.; Melnichenko, N. V. *Chem. Heterocycl. Compd.* **2011**, 1205.
94. Kushnir, O. V.; Dorokhov, O. V.; Melnichenko, N. V.; Vovk, M. V. *Ukrainian Chem. J.* **2011**, *77*, 68.
95. Sukach, V. A.; Tkachuk, V. M.; Rusanov, E. B.; Roeschenthaler, G. V.; Vovk, M. V. *Tetrahedron* **2012**, *68*, 8408.
96. Corbett, J. W.; Pan, S.; Markwalder, J. A.; Cordova, B. C.; Klabe, R. M.; Garber, S.; Rodgers, J. D.; Erickson-Viitanen, S. K. *Bioorg. Med. Chem. Lett.* **2001**, *11*, 211.
97. Briggs, T. F.; Winemiller, M. D.; Collum, D. B.; Parsons, R. L.; Davulcu, A. H.; Harris, G. D.; Fortunak, J. M.; Confalone, P. N. *J. Am. Chem. Soc.* **2004**, *126*, 5427.
98. Parsons, R. L.; Fortunak, J. M.; Dorow, R. L.; Harris, G. D.; Kauffman, G. S.; Nugent, W. A.; Winemiller, M. D.; Briggs, T. F.; Xiang, B.; Collum, D. B. *J. Am. Chem. Soc.* **2001**, *123*, 9135.
99. Jiang, B.; Si, Y. G. *Angew. Chem. Int. Ed.* **2004**, *43*, 216.
100. Fa-Guang, Z.; Hai, M.; Jing, N.; Yan, Z.; Qingzhi, G.; Jun-An, M. *Adv. Synth. Catal.* **2012**, *354*, 1422.
101. Jiang, B.; Dong, J. J.; Si, Y. G.; Zhao, X. L.; Huang, Z. G.; Xu, M. *Adv. Synth. Catal.* **2008**, *350*, 1360.
102. Xie, H.; Zhang, Y.; Zhang, S.; Chen, X.; Wang, W. *Angew. Chem. Int. Ed.* **2011**, *50*, 11773.
103. Yuan, H.-N.; Wang, S.; Nie, J.; Meng, W.; Yao, Q.; Ma, J.-A. *Angew. Chem. Int. Ed.* **2013**, *52*, 3869.
104. Zhang, F.-G.; Zhu, X.-Y.; Li, S.; Nie, J.; Ma, J.-A. *Chem. Commun.* **2012**, *48*, 11552.
105. Zhang, W.; Pugh, G. *Tetrahedron Lett.* **1999**, *40*, 7591.
106. Zhang, W.; Pugh, G. *Tetrahedron* **2003**, *59*, 3009.
107. Ohkura, K.; Ishihara, T.; Nakata, Y.; Seki, K. *Heterocycles* **2004**, *62*, 213.
108. Gauzy, C.; Saby, B.; Pereira, E.; Faure, S.; Aitken, D. J. *Synlett* **2006**, 1394.
109. Savino, T. G.; Chenard, L. K.; Swenton, J. S. *Tetrahedron Lett.* **1983**, *24*, 4055.
110. Peters, G. J.; Bijnisdorp, I. V. *Lancet Oncol.* **2012**, 518.
111. Thomas, J. T.; Terry, A. L.; Catherine, M. W. *J. Med. Chem.* **1994**, *37*, 2437.
112. Mutlib, A.; Chen, H. *Chem. Res. Toxicol.* **2000**, *13*, 775.
113. Hoffmann, C.; Rockstroh, J. K.; Kamps, B. S. *HIV Medicine*; Flying Publisher: Paris, Cagliari, Wuppertal, 2007; p. 134.

BIOCATALYSIS APPLIED TO THE SYNTHESIS OF VALUABLE TRIAZOLE-CONTAINING DERIVATIVES

Aníbal Cuetos,^a Fabricio R. Bisogno^b and Iván Lavandera*^a

^aDepartamento de Química Orgánica e Inorgánica, Instituto Universitario de Biotecnología de Asturias, Universidad de Oviedo, C/ Julián Clavería 8, E-33006 Oviedo, Spain (e-mail: lavanderaivan@uniovi.es)

^bINFIQC-CONICET, Departamento de Química Orgánica, Facultad de Ciencias Químicas, Universidad Nacional de Córdoba, Ciudad Universitaria, CP 5000, Córdoba, Argentina

Abstract. *The use of enzymes applied to organic synthesis is gaining more and more relevance due to the mild reaction conditions needed and high selectivities offered by these catalysts. Herein, examples related to the biocatalyzed synthesis of (chiral) 1,2,3-, 1,2,4- and benzotriazole-based compounds will be described. While in some cases the enzymatic transformation directly modified these derivatives, in other examples it transformed a suitable precursor of an interesting triazole-derived target. Finally, some examples about the rational use of one-pot tandem or cascade protocols to synthesize these heterocycles will also be underlined.*

Contents

1. Introduction
 2. Biocatalytic approaches over triazole-containing derivatives
 - 2.1. 1,2,3-Triazoles
 - 2.1.1. Using hydrolases
 - 2.1.2. Using transferases
 - 2.1.3. Cofactor mimics
 - 2.2. 1,2,4-Triazoles
 - 2.2.1. Using hydrolases: lipases and acylases
 - 2.2.2. Using hydrolases: nucleoside phosphorylases
 - 2.2.3. Using transferases
 - 2.3. Benzotriazoles
 - 2.3.1. Using hydrolases
 - 2.3.2. Using oxidoreductases
 3. Biocatalytic approaches over precursors to obtain triazole-containing derivatives
 - 3.1. Using hydrolases
 - 3.2. Using oxidoreductases
 - 3.3. Using transferases
 4. Novel approaches based on cascade or tandem protocols
 5. Summary and outlook
- Acknowledgments
- References

1. Introduction

Triazole, also known as pyrrodiazole, is one of the most typical organic heterocyclic cores containing two double-bonded five-membered ring structure composed of three nitrogen atoms and two carbon atoms at

(non)adjacent positions. It can exist as two isomeric chemical compounds: 1,2,3-triazole and 1,2,4-triazole. When these heterocycles are fused to a phenyl ring, they give access to benzotriazoles. These derivatives have attracted considerable attention for the past few decades due to their chemotherapeutical uses. Among the different activities they can display, their use as antimicrobial, antifungal, antiviral or anticancer can be mentioned.¹ Thus, compounds such as fluconazole, isavuconazole, carboxyamidotriazole, ribavirin or sitagliptin are just some examples of triazole-based biologically active derivatives which are on the market or in the last phases of clinical studies. Furthermore, these derivatives have also found applications in other fields as peptidomimetics, in conjugation and supramolecular chemistry and in polymer and material sciences.² Also, in coordination chemistry, 1,2,3-triazoles have demonstrated versatility due to chelating properties towards transition metals,³ forming catalytically active complexes.

Among the different synthetic strategies developed for 1,2,3-triazoles, probably the most common is the Huisgen azide-alkyne 1,3-dipolar cycloaddition and their variants due to the high efficiency of this technique.⁴ In fact, the copper-catalyzed reaction (CuAAC) to form 1,4-substituted triazoles is the typical example of the so-called “click” chemistry,⁵ which accounts for clean processes where the atom efficiency is optimum affording quantitatively the desired product. On the other hand, 1,2,4-triazoles can be synthesized through different ways, making use of *N*-acylamidrazone intermediates, through reaction between an amide and a hydrazide (Pellizzari reaction) or between an imide and a hydrazine (Einhorn-Brunner reaction), among others.⁶

Biocatalysis is considered the cornerstone of Industrial Biotechnology, which applies biological systems to more sustainable synthetic routes. Among the outstanding properties that can be underlined about the use of enzymes, the control of the chemo-, regio- and stereochemistry during the course of the chemical transformations under mild reaction conditions is probably the most appreciated.⁷ Hence, the knowledge accumulated so far is resulting in a truly alternative for industry to prepare chemicals, not only at laboratory scale, but also at industrial scale employing a biocatalyzed process as the key step.⁸ As a result of this increasing interest in applying biological systems at the service of more sustainable processes, it is not surprising that also for the synthesis of heterocycles biocatalytic methods are becoming more popular. Herein, we will show different methodologies where enzymes have been involved at some extent in the synthesis of (chiral) triazoles. Thus, in the first section we will focus on enzymatic reactions over 1,2,3-, 1,2,4- and benzotriazole derivatives. Next, some examples describing enzyme-catalyzed transformations over precursors of relevant triazole-based compounds will be underlined. Finally, recent applications of chemoenzymatic tandem or cascade protocols to obtain high-added value triazoles in a more rational and sustainable fashion will be outlined.

2. Biocatalytic approaches over triazole-containing derivatives

2.1. 1,2,3-Triazoles

2.1.1. Using hydrolases

Lipases are able to catalyze regio- and/or stereoselective acylation and deacylation reactions.⁹ In fact, these enzyme-catalyzed reactions represent an important class of transformations in organic chemistry due to their low cost (they do not need any cofactor), their great tolerance to organic solvents and the wide scope of substrates. Carbohydrates are probably the most complex of all polyhydroxylated compounds due to the presence of a great number of stereogenic centers.¹⁰ Several hydrolases (lipases from *Candida antarctica* B,

CAL-B; *Candida rugosa*, CRL; and from porcine pancreas, PPL) were used by Parmar and co-workers¹¹ to perform the regioselective acylation of several 1,2,3-triazole-derived sugars (**1a–3a**, Figure 1), precursors for the synthesis of triazolylacyclonucleosides. Using vinyl acetate (VinOAc) as acylating agent at 42–45 °C, it was observed that both CAL-B and PPL exclusively acetylated the primary hydroxyl group over the secondary one(s) in all these substrates, leading to the formation of monoacetylated sugars **1b–3b**.

The study revealed that the acetylation reaction mediated by CAL-B in diisopropyl ether (DIPE) was very efficient, obtaining 95–98% conversion after 2–8 hours. Moreover, the rate of the acetylation of **1a** was 1.75 and 4-times faster than the rate of the acetylation of **2a** and **3a**, respectively.

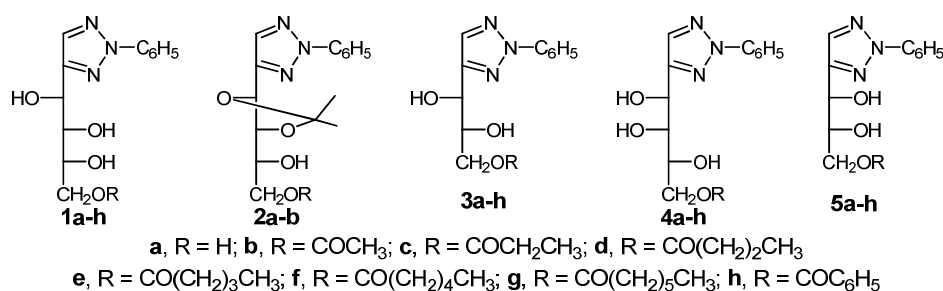


Figure 1. Triazolyl sugar-derivatives obtained by enzymatic acylation reactions.

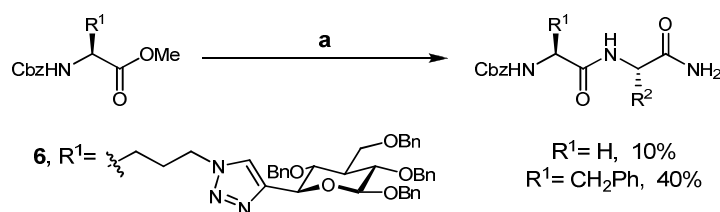
Subsequently, this study (Table 1) was extended to carry out highly selective and efficient CAL-B-catalyzed acylations of triazolyl sugars **1a**, **3a**, **4a** and **5a**, using anhydrides of acetic, propanoic, butanoic, pentanoic, hexanoic, heptanoic and benzoic acids, and 2,2,2-trifluoroethyl butyrate and vinyl acetate as acylating agents.¹² Among the different acid anhydrides accepted by CAL-B in DIPE, butanoic anhydride was found as the most efficient providing the corresponding monoesters at the primary position **1d**, **3d**, **4d** and **5d** in nearly quantitative yields and at short reaction times (1–2.5 hours). This study showed the utility of acid anhydrides as acylating agents. However, for derivatives possessing a longer alkyl chain than butanoic anhydride, the time taken for the reactions was longer, thereby indicating that the increase of the chain length may disturb the finer fitting of the acylating agent in the active site of the enzyme. The benzoic anhydride was found to be a poor acylating agent for all four triazolyl sugars (15–75%). On the other hand, vinyl acetate was a better acetylating agent compared to acetic anhydride, since the yields obtained were much higher (95–97% compared to 15–60%).

Glycopeptides play an important role in various biological processes and are therefore relevant lead molecules for the preparation of new drugs.¹³ In general, the lability of the glycosidic linkage toward acidic and basic conditions is the bottleneck for the synthesis of natural glycopeptides. Moreover, *O,O*- and *N,O*-acetal linkages are prone to enzymatic cleavage. In this sense, as a result of the development of *C*-linked isosteres, 1,2,3-triazole-linked glycopeptide mimics have shown an excellent chemical and enzymatic stability with no detrimental effect on their biological properties.¹⁴ In this sense, Rutjes and co-workers¹⁵ reported the use of a cheap and industrially available alcalase (a proteolytic enzymatic mixture produced by *Bacillus licheniformis*), as the biocatalyst for condensation of *N*-protected acetylenic and azidoamino acid methyl esters as suitable acyl donors with a proteinogenic amino acid amide.

Among the different enzymatic condensations with phenylalanine or glycine amide as nucleophiles under anhydrous conditions, glycotriazolylamino acid methyl ester **6** was attempted (Scheme 1), although the reactions proceeded extremely slow (10–40% after 8 days) and did not lead to a satisfactory yield of the desired dipeptides.

Table 1. Regioselective acylation of triazolyl sugars **1a**, **3a–5a** mediated by CAL-B in diisopropyl ether at 42–45 °C using different acylating agents.

Entry	Substrate	Acylating agent	t (h)	Product	Yield (%)
1		Propanoic anhydride	48	1d	20
2		Butanoic anhydride	2.5	1e	99
3	1a	Pentanoic anhydride	10	1f	85
4		Benzoic anhydride	48	1h	15
5		Vinyl acetate	2.5	1b	97
6		Propanoic anhydride	48	3d	70
7		Butanoic anhydride	0.75	3e	98
8	3a	Pentanoic anhydride	1	3f	97
9		Benzoic anhydride	48	3h	65
10		Vinyl acetate	4	3b	95
11		Propanoic anhydride	48	4d	20
12		Butanoic anhydride	2.5	4e	99
13	4a	Pentanoic anhydride	10	4f	85
14		Benzoic anhydride	48	4h	15
15		Vinyl acetate	3	4b	97
16		Propanoic anhydride	48	5d	40
17		Butanoic anhydride	1	5e	99
18	5a	Pentanoic anhydride	7	5f	82
19		Benzoic anhydride	48	5h	75
20		Vinyl acetate	5	5b	95



a. Alcalase, **6** (1 equiv.), Gly-NH₂ or Phe-NH₂ (1.5 equiv.), ^tBuOH/DMF (5:2 v/v), 35 °C, 8 days

Scheme 1. Alcalase-promoted synthesis of dipeptides.

These results were taken as starting point to study the influence of the carbohydrate moiety in the alcalase-promoted coupling reactions.¹⁶ Thus, the bulky hydrophobic benzyl protecting groups present in **6** were substituted with less hindered acetyl functions, increasing the yield (27–34%) of the coupled product (**7**) in a mixture of *tert*-amyl alcohol and DMF. Nevertheless, shortening the side chain resulted in a significantly enhanced yield of the enzymatic coupling with glycine and phenylalanine amide (**8**), affording the desired dipeptides after few days in good to excellent yields in a mixture of *t*-BuOH and DMF (66–94%, Figure 2). The coupling reactions proceeded relatively slowly, presumably due to the low solubility of the substrates and/or steric factors.

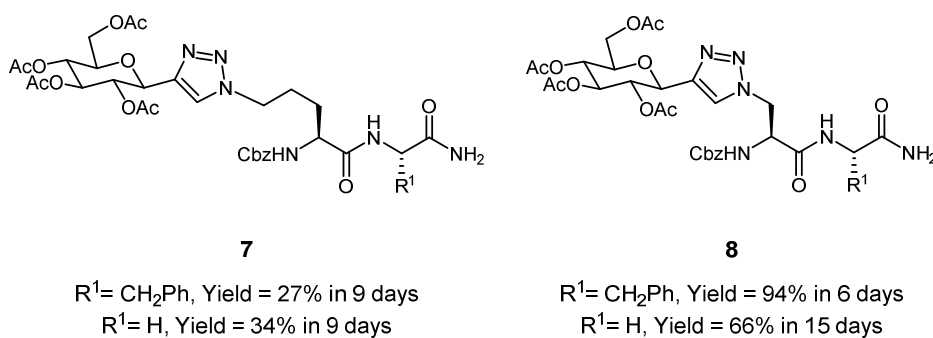
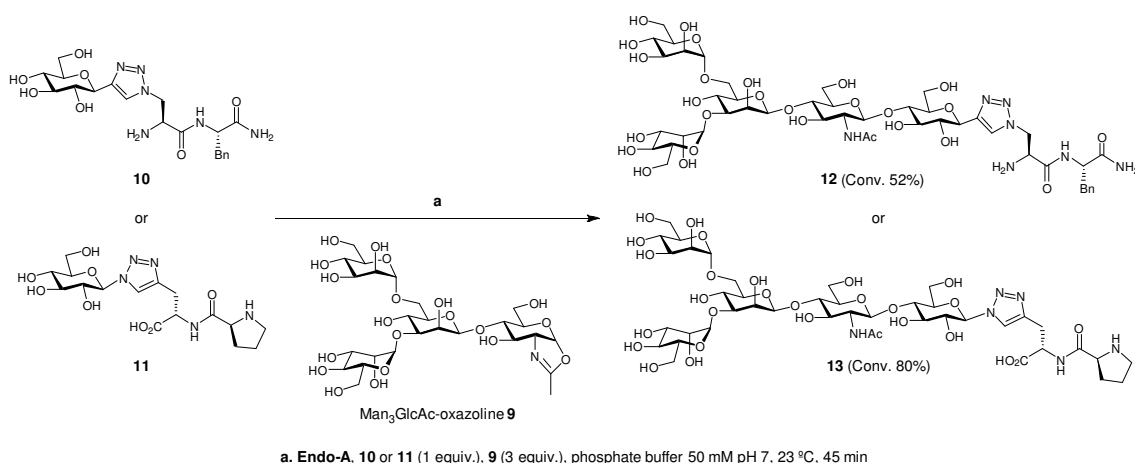


Figure 2. Changing the size of the side chain displayed important variations in the alcalase-catalyzed synthesis of *C*-triazole-linked glucosidic dipeptides.

2.1.2. Using transferases

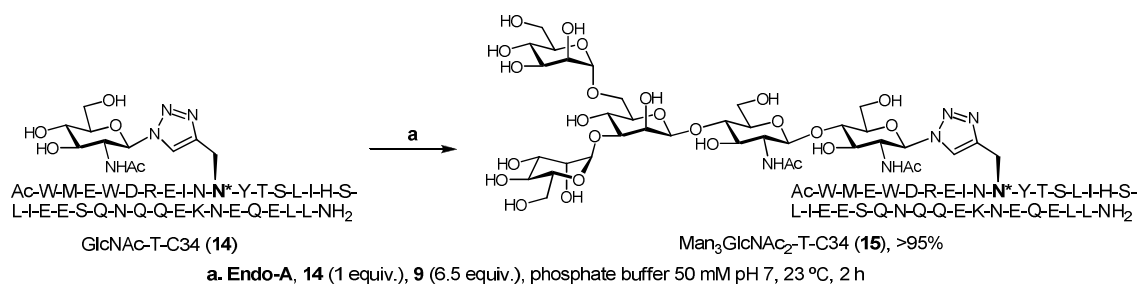
Novel triazole-linked glycopeptides were synthesized *via* endoglucosidase-catalyzed transglycosylation of glucose (Glc)- and *N*-acetylglucosamine (GlcNAc)-containing dipeptides and polypeptides by using a synthetic sugar oxazoline (**9**) as donor substrate.¹⁷ Since endo- β -*N*-acetylglucosaminidase from *Arthrobacter* (Endo A) can recognize both GlcNAc and Glc moieties as acceptor substrates for transglycosylation, the feasibility to glycosylate two 1,2,3-triazole-linked Glc-containing dipeptides was evaluated. Hence, glycopeptides **10** and **11** were chemically synthesized and used with tetrasaccharide **9** in the presence of Endo-A in phosphate buffer 50 mM pH 7 at 23 °C, showing excellent conversions in the transglycosylation processes, affording products **12** and **13** (Scheme 2). *N*-Linked triazole derivative **13** was formed much faster than *C*-linked **12** (conversion of 80% vs 52% respectively after 45 minutes).



Scheme 2. Transglycosylation with triazole-linked Glc-dipeptides.

A plausible explanation for this observed difference may be that the *N*-linked triazole resembled more closely the amide linkage found in the natural *N*-glycopeptides. It must also be mentioned that the hydrolysis of both products mediated by Endo-A was not detected after 24 hours.

This study was extended to the preparation of an *N*-linked triazole with a large glycan moiety and a 34-mer peptide with anti-HIV activity, catalyzed by Endo-A (Scheme 3).¹⁷ The suitability of chemically preformed GlcNAc-T-C34 (**14**), as the acceptor substrate for Endo-A to achieve the transglycosylation reaction with Man₃GlcNAc-oxazoline as the donor substrate, was studied and also compared with the natural *N*-linked counterpart (Scheme 3). After 2 hours, the reaction was complete obtaining the corresponding transglycosylation product. The novel triazole-linked glucopeptide C34 (**15**) showed a decrease in the anti-HIV activity; however its water solubility and protease stability dramatically increased in comparison to the non-glycosylated peptide, making this glycosylated peptide as a valuable candidate for further development.

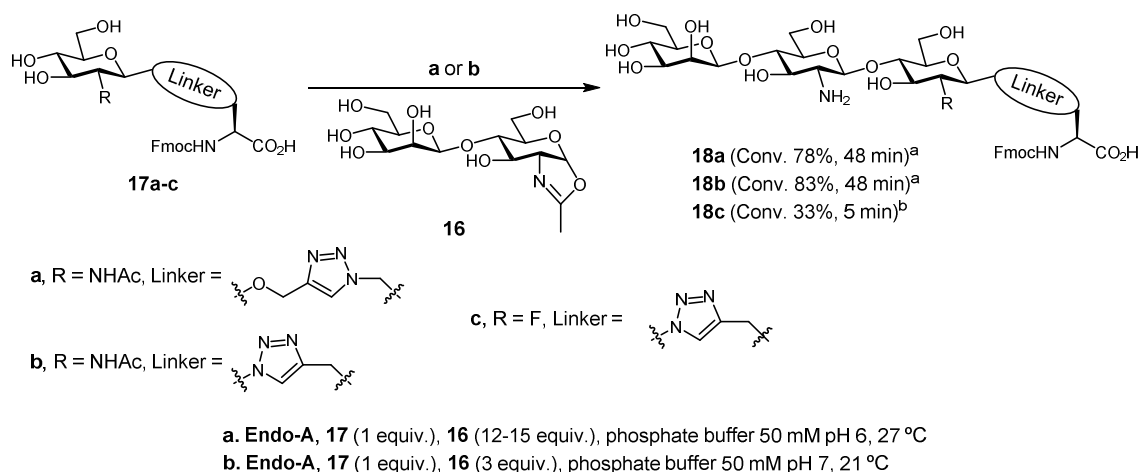


Scheme 3. Enzymatic transglycosylation of a triazole-linked GlcNAc-C34 peptide.

The importance of combining chemical tagging followed by Endo-A-catalyzed elongation was investigated by Davis' group,¹⁸ allowing the access to elaborated glycoproteins. This combined chemo-enzymatic approach consisted of site-selective convergent chemical glycosylation of a protein scaffold with a single GlcNAc (or another sugar), followed by enzymatic glycosylation. Several potential linkages and sugars that could undergo efficient glycosylation were evaluated. These included 1,2,3-triazole-linked proteins,¹⁹ among other "unnatural" as thioether, selenenylsulfide or disulphide.

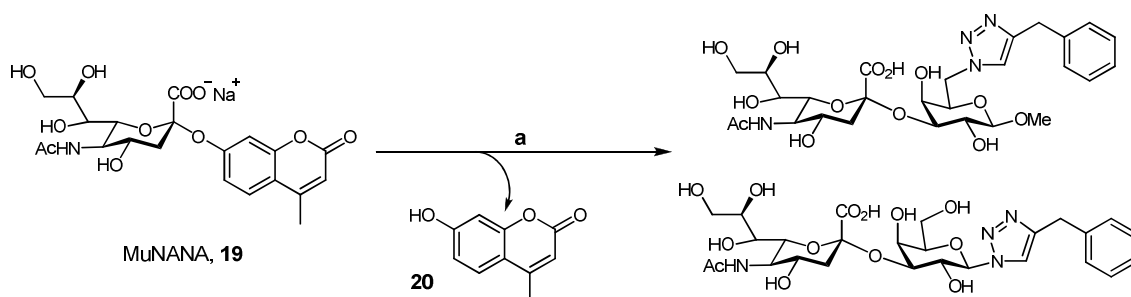
Disaccharide oxazoline **16** was chosen as donor substrate in the glycosylation reaction (Scheme 4). When the elongation with Endo-A was carried out in phosphate buffer 50 mM pH 6 or 7 at 21–27 °C, a wide tolerance to the acceptor linkage was observed beyond the amide. While the natural linkage gave the lowest conversion (25%), better activities were achieved especially for substrates **17a,b**, giving rise to conversions higher than 75%. Interestingly, enzymatic activity was also observed for some examples where the natural GlcNAc moiety was replaced by unnatural sugars such as 2-deoxy-2-fluorosugars (**17c**).

This strategy was also demonstrated on peptide substrates, such *N*- or *C*-triazole-linked peptides derived from two proteins, namely the cancer antigen protein gp90²⁰ and subtilisin from *Bacillus lentus*, that were synthesized and assayed for Endo-A-mediated glycosylation. The corresponding glycopeptides were obtained with >98% conversion in phosphate buffer 50 mM pH 7 at 20 °C after 2–7 hours. A lower reactivity (70% after 8 hours) was observed in the case of the *N*-triazole-glycopeptide. As an extension, novel glycoproteins were formed. Hence, a model protein, NP276 from *Nostoc punctiforme*,²¹ was used to compare the different linkages. Interestingly, the *C*-triazole-linked GlcNAc variant showed activity and 40% of conversion to the glycosylated product was observed. Unfortunately, no product was detected with the *N*-triazole-derived variant. The ease of assembly of triazole-linked glycoproteins, followed by Endo-A extension, made this method as a powerful tool for the production of more complex synthetic glycoproteins.



Scheme 4. Endo-A-catalyzed glycosylation of C- or N-triazole glycoamino acids.

Carvalho, Field and co-workers²² synthesized a library of 46 substrate analogues based on 1,4-disubstituted 1,2,3-triazole galactose derivatives modified at either C-1 or C-6 positions as potential inhibitors of *trans*-sialidase (TcTS) from *Trypanosoma cruzi*. This protozoan parasite is responsible for the Chagas' disease. It utilizes TcTS to transfer sialic acid from the host cell to a mucin-like glycoprotein in order to modify its carbohydrate coat, so then it cannot be recognized by the human immune response system. Therefore, the inhibition of TcTS offers the potential for therapeutic intervention.



a. Cell free extract containing TcTS, **19** (5 equiv.), triazole-sugar (1 equiv.), phosphate buffer 100 mM pH 7.5, 25-30 °C, 4 h

Scheme 5. Examples of the sialic acid transfer reaction catalyzed by TcTS using MuNANA as substrate.

A fluorimetric method was chosen for the determination of the TcTS-activity measuring the cleavage of 2'-(4-methylumbelliferyl)- α -D-N-acetylneuraminic acid (MuNANA, **19**), which releases fluorescent methylumbelliferone (Mu, **20**). In general, triazole-containing compounds showed moderate to low inhibitory effects at 0.5–1 mM concentrations.

Alternatively, these galactose-based compounds might also act as TcTS substrates, inhibiting the cleavage of MuNANA. The experiments were conducted by incubation of an individual member of the triazole-sugar library with TcTS in the presence of MuNANA in phosphate buffer 100 mM pH 7.5. After 4 hours, the incubations showed near complete conversion of all members of the 1,2,3-triazole library to the corresponding sialylated adducts at room temperature (Scheme 5). These experiments showed that although the triazole-sugars were weak TcTS inhibitors, they could compete as substrates for the enzyme.

2.1.3. Cofactor mimics

Nicotinamide adenine dinucleotide (NAD⁺, Figure 3) has attracted major interest because of their prominent biological roles. When it functions as the coenzyme to mediate in an oxidative reaction, the

pyrimidinium ring moiety receives a hydride (H^-) to form NADH, the reduced form of NAD^+ . The adenosine monophosphate part of the coenzyme is believed to endorse the proper binding of NAD^+ in the active site. Over the years, a great variety of NAD(H) analogues have been prepared.²³ One of these examples was reported by Zhao and co-workers,²⁴ where a novel series of NAD analogues (**21a–f**) containing the 1,2,3-triazole moiety instead of the adenine base was synthesized.

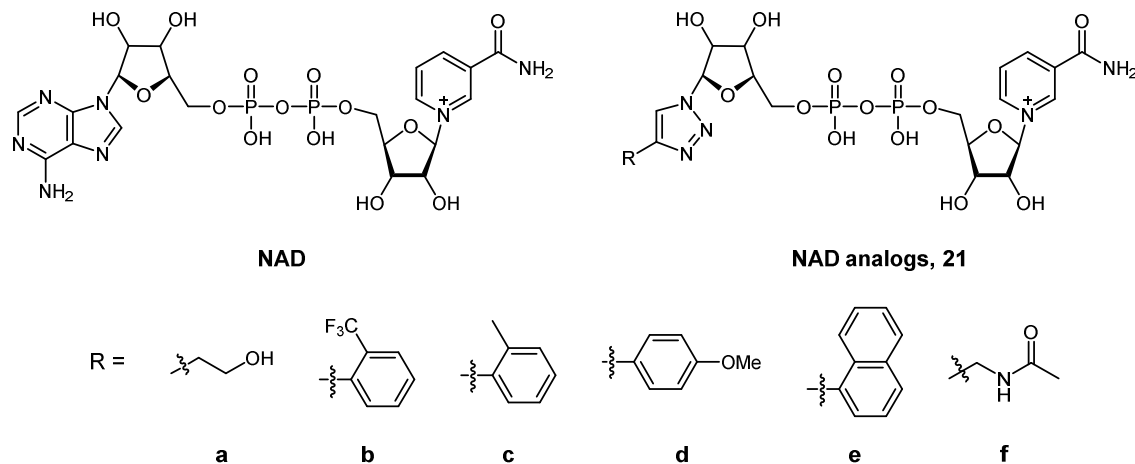


Figure 3. Structure of NAD and 1,2,3-triazole-containing cofactor analogues.

These NAD analogues were tested as cofactors for the recombinant malic enzyme (ME) from *Escherichia coli* in the oxidative decarboxylation of L-malate to yield pyruvate and CO_2 . In these cases, ME activities with the NAD analogues were less than 5% with regards to NAD^+ as cofactor. The highest ME activity was obtained with **21d**.

These NAD analogues were also employed as cofactors for an alcohol dehydrogenase (ADH)-catalyzed oxidation. ADH from *Saccharomyces cerevisiae* was used in the oxidation of ethanol. Noticeable activities were observed with all analogues, especially with **21b**, **21c**, and **21e** (25.3%, 8.5% and 7.9% regarding NAD^+). These results showed that ADH had more flexibility than ME for cofactor acceptance.

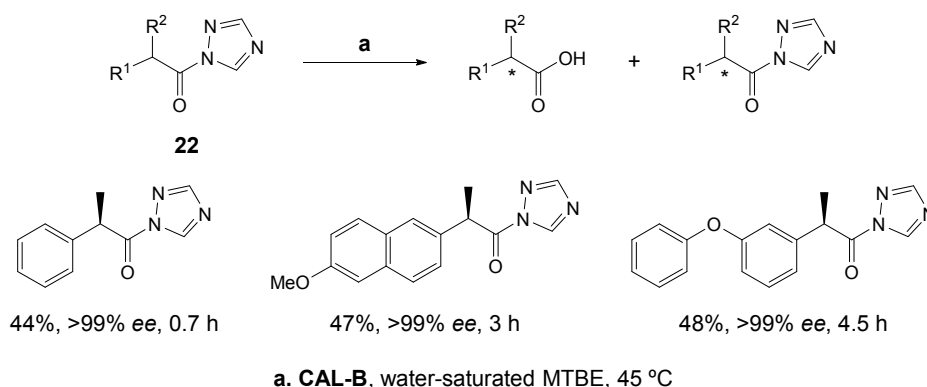
Very recently, the same authors have obtained several ME mutants able to accept the 1,2,3-triazole-derived cofactors with much higher efficiency than the wild-type enzyme.²⁵ Thus, a double mutant of the enzyme was able to accept mimics **21c** and **21e** about 8–9 times better than NAD^+ applied to the decarboxylation of L-malate.

2.2. 1,2,4-Triazoles

2.2.1. Using hydrolases: lipases and acylases

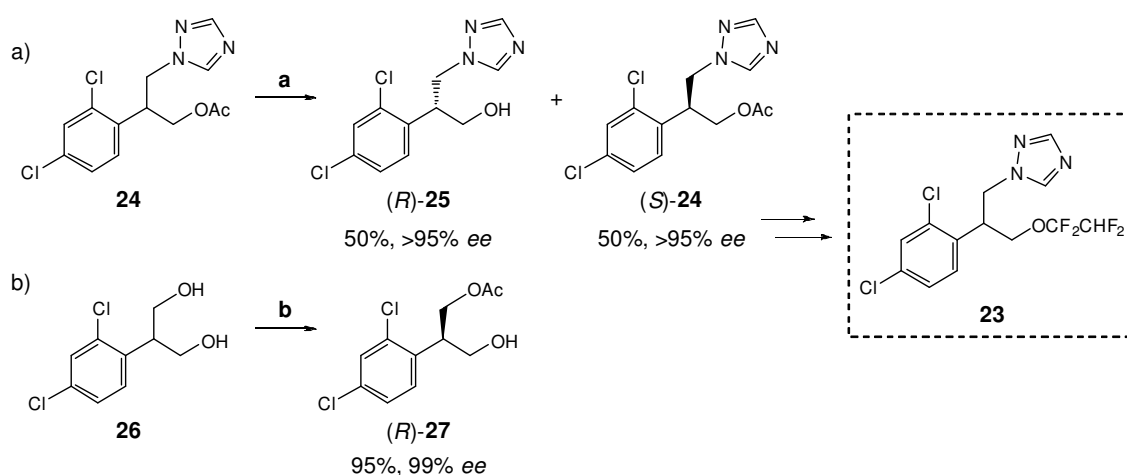
As already mentioned, hydrolases such as esterases, lipases and serine proteases are widely applied as versatile biocatalysts for preparing a great variety of pharmaceuticals and fine chemicals containing a chiral center.⁹ Frequently, the acylation step on the formation of the acyl-enzyme intermediate for the hydrolysis of esters or amides has been found as the rate-limiting step.²⁶ In this sense, the use of activated or irreversible acyl donors or acceptors has been proposed to enhance the enantiomer discrimination towards targeted racemates. Tsai and co-workers have proposed the employment of activated *N*-acylazoles (azolides, **22**), as versatile acylating agents not only acting as better leaving groups but also making the carbonyl carbon more electrophilic and susceptible to the nucleophilic attack. Thus, in a first report (Scheme 6),²⁷ the authors achieved the CAL-B-catalyzed hydrolysis of racemic *N*-profenylazoles, observing that the 1,2,4-triazole

derivatives were very suitable substrates to provide the final profens with excellent enantioselectivities. Among the different parameters studied in this reaction, the water content of the organic solvent appeared as a critical factor, thus achieving the best results with water-saturated methyl *tert*-butyl ether (MTBE) at 45 °C after few hours. This study was further developed comparing several leaving groups with the same substrates obtaining also excellent results for the CAL-B-catalyzed methanolysis in dry MTBE at 45 °C.²⁸ Again, 1,2,4-triazole-derived azolides appeared as the most appropriate ones. In a very recent contribution of the same group, the hydrolysis mediated by CAL-B of racemic *N*-protected proline, pipecolic acid and nipecotic acid azolides, was successfully performed in water-saturated MTBE at 45 °C.²⁹



Scheme 6. *N*-Acylazoles **22** as appropriate acylating agents applied to lipase-catalyzed kinetic resolutions.

2-(2,4-Dichlorophenyl)-3-(1*H*-1,2,4-triazol-1-yl)propyl 1,1,2,2-tetrafluoroethyl ether (tetraconazole, **23**, Scheme 7) is a broad spectrum fungicide, which is highly active against a number of *Ascomycetes*, *Basidiomycetes* and *Deuteromycetes* fungi. It has also been proposed as an agent for crop protection.³⁰ Due to the fact that it was administrated as racemate, Bianchi *et al.* decided to synthesize both fungicide enantiomers to compare their efficiency through two different enzymatic strategies (Scheme 7): by lipase-catalyzed hydrolysis of a racemic acetate precursor (**24**, pathway a) and by lipase-mediated desymmetrization of prochiral diol **26** (pathway b) by acylation.



a. PPL, phosphate buffer 50 mM pH 7.0/dioxane (33:1 v/v), 35 °C, 24 h.

b. PPL/Celite, EtOAc, 25 °C, 16 h

Scheme 7. Enzymatic strategies to synthesize both tetraconazole enantiomers.

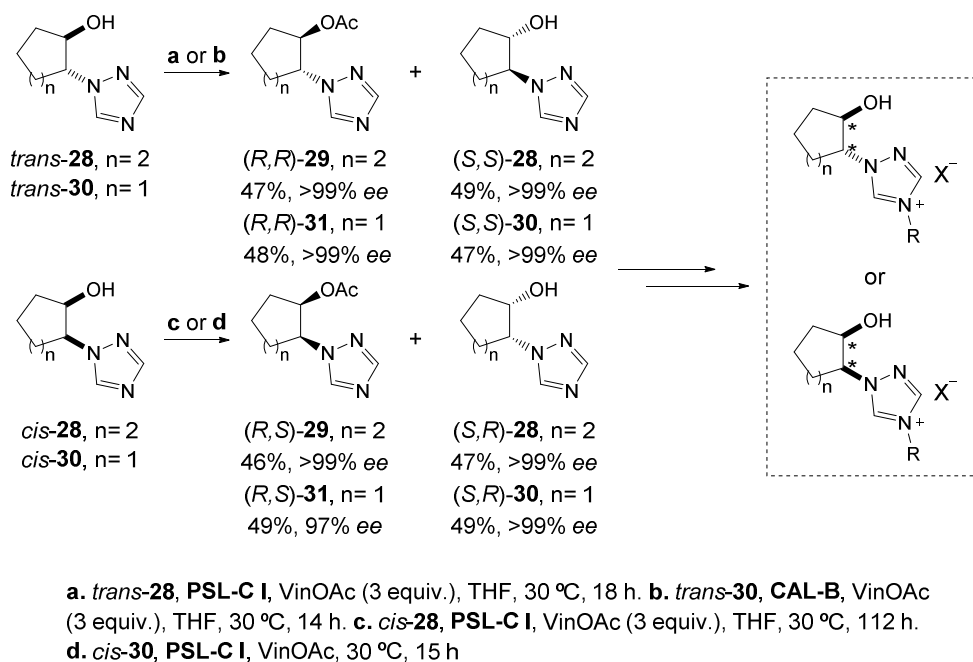
For the first approach, among the different biocatalysts tested, PPL afforded both substrate (*S*)-**24** and product (*R*)-**25** with high *ee* (>95%) after 24 hours in a mixture of phosphate buffer 50 mM pH 7 and

dioxane at 35 °C. In the second case, the transesterification reactions were carried out in ethyl acetate, which acted as both acylating agent and reaction medium. The enzymes were used either in powdered form or supported on Celite[®], finding that adsorbed PPL after fractional precipitation in phosphate buffer (pH 8) with acetone (60% v/v) afforded the monoacetylated derivative (*R*)-**27** in 95% conversion and 95% *ee* after 8 hours at 25 °C. When the precipitation of PPL was done using 50% v/v of acetone, (*R*)-**27** was again obtained in excellent conversion (95%) and in enantiopure form (99% *ee*) after 16 hours in the same reaction conditions. Once synthesized both tetraconazole enantiomers, the authors performed *in vitro* and *in vivo* tests against several fungi, observing that the (*R*)-enantiomer was always more active than the (*S*)-antipode, which did not significantly contribute to the antifungal activity.

The same authors in another contribution showed the lipase-catalyzed acetylation of racemic alcohol **25**, obtaining with PPL in EtOAc at 35 °C both alcohol (*S*)-**25** and ester (*R*)-**24** with excellent *ee* (>95%).³²

Chiral 1,3-amino alcohols bearing rigid cyclic aliphatic backbones in combination with *N*-heterocycles like pyrazole, imidazole or triazole as amino functionality, are important due to their chelating features and also as versatile starting materials for the synthesis of chiral azides, amines and Schiff bases.³³ In this context, Thiel and co-workers synthesized racemic *trans*-2-(1*H*-1,2,4-triazol-1-yl)cyclohexan-1-ol (*trans*-**28**), which was then subjected under CAL-B-catalyzed acetylation conditions using isopropenyl acetate as acylating agent and solvent at 40 °C.³⁴ Unfortunately, acetate *trans*-**29** was obtained racemic, which was ascribed to unfavourable dipolar interactions of the nitrogen group in the 4-position of the heterocycle with the active site of the enzyme or by a fast nonenzymatic side reaction.

In a subsequent contribution, made by Ríos-Lombardía *et al.*, several racemic 2-(1*H*-triazol-1-yl)cycloalkanols (Scheme 8) were resolved through lipase-catalyzed acylation to synthesize a series of chiral-alkylated 1,2,4-triazolium salts and ionic liquids (ILs).³⁵



Scheme 8. Chemoenzymatic synthesis of 1,4-dialkyl-1,2,4-triazolium salts and ionic liquids.

These compounds are salts consisting of a mixture of cations and anions that do not pack well together, with consequently melting points close to room temperature, although they are arbitrarily defined as salts with a melting point below 100 °C.³⁶ ILs have drawn considerable interest for their use in various

analytical techniques, applications in gas-liquid or liquid-liquid extractions, electrochemistry, mass spectrometry and infrared, Raman and fluorescence spectroscopy.³⁷ Additionally, the solubility of gases such as H₂, CO, and O₂ in ILs is generally good, making them attractive solvents for catalytic hydrogenations, carbonylations, hydroformylations and aerobic oxidations.³⁸ The asymmetric synthesis of chiral ionic liquids (CILs) is an attractive and challenging field for organic chemists since they have shown a great ability to induce significant chirality transference in catalytic reactions.³⁹

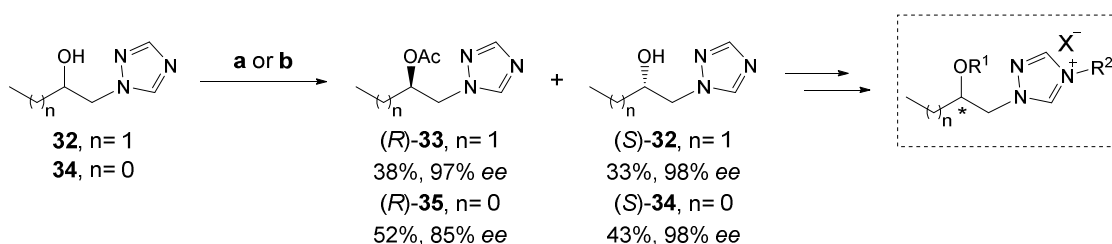
Thus, racemic *trans*-2-(1*H*-1,2,4-triazol-1-yl)cyclopentanol (*trans*-**30**) and the cyclohexyl counterpart *trans*-**28** were obtained and their lipase-catalyzed resolution through acetylation reaction was achieved.³⁵ In this case, both CAL-B and lipase from *Pseudomonas cepacia* (PSL-C I) could efficiently resolve both alcohols using vinyl acetate as acylating agent in dry tetrahydrofuran (THF) at 30 °C after 14–18 hours, depending on the substrate. Therefore, remaining (*S,S*)-**28** and **30** and acetate products (*R,R*)-**29** and **31** could be synthesized with excellent *ee* (>99%). Just for the acetylation of alcohol *trans*-**28**, PSL-C I displayed a higher rate than CAL-B, although with similar selectivity, differently from previous results described by Thiel and co-workers.³⁴ Then, the corresponding isomers *cis*-**28** and *cis*-**30** were obtained and subjected to these lipase-catalyzed kinetic resolution conditions. In general, no reaction occurred when CAL-B was used as the biocatalyst using either three equivalents of vinyl acetate in THF or the ester itself as both reagent and solvent. However, PSL-C I showed an excellent selectivity in the acetylation of the (*R,S*) enantiomers, allowing the isolation of acetates (*R,S*)-**29** and **31** and alcohols (*S,R*)-**28** and **30** in enantiopure form. In the case of the cyclohexyl derivative **28**, the resolution took 112 hours at 30 °C utilizing THF as solvent while shorter reaction times (15 hours) were needed for cyclopentanol **30**. In this case, the acylation was performed also at 30 °C but using VinOAc as acylating agent and solvent.

The synthesis of enantiomerically pure triazolium salts was performed through quaternization of the nitrogen at 4-position in the previously synthesized triazoles using different alkyl or benzyl halides, followed by metathesis of the triazolium salts with different anions [*i.e.*, tetrafluoroborate or bis(trifluoromethylsulfonyl)imide]. Both reactions occurred with very high yields in all cases rendering a family of 30 enantiopure chiral triazolium salts with a significantly large structural diversity. The potential of these salts as asymmetric phase-transfer catalysts for the Michael addition between diethyl malonate and *trans*-chalcone in different organic solvents was then evaluated, observing that although chiral inductions were modest (<23%), the reaction was highly accelerated by most of the tested salts.

In another contribution,⁴⁰ Borowiecki and co-workers resolved again alcohol *trans*-**28** through lipase-catalyzed acetylation in the presence of 3 equivalents of VinOAc, finding that the reactions carried out at 30 °C in 2-methyl-2-butanol run faster than in other organic solvents and that Amano PS-C was a more effective catalyst than CAL-B in terms of activity and selectivity. Thus, after 42 hours (*S,S*)-**28** and acetate (*R,R*)-**29** were obtained in 98% *ee*. From these two chiral precursors, several salts and ILs were synthesized *via* *N*-alkylation and exchange of the halide anion in a similar way as described before.³⁵

The same authors have designed the synthesis of various chiral triazolium ILs (Scheme 9) through the lipase-catalyzed resolution of *N*-(2-hydroxybutyl)-1,2,4-triazole (**32**)⁴¹ and *N*-(2-hydroxypropyl)-1,2,4-triazole (**34**).⁴² Among the different biocatalysts tested for the acetylation of **32**, Amano PS-IM appeared as the best lipase yielding after 6 hours enantiomerically enriched (*S*)-**32** (98% *ee*) and acetate (*R*)-**33** (97% *ee*) using vinyl acetate as acylating ester and 2-methyl-2-butanol as solvent at 30 °C. In the case of alcohol **34**, the lipase-catalyzed acetylations proceeded with lower selectivities, obtaining the best results (enantiomeric

ratio, $E=56$) with native *Pseudomonas fluorescens* lipase (Amano AK) suspended in 2-methyl-2-butanol, with vinyl acetate at room temperature. At different conversions, substrate (*S*)-**34** could be obtained with excellent *ee* (98%) and acetate (*R*)-**35** with 90% *ee*.

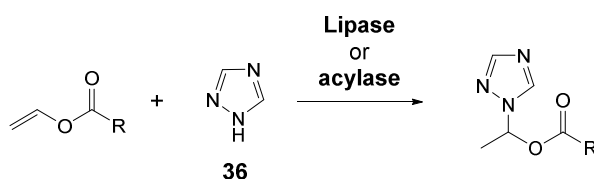


a. 32, Amano PS-IM, VinOAc (5 equiv.), 2-methyl-2-butanol, 30 °C, 6 h. **b. 34, Amano AK**, VinOAc (5 equiv.), 2-methyl-2-butanol, rt, 49 h

Scheme 9. Chemoenzymatic synthesis of triazolium salts and ionic liquids derived from alcohol and acetate derivatives **32–35**.

As an application of these chiral derivatives, various ILs were synthesized through *N*-alkylation with the corresponding alkyl halides and their antimicrobial and antifungal activities were tested against several microorganisms. Among the different information that was obtained from these studies, it appeared clear that these activities were significantly dependent on the alkyl chain length of the triazole, being more toxic as longer the alkyl chain was.

The catalytic promiscuity of enzymes is based on the ability of a single biocatalyst active site to catalyze several chemical transformations.⁴³ Especially hydrolases have demonstrated the ability of catalyzing other reactions such as carbon–carbon, carbon–heteroatom and heteroatom–heteroatom bond formation and oxidative processes.⁴⁴ In 2005, Lin and co-workers demonstrated the ability of a D-aminoacylase from *Escherichia coli*, a zinc binding metalloenzyme which naturally catalyzes the hydrolysis of *N*-acetyl-D-amino acids, to mediate the Markovnikov addition of different azoles (imidazole, pyrazole and 1,2,4-triazole) to vinyl esters (Scheme 10).⁴⁵



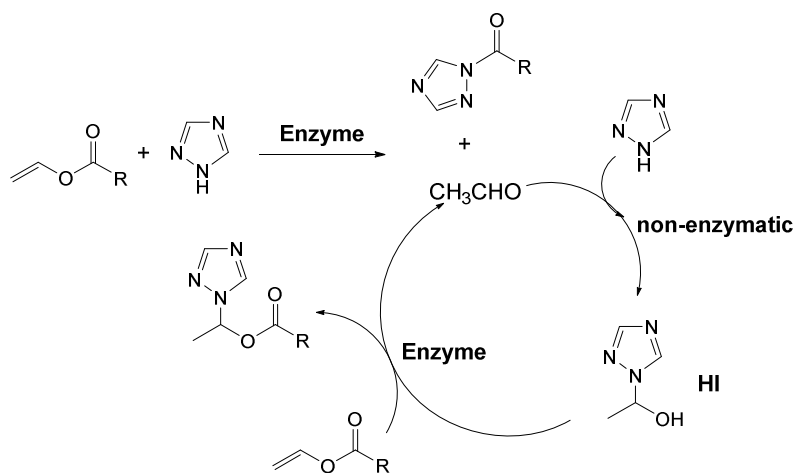
Scheme 10. D-Aminoacylase or lipase-catalyzed Markovnikov addition of 1,2,4-triazole to vinyl esters.

After optimization of the reaction parameters, the addition of 1,2,4-triazole (**36**) was attempted in *n*-hexane using an excess (8 equiv.) of the vinyl ester at 50 °C. In this first report, vinyl acetate and divinyl succinate were tried as substrates obtaining, after 84 to 96 hours, the corresponding Markovnikov products in excellent yields (93% and 90%, respectively), in a very clean manner.

In another contribution, the same authors discovered that also lipases were able to catalyze the aza-Markovnikov addition of different *N*-heterocycles to vinyl esters in organic media.⁴⁶ The best results were achieved when Amino lipase M from *Mucor javanicus* (MJML) was used as biocatalyst. Thus, by using this enzyme in DMSO at 50 °C, **36** reacted with divinyl sebacate (3 equiv.) affording, after 72 hours, the product coming from the monoaddition into one of the two double bonds in 58% yield, being disfavoured the second

addition. This reaction was then combined with a regioselective lipase-catalyzed acylation of a nucleoside. In this case, ribavirin, a potent antiviral drug, was chosen as model substrate to obtain the final adduct. When the monofunctionalized ester (3 equiv.) was treated with ribavirin and CAL-B in acetone for 24 hours at 50 °C, the nucleoside was regioselectively acylated in good yield (67%).

As already mentioned, this aza-Markovnikov addition was firstly assumed as an example of catalytic promiscuity of acylases or lipases,^{45,47} but in a subsequent study of the same group it was discovered that the mechanism of this transformation consisted on two-steps catalyzed by the enzyme plus one non-enzymatic reaction (Scheme 11), so the authors finally ascribed this process as a *pseudo*-promiscuity example.⁴⁸ Hence, the first acylation of the azole with vinyl acetate would be catalyzed by the enzyme, releasing simultaneously acetaldehyde. The nitrogenated heterocycle would act then as a nucleophile attacking the acetaldehyde and forming the hemiaminal intermediate (HI). HI could be stabilized by a hydrogen bonding network in the catalytic site of the enzyme. Then, HI would react with the carbonyl group of another molecule of the vinyl ester which would be bound in the catalytic site. This transesterification accomplished by the enzyme would render the final product.



Scheme 11. Proposed mechanism for the *pseudo*-promiscuous aza-Markovnikov addition of azoles to vinyl esters. This mechanism has been adapted for the reaction of 1,2,4-triazole.

In 2007, Lin and co-workers also showed the efficient promiscuous enzymatic Michael addition of aromatic *N*-heterocycles to α,β -unsaturated carbonyl compounds catalyzed by acylases.⁴⁹ Among the different biocatalysts tested for these aza-Michael additions, two zinc-containing acylases, D-aminoacylase ‘Amano’ from *Escherichia coli* and acylase ‘Amano’ from *Aspergillus oryzae*, were found as the most effective ones. After optimization of the reaction conditions, **36** reacted with methyl acrylate (2 equiv.) in DMSO at 50 °C in the presence of acylase from *A. oryzae*, to obtain the corresponding aza-Michael adduct in 95% yield after 3 hours.

2.2.2. Using hydrolases: nucleoside phosphorylases

Ribavirin (**37**, 1- β -D-ribofuranosyl-1,2,4-triazole-3-carboxamide, also known as virazole, Figure 4) is a base-modified nucleoside effective against a wide spectrum of RNA- and DNA-viruses. It has demonstrated pronounced efficiency in the treatment of hepatitis C virus (HCV) and Lassa fever, as well as influenza of A- and B-types.⁵⁰ The interest for this compound has significantly increased due to its efficiency for the treatment of several diseases in children in their first year of life. Furthermore, the

combination of recombinant interferon alpha-2b with ribavirin is widely employed for the treatment of chronic hepatitis C.⁵¹ In 2011, ribavirin has been approved by the American Food and Drug Administration for the therapy of hepatitis C together with the proteinase inhibitor telaprevir in combination with interferon.

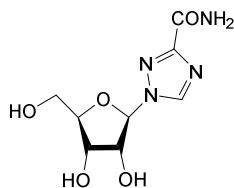
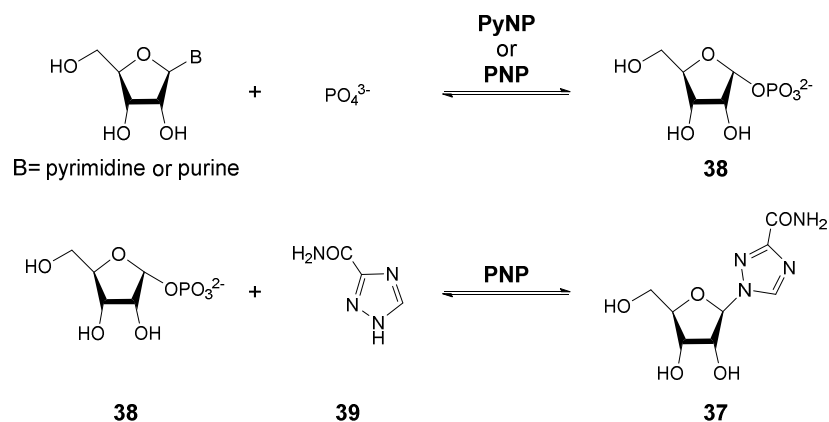


Figure 4. Structure of ribavirin.

Nucleoside phosphorylases (NPs) are intracellular enzymes which can interconvert pyrimidine or purine bases from other nucleosides.⁵² These enzymes achieve this transformation *via* two-step reversible reactions: a) firstly, in the presence of a phosphate anion, the nitrogenated base of the first nucleoside is released forming α -D-ribose-1-phosphate (R-1-P, **38**); b) in the second step, this intermediate reacts with the second nitrogenated base giving access to the final nucleoside derivative with complete β -stereoselectivity (Scheme 12). These biocatalysts are very interesting in biotransformations because purine, pyrimidine or non-natural nucleosides can be obtained in a one-pot reaction from other easily accessible pyrimidine or purine nucleosides. Depending on their substrate spectra, these enzymes can be divided into two main classes: pyrimidine nucleoside phosphorylases (PyNPs), if they accept pyrimidine nucleosides, and purine nucleoside phosphorylases (PNPs), if they react with purine derivatives.



Scheme 12. Two-step mechanism of NPs to synthesize ribavirin.

In 1986, Utagawa *et al.* demonstrated that a purified PNP from *Enterobacter aerogenes* AJ 11125 was able to produce ribavirin from inosine.⁵³ In this case, treating isolated R-1-P (5 equiv.) in the presence of the purified PNP and 1,2,4-triazole-3-carboxamide (TCA, **39**), afforded after 4 hours at 60 °C in Tris-HCl buffer 50 mM pH 8 the desired nucleoside derivative in 75% yield (Table 2, entry 1).

After this seminal contribution, several groups have searched for other enzymes or microorganisms that could synthesize ribavirin with high productivities from easily accessible nucleosides (Table 2). Among the different enzymatic preparations that have been used for that purpose, the following systems can be mentioned:

a) Use of whole cells. Shirae and co-workers devoted many efforts to find suitable microorganisms that could produce ribavirin from easily accessible nucleosides such as pyrimidine (uridine,⁵⁴ cytidine⁵⁴ and

orotidine⁵⁵), or purine (guanosine,⁵⁶ inosine⁵⁶ and adenosine⁵⁷) derivatives (Table 2, entries 2–5). In a subsequent contribution, Sinisterra and co-workers immobilized on agar whole cells from *Enterobacter gergoviae* CECT 875 to obtain ribavirin from uridine (Table 2, entry 6).⁵⁸ In the case of starting from pyrimidinic nucleosides, the supposed pathway consisted of two different phosphorylases: in the first step, a PyNP would form the intermediate R-1-P while in the second step, a PNP would produce ribavirin from this compound. The main problem of this strategy is the low productivity usually achieved.

b) Use of purified enzymes. From previous screenings,⁵⁶ a PNP was purified from *Brevibacterium acetylicum* ATCC 954 and then was tested for production of ribavirin from guanosine or inosine (Table 2, entry 7).⁵⁹ The same authors purified from *Erwinia carotovora* AJ 2992, a microorganism that produced ribavirin from orotidine,⁵⁵ two enzymes, *i.e.*, an orotidine-phosphorolyzing enzyme (PyNP) and a PNP, which coupled could synthesize **37** from orotidine, as previously suggested (Table 2, entry 8).⁶⁰ More recently, Konstantinova and co-workers have employed an immobilized PNP from *E. coli* to obtain ribavirin from guanosine (Table 2, entry 9).⁶¹ The same enzyme has been used to synthesize also some ribavirin analogues (Figure 5) starting from guanosine⁶² or inosine.⁶³ Also with this strategy, the productivity is not high and obviously higher costs and low stability of the purified enzyme can be mentioned as the main drawbacks.

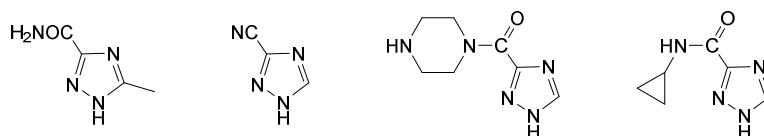


Figure 5. Examples of modified 1,2,4-triazoles accepted by PNP from *E. coli*.

c) Use of overexpressed enzymes. In the last years, some research groups have devoted their efforts to obtain more robust phosphorylases expressed in a host cell, enhancing the process productivity while diminishing costs with regards to the employment of purified enzymes. Furthermore, the immobilization of these whole cells on an adequate support has allowed the recycling of these catalysts. Thus, cross-linked *E. coli* cells overproducing a PNP from the same microorganism were able to synthesize **37** from guanosine (Table 2, entry 10).⁶⁴ Xie *et al.* have described the use of a PNP from *Pseudoalteromonas* sp. XM2107 (Table 2, entry 11)⁶⁵ or from *Bacillus subtilis* (Table 2, entry 12)⁶⁶ overexpressed in *E. coli* to obtain ribavirin from guanosine or inosine. Finally, PNP from *E. coli* MG 1665 was cloned and overexpressed in *E. coli*, forming nucleoside **37** with high productivity starting from guanosine (Table 2, entry 13).⁶⁷

As final approximations to synthesize ribavirin enzymatically, an approach from Hennen and Wong⁶⁸ employing chemically modified bases which can spontaneously undergo hydrolysis in aqueous medium followed by reaction with a PNP, or another from Montserrat and co-workers using a phosphopentomutase starting from furanose 5-phosphates,⁶⁹ can also be mentioned.

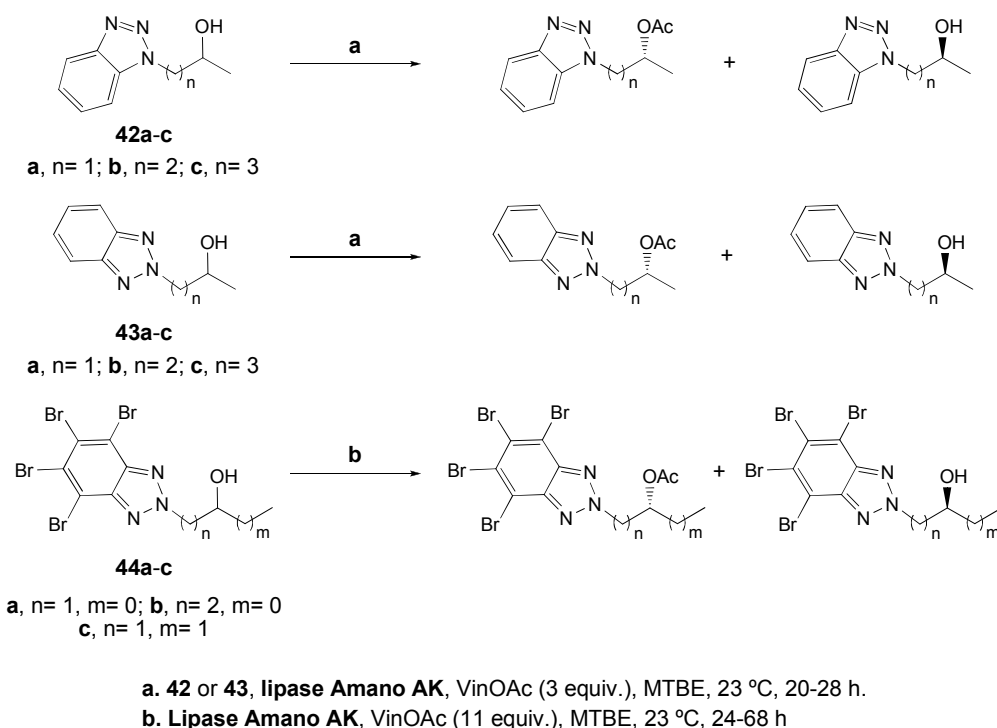
2.2.3. Using transferases

Sitagliptin (**40**) is the active ingredient in Januvia[®], a leading drug for the treatment of type-2 diabetes.⁷⁰ The current industrial synthesis of this compound involves asymmetric hydrogenation of an enamine at high pressure using a rhodium-based catalyst. Apart from insufficient stereoselectivity, the product is contaminated with the metal, necessitating additional purification steps at the expense of the final yield to improve the *ee* and the purity. Savile *et al.* proposed an upgraded synthesis making use of

2.3. Benzotriazoles

2.3.1. Using hydrolases

Due to the known relevance of benzotriazoles, Pchelka *et al.* described the synthesis of enantio-enriched benzotriazol-1-yl-alkan-2-ols **42a–c** and benzotriazol-2-yl-alkan-2-ols **43a–c** through lipase-catalyzed resolution of the racemic alcohols (Scheme 14).⁷⁴ After enzymatic screening, lipase from Amano AK from *Pseudomonas fluorescens* was found as the most suitable catalyst to achieve these resolutions. Then, the effect of several parameters such as the organic solvent, acyl donor, temperature or additive (*e.g.*, crown ethers or thiacycrown ethers) was evaluated on this enzymatic process. After this optimization, the best reaction conditions were obtained using MTBE as organic solvent without any additive employing 3 equivalents of vinyl acetate at 23 °C. Increasing the alkyl chain length linked to the benzotriazole or modifying the position where this chain was connected to the heterocycle, just produced a marginal effect on the lipase selectivity (Table 3, entries 1–6), obtaining both substrate (*S*-configured) and acetate (*R*-configured) with *ee* close to 90% (*E*~30–60).



Scheme 14. Lipase-catalyzed resolutions of benzotriazole derivatives **42–44a–c**.

Table 3. Lipase-catalyzed kinetic resolutions of benzotriazole-derived alcohols **42–44**.

Entry	Substrate	t (h)	Ester (%)	<i>ee</i> (%)	Alcohol (%)	<i>ee</i> (%)
1	42a	20	52	86	48	92
2	42b	23	48	91	52	84
3	42c	26	46	90	54	78
4	43a	21	52	85	48	91
5	43b	23	44	89	56	69
6	43c	28	46	87	54	74
7	44a	42	50	>99	50	>99
8	44b	24	50	>99	50	>99
9	44c	68	50	>99	50	>99

4,5,6,7-Tetrabromo-1*H*-benzotriazole (TBBt) is known as a selective and potent protein kinase CK2 inhibitor.⁷⁵ In order to synthesize TBBt derivatives containing a chiral center, Bretner and co-workers designed a synthetic strategy to get access to various alkanols linked to *N*-2 of the triazole ring (**44a–c**) in enantiopure manner (Table 3, entries 7–9).⁷⁶ After optimization of the reaction conditions, the authors found comparable conditions to the previously described for the unsubstituted derivatives (Scheme 14): lipase Amano AK in MTBE with vinyl acetate (11 equiv.) at 23 °C afforded both substrate (*S*-configured) and product (*R*-configured) with excellent *ee* (>99%).

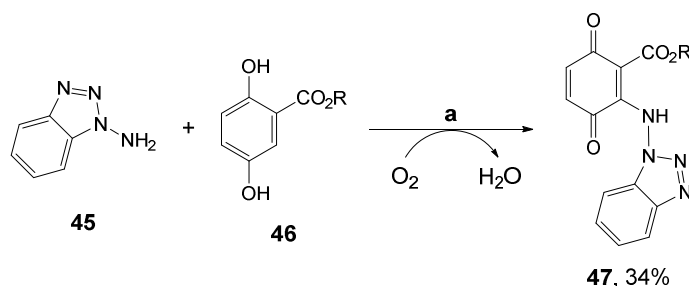
2.3.2. Using oxidoreductases

In the previous work described by Pchelka,⁷⁴ the corresponding ketone precursors were also tried to provide the desired alcohols **42a–c** and **43a–c**. To perform this, baker's yeast was utilized as biocatalyst in water or in mixtures with organic solvents (toluene or MTBE, 95% v/v) at 30 °C, yielding the corresponding *S*-alcohols with moderate to high conversions (29–76%) but unfortunately with modest selectivities (40–67% *ee*).

On the other hand, laccases, copper-containing polyphenol oxidases, are appearing as highly interesting biocatalysts since they can oxidize a considerable range of compounds using molecular oxygen as final electron acceptor.⁷⁷ As possible substrates, polyphenols, methoxy-substituted phenols and diamines can be mentioned. When used in combination with chemical mediators, the substrate spectrum of these enzymes can be broadened including primary or secondary alcohols. Among them, 1-hydroxybenzotriazole (HBT) appears as one of the most typical substances employed,⁷⁸ although in this case it acts just as an electron transfer mediator and finally is discarded as an unwanted by-product.

More recently, Guebitz *et al.* described the laccase-mediated synthesis of tinuvin, a benzotriazole-based UV-absorber acting as photo stabilizer. This type of compounds plays a key role in prolonging the lifetime of polymers and paintings. In this study, laccase from *Trametes hirsuta* was assessed for its ability to catalyze the coupling of methyl 3-(3-*tert*-butyl-4-hydroxyphenyl)propionate with 1*H*-benzotriazole. At low concentrations of the heterocycle, only the homocoupling reaction of the phenol derivative occurred. However, when 1*H*-benzotriazole was applied in a four-fold molar excess, the presence of tinuvin was detected at analytical scale in acetate buffer at pH 3.5–4.5.⁷⁹

Laccases from *Pycnoporus cinnabarinus* and *Myceliophthora thermophila* were used for the synthesis of coupled azole derivatives coming from 1-aminobenzotriazole (**45**) and methyl or ethyl 2,5-dihydroxybenzoate (**46**, Scheme 15).⁸⁰

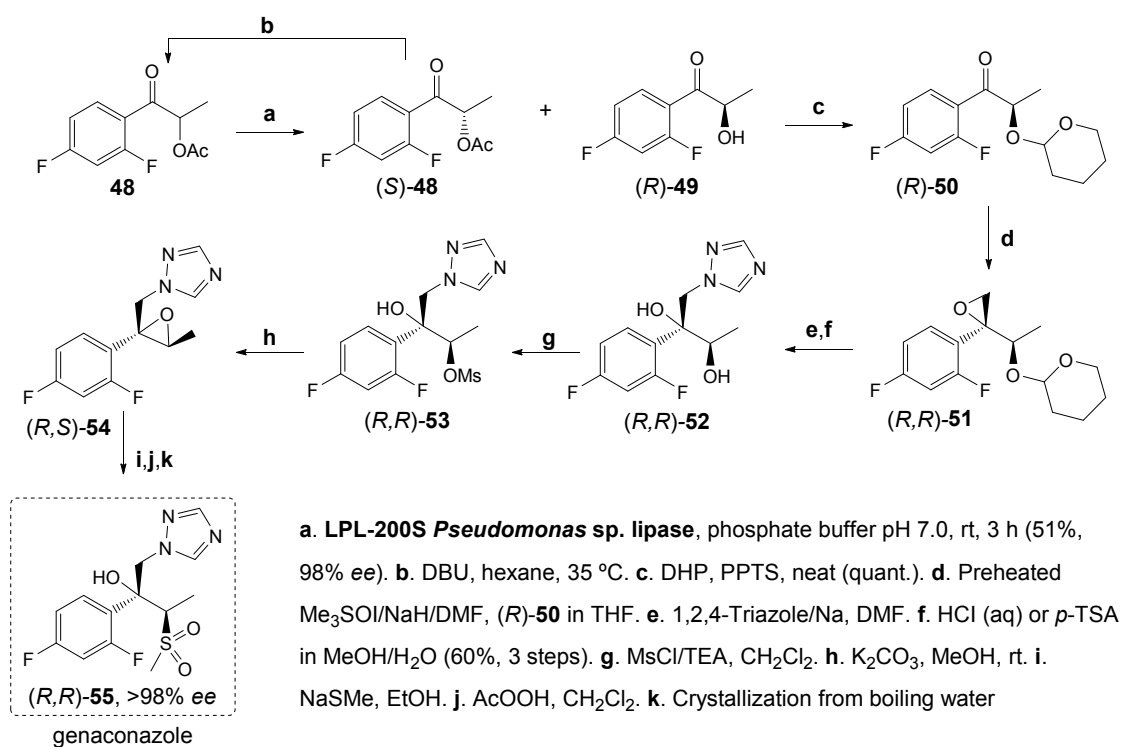


a. **45** (1 equiv.), **46** (1 equiv.), laccase from *P. cinnabarinus*, sodium acetate buffer 20 mM pH 5.0, MeOH (10% v/v), 23 °C, 2 h

Scheme 15. Laccase-catalyzed synthesis of benzotriazole derivatives **47**.

Concerning stereo- and enantioselective synthetic procedures towards this (and related) molecules, researchers have undertaken different routes to establish the relative and absolute stereochemistry. The enzymatic-based methodologies lie on kinetic resolutions of the corresponding precursors employing fungal whole cells or purified hydrolases (Scheme 16).

Thus, Gala *et al.* reported an effective enantioselective synthesis of genaconazole (**55**) employing a set of commercially available lipases (Scheme 17).⁸² The key step was a kinetic resolution of the corresponding α -acetoxy acetophenone derivative (**48**), delivering alcohol (*R*)-**49** with the proper configuration at the carbinolic center (>98% *ee*). An advantage of the described methodology was the possibility of racemization under basic conditions (using 1,8-diazabicyclo[5.4.0]undec-7-ene, DBU) of the remaining acetate bearing the opposite configuration [(*S*)-**48**]. The synthetic chemistry beyond the enzymatic step was already known. Remarkably, an elegant diastereoselective one carbon-homologation with concomitant activation was achieved by reacting (*R*)-**50** with a preheated Me₃SOI/NaH/DMF mixture to afford (*R,R*)-**51**. The authors reported a 60% yield of (*R,R*)-**52** from (*R,R*)-**50** (three steps).^{82a}

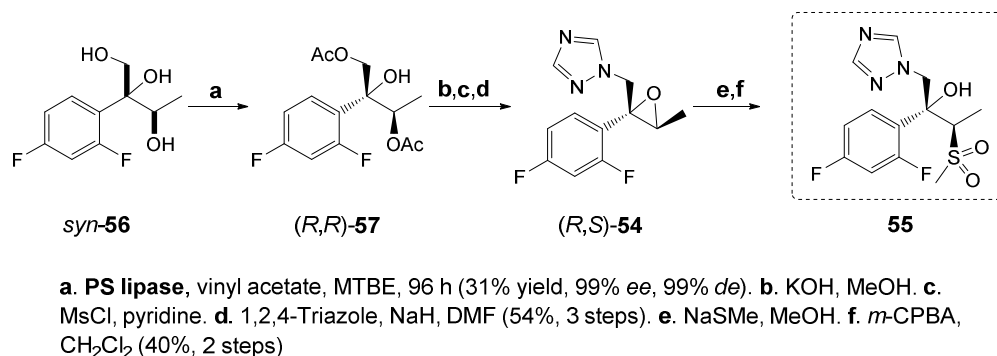


Scheme 17. Enantioselective synthesis of genaconazole employing a lipase-mediated KR and distomer recycling.

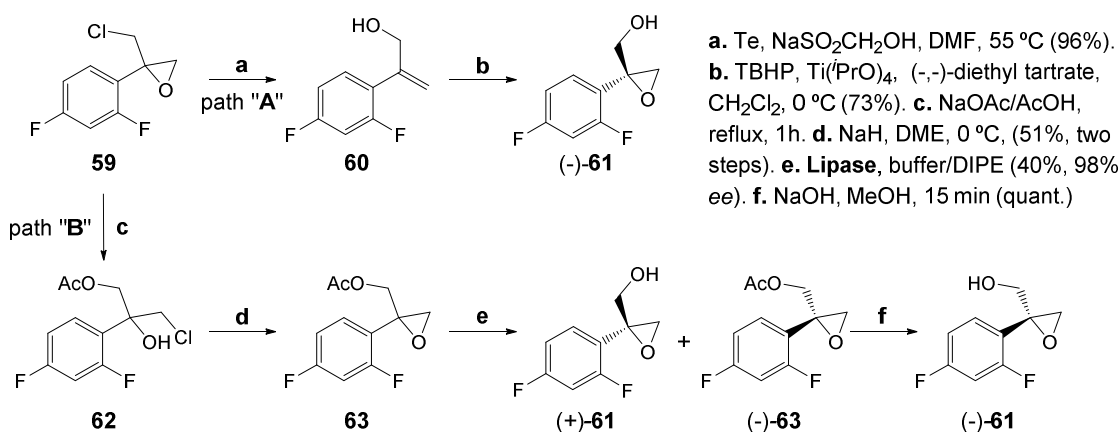
More recently, another chemoenzymatic strategy was adopted by Brenna and co-workers to prepare genaconazole.⁸³ Thus, a lipase-catalyzed kinetic resolution by acetylation of a triol precursor *syn*-**56** was conducted with high level of enantio- and stereoselection (99% *ee*, 99% *de*) using PS lipase in MTBE. The obtained enantiopure diacetate derivative (*R,R*)-**57** was converted into the corresponding epoxy triazole precursor (*R,S*)-**54** and the sulfone moiety was set up at the end of the sequence to give access to **55** (Scheme 18).

In the early 90's, Murakami and Mochizuki patented a versatile enantioconvergent synthetic procedure for the synthesis of antifungal agent D0870 (**58**) employing both metal- and enzyme-catalysis to selectively obtain the suitable chiral precursors.⁸⁴ This is particularly appealing since the mentioned drug has displayed

interesting activity in fluconazole-resistant candidiasis (among other important mycosis). The enzymatic procedure (Scheme 19, path B), became as an alternative to the traditional Sharpless' asymmetric epoxidation of the corresponding allylic alcohol **60** (Scheme 19, path A). Thus, 20 g of racemic epoxide **63** were treated with a lipase in a mixture of buffer and DIPE to obtain both alcohol **61** and remaining acetate **63** in enantioenriched form.



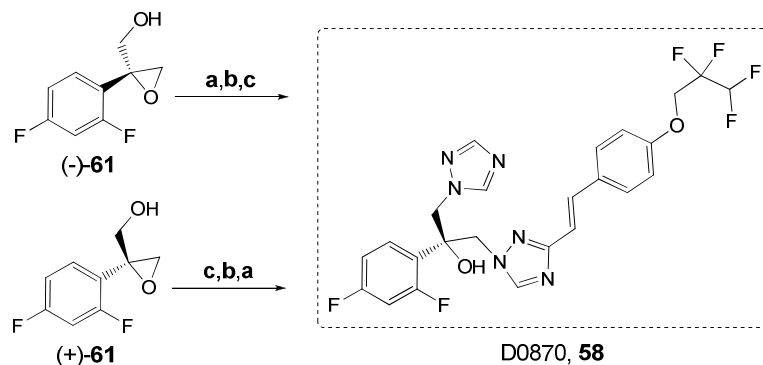
Scheme 18. Lipase-catalyzed kinetic resolution as key feature for the synthesis of enantioenriched genaconazole.



Scheme 19. Enantioselective metal-based (path A) and enzyme-based (path B) catalytic preparation of both enantiomers of chiral precursor **61**.

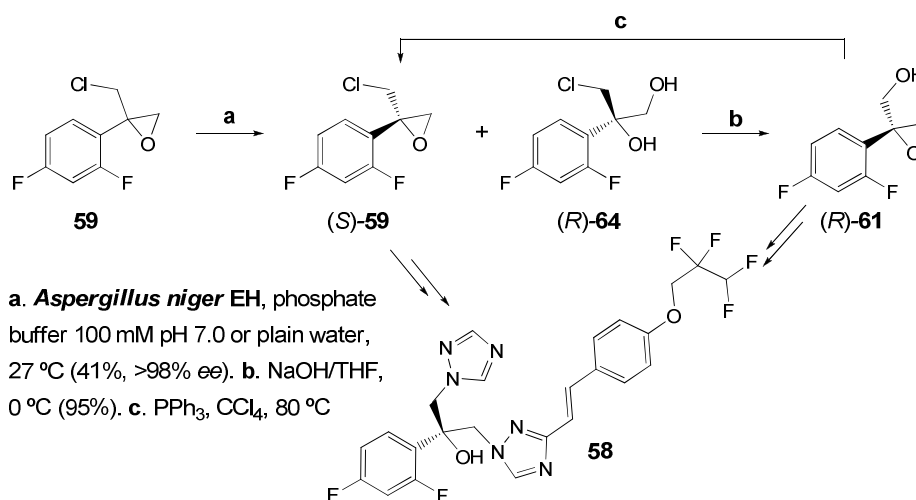
A remarkable feature of this strategy is that both enantiomers of epoxide **61** may be applied for the enantioconvergent preparation of the configurationally-desired D0870 by undertaking different synthetic pathways (*i.e.*, changing the sequence of the 1,2,4-triazole-containing substituents linkage, Scheme 20). Likewise, the intrinsic limitation of 50% maximum theoretical yield can be overcome.

On the other hand, Furstoss *et al.* developed a productive methodology for the synthesis of a chiral precursor of the antifungal agent D0870 with high optical purity (>98% ee).⁸⁵ In this epoxide hydrolase (EH)-based approach (Scheme 21), the kinetic resolution of racemic epoxide **59** *via* hydrolysis was developed using *Aspergillus niger* EH in phosphate buffer 100 mM pH 7 at 27 °C. Additionally, the authors reported a scaling-up of the optimized procedure in a two-phase system with similar results at high substrate concentration (500 g/L) and employing plain water instead of a buffered medium, being the substrate itself the second phase.⁸⁶ Moreover, the reacting enantiomer **64** could be cyclized again affording epoxide **61**, which, in a subsequent step, was converted into (*S*)-**59** overcoming the 50% limitation of the KR process.



a. 1,2,4-Triazole, K_2CO_3 , reflux, 48 h (48% upper sequence, 35% lower sequence). b. MsCl, TEA, Et_2O , rt, 1 h, then NaH, rt, 4 h (87.5% upper sequence, 65% lower sequence). c. 3-Styryl-1,2,4-triazole, K_2CO_3 , 90 °C, 1 h (19% upper sequence, 37% lower sequence)

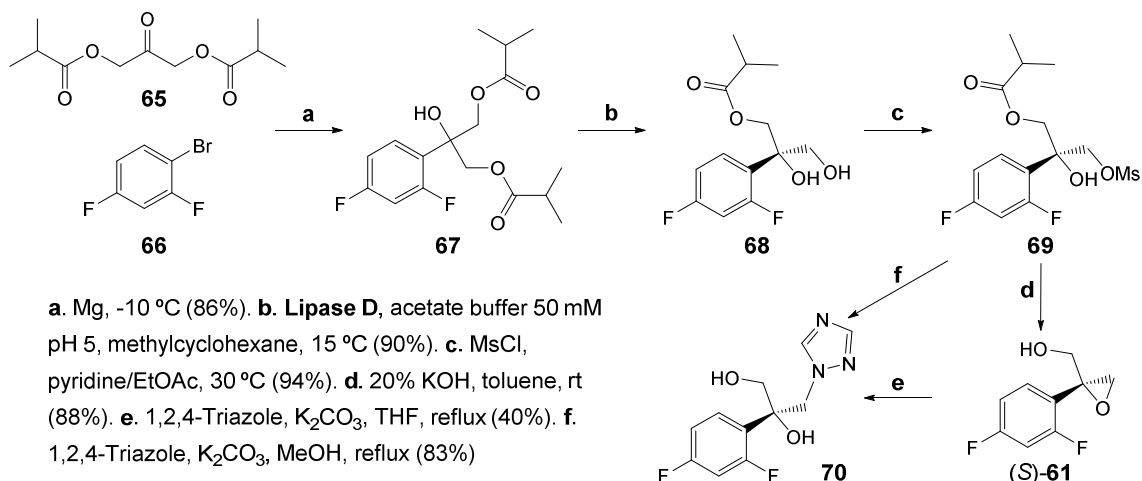
Scheme 20. Enantioconvergent strategy for the synthesis of D0870.



a. *Aspergillus niger* EH, phosphate buffer 100 mM pH 7.0 or plain water, 27 °C (41%, >98% ee). b. NaOH/THF, 0 °C (95%). c. PPh_3 , CCl_4 , 80 °C

Scheme 21. Enantioselective synthesis of a precursor of **58** employing an EH-mediated KR.

Yasohara *et al.* reported a lipase-based protocol to obtain the key precursor **61** in high optical purity (Scheme 22).⁸⁷ Interestingly, the aforementioned 50% maximum theoretical yield could be efficiently circumvented by enzymatic desymmetrization of the corresponding prochiral diester analogue **67** mediated by lipase D from *Rhizopus delemere* in a mixture of acetate buffer 50 mM pH 5 and methylcyclohexane at 15 °C.

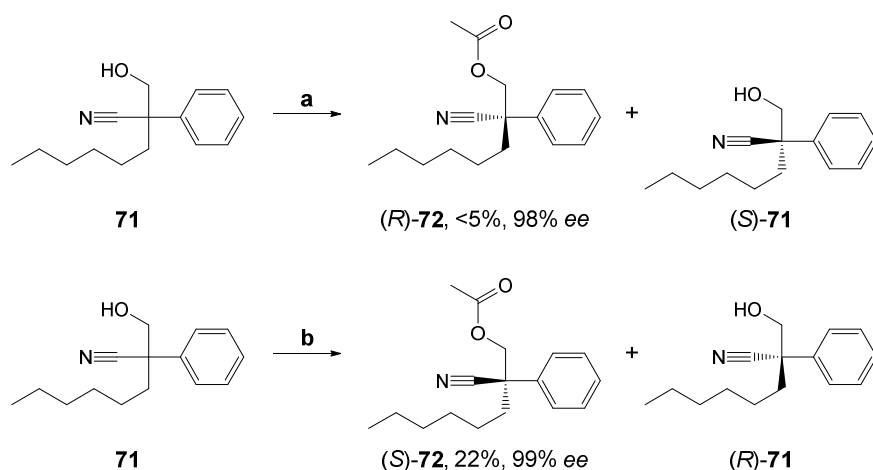


a. Mg, -10 °C (86%). b. Lipase D, acetate buffer 50 mM pH 5, methylcyclohexane, 15 °C (90%). c. MsCl, pyridine/ $EtOAc$, 30 °C (94%). d. 20% KOH, toluene, rt (88%). e. 1,2,4-Triazole, K_2CO_3 , THF, reflux (40%). f. 1,2,4-Triazole, K_2CO_3 , MeOH, reflux (83%)

Scheme 22. *Rhizopus delemere* lipase D-catalyzed desymmetrization for the preparation of D0870 precursor **70**.

In a preparative experiment (starting from 93 g of **67**), **68** was obtained in 90% yield and 96.7% *ee*. This was possible selecting the proper acyl group in the ester moiety, thus preventing the racemization of the obtained monoester **68** by acyl migration. An exhaustive hydrolase and co-solvent screening was earlier reported for the enzymatic synthesis of **68** in high optical purity.⁸⁸ Moreover, chiral intermediate **68** was transformed into the desired 1,2,4-triazole derivative **70** using two different chemical routes (Scheme 22).

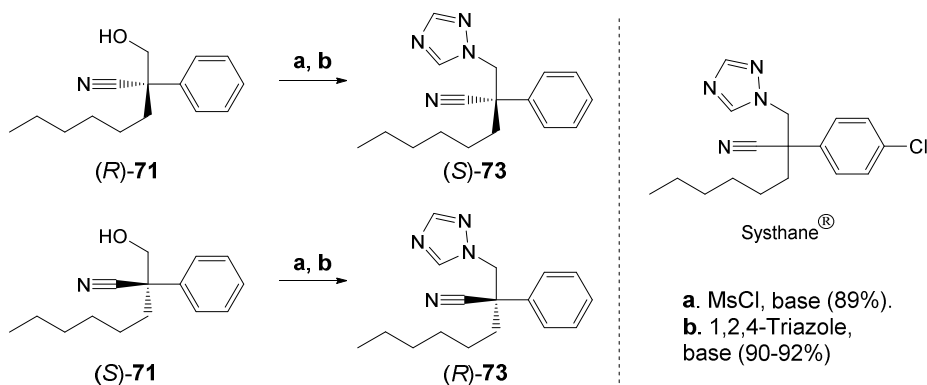
Another valuable 1,2,4-triazole-derived compound is the widely employed fungicide Systhane[®], a useful systemic agent for crop protection that selectively affects the fungal development by inhibition of ergosterol biosynthesis. In 2000, Cheong and co-workers established an enzymatic methodology to prepare a dechlorinated Systhane[®] analogue (Scheme 23).⁸⁹



a. *Candida rugosa* lipase, vinyl acetate (1 equiv.), *n*-hexane, 32 °C (3 cycles). **b.** *Pseudomonas fluorescens* lipase Amano AK, vinyl acetate (1 equiv.), *n*-hexane, 32 °C

Scheme 23. Enantiocomplementary lipase-catalyzed kinetic resolution strategies to synthesize both **71** enantiomers.

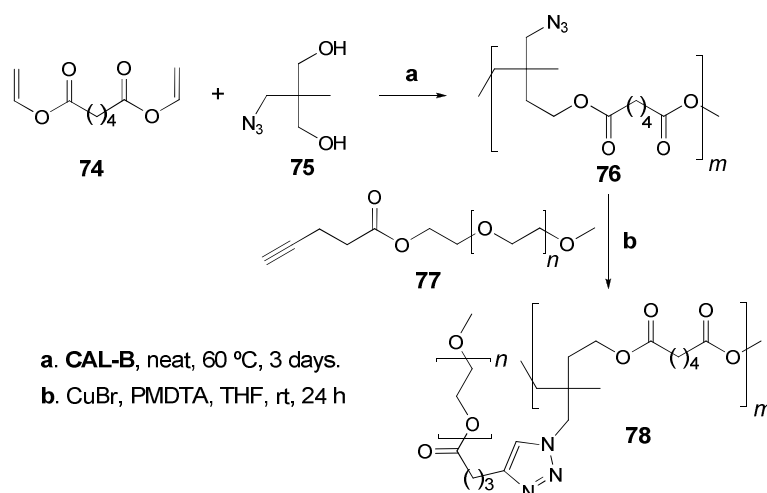
Interestingly, for the resolution of γ -hydroxynitrile **71**, it was possible to find two enantiocomplementary lipases (from *Candida rugosa* and *Pseudomonas fluorescens*, Amano AK) leading selectively to both enantiomers [(*S*)-**71** (99% *ee*) employing CRL and (*R*)-**71** (98% *ee*) with Amano AK]. It must be noted that for *C. rugosa* lipase, the enantioenriched product of the enzymatic reaction was submitted to two further enzymatic resolutions recycling product **72** in order to reach a higher optical purity.



Scheme 24. Synthesis of both enantiomers of a Systhane[®] analogue employing the enantioenriched intermediate previously obtained by enzymatic kinetic resolution.

When trying the *para*-chlorinated phenyl-substituted counterpart of **71**, the presence of the chlorine atom seemed to spoil the kinetic resolution by enzymatic acylation. Further, Systhane[®] analogue **73** was prepared in both enantiomeric forms by easy 1,2,4-triazole substitution of previously activated alcohol as mesylate (Scheme 24).

Regarding 1,2,3-triazoles, Kressler *et al.* efficiently developed a methodology employing an enzyme and metal-catalysis for the preparation of biodegradable polyester graft copolymers.⁹⁰ Likewise, by CAL-B-catalyzed polycondensation of divinyl adipate (**74**) and 2-(azidomethyl)-2-methylpropane-1,3-diol (**75**), the polyester backbone with the pendant azido group **76** was synthesized as a suitable coupling partner (M_n was 3100 g/mol and polydispersity of M_w/M_n was 1.6). Then, monoalkyne poly(ethylene oxide) **77** was coupled by Cu(I)-catalyzed [3+2] cycloaddition in the presence of *N,N,N',N',N'*-pentamethyldiethylene-triamine (PMDTA), thus rendering the expected graft copolymer **78** with $M_n=11,100$ g/mol and $M_w/M_n=2.1$ (Scheme 25). These polyester copolymers may find utility in biomedicine owing to their easy biodegradation and excretion.

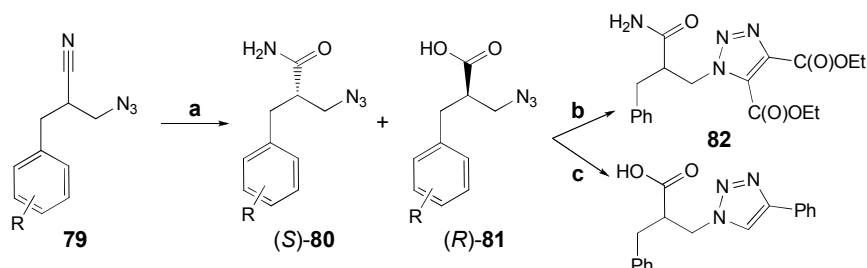


Scheme 25. Graft copolymer preparation by enzymatic polycondensation followed by CuAAC.

By employing bacterial whole cells naturally expressing both nitrile hydratase and amidase enzymes, Wang and co-workers set up a hydrolytic kinetic resolution of a series of diversely substituted azido nitriles (**79**) in phosphate buffer 100 mM pH 7 at 30 °C, thus obtaining the corresponding enantioenriched azido carboxamides (*S*)-**80** (in yields ranging from 41 to 50% and enantioselectivities up to >99% *ee*) and azido carboxylic acids (*R*)-**81** (in yields ranging from 40 to 58% and enantioselectivities up to >99% *ee*, Table 4), resembling a parallel kinetic resolution.⁹¹ Further, the aforementioned chiral compounds were transformed by classical methods into 1,2,3-triazole carboxamides/carboxylic acids **82** in high yields (from 90% to quantitative). The triazole moiety was achieved either by thermal or Cu-catalyzed cycloaddition (Scheme 26).

Recently, Zhao *et al.* reported a practical methodology for the synthesis of triazole-containing nucleoside analogues.⁹² In this case, starting from 0.6 g of peracetylated sugar **83**, *Candida rugosa* lipase successfully catalyzed the regioselective deacetylation of the primary alcohol to form **84** in 65% yield after 3 hours in phosphate buffer 100 mM pH 7, in order to build up the phosphate group later. Once obtained the azido phosphate sugar **85**, the 1,2,3-triazole core was constructed with different substituents by employing the CuAAC reaction affording nucleotides **86** (Scheme 27). The obtained nucleotide analogues were

screened as inhibitors of the *E. coli* NAD-dependent malic enzyme, a highly active protein whose mammalian homologous enzyme can increase in fast proliferating cells and tumors. The results suggested that the 1,2,3-triazole analogues were similar to ATP in their inhibition ability.



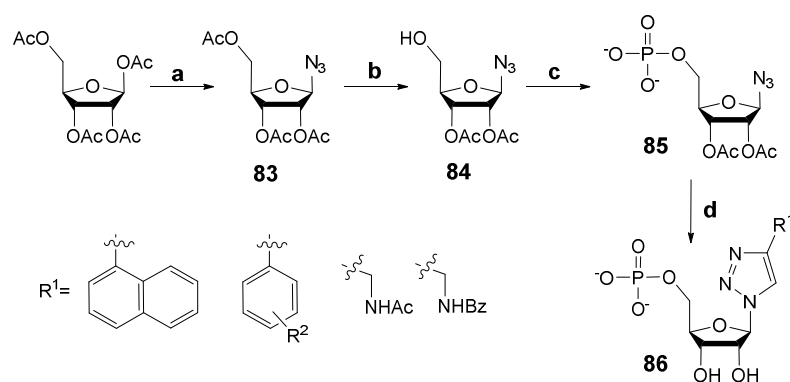
a. *Rhodococcus erythropolis* AJ27060, phosphate buffer 100 mM pH 7.0, 30 °C. **b.** (COOEt)₂C₂, EtOH, reflux, 12 h. **c.** Phenylacetylene, CuSO₄/vit. C, ^tBuOH/H₂O, rt, 2 h

Scheme 26. Chiral 1,2,3-triazole carboxylic acid derivatives (**82**) prepared *via* nitrile hydratase-amidase-cycloaddition sequence.

Table 4. Comparison of the different substitution pattern on the aromatic ring for the nitrile hydratase-amidase sequence.

Entry	Substitution	Conditions ^a	80 (%) ^b	<i>ee</i> (%)	81 (%) ^b	<i>ee</i> (%)
1	C ₆ H ₅	2 mmol, 3.5 h	48	>99.5	49	96.2
2	4-OMe-C ₆ H ₄	2 mmol, 1 h	47	>99.5	48	94.0
3	4-Me-C ₆ H ₄	2 mmol, 4.5 h	48	97.2	49	>99.5
4	4-F-C ₆ H ₄	2 mmol, 4 h	48	>99.5	47	>99.5
5	4-Cl-C ₆ H ₄	2 mmol, 3.5 h	48.5	86.7	44	93.2
6	3-Cl-C ₆ H ₄	2 mmol, 24 h	54	81.2	40	>99.5
7	3-Cl-C ₆ H ₄	1 mmol, 6 h	50	>99.5	47	94.8
8	2-Cl-C ₆ H ₄	2 mmol, 20.5 h	48.5	97.3	48	>99.5
9 ^c	4-Br-C ₆ H ₄	2 mmol, 4.5 h	41.5	93.5	40	95.3
10	4-Br-C ₆ H ₄	1 mmol, 2 h	47	>99.5	46.5	93.6
11 ^d	C ₆ H ₅	12 mmol, 5 h	48	>99.5	51	97.4

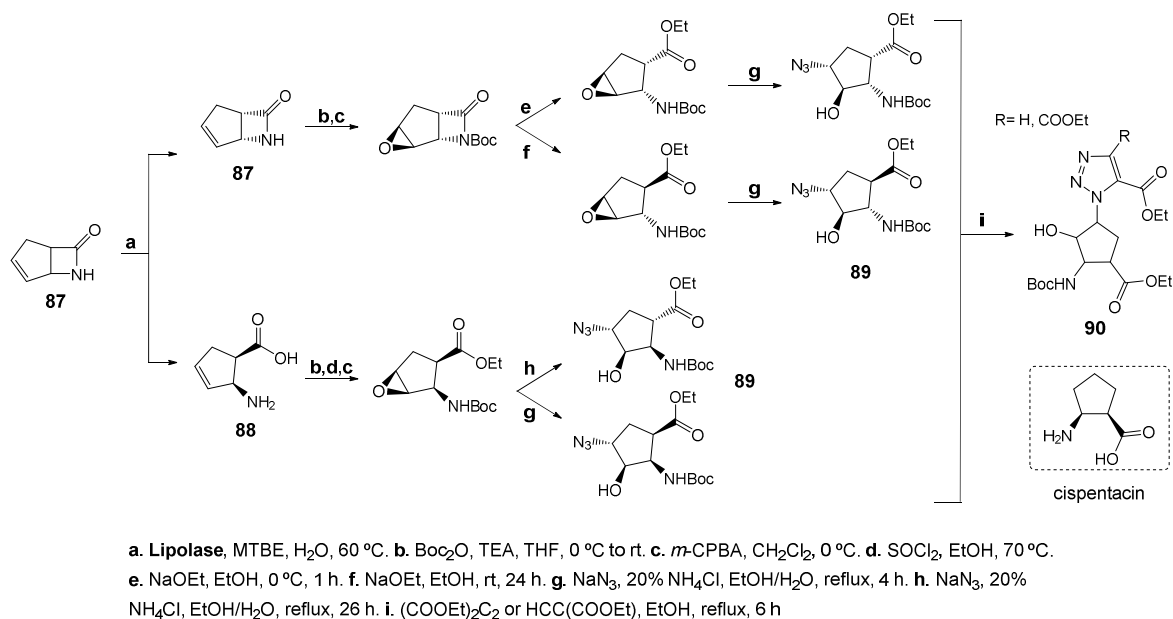
^a*Rhodococcus erythropolis* AJ270 cells (2 g wet weight) in phosphate buffer (50 mL, pH 7.0) at 30 °C. ^bIsolated yield. ^cNitrile (~20%) was recovered. ^dA suspension of *Rhodococcus erythropolis* AJ270 cells (12 g wet weight) in phosphate buffer (300 mL, pH 7.0) at 30 °C.



a. TMSN₃, SnCl₄, CH₂Cl₂, rt (quant.). **b.** Lipase (Sigma), phosphate buffer 100 mM pH 7, DMF, 37 °C (65%). **c.** POCl₃, TEA, THF, 0 °C to rt. **d.** Alkyne, CuSO₄/vit. C, MeOH/H₂O, reflux, 24 h. Then, column chromatography, 60% ^tPrOH/aqueous ammonia as eluent (83-96%, 2 steps)

Scheme 27. Nucleotide analogues **86** containing diversely substituted 1,2,3-triazoles as base featuring lipase-catalyzed regioselective deacetylation as the key step.

In the synthesis of cispentacin analogues, Fülöp *et al.* have successfully exploited the excellent enantioselectivity of Lipolase (*Candida antarctica* lipase B heterologously expressed in *Aspergillus oryzae* and adsorbed in a macroporous resin),⁹³ in the hydrolytic kinetic resolution of unsaturated bicyclic β -lactam **87** (4 g-scale), giving access to enantioenriched amino acid **88** in 48% yield and 98% *ee* and the remaining enantioenriched lactam **87** in 47% yield and 99% *ee*.⁹⁴ Likewise, highly substituted enantioenriched cyclopentane amino carboxylate derivatives were constructed and the azido group introduced by oxirane ring opening (**89**). At a later stage, 1,2,3-triazole moiety was built up by thermal Huisgen [3+2] cycloaddition employing (di)ethyl acetylene (di)carboxylate as coupling partner affording final derivatives **90** (Scheme 28).



Scheme 28. Enantio- and diastereoselective chemoenzymatic pathway toward the preparation of cispentacin analogues starting from an unsaturated bicyclic β -lactam.

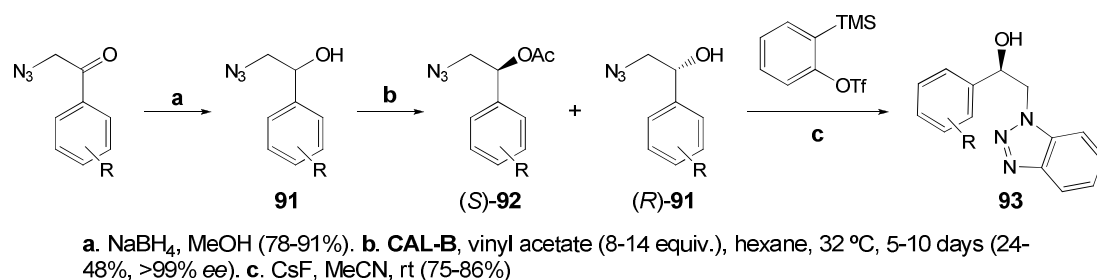
As an extension of the previous work,^{94b} a similar strategy was conducted starting from the racemic Vince lactam (6 g-scale). So, 1,2,3-triazole containing rigid amino esters with the cyclopentane skeleton were synthesized with an enzymatic hydrolytic kinetic resolution as the key feature displaying high enantioselectivity (>99% *ee*).

Recently, Jeller and co-workers reported the synthesis of potentially bioactive chiral benzotriazoles by chemoenzymatic methods.⁹⁵ Thus, starting from the suitable racemic β -azido alcohols **91**, enantioselective lipase-catalyzed acylations permitted the kinetic resolution obtaining both substrate and product (**92**) with high *ee* (>99% in most cases, Table 5).

Table 5. Enzymatic resolution of (\pm)- β -azido phenylethanols **91** using vinyl acetate and immobilized CAL-B in hexane.

Entry	Substitution	91 (%)	<i>ee</i> (%)	92 (%)	<i>ee</i> (%)	<i>E</i>	t (d)
1	C ₆ H ₅	48	>99	48	>99	>200	5
2	4-OMe-C ₆ H ₄	44	>99	45	>99	>200	5
3	4-Br-C ₆ H ₄	55	70	38	>99	>200	10
4	4-Cl-C ₆ H ₄	46	>99	48	>99	>200	7
5	4-NO ₂ -C ₆ H ₄	65	49	24	>99	>200	10

The obtained enantioenriched azido derivatives reacted with *in situ*-formed benzine in order to prepare the desired enantiopure benzotriazoles **93** upon activation with CsF (Scheme 29).



Scheme 29. Preparation of chiral hydroxy benzotriazole derivatives **93** by lipase-catalyzed resolution and azide-aryne [3+2] cycloaddition.

3.2. Using oxidoreductases

Since prochiral ketone reduction may provide maximum 100% theoretical yield of the desired chiral alcohol, ketoreductases surpass hydrolases when chiral *sec*-alcohols are the target. The β -hydroxytriazole core is particularly interesting, not only due to its action as a promising pharmacophore,⁹⁶ but also as β -adrenergic receptor blocker and potential imaging agent.⁹⁷ As an example, an alcohol dehydrogenase-based approach was developed by Hua *et al.* for the synthesis of enantioenriched β -azido alcohols **91** (Table 6, 80–95% yield, >98% ee) and their application toward the synthesis of β -adrenergic receptor blocker analogues **94** by CuAAC reaction with suitable coupling partners (Scheme 30).⁹⁸ It is worth noting that both enantiomers could be achieved since stereocomplementary ADHs [from *Candida magnoliae* (CMCR) and *Saccharomyces cerevisiae* (Ymr226c)] were found displaying excellent selectivity in phosphate buffer 100 mM pH 7. The NADPH cofactor was recycled by using the glucose dehydrogenase (GDH)/glucose system.

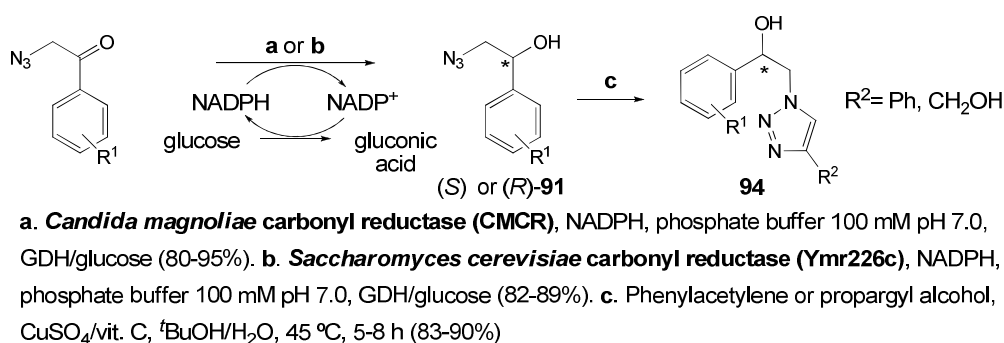
Table 6. ADH-catalyzed reduction of α -azido acetophenones to stereoselectively obtain β -azido alcohols **91**.^a

Entry	Substitution	CMCR			Ymr226c		
		t (h)	Yield (%)	ee (%)	t (h)	Yield (%)	ee (%)
1	C ₆ H ₅	24	92	99 (<i>S</i>)	24	89	>99 (<i>R</i>)
2	4-F-C ₆ H ₄	24	93	>99 (<i>S</i>)	24	84	>99 (<i>R</i>)
3	2,4-F ₂ -C ₆ H ₃	24	90	>99 (<i>S</i>)	24	82	>99 (<i>R</i>)
4	4-Cl-C ₆ H ₄	24	92	>99 (<i>S</i>)	32	85	>99 (<i>R</i>)
5	4-Br-C ₆ H ₄	24	88	98 (<i>S</i>)	24	84	>99 (<i>R</i>)
6	4-Me-C ₆ H ₄	24	85	99 (<i>S</i>)	96	87	>99 (<i>R</i>)
7	4-OMe-C ₆ H ₄	24	88	99 (<i>S</i>)	240	5 ^b	-
8	3-OMe-C ₆ H ₄	24	95	99 (<i>S</i>)	240	19 ^b	>99 (<i>R</i>)
9	4-NO ₂ -C ₆ H ₄	24	84	99 (<i>S</i>)	216	10 ^b	63 (<i>R</i>)
10	3-NO ₂ -C ₆ H ₄	24	82	99 (<i>S</i>)	120	85	>99 (<i>R</i>)
11	4-CN-C ₆ H ₄	24	80	99 (<i>S</i>)	240	<1 ^b	-

^aReactions were performed starting from 170 mg of substrate. ^bDetermined by HPLC, yields were not isolated.

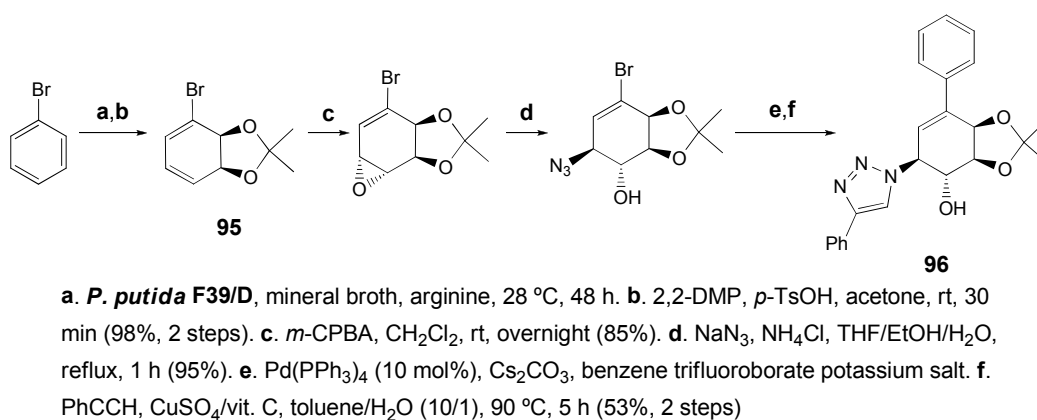
Another class of redox enzymes that has shown great versatility although not commonly found in literature is the dioxygenase family. These enzymes catalyze oxidative reactions introducing both oxygen atoms in the substrate molecule directly from dioxygen. In particular, one of the most popular reactions

catalyzed by them is the stereoselective *syn*-dihydroxylation with concomitant dearomatization of arene substrates.⁹⁹



Scheme 30. Chiral β -adrenergic receptor blocker analogues obtained by stereoselective ADH-catalyzed hydrogen transfer reaction followed by Cu-catalyzed cycloaddition.

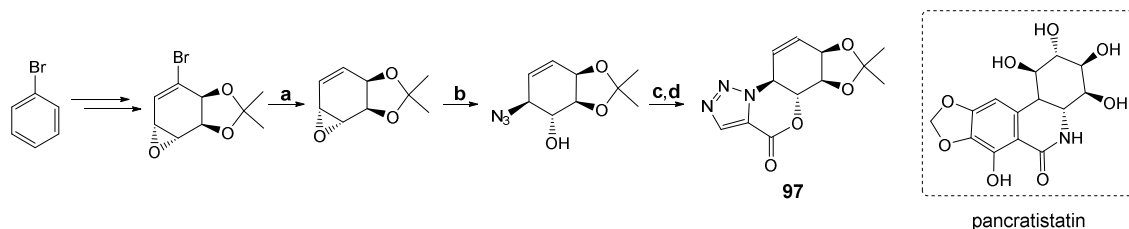
Concerning 1,2,3-triazole derivatives, Gonzalez *et al.* have taken advantage of the aforementioned reaction to obtain enantiopure dienediols as chiral scaffolds for different synthetic purposes. In this line, for the synthesis of conduritol analogues **96**, properly protected enantiopure homochiral dienediol **95**, obtained by aerobic oxidation of bromobenzene (2 g/L) by *Pseudomonas putida* F39/D whole cells, was subjected to several transformations involving some of them transition metal-catalysis (a Huisgen [3+2] cycloaddition and a Suzuki-Miyaura cross-coupling), thus providing great chemical diversity (Scheme 31) in a straightforward manner.¹⁰⁰



Scheme 31. Conduritol analogues **96** constructed from a bacterial metabolite and a combination of different metal-catalyzed reactions.

Later on, by following a similar sequence, more complex conduritol analogues were built up by reacting the suitably protected chiral azido alcohol with the benzene 1,4- or 1,3-diyne coupling partner in a CuAAC reaction.¹⁰¹ The obtained bistriazole-derived compounds were biologically evaluated and displayed interesting antifungal capacities.

To synthesize more complex compounds such as pancratistatin analogues, a similar chemistry rendered outstanding achievements, as demonstrated by Hudlicky and co-workers more than ten years ago.¹⁰² More recently, by combining biocatalysis, metal-catalysis and traditional chemistry, Gonzalez *et al.* constructed tri- and tetracyclic molecules with four defined stereocenters (**97**), resembling the structure of natural phenantridone alkaloids.¹⁰³ The early radical debromination was a key factor for the overall route success (Scheme 32).



a. Bu_3SnH , ABCC, THF, reflux, 4 h. b. NaN_3 , NH_4Cl , THF/EtOH/ H_2O , reflux, 1 h. c. Propiolic acid, DCC, DMAP, CH_2Cl_2 , 0 °C to rt. d. Toluene, reflux, 24 h (56%, from step b)

Scheme 32. Chemoenzymatic strategy for the synthesis of pancratistatin-like triazole derivatives.

3.3. Using transferases

Very recently,¹⁰⁴ two different enzymatic preparations from peach kernel meal and apple seed meal were used to perform reverse hydrolysis or transglycosylation reactions. Using glucose as donor, several alkynyl alcohols and azido-containing alcohols were employed as substrates. Both preparations exhibited relatively broad substrate scope. They were able to accept terminal and internal alkynyl alcohols and several azido alcohols (Table 7). It seemed that azido derivatives had very low toxicity to the glycosidases. In spite of the wide substrate scope, conversions did not exceed 53% in any case after 72 hours.

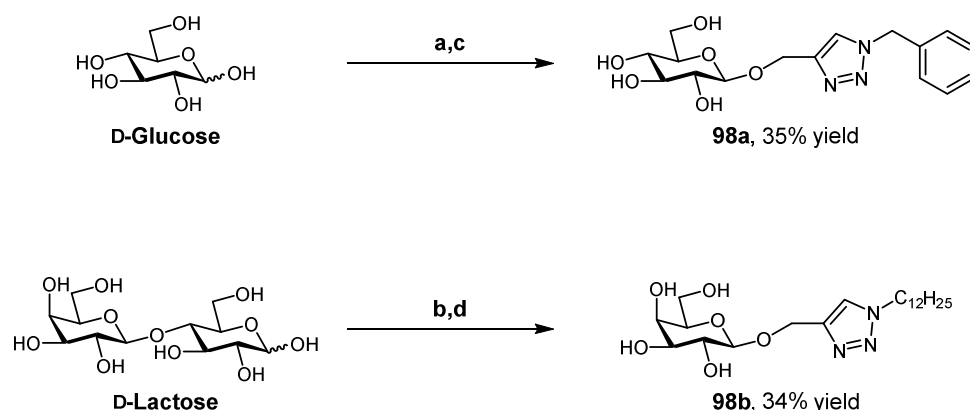
Table 7. Synthesis of β -glucosides using fruit kernel meal by reverse hydrolysis and β -galactosides using β -galactosidase by transglycosylation with several alcohols.

Entry	Substrate	Sugar	Yield (%) ^a		Sugar	Yield (%) ^b
			Peach kernel	Apple seed		β -Galactosidase
1			32	35		36
2			30	31		18
3			17	18		17
4 ^c		glucose	31	27	lactose	21
5			39	45		12
6			53	51		16
7			n.r.	n.r.		6

^a72 h at 50 °C in a mixture $\text{H}_2\text{O}:\text{CH}_3\text{CN}$ (1:9) using 10–30 equivalents of substrate. ^bIn phosphate buffer 20 mM pH 4.5 for 4–24 h at 25 °C. ^cUsing *tert*-butyl alcohol as co-solvent.

The enzymatic glycosidation with lactose was also studied using a commercial β -galactosidase from *Aspergillus oryzae*, affording the corresponding β -galactosides in low yields (up to 36% after 24 hours, Table 7). After isolation of the alkynyl/azido sugar, the [3+2] cycloaddition with several azido/alkynyl compounds achieved near complete conversion and high isolated yield (>85%) towards the corresponding triazole derivatives. Finally, to carry out the sequential one-pot transformation, the reaction crude was

filtered and concentrated after the enzymatic glycosylation. Then, the corresponding coupling substrate was added in the presence of Cu(II) acetate and copper powder in a 1:1 mixture of *tert*-butyl alcohol and water, providing the triazole-derived sugars **98** with moderate yields after 4–24 hours (Scheme 33).



a. *P. persica* kernel meal or *M. pumila* (apple) seed meal, D-glucose (1 equiv.), propargyl alcohol (6.5–25 equiv.), water/MeCN (1:9 v/v), 50 °C, 72 h. **b.** β -Galactosidase from *A. oryzae*, D-lactose (1 equiv.), propargyl alcohol (1.2 equiv.), sodium acetate buffer 20 mM pH 4.5, 25 °C, 4 h. **c.** Copper(II) acetate, copper powder, glycoside (1 equiv.), benzyl azide (1.5 equiv.), ^tBuOH:H₂O (1:1 v/v), rt, 4–24 h. **d.** Copper(II) acetate, copper powder, glycoside (1 equiv.), dodecyl azide (1.5 equiv.), ^tBuOH:H₂O (1:1 v/v), rt, 4–24 h

Scheme 33. Synthesis of triazole-containing glycosides coupling enzymatic reverse hydrolysis (top) or transglycosylation (bottom) and CuAAC reactions.

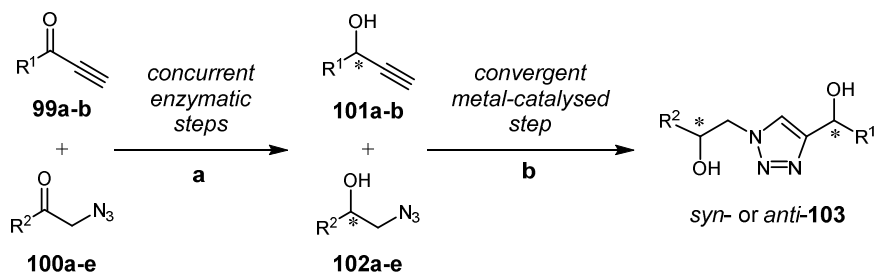
4. Novel approaches based on cascade or tandem protocols

Driven by the need of enhancing the atom economy of chemical transformations, continuous efforts have been focused on the development of (bio)catalytic methods that combine two or more processes in a one-pot multi-step sequential or cascade fashion. Undoubtedly, these transformations present several advantages such as the use of less reagents and solvents, the production of less waste, and also significant time-savings. Moreover, one-pot multi-step protocols avoid the purification of intermediates and decrease the number of operational steps.¹⁰⁵ Recently, many efforts have been pursued to integrate the 1,3-dipolar cycloaddition of azides and alkynes in one-pot or cascade multi-step processes. In this Section, several examples for the preparation of complex molecules *via* enzymatic cascade or sequential approaches will be presented where one step comprises the formation of 1,2,3-triazole derivatives.

Alcohol dehydrogenases, responsible for the stereoselective reduction of carbonylic compounds, are one of the most employed enzymes in this kind of multi-step processes. A recent example shown by Omiro *et al.* made use of plant cell cultures and plant pieces as biocatalysts to reduce prochiral ketones.¹⁰⁶ *Daucus carota* (carrot root) was employed to reduce various substituted acetophenones with an azido group. The biotransformation was carried out in distilled water using fresh carrot cut into thin slices at room temperature, obtaining the *S*-alcohol products with excellent enantioselectivities (>99%) but with moderate isolated yields after few days (4 to 7). Subsequent Cu(I)-catalyzed cycloaddition with alkyne derivatives was performed to afford the enantiopure 1,2,3-triazole alcohols as single products. Although the one-pot protocol was investigated, the cyclization process proceeded faster than the bioreduction avoiding the transformation of the ketone substrate, so the synthesis was performed in a stepwise procedure.

A remarkable example of coupling biocatalysis and CuAAC was recently reported by Gotor and co-workers.¹⁰⁷ A one-pot two-step fully convergent strategy was envisaged where, starting from two achiral

compounds, a pair of suitable chiral precursors could be stereoselectively formed and then assembled *via* CuAAC reaction, giving rise to a single compound bearing two stereocenters (Scheme 34). The influence of different alkynones (**99a,b**) and α -azido ketones (**100a–e**) with aliphatic or aromatic groups was studied using ADHs with stereocomplementary behavior. ADH-A from *Rhodococcus ruber* overexpressed in *E. coli* and LBADH from *Lactobacillus brevis* provided quantitative conversions and excellent *ee* to the corresponding alcohols **101** and **102** in phosphate buffer 50 mM pH 7.5 using 2-propanol (5% v/v) as co-substrate to recycle the nicotinamide cofactor.



a, R¹ = CH₃; **b**, R¹ = (CH₂)₄CH₃

a, R² = C₆H₅; **b**, R² = 2-Np; **c**, R² = (CH₂)₅CH₃; **d**, R² = 4-NO₂-C₆H₄; **e**, R² = 4-OH-C₆H₄

a. ADH-A or LBADH, phosphate buffer 50 mM pH 7.5, 1 mM NAD(P)H, 2-propanol (5% v/v), **99** (1 equiv.), **100** (1 equiv.), 30 °C, 24 h. **b**. Cu wire, CuSO₄ (aq.), 60–80 °C, 24 h

Scheme 34. One-pot chemoenzymatic protocol to synthesize enantioenriched 1,2,3-triazole-derived diols. Np means naphthyl.

Later, the Cu-catalyzed 1,3-cycloaddition reaction was studied finding that comproportionation using a Cu wire with a catalytic amount of CuSO₄ at 60–80 °C was a very simple and economic system to provide Cu(I). Moreover, the Cu(0)-precatalyst could be easily removed and remained active after several cycles. In a final stage, the fully convergent chemoenzymatic approach was achieved furnishing the 1,2,3-triazole-derived diols *syn*- or *anti*-**103** in good yields and with excellent selectivities (Table 8).

Table 8. Examples of 1,2,3-triazole-derived diols synthesized coupling a bioreduction with a CuAAC.

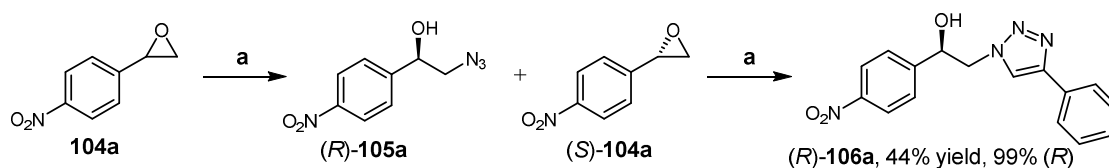
Entry	Structure	Enzyme	R	Product	Yield ^a (%)	<i>ee</i> ^b (%)	<i>de</i> (%)
1			Ph	(<i>R,S</i>)- 103aa	69	99	96
2		<i>E. coli</i>	2-Np	(<i>R,S</i>)- 103ab	82	99	96
3		ADH-A ^c	C ₆ H ₁₃	(<i>R,S</i>)- 103ac	71	99	96
4			4-NO ₂ -Ph	(<i>R,S</i>)- 103ad	78	99	96

5		<i>E. coli</i>	Ph	(<i>R,R</i>)- 103ba	78	99	98
6		ADH-A ^c	2-Np	(<i>R,R</i>)- 103bb	73	99	98
7			C ₆ H ₁₃	(<i>R,R</i>)- 103bc	85	99	98

8			C ₆ H ₁₃	(<i>S,S</i>)- 103bc	82	99	99
9		LBADH	4-NO ₂ -Ph	(<i>S,S</i>)- 103bd	71	99	99

^aIsolated yields are relative to the diastereoisomeric mixture of the final diols. ^b*Ee* values correspond to the major diastereoisomer obtained. ^c*E. coli* means that the enzyme is overexpressed in *E. coli*.

Feringa and co-workers¹⁰⁸ reported an innovative one-pot chemoenzymatic process (Scheme 35), using a halohydrin dehalogenase from *Agrobacterium radiobacter* (HheC). In a first step the biocatalytic azidolysis of racemic aromatic epoxides was achieved through kinetic resolution. The best results were obtained using 2-(4-nitrophenyl)oxirane (**104a**) as substrate. In that case, the reaction with HheC afforded the azido alcohol (*R*)-**105a** with 99% *ee* after 24 hours in phosphate buffer 50 mM pH 7.5. Once optimized the biocatalytic conditions, the [3+2] cycloaddition was studied. The catalyst loading and the scope of the alkyne derivatives were investigated obtaining the best results to form **106a** using 5 mol% of the Cu(I)-catalyst (CuSO₄ plus vitamin C) in the presence of MonoPhos as ligand and 2 equivalents of phenylacetylene (44% yield, 99% *ee* after 24 hours).



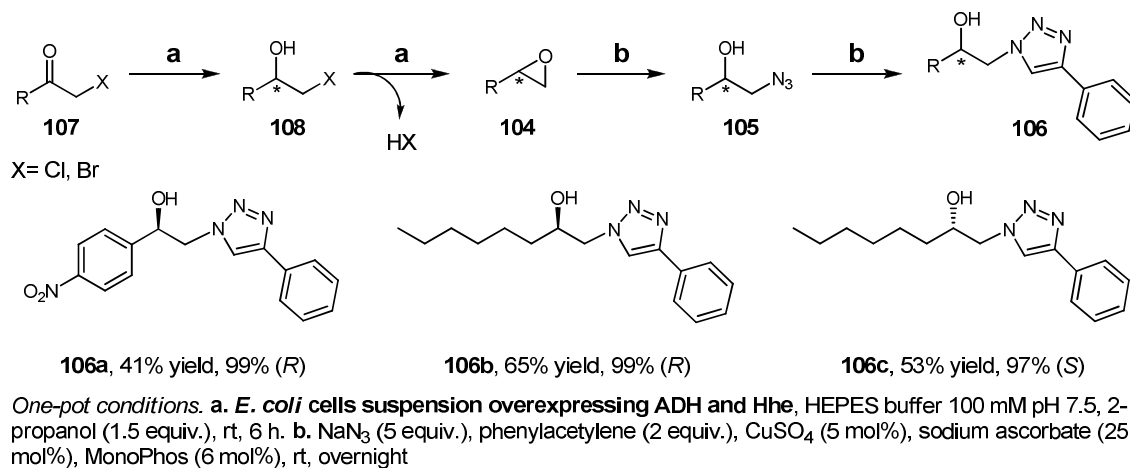
One-pot synthesis. a. Halohydrin dehalogenase HheC, phosphate buffer 50 mM pH 7.5, NaN₃ (0.6 equiv.), CuSO₄ (5 mol%), sodium ascorbate (25 mol%), MonoPhos (5.5 mol%), phenylacetylene (2 equiv.), rt, 24 h

Scheme 35. Chemoenzymatic one-pot tandem reaction coupling an epoxide ring-opening and a 1,3-dipolar cycloaddition.

This method did not allow exceeding the 50% of maximum theoretical yield. Hence, this was overcome in a more complex multi-step catalytic process using “designer cells”.¹⁰⁹ These engineered bacterial cells can overexpress one or more synthetically useful biocatalysts lowering the costs, as there is no need for expensive cofactors enhancing the stability of the enzyme. In this approach (Scheme 36), enantiopure β -hydroxytriazoles **106a–c** were efficiently prepared from simple α -halo ketones **107**, combining the use of “designer cells” and a CuAAC reaction. This biocatalytic tandem process incorporated four reactions: in a first step **107** was stereoselectively reduced to the halohydrin **108** with an ADH; secondly, **108** acted as substrate for a halohydrin dehalogenase which catalyzed the ring-closure towards epoxide **104** and the subsequent ring-opening by the azide anion, forming β -azido alcohol **105**. This compound was converted in the same vessel into the final β -hydroxytriazole **106** in a Cu(I)-catalyzed [3+2] dipolar cycloaddition reaction.

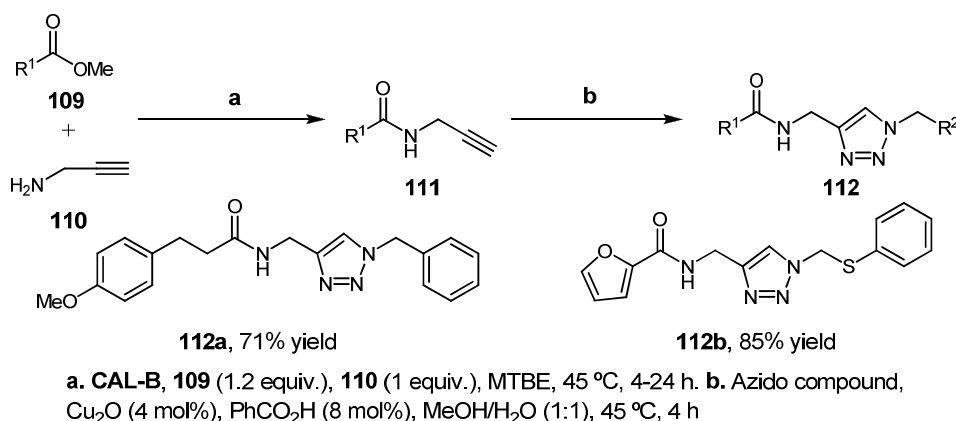
Both enzymes used in this cascade protocol were overexpressed together in the same host, making the process cheaper and applicable on a larger scale. Thus, stereocomplementary alcohol dehydrogenases from *Thermoanaerobacter* sp. (ADH-T) and LBADH were separately co-expressed with halohydrin dehalogenases HheC and from *Mycobacterium* sp. (HheBGP1), respectively. After reaction optimization, several azido alcohols were obtained with moderate isolated yield (35–70%) and excellent enantiomeric excess (96–99%) in HEPES buffer 100 mM pH 7.5, using 2-propanol in a slight excess (1.5 equiv.) as hydrogen donor and sodium azide (5 equiv.).

Then, they coupled in one-pot this system to the [3+2] cycloaddition reaction. After 6 hours of enzymatic bioreduction, sodium azide was added in the second step followed by the introduction of phenylacetylene and the necessary reagents to promote the CuAAC reaction after 30 minutes. With this tandem protocol, enantiopure β -hydroxytriazoles **106** were synthesized with moderate isolated yields (18–65%), indicating that the introduction of the fourth transformation in the same reaction vessel was feasible.



Scheme 36. Multicatalytic tandem process leading to enantiopure β -hydroxytriazoles.

Müller and co-workers¹¹⁰ reported the CAL-B-catalyzed aminolysis of methyl esters **109** with propargyl amine **110** furnishing the corresponding propargyl amides (**111**), which in a second step were consecutively transformed into the amido 1,2,3-triazoles **112** by Cu(I)-catalyzed 1,3-cycloaddition in good to excellent yields. A screening of six commercially available lipases revealed that only immobilized CAL-B on imobead[®] 150 or on an acrylic resin was able to catalyze the amidation reaction after 4–24 hours in MTBE at 45 °C (Scheme 37).

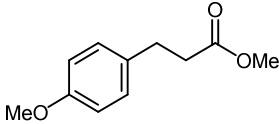
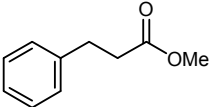
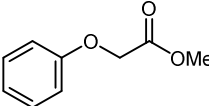
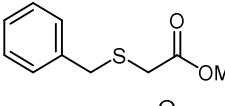
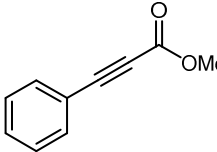
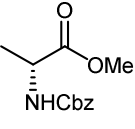
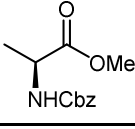


Scheme 37. One-pot sequential chemoenzymatic synthesis of 1,2,3-triazole-derived amides **112**.

The presence of different heteroatoms at α -position of the carbonylic moiety such as oxygen, sulfur and nitrogen was studied achieving high conversions (Table 9). Then, several factors were tuned for the CuAAC transformation, obtaining the best conditions with Cu₂O in the presence of benzoic acid as a bidentate Cu(I) stabilizing ligand in a 1:1 mixture of methanol/water at 45 °C. The sequential one-pot process was carried out with a wide substrate scope furnishing 1,2,3-triazoles **112** with good to high yields (51–85%) after 8–28 hours (Scheme 37).

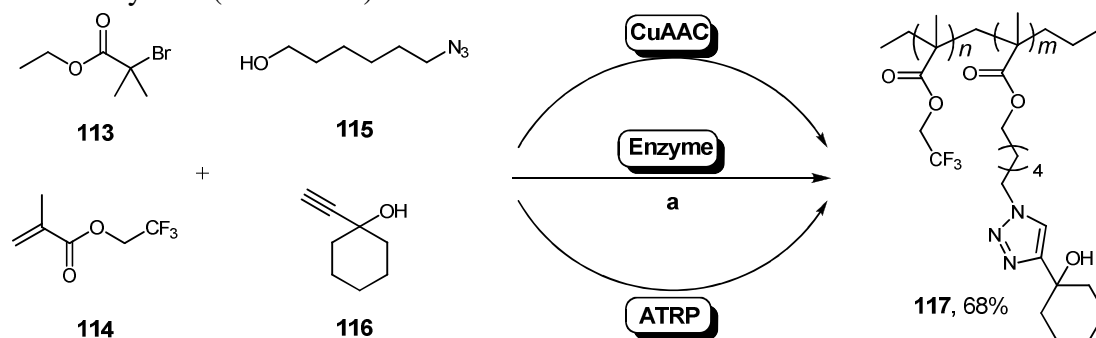
Recently, a one-pot strategy has also been implemented applied to the preparation of triazole-derived functional polymers in a more facile and efficient manner. In this sense, Wei and co-workers described the cooperation of an enzymatic monomer transformation with a controlled radical polymerization (enzymatic-CRP), providing an easy and smart approach to functional chiral polymers.¹¹¹ Moreover, they expanded the scope of the one-pot enzymatic-CRP system into a multi-component polymerization (MCP) system, by introducing an orthogonal alkyne-azide cycloaddition.

Table 9. Propargyl amides **111a–f** synthesized by CAL-B-catalyzed amidation reaction.

Entry	Substrate	Propargyl amide (%)
1	 109a	111a (68) ^a
2	 109b	111b (62) ^a
3	 109c	111c (87) ^a
4	 109d	111d (82) ^b
5	 109e	111e (80) ^a
6	 (R)-109f	(R)-111f (82) ^b
7	 (S)-109f	(S)-111f (87) ^b

^aAfter 24 h. ^bAfter 4 h.

Thus, three simultaneous reactions, including a CuAAC process, a lipase-catalyzed transesterification and an atom transfer radical polymerization (ATRP), were selected to build the above-mentioned tricomponent MCP system (Scheme 38).



a. **113** (1 equiv.), **114** (200 equiv.), **115** (200 equiv.), **116** (220 equiv.), Et₃N (200 equiv.), CuBr (0.5 equiv.), tpy (1.5 equiv.), **CAL-B**, toluene, 45 °C, 24 h

Scheme 38. One-pot CuAAC-enzymatic-ATRP system to prepare designed functional polymers.

Ethyl 2-bromo-2-methylpropanoate (**113**) was used as the ATRP initiator. 2,2,2-Trifluoroethyl methacrylate (**114**) was employed as the acyl donor for the enzymatic reaction and also as monomer for the polymerization. A bifunctional compound, 6-azido-1-hexanol (**115**), was used as the linker associating the lipase-catalyzed transesterification with the CuAAC reaction. Finally several alkynes, e.g. 1-ethynyl-1-cyclohexanol (**116**), were chosen for the cycloaddition transformation. CuBr and 4'-(4-(octadecyloxy)-

phenyl)-2,2':6',2''-terpyridine (tpy) were selected as catalysts for the cycloaddition and ATRP reactions, respectively.

All processes occurred concurrently without interference in toluene at 45 °C, giving rise to the polymers (**117**) with designed functional pendant groups in moderate to high yields (40–68%) after 24 hours. These different reactions cooperated well in a cascade fashion, leading to well-defined polymers with controllable molecular weights, compositions and functionalities.

5. Summary and outlook

There is no doubt about the paramount role of triazole-containing derivatives. Thus, high-efficient techniques have been developed by chemists to synthesize these compounds, such as the Huisgen [3+2] cycloaddition catalyzed by copper. In this sense, recent environmental requirements demanded by society are transforming the way of thinking of industrial companies, which are more delighted to employ (bio)chemical methods that shorten the routes minimizing the amount of reagents, catalysts and solvents wasted, therefore maximizing the productivity and obviously diminishing costs.

Herein we have shown different chemoenzymatic approaches to obtain valuable triazole derivatives. Biocatalysis is able to provide very selective transformations under mild reaction conditions. Among the different biocatalysts tested, hydrolases appear as the most prominent group as they are easily accessible at reasonable prices, do not depend on any external cofactor and can work under water-free conditions accepting high substrate loadings. On the other hand, more recently other enzymes belonging to the oxidoreductase or transferase families are appearing as very promising catalysts to be applied at big scale as, *e.g.* more efficient cofactor regeneration systems or more robust tailor-made biocatalysts, are being developed.

Last but not least, one-pot cascade or tandem protocols reduce operational time, costs and save resources. Therefore, organic chemists increasingly appreciate the advantages of employing biocatalytic concurrent reactions not only applied to multi-enzymatic networks, but also in cooperation with organo- and metallocatalysts. To further expand the synthetic applications of enzymatic reactions (alone or in combination with other (bio)catalysts), new contributions from different multidisciplinary and interdependent areas are required. Consequently as an ongoing engagement, in the near future it is expected a continuous uptake of biocatalysts because of their unparalleled properties.

Acknowledgments

I.L. thanks the Spanish MICINN for personal funding (Ramón y Cajal Program). Funding from the Universidad de Oviedo (UNOV-13-EMERG-07) is gratefully acknowledged. F.R.B. acknowledges INFIQC-CONICET and Universidad Nacional de Córdoba (UNC).

References

1. For recent bibliography, see: (a) Xia, Y.; Qu, F.; Peng, L. *Mini-Rev. Med. Chem.* **2010**, *10*, 806. (b) Agalave, S. G.; Maujan, S. R.; Pore, V. S. *Chem. Asian J.* **2011**, *6*, 2696. (c) Kharb, R.; Sharma, P. C.; Yar, M. S. *J. Enzym. Inhib. Med. Chem.* **2011**, *26*, 1. (d) Kathiravan, M. K.; Salake, A. B.; Chothe, A. S.; Dudhe, P. B.; Watode, R. P.; Mukta, M. S.; Gadhwane, S. *Bioorg. Med. Chem.* **2012**, *20*, 5678. (e) Peng, X.-M.; Cai, G.-X.; Zhou, C.-H. *Curr. Top. Med. Chem.* **2013**, *13*, 1963.
2. (a) Chow, H.-F.; Lau, K.-N.; Ke, Z.; Liang, Y.; Lo, C.-M. *Chem. Commun.* **2010**, *46*, 3437. (b) Juríček, M.; Kouwer, P. H. J.; Rowan, A. E. *Chem. Commun.* **2011**, *47*, 8740. (c) Valverde, I. E.; Mindt, T. L. *Chimia* **2013**, *67*, 262.

3. Yan, W.; Ye, X.; Akhmedov, N. G.; Petersen, J. L.; Shi, X. *Org. Lett.* **2012**, *14*, 2358.
4. (a) Huisgen, R. In *1,3-Dipolar Cycloaddition Chemistry*; Padwa, A., Ed.; Wiley: New York, 1984; p. 1. (b) Breinbauer, R.; Köhn, M. *ChemBioChem* **2003**, *4*, 1147. (c) Meldal, M.; Tornøe, C. W. *Chem. Rev.* **2008**, *108*, 2952.
5. (a) Rostovtsev, V. V.; Green, L. G.; Fokin, V. V.; Sharpless, K. B. *Angew. Chem. Int. Ed.* **2002**, *41*, 2596. (b) Tornøe, C. W.; Christensen, C.; Meldal, M. *J. Org. Chem.* **2002**, *67*, 3057.
6. Moulin, A.; Bibian, M.; Blayo, A.-L.; El Habnoui, S.; Martinez, J.; Fehrentz, J.-A. *Chem. Rev.* **2010**, *110*, 1809.
7. (a) Faber, K. *Biotransformations in Organic Chemistry*; Springer-Verlag: Berlin, 6th Ed., 2011. (b) *Enzyme Catalysis in Organic Synthesis*; Drauz, K.; Gröger, H.; May, O., Eds.; Wiley-VCH: Weinheim, 3rd Ed., 2012. (c) Bornscheuer, U. T.; Huisman, G. W.; Kazlauskas, R. J.; Lutz, S.; Moore, J. C.; Robins, K. *Nature* **2012**, *485*, 185.
8. (a) Wenda, S.; Illner, S.; Mell, A.; Kragl, U. *Green Chem.* **2011**, *13*, 3007. (b) Nestl, B. M.; Nebel, B. A.; Hauer, B. *Curr. Opin. Chem. Biol.* **2011**, *15*, 187. (c) Woodley, J. M.; Breuer, M.; Mink, D. *Chem. Eng. Res. Des.* **2013**, *91*, 2029.
9. Bornscheuer, U. T.; Kazlauskas, R. J. *Hydrolases in Organic Synthesis: Regio- and Stereoselective Biotransformations*; Wiley-VCH: Weinheim, 2005.
10. Collins, P.; Ferrier, R. *Monosaccharides: Their Chemistry and Their Roles in Natural Products*; Wiley: Chichester, 1995.
11. Prasad, A. K.; Himanshu; Bhattacharya, A.; Olsen, C. E.; Parmar, V. S. *Bioorg. Med. Chem.* **2002**, *10*, 947.
12. Bhattacharya, A.; Prasad, A. K.; Maity, J.; Himanshu; Poonam; Olsen, C. E.; Gross, R. A.; Parmar, V. S. *Tetrahedron* **2003**, *59*, 10269.
13. (a) Davis, B. G. *Chem. Rev.* **2002**, *102*, 579. (b) Kobata, A. In *Comprehensive Glycoscience*; Kamerling, J. P., Ed.; Elsevier: Dordrecht, 2007; Vol. 1, p. 39.
14. (a) Dondoni, A.; Marra, A. *Chem. Rev.* **2000**, *100*, 4395. (b) Mizuno, M. *Trends Glycosci. Glycotecnol.* **2001**, *13*, 11. (c) Kumar, D.; Bhalla, T. C. *Appl. Microbiol. Biotechnol.* **2005**, *68*, 726.
15. Groothuys, S.; Kuijpers, B. H. M.; Quaedflieg, P. J. L. M.; Roelen, H. C. P. F.; Wiertz, R. W.; Blaauw, R. H.; van Delft, F. L.; Rutjes, F. P. J. T. *Synthesis* **2006**, *18*, 3146.
16. Kuijpers, B. H. M.; Groothuys, S.; Hawner, C.; ten Dam, J.; Quaedflieg, P. J. L. M.; Shoemaker, H. E.; van Delft, F. L.; Rutjes, F. P. J. T. *Org. Process Res. Dev.* **2008**, *12*, 503.
17. Huang, W.; Groothuys, S.; Heredia, A.; Kuijpers, B. H. M.; Rutjes, F. P. J. T.; van Delft, F. L.; Wang, L.-X. *ChemBioChem* **2009**, *10*, 1234.
18. Fernández-González, M.; Boutureira, O.; Bernardes, G. J. L.; Chalker, J. M.; Young, M. A.; Errey, J. C.; Davis, B. G. *Chem. Sci.* **2010**, *1*, 709.
19. Van Kasteren, I.; Kramer, H. B.; Jensen, H.; Campbell, S. J.; Kirkpatrick, J.; Oldham, N. J.; Anthony, D. C.; Davis, B. G. *Nature* **2007**, *446*, 1105.
20. Doores, K. J.; Mimura, Y.; Dwek, R. A.; Rudd, P. M.; Elliot, T.; Davis, B. G. *Chem. Commun.* **2006**, 1401.
21. Wetting, M. W.; Hegd, S. S.; Hazleton, K. Z.; Blanchard, J. S. *Protein Sci.* **2007**, *16*, 755.
22. Carvalho, I.; Andrade, P.; Campo, V. L.; Guedes, P. M. M.; Sesti-Costa, R.; Silva, J. S.; Schenkman, S.; Dedola, S.; Hill, L.; Rejzek, M.; Nepogodiev, S. A.; Field, R. A. *Bioorg. Med. Chem.* **2010**, *18*, 2412.
23. Paul, C. E.; Arends, I. W. C. E.; Hollmann, F. *ACS Catal.* **2014**, *4*, 788.
24. Hou, S.; Liu, W.; Ji, D.; Wang, Q.; Zhao, Z. K. *Tetrahedron Lett.* **2011**, *52*, 5855.
25. Hou, S.; Ji, D.; Liu, W.; Wanga, L.; Zhao, Z. K. *Bioorg. Med. Chem. Lett.* **2014**, *24*, 1307.
26. See, for instance: (a) Ishida, T.; Kato, S. *J. Am. Chem. Soc.* **2003**, *125*, 12035. (b) Wang, P.-Y.; Chen, T.-L.; Tsai, S.-W.; Kroutil, W. *Biotechnol. Bioeng.* **2007**, *98*, 30.
27. Wang, P.-Y.; Chen, Y.-J.; Wu, A.-C.; Lin, Y.-S.; Kao, M.-F.; Chen, J.-R.; Ciou, J.-F.; Tsai, S.-W. *Adv. Synth. Catal.* **2009**, *351*, 2333.
28. Wang, P.-Y.; Wu, C.-H.; Ciou, J.-F.; Wu, A.-C.; Tsai, S.-W. *J. Mol. Catal. B: Enzym.* **2010**, *66*, 113.
29. Wu, C.-H.; Pen, C.-W.; Wang, P.-Y.; Tsai, S.-W. *Appl. Microbiol. Biotechnol.* **2013**, *97*, 1581.

30. Ruess, W.; Knauf-Beiter, G.; Kueng, R. B.; Kessmann, H.; Oostendorp, M. WO Patent 9701277 A1 19970116.
31. Bianchi, D.; Cesti, P.; Spezia, S.; Garavaglia, C.; Mirena, L. *J. Agric. Food Chem.* **1991**, *39*, 197.
32. Bianchi, D.; Cesti, P.; Golini, P.; Spezia, S.; Garavaglia, C.; Mirena, L. *Pure Appl. Chem.* **1992**, *64*, 1073.
33. Barz, M.; Rauch, M. U.; Thiel, W. R. *J. Chem. Soc., Dalton Trans.* **1997**, 2155.
34. Barz, M.; Glas, H.; Thiel, W. R. *Synthesis* **1998**, 1269.
35. Ríos-Lombardía, N.; Porcar, R.; Busto, E.; Alfonso, I.; Montejo-Bernardo, J.; García-Granda, S.; Gotor, V.; Luis, S. V.; García-Verdugo, E.; Gotor-Fernández, V. *ChemCatChem* **2011**, *3*, 1921.
36. (a) Wasserscheid, P.; Welton, T. *Ionic Liquids in Synthesis*, 2nd Ed.; Wiley-VCH: Weinheim, 2008; Vols. 1–2. (b) Chiappe, C.; Rajamani, S. *Eur. J. Org. Chem.* **2011**, 5517. (c) Domínguez de María, P. *Ionic Liquids in Biotransformations and Organocatalysis: Solvents and Beyond*; John Wiley & Sons: Hoboken, 2012.
37. Sun, P.; Armstrong, D. W. *Anal. Chim. Acta* **2010**, *661*, 1.
38. Sheldon, R. A. *Chem. Commun.* **2001**, 2399.
39. (a) Plaquevent, J.-C.; Levillain, J.; Guillen, F.; Malhiac, C.; Gaumont, A.-C. *Chem. Rev.* **2008**, *108*, 5035. (b) Domínguez de María, P. *Angew. Chem. Int. Ed.* **2008**, *47*, 6960.
40. Borowiecki, P.; Poterała, M.; Maurin, J.; Wielechowska, M.; Plenkiewicz, J. *Arkivoc* **2012**, 262.
41. Borowiecki, P.; Milner-Krawczyk, M.; Brzezińska, D.; Wielechowska, M.; Plenkiewicz, J. *Eur. J. Org. Chem.* **2013**, 712.
42. Borowiecki, P.; Milner-Krawczyk, M.; Plenkiewicz, J. *Beilstein J. Org. Chem.* **2013**, *9*, 516.
43. (a) Bornscheuer, U. T.; Kazlauskas, R. J. *Angew. Chem. Int. Ed.* **2004**, *43*, 6032. (b) Humble, M. S.; Berglund, P. *Eur. J. Org. Chem.* **2011**, 3391.
44. Busto, E.; Gotor-Fernández, V.; Gotor, V. *Chem. Soc. Rev.* **2010**, *39*, 4504.
45. Wu, W.-B.; Xu, J.-M.; Wu, Q.; Lv, D.-S.; Lin, X.-F. *Synlett* **2005**, 2433.
46. Liu, B.; Qian, X.; Wu, Q.; Lin, X. *Enzyme Microb. Technol.* **2008**, *43*, 375.
47. Wu, W.-B.; Xu, J.-M.; Wu, Q.; Lv, D.-S.; Lin, X.-F. *Adv. Synth. Catal.* **2006**, *348*, 487.
48. Liu, B.-K.; Wu, Q.; Lv, D.-S.; Chen, X.-Z.; Lin, X.-F. *J. Mol. Catal. B: Enzym.* **2011**, *73*, 85.
49. Qian, C.; Xu, J.-M.; Wu, Q.; Lv, D.-S.; Lin, X.-F. *Tetrahedron Lett.* **2007**, *48*, 6100.
50. (a) Hayden, F. G. *Antiviral Res.* **1996**, *45*. (b) Crotty, S.; Maag, D.; Arnold, J. J.; Zhong, W.; Lau, J. Y.; Hong, Z.; Andino, R.; Cameron, C. E. *Nat. Med.* **2000**, *6*, 1375. (c) Tam, R. C.; Lau, J. Y.; Hong, Z. *Antivir. Chem. Chemother.* **2001**, *12*, 261.
51. (a) Bellobuono, A.; Monadazzi, L.; Tempini, S.; Chiodo, F.; Magliano, E.; Furione, L.; Ideo, G. *J. Hepatol.* **2000**, *33*, 463. (b) Kwong, A. D.; Kauffman, R. S.; Hurter, P.; Mueller, P. *Nature Biotechnol.* **2011**, *29*, 993.
52. (a) Bzowska, A.; Kulikowska, E.; Shugar, D. *Pharmacol. Therapeut.* **2000**, *88*, 349. (b) Mikhailopulo, I. A. *Curr. Org. Chem.* **2007**, *11*, 317.
53. Utagawa, T.; Morisawa, H.; Yamanaka, S.; Yamazaki, A.; Hirose, Y. *Agric. Biol. Chem.* **1986**, *50*, 121.
54. Shirae, H.; Yokozeki, K.; Kubota, K. *Agric. Biol. Chem.* **1988**, *52*, 1233.
55. Shirae, H.; Yokozeki, K.; Kubota, K. *Agric. Biol. Chem.* **1988**, *52*, 1499.
56. Shirae, H.; Yokozeki, K.; Uchiyama, M.; Kubota, K. *Agric. Biol. Chem.* **1988**, *52*, 1777.
57. Shirae, H.; Yokozeki, K.; Kubota, K. *Agric. Biol. Chem.* **1991**, *55*, 605.
58. Trelles, J. A.; Fernández, M.; Lewkowicz, E. S.; Iribarren, A. M.; Sinisterra, J. V. *Tetrahedron Lett.* **2003**, *44*, 2605.
59. Shirae, H.; Yokozeki, K. *Agric. Biol. Chem.* **1991**, *55*, 493.
60. Shirae, H.; Yokozeki, K. *Agric. Biol. Chem.* **1991**, *55*, 1849.
61. Konstantinova, I. D.; Leont'eva, N. A.; Galegov, G. A.; Ryzhova, O. I.; Chuvikovskii, D. V.; Antonov, K. V.; Esipov, R. S.; Taran, S. A.; Verevkina, K. N.; Feofanov, S. A.; Miroshnikov, A. I. *Russ. J. Bioorg. Chem.* **2004**, *30*, 553.
62. Chudinov, M. V.; Konstantinova, I. D.; Ryzhova, O. I.; Esipov, R. S.; Yurkevich, A. M.; Shvets, V. I.; Miroshnikov, A. I. *Pharm. Chem. J.* **2005**, *39*, 212.

63. Konstantinova, I. D.; Chudinov, M. V.; Fateev, I. V.; Matveev, A. V.; Zhurilo, N. I.; Shvets, V. I.; Miroshnikov, A. I. *Russ. J. Bioorg. Chem.* **2013**, *39*, 53.
64. Barai, V. N.; Zinchenko, A. I.; Eroshevskaya, L. A.; Kalinichenko, E. N.; Kulak, T. I.; Mikhailopulo, I. A. *Helv. Chim. Acta* **2002**, *85*, 1901.
65. Xie, X.; Wang, G.; Xia, J.; Chen, N. *World J. Microbiol. Biotechnol.* **2011**, *27*, 1175.
66. Xie, X.; Xia, J.; He, K.; Lu, L.; Xu, Q.; Chen, N. *Biotechnol. Lett.* **2011**, *33*, 1107.
67. Luo, W.; Liu, Y.; Zhu, X.; Zhao, W.; Huang, L.; Cai, J.; Xu, Z.; Cen, P. *Enzyme Microb. Technol.* **2011**, *48*, 438.
68. Hennen, W. J.; Wong, C.-H. *J. Org. Chem.* **1989**, *54*, 4692.
69. Taverna-Porro, M.; Bouvier, L. A.; Pereira, C. A.; Montserrat, J. M.; Iribarren, A. M. *Tetrahedron Lett.* **2008**, *49*, 2642.
70. (a) Kim, D.; Wang, L.; Beconi, M.; Eiermann, G. J.; Fisher, M. H.; He, H.; Hickey, G. J.; Kowalchick, J. E.; Leiting, B.; Lyons, K.; Marsilio, F.; McCann, M. E.; Patel, R. A.; Petrov, A.; Scapin, G.; Patel, S. B.; Roy, R. S.; Wu, J. K.; Wyvratt, M. J.; Zhang, B. B.; Zhu, L.; Thornberry, N. A.; Weber, A. E. *J. Med. Chem.* **2005**, *48*, 141. (b) Kendall, D. M.; Cuddihy, R. M.; Bergenstal, R. M. *Eur. J. Intern. Med.* **2009**, *20*, S329.
71. Savile, C. K.; Janey, J. M.; Mundorff, E. C.; Moore, J. C.; Tam, S.; Jarvis, W. R.; Colbeck, J. C.; Krebber, A.; Fleitz, F. J.; Brands, J.; Devine, P. N.; Huisman, G. W.; Hughes, G. J. *Science* **2010**, *329*, 305.
72. (a) Malik, M. S.; Park, E.-S.; Shin, J.-S. *Appl. Microbiol. Biotechnol.* **2012**, *94*, 1163. (b) Mathew, S.; Yun, H. *ACS Catal.* **2012**, *2*, 993. (c) Simon, R. C.; Richter, N.; Busto, E.; Kroutil, W. *ACS Catal.* **2014**, *4*, 129.
73. Truppo, M. D.; Strotman, H.; Hughes, G. *ChemCatChem* **2012**, *4*, 1071.
74. Pchelka, B. K.; Loupy, A.; Petit, A. *Tetrahedron: Asymmetry* **2006**, *17*, 2516.
75. Battistutta, R. *Cell. Mol. Life Sci.* **2009**, *66*, 1868.
76. Wawro, A. M.; Wielechowska, M.; Bretner, M. *J. Mol. Catal. B: Enzym.* **2013**, *87*, 44.
77. (a) Burton, S. G. *Curr. Org. Chem.* **2003**, *7*, 1317. (b) Riva, S. *Trends Biotechnol.* **2006**, *24*, 219.
78. (a) Li, K.; Helm, R. F.; Eriksson, K.-E. L. *Biotechnol. Appl. Biochem.* **1998**, *27*, 239. (b) Sealey, J.; Ragauskas, A. J. *J. Wood Chem. Technol.* **1998**, *18*, 403. (c) D'Alfonso, C.; Lanzalunga, O.; Lapi, A.; Vadalà, R. *Tetrahedron* **2014**, *70*, 3049.
79. Schroeder, M.; Pereira, L.; Rodríguez Couto, S.; Erlacher, A.; Schoening, K.-U.; Cavaco-Paulo, A.; Guebitz, G. M. *Enzyme Microb. Technol.* **2007**, *40*, 1748.
80. Hahn, V.; Mikolasch, A.; Wende, K.; Bartrow, H.; Lindequist, U.; Schauer, F. *Biotechnol. Appl. Biochem.* **2010**, *56*, 43.
81. Heeres, J.; Meerpoel, L.; Lewi, P. *Molecules* **2010**, *15*, 4129.
82. (a) Gala, D.; DiBenedetto, D. J. *Tetrahedron Lett.* **1994**, *35*, 8299. (b) Gala, D.; DiBenedetto, D. J.; Clark, J. E.; Murphy, B. L.; Schumacher, D. P.; Steinman, M. *Tetrahedron Lett.* **1996**, *37*, 611.
83. Acetti, D.; Brenna, E.; Fuganti, C.; Gatti, F. G.; Serra, S. *Tetrahedron: Asymmetry* **2009**, *20*, 2413.
84. Murakami, K.; Mochizuki, H. EP Patent 0 472 392 A2 19900824.
85. Monfort, N.; Archelas, A.; Furstoss, R. *Tetrahedron: Asymmetry* **2002**, *13*, 2399.
86. Monfort, N.; Archelas, A.; Furstoss, R. *Tetrahedron* **2004**, *60*, 601.
87. Yasohara, Y.; Miyamoto, K.; Kizaki, N.; Hasegawa, J.; Ohashi, T. *Tetrahedron Lett.* **2001**, *42*, 3331.
88. Yasohara, Y.; Kizaki, N.; Miyamoto, K.; Hasegawa, J.; Ohashi, T. *Biosci. Biotechnol. Biochem.* **2001**, *65*, 2044.
89. Im, D.-S.; Cheong, C.-S.; Lee, S.-H.; Youn, B.-H.; Kim, S.-C. *Tetrahedron* **2000**, *56*, 1309.
90. Naolou, T.; Busse, K.; Kressler, J. *Biomacromolecules* **2010**, *11*, 3660.
91. Ma, D.-Y.; Wang, D.-X.; Zheng, Q.-Y.; Wang, M.-X. *Tetrahedron: Asymmetry* **2006**, *17*, 2366.
92. Hou, S.; Liu, W.; Ji, D.; Zhao, Z. *Bioorg. Med. Chem. Lett.* **2011**, *21*, 1667.
93. Forró, E.; Fülöp, F. *Org. Lett.* **2003**, *5*, 1209.
94. (a) Kiss, L.; Forró, E.; Sillanpää, R.; Fülöp, F. *Tetrahedron: Asymmetry* **2008**, *17*, 2856. (b) Kiss, L.; Forró, E.; Sillanpää, R.; Fülöp, F. *Tetrahedron* **2010**, *66*, 3599.
95. Rocha, L. C.; Rosset, I. G.; Melgar, G. Z.; Raminelli, C.; Porto, A. L. M.; Jeller, A. H. *J. Braz. Chem. Soc.* **2013**, *24*, 2427.

96. Aufort, M.; Hersovici, J.; Bouhours, P.; Moureau, N.; Girard, C. *Bioorg. Med. Chem. Lett.* **2008**, *18*, 1195.
97. Su, S.; Giguere, J. R.; Schaus, S. E.; Porco, J. A. *Tetrahedron* **2004**, *60*, 8645.
98. Ankati, H.; Yang, Y.; Zhu, D.; Biehl, E. R.; Hua, L. *J. Org. Chem.* **2008**, *73*, 6433.
99. Hudlicky, T.; Reed, J. W. *Synlett* **2009**, 685.
100. de la Sovera, V.; Bellomo, A.; Pena, J. M.; Gonzalez, D.; Stefani, H. A. *Mol. Divers.* **2011**, *15*, 163.
101. Carrau, G.; Drewes, C. C.; Shimada, A. L. B.; Bertucci, A.; Farsky, S. H. P.; Stefani, H. A.; Gonzalez, D. *Bioorg. Med. Chem.* **2013**, *21*, 4225.
102. Hudlicky, T.; Rinner, U.; Gonzalez, D.; Akgun, H.; Schilling, S.; Siengalewicz, P.; Martinot, T. A.; Pettit, G. R. *J. Org. Chem.* **2002**, *67*, 8726.
103. de la Sovera, V.; Bellomo, A.; Gonzalez, D. *Tetrahedron Lett.* **2011**, *52*, 430.
104. Lu, W.-Y.; Sun, X.-W.; Zhu, C.; Xu, J.-H.; Lin, G.-Q. *Tetrahedron* **2010**, *66*, 750.
105. (a) Tietze, L. F.; Brasche, G.; Gericke, K. M. *Domino Reactions in Organic Synthesis*; Wiley-VCH: Weinheim, 2006. (b) Ricca, E.; Brucher, B.; Schrittwieser, J. H. *Adv. Synth. Catal.* **2011**, *353*, 2239. (c) Bisogno, F. R.; Lavandera, I.; Gotor, V. In *Kirk-Othmer Encyclopedia of Chemical Technology*; John Wiley & Sons: Hoboken, 2011; p. 1. (d) Pellissier, H. *Tetrahedron* **2013**, *69*, 7171.
106. de Oliveira, C. S.; de Andrade, K. T.; Omori, A. T. *J. Mol. Catal. B: Enzym.* **2013**, *91*, 93.
107. Cuetos, A.; Bisogno, F. R.; Lavandera, I.; Gotor, V. *Chem. Commun.* **2013**, *49*, 2625.
108. Campbell-Verduyn, L. S.; Szymański, W.; Postema, C. P.; Dierckx, R. A.; Elsinga, P. H.; Janssen, D. B.; Feringa, B. L. *Chem. Commun.* **2010**, *46*, 898.
109. Szymanski, W.; Postema, C. P.; Tarabiono, C.; Berthiol, F.; Campbell-Verduyn, L.; de Wildeman, S.; de Vries, J. G.; Feringa, B. L.; Janssen, D. B. *Adv. Synth. Catal.* **2010**, *352*, 2111.
110. Hassan, S.; Tschersich, R.; Müller, T. J. J. *Tetrahedron Lett.* **2013**, *54*, 4641.
111. Fu, C.; Zhu, C.; Wang, S.; Liu, H.; Zhang, Y.; Guo, H.; Tao, L.; Wei, Y. *Polym. Chem.* **2012**, *4*, 264.

2,5-DIKETOPIPERAZINES AS PRIVILEGED SCAFFOLDS IN MEDICINAL CHEMISTRY, PEPTIDOMIMETIC CHEMISTRY AND ORGANOCATALYSIS

Umberto Piarulli and Silvia Panzeri

Università degli Studi dell'Insubria, Dipartimento di Scienza e Alta Tecnologia, Via Valleggio 11, I-22100 Como, Italy (e-mail: umberto.piarulli@uninsubria.it)

Abstract. 2,5-Diketopiperazines (DKPs) are heterocyclic scaffolds, characterized by a rather flat 6-membered ring core in which diversity can be introduced at up to four positions (N1, N4, C3, C6) and stereochemically controlled at two (C3, C6), while they can be prepared from readily available α -amino acids using conventional synthetic procedures, solid-phase and microwave-assisted organic synthesis. In addition, several methods have been developed that allow the decoration of unfunctionalized DKP scaffolds. Thanks to their structural, biochemical and spatial properties, these scaffolds have found wide applications in medicinal chemistry, as peptidomimetic inducers of protein secondary structure elements and in organic synthesis as enantioselective catalysis.

Contents

1. Introduction
 2. Synthesis
 - 2.1. Synthesis of the ring
 - 2.2. Functionalization of the DKPs scaffold
 3. Applications in medicinal chemistry
 - 3.1. DKP as modulator of dopaminergic receptors
 - 3.2. β -turn mimics
 - 3.3. [DKP]integrin ligands
 4. Application in catalysis
 5. Conclusion
- References

1. Introduction

2,5-Diketopiperazines (DKPs), the smallest cyclic peptides (Figure 1), represent an important class of biologically active compounds,¹ while, at the same time, investigations on their synthesis and reactivity have been fundamental to many aspects of peptide chemistry. Once believed to be only protein artifacts or degradation products, they have regained interest thanks to the wide spectrum of their biological properties.²

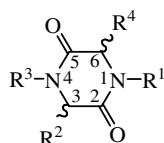


Figure 1. Diketopiperazine structure and numbering.

The structural similarity of 2,5-diketopiperazines to peptides has inspired medicinal chemists to use DKPs to circumvent the limitations of peptides.³ Constraining the nitrogen atom of an α -amino amide into a

DKP ring alters its physical properties, reduces the susceptibility to metabolic amide bond cleavage and induces conformational rigidity. These changes in structural and physical properties, as well as the presence of groups that can act as donors and acceptors of hydrogen bonds, enhance favourable interactions with biological targets. Moreover, DKPs are simple heterocyclic scaffolds in which diversity can be introduced at up to four positions (N1, N4, C3, C6) and stereochemically controlled at two (C3, C6), while they can be prepared from readily available α -amino acids.

Thanks to all these properties, these constrained bifunctional cyclopeptides have emerged as privileged structures⁴ (single molecular frameworks able to provide high-affinity ligands to specific receptors or to be a starting material for heterocyclic diversity-oriented synthesis) for the discovery of new lead compounds and represent a useful toolset for those pursuing research in the areas of medicinal chemistry and design of peptidomimetics. Furthermore, DKP scaffolds are also interesting candidates as organocatalysts.

This chapter covers the main synthetic approaches to diketopiperazines, including the transformations of the DKP ring, and the use of these constrained heterocyclic scaffolds in medicinal chemistry, in β -turn mimicking peptidomimetics and as organocatalysts.

2. Synthesis

2.1. Synthesis of the ring

From the synthetic point of view, DKPs can be accessed through different synthetic pathways. As depicted in Figure 2, there are three logical disconnections of a 2,5-diketopiperazine ring: the amide bond (A), the C–N bond (B) and the C–C bond (C). This last one has been reported only recently, while approaches A and B are both used routinely. Other possibilities are tandem cyclizations forming N1–C2/C3–N4 (D) and C2–N1–C6 (E) bonds, but they are used less frequently.

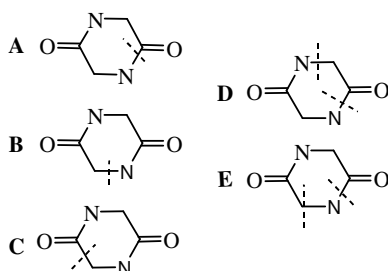
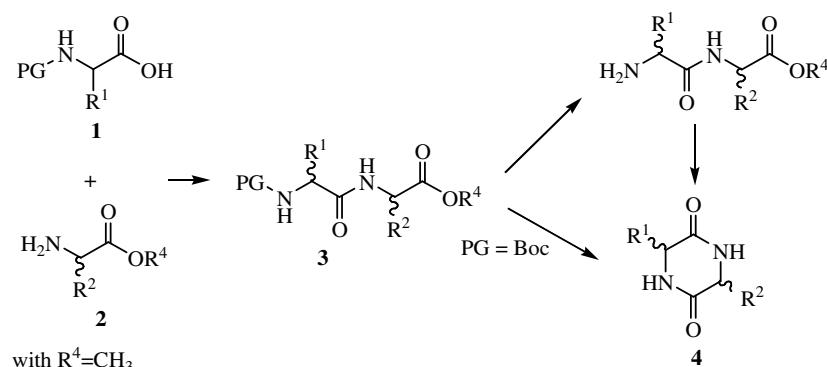


Figure 2. Possible disconnections.

Both solution chemistry and solid-phase synthesis can be found in the literature, for these approaches. Solid-phase synthesis approaches have mainly been used to build combinatorial libraries on a small scale for lead discovery in medicinal chemistry. Unfortunately, the difficulty of scaling up reactions on a solid support hampers this procedure for the large-scale synthesis of 2,5-DKPs.³ Many synthetic approaches are reported in the literature; since comprehensiveness is beyond the scope of this chapter, we will concentrate herein on the construction of the DKP ring *via* amide bond formation by intramolecular ester aminolysis of the corresponding dipeptide esters and *via* multicomponent Ugi condensation.

The synthesis *via* ester cyclization is one of the most commonly used techniques because of its operational simplicity both in solution and on the solid-phase. The synthetic strategy is straightforward: an α -amino acid protected at the amino group **1** is coupled to the free amino group of an α -amino ester **2**. The

resulting dipeptide **3** undergoes spontaneous lactamization after deprotection of the terminal amine to yield the 2,5-DKP **4** (Scheme 1).



Scheme 1. Dipeptide ester cyclization.

The formation of the dipeptide itself is a facile process from commercially available α -amino acids using a large number of coupling reagents. Therefore, 2,5-DKP formation *via* this route is the most commonly used procedure to make this ring system.³

On the other hand, one limitation is that, to achieve cyclization, the amide bond must adopt a *cis*-conformation and, if this is prevented sterically or electronically (secondary amides are known to exist mainly, > 95:5, as the *trans*-conformers, and the barrier to isomerization is quite high), the rate of cyclization can be low. A wide variety of experimental conditions are illustrated in the literature to improve the yield when the cyclization is difficult; however, careful selection of reaction conditions is required to limit racemization. When the cyclization is difficult, heating in an acidic medium is often used to force the ring formation.⁵ Noteworthy, heating in a basic medium is effective but it often leads to racemization.⁶ The cyclization of amino dipeptide esters can also be carried out simply under thermal conditions by refluxing the substrate in high boiling solvents (for example, toluene or xylene).⁷ Refluxing the formate salt of the dipeptide in toluene/*sec*-BuOH has also been shown to be beneficial for cyclization.⁸

Improvement of the yields has been obtained by the use of microwaves: in the work of Luthman *et al.*, a new general and efficient solution-phase synthesis was described.⁹ In contrast to other published methods, this is independent on the amino acid sequence and no epimerization was observed; moreover a comparison with classic thermal heating was performed and it appears that microwave-assisted heating for 10 minutes using water as solvent was the most efficient method of cyclization giving moderate to excellent yields (63–97%) of 2,5-DKPs. In other approaches, microwave irradiation of *N*-Boc dipeptide esters directly caused *N*-Boc deprotection and cyclization to 2,5-diketopiperazines in a fast and efficient manner; this modification has also been used under solvent-free conditions to give indolyl 2,5-diketopiperazine analogues¹⁰ and polysubstituted 2,5-piperazinedione derivatives.¹¹

When the dipeptide cyclization precursor contains a tertiary amide (*e.g.*, the presence of a proline residue or of an *N*-alkylated amino acid), the cyclization step is easier and does not normally require activation by heating or microwaves. On the other hand, the formation of the tertiary peptide bond is more demanding and requires powerful coupling agents and prolonged reaction times. These problems are well described in the synthesis of a small library of bifunctional diketopiperazine (DKP) scaffolds (Figure 3), formally derived from 2,3-diaminopropionic acid and aspartic acid and differing for the configuration of the two DKP stereocenters and for the substitution at the DKP nitrogens.

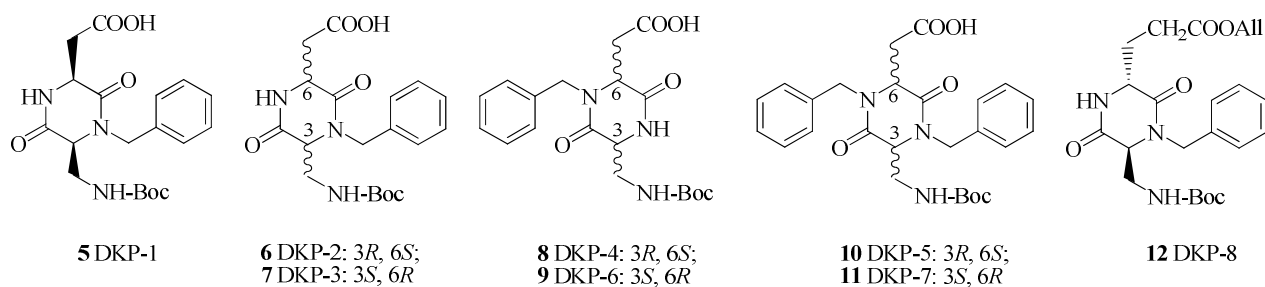
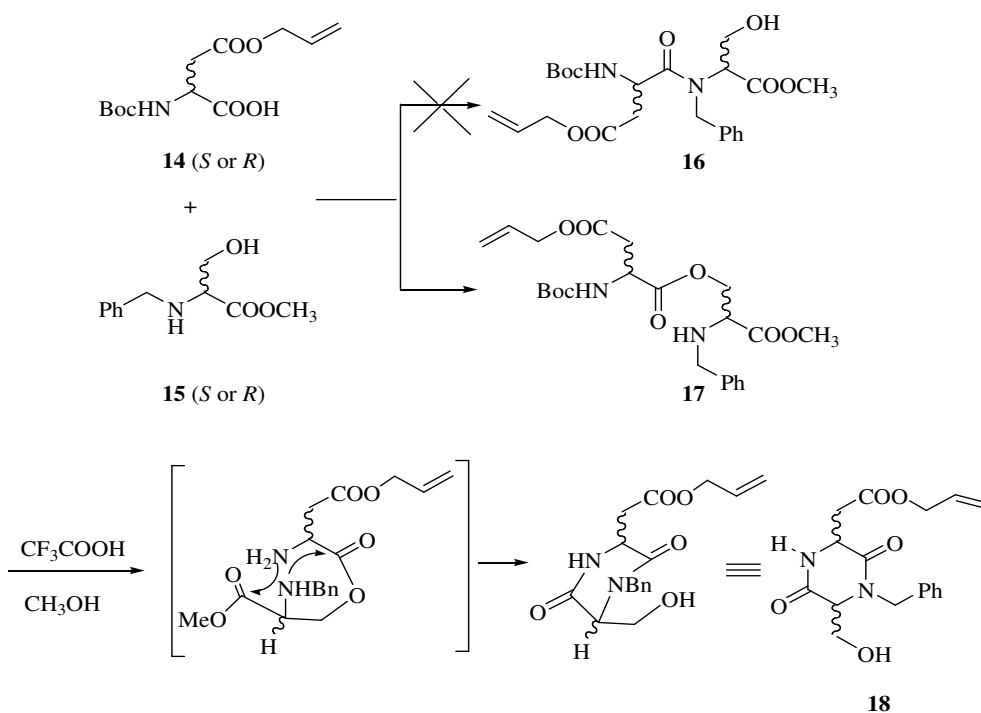


Figure 3. DKP-1 to DKP-8 scaffolds.

Two different strategies were devised for the synthesis of **5–12**, depending on their nitrogen substitution. In particular, **5**, **6** and **7** (bearing a benzyl group at nitrogen N4, Figure 3) were prepared making use of the serine ligation strategy exemplified in Scheme 2,¹² starting from either (*R*)- or (*S*)-*N*-(*tert*-butoxycarbonyl)aspartic acid β -allyl ester **14** and either (*R*)- or (*S*)-*N*-benzylserine methyl ester **15**. Direct coupling of these fragments (HATU, *i*-Pr₂NEt or EDC, DMAP) led to the isopeptides **17** in high yield, rather than forming the expected dipeptides **16**. As a matter of fact, selective *O*-acylation of the unprotected β -hydroxyl group of *N*-benzylserine methyl ester is preferred over the formation of the tertiary amide and the resulting ester bond is stable in solution to *O,N*-acyl transfer. The *O,N*-acyl migration was then triggered by cleavage of the Boc protecting group and treatment with a base, which also promoted the simultaneous cyclization to the diketopiperazine **18** (DKP-OH).

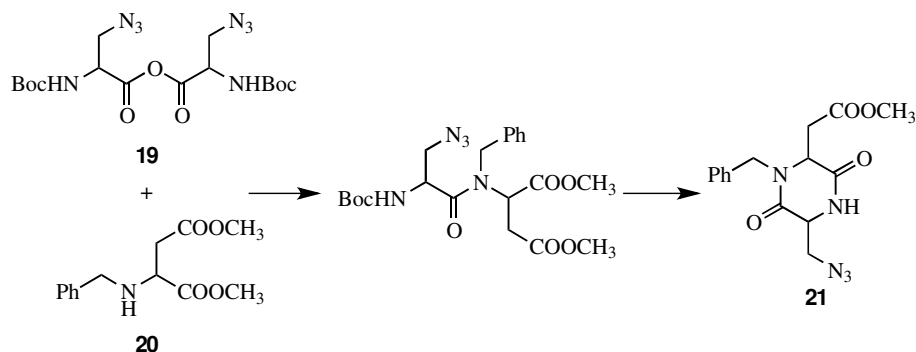


Scheme 2. Synthesis of DKP-1-OH, DKP-2-OH and DKP-3-OH.

The introduction of the nitrogen functionality was then realized through a Mitsunobu-type reaction using hydrazoic acid in toluene, followed by a one pot Staudinger reduction-Boc protection. Final deallylation gave the diketopiperazine derivatives **5**, **6** and **7**.

For the preparation of diketopiperazines **8** and **9** (bearing a benzyl group at nitrogen N1, Figure 3), the coupling of azidoserine to *N*-benzyl-aspartic acid dimethylester **20** was envisaged (Scheme 3). Many different coupling conditions (HATU, PyBrOP, DPPA, acylfluoride and mixed anhydride) were tested to

achieve the condensation but the only successful conditions required pre-formation of the symmetric Boc-azidoserine anhydride **19** (by DCC) and coupling to *N*-Bn-Asp dimethyl ester. In this way, a satisfactory 80% yield was obtained (Scheme 3).

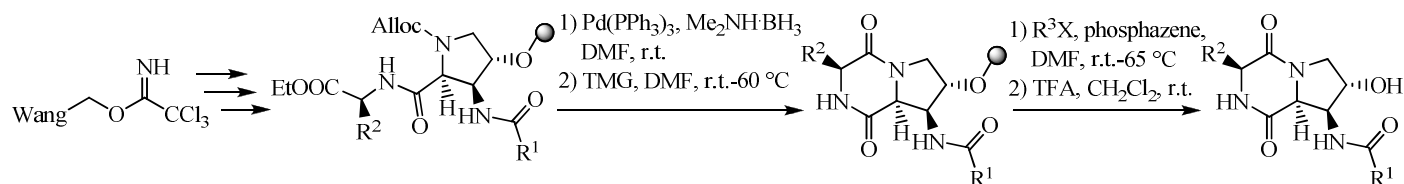


Scheme 3. Coupling of azidoserine to *N*-benzyl-aspartic acid dimethylester and cyclization.

Subsequent Boc cleavage and cyclization to diketopiperazine **21** were nearly quantitative. Catalytic hydrogenation of the azide group, followed by Boc protection of the primary amino group and, as last step, hydrolysis of the methyl ester afforded diketopiperazines **8** and **9**.

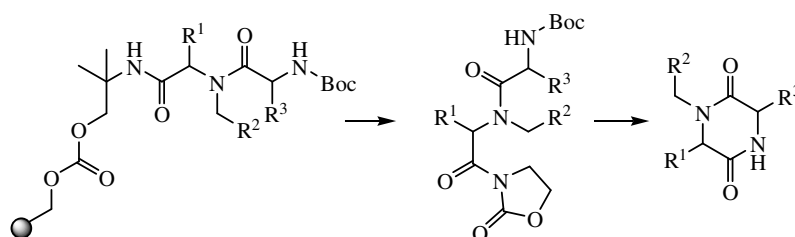
Since its first example in 1965,¹³ the solid-phase synthesis of diketopiperazines *via* amide bond formation met with success in a huge number of examples. Three general strategies are generally followed in this chemistry:

1. Preparation of the solid-phase bound linear dipeptide precursor, cyclization and then cleavage from the resin, as exemplified in Scheme 4.¹⁴ In this case, the cyclization precursor needs a suitable functionality on the side chains for attachment to the solid support.



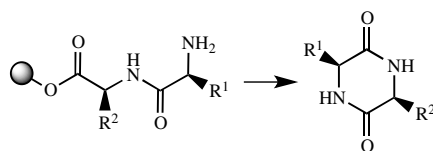
Scheme 4. Preparation of solid-phase bound diketopiperazines.

2. Cleavage of the acyclic precursor from the resin followed by cyclization in solution-phase, as exemplified in Scheme 5 and exploited in the synthesis of 2,5-DKPs libraries.¹⁵



Scheme 5. Solid-phase synthesis of diketopiperazines. Synthesis of the bound precursor, cleavage and cyclization in solution.

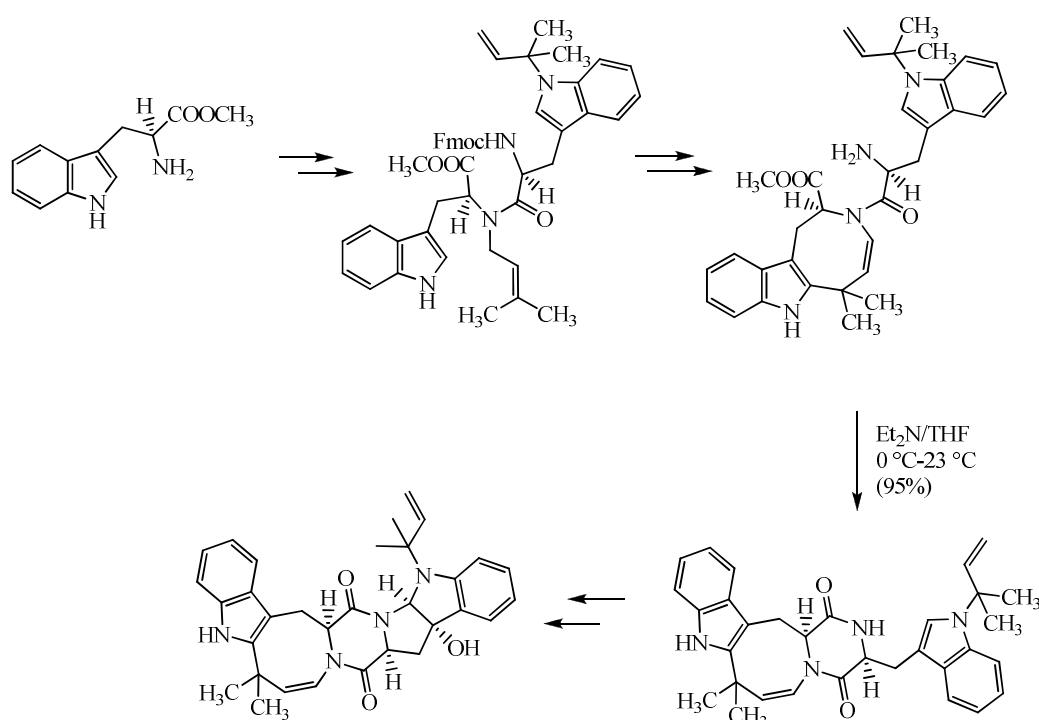
3. Cyclative cleavage of the supported linear dipeptide precursor with concurrent release of the diketopiperazine (Scheme 6).³



Scheme 6. Cleavage-induced cyclization of linear dipeptide.

This approach was studied evaluating various combinations of resins and solvents:¹⁶ high yields of 2,5-DKPs were obtained using both thermal and microwave-assisted heating, irrespectively of the resin and organic solvent employed. The PEGA-Ser resin gave high yields of 2,5-diketopiperazines in water with microwave-assisted heating thus becoming the choice method for the synthesis of libraries of DKPs.

This method was applied to many total syntheses of 2,5-DKP containing natural products, for the ring formation.³ For example, the enantioselective total synthesis of okaramine-N takes advantage of this strategy (Scheme 7).¹⁷



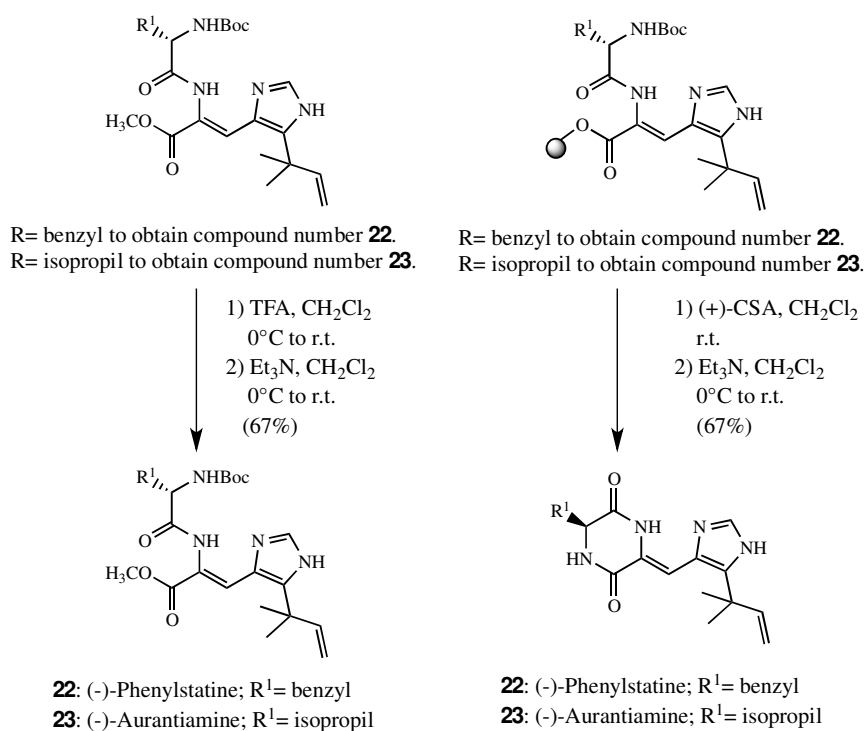
Scheme 7. Base-catalyzed dipeptide ester cyclization in the synthesis of okaramine-N.

Also two natural anti-cancer dehydrodiketopiperazines, namely (–)-phenylahistin **22** and (–)-aurantiamine **23**, have been prepared by this method both in solution and on solid-phase (Scheme 8).^{18,19}

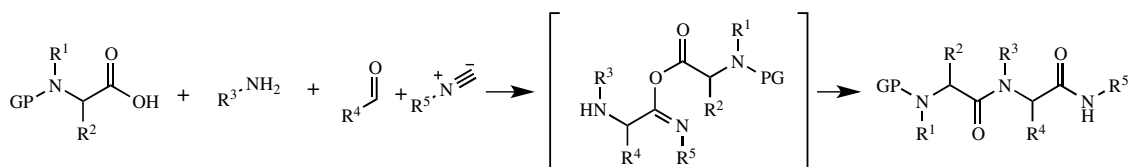
The Ugi reaction offers an alternative method to the formation of a dipeptide cyclization precursor (Scheme 9).²⁰ Using an isonitrile, an acid (or amino acid), an aldehyde and an amine, this reaction can produce a dipeptide in equally high yield.²¹ In this reaction, a new stereocenter is created and, if all reagents are achiral, a racemic mixture of the product is obtained, whereas if chiral reagents are used it is possible to induce the formation of a preferred stereochemistry of the product. Although in principle all four components can be used as chiral starting materials, chiral isocyanides, aldehydes and acids afford only low diastereoselectivities, which reach to moderate to good results using chiral amines.²²

Significantly, this multicomponent reaction offers a number of advantages over the traditional route. In the first place, it allows a greater chemical diversity, even if the commercial access to isocyanides is more

restricted than for the other three components (but the terminal amide produced from this moiety is often removed during the formation of the 2,5-DKP ring without affecting the potential for diversity).



Scheme 8. Diketopiperazine cyclization approaches for the synthesis of (-)-phenylahistin **22** and (-)-aurantiamine **23**.



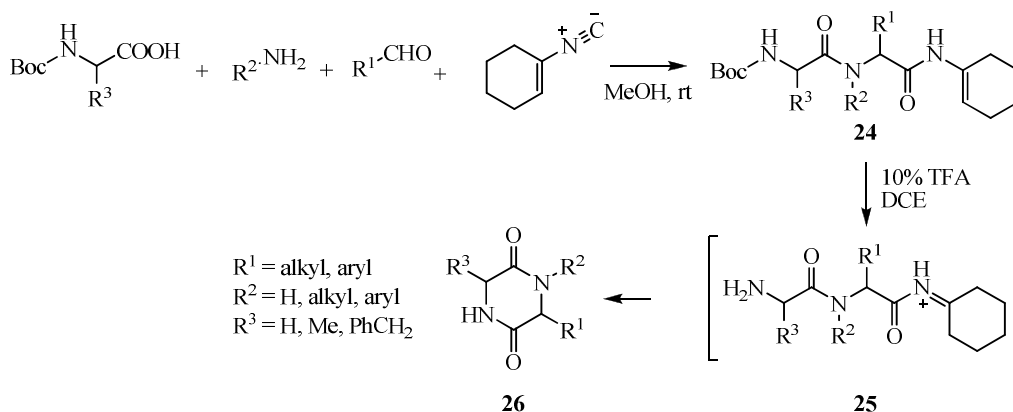
Scheme 9. Ugi reaction.

The major advantage of this technique consists in its modularity and in the fact that the reaction is performed in one pot without the use of expensive coupling reagents. This offers the possibility to generate rapidly high numbers of compounds and as such it has been widely utilized in the preparation of 2,5-DKP libraries.²³

On the other hand, the main disadvantage of the Ugi reaction in the formation of 2,5-diketopiperazines likes in the difficulty of cyclization of the dipeptide. Unlike the previous method, this route produces a C-terminal amide, making the subsequent lactamization step more difficult. To overcome this problem, a number of methods have been developed that facilitate this postcondensational modification (PCM), making the Ugi reaction a credible alternative to the traditional methods.³

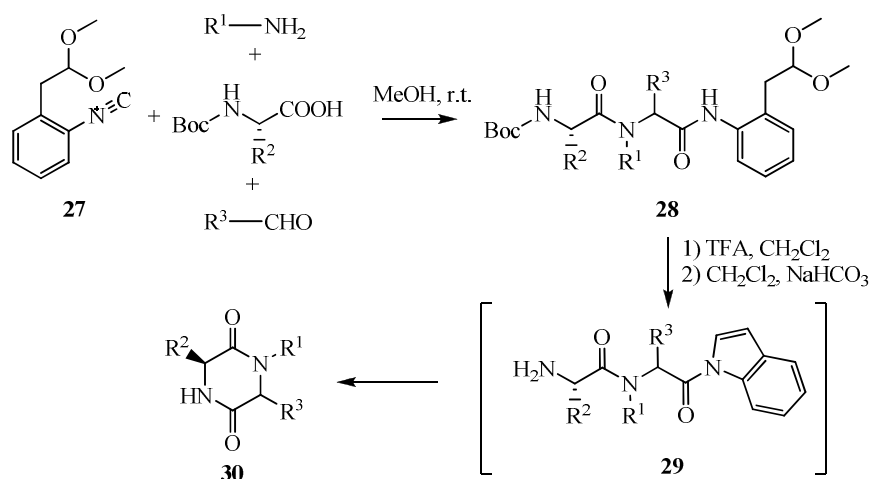
First and most common, the amide is converted to a more labile group to enable cyclization and this can be realized by a judicious choice of the isocyanide reactant, which is the precursor of the terminal amide. Hulme *et al.* adopted the methodology developed in 1995 by Keating and Armstrong,²⁴ who realized the potential of 1-isocyanocyclohexene, using oxygen nucleophiles to form dipeptide esters and acids to form 2,5-diketopiperazines directly.²⁵

In the Ugi reaction, also Boc-protected amino acids and cyclohexenyl isonitrile are used and the typical dipeptide product **24** (Scheme 10) is obtained. Then treatment of this intermediate with acid removes the nitrogen-protecting group and protonates the C-terminal enamide **24**, which generates a transient activated *N*-acyliminium ion. Finally, **25** undergoes ring-closure and the racemic 2,5-diketopiperazine **26** is formed in excellent yield with expulsion of a cyclohexyliminium cation. The major drawback to this methodology consists in the low stability of cyclohexenyl isonitrile.



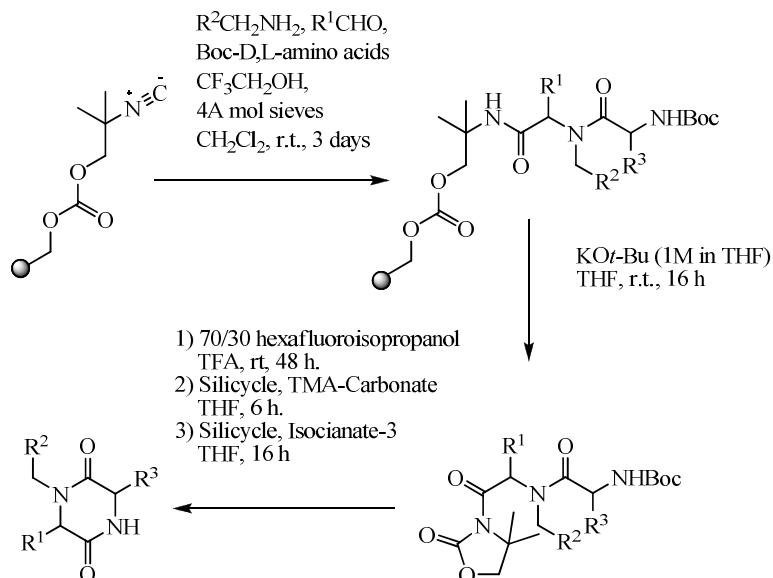
Scheme 10. Cyclization *via* intermediate *N*-acyliminium ion.

Other methods that allow conversion of the isonitrile to a synthetically labile group have been discovered.^{26,27} The synthesis of *N*-substituted 2,5-DKPs reported by Wessjohann *et al.*²⁸ illustrates an example of the use of stable, easily accessible and versatile isonitrile 1-isocyano-2-(2,2-dimethoxyethyl)benzene **27** as a labile group which enable cyclization (Scheme 11). The mildly acidic and chemoselective post-Ugi activation of **28** involving simultaneous indolamide formation and Boc removal gives the active amide **29**, which allows cyclization to **30** without affecting other peptidic or even ester moieties and with stereochemical retention at the stereocenters.



Scheme 11. Cyclization *via* intermediate indolamide.

A resin bound β -hydroxy-isonitrile was used in the solid-phase synthesis of DKP scaffolds *via* Ugi condensation (Scheme 12). In this case, the post condensation modification of the supported dipeptide consisted in a base-catalyzed cyclization to the *N*-acyloxazolidinone and its conversion to the corresponding methyl ester prior than cyclization to diketopiperazine.²⁹



Scheme 12. Cleavage from resin followed by cyclization in solution.

Other approaches have also been used for the solid-phase synthesis of diketopiperazines by Ugi condensation: solid-phase linked isocyanides **31–34** (Figure 4) have been used^{29–31} and the resultant dipeptides can be cyclized off-resin to form 2,5-DKPs.

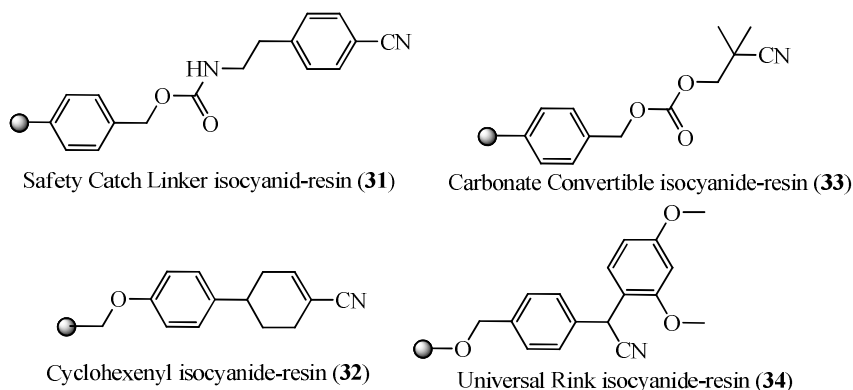
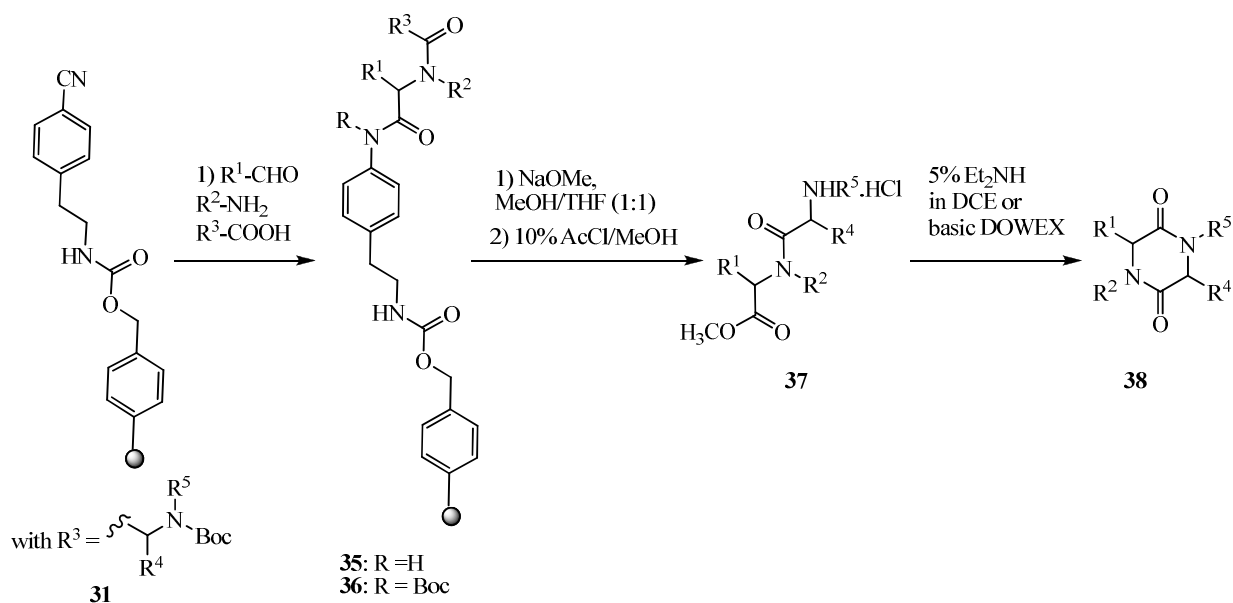


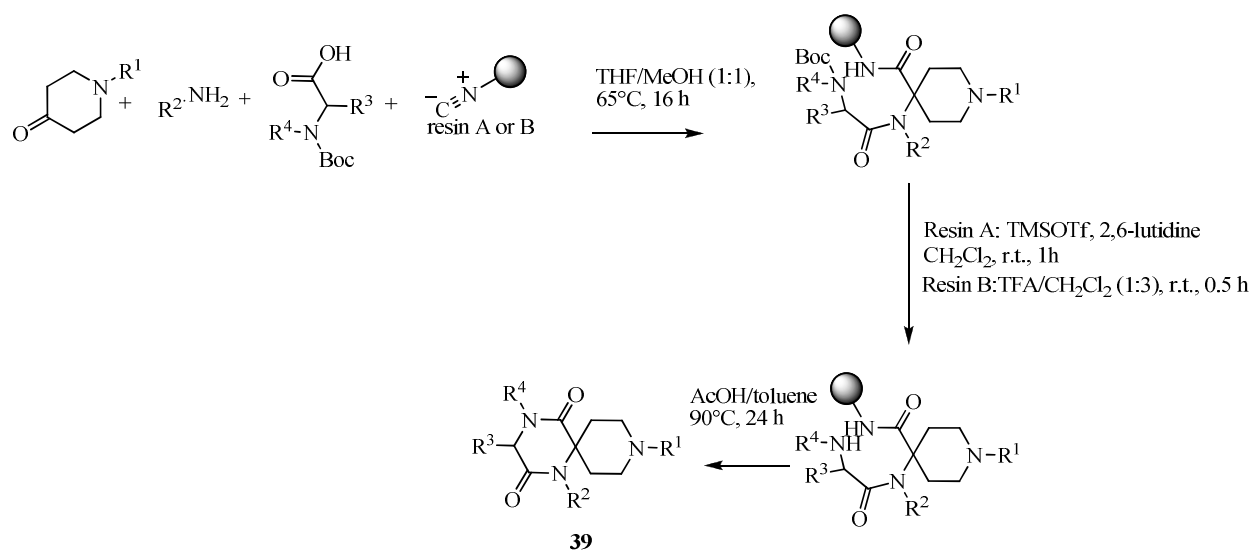
Figure 4. Solid-phase linked isocyanides.



Scheme 13. Off-Resin cyclization.

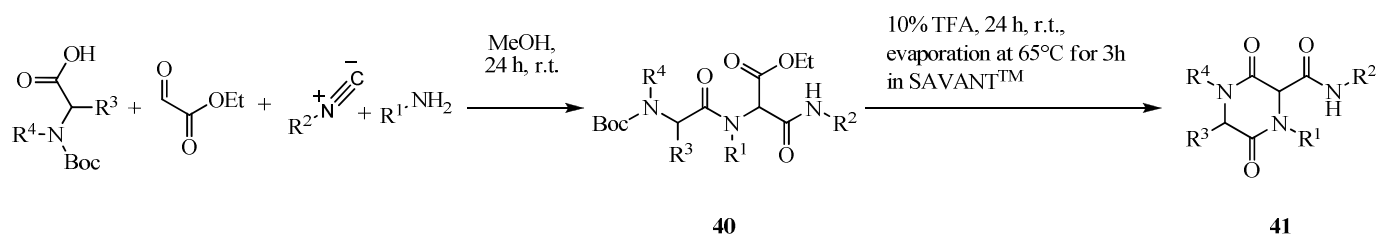
An exemplifying case is the reaction in Scheme 13: resin-bound isonitrile **31** was used with an excess of the other reactants to form biologically relevant constrained 2,5-diketopiperazines in a four-step pathway: isonitrile **31** was converted to the resin-bound dipeptide **35**, then Boc activation of the linker and subsequent facile cleavage of **36** furnished the peptide ester **37**, whose cyclization was achieved under mildly basic conditions to give the 2,5-diketopiperazines **38**.³⁰

A series of CCR5 chemokine receptors antagonists based on the spiro-2,5-DKP scaffold **39** were produced by Habashita *et al.* (Scheme 14) and then developed into the HIV inhibitor Amlaviroc.³² For their synthesis, the initial Ugi reaction required heating to 65 °C, to achieve conversion of the piperidone to the Ugi product; Boc deprotection followed by cyclative cleavage with acetic acid afforded compounds **39**, albeit with varying degrees of epimerization (Scheme 14).



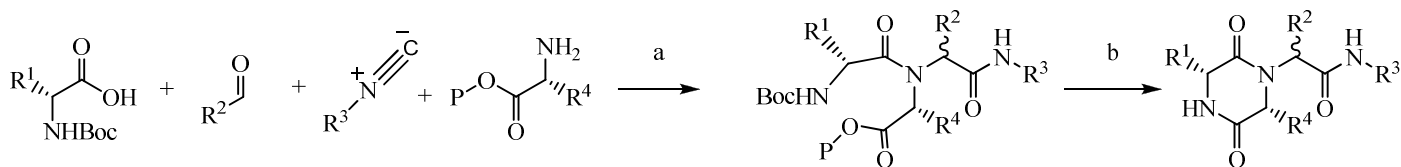
Scheme 14. Cyclative cleavage from resin.

Cyclization conditions have also been developed, which allow the retention of the isonitrile portion in the Ugi condensation product. The first example of such methodology makes use of ethyl glyoxalate as an aldehyde (Scheme 15); an Ugi product (**40**) is formed containing a malonate monoamide derivative, whose cyclization involves the ethyl ester functionality, yielding the 2,5-DKP carboxamide scaffold **41** in excellent yield.³³



Scheme 15. Carboxamide template.

Alternatively, the ester of an amino acid (or a resin bound amino acid) can be reacted under Ugi conditions with an aldehyde, a Boc-protected amino acid and an isonitrile. Boc-deprotection triggers cyclization and formation of a 2,5-diketopiperazine substituted at N4 by a carboxymethyl chain (also called N-4 glycinamides, see Scheme 16). This protocol provides a clean product even if the yields are low.



a) Solid phase P = resin.

1) H₂N aminoacid-resin, R²CHO, CH₂Cl₂, shaken, r.t.; 2) Boc-aminoacid, isocyanide, MeOH added, shaken, r.t.

Solution P = Me.

1) Amine, R²CHO, Et₃N, MeOH, r.t.; 2) Isonitrile, acid, r.t.

b) Solid phase P = resin.

1) 50% TFA/CH₂Cl₂

2) PhMe/EtOH (1:1) shaken with 1% of HOAc or Et₃N

Solution P = Me.

1) TFA or 4N HCl

Scheme 16. N-4 glycinamide template.

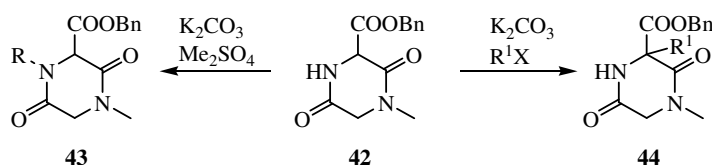
This strategy was applied, in solid-phase or in solution, to the preparation of numerous compounds with potential biological activity as matrix metalloproteinase inhibitors,³⁴ collagenase-1 inhibitors,³⁵ oxytocin antagonists.^{36,37}

2.2. Functionalization of the DKPs scaffold

Several methodologies and many examples have been developed for the selective functionalization of diketopiperazine precursors. In particular, modifications have been proposed for the regio- and stereocontrolled C-functionalization of 2,5-diketopiperazines at C3 and C6. These transformations involve enolate, radical and cationic precursors (and *N*-acyliminium ion) and are sensitive to polar and steric effects. By this methods, alkyl groups, exocyclic double bonds (by aldol condensation), halogens and oxygenated functionalities have been introduced. In most cases, these reactions require the absence of acidic N–H and therefore protection of the endocyclic nitrogens.

The carbonyl groups at C2 and C5 can be reduced to produce piperazine or dihydropyrazine nuclei. Endocyclic *N*-acyliminium ions can also be derived by a reductive strategy and subsequently alkylated inter- or intramolecularly to yield polycyclic systems.

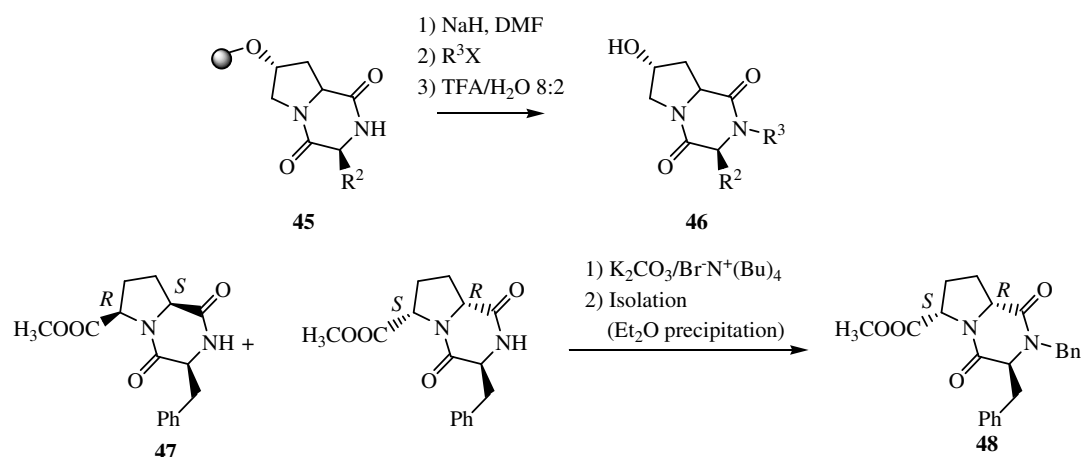
Endocyclic nitrogens can be functionalized by alkylation or arylation. The most common method for alkylation of the lactam nitrogen of 2,5-diketopiperazines is based on the use of sodium hydride as base.^{38,39} However, under conditions where alkylation at carbon can compete, this method can fail. In the alkylation of benzyloxycarbonyl 2,5-diketopiperazine **42** (Scheme 17),⁴⁰ selective methylation of **42** at nitrogen was possible using dimethyl sulphate, giving **43** (R=Me); however, with alkyl halides (Me, Et, Bn, allyl) reaction at carbon was favoured, giving **44** (R¹=alkyl).



Scheme 17. Alkylation of benzyloxycarbonyl 2,5-DKPs.

Also NaH/DMF has been shown to afford epimerization of proline-fused 2,5-diketopiperazines in the alkylation of **45** to **46** (Scheme 18)⁴¹ and this occurs also using milder methods that have been preferred in

recent literature, especially phase-transfer conditions ($\text{Bu}_4\text{N}^+\text{Br}^-$, PhCH_2Br plus K_2CO_3), for example, **47** to **48**.⁴²

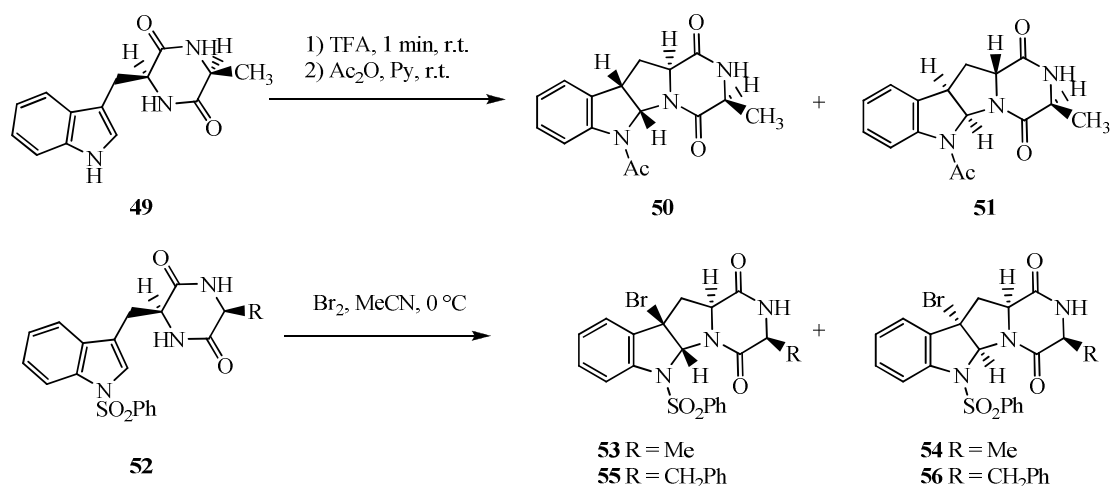


Scheme 18. Alkylation with NaH/DMF or in phase-transfer conditions.

Where sodium hydride gave no *N*-alkylated product, the use of the much stronger phosphazene base BEMP or its polymer supported variant (PS) BEMP was required to give moderate to excellent yields (52–94%).⁴³

KHMDS, although in a stoichiometric amount was also used to generate the amide anion and alkylate the nitrogen.⁴⁴

Different methodologies have been employed for the intramolecular *N*-arylation of 2,5-diketopiperazines. Nucleophilic cyclization of the lactam nitrogen of a 2,5-DKP onto the indole nucleus has been used in the synthesis of biological active 2,5-DKP alkaloids and recent examples of this methodology are shown in Scheme 19.^{45–47}

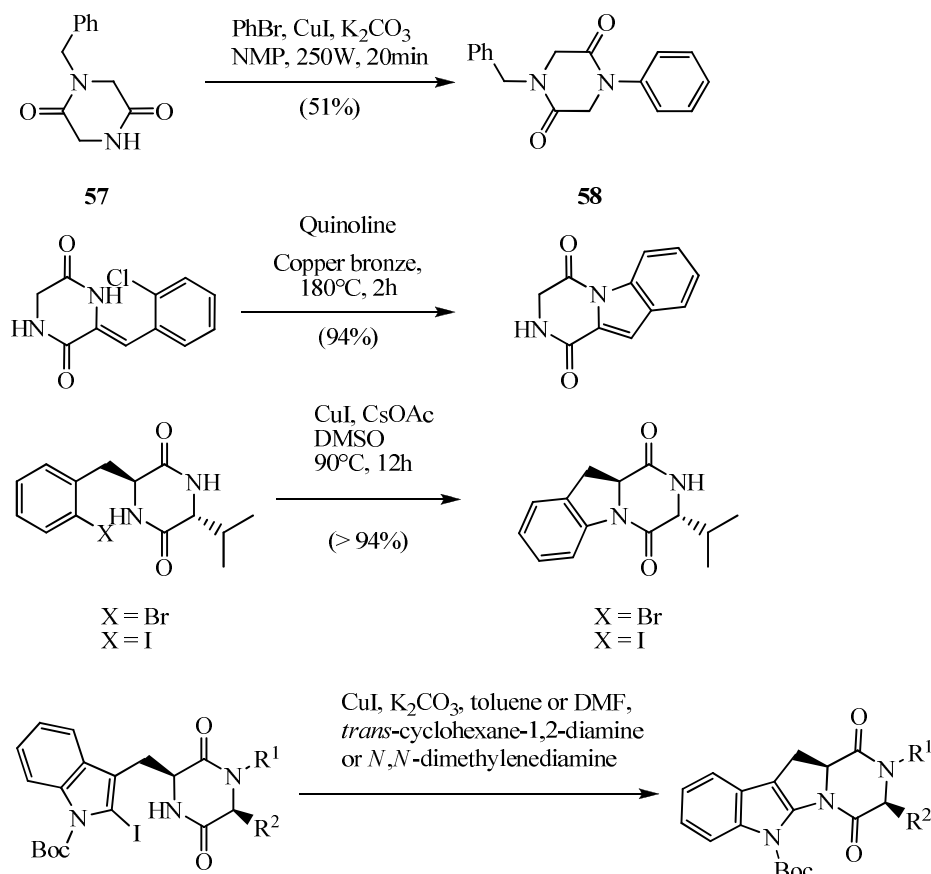


Scheme 19. Intramolecular cyclization onto the indole nucleus.

Brief exposure of *cyclo*-(L-Trp-L-Ala) **49** to neat trifluoroacetic acid gave, after acylation, the tetracycles **50** (45%) and **51** (9%). The major product **50** arises from attack of the lactam N from the bottom (α) face of the indole ring, whereas the minor product **51** occurs from attack to the β -face of the indole ring and epimerization of the α -position, as a result of steric hindrance from the methyl group at C3.⁴⁵ Cyclization of the lactam nitrogen onto the indole ring in **52** in the presence of bromine at 0 °C in aceto-

nitrile gave the tetracyclic bromides **53** (78%) and **54** (19%). The major product **53** was a key intermediate for reductive dimerization in the total synthesis of (+)-11,11'-dideoxyverticillin A.⁴⁸

The *N*-arylation of 2,5-diketopiperazines is usually carried out under the copper-mediated Goldberg reaction (Scheme 20). *N*-arylation under these conditions (copper iodide, potassium carbonate) has been improved by microwave irradiation in NMP.⁴⁹ Reaction of 2,5-DKP **57** with phenyl bromide produces moderate yields of the coupled product **58** (51%) in 20 minutes, while under reflux it took 20 hours. Several improved intramolecular *N*-arylations of 2,5-DKPs have been developed (Scheme 20).



Scheme 20. Copper-mediated Goldberg reaction for *N*-arylation of 2,5-diketopiperazine.

3. Applications to medicinal chemistry

Thanks to their structural properties and their relative metabolic stability, diketopiperazines have found widespread use as valuable scaffolds in medicinal chemistry and as peptidomimetics.

DKPs are biologically active as inhibitor of plasminogen activator inhibitor-1 (PAI-1),^{57–60} as antitumour,^{61–63} antiviral,⁶⁴ antifungal,^{65–67} antibacterial^{68–74} and antihyperglycaemic^{75–77} agents. They are also involved in alteration of cardiovascular and blood-clotting functions.^{2,57–60,82,83} In addition, they have affinities for calcium channels and for opioid GABAergic,⁷⁹ serotonergic 5-HT_{1A}⁸⁰ and oxytocin receptors.^{81–83}

There are many pharmacologically active small molecules that contain the DKP scaffold in their structure. Among these, it is worth mentioning Aplaviroc, a promising CCR5 receptor antagonist now discontinued due to hepatotoxicity⁸³ and Tadalafil (Cialis®), a PDE5 inhibitor.⁸⁴ In this chapter, we will showcase the use of diketopiperazine containing molecules active on dopaminergic receptors and biologically active diketopiperazine peptidomimetics.

3.1. DKP as modulators of dopaminergic receptors

Dopamine is a catecholamine neurotransmitter, whose decreased activity is believed to be associated with several nervous system diseases such as Parkinson's disease, schizophrenia, attention deficit, hyperactivity disorder (ADHD) and restless legs syndrome (RLS).⁸⁵ As a consequence, agonists and antagonists of dopaminergic receptors constitute an interesting research topic. Johnson *et al.*⁸⁶ reported a small collection of molecules derived from L-Prolyl-L-leucylglycinamide (PLG) (Figure 5), a modulator of dopamine D₂ receptor.

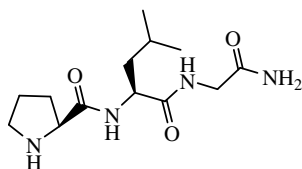


Figure 5. PLG.

Several PLG peptidomimetics were designed⁸⁷ to mimic the postulated bioactive type II β -turn conformation of PLG.^{88,89} In various pharmacological assay systems, peptidomimetic **59** resulted more potent than PLG on D₂-receptors.^{88,90} To understand the correlation between the structure and the high potency of **59**, the diketopiperazine peptidomimetic **61** was synthesized (Figure 6).⁸⁷

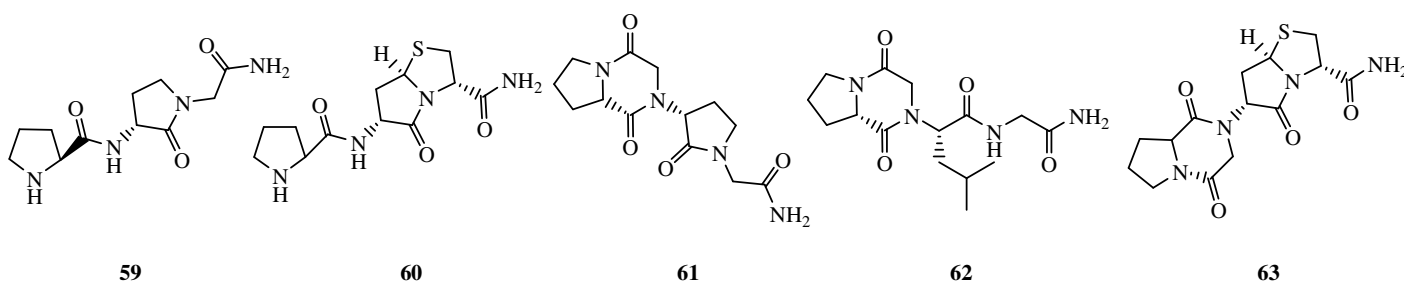


Figure 6. Peptidomimetics of PLG dopamine modulators.

This analogue was designed to mimic a *N*-terminal “C5” conformation involving an intramolecular hydrogen bond between the prolyl nitrogen and the lactam NH, suggesting that the *N*-terminal “C5” conformation might be a factor in the potency of peptidomimetics **59** and **61**. In further studies, diketopiperazines **62** and **63** have also been designed and tested (Figure 6).⁸⁶

The diketopiperazine “C5” conformational mimic was incorporated into the PLG structure in compound **62**, whereas in **63** this structural component was incorporated into the structure of the bicyclic lactam PLG analogue **60**.⁸⁷ Peptidomimetics **62** and **63** were tested in the [3H]spiroperidol/*N*-propyl-norapomorphine D₂ receptor competitive binding assay, showing the same ability to increase the affinity of the dopamine receptor for agonists as previously found for PLG and the PLG peptidomimetics **59** and **61**.^{89–91} On the other hand, **59** produced an increased number of apomorphine-induced rotations than **62**, suggesting that while an *N*-terminal “C5” conformation may play a part in the potency of the γ -lactam peptidomimetics of PLG, it does not appear to be the primary factor.

3.2. β -turn mimics

In the field of peptidomimetics, much effort has been devoted to the design and synthesis of conformationally constrained compounds that mimic or induce specific secondary structural features of

peptides and proteins. Many scaffolds have hence been created which possess the functionalities of peptides (*i.e.*, an amine and a carboxy groups) and well-defined spatial properties, thus reproducing the desired orientation of the growing peptide chain. Bifunctional diketopiperazines, featuring an amino and a carboxy functionalities, can serve this scope and several examples are reported in the literature.

The β -turn is a common feature in biologically active peptides and is defined as any tetrapeptide sequence with a 10-membered intramolecularly H-bond ring, in which the $C\alpha$ (i) to $C\alpha$ ($i+3$) distance varies from 4 to 7 Å (there are at least 14 types of β -turn structures described in literature).⁹² Many β -turn mimics have appeared in the literature and for a broad distinction all these structures can be divided into three classes (Figure 7):¹²

1. internal β -turn, made of scaffolds that mimic a peptide reverse turn;
2. β -hairpin mimics, made of rigid scaffolds that cause a reversal of the peptide chain when incorporated and can promote the formation of parallel or antiparallel β -sheets;⁹³
3. external β -turn inducers, made of rigid templates that constrains the backbone of cyclic peptides thus stabilizing the β -turn conformation.

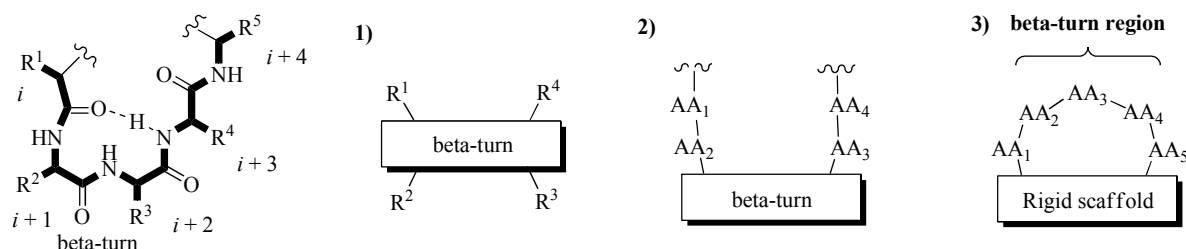


Figure 7. Families of β -turn mimics.

Golebiowski and co-workers synthesized a library of bicyclic diketopiperazines, starting from racemic piperazine-2-carboxylic acid β -turn mimics (general structure **64**, Figure 8).⁹⁴ Later, the same authors synthesized epimeric series of β -turn mimics **64**.^{95,96} Simulated annealing calculations were performed on both epimers of structure **65** to determine their propensity to adopt a β -turn. The data suggest that both *R*- and *S*-epimers of structure **64** fit more closely a type I β -turn. Starting from simple α -amino acids, Kahn and co-workers have also reported the solution-phase synthesis of a conformationally restricted β -turn mimic **66** based on a similar bicyclic diketopiperazine scaffold.⁹⁷

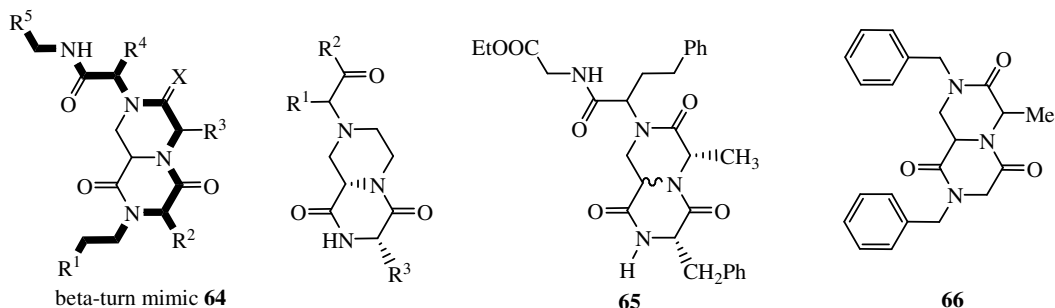


Figure 8. Examples of diketopiperazine-based “internal” β -turn mimics.

A further example is presented in the work of Burgess *et al.*: diketopiperazine scaffolds are used as antagonists of tropomyosin receptor kinase C.⁹⁸ The diketopiperazine scaffolds used in that work (Figure 9) are functionalized at N1 and C3 and the substituents at these two positions were calculated to overlap well with the side chains of the $i+1$ and $i+2$ residues of a type I β -turn.

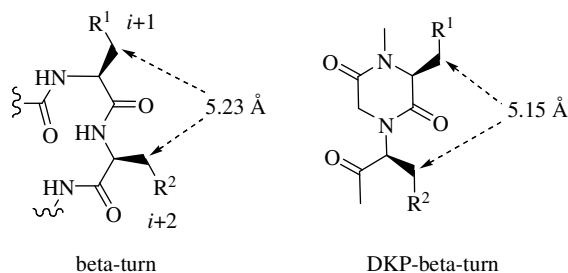


Figure 9. Diketopiperazine mimics of a type I β -turn.

β -turn mimetic **64** has been used to design^{94,95} **67** and **68** (Figure 10), successfully synthesized by a Ugi 4CC component reaction with a solid-phase protocol. Compound **69** was instead prepared by solution chemistry.⁹⁷

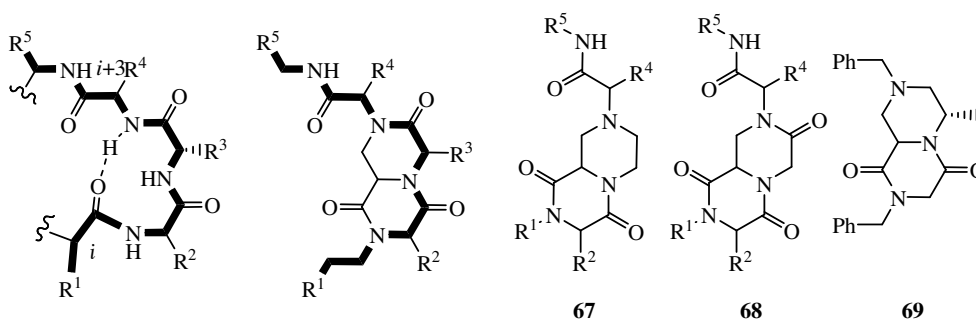


Figure 10. β -turn mimics.

The second class of β -turn mimics consists of a rigid scaffold, which, when incorporated into a peptide or pseudo-peptide chain, causes a reversal of the chain. In strictest terms, these structures themselves should adopt a β -turn conformation but quite often they lack substitution at the important $i+1$ and $i+2$ residues of the turn region or the means to introduce significant diversity at these positions.

The bifunctional DKP scaffold **5** mentioned above, derived from L-aspartic acid and (*S*)-2,3-diaminopropionic acid, bears the amino and carboxylic acid functionalities in a *cis* relationship and, as such, can be seen as a β -turn mimic and promoter of antiparallel β -sheet. In view of these potential properties, the synthesis of several peptidomimetics was performed by solution-phase peptide synthesis (Boc strategy). Conformational analysis of these derivatives was carried out by a combination of ¹H-NMR spectroscopy (chemical shift and NOE studies), IR spectroscopy, CD spectroscopy and molecular modeling and revealed the formation of β -hairpin mimics involving 10- and 18-membered H-bound rings and a reverse turn of the growing peptide chain (Figure 11). The β -hairpin conformation of the longer derivatives (**70** and **71**) was detected also in competitive, dipolar and even protic solvents such as dimethylsulfoxide and methanol, thus showing the high stability of these structures and the very good turn-inducing ability of the scaffold.

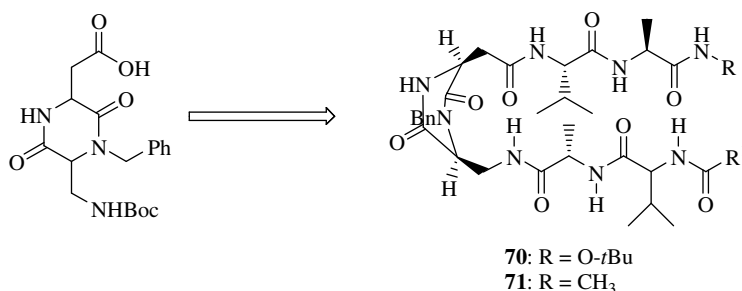


Figure 11. Bifunctional 2,5-DKPs β -hairpin mimics.

Diketopiperazines have been used as external β -turn inducers, where their rigid template constrains the backbone of a cyclic peptide and stabilizes the peptidic residue into a β -turn conformation. An important contribution was made by Robinson and co-workers, who have reported an extensive investigation of proline-based diketopiperazine templates, that were used to stabilize turn and hairpin conformations in cyclic peptides and were used in synthetic vaccine discovery.^{99,100}

Also tricyclic 2,5-DKPs derivatives (**72**, **73** and **74**) as well as heterochiral diproline units (**75** and **76**) (Figure 12) can control the peptide conformation acting as β -hairpin mimics. These 2,5-diketopiperazine templates were incorporated efficiently into cyclic peptide β -hairpin mimics by solid-phase methods and they are used in synthetic vaccine discovery.

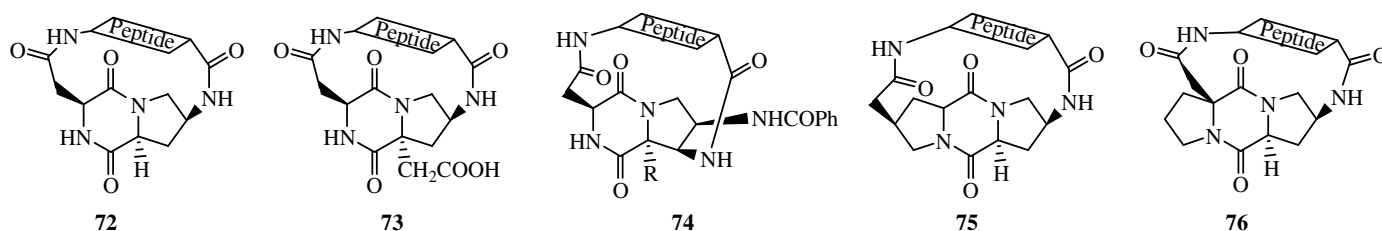


Figure 12. Cyclic β -hairpin mimics.

3.3. [DKP]-integrin ligands

An example of the application of DKPs in medicinal chemistry as peptidomimetic scaffolds is the synthesis of cyclic-peptidomimetic integrin ligands, *cyclo*-[RGD-DKP]- and [*iso*DGR-DKP], with potential applications as anti-cancer drugs. The sequence Arg-Gly-Asp (RGD) has been identified as the common motif used by several endogenous ligands to recognize and bind a group of integrins, including $\alpha_v\beta_3$, $\alpha_v\beta_5$, $\alpha_5\beta_1$, whose key role in angiogenesis, tumour progression and metastasis has been ascertained. Several cyclic peptides and peptidomimetic ligands containing the RGD sequence were prepared and it was shown that nanomolar binding affinities could be reached by a judicious choice of the ring-size and conformational properties of the cyclic ligand. Considering the well-defined conformational properties of diketopiperazines, several ligands based on a diketopiperazine scaffold were prepared and some of these showed excellent binding affinities.

In particular, Robinson and co-workers realized a cyclic RGD ligand containing the *cyclo*-(3-aminoproline-aspartate) moiety. These ligands displayed a submicromolar affinity for integrin $\alpha_v\beta_3$ and this modest binding ability was attributed to the presence of two or more interconverting conformations of the RGD peptide sequence. In a similar approach, Royo, Albericio and co-workers have prepared cyclic peptidomimetics containing *cyclo*-[Lys-Asp] as a template. A solid-phase synthetic approach was followed supporting the DKP scaffold on the resin and cyclizing the linear RGD precursor on the resin. Also in this case, micromolar IC_{50} values were reached.

Recently, Piarulli, Gennari and co-workers reported a new class of cyclic RGD peptidomimetics (Figure 13), containing the bifunctional diketopiperazine (DKP) scaffolds **77–83** and featuring a smaller 17-membered ring.⁴⁴

The *cis*-derivative *cyclo*-[DKP-1-RGD] **77** inhibited biotinylated vitronectin binding to the purified $\alpha_v\beta_3$ receptor at a micromolar concentration ($3.9 \pm 0.4 \mu\text{M}$), while *trans*-derivatives **78–83** ranged from submicro- to subnanomolar concentrations (220–0.2 nM). To investigate the origin of the strikingly different behaviour of the RGD-peptidomimetics, a conformational study was performed by NMR spectroscopy

($^1\text{H-NMR}$ and NOESY spectra of dilute $\text{H}_2\text{O}/\text{D}_2\text{O}$ 9:1 solutions) and by computational methods [Monte Carlo/Stochastic Dynamics (MC/SD) simulations]. These simulations revealed that the highest affinity ligands display well-defined preferred conformations featuring intramolecular hydrogen-bound turn motifs and an extended arrangement of the RGD sequence [$\text{C}\beta(\text{Arg})\text{-C}\beta(\text{Asp})$ average distance ≥ 8.8 Å]. Docking studies were performed, starting from the representative conformations obtained from the MC/SD simulations and taking as a reference model the crystal structure of the extracellular segment of integrin $\alpha_v\beta_3$ complexed with the cyclic pentapeptide Cilengitide. The highest affinity ligands produced top-ranked poses conserving all the important interactions of the X-ray complex.

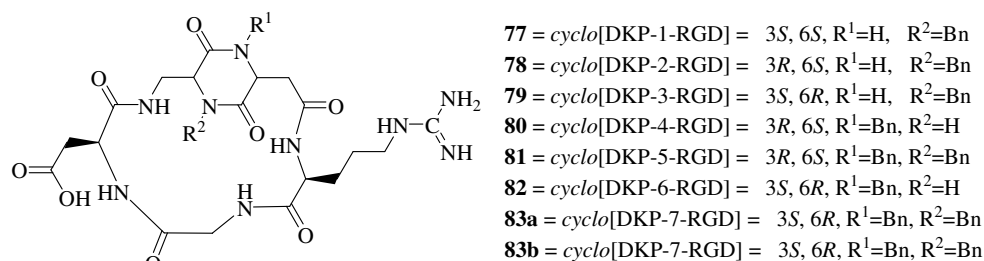


Figure 13. Library of *cyclo*-[RGD-DKP] integrin ligands.

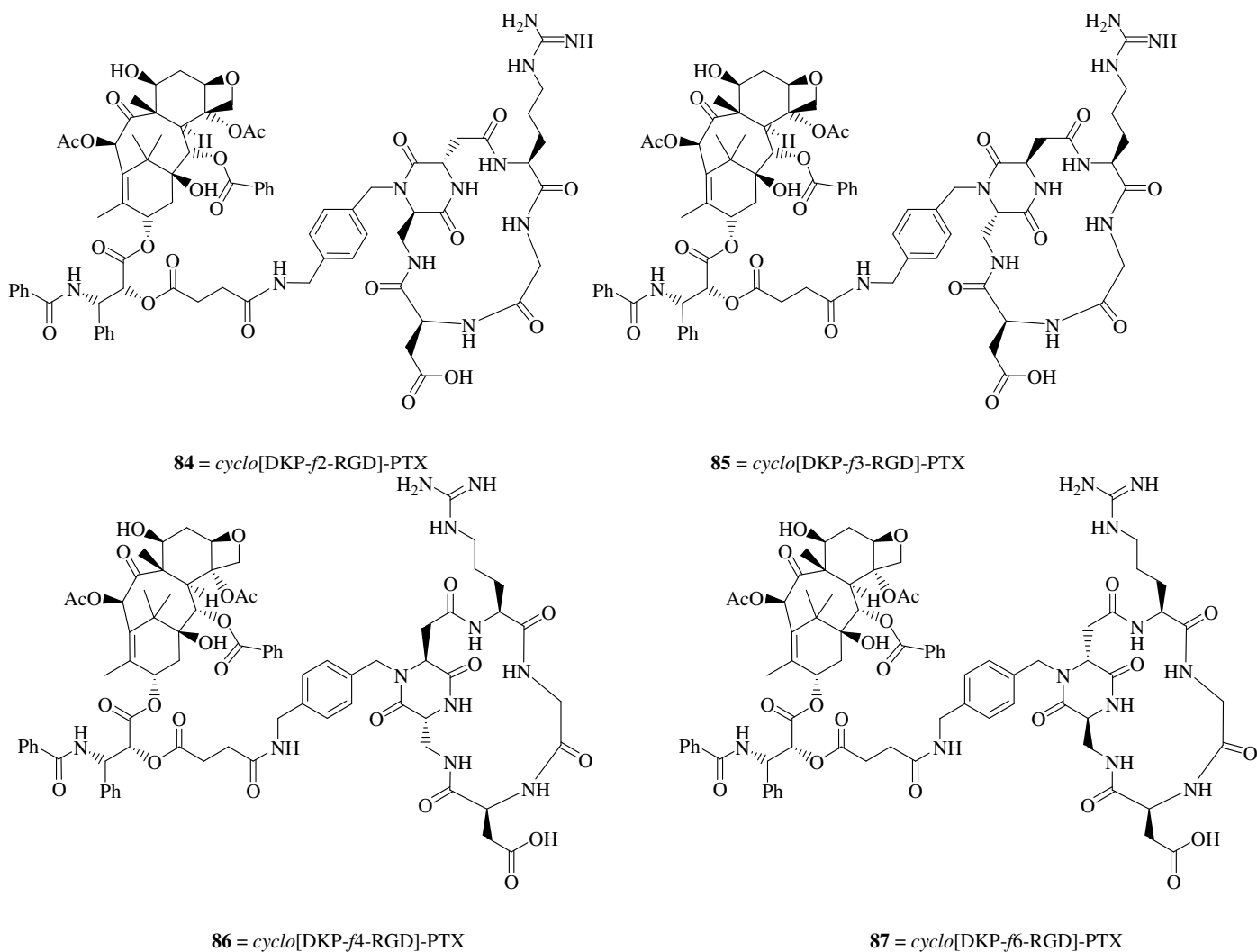


Figure 14. *Cyclo*-[DKP-RGD] - Paclitaxel conjugates.

Considering that α_v integrins are overexpressed on the surface of cancer cells, integrin ligands can be usefully employed as tumour-homing peptidomimetics for site-directed delivery of cytotoxic drugs.¹⁰¹ A

small library of *cyclo*-[DKP-RGD] integrin ligand - Paclitaxel conjugates **84–87** was synthesized (Figure 14).¹⁰³ The *cyclo*-[DKP-RGD] integrin ligands were functionalized with a free amine group suitable for conjugation to Paclitaxel *via* a succinyl linker. All the Paclitaxel-RGD constructs **84–87** showed low nanomolar binding to the purified $\alpha_v\beta_3$ integrin receptor and showed *in vitro* cytotoxic activity against a panel of human tumour cell lines similar to that of Paclitaxel. In tumour-targeting experiments against the IGROV-1/Pt1 human ovarian carcinoma xenotransplanted in nude mice, *cyclo*-[DKP- β_3 -RGD]-PTX **85** exhibited a superior activity than Paclitaxel, despite the lower (*ca.* half) molar dosage used.

Diketopiperazine scaffolds were also incorporated in a second class of cyclic peptidomimetic integrin ligands: *cyclo*-[DKP-*iso*DGR] **88–89** (Figure 15).

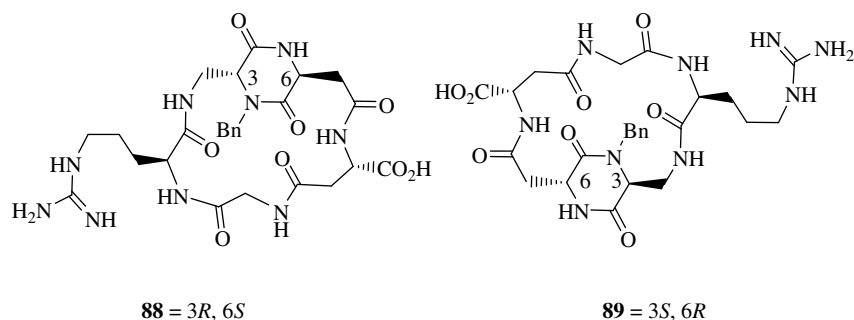


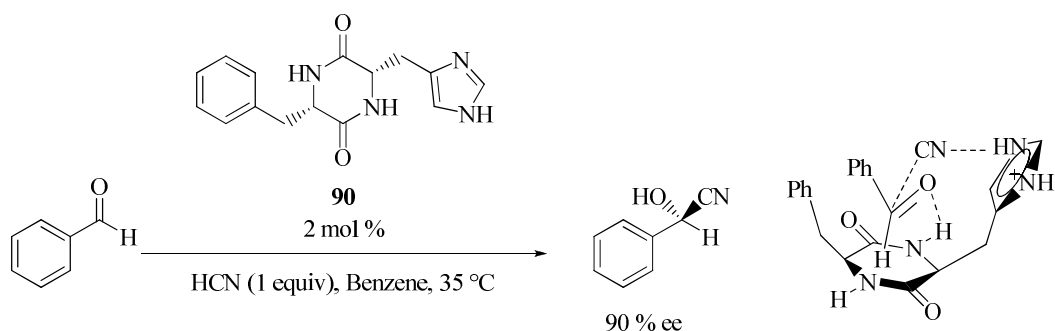
Figure 15. Cyclic *iso*DGR peptidomimetics containing the DKP scaffold.

The *iso*Asp-Gly-Arg (*iso*DGR) sequence is a tripeptidic sequence that originates from a spontaneous post-translational modification of the Asn-Gly-Arg (NGR) motif of the extracellular matrix protein fibronectin,¹⁰² affording a gain of protein function and the creation of a new adhesion binding site for integrins.¹⁰³ With regards to the biochemical, spectroscopic and computational investigations, *iso*DGR sequence can fit into the RGD-binding pocket of $\alpha_v\beta_3$ integrin, establishing the same electrostatic clamp as well as additional polar interactions.¹⁰² Two cyclic *iso*DGR peptidomimetics (Figure 15) containing the bifunctional diketopiperazine scaffolds mentioned above were synthesized, their conformational properties investigated and their affinity to $\alpha_v\beta_3$ and $\alpha_v\beta_5$ integrin receptors measured.¹⁰² The *cyclo*-[DKP-*iso*DGR] ligands **88** and **89** compare favourably with the cyclic peptidomimetic *cyclo*-[(3S,6R)DKP-RGD],^{104,105} as well as with other *iso*DGR cyclopeptides.¹⁰⁶

4. Applications to organocatalysis

Over the last decade, peptides have shown a great potential as organic catalysts, with unique characteristics of reactivity, chemo- and stereoselectivity, which are difficult to achieve with different types of organic catalysts.¹⁰⁷ Their reactivity can be achieved by the use of properly functionalized natural or unnatural amino acids, whereas the rigid backbone of amide bonds and the disposition of the side chains impart well defined three-dimensional conformations typical of the protein secondary structure elements: helices, turns and sheets. An essential role in this process is played by the network of hydrogen bonds among the amino acid residues, as well as with the substrate and reagents, which are only possible in the presence of a number of well defined and organized amino acid residues. A groundbreaking study in the field of organocatalysis with diketopiperazines was published in 1979 by Oku and Inoue showing that cyclic dipeptides are valuable catalysts for the asymmetric addition of hydrogen cyanide to benzaldehyde to give the corresponding cyanohydrins (Scheme 21). Synthetic diketopiperazine **90**, *cyclo*-[L-Phe-L-His], in which

the imidazole group of the histidine residue is catalytically active as a base, afforded *R*-mandelonitrile in 90% *ee* in only 30 minutes.⁵⁵



Scheme 21. Asymmetric addition of hydrogen cyanide to benzaldehyde catalyzed by dipeptides.

A rationale for the stereinduction was provided, whereby the role of histidine is to direct the attack of cyanide to the *si*-face of benzaldehyde while the *re*-face is blocked by the aromatic ring of phenylalanine residue. Further work reported how time, temperature, solvent and crystallization of the catalyst, all play a significant role in an enantioselective reaction. A similar diketopiperazine was used in the asymmetric hydrocyanation of imines (Strecker reaction),^{56,108} although in this case the results have been questioned.¹⁰⁸

The organocatalyzed enantioselective conjugate addition of aldehydes and ketones to electron-poor olefins and particularly nitroolefins has gained momentum in the last few years and many short peptides featuring a terminal proline residue have been applied as selective catalysts. The efficacy of these compounds has been attributed to their ability to adopt a well-defined three-dimensional secondary structure, suitable for the transfer of stereochemical information.

Four peptidomimetics (**91–94**) containing the *cis*-DKP or *trans*-DKP scaffolds formally derived from the head-to-tail cyclization of L-aspartic acid and either (*R*)- or (*S*)-2,3-diaminopropionic acid and either L-Pro or D-Pro were synthesized.¹⁰⁹

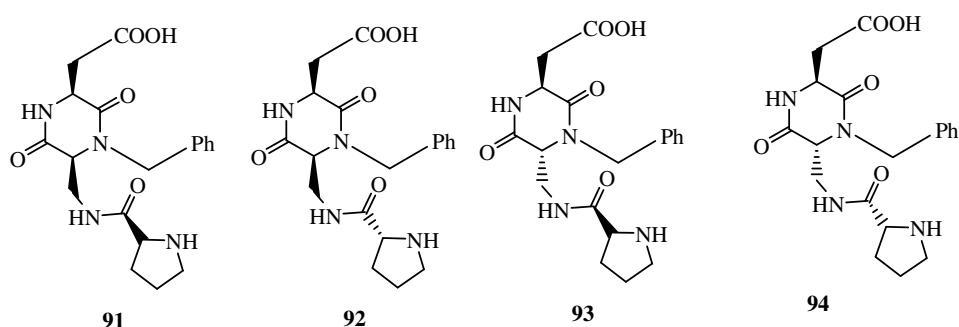
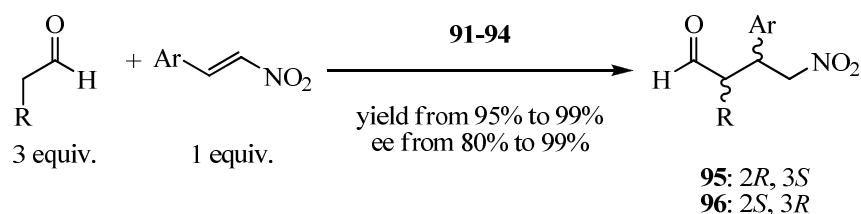


Figure 16. Organocatalysts **91–94**.

Peptidomimetics (**91–94**) were tested as organocatalysts in the conjugate addition reaction of several aldehydes to β -nitrostyrene and (*E*)-2-(furan-2-yl)nitroethene excellent diastereo- (99:1 dr) and enantioselectivities (up to 98% *ee*), particularly for catalysts **91** (containing L-Pro and *cis*-DKP-1) and **93** (containing L-Pro and *trans*-DKP-2), in high yields and under operationally mild conditions. It was shown that the terminal proline residue configuration establishes the absolute configuration of the conjugate addition products: L-Pro gave (*2R,3S*)-**95**, whereas with D-Pro (*2S,3R*)-**96** was obtained. The role of the DKP scaffolds is to tune the degree of selectivity: **93** was the best performing catalyst in terms of

enantioselectivity, whereas better diastereoselectivity was usually obtained with **91**. Catalysts **92** and **94** have a parallel behaviour of **91** and **93**: the more diastereoselective was **92** while **94** gave better *ee* values.¹⁰⁹



Scheme 22. Conjugate addition reaction of aldehydes to β -nitrostyrene.

To rationalize these results, a conformational study of these peptidomimetics was undertaken. A Monte Carlo/Energy Minimization (MC/EM) conformational search for the enamine intermediate derivatives revealed conformations where one face of the enamine moiety is shielded by the diketopiperazine ring and the carboxylic acid is likely to act as a hydrogen-bond donor, activating the nitroolefin acceptor ($-\text{NO}_2$) and directing its approach from the less hindered enamine face.

5. Conclusion

2,5-Diketopiperazines (DKPs) are simple heterocyclic scaffolds, characterized by a rather flat 6-membered ring core in which diversity can be introduced at up to four positions (N1, N4, C3, C6) and stereochemically controlled at two (C3, C6), while they can be prepared from readily available α -amino acids using conventional synthetic procedures, solid-phase and microwave-assisted organic synthesis. DKPs are also widely diffused in nature as part of complex bioactive molecules. In this chapter, we have highlighted different approaches to the synthesis and decoration of DKPs also when this structure is embedded in complex natural structures and showcased their use as interesting scaffolds for medicinal chemistry, in peptidomimetics for mimicking protein secondary structure elements (*e.g.*, β -turns and β -hairpins) and as organocatalysts. In many cases, the properties of these compounds can be rationalized in terms of their conformationally defined three-dimensional structures, which can be assessed by spectroscopic and computational methods. In conclusion, 2,5-diketopiperazines have controverted the common belief to be only protein artifacts or degradation products and they are becoming privileged structures for drug discovery, peptidomimetics and organocatalysis.

References

- (a) Witiak, D. T.; Wei, Y. In *Progress in Drug Discovery*; Jucker, E., Ed.; Birkhäuser Verlag: Basel, 1990; Vol. 35, pp. 249–363. (b) González, J. F.; Ortín, I.; de la Cuesta, E.; Menéndez, J. C. *Chem. Soc. Rev.* **2012**, *41*, 6902. (c) Martins, M. B.; Carvalho, I. *Tetrahedron* **2007**, *63*, 9923. (d) Liebscher, J.; Jin, S. *Chem. Soc. Rev.* **1999**, *28*, 251.
- McClelland, K.; Milne, P. J.; Lucieto, F. R.; Frost, C.; Brauns, S. C.; Van De Venter, M.; Du Plessis, J.; Dyason, K. *J. Pharm. Pharmacol.* **2004**, *56*, 1143.
- Borthwick, A. D. *Chem. Rev.* **2012**, *112*, 3641.
- Evans, B. E.; Rittle, K. E.; Bock, M. G.; DiPardo, R. M.; Freidinger, R. M.; Whitter, W. L.; Lundell, G. F.; Veber, D. F.; Anderson, P. S.; Chang, R. S. L.; Lotti, V. J.; Cerino, D. J.; Chen, T. B.; Kling, P. G.; Kunkel, K. A.; Springer, J. P.; Hirshfield, J. *J. Med. Chem.* **1988**, *31*, 2235.
- Suzuki, K.; Sasaki, Y.; Endo, N.; Mihara, Y. *Chem. Pharm. Bull.* **1981**, *29*, 233.
- Depew, K. M.; Marsden, S. P.; Zatorska, D.; Zatorski, A.; Bornmann, W. G.; Danishefsky, S. J. *J. Am. Chem. Soc.* **1999**, *121*, 11953.
- See, for instance: Bull, S. D.; Davies, S. G.; Moss, W. O. *Tetrahedron: Asymmetry* **1998**, *9*, 321.

8. See, for instance: Woodard, R. W. *J. Org. Chem.* **1985**, *50*, 4796.
9. Tullberg, M.; Grotli, M.; Luthman, K. *Tetrahedron* **2006**, *62*, 7484.
10. Pandey, S. K.; Awasthi, K. K.; Saxena, A. K. *Tetrahedron* **2001**, *57*, 4437.
11. López-Cobeñas, A.; Cledera, P.; Sánchez, J. D.; López-Alvarado, P.; Ramos, M. T.; Avendaño, C.; Menéndez, J. C. *Synthesis* **2005**, *19*, 3412.
12. Ressurreição, A. S. M.; Delatouche, R.; Gennari, C.; Piarulli, U. *Eur. J. Org. Chem.* **2011**, 217.
13. Fridkin, M.; Patchornik, A.; Katchalski, E. *J. Am. Chem. Soc.* **1965**, *87*, 4646.
14. Cabon, G.; Gaucher, B.; Gegout, A.; Heulle, S.; Masquelin, T. *Chimia* **2003**, *57*, 248.
15. Kennedy, A. L.; Fryer, A. M.; Josey, J. A. *Org. Lett.* **2002**, *4*, 1167.
16. Tullberg, M.; Luthman, K.; Grotli, M. *J. Comb. Chem.* **2006**, *8*, 915.
17. Baran, S. P.; Guerrero, C. A.; Corey, E. J. *J. Am. Chem. Soc.* **2003**, *125*, 5628.
18. Couladouros, E. A.; Magos, A. D. *Mol. Diversity* **2005**, *9*, 99.
19. Couladouros, E. A.; Magos, A. D. *Mol. Diversity* **2005**, *9*, 111.
20. Ugi, I. *Angew. Chem. Int. Ed.* **1962**, *1*, 8.
21. Dependence on the aldehyde, see: Armstrong, R. W.; Combs, A. P.; Tempest, P. A.; Brown, S. D.; Keating, T. A. *Acc. Chem. Res.* **1996**, *29*, 123.
22. Ramón, D. J.; Yus, M. *Angew. Chem. Int. Ed.* **2005**, *44*, 1602.
23. Hulme, C.; Gore, V. *Curr. Med. Chem.* **2003**, *10*, 51.
24. Keating, A. T.; Armstrong, R. W. *J. Am. Chem. Soc.* **1995**, *117*, 7842.
25. Hulme, C.; Morrisette, M. M.; Volz, F. A.; Burns, C. J. *Tetrahedron Lett.* **1998**, *39*, 1113.
26. See: Kreye, O.; Westermann, B.; Wessjohann, L. A. *Synlett* **2007**, *20*, 3188, and references therein.
27. Hulme, C.; Chappeta, S.; Dietrich, J. *Tetrahedron Lett.* **2009**, *50*, 4054.
28. Rhoden, C. R.; Rivera, D. G.; Kreye, O.; Bauer, A. K.; Westermann, A. K.; Wessjohann, L. A. *J. Comb. Chem.* **2009**, *11*, 1078.
29. Kennedy, A. L.; Fryer, A. M.; Josey, J. A. *Org. Lett.* **2002**, *4*, 1167.
30. Hulme, C.; Peng, J.; Morton, G.; Savino, J. M.; Herpin, T.; Labauniere, R. *Tetrahedron Lett.* **1998**, *39*, 7227.
31. (a) Chen, J. J.; Golebiowski, A.; McClenaghan, J.; Klopfenstein, S. R.; West, L. *Tetrahedron Lett.* **2001**, *42*, 2269. (b) Hulme, C.; Ma, L.; Romano, J.; Morton, G.; Tang, S.-Y.; Cherrier, M.-P.; Choi, S.; Laubandiere, R. *Tetrahedron Lett.* **2000**, *41*, 1883.
32. Habashita, H.; Kokubo, M.; Hamano, S.; Hamanaka, N.; Toda, M.; Shibayama, S.; Tada, H.; Sagawa, K.; Fukushima, D.; Maeda, K.; Mitsuya, H. *J. Med. Chem.* **2006**, *49*, 4140.
33. Hulme, C.; Cherrier, M.-P. *Tetrahedron Lett.* **1999**, *40*, 5295.
34. Szardenings, A. K.; Harris, D.; Lam, S.; Shi, L. H.; Tien, D.; Wang, Y. W.; Patel, D. V.; Avre, M. N.; Campbell, D. A. *J. Med. Chem.* **1998**, *41*, 2194.
35. Szardenings, A. K.; Antonenko, V.; Campbell, D. A.; DeFrancisco, N.; Ida, S.; Shi, L. H.; Sharkov, N.; Tien, D.; Wang, Y. W.; Navre, M. *J. Med. Chem.* **1999**, *42*, 1348.
36. Wyatt, G. P.; Allen, M. J.; Borthwick, A. D.; Davies, D. E.; Exall, A. M.; Hatley, R. J. D.; Irving, W. R.; Livermore, D. G.; Miller, N. D.; Nerozzi, F.; Sollis, S. L.; Szardenings, A. K. *Bioorg. Med. Chem. Lett.* **2005**, *15*, 2579.
37. Borthwick, A. D.; Davies, D. E.; Exall, A. M.; Livermore, D. G.; Sollis, S. L.; Nerozzi, F.; Allen, M. J.; Perren, M.; Shabbir, S. S.; Woolard, P. M.; Wyatt, P. G. *J. Med. Chem.* **2005**, *48*, 6956.
38. Ohta, A.; Okuwaki, Y.; Komaru, T.; Hisatome, M.; Yoshida, Y.; Aizawa, J.; Nakano, Y.; Shibata, H.; Miyazaki, T.; Watanabe, T. *Heterocycles* **1987**, *26*, 2691.
39. Yoshimura, J.; Yamaura, M.; Suzuki, T.; Hashimoto, H. *Chem. Lett.* **1983**, *7*, 1001.
40. Chai, C. L. L.; Elix, J. A.; Huleatt, P. B. *Tetrahedron Lett.* **2003**, *44*, 263.
41. Bianco, A.; Sonbksen, C. P.; Roepstorff, P.; Briand, J.-P. *J. Org. Chem.* **2000**, *65*, 2179.
42. Guenoun, F.; Zair, T.; Lamaty, F.; Pierrot, M.; Lazaro, R.; Viallefont, P. *Tetrahedron Lett.* **1997**, *38*, 1563.
43. Tullberg, M.; Grotli, M.; Luthman, K. *J. Org. Chem.* **2007**, *72*, 195.
44. Marchini, M.; Mingozzi, M.; Colombo, R.; Guzzetti, I.; Belvisi, L.; Vasile, F.; Potenza, D.; Piarulli, U.; Gennari, C. *Chem. Eur. J.* **2012**, *18*, 6195.
45. Caballero, E.; Avendaño, C.; Menéndez, J. C. *Tetrahedron: Asymmetry* **1998**, *9*, 967.

46. Movassaghi, M.; Schimidt, M. A.; Ashenhurst, J. *Angew. Chem. Int. Ed.* **2008**, *47*, 1485.
47. López-Alvarado, P.; Caballero, E.; Avendaño, C.; Menéndez, J. C. *Org. Lett.* **2006**, *8*, 4303.
48. Kim, J.; Ashenhurst, J. A.; Movassaghi, M. *Science* **2009**, *324*, 238.
49. Lange, J. H. M.; Hofmeyer, L. J. F.; Hout, F. A. S.; Osnabrug, S. J. M.; Verveer, P. C.; Kruse, C. G.; Feenstra, R. W. *Tetrahedron Lett.* **2002**, *43*, 1101.
50. Fischer, P. M. *J. Pept. Sci.* **2003**, *9*, 9.
51. Horton, D. A.; Bourne, G. T.; Smythe, M. L. *Mol. Diversity* **2000**, *5*, 289.
52. Wang, D.-X.; Liang, M.-T.; Tian, G.-J.; Lin, H.; Liu, H.-Q. *Tetrahedron Lett.* **2002**, *43*, 865.
53. Niidome, K.; Migihashi, C.; Morie, T.; Sato, F.; Abstracts of Papers, 225th National Meeting of the American Chemical Society, New Orleans, LA, Mar 23–27, 2003; American Chemical Society: Washington, DC, 2003; MEDI 287.
54. Spatola, A. F.; Romanovskis, P. In *Combinatorial Peptide and Nonpeptide Libraries*; Jung, G., Ed.; VCH: Weinheim, 1996; p. 327.
55. Oku, J. I.; Inoue, S. *J. Chem. Soc., Chem. Commun.* **1981**, 229.
56. (a) Kogut, E. F.; Thoen, J. C.; Lipton, M. A. *J. Org. Chem.* **1998**, *63*, 4604. (b) Iyer, M. S.; Gigstad, K. M.; Namedev, N. D.; Lipton, M. A. *J. Am. Chem. Soc.* **1996**, *118*, 4910.
57. Folkes, A.; Roe, M. B.; Sohal, S.; Golec, J.; Faint, R.; Brooks, T.; Charlton, P. *Bioorg. Med. Chem. Lett.* **2001**, *11*, 2589.
58. Wang, S.; Golec, J.; Miller, W.; Milutinovic, S.; Folkes, A.; Williams, S.; Brooks, T.; Hardman, K.; Charlton, P. *Bioorg. Med. Chem. Lett.* **2002**, *12*, 2367.
59. Brooks, T. D.; Wang, S. W.; Brünner, N.; Charlton, P. A. *Anti-Cancer Drugs* **2004**, *15*, 37.
60. Einholm, A. P.; Pedersen, K. E.; Wind, T.; Kulig, P.; Overgaard, M. T.; Jensen, J. K.; Bodker, J. S.; Christensen, A. *Biochem. J.* **2003**, *373*, 723.
61. Kanoh, K.; Kohno, S.; Katada, J.; Takahashi, J.; Uno, I. *J. Antibiot.* **1999**, *52*, 134.
62. Nicholson, B.; Lloyd, G. K.; Miller, B. R.; Palladino, M. A.; Kiso, Y.; Hayashi, Y.; Neuteboom, S. T. C. *Anti-Cancer Drugs* **2006**, *17*, 25.
63. Kanzaki, H.; Imura, D.; Nitoda, T.; Kawazu, K. *J. Biosci. Bioeng.* **2000**, *90*, 86.
64. Sinha, S.; Srivastava, R.; De Clercq, E.; Singh, R. K. *Nucleos. Nucleot. Nucl.* **2004**, *23*, 1815.
65. Asano, N. *Glycobiology* **2003**, *13*, 93R.
66. Houston, D. R.; Synstad, B.; Eijssink, V. G. H.; Stark, M. J. R.; Eggleston, I. M.; Van Aalten, D. M. F. *J. Med. Chem.* **2004**, *47*, 5713.
67. Byun, H.-G.; Zhang, H.; Mochizuki, M.; Adachi, K.; Shizuri, Y.; Lee, W.-J.; Kim, S.-K. *J. Antibiot.* **2003**, *56*, 102.
68. Fdhila, F.; Vázquez, V.; Sánchez, J. L.; Riguera, R. *J. Nat. Prod.* **2003**, *66*, 1299.
69. Kanokmedhakul, S.; Kanokmedhakul, K.; Phonkerd, N.; Soyong, K.; Kongsaree, P.; Suksamrarn, A. *Planta Med.* **2002**, *68*, 834.
70. Uhegbu, E. E.; Trischman, J. A. Abstracts of Papers, 229th National Meeting of the American Chemical Society, San Diego, CA, Mar 13-17, 2005; American Chemical Society: Washington, DC, 2005; CHED 1151.
71. Sugie, Y.; Hirai, H.; Inagaki, T.; Ishiguro, M.; Kim, Y. J.; Kojima, Y.; Sakakibara, T.; Sakemi, S.; Sogiura, A.; Suzuki, Y.; Brennan, L.; Duignan, J.; Huang, L. H.; Sutcliffe, J.; Kojima, N. *J. Antibiot.* **2001**, *54*, 911.
72. De Kievit, T. R.; Iglewski, B. H. *Infect. Immun.* **2000**, *68*, 4839.
73. Kozlovsky, A. G.; Zhelifonova, V. P.; Adanin, V. M.; Antipova, T. V.; Ozerskaya, S. M.; Ivanushkina, N. E.; Grafe, U. *Appl. Biochem. Microbiol.* **2003**, *39*, 393.
74. Kwon, O. S.; Park, S. H.; Yun, B. S.; Pyun, Y. R.; Kim, C. J. *J. Antibiot.* **2000**, *53*, 954.
75. Song, M. K.; Hwang, I. K.; Rosenthal, M. J.; Harris, D. M.; Yamaguchi, D. T.; Yip, I.; Go, K. V. L. *W. Exp. Biol. Med.* **2003**, *228*, 1338.
76. Hwang, I. K.; Harris, D. M.; Yip, I.; Kang, K. W.; Song, M. K. *Diabetes Obes. Metab.* **2003**, *5*, 317.
77. Kilian, G.; Jamie, H.; Brauns, S. C. A.; Dyason, K.; Milne, P. J. *Pharmazie* **2005**, *60*, 305.
78. Imamura, M.; Prasad, C. *Peptides* **2003**, *24*, 445.
79. López-Rodríguez, M. L.; Morcillo, M. J.; Fernández, E.; Porrás, E.; Orensanz, L.; Beneytez, M. E.; Manzanares, J.; Fuentes, J. A. *J. Med. Chem.* **2001**, *44*, 186.

80. Wyatt, P. G.; Allen, M. J.; Borthwick, A. D.; Davies, D. E.; Exall, A. M.; Hatley, R. J. D.; Irving, W. R.; Livermore, D. G.; Miller, N. D.; Nerozzi, F.; Sollis, S. L.; Szardenings, A. K. *Bioorg. Med. Chem. Lett.* **2005**, *15*, 2579.
81. Liddle, J. PCT Int. Appl. CODEN: PIXXD2; WO 2005000840; A1 20050106; 2005; *Chem. Abstr.* **2005**, *142*, 114102.
82. Brooks, D. P. PCT Int. Appl. CODEN: PIXXD2 WO 2005000311; A1 20050106, 2005; *Chem. Abstr.* **2005**, *142*, 114098.
83. Habashita, H.; Kokubo, M.; Hamano, S.; Hamanaka, N.; Toda, M.; Shibayama, S.; Tada, H.; Sagawa, K.; Fukushima, D.; Maeda, K.; Mitsuya, H. *J. Med. Chem.* **2006**, *49*, 4140.
84. Daugam, A.; Grondin, P.; Ruault, C.; Le Monnier de Gouville, A. C.; Coste, H.; Kirlovsky, I.; Hyafil, F.; Labaudinière, R. *J. Med. Chem.* **2003**, *46*, 4525.
85. Katzung, B. G. In *Basic & Clinical Pharmacology (Tenth edition)*; The McGraw-Hill Companies, Ed.; 2007.
86. Baures, P. W.; Ojala, W. H.; Costain, W. J.; Ott, M. C.; Pradhan, A.; Gleason, W. B.; Mishra, R. K.; Johnson, R. L. *J. Med. Chem.* **1997**, *40*, 3594.
87. Baures, P. W.; Ojala, W. H.; Gleason, W. B.; Mishra, R. K.; Johnson, R. L. *J. Med. Chem.* **1994**, *37*, 3677.
88. Yu, K.-L.; Rajakumar, G.; Srivastava, L. K.; Mishra, R. K.; Johnson, R. L. *J. Med. Chem.* **1988**, *31*, 1430.
89. Subasinghe, N. L.; Bontems, R. J.; McIntee, E.; Mishra, R. K.; Johnson, R. L. *J. Med. Chem.* **1993**, *36*, 2356.
90. Mishra, R. K.; Srivastava, L. K.; Johnson, R. L. *Prog. Neuro-Psychopharmacol. Biol. Psychiatr.* **1990**, *14*, 821.
91. Srivastava, L. K.; Bajwa, S. B.; Johnson, R. L.; Mishra, R. K. *J. Neurochem.* **1988**, *50*, 960.
92. Rose, G. D.; Smith, J. A. In *Advances in Protein Chemistry*; Anfisen, C. B.; Edsall, J. T.; Richards, F. M., Eds.; Academic Press: Orlando, 1985; Vol. 37, pp. 1–109.
93. (a) Gellman, S. H. *Acc. Chem. Res.* **1998**, *31*, 173. (b) Stigers, K. D.; Soth, M. J.; Nowick, J. S. *Curr. Opin. Chem. Biol.* **1999**, *3*, 714. (c) Cheng, R. P.; Gellman, S. H.; DeGrado, W. F. *Chem. Rev.* **2001**, *101*, 3219. (d) Stanford, A. R.; Gong, B. *Curr. Org. Chem.* **2003**, *7*, 1649. (e) Robinson, J. A. *Acc. Chem. Res.* **2008**, *41*, 1278. (f) Perez de Vega, M. J.; Martin-Martinez, M.; González-Muñiz, R. *Curr. Top. Med. Chem.* **2007**, *7*, 33. (g) Haridas, V. *Eur. J. Org. Chem.* **2009**, 5112.
94. Golebiowski, A.; Klopfenstein, S. R.; Chen, J. J.; Shao, X. *Tetrahedron Lett.* **2000**, *41*, 4841.
95. Golebiowski, A.; Klopfenstein, S. R.; Shao, X.; Chen, J. J.; Colson, A. O.; Grieb, A. L.; Russell, A. F. *Org. Lett.* **2000**, *2*, 2615.
96. Golebiowsky, A.; Jozwik, J.; Klopfenstein, S. R.; Colson, A. O.; Grieb, A. L.; Russell, A. F.; Rastogi, V. L.; Diven, C. F.; Portlock, D. E.; Chen, J. J. *J. Comb. Chem.* **2002**, *4*, 584.
97. Kim, H.-O.; Nakanishi, H.; Lee, M. S.; Khan, M. *Org. Lett.* **2000**, *2*, 301.
98. Liu, J.; Brahimi, F.; Saragovi, H. U.; Burgess, K. *J. Med. Chem.* **2010**, *53*, 5044.
99. Pfeiffer, B.; Peduzzi, E.; Moehle, K.; Zurbriggen, R.; Glück, R.; Pluschke, G.; Robinson, J. A. *Angew. Chem. Int. Ed.* **2003**, *43*, 2368.
100. Robinson, J. A. *Synlett* **2000**, *4*, 429.
101. Chen, K. X. *Theranostics* **2011**, *1*, 189.
102. Colombo, R.; Mingozi, M.; Belvisi, L.; Arosio, D.; Piarulli, U.; Carenini, N.; Perego, P.; Zaffaroni, N.; De Cesare, M.; Castiglioni, V.; Scanzani, E.; Gennari, C. *J. Med. Chem.* **2012**, *55*, 10460.
103. Mingozi, M.; Dal Corso, A.; Marchini, M.; Guzzetti, I.; Civera, M.; Piarulli, U.; Arosio, D.; Belvisi, L.; Potenza, D.; Pignataro, L.; Gennari, C. *Chem. Eur. J.* **2013**, *19*, 3563.
104. Dechantsreiter, M. A.; Planker, E.; Mathä, B.; Lohof, E.; Hölzemann, G.; Jonczyk, A.; Goodman, S. L.; Kessler, H. *J. Med. Chem.* **1999**, *42*, 3033.
105. (a) Müller, G.; Gurrath, M.; Kessler, H. *J. Comput.-Aided Mol. Des.* **1994**, *8*, 709. (b) Haubner, R.; Gratias, R.; Diefenbach, B.; Goodman, S. L.; Jonczyk, A.; Kessler, H. *J. Am. Chem. Soc.* **1996**, *118*, 7461. (c) Haubner, R.; Schmitt, W.; Hölzemann, G.; Goodman, S. L.; Jonczyk, A.; Kessler, H. *J. Am. Chem. Soc.* **1996**, *118*, 7881.

106. Frank, A. O.; Otto, E.; Mas-Moruno, C.; Schiller, H. B.; Marinelli, L.; Cosconati, S.; Bochen, A.; Vossmeier, D.; Zahn, G.; Stragies, R.; Novellino, E.; Kessler, H. *Angew. Chem. Int. Ed.* **2010**, *49*, 9278.
107. For recent reviews, see: (a) Colby Davie, E. A.; Mennen, S. M.; Xu, Y.; Miller, S. J. *Chem. Rev.* **2007**, *107*, 5759. (b) Wennemers, H. *Chem. Commun.* **2011**, *47*, 12036. (c) Fanelli R.; Piarulli U. In *Comprehensive Enantioselective Organocatalysis*; Dalko, P. I., Ed.; Wiley-VCH Verlag GmbH: Weinheim, 2013; pp. 97–116.
108. Becker, C.; Hoben, C.; Schollmeyer, D.; Scherr, G.; Kunz, H. *Eur. J. Org. Chem.* **2005**, 1497.
109. Durini, M.; Sahr, F. A.; Kuhn, M.; Civera, M.; Gennari, C.; Piarulli, U. *Eur. J. Org. Chem.* **2011**, *20*, 5599.